

**INVESTIGATION INTO THE EFFECT OF
FIXTURING SYSTEMS ON THE DESIGN OF
CONDITION MONITORING FOR
MACHINING OPERATIONS**

Jabbar Kadhim Abbas
BSc, MSc, PGDR

A thesis submitted in partial fulfilment of the requirements of
Nottingham Trent University for the degree of
Doctor of Philosophy

July 2013

Abstract

The global market competition has drawn the manufacturer's attention on automated manufacturing processes using condition monitoring systems. These systems have been used for improving product quality, eliminating inspection, and enhancing manufacturing productivity. Fixtures are essential devices in machining processes to hold the tool or workpiece, hence they are influenced directly by the stability of the cutting tool. Therefore, tool and fixturing faults play an important part in the inaccuracy of the machining processes causing deterioration of surface roughness.

For the above mentioned reasons, and the limited work in this domain, this thesis develops an experimental investigation to evaluate the effect of fixturing quality on the design of condition monitoring systems. The proposed monitoring system implements multisensors and signal processing methods able to analyse the sensory information and make an appropriate decision. Therefore, several sensors namely force, vibration, acoustic emission, eddy current, power, strain and sound, are combined with a newly suggested approach, named Taylor's Equation Induced Pattern (TIP), and neural networks to detect tool wear and tool breakage. It also evaluates the monitoring system to provide valuable data to show the effect of fixturing quality. Surface roughness of the workpiece has been measured and compared with the sensitivity of the monitoring system, which reflects the state of tool and fixturing conditions.

A novel approach, termed ASPSF, (Automated Sensor and Signal Processing Selection for Fixturing) has been implemented to select the most sensitive sensors and signal processing method. The aim is to reduce the number of sensors needed in the overall system and reduce the cost. New automated detection methods (Principal Component Analysis (PCA), Fuzzy logic, correlation coefficients) have been implemented to prove the capability of the approach. A cost reduction is performed based on removing least utilised sensors without losing the performance of the condition monitoring system. The results prove that the ASPSF is capable of detection the effect of fixturing quality on the design of the condition monitoring system and the trend in surface roughness. Consequently, the findings of this thesis prove that the change in the fixturing quality could have significant effect on the design of the condition monitoring system and the behaviour of the system. Therefore, continuous condition monitoring design process will be needed regularly for every machine, to allow compensation in the change in the characteristics.

Acknowledgements

I would like to present my full gratitude to my supervisor, Dr. Amin Al-habaibeh, for his support, guidance and invaluable advice to achieve the requirements of the thesis. He significantly dedicated and provided necessary critique regarding the research.

I would like also to extend my sincere thanks to my second supervisor, Professor Daizhong Su, for his friendly support in many issues during the research.

I dedicate this thesis to the soul of my father, who I have never seen him, the souls of my mother and oldest brother; they devoted most of their life to serve and take care of me and unfortunately passed to hereafter. Also, many thanks to beloved family who have taken care of me after I lost my parents.

Heartfelt thanks and high respect to my wife, who has participated with me in both my happy and sad moments. Also, thanks for her understanding and endless love, throughout my studies. Even when I felt panicked or disturbed, she encouraged me and said: go on! go on ! you have to continue in the doctoral task which is similar to a marathon running. My kind thanks also go to my lovely children, “*Ali, Nabaa, Mohammed*”, seeing them; I absorb the power to achieve the best position to make them proud as a father.

I would like also to convey thanks to the Ministry of Higher Education/Iraq and Iraqi Cultural Attaché in London for providing the financial means and scholarship facilities, this study would have been impossible without their support and encouragement.

Last but not least, my real thanks and appreciations go to my colleagues and friends in my native country, Iraq and the PhD students in the UK, for their help and wishes for the successful completion of this research.

Awards and Publications

Awards:

The author won the First Prize for the best research in *the First conference of Engineering Sciences /Iraqi Cultural Attaché/ London/ 1&2 October 2011*. A copy of the Prize Certificate is attached in the Appendix A.

Publication list:

ABBAS, J., AL-HABAIBEH, A. and SU, D., 2013. Investigating the Design of Condition Monitoring Systems to Evaluate Surface Roughness under the Variability in Tool wear and Fixturing Conditions. *In: 5th International Conference on Advanced Design and Manufacture (ADM2013), Valencia, Spain, 27-29 September 2013*.

ABBAS, J., AL-HABAIBEH, A. and SU, D., 2011. The Investigation of prediction surface roughness from machining forces in end milling processes. *Key Engineering Materials*. Vol 486, pp. 91-94.

ABBAS, J., AL-HABAIBEH, A. and SU, D., 2011. The effect of tool fixturing quality on the design of condition monitoring systems for detecting tool conditions. *JJMIE - Jordan Journal of Mechanical and Industrial Engineering*. Vol. 5 (1), pp. 17-22.

ABBAS, J., AL-HABAIBEH, A. and SU, D., 2011. Sensor fusion for condition monitoring system of end milling operations. *Key Engineering Materials*. Vol 450, pp. 267-270.

ABBAS, J., 2011, AL-HABAIBEH, A. and Su, D., 2011. The application of multi-Sensor System for condition Monitoring System of Machining Operations. *In: First conference of Engineering Sciences, Iraqi Cultural Attaché/ London/ 1&2 October 2011*.

ABBAS, J., 2011. Measuring the features sensitivity of sensor fusion using neural network in milling operation. *In: Creative Connections: Exploring and Discovering Relationships. Research Practice Course Third Annual Conference, Nottingham Trent University, Nottingham, May, 2011*. Scott, D., Mc, Carron, J., Mandere, M., Warwick, R. and Appiah, S., eds., Nottingham Trent University, Nottingham. pp. 1-5.

ABBAS, J., AL-HABAIBEH, A. and SU, D., 2011. The investigation of prediction surface roughness from machining forces in end milling processes. *In: 4th International Conference on Advanced Design and Manufacture (ADM2011), Kunming, China, 21-23 September 2011*.

ABBAS, J., AL-HABAIBEH, A. and SU, D., 2010. The effect of tool fixturing quality on the design of condition monitoring systems for detecting tool conditions. *In: Seventh Jordanian International Mechanical Engineering Conference (JIMEC'7), Amman, Jordan, 27-29 September 2010*.

ABBAS, J., AL-HABAIBEH, A. and SU, D., 2010. Sensor fusion for condition monitoring system of end milling operations, *In: 3rd International Conference on Advanced Design and Manufacture (ADM2010), UK, 9-11 September 2010*.

List of Figures

Figure 1.1: Error in machine tool and the factors affecting it [10].	3
Figure 1.2: Schematic of ASPSF approach for monitoring the fixturing set-up and tool conditions.	5
Figure 1.3: The change of machining characteristics of milling process.	6
Figure 1.4: The schematic diagram for the structure of the thesis.	9
Figure 2.1: Twelve Degree of freedom for prismatic workpiece.	13
Figure 2.2: Configuration of a tool clamp based on a shape memory alloy.	17
Figure 2.3: A schematic of collet parts.	18
Figure 2.4: The solid collet.	20
Figure 2.5: (a) The split collet (b) Collet chuck system.	20
Figure 2.6: (a) Frictional force M created at the interface between two mating bodies A and B (b) Model of a collet (reproduced from [38]).	21
Figure 2.7: Rigid body and constraint points [49].	26
Figure 3.1: The major influencing parameters on tool wear in machining processes	32
Figure 3.2: The CNC milling machine.	33
Figure 3.3: End mill Cutters.	34
Figure 3.4: Specification of the End mill.	35
Figure 3.5: Cutting tool wear forms in orthogonal metal cutting (reproduced from [69]).	38
Figure 3.6: The relationship between cutting velocity and tool life.	40
Figure 3.7: The relationship between tool wear and tool life with different cutting velocities.	40
Figure 3.8: Parameters that affect surface roughness.	42
Figure 3.9: Workpiece before clamp actuation.	43
Figure 3.10: Axial and radial components of cutting force for surface inclination (reproduced from [84]).	45
Figure 4.1: The general structure of a condition monitoring system (reproduced from [20]).	47
Figure 4.2: Multi-Sensor cutting tool monitoring options.	51
Figure 4.3: Schematic of the X-axis drive and control system (reproduced from [97]).	54
Figure 5.1: Typical curve of tool wear using cutting time.	59
Figure 5.2: Monitoring system for the milling process (reproduced from [18]).	67
Figure 5.3: Representation of neural network based cutting process monitoring.	73
Figure 5.4: Types of contact between the collet and tool surfaces.	76
Figure 5.5: The difference between Rubber collet with other types in gripping part	77
Figure 5.6: Adaptive spindle system (AdSpin) [163].	78
Figure 6.1: The ASPS approach has been modified to produce the ASPSF approach.	85
Figure 6.2: Simplification of complex sensory signal into simple SCFs.	86
Figure 6.3: Example of two measuring sensitivity methods of the SCFs.	87
Figure 6.4: The rank and the selection of SCFs, information obtained from [20].	89
Figure 6.5: Examples of SCFs using linear regression method.	91
Figure 6.6: Examples of SCFs using Sudden Change In Value (SCIV).	92

Figure 6.7:	The essential structure of the ASPSF approach.	94
Figure 6.8:	Schematic diagram of the proposed ASPSF methodology.	95
Figure 6.9:	Diagram of principal component Analysis (PCA).	96
Figure 6.10:	Example of SCFs using Range Value (RV) method.	97
Figure 6.11:	The polynomial equation of the expected tool wear pattern.	98
Figure 6.12:	Steps of the Fuzzy logic approach.	99
Figure 6.13:	Diagram of the structure of the subsequent chapters.	101
Figure 7.1:	The complete experimental setup.	105
Figure 7.2:	Schematic diagram of surface measurement setup.	107
Figure 7.3:	Fixture to insert the Eddy current sensors.	108
Figure 7.4:	Fixture to hold the accelerometers.	108
Figure 7.5:	The equipment of the experimental work.	110
Figure 7.6:	Dynamometer 9257A in milling operation [190].	111
Figure 7.7:	Photo of the Kistler accelerometer [191].	112
Figure 7.8:	AE sensor (Kistler 8152b111) [192].	113
Figure 7.9:	Strain sensor (Kistler 9232A).	114
Figure 7.10:	Eddy current sensor IC 12-02 [195].	114
Figure 7.11:	Sound sensor (microphone).	115
	Photo of Power sensor.12 Figure 7.	116
Figure 7.13:	Structure of a fuzzy logic model.	120
Figure 7.14:	The architecture of the LVQ neural network.	123
Figure 7.15:	The BP neural target division according to $y= X^3$ (function (X3)).	124
Figure 7.16:	The BP neural target division according to $y= X^{20}$ (function (X20)).	125
Figure 7.17:	The architecture of the Back Propagation Neural Network.	126
Figure 8.1:	The essential principles of the ASPSF approach.	129
Figure 8.2:	Schematic diagram of experimental setup for the monitoring system.	130
Figure 8.3:	The two states of the milling tool (fresh and worn tool).	131
Figure 8.4:	Example of the raw signals of the milling process for fresh tool.	132
Figure 8.5:	Example of the raw signals of the milling process for worn tool.	132
Figure 8.6:	The practical steps of the ASPSF approach using linear regression.	134
Figure 8.7:	Example of high, medium and low sensitivity SCF for the tool without sleeve.	136
Figure 8.8:	Example of high, medium and low sensitivity SCF for the tool with rubber sleeve.	136
Figure 8.9:	A graphical presentation of the sensitivity for tool without sleeve.	138
Figure 8.10:	A graphical presentation of the sensitivity for tool with rubber sleeve.	139
Figure 8.11:	The practical steps of the ASPSF approach using PCA.	140
Figure 8.12:	PCA example data, original data on the left, data with the means subtracted on the right, and a plot of the data.	141
Figure 8.13:	A plot of the principle components according to eigenvalue of	143
Figure 8.14:	A plot of the principle components according to eigenvalue of variables in the covariance matrix for tool with rubber sleeve.	144
Figure 8.15:	A graphical presentation of the EVSM for tool without sleeve.	145
Figure 8.16:	A graphical presentation of the EVSM for tool with rubber sleeve.	147
Figure 8.17:	The practical steps of calculating the correlation coefficient between sensitivity and PC.	148
Figure 8.18:	The Correlation coefficient between PCA and Linear regression sensitivity for tools without sleeve.	149

Figure 8.19:	The Correlation coefficient between PCA and Linear regression sensitivity for tools without sleeve.....	149
Figure 8.20:	The relation between the correlation coefficient of PC1 and fixturing system.....	150
Figure 8.21:	The relation between the correlation coefficient of PC2 and fixturing system.....	150
Figure 8.22:	Comparison between the systems sensitivity of tool without sleeve. .	151
Figure 8.23:	Comparison between the systems sensitivity of tool with rubber sleeve.....	152
Figure 8.24:	Comparison between the systems eignvalue of tool without sleeve. .	155
Figure 8.25:	Comparison between the systems eigenvalue of tool with rubber sleeve.	155
Figure 8.26:	The sensor setup used to calculate the cost of the system (prices are based on quation).	158
Figure 8.27 :	As values for the sensory signals of both tools.	166
Figure 8.28:	Asp values for the signal processing methods of both tools.	166
Figure 8.29:	Aev values for the sensory signals of both tools.....	168
Figure 8.30:	Apc values for the principal component methods of both tools.....	169
Figure 8.31:	Comparison between Ac and Ec of both tools.....	170
Figure 8.32:	Surface roughness profile.....	171
Figure 8.33:	Schematic diagram of experimental setup.	172
Figure 8.34:	Surface roughness of forces and workpiece for the tool without sleeve.....	173
Figure 8.35:	Surface roughness of forces and workpiece for the tool with rubber sleeve.....	174
Figure 8.36:	Mean of the surface roughness for the tool without sleeve.....	174
Figure 8.37:	Mean of the surface roughness for the tool with rubber sleeve.	175
Figure 9.1:	Schematic diagram of experimental setup for the monitoring system.	179
Figure 9.2:	The two states of the milling tool (fresh and worn tool).....	179
Figure 9.3:	Example of the raw signals of the milling process for fresh tool.....	180
Figure 9.4:	Example of the raw signals of the milling process for worn tool.	180
Figure 9.5:	Example of high and low sensitivity SCF for the tools without sleeve.....	182
Figure 9.6:	Example of high and low sensitivity SCF for the tools with rubber sleeve.	182
Figure 9.7:	Example of high and low sensitivity SCF for the tools with copper sleeve.....	183
Figure 9.8:	Example of high and low sensitivity SCF for the tools with aluminium sleeves.....	183
Figure 9.9:	A graphical presentation of the sensitivity for tool 1 without sleeve..	185
Figure 9.10:	A plot of the principle components according to eigenvalue of variables in the covariance matrix for tool 1 without sleeve.	186
Figure 9.11:	A graphical presentation of the EVSM for tool 1 without sleeve.	187
Figure 9.12:	The Correlation coefficient between PCA and Linear regression sensitivity for tools without sleeves.....	188
Figure 9.13:	The Correlation coefficient between PCA and Linear regression sensitivity for tools with rubber sleeves.....	188
Figure 9.14:	The Correlation coefficient between PCA and Linear regression sensitivity for tools with copper sleeves.	189

Figure 9.15:	The Correlation coefficient between PCA and Linear regression sensitivity methods for tools with aluminium sleeves.	189
Figure 9.16:	The relation between the correlation coefficient of PC1 and fixturing systems.	190
Figure 9.17:	The relation between the correlation coefficient of PC2 and fixturing materials.	191
Figure 9.18:	The application of Neural Network for SCF data.	192
Figure 9.19:	Example of the SCF data for input training data.	193
Figure 9.20:	SCF testing error ratio using BP neural network for tools with different fixturing systems.	194
Figure 9.21:	SCF testing error ratio using LVQ neural network for tools with different fixturing materials.	194
Figure 9.22:	The application of Neural Network for PCA data.	195
Figure 9.23:	Example of the SCF data of most sensitive sensor.	196
Figure 9.24:	PCA testing error ratio using BP neural network for tools with different fixturing systems.	197
Figure 9.25:	PCA testing error ratio using LVQ neural network for tools with different fixturing materials.	197
Figure 9.26:	Correlation coefficient between training errors of LR and PCA (a) using BP neural network, (b) using LVQ neural network.	198
Figure 9.27:	The sensor setup used to calculate the cost of the system (prices are based on quotation).	199
Figure 9.28:	Comparison between the systems sensitivity for tool 1 without sleeve.	200
Figure 9.29:	Comparison between the systems eigenvalue of tool without sleeve.	202
Figure 9.30:	As values for the sensory signals of tool 1 without sleeve.	208
Figure 9.31:	Asp values for the signal processing methods of tool 1 without sleeve.	209
Figure 9.32:	Aev values for the sensory signals of tool1 without sleeve.	210
Figure 9.33:	Apc values for the principal component methods of tool1 without sleeve.	210
Figure 9.34:	Comparison between Ac and Ec of both tools.	211
Figure 9.35:	The BP neural target division according to the X3 function.	212
Figure 9.36:	The BP neural target division according to the X20 function.	212
Figure 9.37:	The BP neural target division according to the experimental feature (Experimental).	213
Figure 9.38:	The of testing errors for all the tools using different target functions.	214
Figure 9.39:	Surface roughness of workpiece for four types of fixturing materials.	215
Figure 9.40:	Examples of low, medium and high sensitivity SCF for the tools.	216
Figure 9.41:	The correlation coefficient between the sensitivity SCF and surface roughness for different fixturing materials.	218
Figure 10.1:	Schematic diagram of the monitoring system and surface roughness	221
Figure 10.2:	The three states of the milling tool (fresh, one broken tooth and two broken teeth) with four fixturing systems.	222
Figure 10.3:	Examples of the raw signals of the machining process for fresh tools.	223
Figure 10.4:	Examples of the raw signals of the machining process for damaged tools (one broken tooth).	223

Figure 10.5:	Examples of the raw signals of the machining process for damaged tools (two broken teeth).	224
Figure 10.6:	Example of the result for all the SCFs using LR slope method for four fresh tools.	225
Figure 10.7:	A graphical presentation of the sensitivity for fresh tool without sleeve using LR method.	226
Figure 10.8:	A graphical presentation of the sensitivity for tool with one broken tooth, using LR slope method.	227
Figure 10.9:	A graphical presentation of the sensitivity for tool with two broken teeth, using LR method.	227
Figure 10.10:	Examples of SCFs using Range value method for fresh tool without sleeve.	228
Figure 10.11:	A graphical presentation of the sensitivity for fresh tool without sleeve using Range value method.	229
Figure 10.12:	A graphical presentation of the sensitivity for tool with one broken tooth, without sleeve using Range value method.	230
Figure 10.13:	A graphical presentation of the sensitivity for tool with two broken teeth, without sleeve using Range value method.	230
Figure 10.14:	Examples of SCFs using SCIV method for fresh tool without sleeve.	231
Figure 10.15:	A graphical presentation of the sensitivity for fresh tool with, without sleeve using SCIV method.	232
Figure 10.16:	A graphical presentation of the sensitivity for tool with broken one tooth, without sleeve using SCIV method.	232
Figure 10.17:	A graphical presentation of the sensitivity for tool with broken two teeth, without sleeve using SCIV method.	233
Figure 10.18:	Examples of SCFs using CCX3 method for fresh tool without sleeve.	234
Figure 10.19:	A graphical presentation of the sensitivity for fresh tool without sleeve using CCX3 method.	235
Figure 10.20:	A graphical presentation of the sensitivity for tool with 1 broken tooth, without sleeve using CCX3 method.	236
Figure 10.21:	A graphical presentation of the sensitivity for tool with 2 broken teeth, without sleeve using CCX3 method.	236
Figure 10.22:	Steps of the proposed fuzzy logic approach.	237
Figure 10.23:	A graphical presentation of the sensitivity for fresh tool without sleeve using Fuzzy method.	239
Figure 10.24:	A graphical presentation of the sensitivity for normal tool with broken one tooth using fuzzy method.	240
Figure 10.25:	A graphical presentation of the sensitivity for tool with broken two teeth, without sleeve using SCIV method.	242
Figure 10.26:	The LVQ neural network errors of sensitivity feature for fresh tools with deferent fixturing.	243
Figure 10.27:	The average LVQ errors of the sensitivity measuring methods for fresh tools.	244
Figure 10.28:	The LVQ neural network errors of sensitivity feature for tools with one broken tooth for deferent fixturing.	245
Figure 10.29:	The average LVQ errors of the sensitivity measuring methods for tools with one broken tooth.	245

Figure 10.30:	The LVQ neural network errors of sensitivity feature for tools with two broken teeth for deferent fixturing.	246
Figure 10.31:	The average LVQ errors of the sensitivity measuring methods for tools two with broken teeth.	247
Figure 10.32:	Comparison between the average LVQ errors of the sensitivity measuring methods for three tool conditions.	248
Figure 10.33:	The amplitude and variance of first experimental pattern (pattern1)..	249
Figure 10.34:	The amplitude and variance of second experimental pattern (pattern 2).	249
Figure 10.35:	The amplitude and variance of third experimental pattern (pattern 3).	250
Figure 10.36:	The BP neural network errors for fresh tools using different patterns.	251
Figure 10.37:	The training errors of different patterns for tools with one broken tooth.....	252
Figure 10.38:	The training errors of different patterns for tools with two broken teeth.	252
Figure 10.39:	Comparison between the pattern errors for tools with different fixturing systems.	254
Figure 10.40:	Surface roughness of workpiece for fresh tools.	255
Figure 10.41:	Surface roughness of workpiece for tools with one broken tooth....	256
Figure 10.42:	Surface roughness of workpiece for tools with two broken teeth.	256
Figure 10.43:	Average of surface roughness of workpiece for all tools conditions.	257
Figure 10.44:	Comparison between the averages of Ra of workpice for three tool conditions.	258
Figure 10.45:	The relation between Surface roughness and average of sensitivity of features of system for fresh tools.	259
Figure 10.46:	The relation between Surface roughness and average of sensitivity of features of system for tools with one broken tooth.	260
Figure 10.47:	The relation between Surface roughness and average of sensitivity of features of system for tools with two broken teeth.	261
Figure 11.1:	Summary of the overall thesis structure.	265
Figure 11.2:	Graphic illustration of the suggested ASPSF approach.	267

List of Tables

Table 7.1:	The recommended cutting conditions for the carbide and HSS tools. ..	106
Table 8.1:	The machining parameters of the milling process.....	130
Table 8.2:	The Associated matrix of the system for tool without sleeve.	137
Table 8.3:	The Associated matrix of the system for tool rubber sleeve.	138
Table 8.4:	The Eigenvalue Sensory Matrix (EVSM) of the system for tool without sleeve.	145
Table 8.5:	The Eigenvalue Sensory Matrix (EVSM) of the system for tool with rubber sleeve.	146
Table 8.6:	First system with the SCFs sensitivity (LR) slope for the both tools...	152
Table 8.7:	Second system with the SCFs sensitivity (LR) slope for both tools. ..	153
Table 8.8:	Third system with the SCFs sensitivity (LR) slope for the both tools. .	153
Table 8.9:	First system with the PCFs eigenvalue (PCA) for the both tools.....	156
Table 8.10:	Second system with the PCFs eigenvalue (PCA) for both tools.	156
Table 8.11:	Third system with the PCFs eigenvalue (PCA) for the both tools.	157
Table 8.12:	Sensors utilisation for the tool without sleeve using LR.....	159
Table 8.13:	The optimised system (1st and 2nd system) for the tool without sleeve using LR.	159
Table 8.14:	Sensors utilisation for the tool with rubber sleeve using LR.....	160
Table 8.15:	The optimised system (1st and 2nd system) for the tool with rubber sleeve using LR.	160
Table 8.16:	Sensors utilisation for the tool without sleeve using PCA.	161
Table 8.17:	The optimised system (1st and 2nd system) for the tool without sleeve using PCA.	162
Table 8.18:	Sensors utilisation for the tool with rubber sleeve using PCA.....	162
Table 8.19:	The optimised system (1st and 2nd system) for the tool with rubber sleeve using PCA.....	163
Table 8.20:	Comparison between the optimised systems from LR slope and PCA.	164
Table 9.1:	The machining parameters of the milling process.....	178
Table 9.2:	The Associated matrix of the system for tool 1 without sleeve.	184
Table 9.3:	The Eigenvalue Sensory Matrix (EVSM) of the system for tool 1 without sleeve.	187
Table 9.4:	First system with the SCFs sensitivity (LR) slope for the tool 1 without sleeve.	200
Table 9.5:	Second system with the SCFs sensitivity (LR slope) for the tool 1 without sleeve.	201
Table 9.6:	Third system with the SCFs sensitivity (LR slope) for the tool 1 without sleeve.	201
Table 9.7:	First system with the PCFs eigenvalue (PCA) for the tools without sleeve.	202
Table 9.8:	Second system with the PCFs eigenvalue (PCA) for the tools without sleeve.....	203
Table 9.9:	Third system with the PCFs eigenvalue (PCA) for the tools without sleeve.	203
Table 9.10:	Sensors utilisation for the tool 1 without sleeve using LR.....	204
Table 9.11:	The optimised system (1st and 2nd system) for the tool1 without sleeve using LR.	205

Table 9.12:	Sensors utilisation for the tool 1 without sleeve using PCA.	205
Table 9.13:	The optimised system (1st and 2nd system) for the tool with copper sleeve using PCA.	206
Table 9.14:	Comparison between the optimised systems from LR slope and PCA for tools with different fixturing systems.	207
Table 9.15:	The modulus of elasticity (E) and average of surface roughness.	215
Table 9.16:	The most sensitivity of the sensory the system for different tools.	217
Table 10.1:	The machining parameters of the milling process.	221
Table 10.2:	Example of the results of the fuzzy logic evaluation for the SCF of fresh tool without sleeve.	238
Table 10.3:	Example of the results of the fuzzy logic evaluation for the SCF of tool without sleeve with one broken tooth.	240
Table 10.4:	Example of the results of the fuzzy logic evaluation for the SCF of tool without sleeve with two broken teeth.	241
Table 11.1:	The most sensitive sensor(S) and signal processing (SP) in the different machining conditions using fuzzy logic.	273

Nomenclature

Sensory Signals and Sensors

F_x = Cutting force in the x direction measured by a dynamometer (N).

F_y = Cutting force in the y direction measured by a dynamometer (N).

F_z = Cutting force in the z direction measured by a dynamometer (N).

AE = Acoustic Emission Signal/Sensor (V).

AE_RMS = Root Mean Square of the AE signal (V).

Strain= Strain sensor (N).

Mic = Sound Signal (dB).

V_{wx} = Vibration Signal in the x direction measured by accelerometer attached to workpiece table (V).

V_{wy} = Vibration Signal in the y direction measured by accelerometer attached to workpiece table (V).

V_{sx} = Vibration Signal in the x direction measured by accelerometer attached to spindle case (V).

V_{sy} = Vibration Signal in the y direction measured by accelerometer attached to spindle case (V).

V_{sz} = Vibration Signal in the z direction measured by accelerometer attached to spindle case (V).

P_{wr} = Machine Motor Voltage by the Power sensor (V).

E_{dx} = Power of the eddy current sensor in x direction.

E_{dy} = Power of the eddy current sensor in y direction

DOC = Depth of Cut (mm).

R_a = Surface roughness of the machined part (μm).

Signal Processing Methods

std = Standard deviation.

$FFT(f1, f2)$ = Average value of the FFT between frequencies $f1$ and $f2$.

$FFT1 = FFT(20 \text{ Hz}, 2.5 \text{ KHz})$

$FFT2 = FFT(2.501 \text{ KHz}, 5 \text{ KHz})$

$FFT3 = FFT(5.001 \text{ KHz}, 7.5 \text{ KHz})$

$FFT4 = FFT(7.501 \text{ KHz}, 10 \text{ KHz})$

$FFT5 = FFT(10.001 \text{ KHz}, 12.5 \text{ KHz})$

$FFT6 = FFT(12.501 \text{ KHz}, 15 \text{ KHz})$

$FFT7 = FFT(15.001 \text{ KHz}, 17.5 \text{ KHz})$

$FFT8 = FFT(17.501 \text{ KHz}, 20 \text{ KHz})$

$FFT9 = FFT(20.001 \text{ KHz}, 22.5 \text{ KHz})$

$FFT10 = FFT(22.501.001 \text{ KHz}, 25 \text{ KHz})$

Wav_i = Standard deviations of the i th level of the wavelet analysis.

S = Sensor.

SP = Signal Processing Method.

ASPSF Terminology

ASPSF = Automated Sensory and Signal Processing Selection System for Fixturing.

SCF = Sensory Characteristic Feature.

SFM = Sensory Feature Matrix

ASM = Association Matrix

LR= Linear Regression Detection Method.

PCA= Principal Component Analysis Detection Method

RV= Range Value Detection Method.

SCIV = Sudden Change In Value Detection Method.

CCX3= Correlation Coefficient (X3) Detection Method.

CCX20= Correlation Coefficient (X20) Detection Method.

FL= Fuzzy Logic Evaluation and Detection Method.

SU = Sensor Utilisation coefficient (%).

SUA = Overall average utilisation of a monitoring system (%).

S= Number of SCFs used from the sensor.

T= Total number of features in the system.

P= Number of signals produced by the sensor.

ASP_k = Average sensitivity of the *k*th signal processing method.

ASP = Average sensitivity of all signal processing methods implemented in a system.

AS_k = Average sensitivity of the *k*th sensor (or sensory signals).

AS = Average sensitivity of all sensors (or sensory signals) implemented in a system.

Ac = Average of the summation of sensitivity coefficients of the ASM matrix.

d_{ij} = Sensitivity coefficient of a SCF obtained using the machining signal of the *i*th sensor and the *j*th signal processing method.

f_{ij} = The SCF obtained using the machining signal of the *i*th sensor and the *j*th signal processing method.

EVSM= Eigenvalue Sensory Matrix.

PCF= Principal Component Feature.

Ec= Eigenvalue coefficients.

Aev = The average eigenvalue of the *k*th signal.

Classification Systems

LVQ = Learning Vector Quantisation Neural Networks.

TIP = Taylor's Equation Induced Pattern.

BPNN = Back Propagation Neural Network.

Contents

Chapter 1 Introduction.....	1
1.1 Brief Introduction	1
1.2 Problem Definition	2
1.3 Research Aims and Objectives	7
1.4 Thesis Structure	8
1.5 Summary.....	11
Chapter 2 Fixture Design	12
2.1 Introduction.....	12
2.2 Fixturing System.....	12
2.3 Principles of Fixture Design	13
2.4 Type of Fixtures.....	14
2.4.1 Dedicated Fixtures	15
2.4.2 Modular Fixtures	15
2.4.3 Conformable Fixtures	16
2.4.4 Numerically Controlled Fixtures	16
2.4.5 Memory Shaped Alloy Fixture	17
2.5 Fixturing Collet.....	18
2.5.1 Types of Collets.....	19
2.5.2 Mechanism of Collet.....	20
2.5.3 Limitations of Collet.....	22
2.5.4 Parameters Influence Fixtures Performance	23
2.6 Elastic Materials Fixture.....	28
2.7 Conclusion	30
Chapter 3 Tool Life and Wear in End Milling Operations	31
3.1 Introduction.....	31
3.2 Parameters Influencing Tool Wear	31
3.3 Milling Operations.....	32
3.4 End Milling Cutters	34
3.5 Errors in End Milling Operation.....	35
3.6 Tools Wear in the Milling Operation.....	36
3.7 Tool Wear and Fixturing Errors	41
3.8 Surface Roughness in Milling Operation	41
3.9 The Relationship between Tool Wear and Fixturing System.....	43
3.10 Conclusion	45
Chapter 4 Fundamental Principles of Condition Monitoring Systems in Milling Operations.....	46
4.1 Introduction.....	46
4.2 Condition Monitoring Systems.....	46
4.3 Significance of Monitoring Systems	48
4.4 Limitation of TCM System.....	49
4.5 Structure of TCM System.....	50
4.5.1 Tool Condition Monitoring Sensors	50
4.5.2 Signal Processing and Feature Extraction	55

4.5.3 Intelligent Decision Making	56
4.6 Conclusion	56

Chapter 5 A Review of the Implementation of Tool Condition

Monitoring in Milling Processes	58
5.1 Introduction.....	58
5.2 Tool Wear and Monitoring System	58
5.2.1 Tool Wear	58
5.2.2 Online Tool Condition Monitoring.....	59
5.3 Tool Condition Monitoring Methods.....	60
5.3.1 Direct Methods	60
5.3.2 Indirect Methods	63
5.4 Signal processing methods	68
5.4.1 Fast Fourier Transform (FFT)	68
5.4.2 Wavelets Transformation (WT).....	69
5.4.3 Principal Component Analysis (PCA).....	70
5.5 Tool Condition Classification.....	71
5.5.1 Classification using Neural Network (NN)	71
5.5.2 Classification using Fuzzy Logic (FL)	73
5.6 Single and Sensor Fusion.....	74
5.7 Condition Monitoring system and Fixtures	76
5.8 Surface Roughness and TCM	79
5.9 Summery of Identification of Knowledge Gaps.....	80

Chapter 6 Methodology

6.1 Introduction.....	82
6.2 Problem Definition	82
6.3 Problem Domain and Objectives	83
6.4 How the Suggested ASPSF Approach is Conceived.....	84
6.4.1 General stages of ASPS Approach	86
6.4.1.1 Simplification of Complex Signals for Extraction of Features	85
6.4.1.2 Automated Sensitivity Detection	86
6.4.1.3 Association Matrix (ASM)	87
6.4.1.4 Sensor Fusion and Cost Reduction	88
6.4.2 Limitations of the ASPS Approach	91
6.4.3 The suggested ASPSF Approach.....	96
6.5 The Concept of ASPSF Approach.....	93
6.6 Techniques Developed within the Suggested ASPSF Approach	95
6.6.1 Automated Sensitivity Detection.....	95
6.6.2 Principal component Analysis (PCA).....	96
6.6.3 Range Value (RV)	96
6.6.4 Correlation Coefficients for X^n Curves	97
6.6.5 Fuzzy Logic (FL).....	98
6.6.6 Learning Vector Quantisation (LVQ).....	99
6.6.7 Taylor's Equation Induced Pattern (TIP)	99
6.6.8 Surface Roughness (Ra)	99
6.7 The Application of the ASPSF Approach in This Thesis.....	100
6.8 Structure of Subsequent Chapters.....	101
6.9 Summary.....	103

Chapter 7 Experimental Set-up	104
7.1 Introduction.....	104
7.2 Stages of the implemented condition monitoring system.....	104
7.2.1 Workpiece and Cutting Tool	106
7.2.2 Surface Roughness Measuring Device	107
7.2.3 Sensors Installation	107
7.2.4 Sensors and Signals Processing Equipment	107
7.2.5 Data Acquisition Card and Software	110
7.3 The Implemented Sensors.....	110
7.3.1 Force Dynamometers	111
7.3.2 Accelerometers	111
7.3.3 Acoustic Emission	112
7.3.4 Strain.....	113
7.3.5 Eddy Current.....	114
7.3.6 Sound	115
7.3.7 Power	115
7.4 Signal Processing Methods.....	110
7.4.1 Time Domain Methods	116
7.4.2 Frequency Domain Analysis Methods.....	117
7.5 Automated Sensitivity Detection	110
7.6 Making Decision and Pattern Recognition	121
7.6.1 Data Analysis.....	122
7.6.2 Pattern Recognition	124
7.7 Conclusion	127
Chapter 8 Initial Evaluation of ASPSF Approach	128
8.1 Introduction.....	128
8.2 The Experimental work	129
8.3 Signal Simplifications.....	131
8.3.1 Linear Regression (LR) method	133
8.3.2 Principal Component Analysis (PCA) method.....	139
8.3.3 Correlation between LR slope and PCA methods	147
8.4 Selection of Sensory Features.....	151
8.4.1 Selection of Sensory Characteristics Features (SCFs).....	151
8.4.2 Selection of Principal Component Features (PCFs)	154
8.5 System Cost and Utilisation.....	157
8.5.1 System Optimisation.....	158
8.5.2 System Evaluation	164
8.6 Approach to measure surface soughness	170
8.6.1 Proposed Approach.....	170
8.6.2 Implementation of the proposed Approach	172
8.7 Conclusion	175
Chapter 9 The Applications of ASPSF Approach Using Pattern Recognition Systems	177
9.1 Introduction.....	177
9.2 Data Analysis.....	177
9.2.1 Signals Simplifications	180
9.3 Data Training	191

9.3.1	Linear Regression (LR) method	191
9.3.2	Principal Component Analysis (PCA) method.....	194
9.3.3	The Training Error Evaluation.....	197
9.4	System Cost and Utilisation.....	198
9.4.1	Selection of Sensory Features.....	199
9.4.2	System Optimisation.....	203
9.4.3	System Evaluation	208
9.5	Pattern Recognition	211
9.6	Surface Roughness.....	214
9.6.1	Roughness of Machined Surface	214
9.6.2	The Correlation Coefficient.....	216
9.7	Conclusion	218

Chapter 10 The Evaluation of ASPSF Using Broken Teeth of Cutting Tool.....220

10.1	Introduction.....	220
10.2	Experimental Setup.....	220
10.3	Signal Simplification	222
10.3.1	Linear Regression (LR) Method	225
10.3.2	Range Value (RV) Method.....	228
10.3.3	Sudden Change In Value (SCIV) Method.....	231
10.3.4	Correlation Coefficients (CCX3) and (CCX20) methods.....	233
10.3.5	Fuzzy Logic (FL) Method	237
10.3.6	LVQ Neural Network Training	242
10.4	Pattern Recognition	248
10.4.1	Taylor’s Equation Induced Pattern (TIP)	248
10.4.2	Comparison between the Pattern Types	253
10.5	Surface Roughness.....	254
10.5.1	Roughness of Machined Surface	254
10.5.2	Relation between Surface Roughness and Sensitivity.....	258
10.6	Conclusion	261

Chapter 11 Discussion and Conclusion.....263

11.1	Introduction.....	263
11.2	Suggested Solution	263
11.3	Research Aim and ASPSF Approach Implementation.....	265
11.4	Results and Discussion	269
11.5	Contribution to knowledge	274
11.5.1	Conceptual Contribution.....	274
11.5.2	Technical Contribution	275
11.6	Limitation and suggestion for future work	276
11.7	Final Conclusion	276

References278

Appendices1

Chapter 1 Introduction

1.1 Brief Introduction

Manufacturing industries are facing significantly changing market competition driven by customer demands. To survive and remain competitive in a prominent position in the global market, tremendous efforts have been taken to improve product quality. Condition monitoring system of manufacturing processes has gained considerable importance in the manufacturing industry over the preceding last decades. It is one of the essential technologies with a competitive advantage, which is capable of providing means to reduce cost, increase productivity, prevent damage to the machine or workpiece, and significantly influences process efficiency and machined part quality. Machining such as milling, turning, grinding and drilling are material removal processes which have been widely used since the industrial revolution. The performance of machining operations depends on many parameters such as machine, workpiece, tool and fixture. Fixturing technology has been considered as one of the main problems to improve flexibility, productivity and part quality. It is one of the most direct threats to cost effectiveness and operational efficiency, but it is still lagging behind in machining [1].

During manufacturing operations, the role of the operator is mainly to supervise the machine and inspect the process product. But, the operator's reaction time to monitor a problem will not be sufficient for the fast speed at which machining processes take place on recent machine tools [2, 3]. This reason considerably leads to find automated methods to detect the faults of the production process.

Currently, modern automated machining processes have become one of the most promising advanced manufacturing technologies in the industry. In order to fully recognise the potential of these systems, it is essential to monitor and control the performance of the machine intelligently. Among the parameters to be monitored, is tool condition (wear or breakage) which is clearly one of the most significant faults. Tool condition monitoring is to prevent tool failure and reduce down-time [4]. Consequently, there is a real need to design online monitoring system to control the influencing parameters to quality of the machined parts.

This brief introduction clearly highlights the importance of monitoring system, fixtures and tool conditions on the process outcome and the performance of a production system. Therefore, this thesis investigates the effect of fixturing quality on the design of condition monitoring system. The hypothesis is that the collet fixturing quality will change the dynamics of the system introducing different variables and parameters which makes the design of tool condition monitoring a complex task. These aspects of the research work will be described throughout this thesis.

1.2 Problem Definition

Fixtures are essential devices in production systems as they are required in most of the automated manufacturing, inspection, and assembly operations. Fixtures locate precisely a workpiece or a cutting tool in a given orientation and position to allow the machining or measuring process to be accurately performed. There are many standard work holding devices such as jaw chucks, machine holder, drill chucks, collets, which are usually used in workshops for general applications such as manufacturing and measuring [5].

Collets have proven to be as useful on today's CNC equipment, with state-of-the-art control systems, as they were on the early engine lathes and multi-spindle automatic machines since the 1920s [6]. Surprisingly, after more than nine decades of successful applications, there is still no better fixturing element for the new high-technology, high speed spindles than the fixturing collet. Collet remains a proven solution for most metal-working applications, and 90% of machining operations use fixture chucks while the other 10% use hydraulic chucks [7]. However, the field of the fixturing has only recently started to receive the attention and needed to more investigation [8].

For any manufacturer, accuracy of machined components is one of the most critical aspects. Faults in machining can be defined as any deviation in the position of the cutting edge from the theoretically required value to produce a workpiece of a specified tolerance. This is because of the significant changes in the fixturing rigidity or the tool conditions during the manufacturing process [9]. In milling operation, there are four main sources of faults which are kinematics faults, heat

faults, fixturing faults and tool faults. These faults have been shown in Figure 1.1, which produced based on the information from [10].

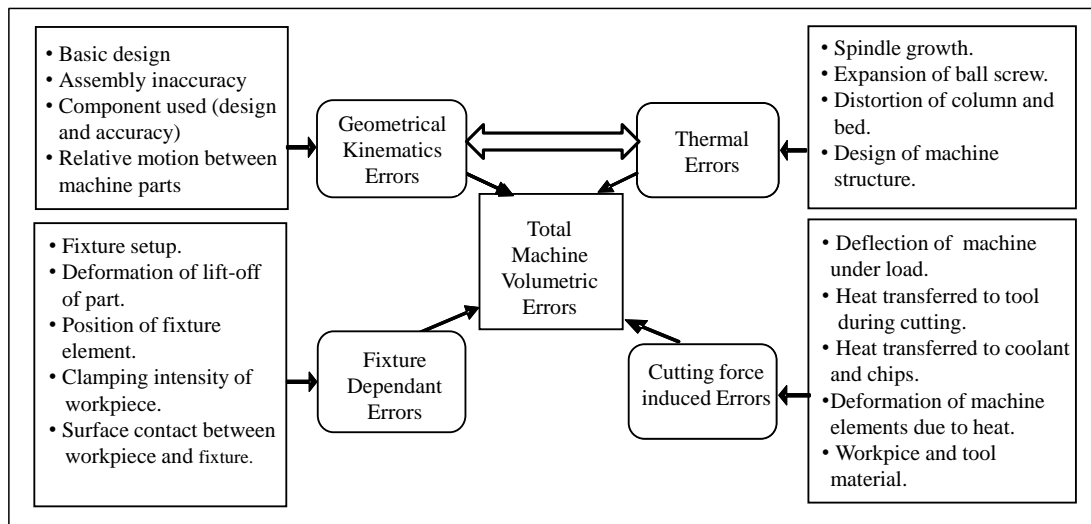


Figure 1.1: Error in machine tool and the factors affecting it [10].

The correct installation of the tool in the collet is important to prevent unnecessary strain on the collet and to ensure a proper fit. Engineers should use a collet designed to fit the tool shank diameter and the tool's flute should not extend into the collet; doing so can score the inside of the surface, as well as force debris into the collet, putting the entire assembly off-balance and potentially damaging the spindle. These errors will affect the stability of machining operation [11]. Consequently, the cutting tool and the collet, which holds it, are a major source of error; in addition to the tool deflection, tool wear, vibration and burr formation.

Although advances in fixture design have significantly improved fixturing accuracy and repeatability, fixture faults (or errors) are still a major reason of quality variation. Where most of the literature on fixture analysis has emphasised the positions of fixture elements on the workpiece rather than the contact condition between the mating surfaces. For machining and assembly processes, fixtures have been developed to provide precise, reliable workpiece location and present rigid collet chucks to reduce the workpiece loose during the machining operation. Therefore, it is very important investigation to search the relationship between clamp performance with product quality and the monitoring system [12]. In addition, considerable investigation has been conducted in the area of machine fault

detection/diagnosis, but relatively little has been done on fixture fault detection and monitoring [13]. The effect of fixturing systems on the design of condition monitoring systems is an area which is not significantly covered in the literature.

Significant research has covered condition monitoring design in the literature. Studies performed in industry have shown that the main causes of downtime are end of tool life (wear) and tool breakage and they account for 40 to 45% of downtime in milling, turning and drilling operations [14]. Hence, condition monitoring is normally used as a strategy to detect or prevent such faults using Tool Condition Monitoring (TCM) [15]. Manufacturers who used TCM systems have documented savings of 3 to 5% of manufacturing costs [16]. Three essential elements are used to create a condition monitoring system, namely sensory devices, statistical methods, determine the tool status systems. Two parameters have affected the performance of the TCM system, which are the quality of the collected data by the sensors and the analysis algorithm that used to evaluate the sensory signals and detect tool status [17].

Much research has been performed concerning the development of reliable TCM. However, several factors have obstructed advances in the development of TCM including inappropriate choice of sensor signals and their utilisation [18]. In order to address the drawbacks in condition monitoring, reference [19] presented a novel approach, termed (ASPS), to deal with these problems. Automated Sensor and Signal Processing selection approach (ASPS) in selecting the sensors and signal processing techniques is implemented for monitoring the tool conditions in milling processes. The sensitivity to tool wear is extracted for each sensory signal based on the absolute slope of the Linear Regression (LR) method. The aim is to reduce the number of sensors needed in the overall system and reduce the cost. Another researcher [20] has employed this approach to develop an effective sensor fusion model for turning processes for the detection of tool wear. Despite the ASPS approach can provide a solution for monitoring the fixturing system, there are some limitations in relation to the sensory sensitivity detection. These limitations will be described in Chapter 6.

So far, however, there has been little discussion about the effect of fixturing type and quality on machining signals and hence the design of the condition monitoring

system [1]. Also, there is limited research to address the relationship between the online condition monitoring system and the fixturing quality (either fixturing type or fixturing material). The key question with this research is that; what is the effect of the fixturing setup on the efficiency of the condition monitoring system? can the monitoring system detect the changes of the fixturing system which also influence the tool condition?

Therefore, the domain of this research is in implementing a novel approach, termed ASPSF (Automated Sensor and Signal Processing Selection for Fixturing) for selecting the sensors and signal processing techniques essential for monitoring the setup and conditions of fixturing system in milling processes. As will be described later, the ASPSF approach utilises the ASPS approach and modifies it to investigate the effect of fixturing system on the design of condition monitoring system. Through the ASPSF approach, a wide range of novel signal analysis and simplification techniques is used to confirm and assess the research methodology for selecting sensors and signal processing methods and detect the relationship between the changes of the process setup and the design of condition monitoring system as shown in Figure 1.2.

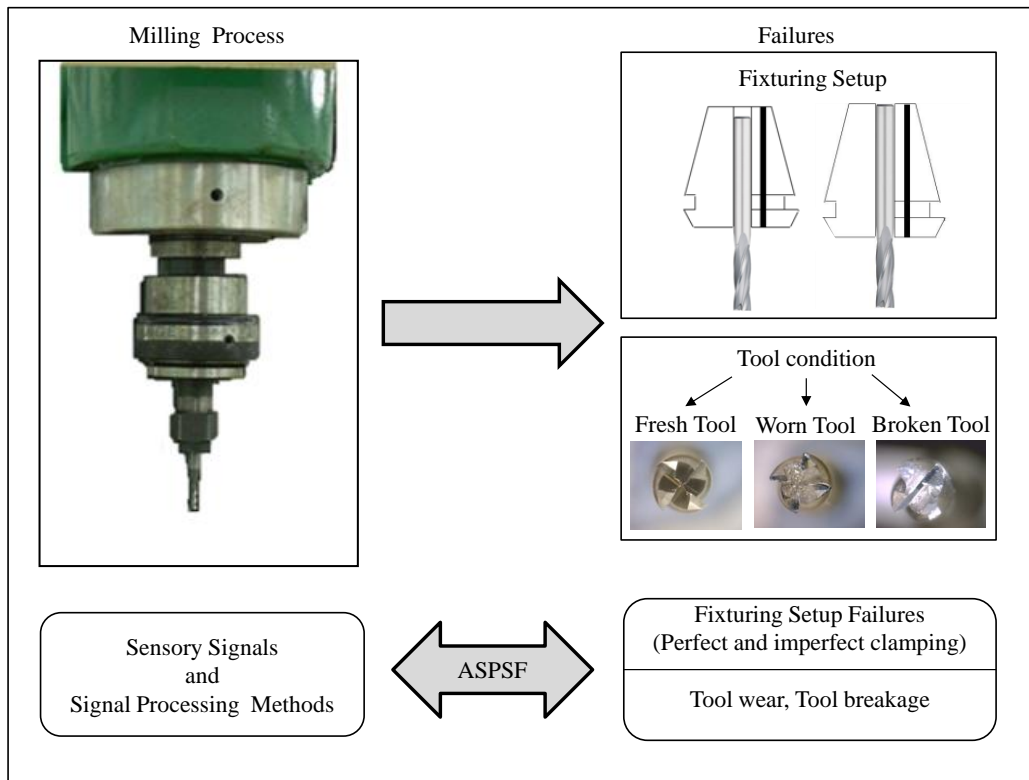


Figure 1.2: Schematic of ASPSF approach for monitoring the fixturing set-up and tool conditions.

Briefly, this research will provide the designer of monitoring systems with the details of the next stage for operating the system if any change in machining characteristics (i.e. fixturing status, tool conditions) has occurred in the machining process. This system allows for the detection of subtle changes from normal to abnormal conditions as illustrated in Figure 1.3. The key question is does the change in machining system characteristics have an effect on the behaviour of condition monitoring system?

The fixturing system is the main parameter of the machining characteristics, and will be investigated throughout this thesis.

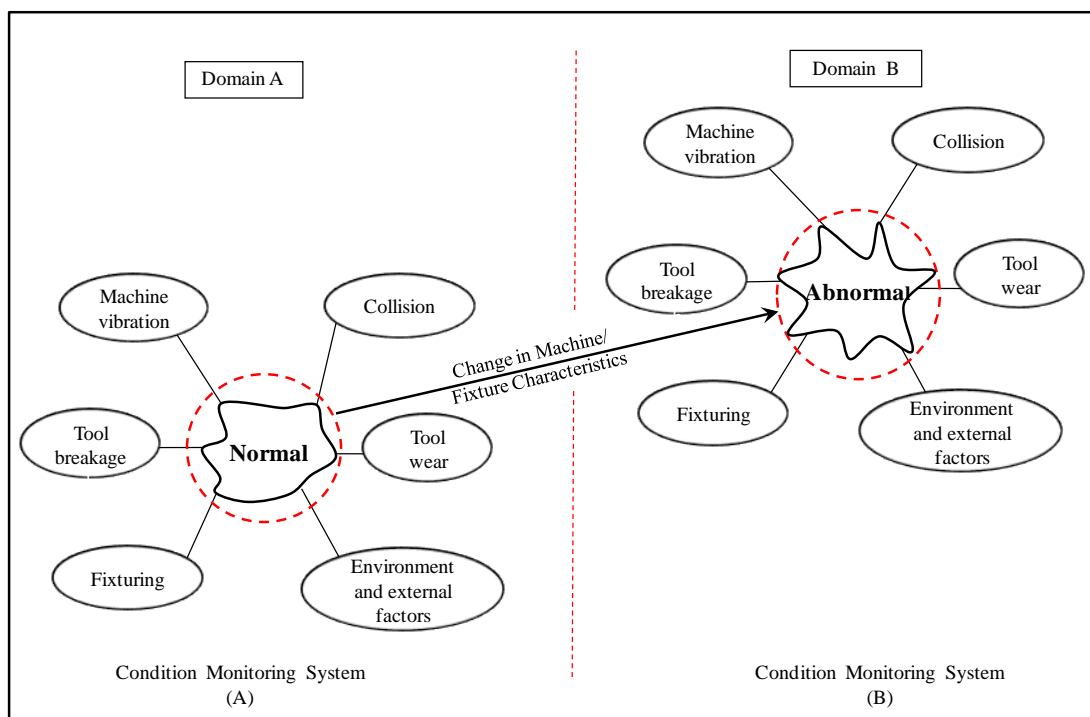


Figure 1.3: The change of machining characteristics of milling process.

As seen from the previous discussion, it can be concluded the following issues:

1. There is limited literature on the relationship between fixture type, material and other design parameters on the quality of the manufacturing operation and efficiency of the fixturing system.
2. Most researchers have used one type of fixture (i.e. collet) in the investigation of monitoring system in machining operation, while the effect of variation of tool holder with workpiece material on performance of the monitoring system is still a weak point in this area of research. The application of sensor fusion is also very limited in this area.

3. Fixturing capability depends on unautomated evaluations which are relatively imprecise in the complex manufacturing processes (as milling and drilling). This depends mostly on the information and skill of the operator and is both time-consuming and costly. Computers are used to support manufactures in evaluating the fixture performance. Therefore, the required approach will be created in this research to study the parameters which are included in the experimental work.

4. Most studies in the industry have only been carried out in developing the monitoring system to detect the faults and abnormalities of the machine tool and the tool. However, little investigation has been done on fixture fault detection and monitoring. Therefore, there is a real need to create an effective detecting system to deal with the fixturing problems.

5. Generally, the real surface roughness does not consistent with that obtains from theoretical calculation. Also, the monitoring of surface finish is often done by manual inspection of workpiece surface using profilometer which is time consuming and very costly. Therefore, surface roughness monitoring in industry needs to a new approach to predicate it continually.

1.3 Research Aims and Objectives

The main aim of this research is to investigate the effect of the fixturing system on the design of the monitoring system in order to classify tool conditions regarding to the collected data. The investigation, as a result, will address the following issues:

- Address the limitation of literature about the tool holder and then study the effect of the fixturing system (type or material) on the efficiency of monitoring system.
- Detect any faults or abnormalities that may occur during the machining operation using sensor fusion which is designed to monitor the health of the manufacturing process with regard to changing tool conditions.
- Evaluate the stability of the fixturing system and the efficiency of the monitoring system regarding to the surface roughness of the work piece.
- Since the manual measuring method for the surface roughness is time consuming and relatively expensive, part of the proposed monitoring system will be

employed to predict the roughness of the machined surface using the output of the force sensor.

The aim of the research is supported by the following objectives:

1. Conduct literature review in relation to fixturing system, milling process, tool wear and surface roughness, condition monitoring and applications.
2. Investigate, in detail, the limitation in current condition monitoring system.
3. Propose an experimental setup to investigate the effect of collet design/type on machining operations.
4. Conduct experimental work to evaluate the effect of fixture type/material on product quality and the capability of the condition monitoring system using different materials, machining parameters and collet types.
5. Perform the experiment work on the appropriate and available equipment to achieve more accurate and precise results.
6. Select the sensitive and applicable sensors to build the fusion model and cover the most important parameters which affect the machining process.
7. Analyse the data needed to simplify the complex signal to obtain the useful information.
8. Use the accurate and reliable methods to determine the most sensitive sensor and concentrate on how to reduce the cost of the proposed system.
9. Investigate the relationship between the surface roughness of workpiece and the sensitivity of the sensory signals to assess the capability of the proposed monitoring system.
10. Test the validation of sensitivity measuring methods to measure their efficiency to detect the most sensitive features using an independent evaluation method.
11. Investigate current condition monitoring design systems, including the ASPS approach [19]; and evaluate their suitability to study the effect of fixturing system on the design of condition monitoring system.
12. Create a new technique to improve the detection of the classification of the tool status and design a general target more correlate to the pattern recognition.

1.4 Thesis Structure

The structure of thesis is organised in 11 chapters to cover the whole aspects and problems and the suggested approach, which are presented by the author as

illustrated in Figure 1.4. This structure is carefully built to keep the flow and the sequence of ideas related to the subject.

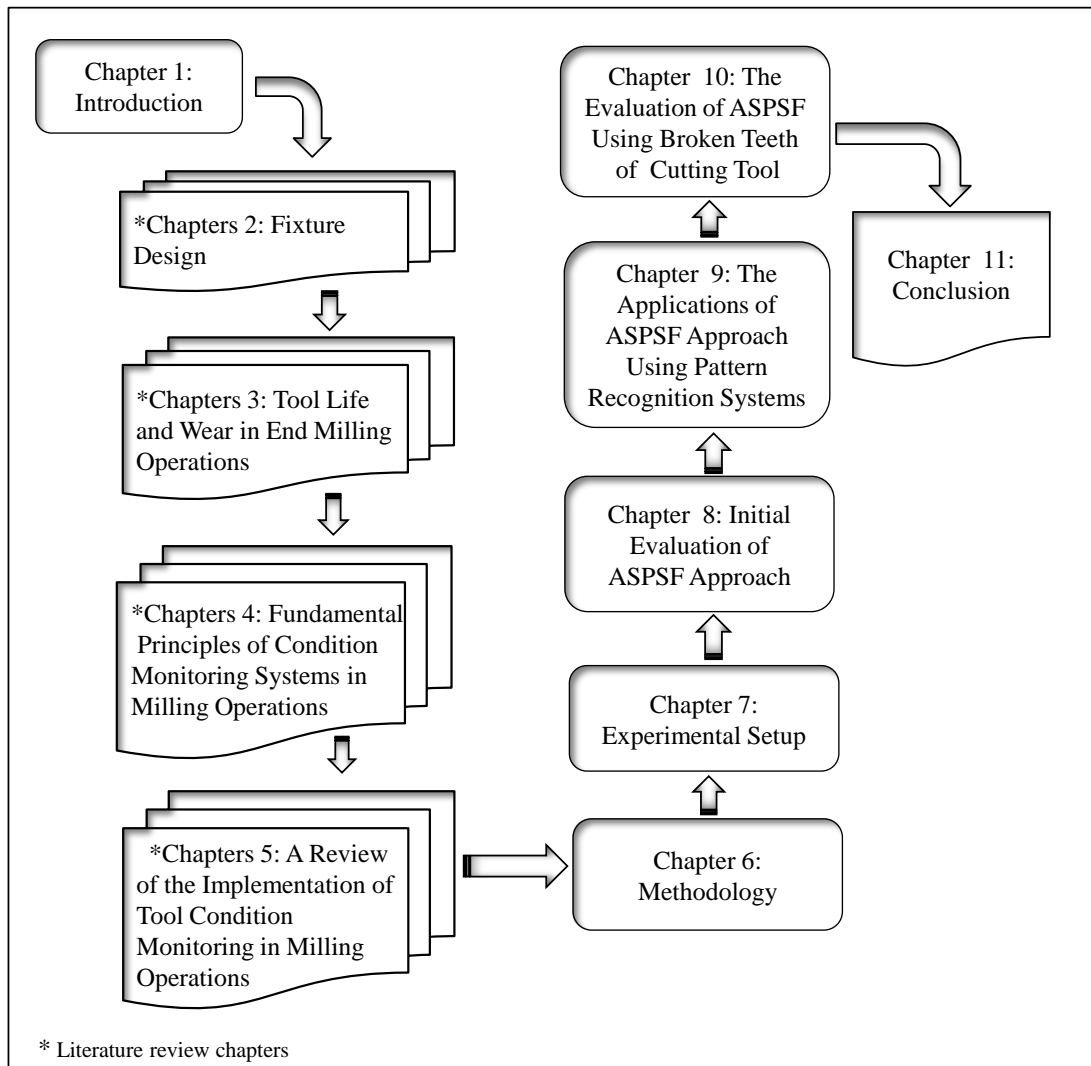


Figure 1.4: The schematic diagram for the structure of the thesis.

A brief description of the content of each chapter is presented below:

Chapter 1 presents the real need to create a fully automated manufacturing system and the effect of fixturing system on this demand which depends on the condition monitoring system. The aim and objectives of this thesis are also introduced in this chapter.

Chapter 2 looks at the literature concerning fixture design and provides the fundamentals of the fixturing work and application. It presents the discussion of the details of using rubber as elastic material in the fixturing system. Therefore, this

chapter totally aims to address the limitation of the research about the fixturing systems.

Chapter 3 aims to introduce the concept of tool life and wear in end milling operations. It is generally given the principles of end milling processes and tools. This chapter shows also the effect of the fixtures on tool wear and surface roughness.

Chapter 4 describes the concept of condition monitoring systems which is applied in the industry. It explains the basic information for the application of the monitoring technology related to the current area of research.

Chapter 5 demonstrates the application of implementing tool condition monitoring in the milling process to monitor tool condition and fixturing systems. This chapter shows an overview of the studies implemented in condition monitoring and outlines the problems and limitations of these studies.

Chapter 6 introduces the overall methodology of the thesis. It introduces the new ASPSF approach and explains its technicalities. It presents the objectives of the research, and also provides a brief description of the steps of implementing the proposed approach. The chapter defines the structure of the following chapters of the thesis.

Chapter 7 describes technically the experimental set-up. It states the equipment used to implement the proposed system and also defines the software used to collect the data. The equipment includes CNC milling machine, condition signals devices, fixtures to hold the sensor, surface roughness measuring apparatus and data acquisition system. In this chapter, a brief description for the sensors and signal processing methods will be presented. Following this, the techniques to address the pattern recognition of data are outlined.

Chapter 8 presents the initial evaluation of ASPSF. It explains the fully details of application the ASPSF (Automated Sensor and Signal Processing Selection System for Fixturing) approach and how this approach can achieve the requirements of the condition monitoring system. In this chapter, the ASPSF approach is implemented through the tool wear with changing the fixturing system. Furthermore, a novel approach will be presented to predict the surface roughness.

Chapter 9 describes the applications of the ASPSF approach using pattern recognition systems. In this chapter, more applications of the proposed approach and more extended sensors and fixturing systems are presented to show the practical

validation of the monitoring system. Roughness of the machined surface is measured to assess the approach. Also, a suggested method will be used in conjunction with pattern recognition systems.

Chapter 10 introduces the evaluation and a new application of ASPSF using tools with broken teeth and investigates the surface roughness. A wide range of the sensitivity measuring methods are applied with more experimental work. Here the ASPSF approach is implemented through the tool with broken teeth to investigate the phenomena of tool breakage. A novel approach is presented to define the pattern of the tool conditions. Surface roughness measurements, also investigated here with the procedures of collecting sensory signals.

Chapter 11 summarises the overall findings of the thesis. It presents the research objectives and discussion the results of the ASPSF approach. The main contribution to knowledge with the conceptual and technical has been described. Finally, it presents the final conclusion, suggestion and limitation in relation to the research presented in this thesis.

1.5 Summary

This Chapter has highlighted the current problems related to fixturing systems and their effects on the design of the condition monitoring systems. The structure of this thesis has also been presented.

Chapter 2 Fixture Design

2.1 Introduction

Since this thesis addresses the relationship between condition monitoring design and fixturing system, the author feels it is essential to highlight the basic principles, applications and problems in these systems. Therefore, this chapter will introduce the main aspects to consider in fixture design, the main parameters which affect performance and limitations of the fixture device as a weak point in the manufacturing system. The limitation of literature on fixture is also addressed here. The main types of the fixturing system are described with focus on collet fixture as a main tool holder in the milling process. This chapter also presents a new technology of using flexible material in fixturing system.

2.2 Fixturing System

In process planning, the correct selection of fixturing type represents an important specification in addition to cutting tool requirements. This is to ensure that products meet the market needs and are capable of being produced and mounted in a cost effective and reliable way. The arrival at an appropriate fixture design traditionally consists of several stages including the detailed study of a workpiece specification, searching for any existing similar designs, and manual selection of fixture elements based on catalogues and items available in the shop. This procedure depends largely on the knowledge and experience of a tool designer and is both time-consuming and expensive [21].

Fixtures have significant effect on manufacturing quality, productivity, and the cost of products. Practically, the manufacturer could be consumed a 10–20% of the total cost of a manufacturing system as the costs associated with fixture design. Therefore the appropriate fixture design is vital to improve the product quality in terms of precision, accuracy and finish of the machined part [22].

The fixturing development is considered as particularly difficult procedures, since it is included in different concepts of product improvement set: design, process planning, machining and assessment. The most of fixtures designs are performed for a particular workpiece, as dedicated fixtures. Currently, many companies need the

fixturing systems to be more multi-use because of the trend in manufacturing supporting a larger component diversity, dimensions and quality. They can allow a variety of parts to be held during machining and assembly, thus minimising cost for dedicated fixtures and reducing the inventory of a multiplicity of fixtures [23].

2.3 Principles of Fixture Design

A usual fixture design for workpieces consists of three essential elements: locators, clamps and supporters. Locators are used to place the workpiece in equilibrium. Hence, the main duty is to remove all degrees of freedom. However, clamps are employed to hold the workpiece strongly against the locators during the machining process. The primary design factors of fixture clamps comprising external cutting force and tool direction have to be taken into account during a fixture design process. Supporters are added to improve the stability of the workpiece. The function of these fixturing elements can be determined manually or analytically [24]. An unconstrained workpiece will have 12 degrees of freedom in three dimensional spaces, because its movements can follow along the positive and negative directions of the X, Y and Z axes in addition to the clockwise and counter-clockwise rotations around the three axes as clarified in Figure 2.1. During the machining process, the degrees of freedom of movement of the workpiece must be controlled by the locators and clamps.

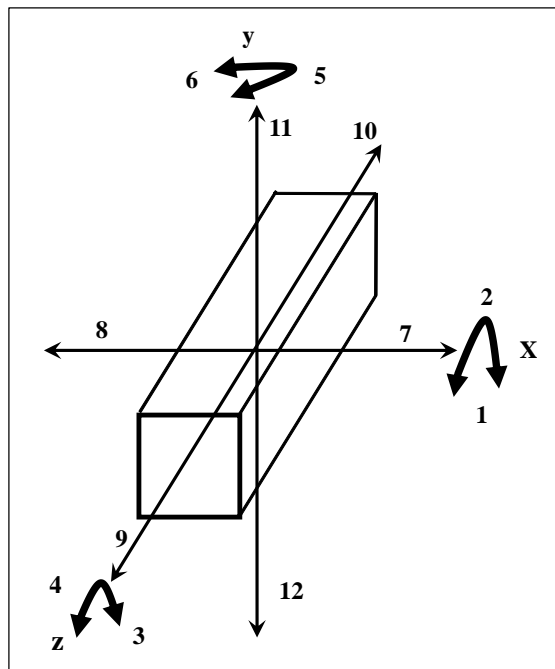


Figure 2.1: Twelve degrees of freedom for prismatic workpiece.

The main guidelines with respect to the determination of locating and clamping locations have been described as follows [24]:

1. The datum of the fixture which is normally defined as the surfaces with the largest area should be made precisely to achieve the higher percentage of parallel and perpendicular. This is to avoid the error in holding the parts.
2. The locators should be placed in maximised of the contact area to achieve a higher stability and to grip most of the part body.
3. It is mostly better that the locators are fixed on the interior points of the fixture to reduce deflection of the workpiece.
4. The vertical locators are advised to form a triangle shape to keep the centre of workpiece gravity in the middle point to avoid instability.
5. The clamping forces should be directed to opposite the corresponding vertical and horizontal locators to prevent extreme torque.
6. The layout of the locator must be prepared to against the highest cutting force applied by manufacturing process [25].
7. For the general fixtures, the angle between perpendicular surfaces should be between 90° and 120° to avoid presence over-located.
8. For providing a higher stability, it is recommended to use the available holes which are existed in the workpiece; therefore the locators with the fitting dimension can be used.
9. Unfixed locators or the supports with floating mechanism could be applied to prevent the deflection or instability due to increase the cutting forces [26].

2.4 Type of Fixtures

A fixture is mostly fastened to a machine head or machine table in a fixed position. It does not contain special arrangements for guiding the cutting tool, if so; it will be called a Jig. There are many standard work holding devices such as vice, jaw chucks, drill chucks, collets, which are commonly used in workshops and are usually kept in stocks for general applications. The production of collets at Harding (New York) occurred in the 1890s, with many of the applications at that time focusing on the watch making and adjusting the position of a large body attached to a column or shaft. They are used as an alternative to the nut-screw combination due to the screw

thread can result in a considerable reduction of the effective diameter of the column and therefore of its strength [27].

Generally, it is possible to divide the type of the fixturing system according to the stage of the application development in the industry as briefly described [8]:

2.4.1 Dedicated Fixtures

This form of fixturing is possibly the oldest fixturing method. They are called dedicated because they are designed for fixturing one particular workpiece and, probably, one workpiece for only one stage of the manufacturing process. This lack of flexibility is the main disadvantage of dedicated fixtures. Therefore, when multiple fixtures are used, the expected change-over from one fixture to the next during the manufacturing cycle introduces an extra bottleneck and increases the production down-time. Despite these drawbacks, dedicated fixtures are still used in large- and small-batch production sites, where increased accuracy is the prerequisite for the final result. Efforts are therefore focused on developing alternative fixturing concepts or tools that assist the fixture designer and accelerate the design process. Consequently, several Computer Aided Fixture Design (CAFD) tools for rapid concept generation and verification have been proposed.

2.4.2 Modular Fixtures

Modular fixtures are perhaps the first method to tackle the drawbacks of dedicated fixtures and may be the most industrially applicable and flexible fixturing method available. The dates of concept of modular fixtures were proposed and back to the Second World War. Modular fixturing systems are fixtures that consist of a number of standard elements, called modules, which can be used in various combinations to create fixture assemblies that can accommodate different workpieces. The modules include various forms of clamps, locators, supports, base plates and connections.

The main advantage of modular fixtures is that standard elements can be re-used to build a large variety of different set-ups. This renders modular fixtures most appropriate for highly-flexible manufacturing environments, such as workshop facilities. However, the main shortcoming of these fixtures is large amount of knowledge and time needed for fixture planning and difficulty to hold parts with very complicated geometry.

2.4.3 Conformable Fixtures

Conformable fixture is another flexible fixturing method which is commonly referred to as pin-array fixtures or pin-type fixtures. In principle, they comprise a bed of independently adjustable pins that either manually or automatically conforms to the surface of the workpiece, providing support and localization to the workpiece. The part is then clamped from the opposing side. The clamping mechanism can vary from a simple structure to another pin-array formation that is pneumatically or hydraulically actuated. Another concept of reconfigurable fixtures that has received considerable research attention is based on phase-change materials. The term “phase-change” involves the utilisation of the transition from one material state to another, usually from liquid to solid. In detail, these fixtures arrange a bed filled with a material, which constitutes the fixturing medium. When the medium is in liquid state, the workpiece can be inserted and localised. Clamping takes place through solidification of the medium [8].

2.4.4 Numerically Controlled Fixtures

Numerically-controlled (NC) fixtures belong to a classification of fixturing concepts that meanings away from the traditional static methods and moves towards the idea of a gripper. These fixtures are possibly the first step towards more intelligent methods. The flexibility here lies within the ability to automatically adjust the layout of the fixture, in order to grasp parts with different geometrical features. Numerically-controlled fixtures are identified by their ability to automatically reposition their locating, clamping or supporting elements. In general, the clamping elements of this NC fixture are situated at the side of the workpiece and are positioned on slides with vertical orientation.

Collets have proven to be as useful on today’s CNC equipment, with state-of-the-art control systems, as they were on the early engine lathes and multi-spindle automatic machines from the 1920s. Unpredictably, it might be noticed that when checking back what has developed with machining and equipment technology, it is as though the basic collet was suspended in design time and space. However everything around it was required to engage to productivity improvements [28]. In addition, there is a common misconception that collets are limited to hold multi- shaped products. Currently, and after around 100 years of successful applications there is still no

better fixturing element for the modern automated technology, high speed spindles machine than the fixturing collet. Collet remains a verified solution for most machining applications [29].

Reference [30] presented a novel approach to improve the quality of machined surfaces on wood cutting machine by presenting additional cutter head movement. It is shown that changing slightly the position of the tool reduces waviness height significantly. This approach could be a further development of NC fixturing (i.e. dynamic changing of tool position for smooth machining).

2.4.5 Memory Shaped Alloy Fixture

In developing micro-spindle units, a critical problem is miniaturisation of the tool clamp. As an interesting study, reference [31] developed a novel tool clamp based on shape memory alloy (SMA), which allows further miniaturization. An SMA that is deformed in a low-temperature phase can recover its original shape upon heating to the reverse transformation temperature. The tool clamp can be simplified by using an SMA ring consists of only two parts: a tool holder in the end of the spindle, and a closed SMA ring as shown in Figure 2.2. The SMA ring is placed around the outside of the tool holder. A serious weakness with this method is that it needs a heating source to use the SMA ring, which may be affected by the changing of the temperature.

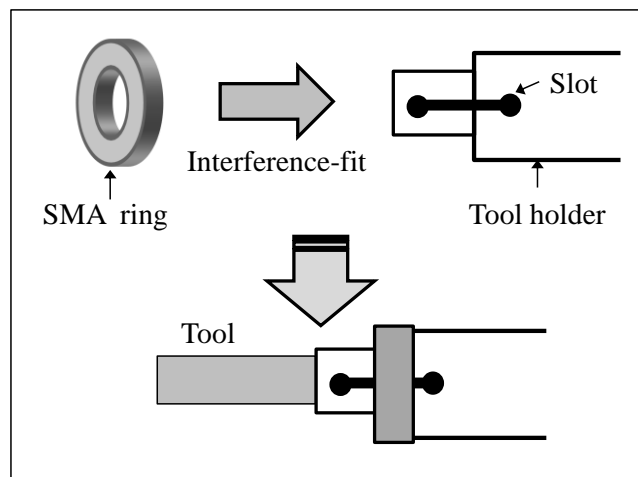


Figure 2.2: Configuration of a tool clamp based on a shape memory alloy.

The prediction of contact forces in a frictional workpiece-fixture system is an important problem that has been addressed in [32]. They presented an elastic contact model to describe the non-linear coupling between the contact forces and elastic

deformations at the contact point. The results indicated that all contact forces can be accurately predicted in the frictional workpiece-fixture system.

2.5 Fixturing Collet

Nowadays, complex manufacturing environment and maintaining operations at optimum levels will require a significant degree of attention, effort and priority. This is particularly accurate of the higher technology elements such as machine controls, hardworking mechanical structures, programming and general equipment reliability. On the other hand, there are certain manufacturing components that are robust and consistent yielding a long life time of usage. This attention it is not certain when the first collets were employed, but it has been established that fixturing collets were available before the turn of the last century. Collet is an essential component of fixturing in workshop which holds tool or workpiece in machining operations.

Collet is described as a cone shaped sleeve which generally used for holding circular or rod such as pieces in various machines typically in most machining process [33]. It has usually a cylindrical inside and a conical outside and has slit edges extend its length to allow it to enlarge and contract. Therefore, to achieve the clamping, the collets are designed that either to be pulled or pushed into a matching conical housing. When it is inserted into the housing, it contracts and holds the surface of the inner cylinder. Collet is an adjustable metal part that is used to tightly grip a tool or any workpiece. Collets enlarge spindle applications as shown in Figure 2.3.

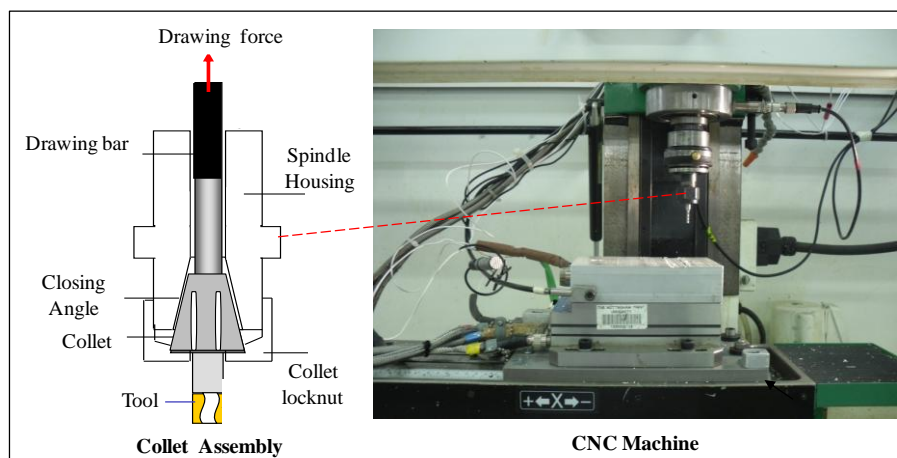


Figure 2.3: A schematic of collet parts.

This capability of the continuing power of the collet is recognised to do the fixturing function in spite of the simplicity of the device. The collet is a small but powerful component for the machine tool industry, including all of the following features:

- The ability to accurately hold a workpiece or a tool, resisting both rotational forces and multi-directional cutting loads [34].
- The ability to increase the actuation force, converting it into workpiece or tool clamping.
- The essential ability to rapidly release the workpiece or the tool.
- The capability to work at high repetition levels without loss of accuracy or material failure.
- The capability to work at a different range of rotational speeds with minimal loss of gripping force.

2.5.1 Types of Collets

There are two basic types of collets used on milling machines.

2.5.1.1 Solid Collets

The solid collet is the most rigid type of tool holding collet. The solid type of collet is usually stated to an end mill holder. This collet type has a precision ground shank which fits accurately into the spindle of the milling machine. The collet is held in the machine using a draw-in bolt which runs through the centre of the spindle.

Furthermore, to adapt the shank of the cutter, the solid collet also has a precision ground hole in it. The cutting tool, in a solid collet, is fixed strongly by using a set screw which is constricted on the ground or cast into the shank of the tool. Solid collets are especially used in the probability that the cutting forces could be caused the tool to slip in case of using a less rigid type of tool holder. Typically, the applications for the solid collet would be clamped carbide cutter and performed a hard machining using the T-slot or dovetail tools [35]. Solid collets made in many different sizes, each size is including a precision ground to take different size of tool holder shanks and cutters as shown in Figure 2.4.



Figure 2.4: The solid collet.

2.5.1.2 The Split Collet

Split collets are the most popular and widely used on vertical milling machines. The first type of split collet as shown in Figure 2.4a, the tapered neck of the collet is pulled into the spindle taper of the machine using the draw bar or draw bolt on the machine spindle. The pulling in of the collet reasons the split collet to contract down onto the shank of cutter. Split collets are a very effective tool clamping method, however under heavy cutting forces; they may have a trend to slip. Figure 2.5b is shown another type of split collet system where the tool slippage phenomena could be minimised due to the slots in this type is provided the holding system to work effectively [36]. Moreover, the adjustable element (Lock nut in the Figure 2.5b) improves the ability of the collet to adjust and grip the tool firmly.

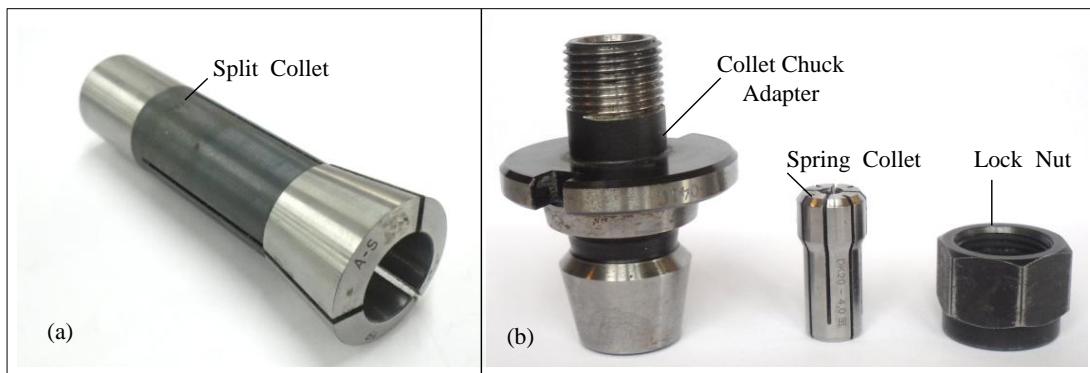


Figure 2.5: (a) The split collet (b) Collet chuck system.

2.5.2 Mechanism of Collet

Recently, collets have been used in a variety of applications in automated machines. These collets are too large for trial and error methods of manufacture; therefore it is essential to find quantitative expressions for their properties if they are to be included as predictable elements in a detailed design. A major particular concern is

the capability of a collet to hold a tool stationary opposite to axial forces in either direction and yet be able to relief its hold with a minimum of force. Also it is important to find the distance which the collet must move into its housing in order to secure the tool.

The achievement of a collet has been developed based on a theory of using the normal laws of friction to present the requirement of the control of grip, the simplicity of relief and the interface stresses on the cone angle, the interface coefficients of friction and the practical axial forces.

Figure 2.6a shows the schematic model of the theory, since the block A is held against base B with applied force N . When the force F forms up from zero, the frictional force M forms up to become equal and opposite to F , therefore no movement follows. This remains until M ranges its limiting value of μN where μ is the coefficient of friction at the interface of mating surfaces AB. The sliding takes place when $F > \mu N$, however if F is reduced, correspondingly M is reduced. There is no sliding taken place until $F < -\mu N$. Thus, M is a self-adjusting force which is always just enough to avoid or stop the motion, until it increases over limiting value. The collet is assumed to contain a set of axial slots accordingly that it is designed by a set of slices held together weakly by slight bridges at their ends. Consequently, therefore it is characterised by a slice B of angle θ in a tapered housing A and build against a tool C as exemplified in Figure 2.6b. Forces F push B into A whereas forces f challenge to slide C through B. μ_1 and μ_2 are the interface coefficients of friction, meanwhile M_1 and M_2 are frictional forces against motion. The balancing of the effective forces N_1 and N_2 performing on A and C is ensured by the axial symmetry of fixturing collet [37].

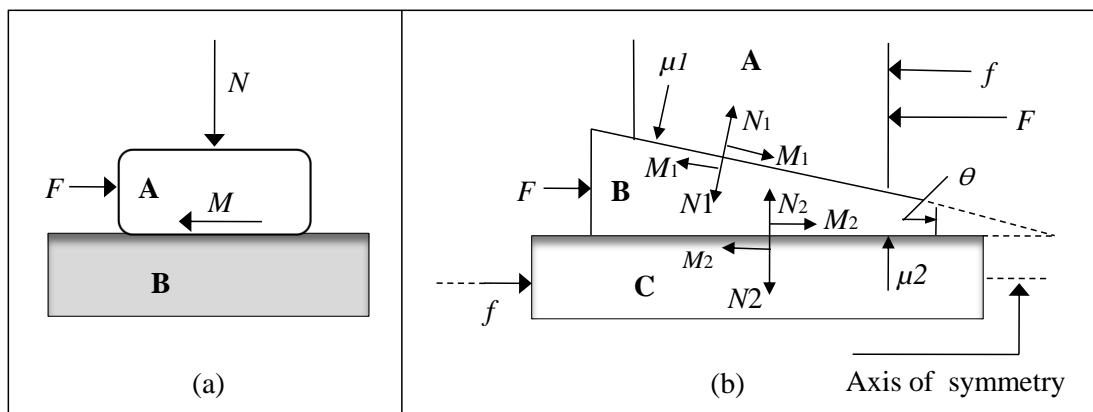


Figure 2.6: (a) Frictional force M created at the interface between two mating bodies A and B (b) Model of a collet (reproduced from [37]).

The criteria for an effective collet are as follows:

1. No slipping at BC with F fixed at F_a and with f up to the design maximum of $\pm f_{max}$.
2. Easy relief when F is declined from F_a to zero, i.e. Slippage of the tool is achieved with small negative values of f .
3. Normal interface stress ranges when F_a and f_{max} acting together.

2.5.3 Limitations of Collet

The tool holding collet is the standard work holding device for most CNC machine users and it is versatile enough to be used in a wide range of machining applications. However, it is not the best fixturing chuck for all types of work. The jaw chuck is an alternative fixturing device that also uses mechanical force to hold the part being machined especially in drilling operations.

Numerous factors are considered into the determination of which type of fixture would work better. When evaluating a collet chuck against a jaw chuck for a given industrial application, take all of the following parameters into consideration [38]:

1. Spindle Load Capacity and speed.
2. Operation to be performed.
3. Workpiece Dimensions.
4. Types of Materials.

2.5.3.1 Spindle Load Capacity and Speed

The allowable spindle weight is based on bearing load capacity. Therefore, if the combination of the collet and the workpiece designs are overloaded, there is a risk of exceeding this limit. However, jaw chucks tend to be more massive than comparable collet chucks, making the collet chuck an appropriate choice where weight control is needed. A collet chuck is considered a better choice for milling process especially at high ranges of the spindle speed due to the mass of the collet which provided the same spindle horsepower and fast to accurate up to the required speed. This will reduce the cycle time and increase the productivity.

2.5.3.2 Operations to be performed

There is increasing concern that collet fixture is being more advantages due to the fact that holding forces all around the circumference of the workpiece instead of just

at the selected contact area as in other fixtures. This will lead to the tight concentricity, which is important particularly for the second machining process when the accuracy and precession are of significance. A jaw chuck generally obtained a tool runout within 0.0006 to 0.0012 inch, while a collet usually obtained 0.0005 inch or less. The collet fixture can be also adjusted for concentricity during setting to further develop secondary process accuracy.

2.5.3.3 Workpiece Dimensions

Collet fixtures are limited in the variety of workpiece sizes, and can be used on since they are suited to workpiece diameter less than 3 inches. They may also impose a limitation on the tool length, especially in the range of the z axis, therefore sometime this situation dictated to use the jaw chuck. Therefore, in the case of the smaller size of the workpiece, it is preferred to use the collet as actuation stroke is shorter and his action faster, while using the jaw chuck for the workpiece with vary significant size [38].

The collet chuck considerably decreases the idle time that is used to change the holder in case of the change between very large and very small lot sizes due to the collet can be in a quick changed in 15-20 seconds. In contrast, the swapping of the jaw for the standard jaw chucks takes around 15-20 minutes.

2.5.3.4 Types of Materials

For hot rolled steel, castings, forgings and extrusions, the standard jaw chuck tends to work better than the collet because of the diameter variations essentially in all of these types of workpices. However, cold rolled material could be more consistent in size and therefore better appropriate to collet chucks. The collet designed for non-round cross sections can be used for the extruded bars [39].

2.5.4 Parameters Influence Fixtures Performance

2.5.4.1 Clamping Force

The main factor to the success of any machining operation is the clamping the workpiece in the best state condition. A serious design factor with regard to fixturing the workpiece is the selection of the clamping force.

Practically, the clamping loads are mostly setting to more 10 times than that need to prevent the slipping of the workpiece. This is due to the inaccessibility of the analytical tools to evaluate and computing the minimum clamping load. Therefore, more flexible and higher performance fixturing systems are required to improve the accuracy of machined components [40]. However, there has been little research reported with regard to the development of models to predict minimum required clamp pre-loads in light of fixture-workpiece system. Therefore, reference [41] presents a linear clamp pre-load model to compute the minimum required pre-loads needed to avoid the workpiece slip at the fixture-workpiece joints opposite to a variety of external loads.

The minimum clamping forces to secure a workpiece are changed continuously during the machining processes. Therefore, the reference [42] attempted to design an Intelligent Fixturing System (IFS) to provide dynamic clamping forces during the entire machining and fixturing process. The clamping force distribution between a jaw chuck and a cylindrical workpiece had been measured by references [43, 44]. Measuring techniques for the contact pressure between elastic bodies are developed. For instance, ultrasonic method has been used to measure the contact pressure in bolted joints, in which it is extended up to 50MPa [45]. However, it is difficult to find a small ultrasonic transducer which can be built in a tool shank. A new technique [46] using strain gauge is designed to detect the contact pressure in the collet chuck holder by using cylindrical bar similar to a hob to cut spur gear teeth.

2.5.4.2 Coefficient of Friction

To assist the selection of proper clamping forces, analytical methods [47] have been developed to predict fixture-workpiece reaction forces and/or determine the minimum clamping forces necessary to keep the workpiece from slipping within the fixture during machining. These models assumed that the forces at the joints of fixture-workpiece observe Coulomb's law of friction. This law states that the friction force is proportional to the normal load, the force perpendicular to the sliding surface which presses the two solids together. The proportionality factor is called friction coefficient.

Furthermore, the predictions provided by these models are very sensitive to the assumed coefficients of friction. Consequently, in order for these models to be used

with confidence, the coefficients of friction for the fixture-workpiece joints modelled must be identified further with their expected ranges of variation.

Typically, the main source of the coefficient of friction data is handbooks. In general, accurate values of coefficients of friction for fixture-workpiece joints can be obtained through experimentation that investigates the geometric-tribological-loading conditions of the joints.

2.5.4.3 Number of Contact Point

The machining and clamping forces significantly affect the workpiece location accuracy and hence the machined part quality, therefore the workpiece motion arising from localised elastic deformation at the contact point of the workpiece-fixture. Generally, the contact problems with friction are complex in terms of the contact surface can encourage slipping, sliding, and rolling or tension relief depending on the amount of the normal and tangential forces at the contact interface. Although, the literature is significant of research on friction and its application, but it lacks research that investigates the contact between workpiece-fixture systems. However, it is noticed that many joints in machine tools and their characteristics have direct effect upon the static and dynamic performance of the machine tool. Reference [45] classified the joints into three kinds according to the joints stiffness including open, semi closed and closed type. A bolted joint and a sliding joint belong to an open type, and a tapered joint is a closed type. A joint between a workpiece and three jaw chuck is a semi-closed type. The form of closure grasp is needed to constrain a rigid workpiece by surrounding the part surface with mechanical fingers. Reference [48] reported a new and convenient synthetic procedure to develop an efficient algorithm for examining the form closure grasp conditions by applying linear programming techniques. Fingertip locations are determined to achieve the form of closure grasp specified the geometry of a workpiece as illustrated in Figure 2.7.

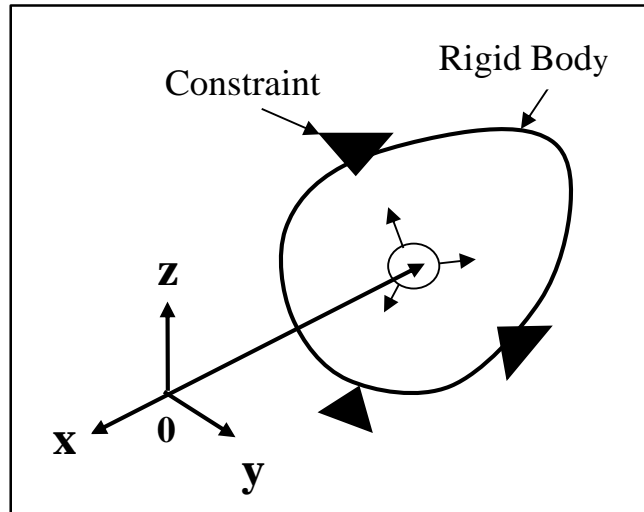


Figure 2.7: Rigid body and constraint points [48].

For simple workpiece geometries, designers mostly depend on the self-experience to ensure that constraint requirements are implemented. Nevertheless, for complex workpieces, it is virtually incredible to validate total restraint without prototyping the fixture. An alternative to prototyping is full constraint analysis if a workpiece is totally clamped by contact area geometry. Reference [49] demonstrated that algebraic analysis has been providing that a minimum of seven points of contact are needed to form close a workpiece in three dimensions, and as extended to this analysis, by adding friction.

2.5.4.4 Modelling

To ensure the dynamic stability of a fixtured workpiece during machining, reference [50] presented a model-based structure for determining the minimum required clamping forces. As shown in Figure 2.8, three types of contact status are possible including full stick, macro-slip, and lift-off. Since full constraint of the workpiece by the fixture must be satisfied during the machining operation, lift-off of the workpiece from any fixture element and macro-slip of the workpiece at any contact at any instant are indicators of an unstable workpiece. The developed approach exposes that the minimum required clamping forces for dynamically stable fixturing are significantly affected by the fixture-workpiece system dynamics. The main limitation with this explanation is that it does not explain what the role of the clamping force to keep the stability between the mating surfaces of workpiece and the fixture.

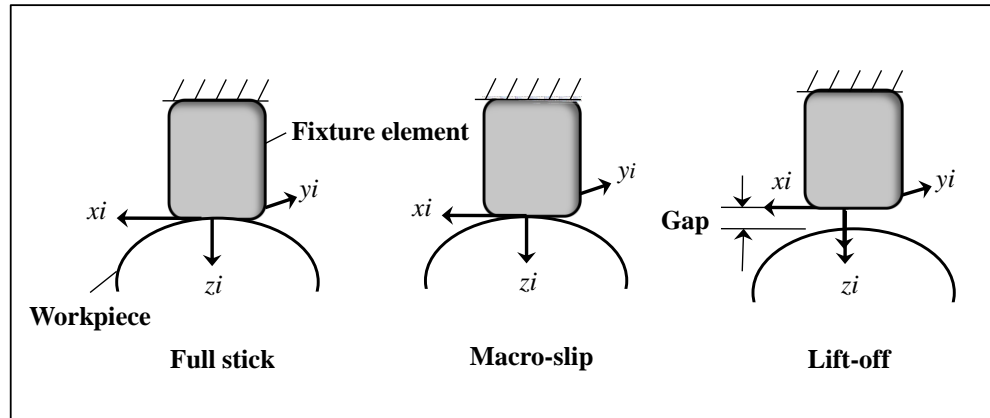


Figure 2.8: Dynamic contact interaction between the workpiece and fixture.

2.5.4.5 Slip

Reference [51] addressed the influence of the partial slip phenomenon on the dynamic motion of a spherical workpiece held in a fixture with application to machining fixture design. The model studies the effect of interfacial slip damping arising from partial slip at a spherical-planar frictional contact exposed to a constant normal load and oscillating tangential load. The model designed to search both single and multiple contact probabilities. Experimental results agree with those predicted by the model, and the effect of the partial slip phenomenon on workpiece dynamic motion is significant and should not be ignored.

2.5.4.6 Force/deformation

Deformation of the workpiece may cause dimensional problems in machining. Supporters and locators are used in order to reduce the error caused by elastic deformation of the workpiece. The optimization of support, locator and clamp locations is a critical problem to reduce the geometric error in workpiece machining. A genetic algorithm based approach is developed to optimize fixture layout through integrating a finite element code to compute the objective function values for each generation [52]. Based on the fixturing principle there are two locating planes for accurate location containing two and one locators shown in Figure 2.9. Therefore, there are two sides clamping against each locating plane. The results show that the optimized designs do not have any apparent similarities although they provide very similar performances. One of the explanations tends to overlook all the effected parameters in the design of the model, such as the friction between the locators and the surface of the workpiece.

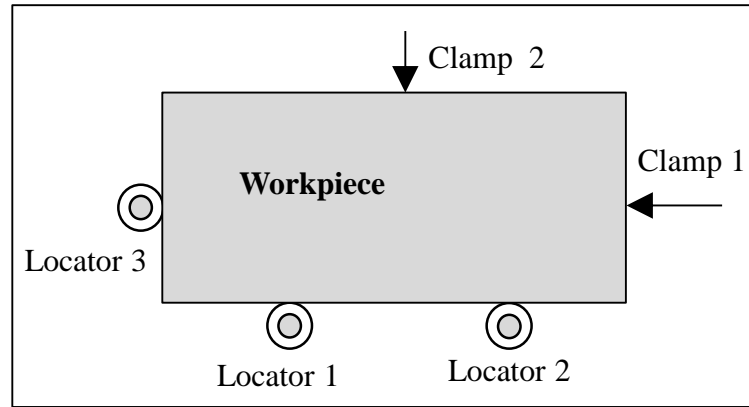


Figure 2.9: Locating layout for 2D prismatic workpiece.

2.6 Elastic Materials Fixture

Recently, under the influences of globalisation, manufacturing companies are required to qualify continuously changing demands in terms of product volume, a wide range and rapid response. The elastic grippers become one of the influenced factors on direct contacts with the product especially in the robotic technology applications. In the past, most grippers were designed for dedicated functions, and could not be revised for other shape, size and weight conditions. Currently, a variety of elastic gripper designs were proposed to overcome such limitations. But, the high cost is an obstacle in addition to maintenance concerns and restrictions to few materials and applications. Despite these drawbacks, cost effective elastic gripper designs have been always required as for the automated manufacturing system [53]. The requirements for the preferred elastic gripper system can be summarised as follows [54]:

- Ability to handle parts with different shapes, sizes and weights by changing the rubber-pocket pressure.
- Robust and highly precise and repeatable in terms of location positioning by multiple pins embedded into the upper plate are envisioned.
- Effective cost, and simple to employ and maintain.

Rubber material is employed in a wide range of technical applications. These elastomers are the essential component of tyres, pneumatic springs or rail brakes, and recently used in the fixturing application. Generally, due to the importance of elastomer components in engineering applications, the accurate prediction of the

mechanical behaviour under effective conditions is a related subject in industry. Therefore, an appropriate approach has to present for dissipative features and large deformation of the material. Reference [55] used the industrial components to improve the performance of the fixturing systems. These components are made of the filled rubber material which is combined from: natural rubber and polybutadiene rubber (NR+BR) filled with 36% carbon black. These fixtures mounted to reduce the transmitted energy to receive structures, consequently the rubber materials prove their efficiency to provide insulation and to meet fixturing requirements.

The particular mechanical characteristics of rubbers influenced their frictional behaviour, as rubber has low elastic modulus and high elongation. Therefore, its microscopic contact area is large as the rubber adjusts to the shape of the surface asperities of the counter material, presenting in consequence high friction in dry conditions as shown in Figure 2.10. In contrast, the main statement of Coulomb's model is that the friction coefficient is independent of the vertical load and the macroscopic area of contact. In detail, the ratio of real area of contact (A_r -interaction between the asperities of the two bodies in contact) to apparent area of contact (A_p -macroscopic area) remains constant when the vertical load increases [56]. In the case of rubbers, this ratio of real to apparent area of contact (A_r/A_p) varies when the vertical load and therefore the contact pressure increases.

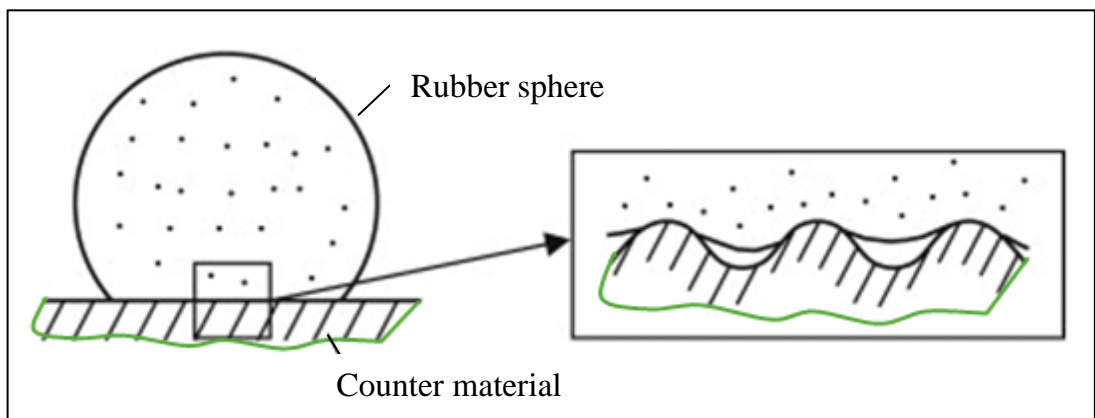


Figure 2.10: Contact area at (a) macroscopic level and (b) microscopic level [56].

Reference [57] presents a methodology for obtaining pressure dependent friction laws from experimental tribometer tests on rubber-metal contacts. Tribometer experiments are simulated for investigating the area of contact and producing an estimation to the contact pressure distribution in the test. The material chosen for the

rubber–metal tribometer tests was 75°IRHD (EPDM type) for the rubber and 6262-T9 aluminium alloy for the counter material. The proposed methodology is applied to evaluate of experimental results from tribometer tests running either in flat on flat or flat on cylinder structures. The result indicates that the flat and cylindrical counter materials have been produced very similar surface morphologies and, therefore, this result is agreement with theoretical pressure-dependent friction law.

In this thesis, the elastic material (rubber, for instance) will be investigated by using elastic fixturing systems to investigate the influence of using these materials on the efficiency of the fixturing system and the proposed monitoring system.

2.7 Conclusion

The fixtures are considered as main parts which are used to support and ensure the constraint the workpiece or tool during the manufacturing processes. There many types of fixturing systems employed in industry. One of these fixtures is the collet; a very important device to clamp the parts effectually, but with many limitations of use when it comes to spindle speed and workpiece material and size. Some parameters can influence the efficiency of the fixture or collet such as clamping force, coefficient of friction, number of contact points and material. Although significant research has been done in developing different fixturing systems based on different techniques, the influence of fixturing design and its instability on condition monitoring system is extremely limited.

Chapter 3 Tool Life and Wear in End Milling Operations

3.1 Introduction

Tool wear has a great influence on the economics of the machining operations. Therefore, knowledge of their mechanisms and capability of predicting tool life are important and necessary in metal cutting. This chapter focuses on the gradual tool wear formation and tool breakage, in the milling operation, associated with the effects of tool and tool holder dynamics and materials as a fixturing system. Moreover, surface roughness is significantly influenced by changing the conditions of the cutting tool. Therefore, this chapter presents the concept of tool wear in milling process and its relation to fixturing and surface roughness.

3.2 Parameters Influencing Tool Wear

The practical parameters that affect the wear of a cutting tool are illustrated in Figure 3.1 and can be summarised in four major groups, as follows:

1. The material of the workpiece and its physical properties (mechanical and thermal properties, hardness, microstructure, etc.), which can determine cutting forces and energy for the applied machining conditions.
2. The interface conditions: in 80% of the industrial manufacturing applications, coolants are used to decrease cutting temperatures and to be expected to reduce tool wear [58].
3. The cutting tool: tool parameters such as tool material, tool coatings, and tool geometric design need to be correctly chosen for different processes (roughing, semi-roughing, and finishing). The optimal performance of a cutting tool requires an accurate combination of the above tool parameters and machining conditions (cutting speed, feed rate, depth of cut, etc.).
4. The dynamic features of the machine tool, affected by the machine tool structure and all the components taking part in the manufacturing process, play an important role for successful cutting.

The instability of the cutting processes with large vibrations generate a fluctuating overload on the cutting tool and mostly encourage the early malfunction of the cutting edge by tool chipping and excessive tool wear.

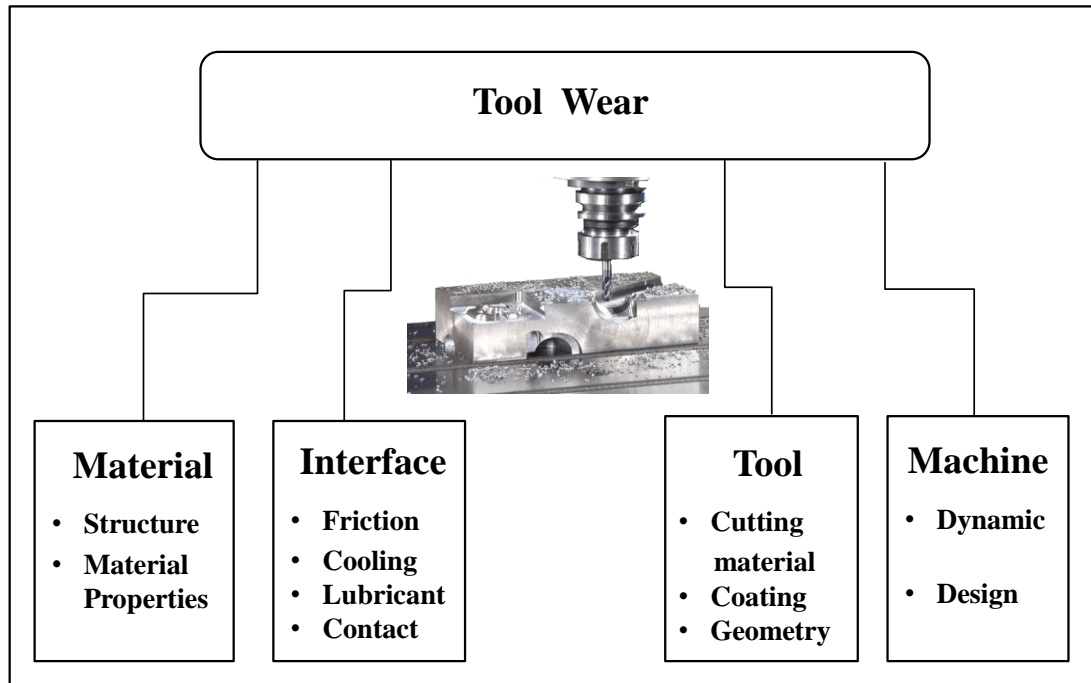


Figure 3.1: The major influencing parameters on tool wear in machining processes.

3.3 Milling Operations

Milling operations are considered one of the most common manufacturing processes in industrial technology. Typically, milling is used to manufacture different and complex objects that are three dimensional geometry with many added features (i.e. holes, slots and pockets). As this process produces the parts with high finishing quality, it is mostly used to manufacture the prototypes for future products. Another application of milling is the production of tooling for other processes. For instance, three-dimensional moulds are usually milled. Milling is also generally used as a secondary process to provide or improve features on parts that are manufactured using different processes.

Milling machines are essentially classified as vertical or horizontal to create irregular surfaces by feeding the workpiece against a rotating cutter containing a number of cutting edges. The milling machine consists mainly of a motor driven spindle, which mounts and revolves the milling cutter, and a moveable machine table, which mounts and feeds the workpiece. Most milling machines have self-

contained electric drive motors, coolant systems, variable spindle speeds, and power-operated table feeds.

The cutter head generally contains the milling machine spindle which is attached to the ram. The cutter head can be swivelled from a vertical spindle position to a horizontal spindle position or can be fixed at any desired angular position between vertical and horizontal. The recent milling machine (Computer Numerical Control (CNC)) is connected by the computerised system to control the machining conditions and implemented the manufacturing program as shown in Figure 3.2.



Figure 3.2: A CNC milling machine.

Milling cutters are usually made of High Speed Steel (HSS) and Carbide which are available in a great variety of shapes and sizes for various purposes. Generally, the operator should know the names of the most common classifications of cutters, their uses, and the sizes best suited to the work to avoid the problem of the inaccurate selection for the tool [58]. This can be achieved by following the instruction of the tool manufacture that provides the required information about the tool and their machining conditions.

3.4 End Milling Cutters

The end milling cutting tool, also called an end mill or end mill cutter, has teeth on the end as well as the periphery. The smaller end milling cutters have shanks for collet mounting or direct spindle mounting. For the small cutters, they may have either a straight or tapered shank. End milling cutters may have straight or spiral flutes. Spiral flute end milling cutters are classified as left hand or right-hand cutters depending on the direction of rotation of the flutes. Straight flute end milling cutters are generally used for milling either soft or tough materials, while spiral flute cutters are used mostly for cutting steel large end milling cutters (normally over 2 inches in diameter) are called shell end mills and are fixed on the face to be bolted for mounting on a separate shank or mounting on an arbour, such as plain milling cutters as shown in Figure 3.3.

Furthermore, the most common end milling cutter is the spiral flute cutter containing four flutes. Two-flute end milling cutters, referred to as two-lip end mill cutters, are used for milling slots and keyways if there are no drilled holes provided for starting the cut. The helical cutter teeth are used particularly for face milling operations requiring the facing of two surfaces at right angles to each other [59].

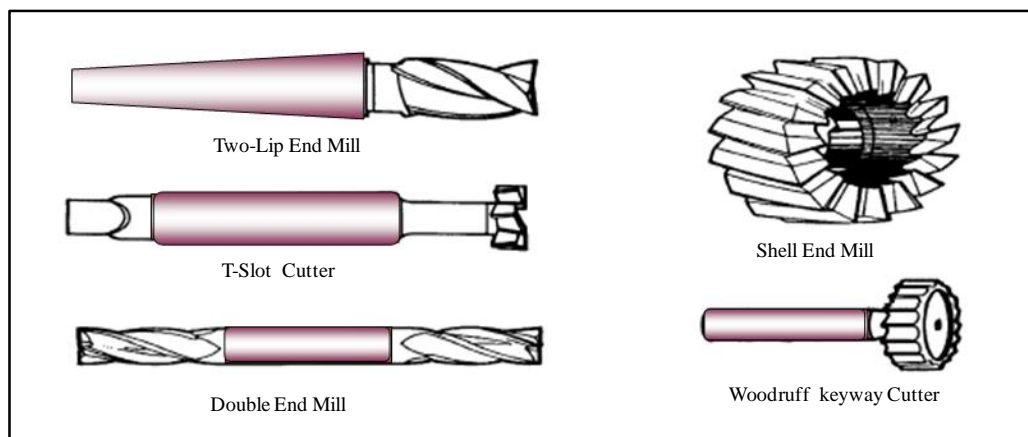


Figure 3.3: End mill Cutters.

The specification of the end mill cutter [60], are described in the following points, which is necessary to be defined as it will be used in the experimental work.

- Shank is projecting portion of cutter which locates and drives the cutter from the machine spindle or adapter as shown in the Figure 3.4.

- Tooth is the cutting edge of the End mill. Tooth face, also known as the rake face, the portion of the tooth upon which the tooth meets the part.
- Length of cut (Flute Length) is the effective axial length of the peripheral cutting edge which has been relieved to cut.
- Flute is a space between cutting teeth providing chip space and regrinding capabilities. The number of cutting edges is sometimes referred to as "teeth".
- Clearance angle is the angle formed by the cleared surface and line tangent to the cutting edge.
 - Clearance: Primary (1st angle, 5° - 9°) - Relief adjacent to the cutting edge.
 - Clearance: Secondary (2nd angle, 14° - 17°) - Relief adjacent to cutting edge
 - Clearance: Tertiary (3rd) - Additional relief clearance provided adjacent to the secondary angle.

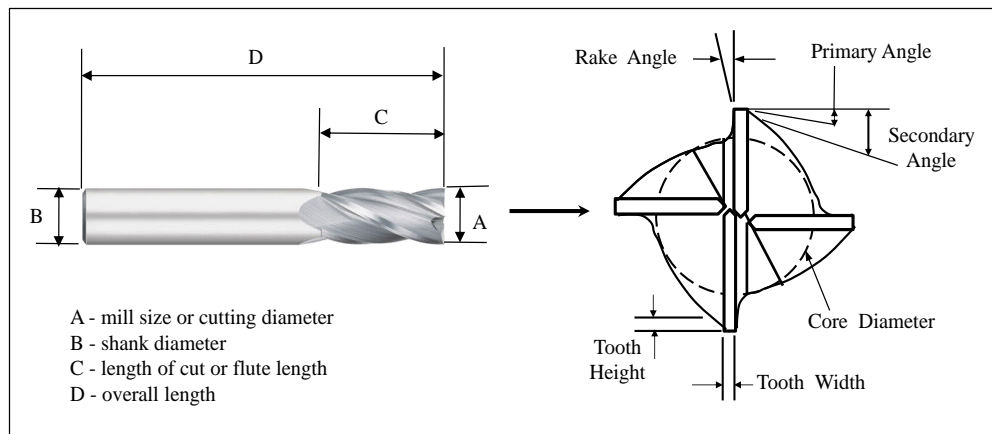


Figure 3.4: Specification of the End mill.

3.5 Errors in End Milling Operation

Accuracy of machined components is one of the most critical considerations for any workpiece manufacturer. It could be defined as the degree of agreement or achievement of a finished product with the required dimensional and minimum geometrical accuracy error [61]. On the other hand, theoretically it can be explained as any deviation in the position of the cutting edge from the required value to make a workpiece of the specified tolerance. The amount of error in a machine gives a

measure of its accuracy which expressed the maximum translation error between any two points in the production of the machine. This widely depends on the available resolution of the system positioning that can be difficult produced more accurate than what it made for. Therefore, there will be no further feedback to improve the positioning within more over the designed range.

However, another important issue is the errors that occur between the measurement point and the feedback point [62]. The suggested way to keep track of the errors is to create an error account. An error account allocates sources among the different components of a machine. It is a system analysis tool used for the prediction and control of the total error of a system. An error account essentially addresses two fundamental issues. One involves obtaining the influence of different sources of error on the accuracy of the machine. The other involves taking a set of specifications and determining the permissible level of each source and the difference will be taken in the consideration till reach to the optimised system.

Specifically, errors may contain two categories quasi-static errors and dynamic errors. Quasi-static errors are those geometric/kinematic between the tool and the workpiece that are slowly varying with time and related to the structure of the machine tool itself because thermally induced strains in the machine structure. The other is Dynamic errors that are caused by sources such as spindle error motion, vibrations of the machine structure, controller errors etc. These are more dependent on the particular process conditions of the machine. Quasi-static errors account for about 70 % of the total error of the machine tool, and therefore, a major focus of error compensation has been investigated in research [63].

3.6 Tools Wear in the Milling Operation

Generally, tool wear is defined as the loss amount of tool material due to physical (mechanical) and chemical interactions between the cutter and workpiece, this leads to remove small parts of material from the used cutter. Tool wear is an extremely complicated process associated with many parameters such as contact stress between mating surfaces, material properties of the workpiece and cutting tool, temperature on the cutting edge, and cutting conditions [64]. Sometimes when high temperature and high contact stresses at the tool-chip interface, the chip maintains a very close contact with the tool on the rake surface and flank surface through an interfacial

layer or built up edge [65]. Therefore, tool wear in the metals cutting is supposedly due to adhesion and diffusion of tool material into the flowing chip at the interface of tool-chip.

Tool wear is the leading cause of vibration of the machine tool and weakening of surface roughness and dimensional accuracy of the workpiece. Hence, it causes tool breakage and workpiece damage. These rapid changes are having a serious effect on the progress of machining process. In the last decades, automated machining operation has been progressing intensively and unattended process of machine tools is widely introduced in many machine shops. Therefore, these aspects and the problems have been encouraged the researcher [66] to seek a detecting system to monitor these conditions and realises high efficiency and automation of machining process.

Tool wear can be classified into several types, and summarised as follows [67]:

- Adhesive wear associated with shear plane deformation. Generally, adhesion means the recombination made when the tool and the workpiece material derived into contact with distance of atoms. Therefore, it is called cold welding phenomena caused by the plastic deformation of the actual contact area of mating surfaces under pressure and temperature. Consequently, the relative motion of adhesion points on these surfaces, it reasons adhesive wear when the grain is taken away by shear or tension.
- Abrasive wear resulting from hard particles cutting action, therefore it is defined as the damage on a surface, which occurs because the motion relative to the surface of harder asperities at the interface. Specifically, the adhesive layer could be occurred in the whole cutting process, and directly allows the cut by the hard inclusions in the workpiece material on the tools. The hard inclusions in the workpiece surface will press into the friction surface and generates the trough-shaped indentation by the increasing the abrasive grooves.
- Diffusion wear occurring at high temperatures. The close contact between the tool-chip and tool-workpiece makes an ultimate environment for the atoms in the tool material with the external diffusion through the tool-chip interface.
- Fracture wear or Debonding failure happened due to fatigue. It is a complex process and formed by the part of tool material detaching under the joint action of the abrasive wear, adhesive wear, and diffusion wear. The fracture wear has different forms due to the differences of tool materials.

The tool wear structure may depend totally on the machining conditions, mainly cutting speed and the undeformed chip thickness, and a combination of the abovementioned wear mechanisms. A variety of forms of wear-land pattern and existing cutting speed are shown in Figure 3.5 for metal cutting process. The more largely occurring forms of cutting tool wear usually identified as the principal types of tool wear in metal cutting using single-point tools are nose, flank, notch and crater wear.

Nose wear or edge rounding occurs mainly through the abrasion wear mechanism on the cutter major edges resulting in an increase in negative rake angle. Nose wear can be dependent entirely on the implemented cutting conditions with the lost of tool sharpness throughout plastic or elastic deformation. At high cutting speeds, the edge deforms plastically and may be lost of the entire nose. Edge chipping and cracking occurs during periodic breaks of the built-up edge in interrupted cuts with brittle tool and thermal fatigue. Catastrophic failure may be also happened if the nose is considerably worn or as a consequence of the utilisation of inappropriate machining conditions and brittle tools such as ceramics and cemented carbide [68].

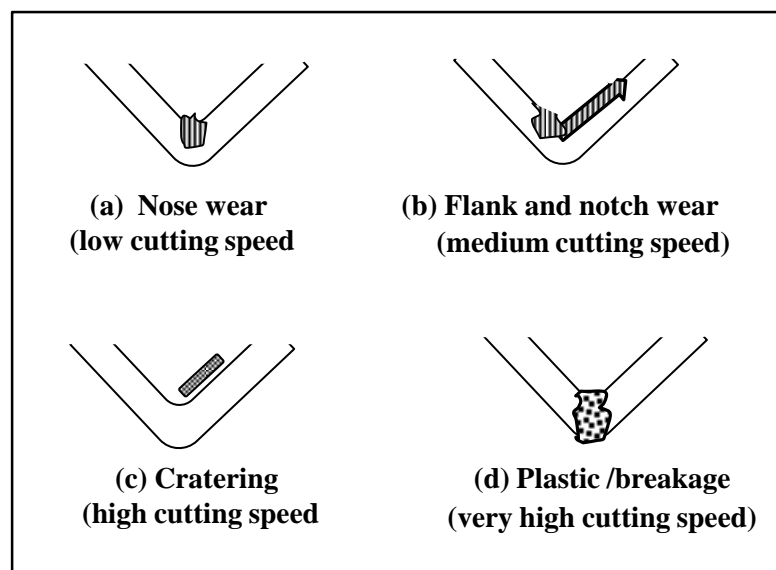


Figure 3.5: Cutting tool wear forms in orthogonal metal cutting (reproduced from [68]).

However, choosing suitable machining methods and tooling systems is important to achieve dimensional accuracy and surface quality. In addition, cutting parameters, cutter characteristics, material of tool and work piece, chip formation, tool wear and

the vibration of the tool and work piece configuration are parameters that significantly affect production performance. The most critical one among these mentioned parameters is the tool life. Tool wear can be visually measured using a microscope [69]. However, in practice, tool life is estimated by Taylor's equation instead of making cumbersome measurements.

The cutting conditions have significant importance since they effected on the metal removal rate and production rate. These conditions included feed, speed, and depth of cut which are built in Taylor's equation [69]:

$$VT^n = C \quad (3.1)$$

Where T = Tool Life (min) V = Cutting speed (mm/min)

n and C are constants that depend on feed, depth of cut, work material, and tooling material, but mostly on material (workpiece and tool).

It can be expressed the above equation of tool life in terms of the cutting variables as follows:

$$T = CV^k f^l D^m \quad (3.2)$$

f = Feed per tooth (mm/tooth) D = Axial depth of cut (mm)

k, l, m = Constants for a given tool-work combination and tool geometry and to be estimated using experimental work.

A common approach for assessing machining performance is tool wear/tool life. Tool wear is a time dependent process. As cutting proceeds, the amount of tool wear increases gradually. Tool wear must not be allowed to go beyond a certain limit in order to avoid tool failure. However, tool life is the length of time that a cutting tool can work satisfactorily before it begins to fail.

Tool wear/tool life is one of the most significant and necessary parameters required for process planning and total machining economics. A review of several theoretical and experimental techniques for predictive assessment of tool-wear and tool-life are described in reference [70].

The trend in tool wear/tool life modelling has been to extend Taylor's equation. This is mainly due to the direct relationship between cutting speed and tool-life as shown in Figure 3.6.

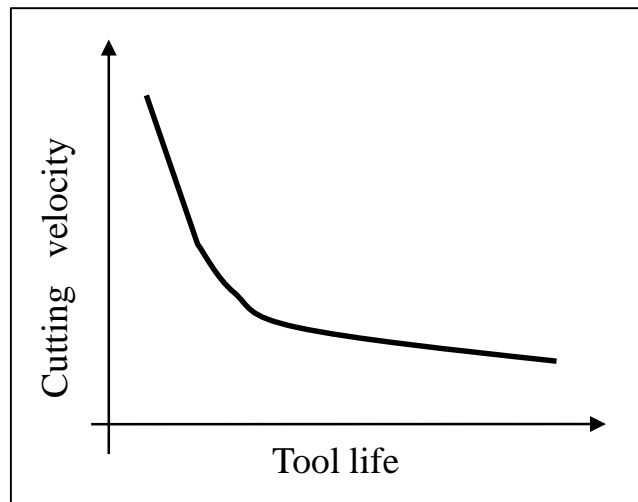


Figure 3.6: The relationship between cutting velocity and tool life.

This relationship holds appropriate for all machining operations and is considered as a basis for more advanced models. However, there is a serious drawback with the use of Taylor's equation, because it does not inform directly the relationship between tool wear and tool life. Empirical attempts [71] have been presented to define this relationship in terms of the variation in cutting speed as shown in Figure 3.7. It can be observed that the tool wear is proportional to the time of machining.

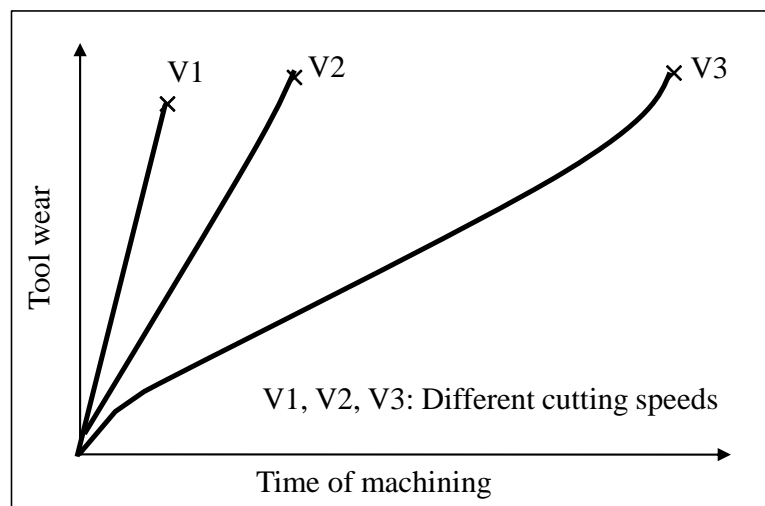


Figure 3.7: The relationship between tool wear and tool life with different cutting velocities.

These curves of the relationship between tool wear and tool life have been taken in the methodological consideration of this thesis.

3.7 Tool Wear and Fixturing Errors

Currently, it can be seen that both the tool wear and fixturing errors have played a critical role in creating inaccuracy of the manufactured parts. Taken together, fixture set-up and geometric imprecision of the locating elements are caused to errors in fixturing, especially where the contact area is small between the fixture and workpiece. Therefore, it is important to create more attention to the workpiece displacement which is dependent on some factors including place of the fixturing elements, clamping system, clamping strength, and type of contact surface. Thus workpiece displacement could be a major cause of machine error.

On the other hand, the fixture also contributes to machining imprecision by generating the deformation of thin-walled parts under the influence of the clamping force. Therefore, the main aim of the recent research is trended to focus on the basic design of fixture such as locator and clamp, their placement, and the clamping sequence. Many suggestions have been presented to address this error such as increasing the clamping force to prevent the separation of the workpiece, and reducing the depth of cut during machining processes [72]. Therefore, the general aim is built the fixture forms as an integral part of the machine tool and thus contributes to its based accuracy. Another suggestion is presented by reference [30] to improve the quality of wood machined surfaces using NC fixturing system.

3.8 Surface Roughness in Milling Operation

Surface roughness is considered as one of the most important parameters to determine the quality of machined parts. Surface roughness is defined as a group of irregular waves in the surface, measured in micrometres (μm). There are various simple surface roughness amplitude parameters used in the industry, such as roughness average (Ra), and maximum peak-to-valley roughness (Rmax) [73]. The parameter Ra is used in this study. The quality of the machined surface has a very important role especially in the production of complex shapes such as precision moulds which need to high resistance of deformation and corrosion [74].

Many investigations have been performed to verify the relationship between surface roughness and cutting parameters such as cutting speed, feed rate and depth of cut. Practically, many influences which usually have an effect on surface roughness including vibration and inaccuracies in the machine tool, abnormalities in feed

mechanism, imperfection in the structure of workpiece materials and surface damage produced by chip flow [75]. Surface roughness is affected also by other variables [76], such as the mechanical properties of the material, the geometry of the milling cutter, the runout errors of the tools and the vibration produced during the process as illustrated in Figure 3.8.

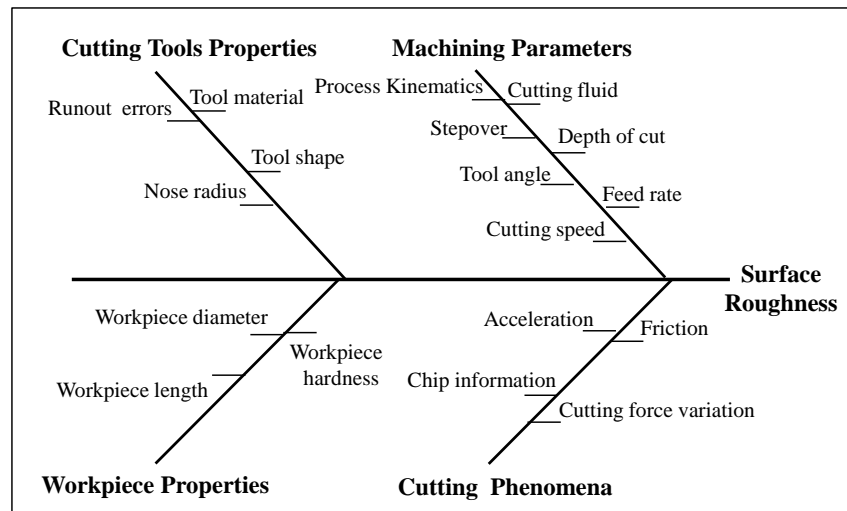


Figure 3.8: Parameters that affect surface roughness.

Surface roughness measurement is divided into two categories: direct and in-direct measurement. Direct measurement of the machined surface which is directly proposed by light scattering, ring field capacitance or ultrasonic sensing, stylus type gage is the most common direct measuring instrument. In indirect methods, surface roughness is derived using parameters of machining process such as acceleration. Although the indirect methods showed less accurate prediction than direct method, the indirect methods are more practical to be implemented in the in-process measurement [77]. The modelling and prediction problems of surface roughness of a workpiece by computer vision in machining operations have received a great deal of attention [78]. However, since the roughness of the machined surface is an important quality measure in metal machining, therefore it is important to monitor and control surface roughness over time during the machining operation. Monitoring surface roughness is mostly performed by manual inspection of workpiece surface using profilometer which is taken a long time and needs to the skilled operator. For the specific production, sometimes the inspection of the surface roughness applied 100% on all products; this will increase the cost of the workpiece [79].

Surface roughness needs to be investigated with regard to the effect of the change of cutting tool condition and the stability of the machine under the observing of the monitoring system.

3.9 The Relationship between Tool Wear and Fixturing System

In the past years, many researchers have studied the end milling process since they investigated the effect of vibration, deflection of the workpiece-tool system in the end milling process on surface roughness. Nevertheless, other established a mathematical model that predicts the surface roughness after end milling. The most critical point is the relationship between the holding device and the workpiece or tool.

Generally, in the analysis of the workpiece-fixture displacement, it is assumed that both of the mating objects are rigid everywhere except with the contact region. Most of the research suggests that the best shape of the locators and the clamps is spherical tips to make sufficient contact. This may be to increase the area of contact and reduce the deformation of the workpiece, and to stand against the change of the machining conditions such as tool wear. For example, reference [72] presented a set-up for the workpiece which clamped by the locators as shown in Figure 3.9. This recognised a reference for the frame of the workpiece with respect to the frame of fixture reference. However, throughout the machining process, the workpiece is displaced within the fixture. This displacement is emerged because a combination of localised deformation, slip and lift-off at the contact regions. This finding supports the idea that the most of the workpiece-fixture errors happen at the contact points.

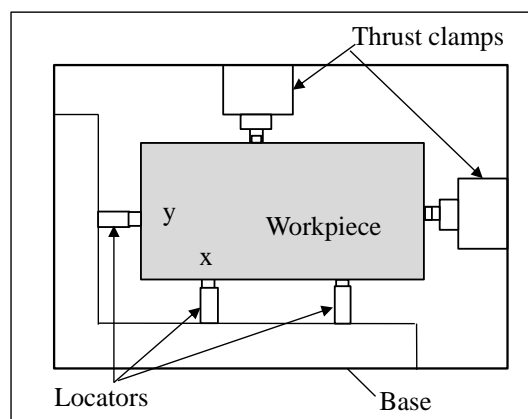


Figure 3.9: Workpiece before clamp actuation.

The tool geometry could have a significant effect on process vibration. Reference [80] has studied the effect of material and geometry on the tool wear characteristics of cutting tools during the milling process. The wear investigations in this case are more complex than in other machining operation and the cutting conditions are influenced by the location of the cutter with respect to the workpiece. The conclusion is the chip cross-section changed due to the fluctuations of contact between the tool and workpiece. Reference [81] interpretation overlooks much for this problem as it investigates the effect of tool holder geometry (70° and 90°) on cutting performance in terms of tool life and tool wear when machining of nickel-based alloys 242. It was found that during machining of workpiece with a tool holder providing geometry of 90° shoulder cutting, the tool wear rate progressed more rapidly compared to the 70° -tool holder. Generally, the cutting inserts were rejected mainly due to intensive wear on the flank face and the surrounding area.

Tools for semi-finishing and finishing operations, particularly for medium and large moulds, must generate complex forms using end mills. These final processes normally use tools with small diameters, small feed per tooth, radial and axial depth of cut and higher tool rotation and feed velocity than in conventional processes. This encouraged reference [82] to suggest that these tools may be either solid (mainly for small diameters) or with inserts. The results show that the selection of the tool materials is necessary to minimise the friction coefficient between chip and tool and consequently reduce the tool wear and improve surface roughness.

Furthermore, reference [83] contributes a work to a better understanding of the milling process and of the wear mechanisms of tools used in semi-finishing operations of hardened steels for dies and moulds. The work evaluates the influence of the inclination of machined surfaces as indicated in Figure 3.10. The finding indicates that with inclined surfaces, the problem of cutting speed is absent since the effective tool diameter is increased. The angle between the tool axis and the surface exerts a strong influence on the components of the cutting force. When the tool axis is parallel to the surface (90°), only tangential and radial components of force are present. The main conclusion has been presented that the inclination of the machined surface strongly influences tool life, and tool wear involves different mechanisms. Hence, the way tool wear-vs-machining time behaves could be different and dependent on the above factors.

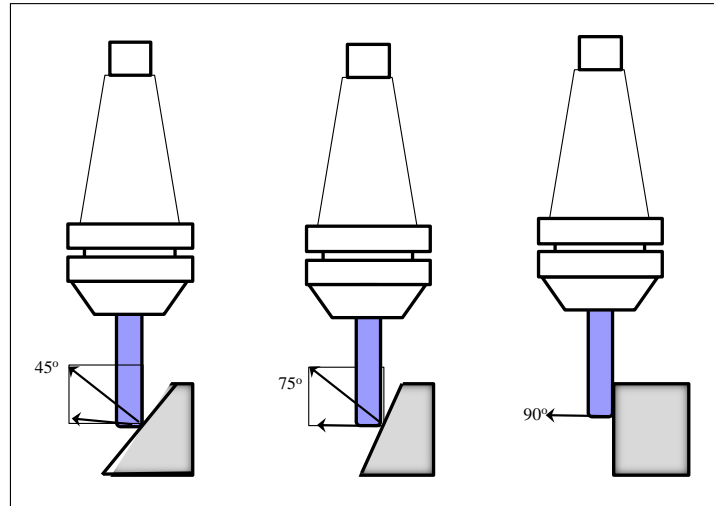


Figure 3.10: Axial and radial components of cutting force for surface inclination (reproduced from [83]).

3.10 Conclusion

Milling process is one of the most common and complex process in machining operations. The quality of the machined parts is influenced by many parameters including machine, tool wear, fixture, workpiece and cutting conditions.

Tool wear plays an important role in the quality of the workpiece and surface finish. Therefore, monitoring tool wear to predict surface finish is important for quality control. Tool wear/life in milling is a complex process and influenced by many factors. The tool wear/life-vs-machining time is not consistent and can be influenced by many factors; hence, it is important to investigate how the expected tool wear performance would influence the prediction of tool wear.

Chapter 4 Fundamental Principles of Condition Monitoring Systems in Milling Operations

4.1 Introduction

Nowadays, the global market competition has drawn the manufacturer's attention on automated manufacturing systems using condition monitoring. The Condition Monitoring (CM) has been used as a method to improve products quality, eliminating inspection, and enhancing manufacturing productivity. The main goal of condition monitoring also is eliminating accelerated tool wear, tool breakage and poor surface finish. In this chapter, the concept of condition monitoring is presented with its importance. The limitation of the CM is also addressed.

4.2 Condition Monitoring Systems

Traditionally, the ability of an operator to define the condition of the process is built based on his knowledge and senses (i.e. vision and hearing). This ability now is the expected role of the monitoring system. Currently, most of machining processes are fully automated and carried out under the supervision of safety screens. Typically, the role of the operator is to supervise and also to load and unload of the parts for several machines in a manufacturing cell. One of the limitations of this process is that the operator does not monitor continuously and his reaction time to any problem will not be sufficient, especially in a high speed machining. This reason considerably leads to find an automated method to detect the faults of the production process. Therefore, a Tool Condition Monitoring (TCM) systems are proposed in literature to identify and respond, on line, to any abnormalities in process, it is also should take a suitable action [84]. Figure 4.1 shows the general structure of a TCM which consists of sensors, signal processing stages, and decision making systems. The decision making system is used to interpret the sensory information and to decide on the required corrective action.

The tool condition monitoring system depends on two basic elements including the number and type of the used sensors. This is important to determine the quality of

the data acquired, and the associated signal processing and simplification methods which are employed to analyse the sensory information and determine status of tool. The first element affects the cost of the system since it involves expensive hardware, while the second element influences the effectiveness and the speed of the system. It is important to design a condition monitoring system with a high efficiency, short development time, and with a suitable number of sensors [84]. By choosing appropriate number of sensors and associated signal processing methods, a minimum classification error of process abnormalities can be reached.

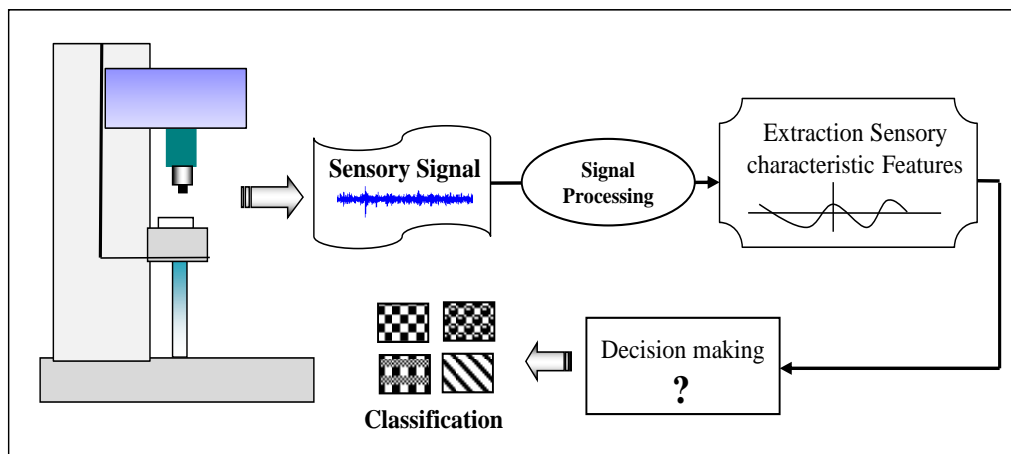


Figure 4.1: The general structure of a condition monitoring system (reproduced from [19]).

For more than several decades, the creation of effective, efficient and on-line tool condition monitoring systems (TCMSs) have been observing importance in industry and manufacturing research. Therefore, researchers have dedicated much time and effort in developing these systems. However, only limited reliable TCMSs have been established for industrial applications. This is mainly due to the nature of the monitoring signals, difficulties to define or find the nonlinear relationship between the measured features and tool wear, and to economic reasons [85]. Other methods are more simplistic and fast to use, however they are mostly more sensitive to changes in cutting conditions and less sensitive to tool wear.

Many researchers participated in the development of TCMSs have focused on the problem of extracting the most valuable information from the monitoring signals. As a result, several new signal processing techniques are investigated, in order to achieve more efficient and accurate estimation methods in designing an effective TCM. There is also a trend in the manufacturing research community of several

needs in the development of a TCM to be used in the practical applications. The developed TCM can be reached the following achievements [86]:

- An agreement between the number of the used sensors and their cost, and the performance of the TCM.
- A sufficiently less computation time that permits to change the tool before the wear exceeds the accepted limit.
- The used sensors that do not disturb the production process.

4.3 Significance of Monitoring Systems

The aim of an automated system is to allow machines to continue working as long as the conditions of the process are satisfactory. This already is becoming a practical reality. Complex automated manufacturing systems mean that individual units are extremely interdependent. Therefore, a fault or a breakdown could mean a full stoppage of a manufacturing cell, thus affecting productivity of the complete production system. The need to the process monitoring system is not only to detect tool wear and tool breakage at an early stage, but also to present a process assessment and optimisation parameters. The system can be implemented to improve machine utilisation and thus reduce the machining cost. In the next sections, the importance and limitations of the monitoring system are presented in detail.

To avoid the damage to the machining system (i.e. tool, tool holder and machine), it is required to have resources that have the ability to promptly detect an actual or forthcoming tool breakage. This could be achieved by making in-process measurements existing by continuous monitoring of the metal-cutting process. It has estimated that the development of this monitoring system to reliably detect tool condition could result in an increase of cutting speed, a decrease in cutting time, savings in tool changing time, and overall savings of 10 to 40% [87].

In a metal cutting process, TCM systems cover monitoring the machine and the cutting process dynamics, cutting tools and workpiece to achieve optimum performance of the process [88]. Therefore, as a serving, the TCM systems can be briefly observed the following purposes:

1. Detect the fault in the process for cutting tool and machine.
2. Check and maintain the stability of the manufacturing process.

3. Provide a compensatory mechanism for tool wear progress which keeps the tolerance of the machined workpiece in acceptable limits.
4. Create an avoidance system of machine tool damage.

Simply the continuing of the production process through rest breaks alone could give around 10-12 % more parts per shift [89]. This means that the payback period for installing the monitoring system is relatively very short. This advantage even without considering additional benefits such as detecting tool wear or tool breakage, collision control, and so on, the system can repay its cost exclusively by accessing the production through operators breaks.

Another advantage can be observed from the monitoring system is the product quality improvement, since the automated machines remain in a stable thermal conditions. Generally, the existing conditions of the operation, it is possible to realise gradual improvements. This development supports the manufacturing process to have better quality, and reduce the costs.

4.4 Limitation of TCM System

Much research has been performed concerning the development of reliable TCMs. However, due to the obvious complexity of the process, the current systems have some significant limitations. Several factors have obstructed advances in the development of TCM including inappropriate choice of sensor signals and their utilisation. The lack of an efficient TCM system may include excessive power take-off, inaccurate tolerances, irregularities and uneven workpiece surface finish. As a result, the machine tool and/or machine peripheral damage which suffer from unnecessary costs. One of the primary reasons for the lack of industrial application of TCM is due to the fact that these systems have been developed based mainly on mathematical models with perhaps limited number of experimental work. These models require enormous amounts of experimental data for validation. Another possible interference, generally, lies in the nature and features of the applied sensor signals, which tend to be non-linear and therefore difficult to model. The random behaviour can be related to the significant variation and non-homogeneities that occur in the operating part [88]. Also, there are complications involved in designing TCM that take account of the noise sources.

Usually, most machining processes can be classified as having one or more of the following characteristics:

1. Difficult to organise into behaviour due to non-homogeneities in workpiece material.
2. Sensitivity of the process parameters to machining conditions.
3. Non-linear relationship of the process parameters to tool wear.

The disturbances of aforementioned sources could lead to misleading information, hence limiting the precision of the condition monitoring system. Therefore, when unexpected disturbances occur, a TCM should to be capable of analysing and recognising the fault and cancel any disturbance with specific level of confidence.

Many attempts to develop the TCM to detect rapid changing and unpredictable environment have been done. The major drawback is still to the implementation real adaptive, self-calibrating, condition monitoring system that is more sensitive to faults and less sensitive to disturbances and noise. There is a limitation for selecting a suitable sensor and signal processing for online monitoring with complex machining scenarios. This problem can be avoided by using influencing parameters of the machining process that show sensitivity to tool wear or tool breakage. For milling processes, it can be noticed that the majority of researchers developing the TCM have used torque, thrust force, vibration and strain, while other researcher used temperature and sound and acoustic emission (AE) [18].

4.5 Structure of TCM System

Typically, most approaches which are used in tool condition monitoring are constructed upon three major elements; sensors, feature extraction and decision making as illustrated in Figure 4.1. This section will discuss these elements and the limitations associated with them.

4.5.1 Tool Condition Monitoring Sensors

A wide range of sensors has been used to monitor the parts of machine tool that are more expected to produce unique signals related to process or machine conditions. The monitoring of cutting tools has included approaches to tool identification, tool wear monitoring, tool breakage and tool life.

Since the indirect signal measurement of the tool performance is easier than the direct measurement, the practical approaches for tool condition monitoring are implemented using indirect measurements. Significant connection exists between the sensors used for tool monitoring during machining operations [90]. Figure 4.2 illustrates the most approaches used. Most of these approaches have usually placed additional sensors on the machine.

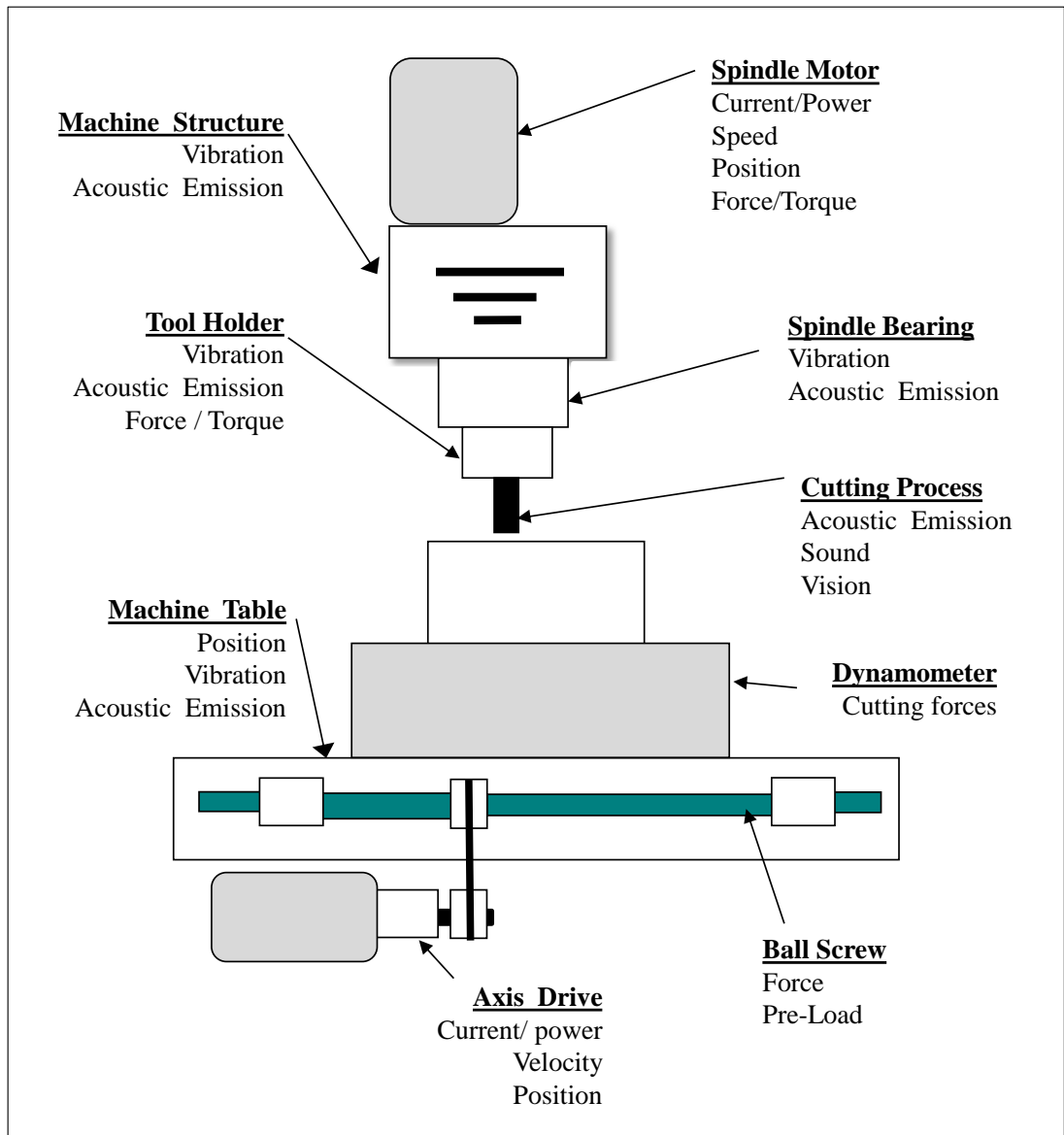


Figure 4.2: Multi-sensor cutting tool monitoring options.

4.5.1.1 Cutting Force

One of the most significant current approaches in condition monitoring is based on the measurement of cutting forces. Force measurements are generally taken using a

dynamometer mounted between the workpiece and machine table during cutting process as shown in Figure 4.2. This dynamometer measures the cutting force in three perpendicular directions including the X, Y and Z axis. However, in the end milling process, the Z axis cutting force component contains little information but the X and Y axis signals have been exposed to provide more accurate information for the process. A serious weakness with this dynamometer, however, is the physical and cost limitations. These limitations have encouraged the researcher to seek indirect measuring the cutting force and develop a range of tool holder mounted dynamometers which could reduce some of the limitations [91].

4.5.1.2 Spindle System Condition

Spindle parameter such as motor torque is the most common approach for monitoring various tool condition monitoring. This approach is based on cutting experiments which are performed to obtain an understanding of the variations of the signals during machining process. Then, the machine controller aims to hold the parameter at or around the optimum value by controlling the machining process.

The spindle motor torque is predicted using a geometric model of the tool and workpiece interaction. It is able to quantify the metal removal over discrete time intervals. The transfer function of spindle torque to current is normally calibrated using a force dynamometer. Within this overall approach, several methods have been developed. The torque extrapolated from the spindle current measured on-line. The aim is to compare the estimated spindle torque to the actual torque during end milling therefore any deviation around a pre-set value will indicate a range of faults, including tool wear or breakage [92]. This approach will serve as a base for future studies, where they developed a monitoring of spindle shaft vibration to measure the tool wear during milling process. A concern is recognised that the bandwidth of the spindle motor servo enforces limiting factors to affect both spindle speed and number of cutting edges on the tool. Also, in some cases spindle power might not be sensitive to tool conditions when using a small tool on an over-rated spindle motor.

4.5.1.3 Acoustic Emission

Acoustic Emission (AE) is a very high frequency oscillation or stress wave, generated when deformation occurs as metals are cut or fractured. The acoustic

emission is a very high frequency stress wave generated when plastic deformation occurs (chip creation) as a result to the interaction between the operating part and the tool. The AE is found successful in applications related to tool monitoring during machining processes. It is still less straightforward in milling since the pulse shock loading arises during the entry and exit of each individual tooth to the workpiece. Those pulses also generated during tooth fractures.

Another limitation in using the AE is related to the discontinuous nature and variability of the process. To overcome this limitation, an approach is suggested to monitor cutting tool wear using both AE and vibration monitoring as outlined in [93]. The approach suggests that progress in the application of AE in this area may be forthcoming and could be implemented by using optical probing to measure the AE from the rotating tool holder during machining process [94].

4.5.1.4 Feed Axis System Condition

This approach is based upon the actions of the axis system used to move the workpiece past the rotating tool. The monitoring strategy involved monitoring of the armature current of the DC motors on the X and Y axis drives. Same limitations emerge with the use of monitoring the axis motor current as with monitoring the spindle motor. The bandwidth of the system is limited by the characteristics of the servo since the bandwidths of 100 Hz are too low compared the possible tooth passing frequency of 400 Hz or higher in milling applications.

A method is developed to use this approach for detecting the tool breakage by comparing the actual cutting force measured using a table dynamometer. It then became possible to detect tool breakage from direct measurements of the axis drive armature current. The cutting force is considerably more than the friction forces within the drive system [95].

Many experiments are conducted to form inter-relationships between tool condition (i.e. wear or breakage) and various control signals within the X axis DC motor feed drive system. The parameters of the axis are monitored including armature current, motor tachometer and the velocity command signal from the machine controller as illustrated in Figure 4.3. This system enables to detect a broken or worn tool from a sharp tool by considering the variance of the tachometer or motor current individually [96].

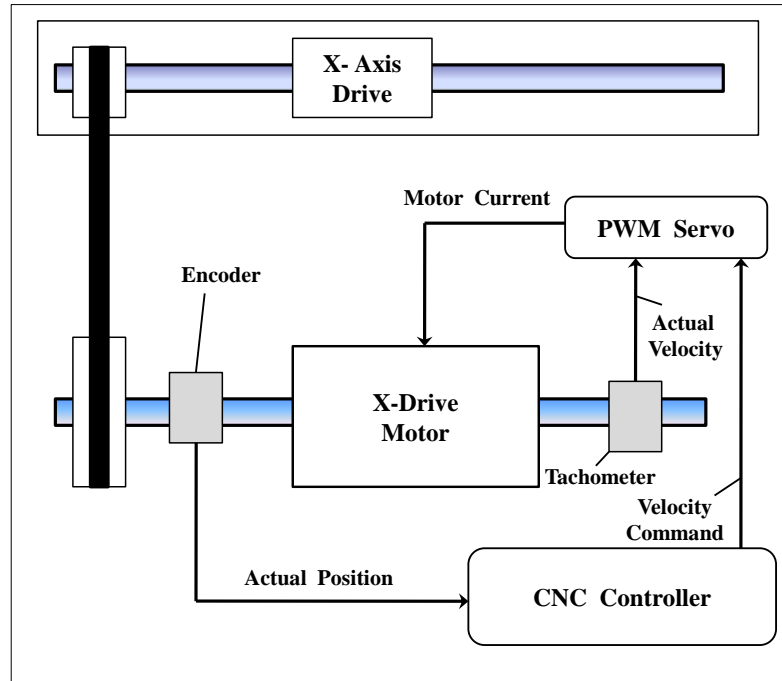


Figure 4.3: Schematic of the x-axis drive and control system (reproduced from [96]).

4.5.1.5 Recent TCM Approaches

Further to the aforementioned approaches, vibration analysis is a successfully and widely used condition monitoring tool for machines and processes. However, in the setting of milling monitoring, its application is slightly limited by the nature of the process due to the noisy signals arising with the vibrations during to the cutting process. It is reflected a good indicator especially in a real time for tool breakage monitoring. A multi-sensor approach (fusion model) has also become increasingly more applicable in TCM comparing with other existing methods. Multi-sensor approach has developed a massive rise in the data acquisition and computing capabilities presented to achieve an on-line monitoring of the manufacturing process. A combination of the sensory techniques to create effective monitoring system has been presented in literature [19]. The amount of information generated by this approach associated with the application of artificial intelligence, such as ANN to control large amount of sensor inputs [97].

4.5.2 Signal Processing and Feature Extraction

The critical step in tool monitoring is how to extract valuable information from the implemented sensors. The accurate interpretation of data could significantly produce a reliable level of information for the decision making process [98].

End milling process, similar to many machining operations, could be characterised using deterministic model or stochastic model. The deterministic model assumes the process parameters are stable and can be easily predicted while the stochastic model assumes random variation in the process [99]. It is assumed that real life operations have stochastic nature and hence it is important to develop the efficient signal processing and feature extraction to ignore the random variation and focus on features related to the faults and process/machine health.

The traditional technique of observing signals is to view them in the time domain. The time domain is a record of what happens to a parameter of the system versus time. Another technique, which is the frequency domain, used for analysis of signals with respect to frequency, and it shows how much of the signal's energy is present at each frequency. Signal processing in time domain and frequency domain are normally used to extract useful features from the signals.

There are several time domain features that can be extracted from raw sensor data such as maximum, minimum, standard deviation and average. All the time domain-features avoid the complexity of pre-processing (i.e. they do not require the difficult task of framing, windowing and filtering), therefore they do not consume processing power and time. However, they are not robust to measurement and calibration errors. The frequency domain features (i.e. frequency spectrum energy and maximum of frequency spectrum) require pre-processing and Fast Fourier Transform (FFT) of sensory signals. The frequency domain features greatly depend on user knowledge about the characteristics of features. Also, fourier transform of a signal does not contain any local information about the signals. Generally, the features extracted from the absolute values of the raw measurements are more robust to noise and calibration errors than the features extracted directly from the raw measurements [100].

Wavelet analysis is an exciting new method for solving the problems in the previous methods by combining the applications in time and frequency domains.

Wavelet transform is better than the existing minutiae based methods and it takes less response time which is more suitable for online verification with high accuracy. The modern applications of wavelet theory as diverse as signal processing, image processing and pattern recognition [101].

4.5.3 Intelligent Decision Making

An Intelligent TCM system is defined as an integrated system consists from multi-sensors, signal processing method and intelligent decision making technique, these requirements are necessary for automatic manufacturing process.

In recent years, intelligent monitoring systems for tool breakage detection have gained more attention because they can better expect the correct mapping pattern for the input and output of a dynamic system directly. This feature is too difficult in the physical model which requires the derivation of very complex mathematical equations concerning measures that are difficult to determine. Many researchers moved from the predictive methods to intelligent discriminator systems, such as Expert systems, Fuzzy sets, novelty detection, and Artificial Neural Network (ANN). The intelligent system uses their ability to describe high non-linear characteristics of manufacturing processes, superior learning, noise destruction, and parallel computation abilities [102].

However, the disadvantage of some of the decision making systems that they would require significant training and they could be very dependent on their structure and configuration [103].

4.6 Conclusion

TCM systems are important to detect faults which may occur during the machining process. Consequently, this leads to improve the quality of the product, save the energy, increase the productivity, reduce the totally cost. The successful of the TCM application depends on the number and type of the used sensors, and on the quality of signal processing and decision making stage. This is additional to the dependency on the reliability of the hardware and data acquisition systems.

Many approaches have been implemented regard to the environment of the milling machine tool including cutting force, spindle system, acoustic emission, vibration

and fusion model. For feature extraction, many techniques have been applied state from time series, frequency component such as the FFT, wavelet, those currently combined with artificial intelligence system such as neural network and/or fuzzy logic. Overall, it seems to be a possibility that the next generation of monitoring tools can be developed to engage into the control strategies implemented in the advanced machine tools design. The research in this topic is continuing to provide more reliable, robust and responsive tool condition monitoring systems which are needed in recent manufacturing systems. They still needed for more development if really automated machining process is to develop further.

Chapter 5 A Review of the Implementation of Tool Condition Monitoring in Milling Processes

5.1 Introduction

Reliable techniques for on-line tool condition monitoring (TCM) are required for automated manufacturing; therefore TCM systems in machining process have become the topic of investigation over the past decades. This chapter reviews the condition monitoring application presented in industry and academic research. It also covers the implication and the concern with implementing such condition monitoring systems. The techniques used for signal processing and classification of the pattern recognition for the data have been displayed in the context of this chapter. The investigation focuses on four challenging issues including fixturing system, tool wear and breakage in milling, surface roughness and condition monitoring systems. Finally, this chapter summarises the knowledge gaps which this literature survey reveals, and which are addressed in this thesis.

5.2 Tool Wear and Monitoring System

The current demand for higher manufacturing efficiency has led to an increased need for research aimed at machine tool condition monitoring. This is to prevent downtime due to tool failure, and is also a very important economical consideration. The cost of a tool failure can be significant compared to the price of the cutting tool.

5.2.1 Tool Wear

In general, from reference [104], it can be observed that the development of the tool wear is relatively rapid in milling, and it is sometime un-useful for up machining. It is common that the pattern that explains the wear progress within the cutting time can be divided into three different regions as illustrated in Figure 5.1. In the first region, the wear develops rapidly in the form of an exponential curve and then gradually decreases to a constant rate. While, the steady state of the wear presented in the second region of the wear curve can be viewed as linear to the cutting time. The third region simulated the failure region but it can be observed that different

wear curves depend on the different combination of tool-workpiece materials. It can be established that third period is very short and could be detected (tool breakage) in the early stages of the cutting especially when the machining conditions are not selected according to instruction of the tool manufacturer.

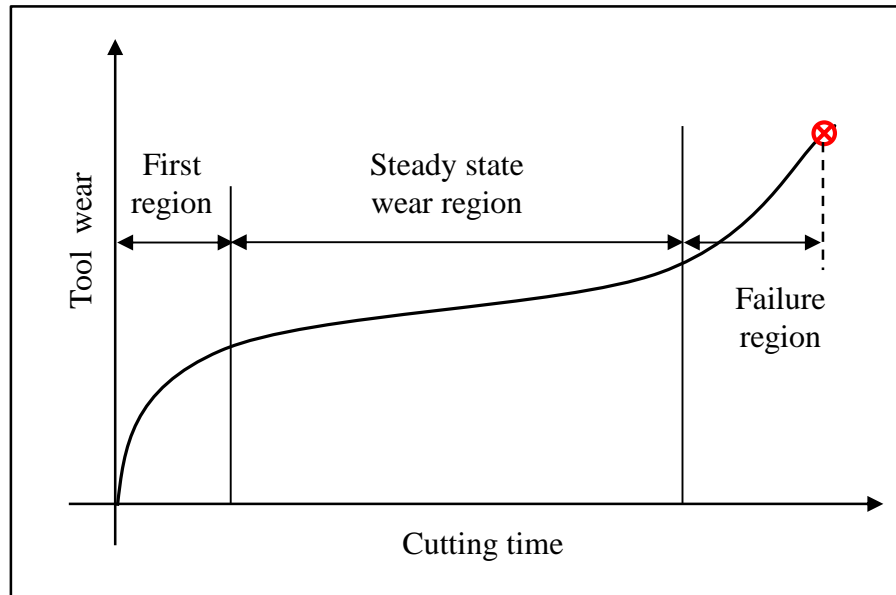


Figure 5.1: Typical curve of tool wear using cutting time.

Reference [105] demonstrated that tool faults contribute to downtime of machining centres with average of 7%, also this estimation could be increased to 20% as reported by [106]. Furthermore, unexpected breakages may happen at any time, catastrophic failure affecting other constituents in the system. However, by designing an effective tool wear monitoring system such failures can be avoided, and obtain a maximum utility from the cutting tools [107].

5.2.2 Online Tool Condition Monitoring

It is therefore, the main objective of automated condition monitoring systems is to improve the quality of manufactured products by employing a detection system for faults within the process and machine. Various signals are emitted from the machine tool throughout the machining process. However, these signals could provide a valuable input to the monitoring systems, in spite of the considerable amount of noise generated. Therefore, the signals would require processing for monitoring purposes. This leads the researchers to search for an effective method to extract

useful information from the data of sensory signals. This process normally requires several stages of signal processing and data analysis to extract abnormal patterns. Generally, the performance of the condition monitoring system is significantly depends on the number and type of sensors and the associated algorithm methods employed to extract useful information from signals. These factors are based to design of an effective, automated fusion model and reduction in cost of monitoring systems [105]. Hence, it could possibly be hypothesised that the setup of a monitoring system in the milling process needs to consider all the above aspects.

5.3 Tool Condition Monitoring Methods

The development of reliable condition monitoring techniques is based on a considerable amount of research which was carried out earlier in the research program in order to construct the fundamentals of a detection system [108]. These techniques can be categorised into two main groups:

5.3.1 Direct Methods

Direct methods involve direct measurements from the tool. The tool condition (i.e. wear) is directly captured by assessing the changes of actual geometrics arising from worn area on the tool cutting. Direct measurement of tool wear requires that either the tool be removed from the machine after a certain period of time or a measuring device be installed on the machine. However, both of these alternatives are not reasonable in automated machining processes increasing machine downtime and affect productivity. Furthermore, direct measurements are difficult to implement because of the continuous contact between the tool and the workpiece, practically in the presence of coolant fluids. Therefore, although the direct methods are probably more accurate than the indirect methods, the indirect methods have been preferred over the direct methods and most of the research in this field is concentrated on them. Most of these are applied as off-line methods where the process is interrupted to carry out the control. The most common direct sensing techniques are described into the next sections.

5.3.1.1 Optical Direct Method

The application of this method depends on a measurable parameter that can be included with the visual inspection on the used component. For example, to measure

the wear, an inspection of tool thickness will be performed before and after the machining [109]. In general, these sensors depend on the higher reflective properties of the wear area, compared to the unworn surface, to derive various morphological parameters that characterise tool wear. The majority of the research work has tracked the measurement of flank wear whereas few researchers have attempted to measure both flank and crater wear. Flank wear regions can be imaged with a CCD camera; however, in order to derive valuable information from within the crater, the projection of a structured light pattern onto the tool is required. The CCD camera is coupled to an expert system to assess tool life in flexible manufacturing cells [110]. One problem with this method is that due to the hostility of the machining environment (lubricant, built-up edge or metal deposits on the cutting tool), vision sensors are restricted to user use between cutting cycles when the tool is removed from the workpiece (i.e. off line process) [111]. The new trend is to use the digital camera wired or wireless transmission (Wi-Fi) in monitoring system.

5.3.1.2 Laser Vibrometry Method

Laser Vibrometry is one of the non-contact and remote measurement methods normally adopted for milling tool vibration measurements during the manufacturing process. It is employed for precisely measuring velocity and displacement of vibrating surface without any physical contact. The vibrometer automatically collects vibration data from a user defined surface and presents it for visualisation and analysis [112]. Laser Doppler Vibrometry (LDV) presents an attractive solution for radial vibration measurement which is taken directly from a rotor surface. Reference [113] combined an experimental study of the cross-sensitivity encountered in LDV measurements of rotor radial vibration with a quantitative evaluation of measurement errors, including sensitivities to other motions. The evaluation of the effects of misalignments and other motions, for both rough and polished-circular rotors, is made possible by a recently developed structure for a comprehensive mathematical prediction of measured velocity. The simplicity in modelling enhances further importance to the finding that this modelling framework can be applied universally for laser vibrometry applications.

5.3.1.3 Radioactivity Method

In machining processes, most of the wear particles of cutting tools are carried away following to the chip. Therefore, a suitable way for measuring wear could be to track these lost particles. Radioactive sensors have been employed to measure the volumetric overall loss of the tool material. In most cases, the tools are made radioactive by irradiation in atomic reactors. The idea of this method is used a small amount of radioactive material is fixed on the face of the tool, throughout of cutting process; the worn tool material will transfer to the chips. By using radioactive sensors monitoring, the amount of radioactive material deposited on the chips can be evaluated and the tool wear assessed [114]. However, the limitations of this method are related to the total amount of the wear which is too small percentage compared to the chips which have to be collected and measured for their radioactivity. Therefore, it is difficult to utilise radioactive methods as an on-line wear monitoring system. Also, some concerns over the environmental and health limit use this technique for workshop.

5.3.1.4 Proximity Method

Proximity sensors (i.e. inductive, capacitive and infrared) estimate tool wear by measuring the change in the distance between the tool's edge and the workpiece. All these sensors depend on the idea of generating an output related to the distance between the sensor and the target. This distance can be measured by electric micrometres and pneumatic touch probes [115] or can detect the light reflected by the target using Proximity type photoelectric sensors [116]. However, this method suffers from a serious drawback. The measurement is affected by the thermal expansion of the tool, deflection or vibration of the workpiece and the deflection of the cutting tool due to the cutting force. Also, for monitoring the cutting tool, particularly the accessible detecting only from one direction.

5.3.1.5 Wireless Temperature Method

The determination of temperature at the cutting tool, workpiece or chip could significantly be used to assume the process temperature. Reference [117] contributed a design of sensor which combines the implanted wireless thermocouple, in conjunction with the transmission of wireless signals. The tool is surrounded by a

thermocouple sensor relays a signal to a thermocouple module allowing for cold junction referencing, amplification and filtering of the analogue voltage signal. The signal is then transferred to a transmission (ADC) module which converts the analogue signal to a digital pulse code modulator representative signal. The success of this method mostly depends on the environment of the process which effects on the temperature of the machining process.

5.3.1.6 Resistance Method

It is noticed that electrical resistance increases between the interfaces of the tool and workpiece. Gradually, increasing the tool wear leading to an increased contact area. Therefore, resistance measurement employed in detecting the tool wear in machining process, but it is considered an ineffective method because of the resistance change due to the variation in temperature and cutting forces throughout the machining process.

This effect may be limited in the micro-machining operation, therefore, reference [118] suggested a new transition resistance sensor for monitoring of micro machining processes with a high number of revolutions up to 160.000rpm. Since, the micro-machining operations are not sufficiently provided with suitable setting equipment and the process is not perfectly controlled as the process parameters cannot be detected due to the extremely limited working zone and the high spindle speed. Various applications such as in process detection of tool wear are introduced. This method needs further improvements to be used in the automatic control of the micro-cutting processes.

5.3.2 Indirect Methods

The indirect methods often use cutting parameters such as cutting force, vibration, acoustic emission, temperature and power measured during the cutting process. Besides the indirect method used, the selection of parameter is also very important to design an effective condition monitoring system. However, the parameter that is useful for one method could be inappropriate choice for the other. Furthermore, detecting mechanisms including a single sensor could be infrequently making reliable results for the tool condition. Therefore, it is better to employ multiple

sensors to observe the same process in order to detect the tool wear status with high accuracy rates using a sensor fusion model [108].

Indirect methods, which are concerned in this thesis, are usually indirect on-line methods.

The main indirect methods are:

5.3.2.1 Force Sensor

Among the indirect on-line tool wear monitoring methods, cutting force, an indicator of tool condition, is one of the most widely used variables. Indeed, it is noticed that cutting forces increase gradually with tool wear. Exploring the relationship between tool wear propagation and cutting force variation is of great importance to the development of an effective tool condition monitoring strategy. Reference [107] presented an experimental study of variations in the tool wear propagation and cutting force in the end milling process. The experimental results showed that significant wear is the major failure mode affecting the tool life.

The cutting forces have a direct influence on heat generation, tool wear or failure, quality of machined surface and accuracy of the operating parts. Therefore, reference [119] provided in-depth analysis of the work showing that milling dynamometer can measure quasi-static and dynamic cutting forces, and torque by using strain gauge and piezo-electric accelerometer has been designed and constructed.

An online monitoring of the cutting tool wear level is very necessary to prevent any deterioration. However, there is no direct manner to measure the cutting tool wear online. Therefore, reference [120] adopted an indirect method to estimate the wear measurement of one or more physical parameters appearing during the machining process such as the cutting force. The cutting forces are measured by means of a force dynamometer, while the tool wear is measured in an off-line manner using a binocular microscope. In some cases Renishaw contact sensor can be used to measure tool wear.

Despite the importance of micromachining operations in industry and the extensive research conducted in the past, there are few dynamometers capable of measuring the lowest frequencies that exceed the excitation frequency enabling the process

force measurement of micromachining operations. Hence, applications with high spindle speeds require a dynamometer whose lowest frequency value is maximised. Reference [121] contributed an innovative piezoelectric dynamometer (MicroDyn) providing the base for measuring high frequency signals in micro machining processes with rotational speeds of more than 100,000 rpm, resulting in a high excitation frequency. Consequently, the interference of the excitation frequency of those processes with the natural frequency of designed dynamometer makes it impossible to measure machining forces within a wide frequency range.

For development with the on-line monitoring equipment (hardware) and real-time data analysis and optimisation software, reference [122] has presented an intelligent system that commenced with experiments using a force dynamometer. The monitoring system is connected with the PC which including data processing, analysis and optimization.

5.3.2.2 Vibration Sensor

In the condition monitoring of rotating machine, vibration sensors are the most used type of signal, but they do not achieve agreement in the area of the monitoring of cutting tool wear. This is mainly due to the other surrounding sources of vibration. Though, it is clear that cutting with a worn tool leads to higher variations of the effect on the tool; this obviously stimulates the tool to vibrate. The advantages of vibration measurement include ease of implementation and the fact that no modifications to the machine tool or the work piece fixtures are required. Vibration monitoring is mainly used to detect tool condition, surface quality, and dimensional deviations in machining applications. Generally, the vibration amplitude caused by interaction of a new tool and work piece is small compared to worn tool.

Reference [123] developed a reliable monitoring system for industrial application based on the analysis of the structure of the tool vibration signals using singular spectrum analysis (SSA) and cluster analysis. This technique of time series analysis decomposes the acquired tool vibration signals into an additive set of time series.

Following this, reference [124] explored the use of data mining techniques for tool condition monitoring in metal cutting using SSA which is performed on vibration signals measured on the tool holder. The main aim is to avoid the lack of large training data set was compensated by application of cross validation. This highlights two important aspects: strong significance of information in high frequency

vibration components, and benefits of the combining SSA and band-pass filtering to remove undesirable components (noise).

5.3.2.3 Acoustic Emission Sensors

During the cutting process, the workpiece is machined by removing unwanted material (chip) via plastic deformation. The acoustic emission is defined as transient elastic energy released in the deformation, phase transformations and the cracking mechanisms. In rotating machine with very small tool diameters, where the monitoring by cutting forces and motor current is not applicable because of their very low levels, the alternative sensor is of acoustic emissions.

Recently, AE sensors designed for detecting tool breakage have been successful. This result may be explained by the fact that the frequency range of the AE signal is much higher than machine vibrations and environmental noises [125].

It is a simple process to mount the AE sensor on the workpiece side for monitoring the milling and drilling processes which use multipoint rotating cutting tools. However, the difficulty occurs in transmitting the detected signal from the rotating part. Although transmission may be made by radio signal, there are few workable methods that have been developed to transmit the sensor signal from the rotating spindle to the fixed part using optical methods [16]. However, such techniques are still not economically usable due to either the reliability of the system, or the basic cost of the devices and the change in the construction of machine head.

As one of the practical solutions to meet the requirement in terms of the signal transmission, reference [17] has developed the application of the acoustic emission (AE) sensor for monitoring the cutting process. The coolant stream is successfully used as a medium for transmitting the AE wave in the milling process monitoring. This sensor is mounted in the special holder with other necessary devices. Figure 5.2 illustrated the proposal to effectively utilise the cutting fluids as the medium for transmitting the AE signal. The AE sensor is attached to the cutting fluids supply nozzle so that the AE signal generated at the cutting point can be transmitted through the fluids and consequently detected by the sensor. By applying this method, it has become possible to take the AE signal from the rotating tools. But, the concern on this method is the effect of the noise of the fluid flow and machine bearing.

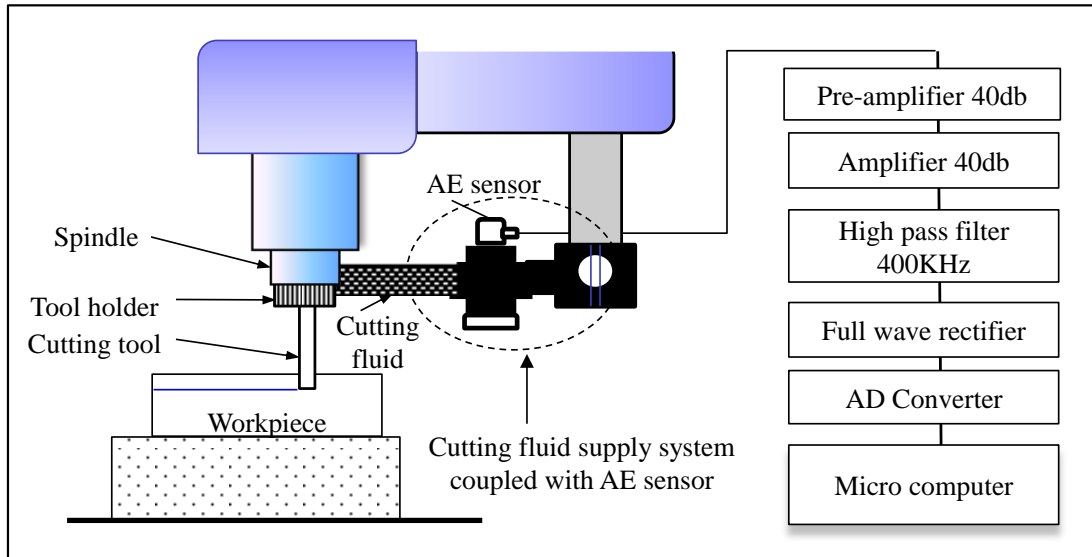


Figure 5.2: Monitoring system for the milling process (reproduced from [17]).

Micromilling processes can make miniaturised products with high relative accuracy. While micromachining operations are different than conventional macromachining processes, it is important that the modelling of micro end milling forces incorporates the dynamics of the tool, ploughing and elastic recovery. Reference [126] examined the mechanistic modelling of shearing and ploughing domain cutting regimes to accurately predict micro-cutting forces for micromilling with spindle speeds up to 160,000 rev/min with a cooling system that steadies the temperature at high rotations. The tool dynamics are indirectly identified by performing dynamometer and AE coupling analysis.

5.3.2.4 Power Sensor

Apart from these main types of signal used for indirect monitoring, the electric power consumption is often a properly accurate measure of the deterioration of tool condition. It reflects a situation of tool condition change throughout the machining process. The spindle motor power monitoring system is considered one of the most applicable systems for plant floor applications because it is relatively simple and its mounting hardly affects the machining operation. In the last three decades, researchers have utilised many machining variables such as spindle motor power (current) [127-129].

Power sensors are often used in combination with other sensors. For example, if the change in the consumed current would not be sufficient to be detected. Therefore,

modifying a blind sources separation technique has contributed to separating those source signals obtained by milling operations. This method based on wavelet transform and independent component analysis has been developed by [130]. The source signals related to a milling cutter and spindle are separated from a signal of single channel power. The experiments with different tool conditions illustrated that the separation strategy is reliable and encouraging for machining process monitoring.

5.3.2.5 Sound Sensor

When the milling process is stable, the system is controlled by forced vibrations produced by periodic forces which will increase as a result of the interaction between the cutting tool and the workpiece during the machining process [131]. Correspondingly, vibrations arise from this interaction will generate a sound. This sound is a transmission of mechanical energy contains information about the process. Experienced operators can have ability to extract information from it and correct or modify the cutting parameters. Reference [132] developed an approach to collect the milling process sound through a sound sensor (microphone) placed inside the machine-tool enclosure. Frequency range is normally related to the sound range 20 Hz - 20 kHz, but some research has analysed wider ranges 0.5 Hz - 40 kHz. Generally, the sound sensor reflects similar behaviour as a accelerometer sensor as both depend on the vibration of the machining process.

5.4 Signal processing methods

5.4.1 Fast Fourier Transform (FFT)

The most common approaches regarding indirect methods of cutter tool monitoring are analysis of accelerations signal, dynamic forces and acoustic emissions. Fast Fourier Transformation (FFT) is widely used in order to present cutter tool wear or tool fault in the frequency domain.

If the FFT is taken into account, the second harmonic is an indicator of tool wear estimation. Another approach uses the increase of energy in the frequency domain as an indicator of cutter tool conditions. However, a question arises as to whether a

change of cutter tool geometry is as a result of wear or as a tool fault that can be observed in the frequency domain.

The limitation of FFT consists in the impossibility of processing non-linear and non-stationary data [101]. Since the Fourier transform approach has certain serious theoretical drawbacks in processing machining signals. It is the integration for all times. This fact makes it difficult to analyse any local property of the signal. Another shortcoming of the FFT is presentation of results only in frequency domain. However, the manufacturing process is described as a non-linear and non-stationary process. The signal processing methods used to analyse non-stationary signals are appropriate for cutting process monitoring. Therefore, reference [133] studied the relation between cutter tool wear and acceleration signal in frequency and time-frequency domain using a new method, Hilbert–Huang Transform (HHT) which presented data locally without harmonics. The idea is processed the data by short-time Fourier transform the cutter tool wear or tool fault is detected by increasing the power in the power spectral density. While by using HHT, the acceleration signals change the frequency in the marginal spectra as a result of geometric change of the cutter tool. Also, it is applied to the cutter tool wear and tool fault monitoring and compared to the FFT.

5.4.2 Wavelets Transformation (WT)

The reliability and applicability of tool breakage detection to assist in advancing high availability levels of sophisticated manufacturing systems, in conjunction with high quality levels of manufactured components, are considered in the resent research. In order to improve robustness of the tool from wear and breakage, the signal processing method of spectral analysis is the most commonly used technique in tool breakage detection. Yet, although it is resolution is good in the frequency domain, it has an inadequate time domain resolution. Also some signal information in time domain is lost in the spectral analysis process. The wavelet transforms (WT) which is localized in both time and frequency to detect a small change in the input signals. In addition, it requires less computation than FFT.

Continuous wavelet transformer is recognised as effective tools for both stationary and non-stationary signals. However, much of the information is superfluous and computationally very slow [134]. Discrete wavelet transform (DWT) uses an analysing wavelet function. DWT is able to simultaneously sample in both

frequency and time domains so that it can extract more information, which can be used to analyse tool breakage monitoring signals [135]. Reference [136] presented an effective algorithm for tool breakage monitoring system based on DWT of an acoustic emission (AE) and an electric feed current signal. The experiment results show overall 98.5% reliability and the good capability of real-time monitoring of the proposed for detecting tool breakage during machining process.

Among many machining condition monitoring systems, a spindle motor power monitoring system is considered as one of the most popular systems for plant floor applications. However, in practice, power signals are mixed with many signal sources relevant to cutting tool, which contaminate with each other in feature extraction processes and decrease the monitoring reliability. Reference [137] presented a new method based on the wavelet transform for the detection of tool damage. It is assumed that the vibration signal of the original structure of tool without any defect is already known. When the defects are presented, the vibration signals of the defected tool are then recorded. After comparing the DWTs of these two sets of vibration signals in the space domain, it could be used to detect the presence of defects; their number and location.

5.4.3 Principal Component Analysis (PCA)

Principal Component Analysis (PCA) is technique of identifying patterns in the correlated data, and expressing the data to highlight their similarities and differences. The main advantage of PCA is that once the patterns in data have been identified, the data can be compressed, i.e. by reducing the number of dimensions, without much loss of information. The methods involved in PCA are discussed below [138]:

1. Getting some data
2. Normalization of data
3. Calculation of covariance matrix.
4. Interpretation of covariance matrix.

Reference [139] proposed a signal processing method used on PCA and wavelet analysis, aiming to reduce the dimension of the data and obtain both frequency and time localisation information which could help to find abnormal phenomenon quickly and orient the position and the time of faults exactly in the complex textile

machinery systems. At first, the original signals are simplified by principal component transform, which was conducted by calculating the eigenvalue and eigenvector of correlation coefficient matrix, and by defining the first few Principal Components (PCs) containing most of the variables according to the contribution and cumulative contribution rates. Secondly, the restructured signals are decomposed into approximate and detailed ones for obtaining meaningful captures of instantaneous frequency by wavelet analysis. From practical application, this signal processing method was validated.

In addition, PCA is used for fault diagnosis based on different sensors. For example, the basic theory of principal component analysis and its basic procedures for fault detection are introduced the sound signal pre-processing is depicted, multi-domain feature vector is extracted from time, time-frequency and frequency domain, faults are diagnosed with principal component analysis method [140].

In the current research, the PCA is used to design an effective fusion model to detect the faults of tool and fixturing system.

5.5 Tool Condition Classification

5.5.1 Classification using Neural Network (NN)

An Artificial Neural Network (ANN) is a mathematical or computational model based on biological neural networks. It consists of an interconnected group of artificial neurons and processes information using a connectionist approach to computation. In most cases an ANN is an adaptive system that changes its structure based on external or internal information that flows through the network during the learning phase. An ANN usually organises its units into several layers. The first layer or input layer, the intermediate layers or hidden layers, which are not always present because they are sometimes not needed, and the last or output layer. The information to be analysed is presented (or fed) to the neurons of the first layer and then propagated to the neurons of the second layer for further processing.

These results are propagated through each layer, converting the information into the network output in the final layer. The goal of an ANN is to discover some association between input and output patterns. Many different neural network structures have been developed to achieve different learning and processing speed

capabilities. Neural networks are classified as supervised and unsupervised according to their learning characteristics. The decision is greatly dependent on the data obtainable for training the networks. If there is a target class or output for each pattern, then a supervised neural network can be used such as Back Propagation Neural Network (BPNN). However, when the input data do not have target output specified previously, then “unsupervised” neural networks have to be implemented. Unsupervised neural networks, such as Learning Vector Quantisation (LVQ) use a special algorithm to group similar patterns in the input data space into similar output classes [141].

Tool condition monitoring is necessary to obtain good quality product. The relationship between sensor and tool wear is investigated during end milling. For this purpose, reference [142] conducted an experiment using an acceleration sensor assembled on a machinery analyser. Tool wear was measured by a toolmaker's microscope where it was observed that there was an increase in vibration amplitude with increasing tool wears. However, the problem of associating such an approach with the milling process makes it very difficult to detect the levels of tool wear especially when considering the use of intelligent sensor based monitoring systems within an automated machining environment. Therefore, another approach is needed for the decision making process in order to support tool condition monitoring is the application of neural networks. Reference [143] presented a review of the application of neural networks as outlined in Figure 5.3. Where the sequence of the monitoring process start from the transfer the data from the machining process through the sensors to the computer system. The feature extraction technique will obtain the useful information, and then the data will be trained and tested using neural network to determine the tool stats. It is identified that the development of accurately on-line monitoring system capable of operating within the milling environment is needed further investigations.

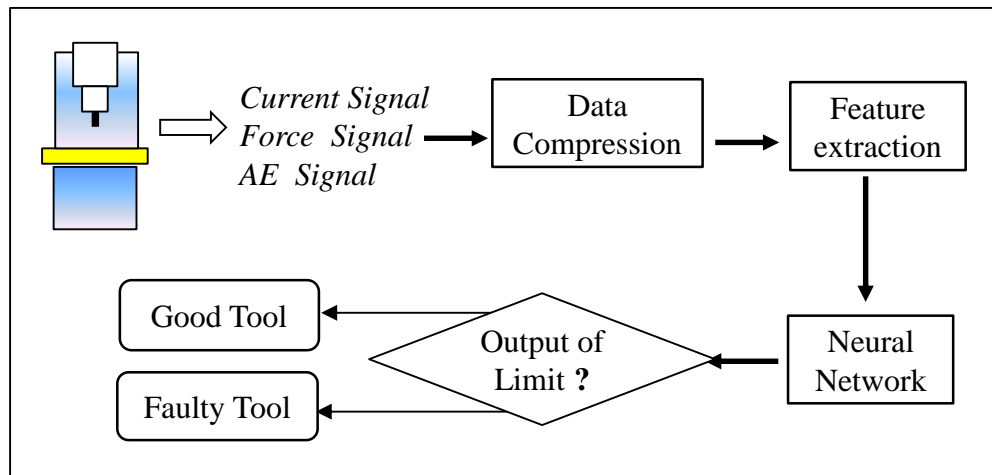


Figure 5.3: Representation of neural network based cutting process monitoring.

5.5.2 Classification using Fuzzy Logic (FL)

A fuzzy logic is an artificial-intelligence-based method has also proved a useful classification technique to tool wear monitoring strategies when combined with multiple sensor inputs. A fuzzy clustering algorithm is used for online tool wear classification. This approach develops the online capabilities of the system which have yet to be established as all analysis is carried out off-line. The application of fuzzy pattern recognition techniques is described to identify and classify tool wear as part of an on-going research activity. Reference [144] presented a method for tool wear monitoring based on fuzzy logic handling multi-sensor inputs, and monitoring the spindle motor power and the cutting forces. During a classification stage, cutting experiments are carried out utilising various tools with known wear.

Skilled human operators are shown to be better than model-based controllers in machining control, therefore fuzzy logic control, is a practical alternative to model based control schemes. Reference [145] employed this fact and proposed a fuzzy-logic control of cutting forces in CNC milling processes using motor currents as indirect force sensors.

Reference [146] performed a comparison between experimental results and consistent fuzzy rule-based model for estimating the cutting forces. For experimental work, a dynamometer and strain gauge are used to measure static and dynamic cutting forces. Experimental results are compared with the predicted fuzzy model; the difference between experimental and predicted results is around 99.6% due to possibly the inaccurate editing for the role of the fuzzy logic. The developments are

continuous to achieve good results with this approach. Therefore, reference [147] conducted with the advance of a tool wear condition-monitoring technique based on a two stage fuzzy logic scheme. For this, signals acquired from various sensors are processed to make a decision about the status of the tool. In the first stage of the proposed scheme, statistical parameters derived from thrust force, machine sound and vibration signals are used as inputs to the fuzzy process. The fuzzy output values of this stage are then taken as the input parameters of the second stage. Finally, outputs of this stage are taken into a threshold function, the output of which is used to assess the condition of the tool.

Fuzzy logic approaches are applied for the micromilling processes, as extreme forces and vibrations significantly affect the overall quality of the part. In order to improve the part quality and longevity of tools, so reference [148] examined the factors affecting tool wear using various sensors including accelerometers, force and acoustic emission sensors combined with an optical microscope to measure the real tool condition in micro-milling. The signals are fused through the neuro-fuzzy method to determine whether the tool is in good shape or is worn.

Overall, the applicability of fuzzy logic analysis to monitor tool wear has yet to be established within an industrial context. Correspondingly, the application of the approach as a means of decision making within a tool breakage monitoring system also requires further investigation.

5.6 Single and Sensor Fusion

Generally, the use of a single sensor signal in the development of a tool condition monitoring system is still insufficient in recognising the complex and diverse nature of the cutting process. Such models are frequently less robust, less reliable and often not capable of whole tool condition monitoring due in part to the lack of information to make a reliable decision on tool condition monitoring from a one sensor alone [149]. However, the utilisation of multisensory systems for TCM is proposed to fuse the informational power of each unique sensor to provide complementary and redundant information about conditional changes in cutting tools, which is referred to as sensor fusion. In these multisensory systems, signal processing techniques extract sets of features that are sensitive to the tool condition

as explained by references [150,151]. Reference [152] also has interferenced with the concern of a single sensor and proposed many investigations to overcome the limitations of sensor methods, by using multisensory (sensor fusion) to create a stronger correlation between indirect signals and actual tool condition. These investigations show that multisensory systems could provide additional signals for better predictive findings.

In the last decades, various pattern classification methods have been applied in the application of multisensory TCM to ensure high level of accuracy in prediction or classification results. Some research has emphasised pattern recognitions that can be an effective sensor fusion strategy in TCM. However, the level of complexity and robustness of the TCM model has been rarely part of the design objectives as presented by references [153].

An important point of consideration is that under different cutting conditions, a time series of signal from a single sensor may not be able to provide sufficient information to create reliable decisions with high degree of certainty on the state of manufacturing processes. Consequently, reference [154] developed a multisensory system by combining the capability of AE methodology, and force and torque methodology for the monitoring of end milling operations. Multi-sensor systems remove the above drawback since loss of sensitivity in one sensor domain can be offset by information from other sensors within the system, thus allowing high decision making capability over a wide range of process conditions to be possible.

Recently, the advances in process monitoring and signal processing have encouraged the effectiveness of sensor systems closer to industrial implementation. Particularly, a wide range of sensors that can recover information about the machining process such as tool condition and surface roughness has been implemented. Reference [155] supported this idea and reported that significant reduction in cutting errors can be achieved by the utilisation of sensor systems for the monitoring of machine manufacturing processes. As new effort to use a fusion sensors, reference [156] studied the application of the multisensory (i.e. force sensors and accelerometers) for monitoring the machined roughness at varying cutting parameters. Taken together, a Laser Doppler Vibrometry (LDV) is used to correlate signal values with surface roughness values. With these advances in process technology and monitoring, an intelligent tool condition monitoring (TCM) method using

multisensory systems has attracted closer attention from academic and industrial research because successful application of TCM during machining can improve the probability of producing high quality parts and protects the manufacturing systems.

5.7 Condition Monitoring System and Fixtures

An analysis enables the deformation of the joint to be predicted together with distributions of stress and strain in the contact layer at joint interface. The influence of geometrical features, defined by the shape and the dimension of contact area (joint) on stress and strain levels is considered as a critical issue in the fixturing system. This is because the concentrations of stress and strain can be reduced leading to optimisation of the performance and reliability of the clamping process.

The author [157] worked in the area of fixturing design (collet) and stated that initially the nature of contact between mating surfaces were identified to be full, partial and pointed contact as shown in Figure 5.4. The real target is to reach to the full contact case by increasing the applied load, but less maintaining a load than the yield stress for the work piece or tool to avoid the plastic deformation.

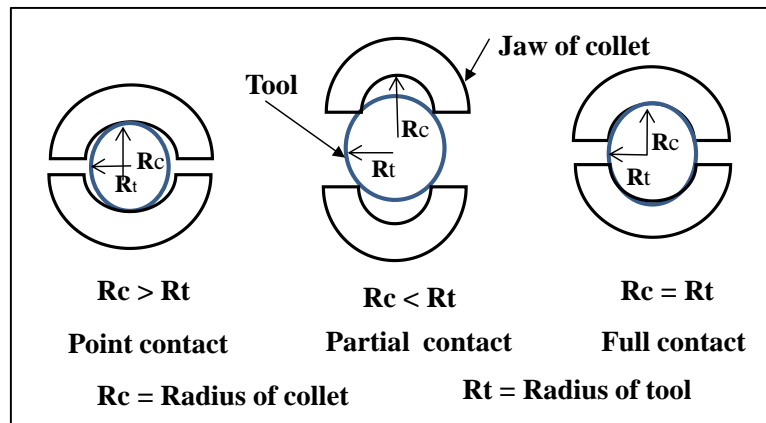


Figure 5.4: Types of contact between the collet and tool surfaces.

When a workpiece is clamped in a fixture and the contact between the workpiece and the fixture elements changes, its frequency response will also change. Reference [158] investigates the signal variations between normal and abnormal clamping conditions of the fixture on the workpiece using an expanding sleeve between the machine tool spindle and the tool holder, the uniform contact or the triple-contact will be achieved. This added stability considerably increases cutter life, while

allowing cutting tools to operate effectively at much heavier feed rates. However, to realise this advantage, contact tooling must be used with fully automated machine and monitoring systems.

Currently, continuous attempts are being made to develop the models and use the rubber (as elastic material or composite with ductile materials) that exhibit extensive non-linear deformation before failure [159]. In the industrial, some of the company [160] used this advantage of the rubber and used it as a collet to hold the cutting tool in the process. Conventional split-steel collets provide maximum gripping efficiency only at actual bored or nominal capacity. They lose parallelism when chucking bars due to the size over or under this capacity. This significantly reduces gripping strength and accuracy. Rubber collets are used in some machining operations (e.g. tapping) to avoid the problem of contact and the flexibility of rubber can provide the freedom of the steel slot to create full contact with shaft or tool as shown in Figure 5.5.

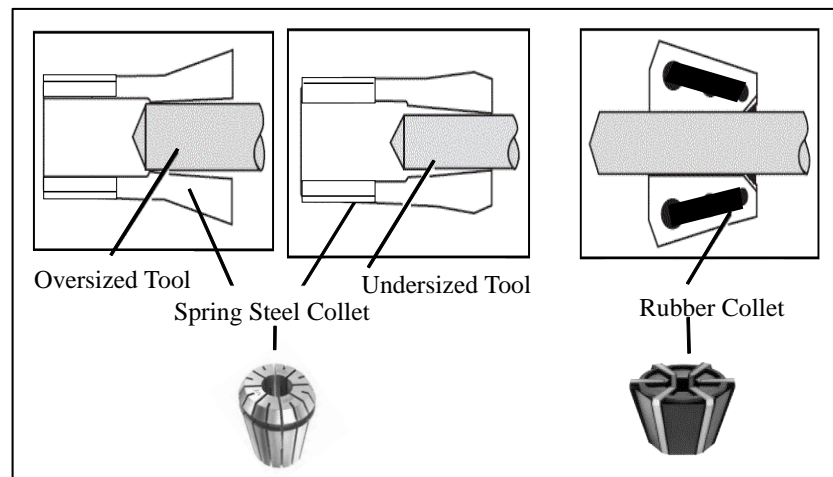


Figure 5.5: The difference between rubber collet with other types in gripping parts.

In applying the monitoring system to the machining process including fixturing system, reference [1] presented an experimental design and evaluation of a pin-type universal fixturing system. The fixturing system is designed for holding complex shaped aerospace components during machining processes. The experimental investigation is performed by comparing the pin-type clamping system with a dedicated clamping system during the machining of aluminium and steel parts. Force signals are monitored during machining. According to the evaluation of the force signals, the results prove that the pin-type clamping system can be recognised

for machining different complex shaped components with performance comparable with a dedicated clamping system. In order to obtain enough sensing data, special attention should be paid to the sensor allocation optimisation within the rigid fixturing system to ensure and improve diagnosis, lowering sensing cost and reduce down-time. Reference [161] investigates both theoretically and experimentally the effect of sensor allocation optimisation on the diagnosis ability of a multi-station manufacturing system. The effective diagnostic ability depends on three parameters, namely detection, location, and insulation.

Various developments in production technology lead to increasing automation, flexibility and productivity. As a first component, generated a sensory fixture system has been developed, which includes different sensors and allows multi-sensors fusion. The integrated sensors can likewise be utilised for monitoring. Using these two components in one set-up, a milling machine provides sensory capability at both sides of the process. This translates to a first step towards sensory machine tools and comprehensive process control comparable with manual processing in which the tool and workpiece are hand guided. Reference [162] described the combined application of the sensory fixture and the spindle for process monitoring. Since three piezo-actuators have been arranged around a conventional spindle in a parallel kinematics configuration. This allows the movement of the spindle in three degrees of freedom in a range of $\pm 100 \mu\text{m}$. The structure permits only displacements in z -direction and rotations about the x - and y -axis. Thus, the tool tip can be moved inside a prismatic space as shown in Figure 5.6. However, the research of the fixturing controlling by condition monitoring system still needs for future development.

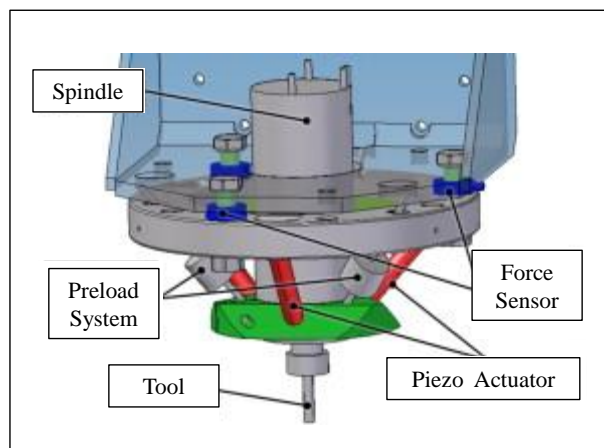


Figure 5.6: Adaptive spindle system (AdSpin) [162].

5.8 Surface Roughness and TCM

One of the most significant aspects of cutting processes is surface quality of the produced workpiece, since it is mostly considered as a final stage in the production cycle for improving the surface finish and dimensional and geometrical properties of the workpiece. Therefore, to provide the desired surface quality, it is important to determine the influencing factors which include workpiece material and cutting tool, the cutting conditions and process phenomena [163, 164].

In end milling operations, theoretical surface roughness is generally dependent on cutting conditions, workpiece materials and cutting tools [165]. However, the following equation is used to calculate the theoretical roughness [166]:

$$Ra = \frac{f_z^2}{32(R \pm \frac{f_z \times z}{\pi})} \quad (5.1)$$

Where Ra is the surface roughness (μm), f_z is feed per tooth (mm/tooth), z is number of teeth in the cutter, R-radius of the cutter, \pm ve sign to up and down milling respectively.

The actual surface roughness is usually larger than the theoretical surface roughness values obtained by these formulae, because, it does not take into account built up edge formation, deflection and vibration which are usually a function of cutting conditions like speed and axial depth of cut. This limitation refers to the real need to find an approach to measure the surface roughness.

In the past, researchers have created many attempts to improve the conditions of milling and the surface roughness quality in CNC machines by mathematical studies. On the other hand, an estimation of the surface roughness has been proposed considering the significance of runout tool errors which are a result of imperfect fixturing systems [167]. These runout errors create a forced vibration detected by a dynamometer mounted over the support workpiece surface [168].

The surface roughness of a workpiece is modelled and predicted by using computer vision methods. However, the difficulty occurs in obtaining the actual surface roughness from surface images [169]. To be able to predict the surface roughness of the machined part, it is necessary to develop a model that includes the influence of cutting conditions, tool errors and the properties of the workpiece material and

cutting tool. Reference [170] proposed useful models for determining surface roughness from process parameters such as feed, cutting speed and depth of cut, but neglected to include the effect of tool errors.

References [171, 172] presented models that make it possible to predict surface roughness as a function of tool errors such as radial and axial runouts in milling operations with square insert cutting tools. However, these models did not carry out the statistical analysis of tool errors and therefore did not represent the sensitivity of surface roughness to variations in these errors.

One of the main factors that affect the surface finish of the machined part in milling operations are such as reference [173] investigated the effect of tool errors by studying the defects in the location of the cutting tool teeth. The study found that the main parameters to generate these defects are imprecision in the tolerances of the cutting tool inserts and seats, inaccuracy in the fixturing of the indexable inserts.

Reference [174] presented the application of neural networks algorithm to perform the adaptive surface roughness control in end-milling operations. Moreover, reference [175] created a model dealing with the prediction of the machined surface by assuming that the milled surface has the same profile as the profile of the deflected cutting tool during the milling process. The efforts of roughness prediction are continuous, as reference [176] proposed a method to compare the usefulness of data from CNC machine tools and external sensor data for the indirect evaluation of surface roughness in vertical milling operations. Therefore, it can be observed that the research for surface roughness requires more development.

5.9 Summary of Identification of Knowledge Gaps

The fixturing system (tool holder) is influenced directly by the stability of the tool. Moreover, due to the complex structure of tool wear mechanism, unpredictable breakages may occur at any time which might also lead to catastrophic failure affecting other components in the system. A considerable amount of research has been carried out so far to develop reliable condition-monitoring techniques. These techniques can be categorised into two main groups: direct methods and indirect methods. One of the most effective indirect methods is design sensor fusion models for monitoring tool condition and selection of a suitable sensor to detect the changes in machining processes. However, the studies are still limited with regard to

investigation of the overall effect and monitoring of the fixturing system during the machining process.

From the conducted survey of the literature for the related research in terms of the monitoring system, tool conditions, fixturing system and surface roughness, either in academic or in industrial fields, it can be observed a series of gaps within the knowledge which has been generated from the reviewed work. These can be summarised in the following list:

1. There is limited research focusing on the problems generated by the incorrect use of the fixturing system.
2. There have been many attempts to design a condition monitoring system to detect the tool condition in milling processes. However, there is limited work on including the fixturing system in the element of the automated manufacturing system.
3. The efforts of using a multisensors model require further developments to improve the technique of the sensory system and the feature extraction. The fusion model is rarely used for fixturing system.
4. Most significant current research deal with a new approach by combining the indirect monitoring methods with those direct or real measurements of the cutting process variables. So far, however, there has been little discussion about applying this approach for fixturing system monitoring.
5. Surface roughness as a reflection of the part quality needs to be predicated with a practical approach to avoid the manual measurement.

These concerns need to be investigated within an effective sensor fusion to deal with the aforementioned issues which are taken into serious consideration for the whole trend of the thesis.

Chapter 6 Methodology

6.1 Introduction

This chapter outlines the research methodology. It summarises the drawbacks in research and industry in relation to the design of condition monitoring systems and its relationship to fixturing quality. The condition monitoring system has been used for detecting the milling process faults such as tool wear and tool fixturing. It also presents the research aim, objectives and the implemented condition monitoring methodology. The chapter explains the general stages of the proposed approach. In addition, it presents how the following chapters are structured to assess the planned methodology.

6.2 Problem Definition

From the previous literature review chapters, the knowledge gaps can be summarised as follows:

1. There are many attempts to design a condition monitoring system to detect the tool condition monitoring in milling process. But there is a lack of understanding in the effect of the fixturing system on the condition monitoring systems. Also, there is limited research in studying the relationship between the online condition monitoring system and the fixturing quality (either fixturing type or fixturing material).
2. The efforts of using a sensor fusion model would need further developments, particularly when addressing fixturing systems.
3. Most significant current research deals with a new approach by combining the indirect monitoring methods with those direct or real measurements of the cutting process variables. So far, however, there has been little discussion about applying this approach for fixturing system monitoring.
4. Surface roughness as reflection of the part quality needs to be predicated with practical approach to avoid manual measurement techniques.

Therefore, it can be concluded that a limited research has been done on the effect of fixturing system on the design of condition monitoring system. Therefore, this thesis is targeted towards the investigation of the effect of fixturing system on the condition monitoring system and, if there is any effect, how then the designer can address such effect.

The schematic of the investigated problem is illustrated in Figure 1.3. This research will investigate the difference in the system's behaviour and the changes in the machining characteristics on the design of condition monitoring system.

The key question is does the designer have the ability to adjust the monitoring system in normal case (domain A) and recalibrate it when the change of parameters becomes abnormal (domain B) if influenced by change in machine characteristics?

6.3 Problem Domain and Objectives

The aim of this research is to investigate the effect of fixturing system (collet) on the capability of condition monitoring system using sensor fusion model. Much research has been performed to develop reliable TCM. However, several factors have obstructed advances in the development of TCM including inappropriate choice of sensor signals and their utilisation [18]. The ASPS approach [19] has been presented to select the most sensitive sensors and signal processing techniques for monitoring the tool conditions in milling processes. Despite the ASPS approach can provide a solution for monitoring the fixturing system, there are some limitations in relation to the sensory sensitivity detection methods implemented. Therefore, the domain of this research is in developing and modifies the ASPS approach to address and solve the fixturing problems. The outcome is a novel approach, termed ASPSF (Automated Sensor and Signal Processing Selection for Fixturing) in selecting the sensors and signal processing techniques essential for monitoring the setup and conditions of fixturing system in milling processes to address fixturing quality. Through the ASPSF approach, a wide range of novel signal analysis and simplification techniques are used to confirm and assess the research methodology for selecting sensors and signal processing methods and to detect the relationship between the changes of the process setup and the design of condition monitoring systems.

The overall aim of this thesis is to construct a condition monitoring system for detecting fixturing quality, at reduced cost, using an effective sensor-fusion model

with reduced experimental work. This investigation will address the limitation of literature review for the fixturing system as an important part during the manufacturing process, also to monitor the fitness and the clamping rigidity to reduce the loose of the cutting tool. This investigation, as a result, will address the following issues:

- Address the limitation of literature about the tool holder and then study the effect of the fixturing system (type or material) on the performance of monitoring system.
- Detect any faults or abnormalities may occur during the machining operation using sensor fusion which is designed to monitor the health of the manufacturing process with regard to changing tool conditions.
- Evaluate the stability of the fixturing system and the efficiency of the monitoring system regarding to the surface roughness of the work piece.
- Since the manual measuring method for the surface roughness is time consuming and relatively expensive, part of the proposed monitoring system will employ to predict the roughness of the machined surface using the output of the force sensor.

As milling is a complex process with regard to extracting the information from the used sensors, the ASPSF approach will be used to address the effect of milling machine setup on the design of the condition monitoring system. Fixturing type and material will be taken as a case study to explore the feasibility of the proposed model.

6.4 How the Suggested ASPSF Approach is Conceived

This research builds on the knowledge gaps in the industry and research to design the condition monitoring system. The knowledge gap highlights that there is no unique design of monitoring in relation to detect the faults of the fixturing quality.

Furthermore, the main obstacles facing the designers of monitoring systems are selecting the required number of sensors and effective signal processing method. However, the reference [19] has presented the ASPS approach to select the sensors and signal processing techniques for monitoring the tool conditions in milling processes. Another reference [20] has employed this approach to develop an effective sensor fusion model to measure the sensitivity to tool wear for turning processes. The ASPS approach will be developed and improved to be used in this research as shown

in the Figure 6.1. This section will describe the general stages of the ASPS approach, and the limitations to be addressed in this thesis.

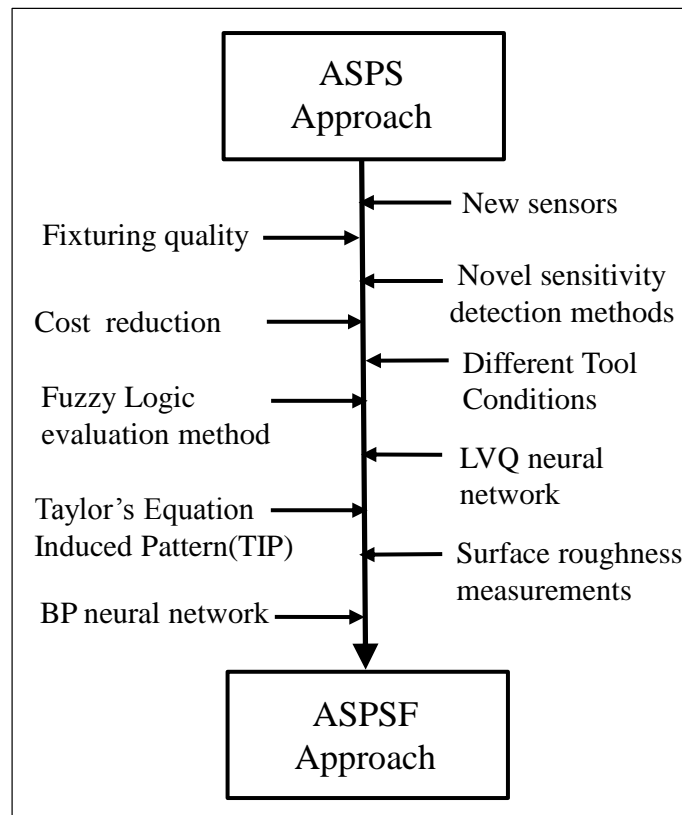


Figure 6.1: The ASPS approach has been modified to produce the ASPSF approach.

6.4.1 General stages of ASPS Approach

The ASPS approach can be implemented using the following stages:

6.4.1.1 Simplification of Complex Signals for Extraction of Features

The raw signals which are collected from complex processes (e.g. milling) need to be processed start by removing the signals from a complex shape into a group of simplified Sensory Characteristic Features (SCFs), see Figure 6.2. SCFs can be obtained from any signal processing technique or a combination of signal processing techniques as long as the output is, or can be presented as, a real number. Several numbers of SCFs can be calculated when taking samples of the complex signals at constant intervals and processes these signals using a broad variety of signal processing methods. During the processing time, these sensory signals can be simplified into a number of SCFs [20]. The SCFs could be a perfect means to explore

the essential information regarding the presented process conditions. Several processing methods can be achieved SCFs since the output is a real number or entered as a real number, see Figure 6.2.

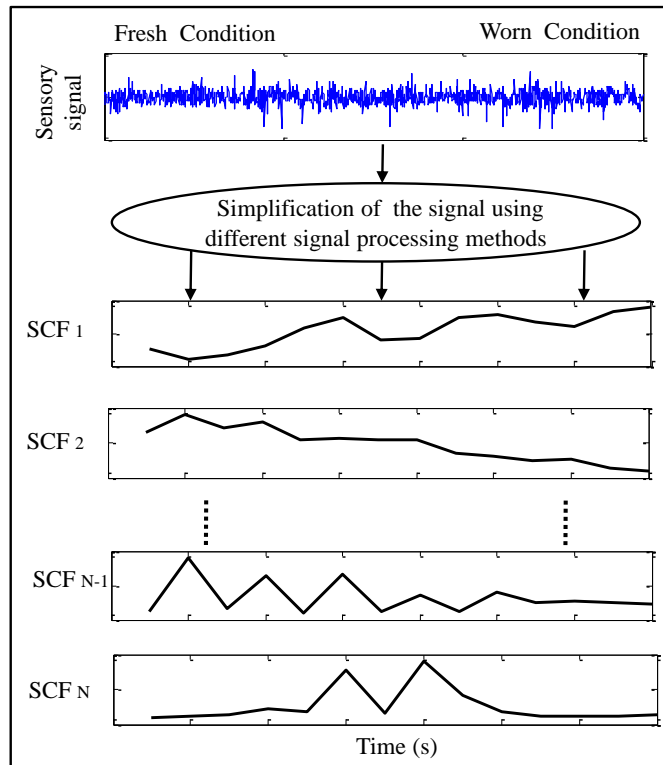


Figure 6.2: Simplification of complex sensory signal into simple SCFs.

6.4.1.2 Automated Sensitivity Detection

A sensitive sensory characteristic feature (SCF) could, depending on its information content, include an important amount of information about the state of the process which could lead to superior recognition. It is expected to react to the change in process conditions by an important change in its value. The sensitivity of a SCF can be evaluated by several methods such as:

1. The use of manual observation and visual inspection of the signals.
2. The use of a classification system as they are automated processes with complete independence such as neural networks, etc.
3. The use of statistical techniques to detect the change in the SCFs levels.

The change in SCFs can be detected visually. Figure 6.2 shows a simplification of a complex sensory signal into simple sensory characteristic features (SCFs), SCF₁ is increasing gradually between the two conditions of the process. In addition, SCF₂ is

decreasing gradually between the conditions of the process when the process changes from one condition to the other. SCF_{N-1} and SCF_N could be changing randomly between the process conditions with time. These sensory characteristics features (SCF_{N-1} and SCF_N) are identified as insensitive SCFs while both SCF_1 and SCF_2 are identified as sensitive SCFs [177]. The detection of the sensitivity of the SCFs has to be automated in order to develop a rapid and structured methodology of selecting sensors and signal processing methods. Several methods can be utilised for sensitivity measurements. For example, Figure 6.3 shows an example of methods which can be used for sensitivity detection measurement, such as the slope of a linear regression and sudden change in value.

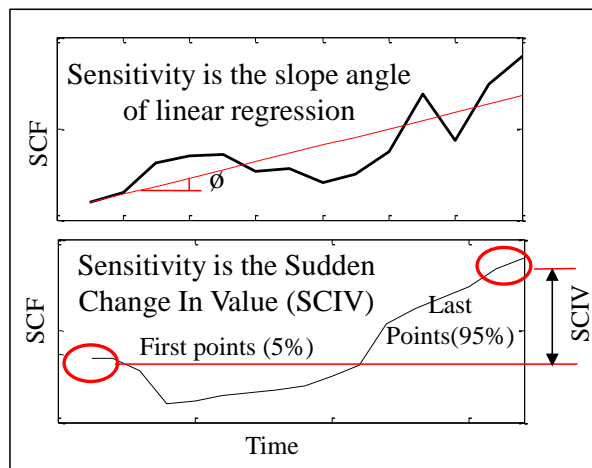


Figure 6.3: Example of two measuring sensitivity methods of the SCFs.

6.4.1.3 Association Matrix (ASM)

The following stage of ASPS is used the sensitivity values for every sensory signal and signal processing method to construct another matrix which is called the Association Matrix (ASM). The Association Matrix (ASM) is a matrix which associates the obtained sensitivity values (eg. in Figure 6.3) for the corresponding sensory features [20]. It gives a simple presentation of the sensitivity values associated with each feature (f_{ij}). The ASM for a fault y is defined as follows:

$$ASM_y = \begin{bmatrix} f_{11} & f_{12} & f_{13} & f_{14} & \cdots & f_{1m} \\ f_{21} & f_{22} & f_{23} & f_{24} & \cdots & f_{2m} \\ f_{31} & f_{32} & f_{33} & f_{34} & \cdots & f_{3m} \\ \cdots & \cdots & \cdots & \cdots & \cdots & \cdots \\ f_{n1} & f_{n2} & f_{n3} & f_{n4} & \cdots & f_{nm} \end{bmatrix} = f_{ij}$$

where $1 \leq i \leq n$ and $1 \leq j \leq m$

The element f_{ij} is called the sensitivity coefficient of the machining feature obtained using the machining signal of the i th sensor and the j th signal processing method.

The essential evaluation for the most appropriate sensor and signal processing method can be provided by using ASM since each column is associated with one signal processing method while each row is associated with one sensor. Basically, the sensory characteristic features with relatively high sensitivity coefficient are the most sensitive to fault detection and they are the most appropriate features to be used. Therefore, the related sensory signals and signal processing methods are the most appropriate ones and then selected as an initial monitoring system.

6.4.1.4 Sensor Fusion and Cost Reduction

A group of high-sensitivity SCFs should be used in combination to design a monitoring system with high sensitivity and consistency. When all SCFs extracted from the sensors are ranked according to their sensitivity values, the highest sensitive number of SCFs can be used together to construct the preliminary monitoring system. The number and type of sensors can be used easily to calculate the cost of the system. The value of the highest sensitive number of SCFs can be selected based on the cost of the system, the required quality of interpretation, the speed of signal processing and the implemented decision making method. The value chosen in this research is 10 based on a previous implementation of the ASPS approach for turning processes and on using a decision-making method in the turning process [20]. The last value is also found satisfactory in providing sufficient monitoring capability with reasonable signal processing speed.

Consider Figure 6.4 where m sensors are processed by n signal processing methods to create $(m \times n)$ sensory characteristic features. These features need to be calculated during the process in order to classify the sensitivity of the SCFs to the process states. The SCFs are arranged in order of sensitivity and the most sensitive number of SCFs is selected to produce the initial condition monitoring system, the cost of the system can be calculated based on the sensors of the selected SCFs.

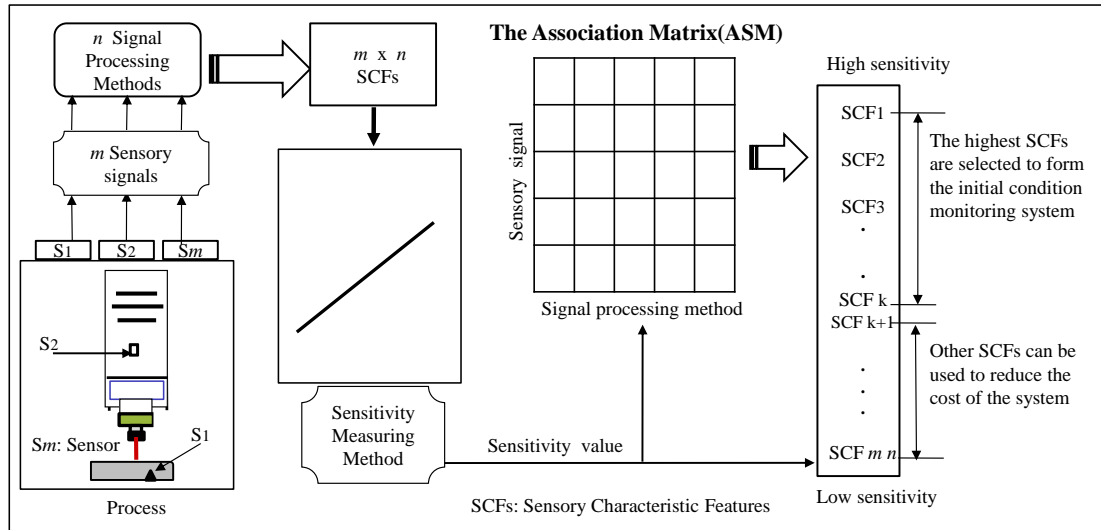


Figure 6.4: The rank and the selection of SCFs, information obtained from [19].

Efficient design of condition monitoring systems is thus accomplished within shorter development time, and more economically by minimising the number of sensors used. Therefore a cost reduction stage has been implemented in order to minimise the cost of the system. The cost reduction of the system is performed by eliminating sensors which do not significantly contribute to the selected number of SCFs by removing their SCFs from the system and replacing them from SCFs which come next on the rank, see Figure 6.4, from sensors already in the system without having to significantly reduce the overall sensitivity of the system (i.e. the new SCFs should still have relatively high sensitivity). The contribution of a sensor in a system is defined as the utilisation of a sensor. It is defined as the number of SCFs used in a system from that sensor relative to the total number of SCFs used in the overall system. More details are presented in the following chapters. Assume, for the process shown in Figure 6.4, that the first sensitive number SCFs are found from sensors (S_1 , S_3 , S_5 , S_i , S_{n-1} , S_n). Therefore, the cost of the sensors in addition to their signal conditioning devices will be considered as the cost of the hardware. Assume CS_j is the cost of the j th sensor and its signal conditioning devices and all the associated hardware [20].

Therefore, the cost of the system will equal to:

$$\text{Cost} = CS_1 + CS_3 + CS_5 + CS_i + CS_{n-1} + CS_n$$

Assume that the sensor S_{n-1} contributes in only h SCFs where h is much less than the contribution of the other sensors. Then that SCF from the S_{n-1} can be removed from

the system and replaced by another h SCF from the other sensors (S_1, S_3, S_5, S_i, S_n) as long as these new SCFs have relatively high sensitivity on the rank. Consequently, the cost of the new system will be:

$$\text{Cost} = CS_1 + CS_3 + CS_5 + CS_i + CS_n$$

Where the new system is reduced by CS_{n-1} .

The number of sensors is reduced, even if the number of SCFs in the system is still not changed, and therefore the cost of the system is also reduced. This removal process can be very efficient as long as:

- The new SCFs have high sensitivity so that the overall system performance does not decline.
- The eliminated sensor is relatively expensive.

In the subsequent chapters, much more details will be explained the previous discussion.

6.4.1.5 Data Analysis and Pattern Recognition

A machine condition monitoring problem will be finally transformed into a pattern recognition problem to identify, from the sensory signals, the machine or process conditions. Five types of pattern recognition systems have been used to demonstrate the application of the ASPS approach by previous researchers [19, 20]. Novelty detection and Learning vector quantisation neural networks (LVQ) are implemented in order to compare their result directly. The application of two systems is used to compare their result in order to evaluate the ASPS approach independently from specific pattern recognition.

6.4.2 Limitations of the ASPS Approach

The researcher [19] has extracted the sensitivity for each sensory signal based on the absolute slope of the Linear Regression (LR) method. The aim is to reduce the number of sensors needed in the overall system and reduce the cost. As shown in Figure 6.5, both signals (SCF1 and SCF2) have different levels of the sensitivity utilising the linear regression method.

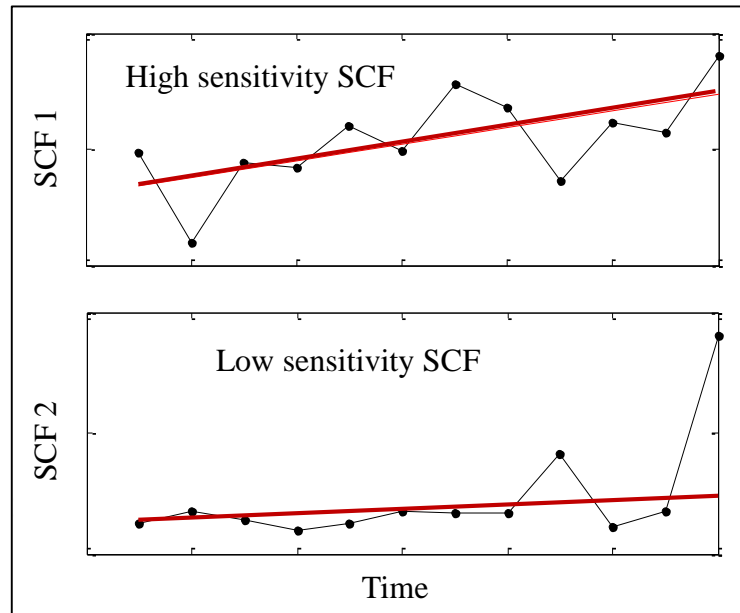


Figure 6.5: Examples of SCFs using linear regression method.

So far, this method has been applied to obtain the slope of the SCF pattern to measure the sensitivity. However, as can be seen from Figure 6.6, sometimes sensitive features are considered to have low sensitivity.

Another reference [20] has employed this approach to develop an effective sensor fusion model for turning processes based on the Sudden Change In Value (SCIV). The SCIV method used to measure the sensitivity of the sensory characteristic feature. This value is obtained from the absolute difference of 5% of the mean of the first points and 0.95% of the mean of last points. Figure 6.6 shows examples of the sensory characteristic feature (SCF). One major issue in this method is concerned with the lack of investigating the changes of the features for the points between the first and last group of points, see Figure 6.6 for example.

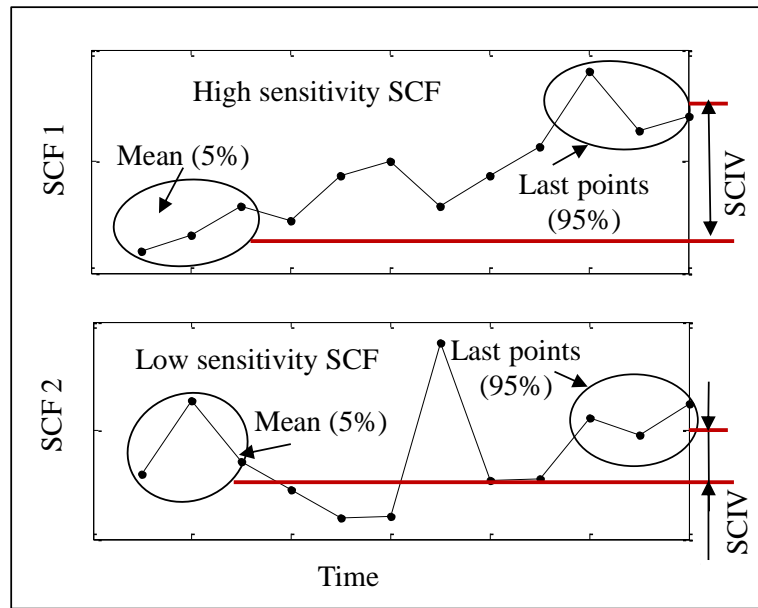


Figure 6.6: Examples of SCFs using Sudden Change In Value (SCIV).

The sensitivity measuring methods which are used by the previous researchers are not always suitable to address the relation between the fixturing system and the design of the monitoring system.

6.4.3 The Suggested ASPSF Approach

Therefore, ASPSF approach is used to address the current drawback in the ASPS approach and extend its application for the relationship between fixturing quality and the design of the condition monitoring system.

In the implemented machining process, different types of the fixturing systems will be used to hold the cutting tool. The signals of the sensory automatically transferred to the PC for processing. Therefore, the ASPSF objective is to extract sensory characteristic features (SCFs) obtained from the sensory signals using different signal processing methods and to find out the sensitivity of such features on the machine which has gone abnormal. If a specific feature from a specific sensor shows high sensitivity to the fault this simply means this SCF is useful in detecting or evaluating the fault of the fixturing system or address the tool condition. Therefore, ASPSF will provide the condition monitoring designer by the quality information to calibrate the characteristics of machining parameters. Consequently, the designer has the ability to adjust the monitoring system in normal case and recalibrate it when the change of parameters becomes abnormal.

This approach is considered the author's main contribution which is established to combine previous points with the idea of developing a generic structured sensor-fusion model using the following three techniques:

1. Evaluating the new ASPSF approach (Automated Sensor and Signal Processing Selection for Fixturing).
2. The automated simplification of complex signals into simple sensory characteristic features (SCFs).
3. Automated detection techniques of sensitive SCFs and hence the associated sensors and signal processing methods.

The details of the main techniques developed will be described in the following sections with more technical description and examples in the subsequent chapters.

6.5 The Concept of ASPSF Approach

The main idea of the implemented approach is described in this section. Specifically, further detailed procedures for the implemented approach will be described in section 6.6 of the current chapter and with more detail and experimental examples in the subsequent chapters of this thesis. The aim of the implemented approach is to design a condition monitoring system for fixturing using an automated simple procedure to detect the sensory characteristic features which are most sensitive to the process states or faults and show less sensitivity to other process operating variables and parameters. The ASPSF approach is based on the ASPS approach and on conducting studies to prove that there is a dependency between a measured sensory value (SCF) and the monitored state or physical phenomenon [178]. The cost of the system should also be considered; the expensive sensor should be eliminated from the system when a low-cost sensor can be used to do the same task instead of an expensive sensor.

Figure 6.7 shows the basic principle of an ASPSF approach. It analytically relates the sensory signal and the signal processing methods used to the state or the physical phenomenon which needs to be detected or evaluated.

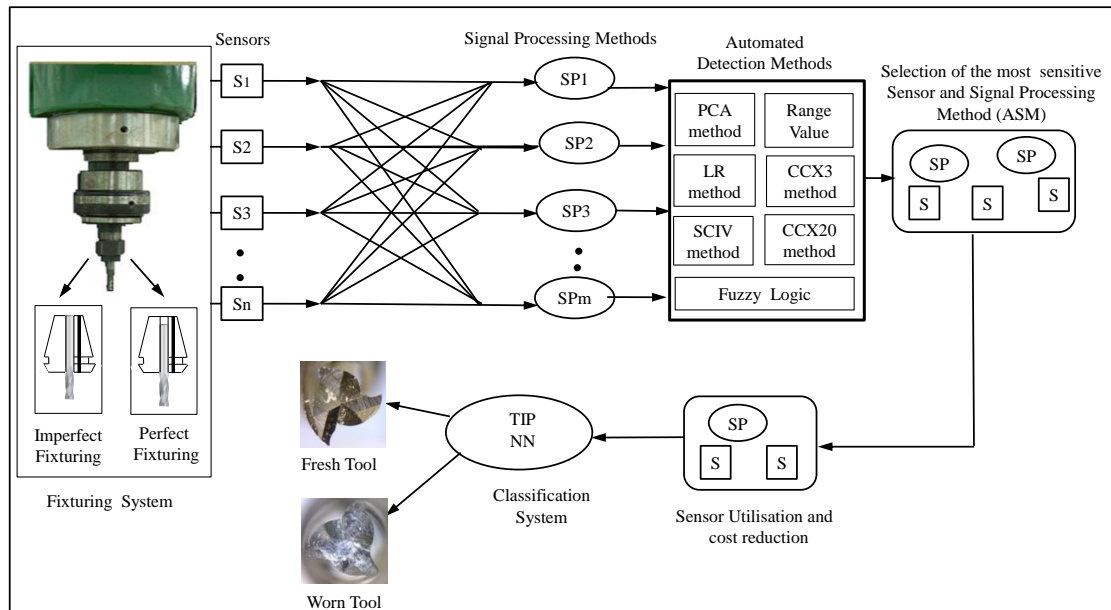


Figure 6.7: The essential structure of the ASPSF approach.

Similar to the original ASPS approach, the ASPSF approach starts by defining the operation to be monitored and its states (e.g. normal or abnormal condition). Then, several sensors are installed for process monitoring in order to produce sensory signals that contain information about the process. The following stage of the proposed approach is for extracting sensory characteristic features (SCFs) obtained from the sensory signals using a wide range of signal processing methods and then discovering the sensitivity of such features on the investigated process state. If a specific feature from a specific sensor shows high sensitivity to the fault, this means this sensory characteristic feature is useful in detecting or evaluating that fault. A particular number of sensitive sensors and signal processing methods are then selected as an initial monitoring system. Cost reduction can then be performed based on the number of SCFs extracted from the selected sensors. Consequently, and to reduce the cost, the sensor might be eliminated from the monitoring system if extracted numbers of SCFs from a sensor are insignificant. More details about the main concept of the ASPSF approach are explained in the next sections of this Chapter.

As shown in Figure 6.8, the ASPSF implements new techniques as described in the next sections.

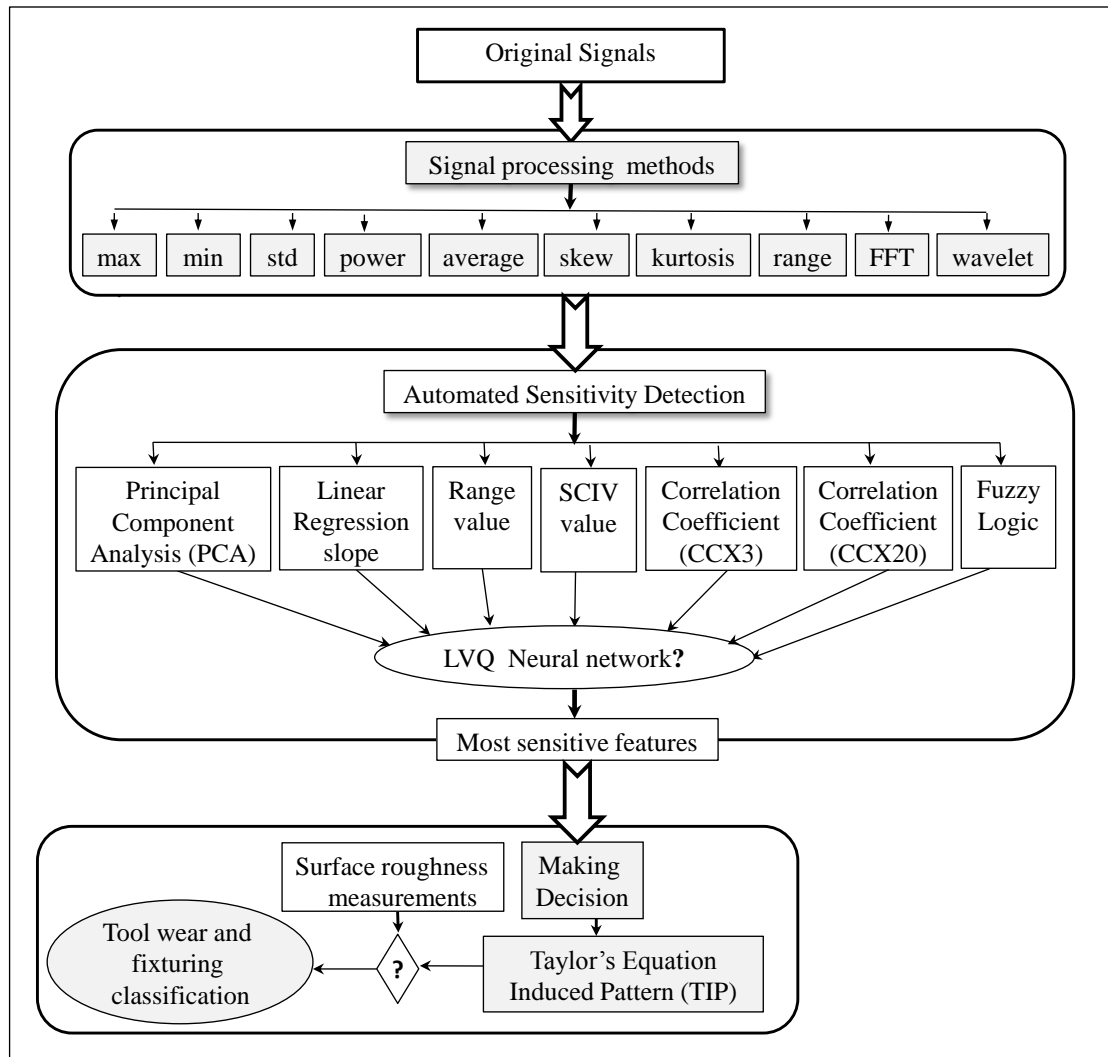


Figure 6.8: Schematic diagram of the proposed ASPSF approach and methodology.

6.6 Techniques Developed within the Suggested ASPSF Approach

This thesis utilises different sensors such as force, accelerometer, acoustic emission, power, eddy current, strain and sound sensor. It also utilises several signal processing methods such as maximum, minimum, standard deviation, range, average, power, skewness, kurtosis, Fast Fourier Transform (FFT) and wavelet.

6.6.1 Automated Sensitivity Detection

Several measuring sensitivity methods have been developed in this thesis and implemented to measure the sensitivity of the sensory features. These methods are Principal Component Analysis (PCA), Range value (RV), Correlation Coefficients

(CCX3 and CCX20) and Fuzzy logic. All these methods are considered as statistical methods modified to be used in detecting the sensitivity of the SCF. Linear regression method and Sudden Change In Value method will also be used and evaluated throughout this thesis. LVQ neural network will be used to measure the capability of each method and defines the most accurate method. A brief definition for each method is provided in the following sections.

6.6.2 Principal component Analysis (PCA)

Principal Component Analysis (PCA) [179] is a linear transformation method used to identify dimensions of maximum variation within a data set. The data is transformed into a space spanned by a set of orthogonal vectors called Principal Components (PCs), which are aligned along the axes of maximum variation. The first PC is the dimension with maximum variation with each further PC corresponding to less variation than the previous [180].

Diagrammatically, the concept of the PCA can be shown as in Figure 6.9. The uncorrelated property of the components is highlighted by the fact they are perpendicular, i.e. at right angles to each other, which mean the indices are measuring different dimensions in the data.

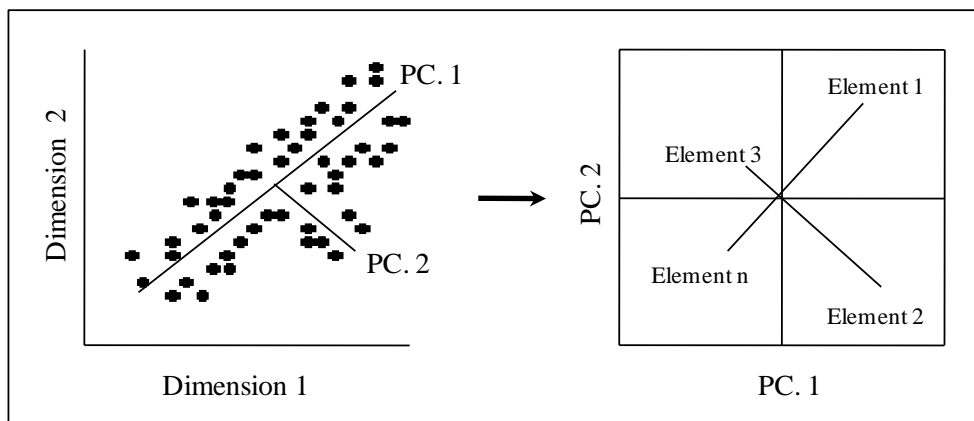


Figure 6.9: Diagram of the Principal Component Analysis (PCA).

Simply, the steps of implementing the PCA start by subtracting the mean of the data from the original dataset and then finding the covariance matrix of the dataset. The following step is calculating the eigenvalue which equals to the distance between the zero mean and each variable of the row data. The biggest value is indicated the more effect on the data. Therefore, it is useful to select which sensor has more performance during the machining. Each eigenvalue of the used sensor is combined to create the

Principal Component Feature (PCF). All the PCFs are arranged to form the Eigenvalue Sensory Matrix (EVSM) which will be fully described in Chapter 8, Section 8.3.2. Further information about the PCA in general can be found in reference [181].

The advantages of the PCA are summarised as follows:

- 1- It is a way for identifying patterns in data, and expressing the data in such a way as to highlight their similarities and differences. Since patterns in data can be hard to find in data of high dimension, where the luxury of graphical representation is not available, PCA is a powerful tool for analysing data.
- 2- The other main advantage of PCA is that once you have found these patterns in the data, and you compress the data, i.e. by reducing the number of dimensions, without much loss of information.

6.6.3 Range Value (RV)

The Range Value (RV) method used to measure the absolute difference between the last point and first point of the feature as illustrated in Figure 6.10. This is to explain the range of the change of the signal pattern.

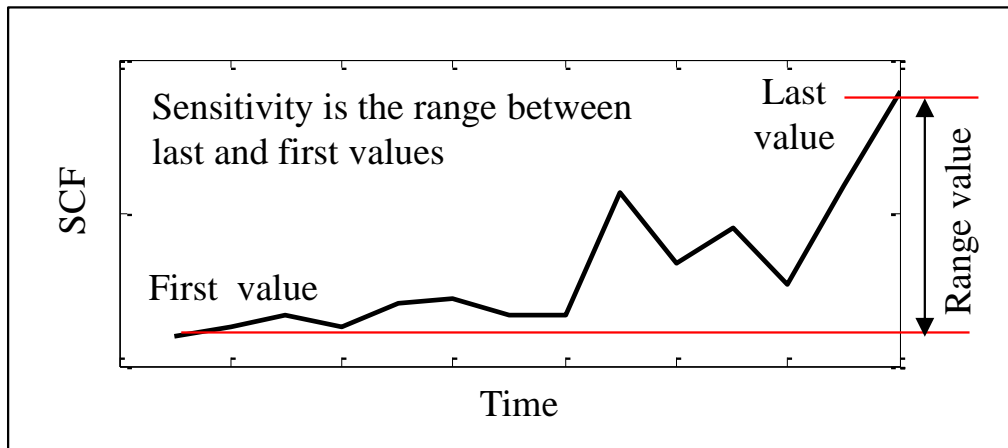


Figure 6.10: Example of SCFs using Range Value (RV) method.

6.6.4 Correlation Coefficients for X^n Curves

Based on Taylor's equation [69], tool wear can be expressed as:

$$y = X^n \quad (6.1)$$

For $n = 3$ and $n = 20$, see wear curves in Figure 6.11.,

In this thesis, the correlation between SCFs and Taylor's equation is investigated.

$y = X^3$ is named CCX3,

and $y = X^{20}$ is named CCX20.

In this case, high correlation will mean high sensitivity to the process states or faults.

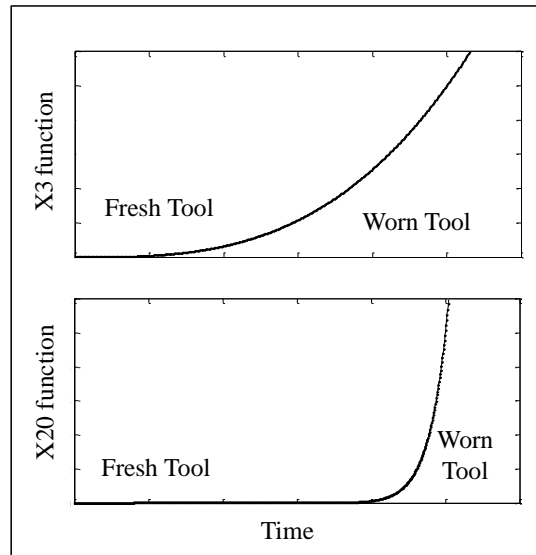


Figure 6.11: The polynomial equation of the expected tool wear pattern.

6.6.5 Fuzzy Logic (FL)

As described in the aforementioned sections, that there are different methods to measure the sensitivity of the features. In this thesis, a fuzzy logic [182, 183] has been used to characterise the sensitivity of the features when all the sensitivity measuring methods are combined together. This will be implemented by a membership function (0--1) which associates with each element of universe and represents the grade of membership specify for the condition each case [184]. As illustrated in Figure 6.12, the features obtained from each method have been interred in the fuzzy logic rules, these rules to evaluate each type of the method and then the results of the rules are combined to determine the most sensitive features.

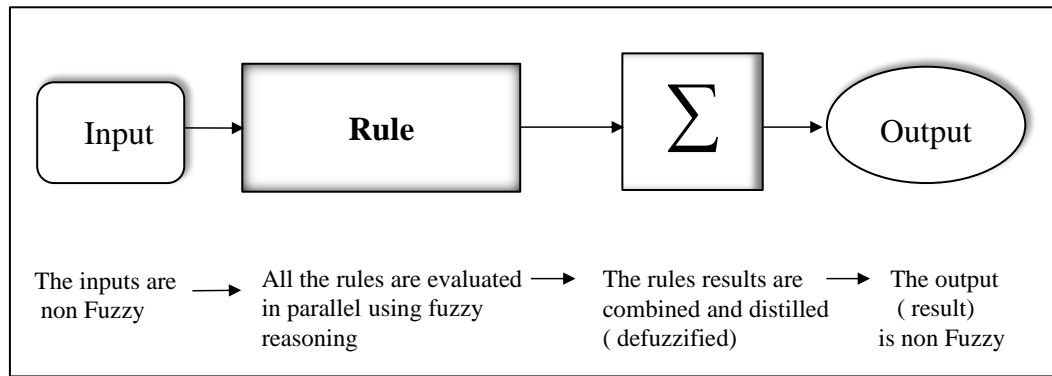


Figure 6.12: Steps of the fuzzy logic approach.

6.6.6 Learning Vector Quantisation (LVQ)

Learning Vector Quantisation is implemented in this research work. LVQ which implements a competitive neural network. LVQ neural network will be trained and tested with various experimental cases to evaluate the effect of different factors on the identification performance. Learning vector quantization is a nearest-neighbour pattern classifier based on competitive learning [185]. A LVQ network will be used in this research to evaluate all the measuring sensitivity methods and define the most accurate method among them.

6.6.7 Taylor's Equation Induced Pattern (TIP)

Taylor's equation will also be used for another novel application, which is to determine the capability of the group of SCFs to detect tool wear. This technique will be termed as Taylor's Equation Induced Pattern (TIP) to represent the pattern of the signal and to detect the moment of changing the tool conditions. This technique is also evaluated by using a supervised neural network, as Back Propagation Neural Network (BPNN). Consequently, the application of this system is used to compare the TIP results in order to evaluate the ASPSF approach independently from specific pattern recognition.

6.6.8 Surface Roughness (Ra)

Research over several decades in industry has reported that surface roughness is a reliable indicator to measure the quality of the machined surface. Therefore, the current research will concentrate on the investigation of using this indicator as a reflector to the sensitivity of the sensory system. In other words, the author will seek

how the change of the surface finish will affect the sensitivity of the monitoring system. More details are described in Chapters 8, 9 and 10.

6.7 The Application of the ASPSF Approach in This Thesis

The approach has been tested on three stages:

STAGE 1: (Chapter 8) Initial implementation of the ASPSF approach

A self-learning methodology can be considered this part of thesis for the classification of the system normal and abnormal states and the selection of the most sensitive sensors and signal processing methods for detecting machining faults in milling. The ASPSF approach is performed by mounting multi-sensors (force, vibration, acoustic emission, sound and strain) on the machine tool. Two types of the fixturing are used as perfect and imperfect clamping. The Experimental evaluation will be described in Chapter 8. Furthermore, a novel approach will be presented to predict the surface roughness.

STAGE 2: (Chapter 9) Initial implementation of the ASPSF approach using pattern recognition systems

A new group of multi-sensory signals (eddy current, accelerometers, power) has been installed on the machine tool to perform the ASPSF approach for milling operations using different fixturing systems. Surface roughness tester used to measure real roughness of the workpiece. The ASPSF approach is performed for evaluating the surface roughness of machined parts. This part of thesis also investigates the correlation coefficient between the SCF and the surface roughness for rapid design of monitoring system using four types of fixturing system. The experimental evaluation will be described in Chapter 9.

STAGE 3: (Chapter 10) The evaluation of ASPSF using broken teeth of tool

In this part, the new methodology has been implemented to apply the ASPSF approach using the tools with different number of broken teeth, and different fixturing systems. The correlation between SCFs and surface roughness of the machined parts

has been investigated. Neural networks are used for evaluating the methodology. The experimental evaluation will be described in Chapter 10.

6.8 Structure of Subsequent Chapters

The subsequent chapters of this thesis are organised to investigate the applicability of the ASPSF approach for designing condition monitoring systems for detecting the machine/fixture abnormalities in milling processes and to explain, in detail, the main steps for the approach. The following chapters are outlined in order to provide a logical basis for testing the assumptions and describing the outcomes. A simplified flow diagram of the basic structure of the subsequent chapters as illustrated in Figure 6.13.

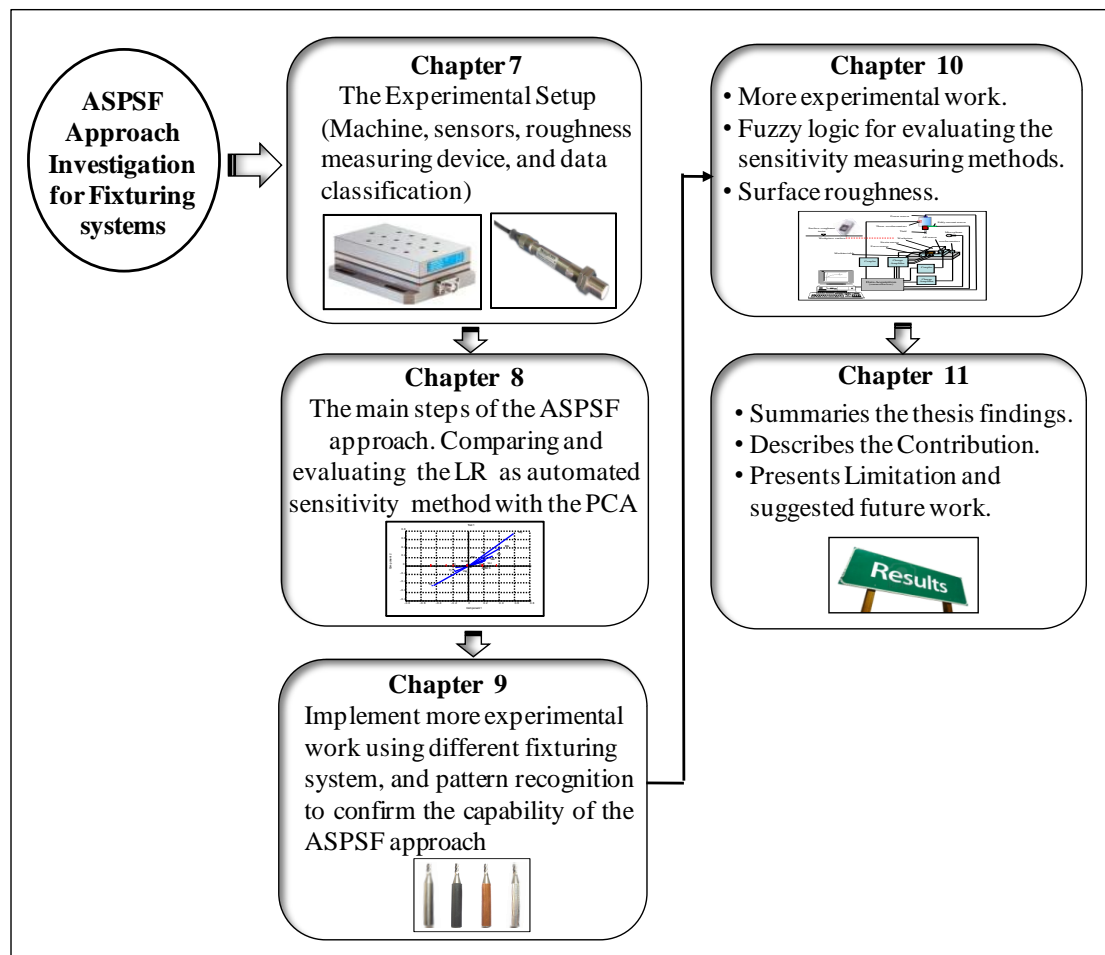


Figure 6.13: Diagram of the structure of the subsequent chapters.

Chapter 7 describes the general experimental set-up which has been performed to prove the capability of the ASPSF approach for fixturing processes. It describes the machine tools used, the faults investigated and the data acquisition software.

This chapter also describes the components of the implemented monitoring system. It presents the tools used in designing the monitoring system including sensors, signal processing and simplification methods, and classification techniques including neural networks and Taylor's Equation Induced Pattern (TIP).

The chapter outlines the tools which have been used to prove the applicability of the methodology for fixturing systems and milling processes.

Chapter 8 explains how the ASPSF approach can be used to design a monitoring system for a fixturing process with eight sensory signals such as force, strain, acoustic emission, accelerometer and sound. The main aim of the chapter is to describe the details of the ASPSF approach in a practical way aided by real experimental tests. The chapter presents a monitoring design for monitoring fixturing and gradual tool wear in milling processes. Furthermore, a novel approach will be presented to predict the surface roughness. Generally, the chapter introduces the following points:

1. The common problem of selecting the most appropriate sensors and signal processing method for designing a condition monitoring system in milling.
2. The basic main steps of the ASPSF approach for eight sensory signals. It describes how the SCFs are created and how they can be arranged in order to calculate their sensitivity for fixturing rigidity and gradual tool wear detection.
3. The capability of linear regression analysis to detect the sensitivity of SCFs. The response of the SCFs is visually investigated and compared to the Principal Component Analysis (PCA).
4. The method of choosing the most sensitive SCFs and PCFs to form the required condition monitoring system.

Chapter 9 presents further applications of the suggested ASPSF approach described in Chapter 9. The chapter presents more experimental work to prove the capability of the ASPSF approach in designing a condition monitoring system by selecting the most sensitive sensors and signal processing methods with reduced cost and less experimental work. All these concepts are compared with the PCA method. The aim of this chapter is to confirm the theory and the technique established in Chapter 9 using pattern recognition methods.

Chapter 10 presents the tool with broken teeth and the correlation between SCFs and surface roughness of the machined parts of the ASPSF approach. Neural networks are used for evaluating the methodology. It builds on the results found using

pattern recognition systems and dependency. The chapter addresses the following key issues:

1. Select the most accurate sensitivity method using fuzzy logic and then evaluate all these methods using LVQ neural network. Taylor's Equation Induced Pattern (TIP) and Back Propagation (BP) neural network are used to prove the results.
2. Address the composite relation between the tool conditions, fixturing system and efficiency of the condition monitoring system.
3. Address the relation between the surface roughness and sensitivity of monitoring system.

Chapter 11 reviews the implementation of the suggested methodology. It also considers whether the results in previous chapters prove that ASPSF is a re-usable designed methodology for selecting sensors and signal processing methods with reduced cost and experimental work for fixturing and tool wear, tool breakage in the milling process. It clarifies how novel approach has been created and tested. It also presents the contribution of the researcher, estimates unresolved problems and recognises limitations on the methods. Experiments and outcome are clearly detailed and future work is suggested to assistance following researchers.

6.9 Summary

The implemented methodology of this research work has been summarised and investigated in this chapter. The aim is to develop an organised structured methodology for the design and implementation of the ASPSF approach of condition monitoring systems for machining operations with experimental conformation for investigation the effect of tool condition and fixturing on milling processes using monitoring system. The problems of condition monitoring design have been described and compared with the current practice in the field. This has covered the way the ASPSF approach is concerned and its new features and techniques. The general steps of the ASPSF approach have been described. The purpose of the following chapters has described in light of the suggested methodology.

Chapter 7 Experimental Set-up

7.1 Introduction

The elements and stages of the implemented condition monitoring system in this research are covered in this Chapter. This Chapter provides further details regarding the machine tool, workpiece and cutting tool. It also presents the surface roughness measuring device and the condition monitoring system set-up including the placement of sensors, the data acquisition system and programmed software. A brief description of sensors, signal processing methods and pattern recognition systems utilised for developing the proposed model (as defined in chapter 6, section 6.4) is presented. A force dynamometer, accelerometers, eddy current, sound, strain, acoustic emission and power sensors are used for monitoring the machining process. Different types of signal processing methods are used to process the raw signals in the time and frequency domains to extract the Sensory Characteristic Features (SCFs). The sensitivity of the sensory characteristic features is calculated using automated sensitivity methods to evaluate physical phenomena. All pattern recognition techniques used in developing the model including neural networks and the Taylor's Equation Induced Pattern (TIP) classification method are addressed in the last part of this chapter.

7.2 Stages of the implemented condition monitoring system

As described in Figure 7.1, the procedures of research work have been implemented on four stages as follows:

- 1. Machining Process:** this stage provides information about the machine tool, workpiece and cutting tool, roughness measuring device, and sensors installation. The implemented sensors and signals processing equipment will be also presented. It is also described data acquisition card and Software.
- 2. Signal Processing:** the sensory signal will simplify using statistical methods in time domain, and FFT and wavelet in frequency domain.

3. Automated Sensitivity Detection: All the automated measuring sensitivity methods and LVQ neural network to evaluate these methods will be described.

4. Making Decision and Classification: Taylor’s Equation Induced Pattern (TIP) and BP neural networks classification methods are presented.

The complete experimental setup is illustrated in Figure 7.1, and will be described in the next sections.

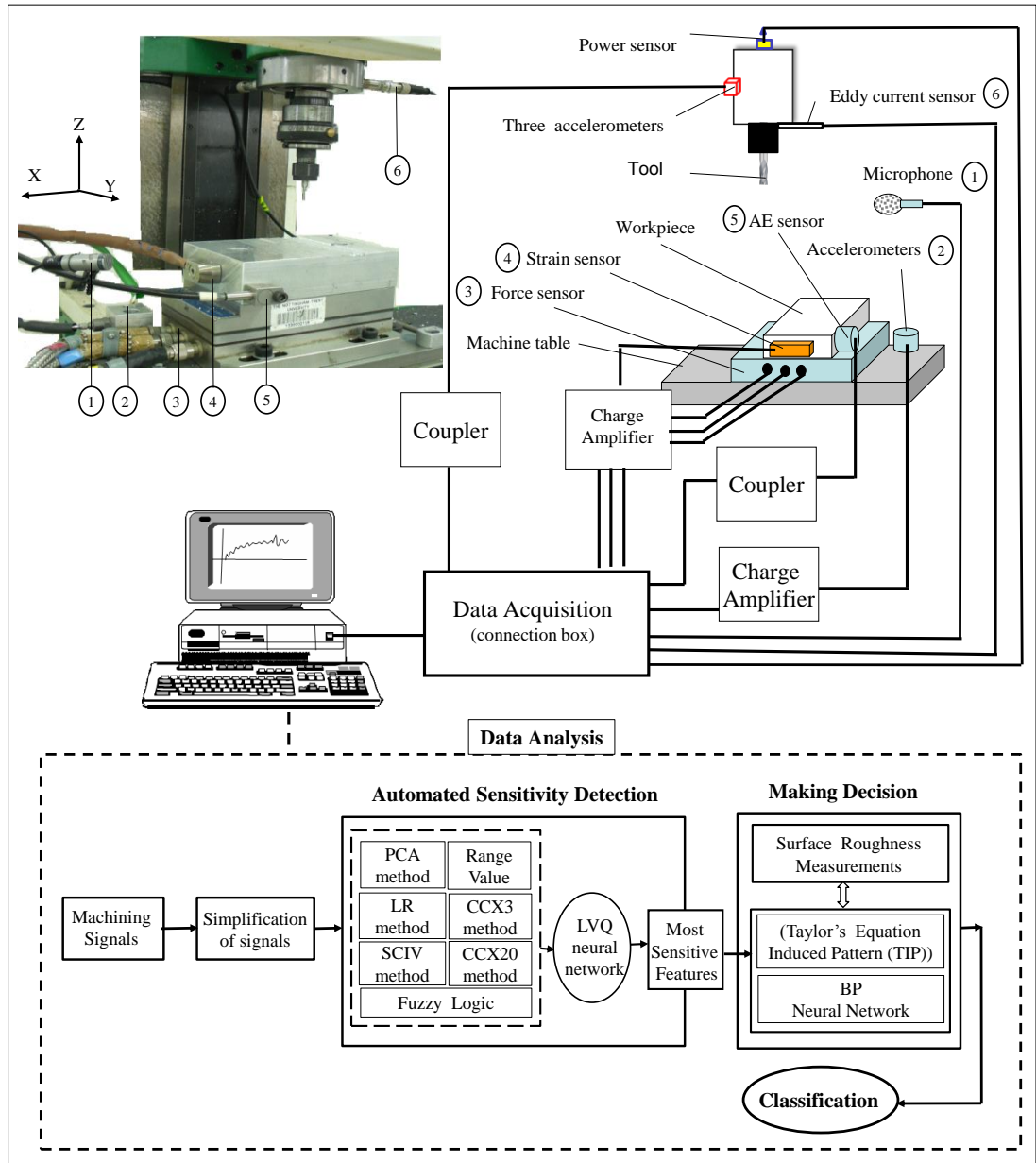


Figure 7.1: The complete experimental setup.

7.2.1 Workpiece and Cutting Tool

The experimental work is performed on a CNC milling machine type DENFORD. To present and simulate a real environment, the experimental work is designed by using the milling process of aluminium workpiece with a gradual tool wear test. The use of workpiece materials with low specific weight is an effective way of reducing the weight of structures. Aluminium alloys (aluminium AA6262) are among the most commonly used lightweight metallic materials as they provide a number of different interesting mechanical and thermal properties. Furthermore, they are relatively easy to shape metals, especially in material removal processes, such as machining [186]. The dimensions of the aluminium workpiece are (150 x 100 x 40 mm).

For the cutting tools, two material types have been used, namely, Carbide and High Speed Steel (HSS) tools. Carbide tool (or tungsten carbide) is made from a composite material containing equal quantities of tungsten and carbon powder, but it can be pressed and formed into shapes for use in industrial machinery. Carbide tool maintain a sharp cutting edge better than other tools, and they are very abrasion resistant and can also withstand higher temperatures than high speed steel tools. High speed steel tool consisted of 2% carbon (C), 2.5% manganese (Mn), and 7% tungsten (W). It can withstand higher temperatures without losing its hardness; therefore this property allows HSS to cut faster than high carbon steel, hence the name high speed steel. Carbide and HSS tools are the common cutters used generally in milling operation; therefore they will be used in this research.

For the selected tools, the recommended machining values are as follows: feed-rates, 215–260 mm/min while Depth Of Cut (DOC) varied from 0.2 to 0.4mm [187]. Cutting speed is selected based on the toughness of the workpiece to be machined. Based on the tool’s manufacture instructions, the recommended cutting conditions for the carbide tools and HSS tools are described in Table 7.1.

Table 7.1: The recommended cutting conditions for the Carbide and HSS tools.

Type of Tool	Spindle Speed	Feed Rate	Depth of Cut (DOC)
Carbide tools	2490 RPM	250 mm/min	0.22-0.36 mm
HSS tools	2860 RPM	215 mm/min	0.36 mm

7.2.2 Surface Roughness Measuring Device

Surface roughness is considered as the character of the machining quality, therefore roughness test used to investigate the change in the roughness of the machined surface [188]. Surface roughness measuring device will be performed in the current experimental work as shown in Figure 7.2. Therefore, a Mitutoyo (SJ-210) apparatus is used for the surface roughness measurements [189]. The measuring process by the roughness tester is tracking the machining process where the workpiece surface width (100 mm) divided to 5 divisions (20 mm per division) of machining and those will be measured later using the tester as the stylus movement length is 17.5mm. The measurements of surface roughness will be compared later with the progress of tool wear. Figure 7.2 illustrated the machining and roughness measurements.

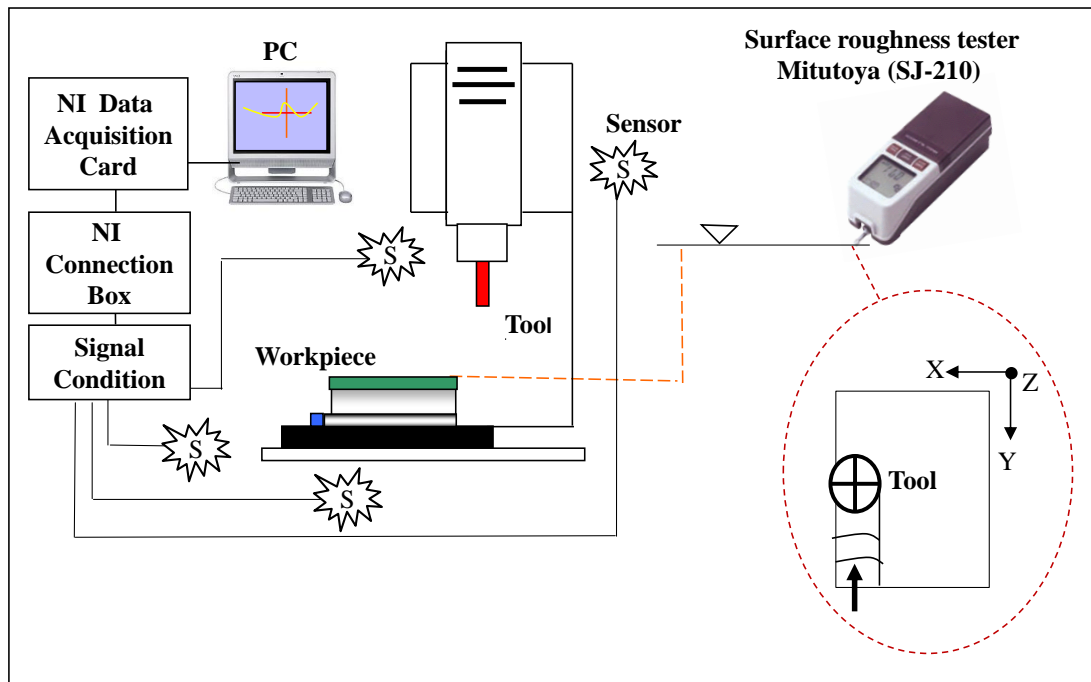


Figure 7.2: Schematic diagram of surface measurement setup.

7.2.3 Sensors Installation

To hold the sensor on the milling operation to detect the changes of tool condition, it is very important to make the required holder to fix the sensor in a suitable position. The main point of the difficulties in monitoring the rotating system is the limitation on fixing the sensor on the moveable and rotating spindle. Therefore, specific fixture has been designed and made in the workshop at the Nottingham Trent University. It

is attached precisely to the spindle case using a strong bond (Epoxy), and then the eddy current sensors have been inserted as shown in Figure 7.3.

Figure 7.4 shows the fixture to hold the accelerometers in three axes (x, y, and z). This fixture has been attached mechanically to the spindle case, and is used to hold the sensors to detect the vibration of the spindle. The other fixture has been attached to the workpiece, with same design and function. The robust attach will increase the reliability of the collected signals.

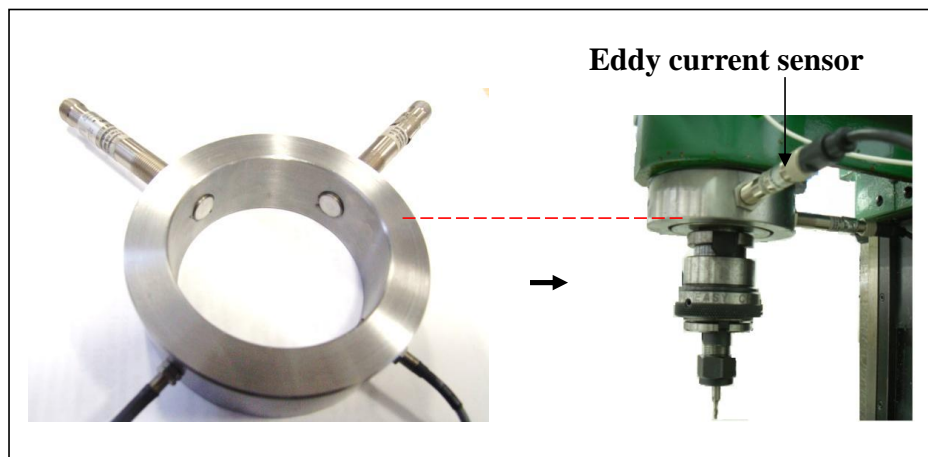


Figure 7.3: Fixture to insert the eddy current sensors.

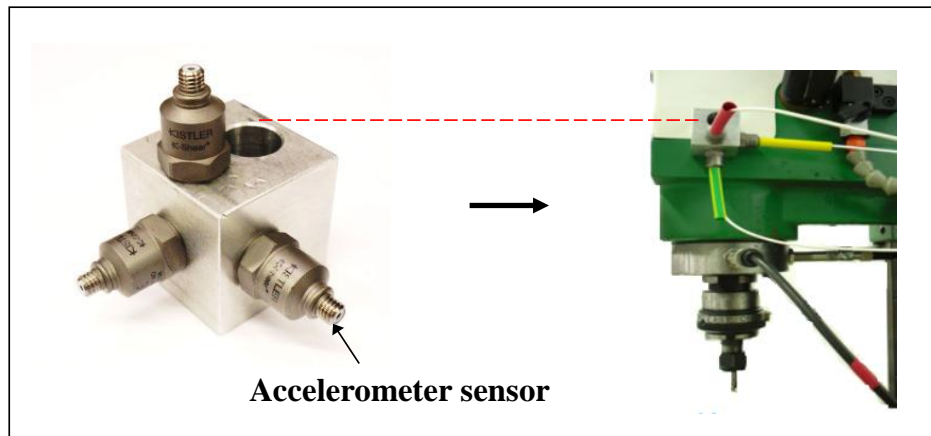


Figure 7.4: Fixture to hold the accelerometers.

7.2.4 Sensors and Signals Processing Equipment

A wide range of sensors are installed on the machine tool to develop a unique combination of sensory systems to detect the faulty and abnormal conditions of the machining process. These sensors are connected on the holder of workpiece,

machine spindle case and cutting tool. Therefore, they will be detecting faults in the workpiece and cutting tool.

The force signals are monitored using 3-component Dynamometer (Kistler 9257A) and the cutting tool is fixed on the dynamometer bolted rigidly on the machine movable table so that the workpiece speed and the feed components of the cutting forces can be measured. The vibration signals are monitored using an accelerometer (B&K4366) which is mounted close to the workpiece and tool in order to measure the radial acceleration due to the workpiece-cutting tool system vibration. Both the force dynamometer and the vibration accelerometer are connected to a 4-channel charge amplifier (Kistler 5070A).

The acoustic emission signals are monitored using an AE-Piezotron Sensor (Kistler 8152B) which is mounted close to the workpiece and is connected to AE piezotron coupler (Kistler 5125B) which gives the AE signals and the RMS of the AE signals. The four vibration accelerometers (Kistler 8704B) which three of them are attached to the machine spindle case, and the fourth one is attached perpendicularly to the movable workpiece table, together are connected to a coupler (Kistler 5134B).

The dynamic and quasistatic force signals are monitored using a strain sensor (Kistler 9232A) which is mounted at the side of the workpiece and it is connected to a charge amplifier (Kistler 5001). The sound signals are monitored using a Back Electret Condenser Microphone (Yago EM-400) which is mounted in a post on the machine moveable table and is connected directly to the DAQ card. Eddy current sensors (IC12-02) are connected to power supply (PDA 3502 A) with 12 volts. Power sensor (IP-151) is connected directly to the connection box, then to the data acquisition card. The signals are monitored using data acquisition card NI PCI-6071E from National Instruments using special data acquisition software written using the National Instrument CVI programming package and a computer. Matlab software is used for the complete analysis of this research. Figure 7.5 shows a photo of the equipment used in the experimental work.

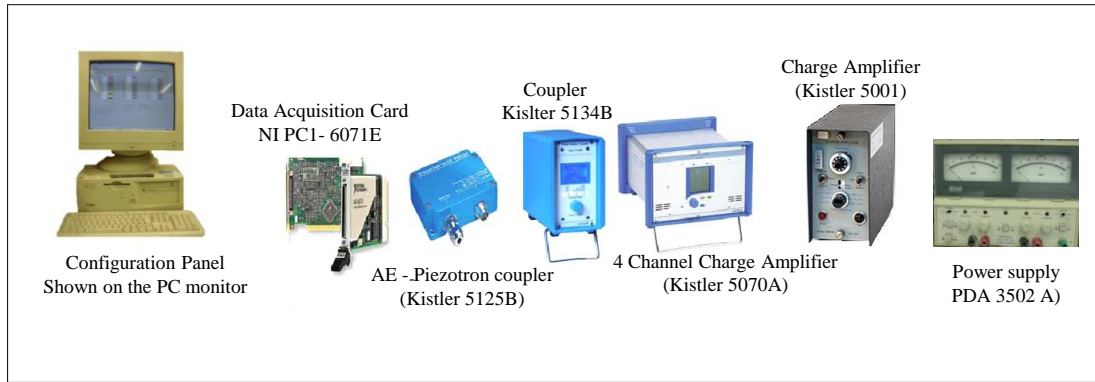


Figure 7.5: The equipment of the experimental work.

7.2.5 Data Acquisition Card and Software

The data acquisition card used is the NI-6071E from National Instruments, a multifunction analogue, digital, and timing I/O boards for PC AT. The card has 12 bits ADCs with 64 analogue input single ended or 32 differential with a guaranteed sampling rate up to 50k sample. The analogue input used configured as differential inputs because of the low voltages level involved, noisy environment, and long wires used in connecting the signals to the data acquisition card. The analogue channel is used to acquire the machining data using a sampling rate of 15000 or 16000 samples per channel. The card is used in a bipolar mode of ± 10 V with a board gain of 0.5. Hence, for 12 bit data samples the resolution is up to 9.76 mV. The data acquisition card is programmed using Labview/ CVI from National Instrument, a developed software package for data acquisition and monitoring. LabWindows/CVI is a enhanced ANSI standard C programming language.

The data acquisition software enabled the capture of the required signals to the PC hard disk for off-line analysis using Matlab. The software saves the data in text format for simple use by Matlab for analysis.

7.3 The Implemented Sensors

The sensors used in this research are force dynamometer, strain sensor, accelerometer sensor, eddy current sensor, power sensor, acoustic emission sensor and microphone for measuring sound.

7.3.1 Force Dynamometers

Piezoelectric force sensors are mostly used for dynamic-force measurements such as oscillation, impact, or high-speed compression or tension. Any force applied to the piezoelectric sensing element produces a separation of charges within the atomic structure of the material, generating an electrostatic output voltage. These sensors are widely used in the practical investigation due to being less dependent on the structure of the cutting machine and that the cutting forces can be easily simulated. Dynamometer mainly consists of three-component force sensors fitted under high preload between a base plate and a top plate. Each sensor contains three pairs of quartz plates, one sensitive to pressure in the z-direction and the other two responding to shear in the x and y-directions, respectively [190].



Figure 7.6: Dynamometer 9257A in milling operation [190].

Kistler dynamometer 9257A that measures the horizontal and vertical components of the cutting force will be used in the proposed research as in Figure 7.6. A base plate of dynamometer (Kistler type 9257A) is attached to the movable table of the milling machine. The workpiece is mounted on the top plate of the dynamometer to allow indirect measurement of the milling forces to which it is subjected.

7.3.2 Accelerometers

Accelerometers or vibration sensors are used for measuring acceleration. The main reason for using the vibration for monitoring machine tools and processes is that they are simple, precise and affordable. In addition, they are easy to use and no

significant modification to the machine is generally required. Meanwhile, the limitations of the vibration methods are dependency of the vibration signals on cutting conditions, workpiece materials and machine structure.

The accelerometer mounting position in milling operations has been proposed in a number of studies. In this study, the sensors are mounted on the base of the workpiece in x, y axis, also three sensors on the case of rotating machine spindle in three axes (x, y, and z). These positions are determined to be suitable locations to detect the vibration from the cutting tool. After the mounting positions are decided, special fixtures have been made with thread hole to hold the sensors on the fixtures. Vibration monitoring has been found useful in machine tools as well as continuous process industries [191].

Figure 7.7 shows a photo of the one of Kistler accelerometers (8704B) used in this research.



Figure 7.7: Photo of the Kistler accelerometer [191].

7.3.3 Acoustic Emission

Acoustic Emission (AE) has been used for materials research in monitoring stresses from AE events emitted from crack initiation, structural defects, measurements, and other material anomalies [192]. From this work it was found that most materials emit sounds or stress waves as they are deformed, these sounds provide the very nature of plastic deformation under different intensities which inherently give warning signals for impending failure of a specific material. Recently, acoustic emission based monitoring systems are finding increased applications in condition monitoring. Acoustic emission and audible sound waves which are created during

machining have been found useful in several researches for the classification of process condition, especially with following specification [192]:

- High sensitivity and wide frequency range.
- Inherent high pass-characteristic.
- Insensitive to electric and magnetic noise fields.
- Robust, suitable for industrial use.
- Ground isolated: prevents group loops.

Figure 7.8 shows a photo of the Kistler AE sensor (8152B) used in this research which is attached to the workpiece.



Figure 7.8: AE sensor (Kistler 8152b111) [192].

7.3.4 Strain

The dynamic and quasistatic forces on fixed or moving machine parts are measured by using strain sensor. The sensor has ability to measure the force-proportional strain at machine tool or structural surfaces (indirect force measurement). The high sensitivity and acceleration-compensated design of the sensor allows process monitoring on fast running process machinery (e.g. presses, automatic assembly machines). The strain of the basic material acts using the two contact surfaces on the sensor as a change in distance. The sensor enclosure serves as an elastic transmission element and converts the change in distance into a force. This sensor has many advantages compared with the common wire strain gauge technology state in the high sensitivity, significant overload resistance and practically unlimited life

even under fluctuating loads [193]. Figure 7.9 shows a photo of the Kistler strain sensor (9232A) used in this research.



Figure 7.9: Strain sensor (Kistler 9232A).

7.3.5 Eddy Current

These sensors operate with magnetic fields. The driver creates an alternating current in the sensing coil in the end of the probe. This creates an alternating magnetic field which induces small currents in the target material; these currents are called eddy currents. The eddy currents create an opposing magnetic field which resists the field being generated by the probe coil [194]. The interaction of the magnetic fields is dependent on the distance between the probe and the target. As the distance changes, the electronics sense the change in the field interaction and produce a voltage output which is proportional to the change in distance between the probe and target. The target in the current research is the rotating spindle of the milling machine; therefore a round fixture has been attached to the spindle case to amount the sensor. Figure 7.10 shows the photo of Eddy current sensor (IC 12-02) which is used in the research [195].



Figure 7.10: Eddy current sensor IC 12-02 [195].

7.3.6 Sound

The sound signal during a cutting process based on the concept of sensing tool condition has been used more than three decades ago [196]. Several studies using sound signals and their results indicate the correlation between tool condition and the sound emitted during the machining process [197]. It has been reported that tool wear is correlated with an increase in the amplitude of the high frequency bands of the sound signal. In this research, a sound signal is used to extract valuable information correlated with fixturing and tool condition. The main limitation of using this signal in the development of a condition monitoring system is the ambient noise, as has been identified and studied in several research papers [175].

These papers conclude that in the region between 0 and 2 kHz the influence of the environment and of the noise either from adjacent machines, motors, conveyors, or from processes may contaminate the signals. Nevertheless, they conclude that this effect can be moderated by using noise cancellation methods in the signal processing algorithm. A photo of the microphone (EM-400) which used in this thesis has shown in Figure 7.11.



Figure 7.11: Sound sensor (microphone).

7.3.7 Power

A power sensor is used to monitor the load on the motor that is driving the machines spindle which can give valuable information related to the load on the motor. The major advantage of the motor related parameters to detect malfunctions in the cutting process is that the measurement apparatus does not disturb the machining process and the power sensing use the motors current as an indirect sensor of cutting force [198]. Figure 7.12 shows the power sensor which used in this research.



Figure 7.12 Photo of power sensor.

7.4 Signal Processing Methods

This research work has been used maximum, minimum, standard deviation, range, average, power, skewness, kurtosis for analysis in the time domain. It also has used FFT1, FFT2, FFT3, FFT4, FFT5, FFT6, FFT7, FFT8, FFT9 and FF10 for analysis in the frequency domain. The following paragraphs outline each method used.

7.4.1 Time Domain Methods

More details about the following methods are described in [199].

1. Arithmetic mean (μ): The mean of amplitude values of raw data signal. The mean of n amplitude values of a signal $[x_1, x_2, \dots, x_n]$ is

$$\mu = \frac{1}{n} \sum_{i=1}^n x_i \quad (7.1)$$

2. Standard Deviations (std) which is normally represented by the Greek symbol σ , where σ measures the variation of the data from the average. It is defined as:

$$\sigma = \sqrt{\left(\frac{\sum_{k=1}^N (x_k - \mu)^2}{N - 1} \right)} \quad (7.2)$$

3. Skewness (*Skew*): The 3rd central moment and is a measure of the asymmetry of the probability distribution of the signal raw data. It is expressed as:

$$Sk = \frac{1}{n} \frac{\sum_{i=1}^n (x_i - \mu)^3}{\sigma^4} \quad (7.3)$$

4. Kurtosis (*Ku*): Fourth central moment and is a measure of the peakedness of the probability distribution of the signal raw data:

$$Ku = \frac{1}{n} \frac{\sum_{i=1}^n (x_i - \mu)^4}{\sigma^4} \quad (7.4)$$

5. Power (P): Signal power is defined as the measured area under the rectified signal envelope. This is another measurement of the signal amplitude; however, it is sensitive to amplitude as well as duration, and it is less dependent on operating frequency. Power is defined as:

$$P = \frac{1}{n} \sum_{i=1}^n x_i^2 \quad (7.5)$$

7.4.2 Frequency Domain Analysis Methods

Fourier Transformation

In order to confirm the presence of certain frequencies, it is important to break down the signal into its frequency spectrum. Because of this the frequency content of a signal is not regularly clear from the time domain. The discrete Fourier transformation (DFT) algorithm is used to exchange a digital signal from time domain into a signal in the frequency domain. The discrete Fourier transformation is a very computationally intensive algorithm which contains a huge number of mathematical operations, though when the length of the signal is a power of two, then Fast Fourier Transformation (FFT) can be used which reduces the computation necessary to make the transformation from time domain to frequency domain [200].

$$X[k] = \sum_n^{N-1} x[n] W_N^{nk} \quad (7.6)$$

For $k = 0, 1, 2, \dots, N-1$

Where:

$$W_N = e^{-j2\pi/N}$$

Wavelet Analysis

Fourier transformation has an important disadvantage as the transformation process from the time domain to frequency domain removes the time information. Consequently, when looking at a frequency spectrum, it is not possible to know when an exact event has happened. Wavelet analysis provides an alternative technique of breaking a signal down into sub-signals or levels with different

frequencies which carry the time information. In wavelet analysis, the length of the signal, i.e. number of values contained in the signal, determines how many wavelet levels there will be in the decomposition. In general, for a signal of length N , where $N = 2^n$ there are $n+1$ wavelet levels. The shape of the wavelet levels depends on the mother wavelet signal which is used to build these levels. Wavelet analysis involves breaking the signal into sub-signals, each of which is generated from a combination of shifted and scaled wavelet signals. For every level the number of wavelet signals used to construct the signals equals 2^n where n is the level number. The standard deviation (std) of the wavelet levels is used as sensory characteristic features for the condition monitoring system. The standard deviation of each level reflects the actual contribution of that level in building the original signal [200].

7.5 Automated Sensitivity Detection

Linear Regression (LR)

Linear regression is used to find the linear equation which best represents the linear relationship between two variables. The first variable is the independent variable which could be the degree of tool wear, etc. The second variable is the dependent variable and this variable is a sensory characteristic feature which changes according to the change in the independent variable. The line is obtained by using the least squares straight line fitting. The least squares line is defined as [20]:

$$y^1 = b_a + b_1 x_1$$

Where:

$$b_1 = \frac{N \sum_{i=1}^N x_i y_i - \left(\sum_{i=1}^N X_i \right) \left(\sum_{i=1}^N Y_i \right)}{N \sum_{i=1}^n y^2_{i1} - \left(\sum_{i=1}^N X_i \right)^2} \quad (7.7)$$

$$b_a = \bar{y} - b_1 \bar{x} \quad (7.8)$$

Equation 7.8 represents the slope of the least squares straight line. The absolute value of b_1 is to find out the most sensitive sensory feature to the independent variables (e.g. degree of cutter wear) of machining parameters.

Sudden Change in Value (SCIV)

The Sudden Change In Value (SCIV) statistical method is used in this research to find the average difference between the first group of points and the last group of points. The first variable is the average value of the first (5%) of samples. While the second variable is the average value of the last (95%) of samples, see Figure 6.7 in the previous chapter. The sudden value is the difference between the two averages [21]. SCIV is defined as:

Last values = maximum of mean (Last point - (0.05* Last point)).

First values = mean of the (0.05* Last point).

SCIV = Last values – First values.

Range Value (RV)

The Range Value (RV) statistical method is used in this research to find the difference between the first value and the last value. RV is defined as:

RV= Last Value – First Value.

Correlation coefficients (CCX3 and CCX20)

Based on Taylor's equation [69]:

$$y = X^n$$

where y is wear level, n is a constant, X is machining time.

This research has used $n= 3$ and $n= 20$ to develop two types of generic wear curves, namely $y= X^3$ and $y= X^{20}$ which are named CCX3 and CCX20 respectively.

The correlation coefficient is obtained from the correlation between the pattern of the constant functions individually and the pattern of the feature (SCF) to generate the correlation coefficient (CCX3) and the correlation coefficient (CCX20) as shown in Figure 6.12 in the previous chapter. This correlation will provide a representative to the trend of the feature pattern as the high correlation indicates high sensitivity of the feature to detect the change of the tool condition.

Fuzzy Logic (FL)

Fuzzy Logic is a particular area of concentration in the investigation of artificial intelligence and is constructed on the value of that data which is neither absolutely

true nor false [184]. The data which operators use in their everyday lives to base natural decisions and apply general rules of practical information can and should be applied to those control situations which demand them. Developed knowledge can be a great way to avoid the unwanted effects of the system reaction.

In the current research, fuzzy logic will be used to implement the controlling of the sensitivity measuring method to select the most sensitive feature. A fuzzy logic model with its fundamental input-output relationship consists of four components namely, the fuzzifier, the inference engine, the defuzzifier, and a fuzzy rule base as shown in Figure 7.13. In the fuzzifier, inputs are fuzzified into linguistic values to be associated to the input linguistic variables. After fuzzification, the inference engine refers to the fuzzy rule base containing fuzzy IF-THEN rules to derive the linguistic values for the intermediate and output linguistic variables [183]. Once the output linguistic values are available, the defuzzifier produces the final values from the output linguistic values.

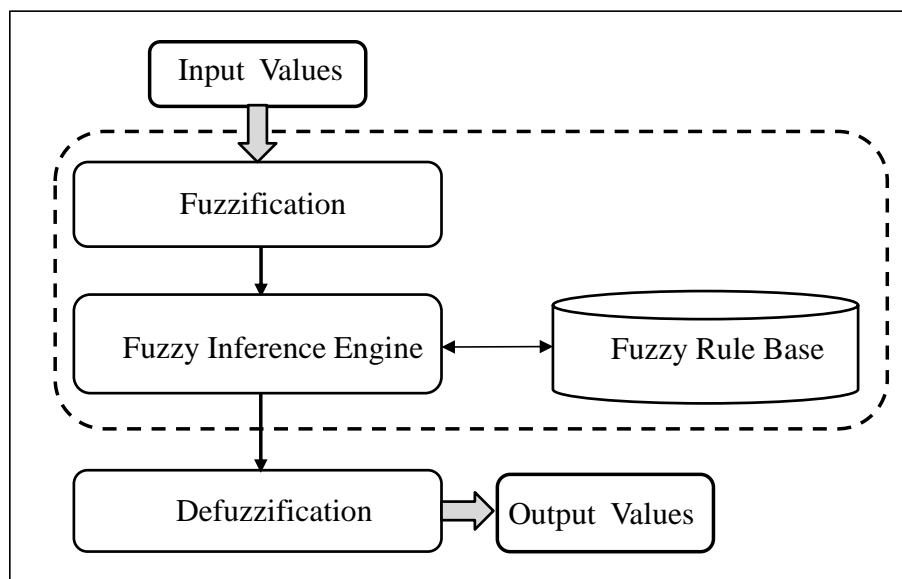


Figure 7.13: Structure of a fuzzy logic model.

Principal Component Analysis (PCA)

PCA is a multivariate statistical technique used to reduce the number of variables in a data set into a smaller number of dimensions. In mathematical terms, from an initial set of n correlated variables, PCA creates uncorrelated indices or components, where each component is a linear weighted combination of the initial variables. For example, from a set of variables X_1 through to X_n :

The formula for covariance is very similar to the formula for variance. The formula for variance could also be written as [181]:

$$\text{var}(X) = \frac{\sum_{i=1}^n (X_i - \bar{X})(X_i - \bar{X})}{(n-1)} \quad (7.9)$$

For two dimensions can be described as:

$$\text{cov}(X, Y) = \frac{\sum_{i=1}^n (X_i - \bar{X})(Y_i - \bar{Y})}{(n-1)} \quad (7.10)$$

The $\text{cov}(X, Y)$ is a covariance matrix which is squared matrix, therefore it is possible to calculate the eigenvalue and eigenvector as it will indicate the useful information about the effect of each variable on the data. Eigenvector (v) is a non-zero vector that after multiplying by the matrix, remain parallel to the original vector. For each eigenvector, the corresponding eigenvalue (λ) which is a factor or real number to scale the eigenvector when multiplied by the matrix as showing on equation 7.11. In other words, the eigenvalue will define the length of the variable of the row data. It is possible to measure the eigenvalue by the following equation:

$$[\text{cov}(X, Y)][v] = \lambda[v] \quad (7.11)$$

For the purpose of measuring the significance of the sensor in current research, eigenvalue will be used to evaluate the important of each sensor. The theory is based on the discussion represented in chapter 6, section (6.6.2). More details regarding the application of this method are shown in Chapter 8.

7.6 Making Decision and Pattern Recognition

A machine condition monitoring problem will be finally transformed into a pattern recognition problem to identify, from the sensory signals, the machine or process conditions. For data analysis, unsupervised neural network Learning Vector Quantisation (LVQ) has been used two types of pattern recognition systems to demonstrate the application of the ASPSF approach. The application of these systems is used to compare their result in order to evaluate the ASPSF approach independently. Taylor's Equation Induced Pattern (TIP) and Back Propagation Neural Network (BPNN) are implemented in order to compare their results directly.

These methods are implemented to compare the result of each monitoring system. More details about these methods are briefly described in the following sections. The ASPSF approach is not limited to these methods but can be implemented with other methods such as the Self-Organizing Neural Networks and the Radial Basis Neural Network (RB), etc.

7.6.1 Data Analysis

Data analysis is an important stage of the research process which is generally defined as a process that converts raw data into information and knowledge to explore the relationship between variables. Unsupervised neural network, such as LVQ uses a special algorithm to group similar patterns in the input data space into similar output classes. The functional behaviour of the whole system is determined mainly by the pattern of connectivity of the nodes. As a system, they are capable of performing some high level functions such as adaptation, generalisation and target learning. These capabilities are particularly attractive for tool wear monitoring applications. The method developed and applied in this work, is the Learning Vector Quantisation (LVQ) which implements a competitive neural network. LVQ neural network will be trained and tested with various experimental cases to evaluate the effect of different factors on the identification performance. Learning vector quantization is a nearest-neighbour pattern classifier based on competitive learning. A LVQ network contains an input layer, a Kohonen layer which learns and performs the classification, and an output layer. The input layer contains one node for each input feature, the output layer contains one node for each class. Figure 7.14 illustrates the structure of LVQ neural network. During the training process of the LVQ, the euclidean distance from a training vector, x , to each node's weight vector, w_i , in the Kohonen layer is computed according to the formula:

$$d_i = \|w_i - x\| = \left[\sum_{j=1}^n (w_{ij} - x_j)^2 \right]^{1/2} \quad (7.12)$$

The nearest node is declared to be the winner, and its weight vector is adjusted according to whether the winning node is in the class of the training vector:

If the winner is the correct class, then $w_{i+1} = w_i + \alpha(x - w_i)$;

If the winner is not the correct class, then $w_{i+1} = w_i - \lambda(x - w_i)$,

where w_{i+1} is the weight vector after adjustment, w_i the vector before adjustment, α and λ are learning parameters. A brief description of the algorithm is given below [185]:

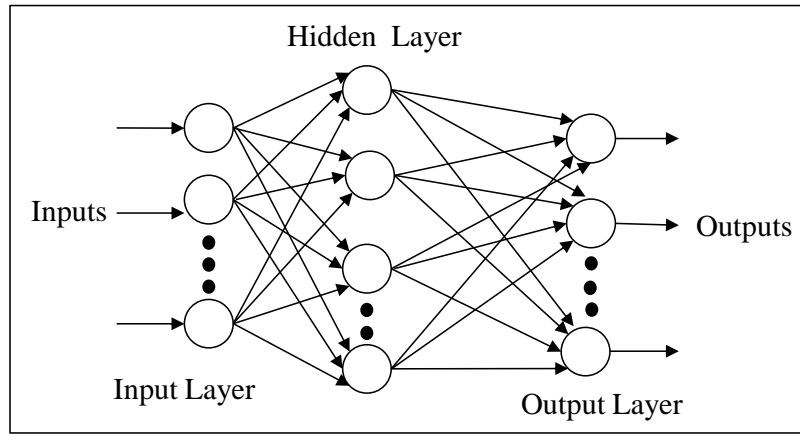


Figure 7.14: The architecture of the LVQ neural network.

For each input sample, the two closet weights vectors w_i and w_j are first found by using the Euclidean distance criterion. Assume the distances from w_i and w_j to x are d_i and d_j , respectively. If the two closest weight vectors belong to different classes, one of them is correct. Furthermore, if the input sample x is located inside the window between the two closest weight vectors, then:

$$w_i(t+1) = w_i(t) - \alpha(t)(x - w_i(t)) \quad (7.13)$$

$$w_j(t+1) = w_j(t) - \alpha(t)(x - w_j(t)) \quad (7.14)$$

Let t denote the number of training set iterations. The window is defined in terms of relative distances d_i and d_j from w_i and w_j to x , respectively, having a constant ratio. Then the input vector x is defined to be within the windows if $\min(d_i/d_j, d_j/d_i) > s$, with $s = (1 - w)/(1 + w)$.

During testing, LVQ classifies an input vector by assigning it to the same class as the output unit has its weight vector closest to the input vector. To reduce computing time and simplify the structure of LVQ neural network, five neurons are set in the Kohonen (hidden) layer, which is useful to eliminate the subclusters of each class.

7.6.2 Pattern Recognition

7.6.2.1 Taylor's Equation Induced Pattern (TIP)

Since the best measuring sensitivity method has been defined, the feature (SCF) will be arranged according to the sequence of this method, that is will lead the investigation to the next stage of the monitoring system which is the pattern recognition. In general, therefore, it seems that it is important to classify the status of the tool from fresh to worn then making the decision. The key problem is how could one define the tool status when the tool has moved from being fresh, to semi-worn to worn?

To solve this problem, as discussed previously, Taylor's equation is used as a generic pattern for that which is a novel way to address this problem. These patterns are derived from the general aspect of the Taylor's equation as explained in chapter 3, section 3.7. Therefore, this technique will be called as Taylor's Equation Induced Pattern (TIP). To plot these patterns, two types of constant functions X3 and X20 are employed to do that as shown in Figures 7.15, and 7.16. These patterns are considered as templates to divide the target of neural network. Here, Back Propagation (BP) Neural Network will be implemented for the data training and testing since it is supervised method and definitely needs to determine the target in advance.

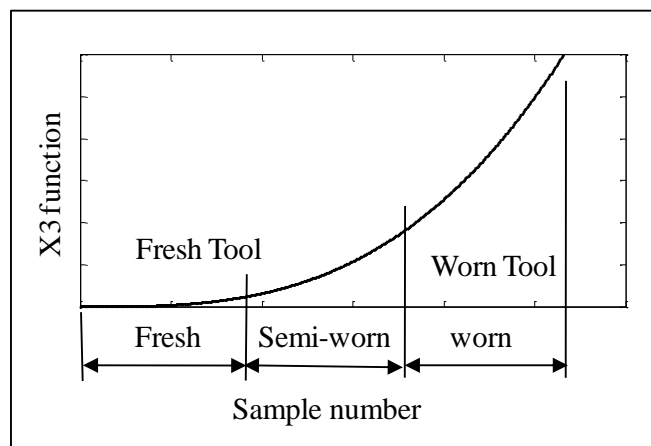


Figure 7.15: The BP neural target division according to $y = X3$ (function (X3)).

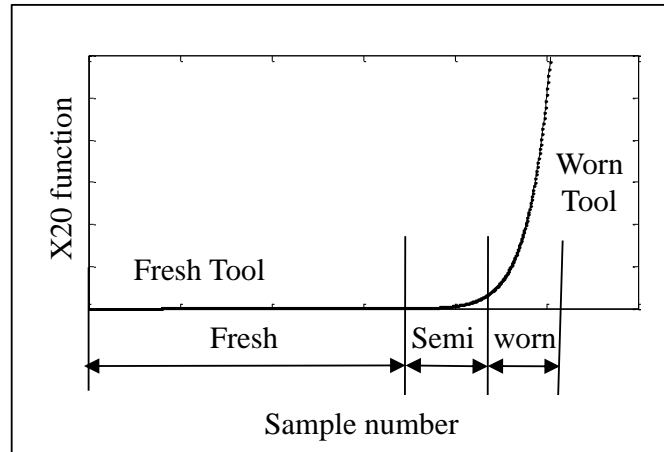


Figure 7.16: The BP neural target division according to $y = X20$ (function (X20)).

Figure 7.15 shows the first constant function (X3 function) divided the tests to three equal sections, meanwhile Figure 7.16 shows the second constant function (X20) which is divided to different sections length (77 % fresh, 12% semi-worn, 11% worn). The experimental sensory feature (Experimental) divided to the empirical number extracted according to the features pattern.

7.6.2.2 Back Propagation Neural Network (BPNN)

The back propagation algorithm is a supervised learning method which was first proposed in 1969, but was ignored because of its demanding computations until the mid-1980s. It is more useful for feed-forward networks (networks that have no feedback or simply, that have no loop connections). The term is an abbreviation for backwards propagation of errors. Back propagation requires all transfer functions used by the artificial neurons (or nodes) to be differentiable. Back propagation is used to calculate the error gradient of the network with respect to its modifiable weights. This gradient is almost used in a simple stochastic gradient descent algorithm to find weights that minimize the error. Back propagation may have practical problems of getting trapped in local minima and knowing when the procedure has converged. It is important to note that back propagation networks are necessarily multilayer perceptrones usually with one input, one hidden, and one output layer. Generally, BP neural network as a classifier model is simple to use, but this model works as a black box.

Figure 7.17 illustrates the architecture of the back propagation neural network, as the learning has two phases.

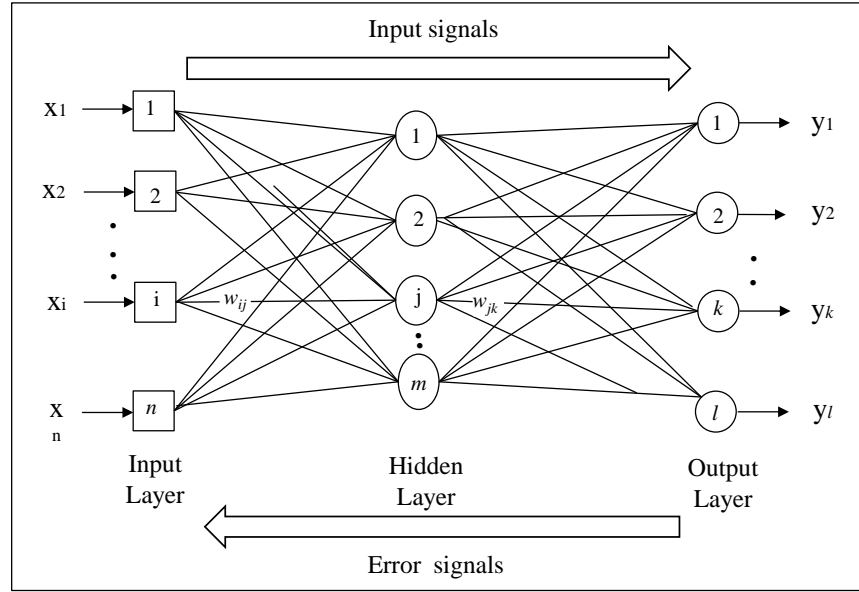


Figure 7.17: The architecture of the Back Propagation Neural Network.

First, a training input pattern is presented to the network input layer. The network then propagates the input pattern from layer to layer until the output pattern is generated by the output layer. If this pattern is different from the desired output, an error is calculated and then propagated backwards through the network from the output layer to the input layer. The weights are modified as the error is propagated. As in the above figure the inputs signal pattern $(x_1 \ x_2 \ \dots \ x_n)$ are propagated through the network from the left to right, and the error signal $(e_1 \ e_2 \ \dots \ e_n)$ from the right to the left. The neuron determines its output in a manner including two stages. First, it computes the net weighted input as [202]:

$$X = \sum_{i=1}^n x_i w_i - \theta \quad (7.15)$$

Where n is the number of inputs, and θ is the threshold to the neuron. Next, this input value is passed through the activation function as a sigmoid activation function:

$$Y = \frac{1}{1 + e^{-x}} \quad (7.16)$$

The derivative of this function is easy to compute and guarantees that the neuron output is bounded between 0 and 1. The error signal at the output of neuron k at iteration p is defined by:

$$e_k(p) = y_{d,k}(p) - y_k(p) \quad (7.17)$$

Where $y_{d,k}(p)$ is the desired output of neuron k at iteration p . After this, for example, neuron k which is located in the output, is supplied with a desired target. Hence, straightforward procedure is used to update weight w_{jk} . The rule for updating weights layer at the output layer according to the following equation:

$$w_{jk}(p+1) = w_{jk}(p) + \Delta w_{jk}(p) \quad (7.18)$$

Where $w_{jk}(p)$ is the weight between neuron j in the hidden layer and neuron k in the output layer at iteration p , and the $\Delta w_{jk}(p)$ is the weight correction.

The aforementioned procedure is employed in the current research to find the most accurate pattern which achieves the lower ratio of the training error using the BP neural network.

7.7 Conclusion

This chapter described the general experimental setup of this research work. It described the elements and stages used to implement the experimental condition monitoring systems, including CNC milling machine, workpiece materials, cutting tools, sensors installation, surface roughness measurements, software and the data acquisition system. Correspondingly, it also presented the sensor types and their position focusing on cutting tools. The signal processing methods and artificial intelligence recognition system have been illustrated.

Different types of signals, including force, accelerometer (vibration), AE, strain, eddy current, sound and power are used to obtain the information about the process. Roughness tester is also used in experiments to measure the quality of the machined surface. To extract the Sensory Characteristic Features (SCFs) for the design process of the monitoring system, time and frequency domain signal processing methods are used. The most appropriate sensory features are chosen by the ASPSF approach to be introduced to the pattern recognition system to identify process faults. For data analysis, unsupervised neural network, Learning Vector Quantisation (LVQ) is implemented to explore the relation between the investigated variables. Two types of pattern recognition system, Taylor's Equation Induced Pattern (TIP) and back propagation neural network, are used in this investigation to categorise process states independently.

Chapter 8 Initial Evaluation of ASPSF Approach

8.1 Introduction

This chapter describes the initial evaluation and implementation of the Automated Sensor and Signal Processing Selection for Fixturing (ASPSF) approach. In this chapter, it is outlined how the ASPSF approach can be utilised to develop a sensor fusion model of a condition monitoring system to detect the effect of the changes of the fixturing setup on the condition monitoring system design. The details of the ASPSF approach is introduced using different types of fixturing materials combined with gradual tool wear depending on multi-sensor signals during a milling operation. This chapter uses force, strain, accelerometer, acoustic emission, sound sensors to examine the suitability of the ASPSF condition monitoring. It covers the main stages of the ASPSF approach, the Association Matrix (ASM) and the Eigenvalue Sensory Matrix (EVSM) of the wear test, the sensitivity detection, the selection of the most sensitive SCFs and PCFs for a condition monitoring system, and the cost of the implemented monitoring system. The implementation of the ASPSF approach will answer the following questions:

1. What is the effect of the changes in fixturing on the machining signals and hence the design of the monitoring system?
2. What is the relationship between ASPSF approach and PCA for detection of sensitive information?
3. Can the surface finish be predicted from the sensor signals (Cutting force)?

The essential principles of the ASPSF approach are diagrammed in Figure 8.1. It is designed to systematically relate the sensory signal and the signal processing methods created to the faults which are to be detected taking into consideration the fixturing setup.

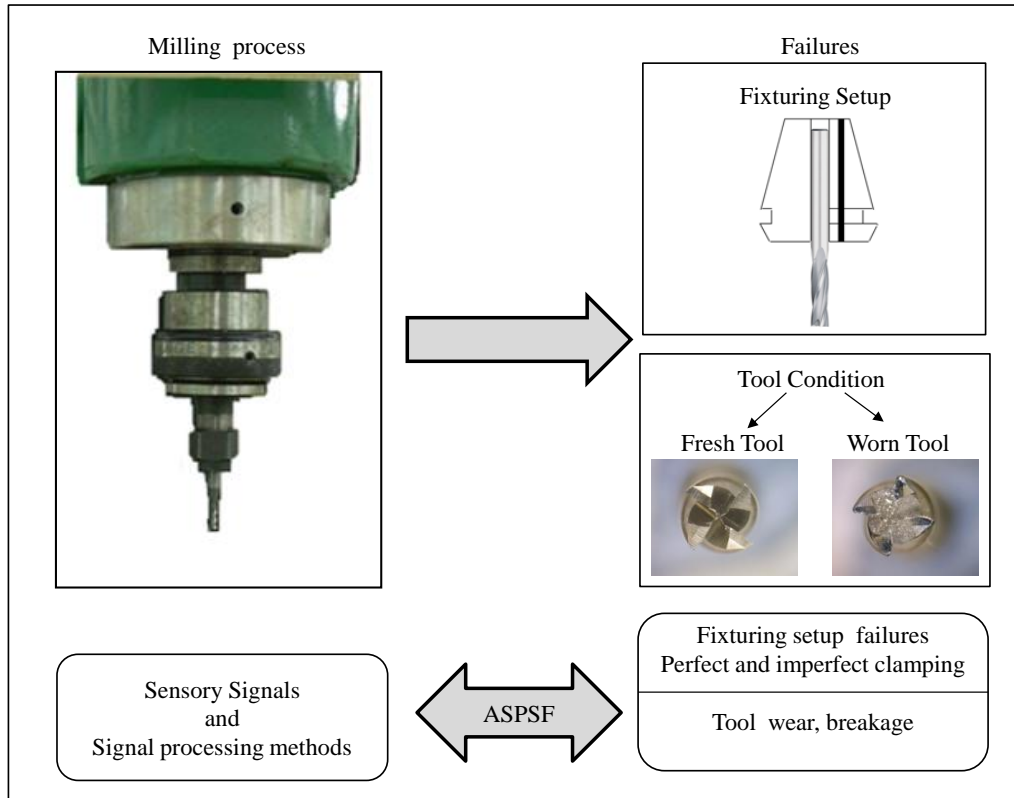


Figure 8.1: The essential principles of the ASPSF approach.

8.2 The Experimental work

In this chapter, the experimental work is conducted to examine the behaviour of the signals for different fixturing types, material and monitor tools status (fresh and worn), and then to find the most sensitive sensory characteristic features to fixturing and tool failures. As illustrated in Figure 8.2, the experimental work of the condition monitoring system of this study is performed on a milling CNC machine type (DENFORD). Several sensory signals are used in this study including cutting forces (F_x , F_y and F_z), strain, accelerometer (Vwy), acoustic emission sensor (AE), and microphone (Mic) for measuring sound. The force signals are monitored using 3-component dynamometer (Kistler 9257A) and the work piece is fixed on the dynamometer. The dynamic and quasistatic force signals are monitored using a strain sensor (Kistler 9232A). Both the force dynamometer and the strain sensor are connected to a 4-channel charge amplifier (Kistler 5070A). The AE sensor (Kistler 8152b111) is attached to the workpiece to monitor AE signals transmitted during machining and connected to AE coupler (Kistler 5125B). The accelerometer (B&K4366) are mounted on the moveable table of machine and connected to charge

amplifier (Kistler 5001). Sound signals are collected using a microphone (EM400) placed in direct vicinity of the workpiece. All the wires and cables of the sensors are connected to a National instrument connection box (SCB-100). The signals are monitored using data acquisition card NI PCI-6071E from National Instrument using special data acquisition software written using the National Instrument (Lab windows/ CVI) programming package. The experimental work is performed on milling machine using Aluminium workpiece. The milling process is carried out at the conditions as shown in the Table 8.1.

Table 8.1: The machining parameters of the milling process.

Machining condition	Specifications
Feed rate	250 mm/min
Depth of cut	0.22 mm
Coolant type	No coolant (Dry)
Spindle speed	2490 RPM
Diameter of tool	3 mm
Material of tool	Solid Carbide (End mill Solid Carbide)
Type of tool	End mill Tool (4 Flutes, Uncoated)

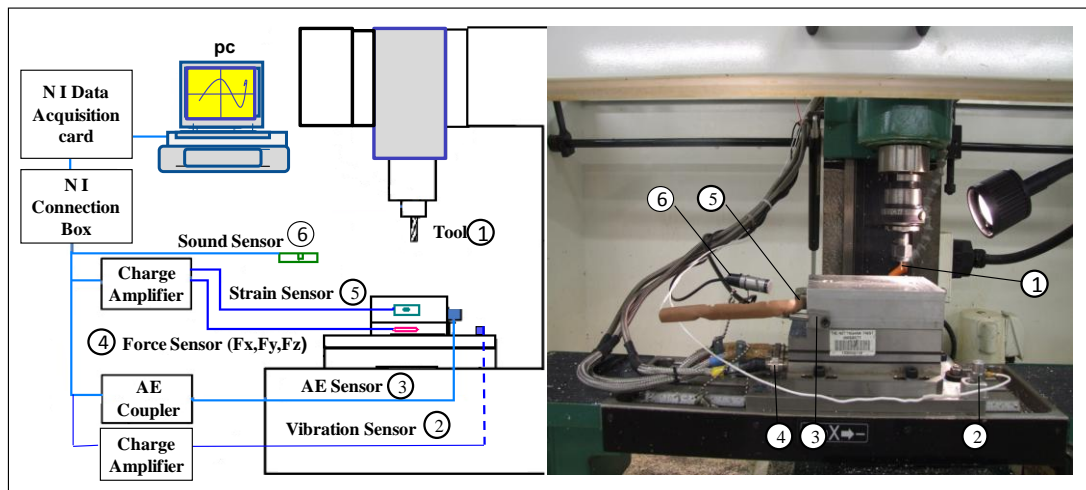


Figure 8.2: Schematic diagram of experimental setup for the monitoring system.

To emulate a fixturing system with low rigidity, the shank of the tool is covered by rubber with thickness of 1 mm as shown in Figure 8.3 where the tests start with a fresh tool and finished with completely worn tool.

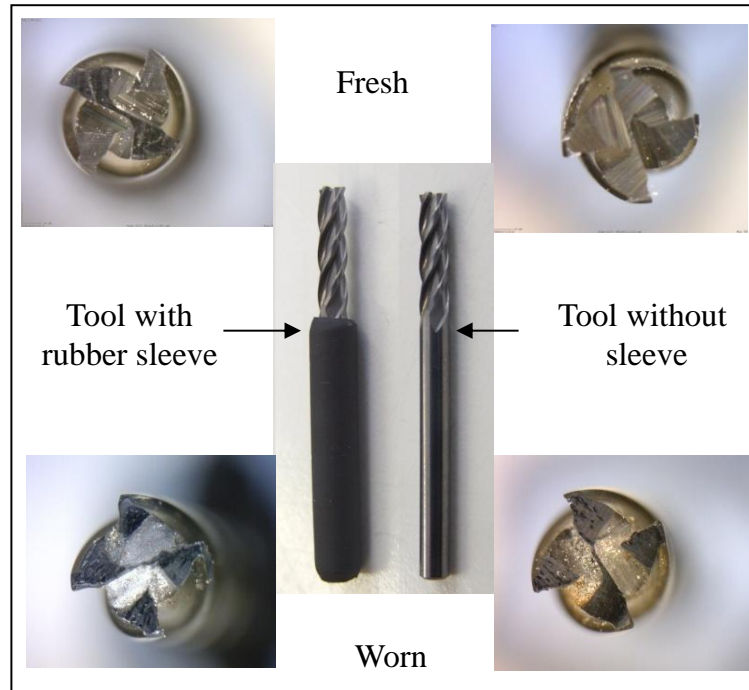


Figure 8.3: The two states of the milling tool (fresh and worn tool).

8.3 Signal Simplifications

One of the complex machining processes is milling, and it is assumed that complex sensory signals presented as a function of time as shown in Figure 8.4 and Figure 8.5. It can be noticed that the author assumed that the process starts with a healthy condition (fresh tool), and gradually or suddenly the state of the process changes with an introduced fault (worn tool). Previous researchers [20] used the visual inspection as a signal simplification method to evaluate the performance of the sensors, but the limitation of this method it is not automated and depends on the experience of the inspector. It is relatively clear these machining signals have been found difficult to predict the most sensitive signals to fixturing rigidity and tool wear directly from the unprocessed data.

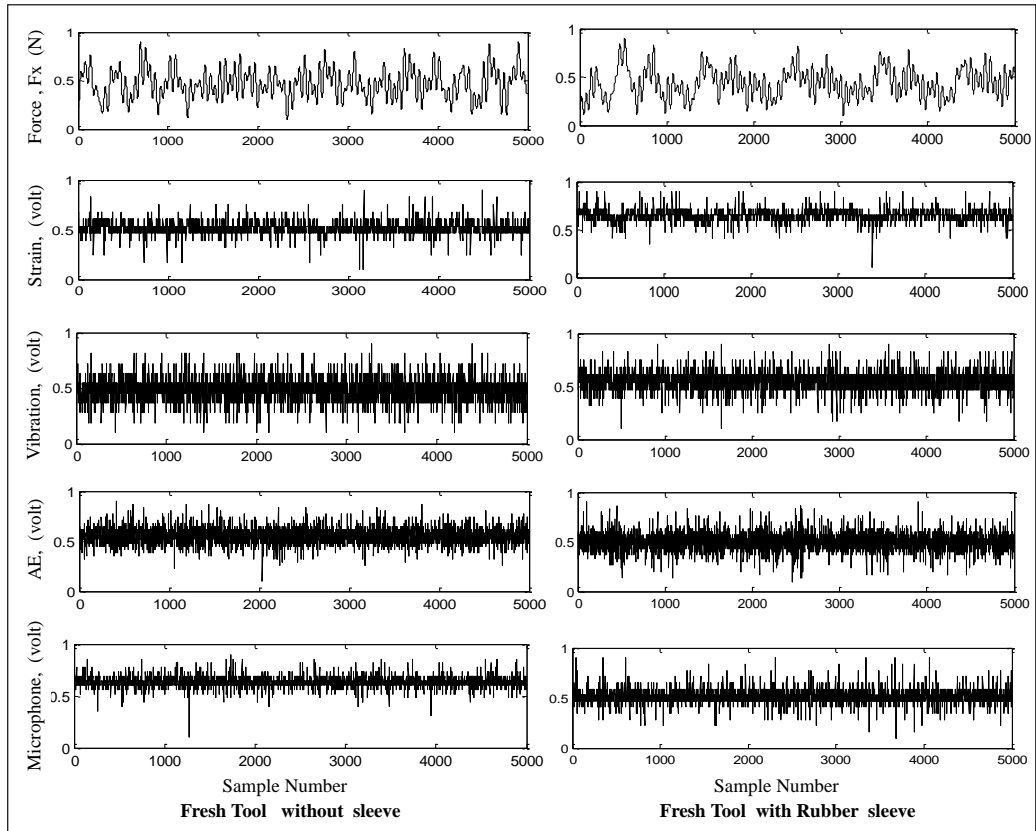


Figure 8.4: Example of the raw signals of the milling for fresh tool (normalised).

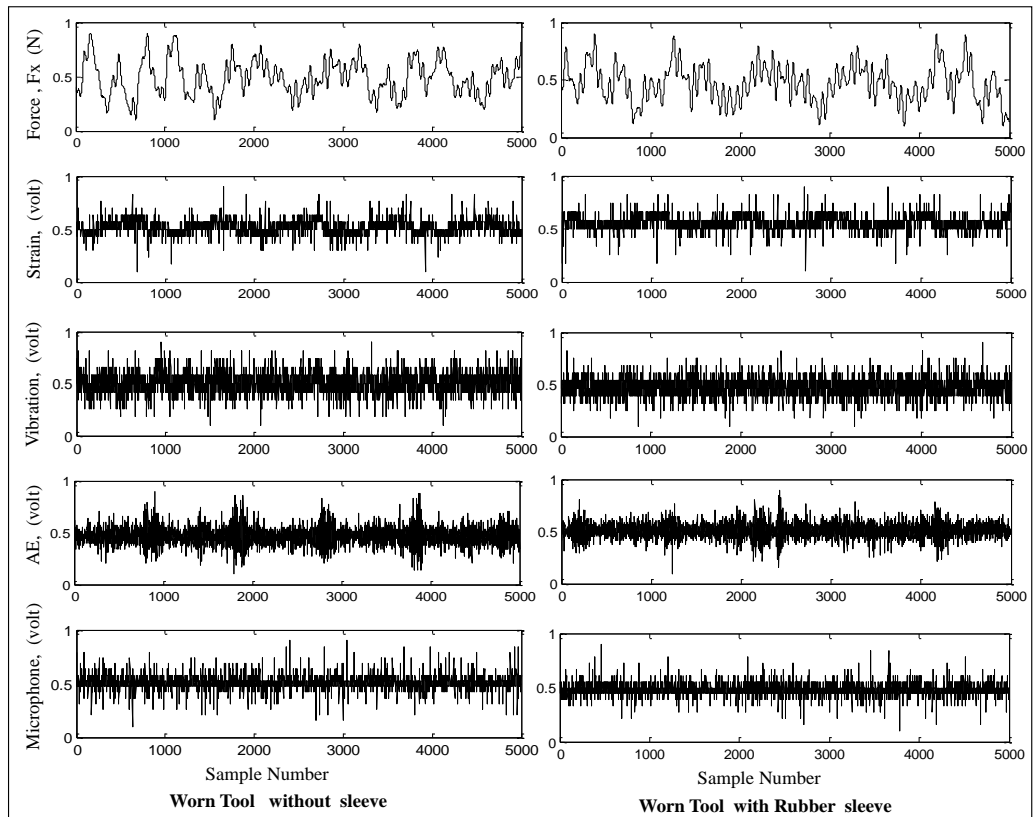


Figure 8.5: Example of the raw signals of the milling for worn tool (normalised).

It can be observed from Figures 8.4 and 8.5 that the vibration amplitude of some signals has increased for the worn tool, as in the cutting forces signals. In addition, the level of some sensory signals has changed such as the acoustic emission (AE) signal. It may be difficult to assess the state of the process from the produced signal, therefore the first step is to transfer signals from its complex form into a group of simplified sensory signals denoted Sensory Characteristic Features (SCFs). For example, if a milling process sensory signal can be transformed into a group of SCFs with relatively simple nature with less variation, then it is expected to be much easier to retrieve the necessary information which presents the state of the process based on the change in the level of the extracted SCFs. Another indicator of signal simplification is Principal Component Feature (PCF) which is obtained by using the Principal Component Analysis (PCA) method as described in the following sections. A sensitive SCF or PCF is a feature which includes a significant amount of information regarding the condition of the process. This should lead to better recognition. The sensitivity of the SCFs and PCFs respectively for this experimental work in this chapter is evaluated by the following methods:

1. Linear Regression (LR) method.
2. Principal Component Analysis (PCA) method.

8.3.1 Linear Regression (LR) method

In order to reduce the cost and development time, the automated design method of condition monitoring systems will be used along with multisensors and features extraction to select the most appropriate sensor and its associated signal processing methods in order to reduce cost and development time. Therefore, in this section the practical steps of the ASPSF approach for the same eight (Fx, Fy, Fz, strain, Vwy, AE, AERMS, and Mic) sensory signals are described. The theoretical ideas of the ASPSF approach are presented in Chapter 6. Briefly, assuming that the monitoring system has m number of sensory signals which can be processed by n number of signal processing methods to produce a sensory characteristic features (SCFs). For example, a sensory characteristic feature extracted from the std value of the Fx sensory signal can be presented as SCF (Fx, std). The sensory feature matrix (SFM) can be calculated for every set of signals, or machining samples, during the

machining process. For any sensory characteristic feature, it is possible to study its behaviour in relation to fixturing setup and tool status.

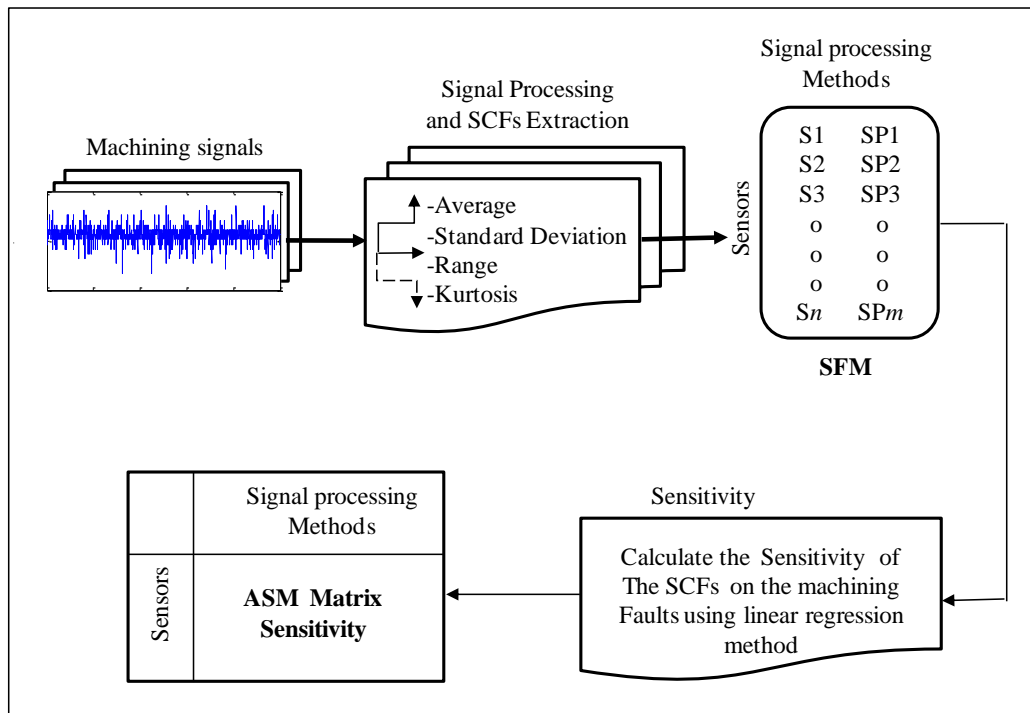


Figure 8.6: The practical steps of the ASPSF approach using linear regression.

A schematic diagram of the practical steps of the ASPSF approach is utilised in Figure 8.6. The sensory signals are simplified and processed to give specific sensory characteristic features arranged in the SFM which can be used to calculate the sensitivity of every feature on tool conditions. The sensitivity coefficients are then arranged in the Association Matrix (ASM) for further analysis. After calculating the sensitivity of each sensory characteristic feature on the machining conditions, tool status level in this case, another matrix is constructed. The ASM is a matrix which associates the obtained sensitivity values for the corresponding sensory features. It gives a simple presentation of the sensitivity values associated with each feature. The sensitivity coefficient of the machining feature is obtained using the machining signal of the sensor and the signal processing method. The ASM gives the key evaluation for the most appropriate sensor and signal processing method to be used since each column is associated with a signal processing method while each row is associated with a sensor. Therefore, the sensory characteristic features with relatively high sensitivity coefficient are the most sensitive to the cutting conditions

and they are the most appropriate features to be used. Therefore, the related sensory signals and signal processing methods are the most appropriate ones to use.

Since the importance of a feature is in its relative value compared to others, a normalising process is performed using equation 8.1 below so that any sensory characteristic feature will have a value between 0.1 and 0.9 making it possible to compare all calculated sensory features relative to each other [175]. There is no specific reason for using this type of normalising and any other normalising values could be used. The only reason is that such values are expected to have better effect on the classification systems [170]. Also, in order to be able to compare the sensitivity of SCFs of this test with the sensitivity of SCFs in similar tests, all features are normalised using the same equation [188].

$$x = 0.1 + \frac{0.8}{\max - \min} (x_i - \min) \quad (8.1)$$

Where:

max: is the maximum value of a sensory characteristic feature.

min: is the minimum value of a sensory characteristic feature.

Then, the raw signals are processed using several time domain signal processing methods to extract the Sensory Characteristic Features (SCFs). The signal processing methods used are maximum (max), minimum (min), standard deviations (*std*), the average (μ), the range, the skewness (skew), kurtosis value (*K*) and power as explained in Chapter 7. The 8 signal processing methods are used to process the 8 sensory signals to construct an Association Matrix (ASM) of (8 × 8) which allows the investigation of 64 sensory characteristic features (SCFs) for the design of the monitoring system. The SCFs are arranged according to their sensitivities to tool status based on the absolute slope of the linear regression method as shown in Figure 8.7. Figures 8.7, 8.8 present examples of high, medium and low-sensitivity SCFs to tool wear for two types of fixturing sleeve materials, namely steel (without sleeve) and rubber sleeve respectively.

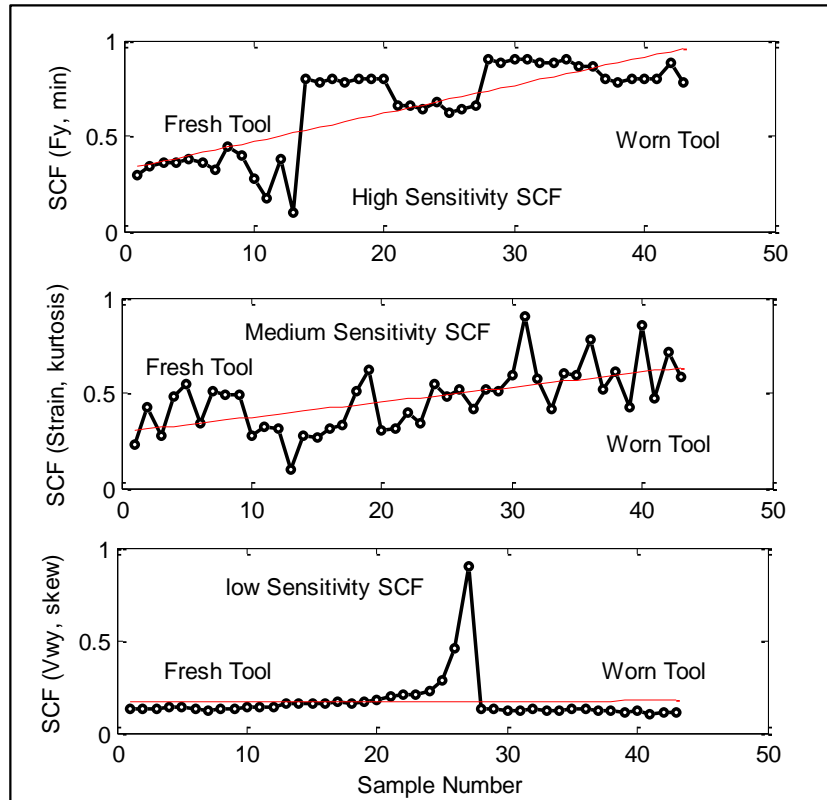


Figure 8.7: Example of high, medium and low sensitivity SCF for the tool without sleeve.

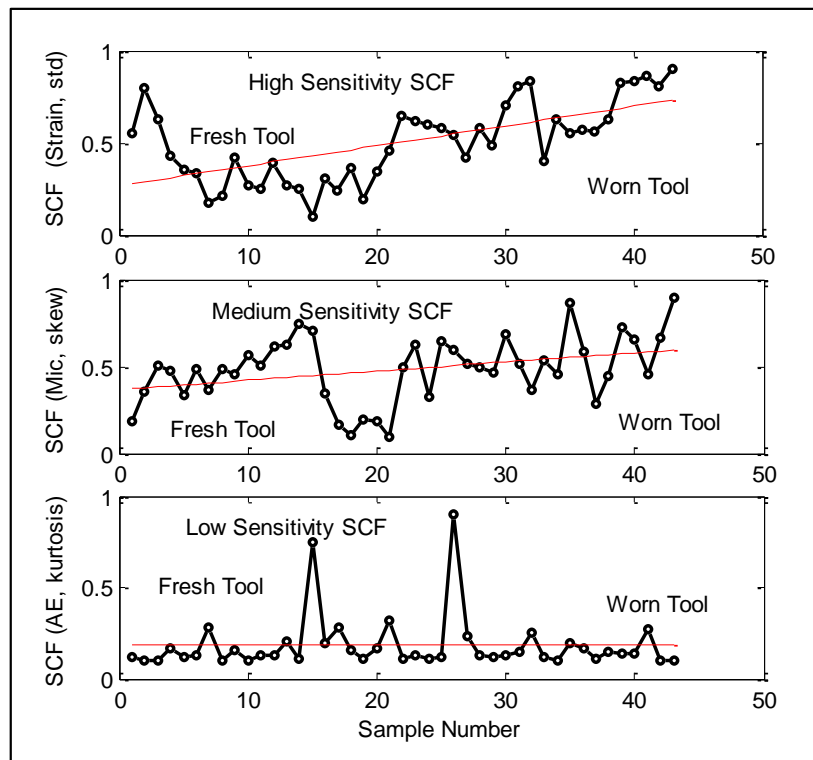


Figure 8.8: Example of high, medium and low sensitivity SCF for the tool with rubber sleeve.

The SCFs are visually inspected and it has been found that SCFs with high absolute slope show higher sensitivity to the fault. The above figures present examples of the highest and lowest sensitive SCFs for this particular tool wear test where sensitivity values are the linear regression slope of the normalised features. The whole SCFs are arranged to create the Association Matrix (ASM) for the tool without sleeve as shown in Table 8.2. This matrix will provide an opportunity to visually inspect the sensitivity of the all used sensors.

Table 8.2: The Associated matrix of the system for tool without sleeve.

Sensor	Signal Processing Method							
	max	min	std	power	average	skew	kurtosis	range
Fx	0.048	0.415	0.257	0.323	0.637	0.111	0.120	0.379
Fy	0.450	0.701	0.528	0.043	0.650	0.014	0.287	0.610
Fz	0.406	0.214	0.242	0.124	0.129	0.005	0.490	0.450
Strain	0.060	0.171	0.324	0.294	0.254	0.040	0.422	0.229
Vwy	0.154	0.155	0.052	0.264	0.155	0.012	0.030	0.044
AE	0.242	0.301	0.364	0.303	0.027	0.362	0.131	0.270
AERMS	0.447	0.373	0.422	0.295	0.385	0.182	0.029	0.415
MIC	0.070	0.014	0.082	0.049	0.136	0.146	0.023	0.043

Figure 8.9 presents images of the Association Matrix (ASM) which includes the sensitivity of a few SCFs implemented in this monitoring system. The ASM presents for each sensor and signal processing method (SCF) the sensitivity to detect the machining faults, where high sensitivity indicates high capability to detect the fault. The numbers with small value in Table 8.2 show in black in the images in Figure 8.9. This mean low sensitivity, numbers with medium values are shown in red which means medium sensitivity, and numbers with high values are shown in white which means high sensitivity.

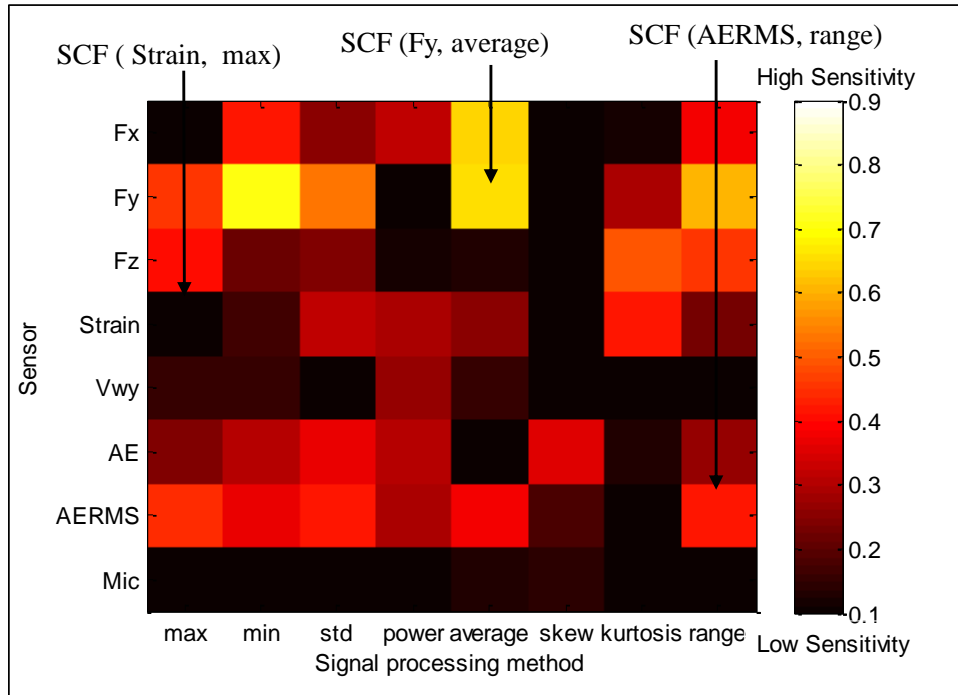


Figure 8.9: A graphical presentation of the sensitivity for tool without sleeve.

By using the same methodology to create the ASM matrix for the tool without sleeve, Table 8.3 presents the values of the sensory sensitivity for all features of the system to monitor the tool with rubber sleeve. Similarly, this table is used to present the images of the sensitivity as shown in Figure 8.10.

Table 8.3: The Associated matrix of the system for tool rubber sleeve.

Sensor	Signal Processing Method							
	max	min	std	power	average	skew	kurtosis	Range
Fx	0.260	0.082	0.182	0.243	0.473	0.132	0.053	0.188
Fy	0.567	0.577	0.015	0.276	0.589	0.032	0.126	0.018
Fz	0.021	0.108	0.005	0.004	0.008	0.052	0.033	0.024
Strain	0.383	0.153	0.553	0.275	0.283	0.543	0.304	0.445
Vwy	0.113	0.110	0.248	0.159	0.111	0.050	0.548	0.102
AE	0.066	0.009	0.071	0.060	0.454	0.000	0.004	0.047
AERMS	0.022	0.299	0.058	0.018	0.096	0.037	0.140	0.015
MIC	0.404	0.398	0.551	0.560	0.004	0.294	0.492	0.455

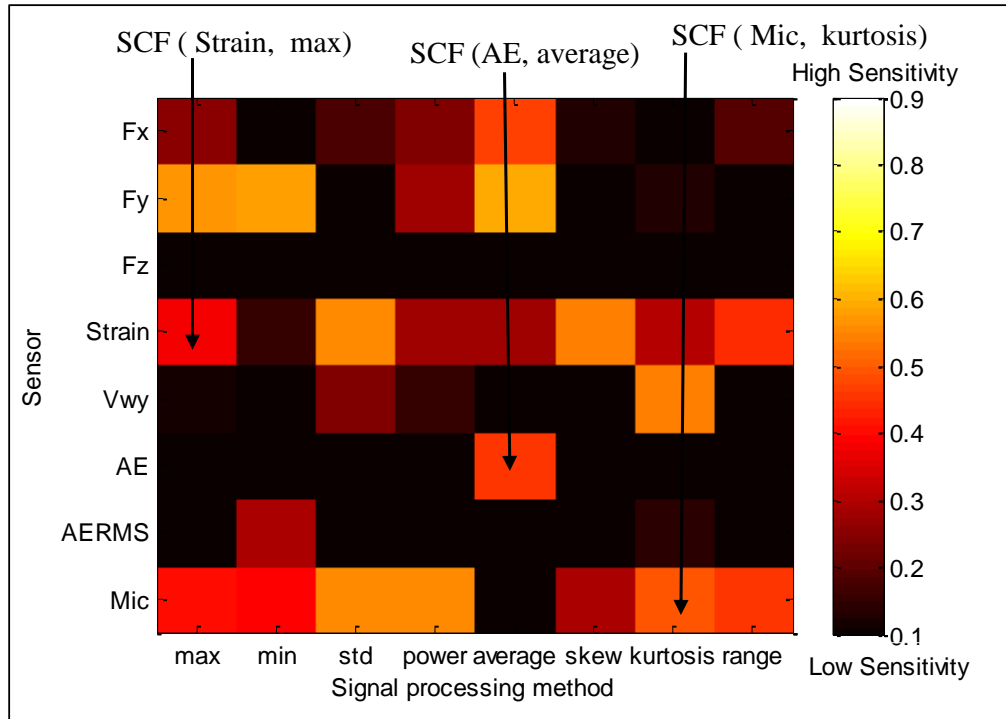


Figure 8.10: A graphical presentation of the sensitivity for tool with rubber sleeve.

It can be noticed from Figures 8.9, 8.10 that the change in the characteristic of the fixturing system has caused change in the most sensitive sensors and signal processing systems that can be used to detect tool wear. For example, with normal fixturing system, force signals (Fy) and force (Fx) are found to be the most sensitive to detect tool wear. However, with the rubber sleeve system, force sensor (Fy) and sound signals are found to be the most sensitive signals to detect tool wear.

8.3.2 Principal Component Analysis (PCA) method

One of the difficulties inherent in multivariate statistics is the problem of visualizing data that has many variables. Some of the software, such as Matlab, can be used to display a graph of the relationship between two or three. But when there are more than three variables, it is more difficult to visualise their relationships.

Generally, in data sets with many variables, groups of variables often move together. One reason for this is that more than one variable might be measuring the same driving principle governing the behaviour of the system. In many systems there are only a few such driving forces. But an abundance of instrumentation enables you to measure dozens of system variables. When this happens, it is can be simplified the problem by replacing a group of variables with a single new variable.

Principal component analysis is a quantitatively rigorous method for achieving this simplification. The method generates a new set of variables, called Principal Components Analysis (PCA). Each principal component is a linear combination of the original variables. All the principal components are orthogonal to each other, so there is no redundant information. The principal components as a whole form an orthogonal basis for the space of the data. The first principal component is a single axis in space. When you project each observation on that axis, the resulting values form a new variable, and the variance of this variable is the maximum among all possible choices of the first axis. The second principal component is another axis in space, perpendicular to the first. Projecting the observations on this axis generates another new variable. The variance of this variable is the maximum among all possible choices of this second axis.

By examining plots of these few new variables, researchers often develop a deeper understanding of the driving forces that generated the original data.

In general, the raw data does not make enough sense without processing analysis, and according to the above basis, it is suitable to use the principle component in this research, due to the fact that it is necessary to show the effect of the variables on the data, this will provide the researcher the ability to determine which variable (e.g. sensor) is more effective to detect the changes during the machining operation. The theoretical concept of the principal component has described in the previous chapter.

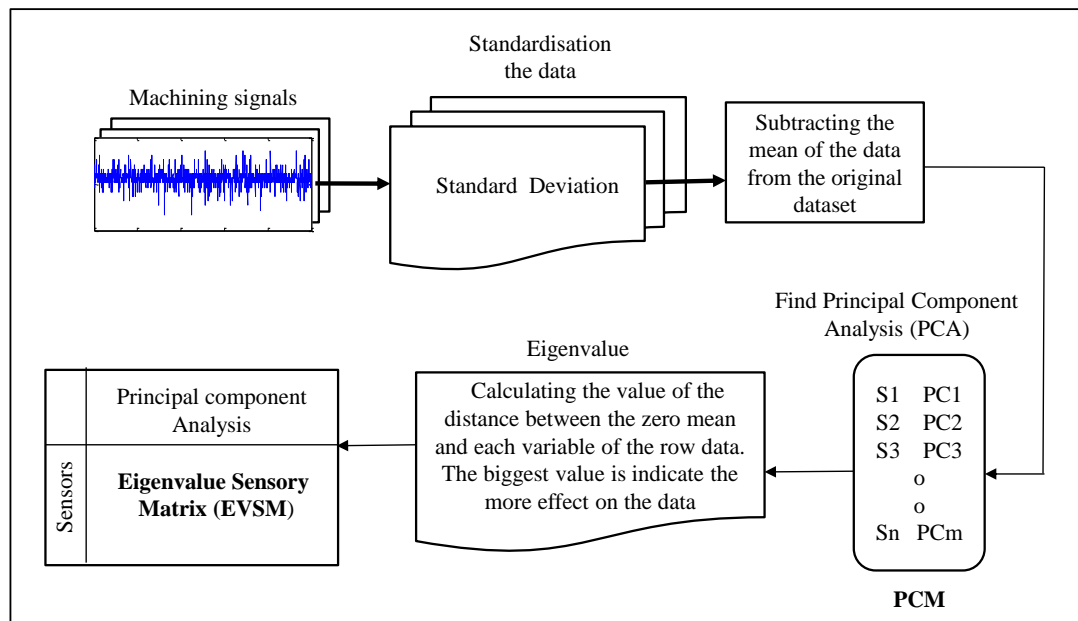


Figure 8.11: The practical steps of the ASPSF approach using PCA.

Figure 8.11 explains the practical steps of implementing the principal component analysis. The raw data is the same which was used in the previous section. The first step is arranged the raw data to be more appropriate, which mean that the variables are measured in the same unit. Standardising the data is often preferable when the variables are in different units. The normalisation the data by dividing each column by its standard.

The second step, and for PCA to work properly, it is important to subtract the mean from each of the data dimensions. The mean subtracted is the average across each dimension. Therefore, all the values have (the mean of the values of all the data points) subtracted, and all the values have subtracted from them. This produces a data set whose mean is zero as shown in Figure 8.12.

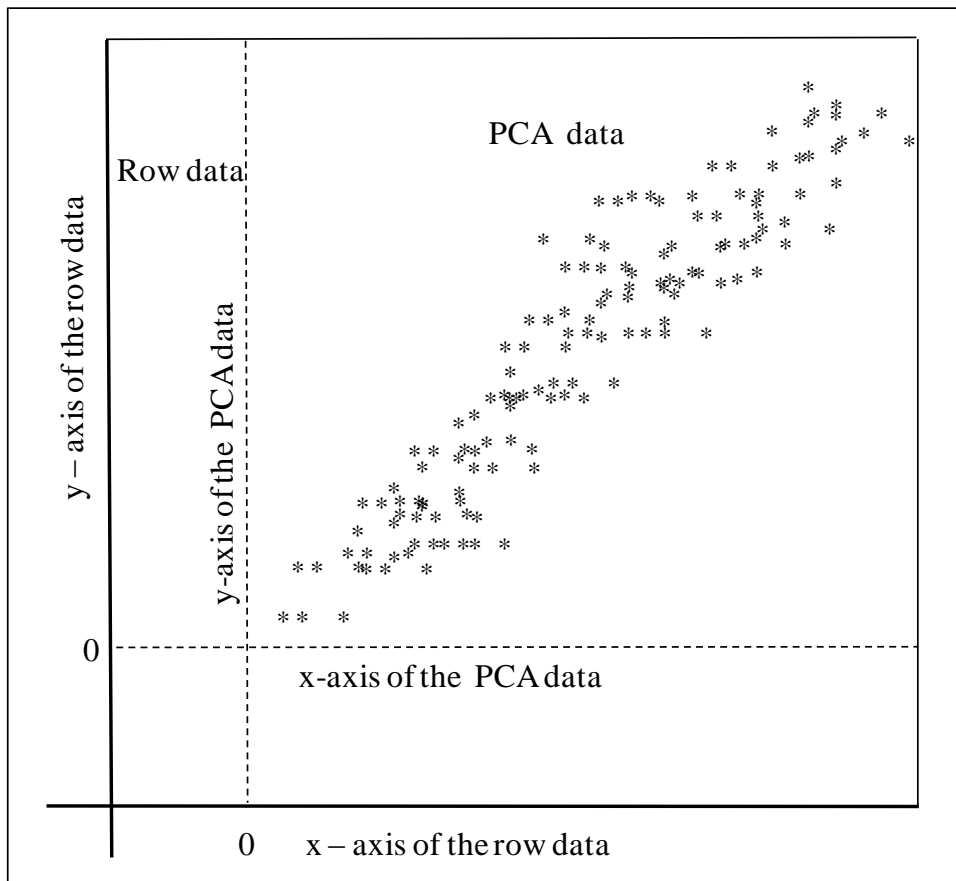


Figure 8.12: PCA example data, original data on the left, data with the means subtracted on the right, and a plot of the data.

In the third step, the covariance will be calculated, as explained in the Chapter 7. Covariance is always measured between two dimensions. Consequently, as a data set with more than 2 dimensions, there is more than one covariance measurement that

can be calculated. For example, from a 3 dimensional data set (dimensions x, y, z), it could be calculated cov (x, y), cov (x, z) and cov (y, z). Basically, the dimension of the data equals to the number of data variables, hence, for an (n) dimensional or variable data set; it is possible to calculate different covariance values as in the following equation:

$$\text{Number of covariance values} = \frac{n}{(n-2) \times 2} \quad (8.2)$$

Where: n is the number of variable of the row data.

A useful way to get all the possible covariance values between all the different variables is to calculate them all and put them in a matrix. In the current research, it is called Principal Component Matrix (PCM). This matrix with n row and n column, so it is a squared matrix and arranged as follows:

$$\text{PCM}^{n \times n} = [\text{cov}(X_i, X_j)_{n \times n}] \quad (8.3)$$

Where

X_i is the first variable (first sensor).

X_j is the second variable (second sensor).

In the following equation (8.4), there is an example of how to calculate the covariance for three accelerometer sensors (Fx, Fy, and Fz). The first value in the PCM matrix is obtained from the covariance between first sensor (Fx) and itself, and the second value resulted from the covariance between the second sensor (Fy) and first one (Fx), and so on. Therefore, as eight sensors used in this research, the whole dimensions of the PCM matrix is (8 x 8).

$$\text{PCM}^{3 \times 3} = \begin{bmatrix} \text{cov}(F_x, F_x) & \text{cov}(F_x, F_y) & \text{cov}(F_x, F_z) \\ \text{cov}(F_y, F_x) & \text{cov}(F_y, F_y) & \text{cov}(F_y, F_z) \\ \text{cov}(F_z, F_x) & \text{cov}(F_z, F_y) & \text{cov}(F_z, F_z) \end{bmatrix} \quad (8.4)$$

A covariance is created the PCA more effective in ASPSF for calculating the relation between the variables of data, and this provides the proposed method more support than linear regression which depends on measure the sensitivity for each variable (sensor) individually.

The fourth step is implemented by calculating the eigenvectors and eigenvalues for the PCA matrix since it is square. The concept of the eigenvector and eigenvalue is defined in chapter 7. This gives the components in order of significance. To be precise, if you originally have n variables in the row data, and so you calculate n eigenvectors and eigenvalues. Eigenvector determine the location of the variables on the n - variables space, meanwhile the eigenvalues evaluate the distance between the variable and the mean zone. In general, once eigenvectors are found from the covariance matrix, the next step is to order them by eigenvalue, highest to lowest. That is meaning the eigenvector with the large eigenvalue is pointed as the most significant relationship between the data variables.

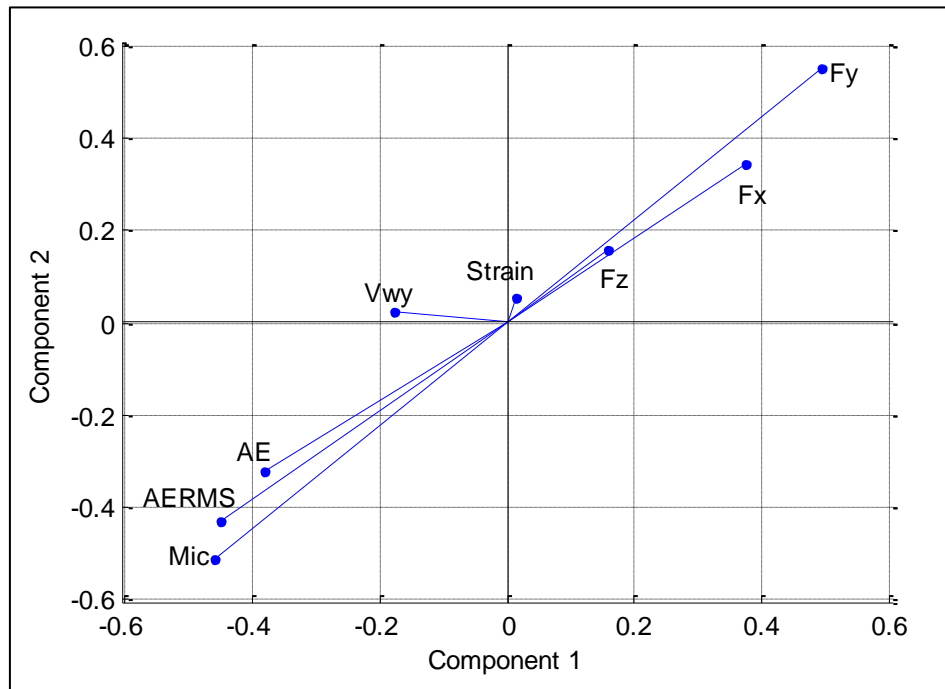


Figure 8.13: A plot of the principle components according to eigenvalue of variables in the covariance matrix for tool without sleeve.

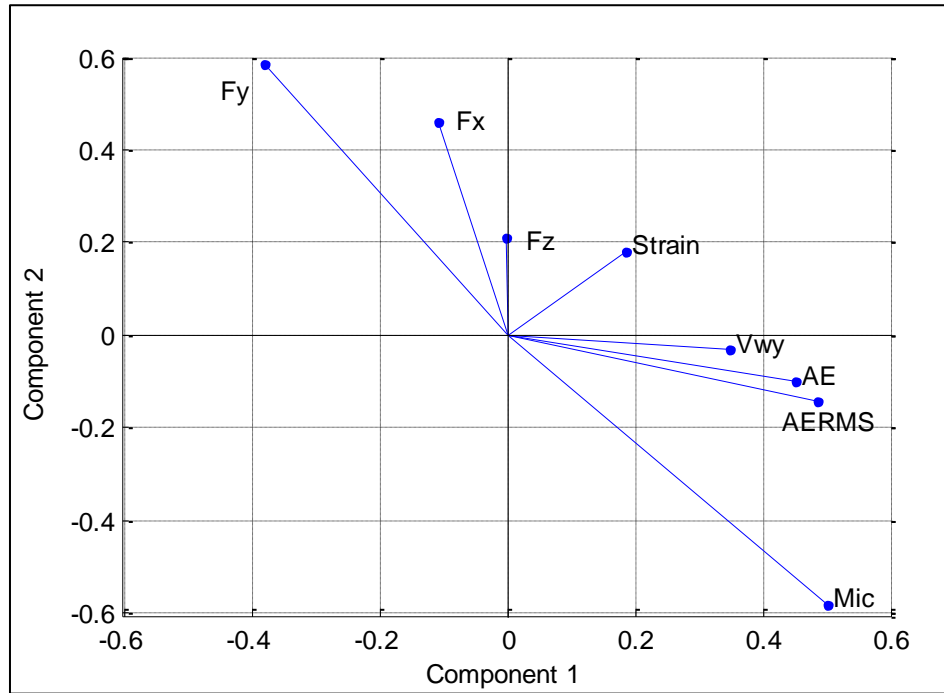


Figure 8.14: A plot of the principle components according to eigenvalue of variables in the covariance matrix for tool with rubber sleeve.

Figures 8.13 and 8.14 illustrate the application of the above procedure in this research, and visually show that the force sensor (Fy) has the maximum eigenvalues for tool without sleeve, and tool with rubber sleeve. This means that the force sensor is most sensitive to the changes of the machining process for both cases. Sound sensor (Mic) is also achieved the second most sensitive sensor in both cases. Aforementioned figures display the variables in two dimensions and there is ability to show the results in three dimensions.

In the final step, all eigenvalues are arranged in a matrix, where the sensors in the column, and principal components in the row. This matrix is called Eigenvalue Sensory Matrix (EVSM) as shown in Table 8.4, and it is assumed to ignore the sign of the eigenvalue which is indicate the position of the variable due to the investigation depends on the value not on the sign. This will create a matrix similar with that one constructed in the linear regression (ASM). In the current research, the first and two principal components (PC1 and PC2) will be used because they are most accurate and relate to the original data.

Table 8.4: The Eigenvalue Sensory Matrix (EVSM) of the system for tool without sleeve.

Sensor	Principal component Analysis							
	PC1	PC2	PC3	PC4	PC5	PC6	PC7	PC8
Fx	0.412	0.704	0.563	0.611	0.768	0.693	0.781	0.579
Fy	0.318	0.872	0.298	0.423	0.051	0.391	0.225	0.010
Fz	0.020	0.092	0.150	0.208	0.022	0.182	0.006	0.153
Strain	0.404	0.053	0.105	0.182	0.024	0.171	0.031	0.014
Vwy	0.405	0.011	0.101	0.254	0.049	0.142	0.045	0.013
AE	0.407	0.026	0.212	0.270	0.138	0.049	0.166	0.027
AERMS	0.410	0.042	0.285	0.300	0.139	0.031	0.184	0.080
Mic	0.411	0.105	0.651	0.380	0.604	0.006	0.524	0.730

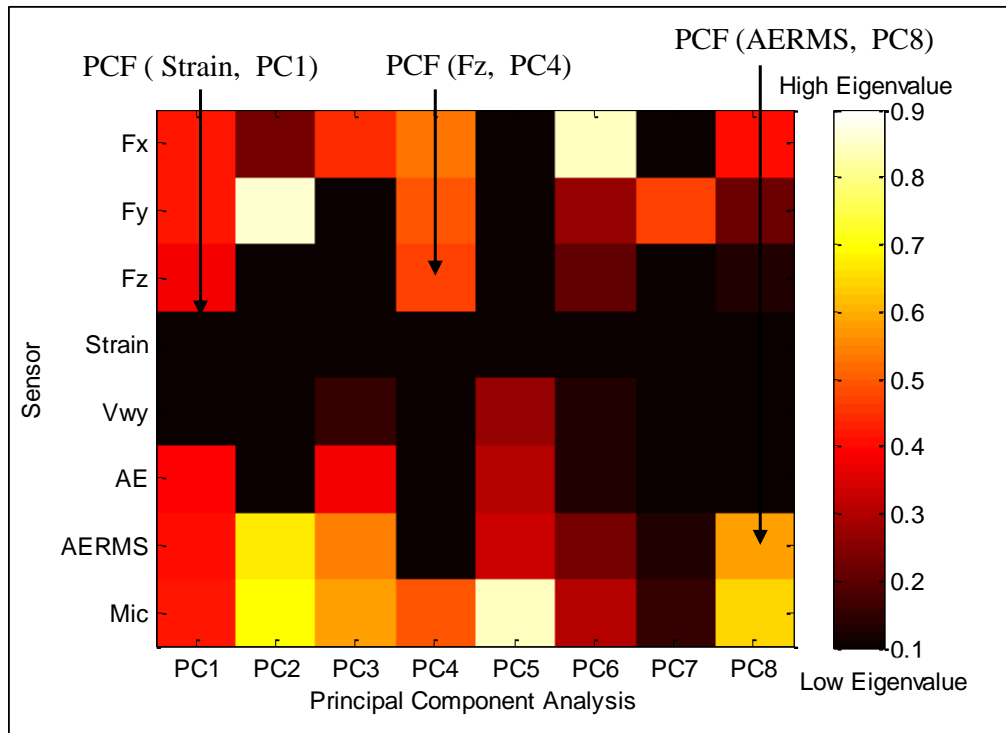


Figure 8.15: A graphical presentation of the EVSM for tool without sleeve.

Figure 8.15 shows the image of the eigenvalue sensory matrix (EVSM) for the tool without sleeve, where the high value is presented in white, while the low eigenvalue in black. It is possible to consider the eigenvalue of the PC as a feature for each sensor; therefore, the each sensor in each PC will has Principal Component Feature (PCF). In the above figure, it can be seen that the feature of the force sensor (Fz) in the fourth principal component (PC4) is PCF(Fz, PC4), and it is same for the strain

sensor in first principal component which is PCF(Strain, PC1) and so on. However, the PCF(Fy, PC2) is the most sensitive feature for the tool without sleeve.

For the tool with rubber sleeve, Table 8.5 presents the eigenvalue matrix in the same arrangement for the sensor and the principal component.

Table 8.5: The Eigenvalue Sensory Matrix (EVSM) of the system for tool with rubber sleeve.

	Principal component Analysis							
Sensor	PC1	PC2	PC3	PC4	PC5	PC6	PC7	PC8
Fx	0.423	0.229	0.443	0.530	0.089	0.840	0.112	0.409
Fy	0.423	0.850	0.031	0.490	0.044	0.268	0.465	0.217
Fz	0.379	0.010	0.029	0.466	0.026	0.205	0.108	0.137
Strain	0.012	0.009	0.005	0.084	0.035	0.015	0.064	0.105
Vwy	0.012	0.018	0.152	0.007	0.268	0.129	0.013	0.047
AE	0.398	0.098	0.385	0.023	0.307	0.133	0.051	0.040
AERMS	0.402	0.669	0.547	0.093	0.336	0.227	0.137	0.580
Mic	0.423	0.690	0.575	0.496	0.842	0.306	0.154	0.644

Similarly, the procedure for the image of the tool without sleeve, Figure 8.16 presents the visual matrix of the sensor and the principal component. The feature for the force sensor (Fy), for instance, in the second principal component (PC2) and it will obtain the PCF(Fy, PC2), also the feature for the acoustic emission sensor (AE) in the fourth principal component (PC4) is PCF(AE, PC4). However, it can be seen that the force (Fy) and sound signals are the most sensitive signals for the tool with rubber sleeve to detect tool wear.

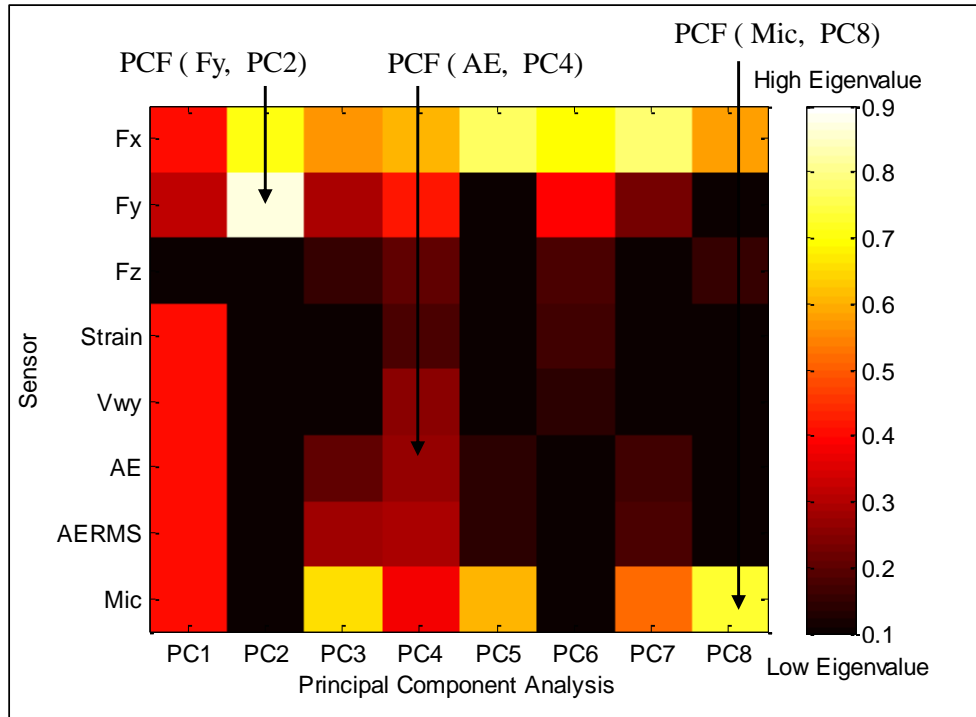


Figure 8.16: A graphical presentation of the EVSM for tool with rubber sleeve.

8.3.3 Correlation between LR slope and PCA methods

The correlation coefficient is a quantity that gives the quality of a least squares fitting to the original data or to define the relation between two cases [186]. In this research, it is used to calculate the relation between the sensor sensitivity using linear regression and the sensitivity using Principal Component Analysis (PCA). The calculation process correlation is started by preparing the required data from the ASM matrix and covariance matrix. Figure 8.17 shows the practical steps of calculation the correlation coefficient between the sensitivity and principal component. Where the ASM matrix using linear regression is constructed from the 8 signal processing methods as a column and 8 sensors as a row, therefore it is possible to measure the average of the sensitivity values for each sensor individually. All the 8 sensitivity average values for the sensors will be putted in one column.

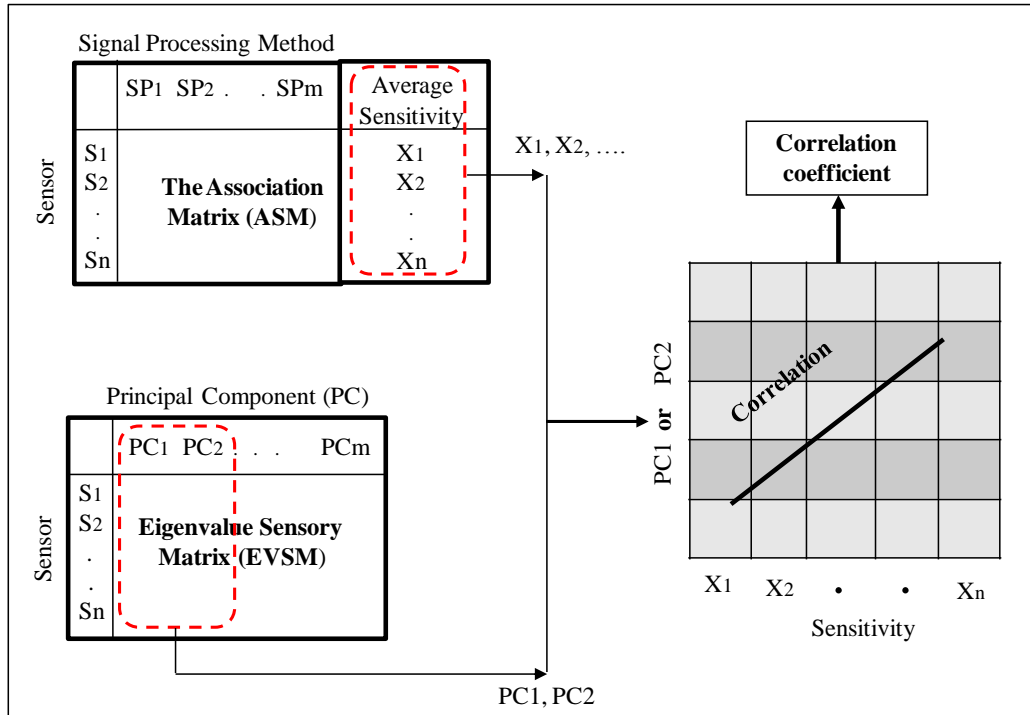


Figure 8.17: The practical steps of calculating the correlation coefficient between sensitivity and PC.

With regard to the covariance matrix using PCA and as described in the previous section this matrix is squared matrix and constructed from the 8 principal components and 8 sensors as a row with same sequence as in ASM matrix use linear regression. As the principal components are arranged in order of significance, the first and two principal components (PC1 and PC 2) will be used in this research. Each principal component has eigenvalues for eight sensors, and this value determines the sensor significant which qualified to the sensor sensitivity. Consequently, the correlation coefficient will be calculated from the relationships between the sensitivity of the sensors and the PC1, PC2 individually as will be illustrated in the following Figures.

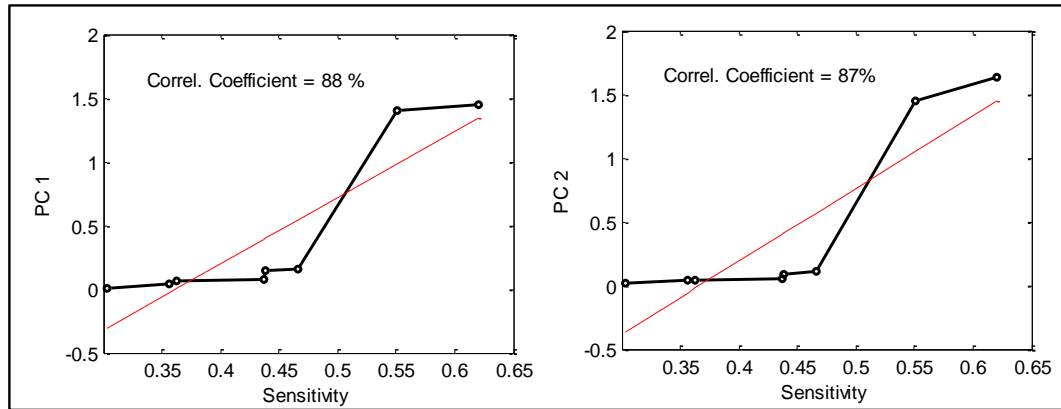


Figure 8.18: The correlation coefficient between PCA and Linear regression sensitivity for tool without sleeve.

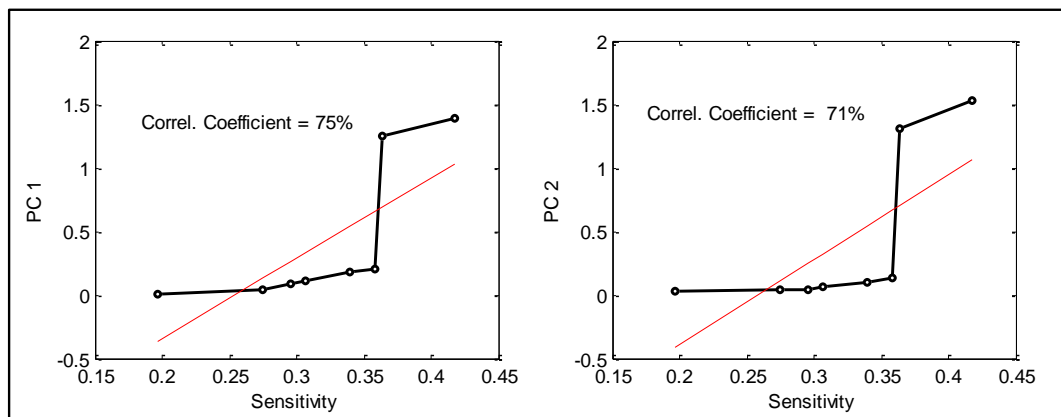


Figure 8.19: The correlation coefficient between PCA and Linear regression sensitivity for tool with rubber sleeve.

Figures 8.18, 8.19 show the correlation coefficient between the sensitivity using linear regression and the sensitivity using the PCA for tool without sleeve, tool with rubber sleeve respectively. In Figure 8.18, this relationship has been plotted for the tool without sleeve, and the correlation coefficient between the mean sensitivity and first principal component (PC1) is 88%, meanwhile it is 87% between the sensitivity and second principal components (PC2). The correlation coefficient for the tool with rubber sleeve is much lower than for the tool without sleeve, where it is 75%, for sensitivity and PC1, whereas the relationship between sensitivity and PC2, it is 71% as shown in Figure 8.19.

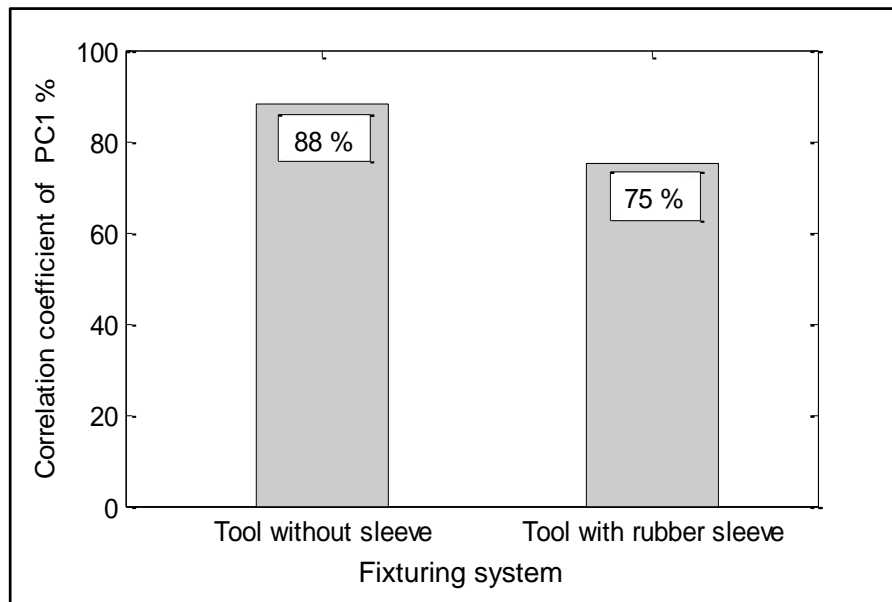


Figure 8.20: The relation between the correlation coefficient of PC1 and fixturing system.

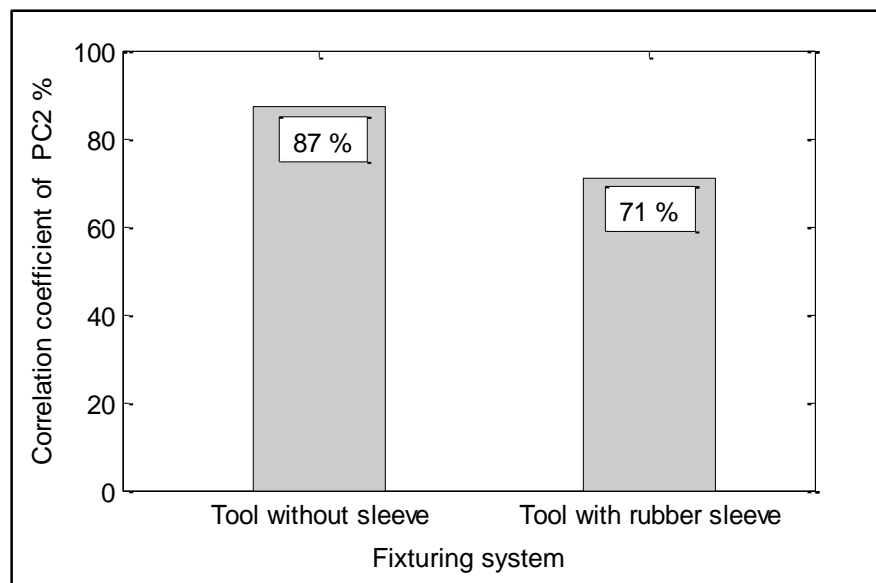


Figure 8.21: The relation between the correlation coefficient of PC2 and fixturing system.

Figure 8.20 shows the concluding relationships between the correlation coefficient of PC1 and the fixturing systems (both types of tools, with and without sleeve). Where the bar chart proves the aforementioned findings as the correlation decreased with the used material less rigidity (less modulus of elasticity) as the maximum correlation for the tool without sleeve (88%), following by the tool with rubber sleeve (75%) respectively. Figure 8.21 presents similar results for the correlations of

PC2, where they are (87%, 71%) for the tool without sleeve and the tool with rubber sleeve. From the analysis and above figures, it is can be concluded that the fixturing type and material could play a significant role in the result of sensitivity level.

8.4 Selection of Sensory Features

8.4.1 Selection of Sensory Characteristics Features (SCFs)

In order to assist the classification system to be fast implemented and to provide useful classification, it has been decided based on previous applications of the ASPS approach (turning process) [20] to base the application and the design of the ASPSF condition monitoring system of this test on a set of 10 SCFs. The sensory characteristic features are grouped into 3 systems, with 10 features in each. A Matlab computer program is used to arrange the ASM features according to the absolute Linear Regression (LR) and arrange every 10 as a separate system. The three systems have the average sensitivity as shown in Figure 8.22 and Figure 8.23 for the tool without sleeve and tool with rubber sleeve. It can be observed that the first system has the most sensitivity features for fixturing system stability and tool wear detection compared to the other systems.

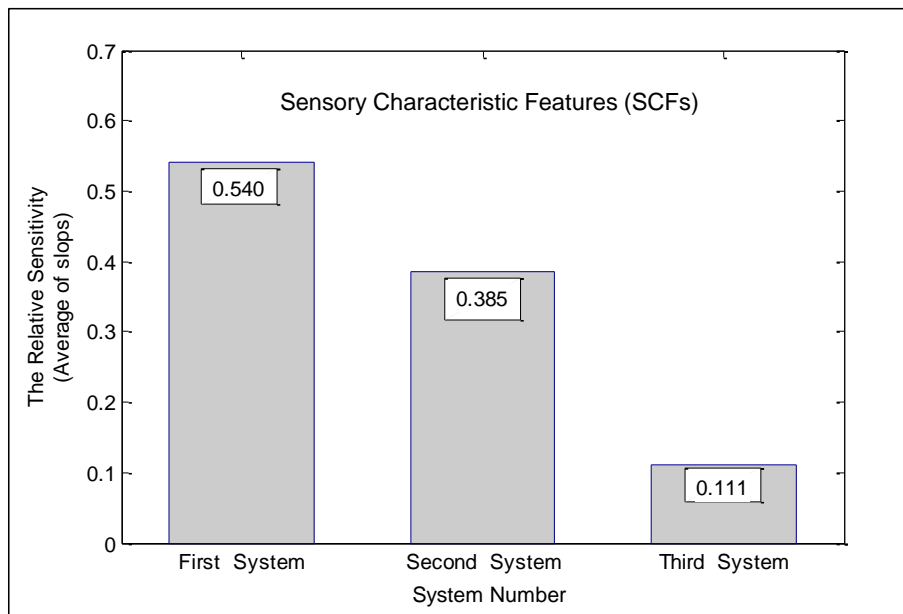


Figure 8.22: Comparison between the systems sensitivity of tool without sleeve.

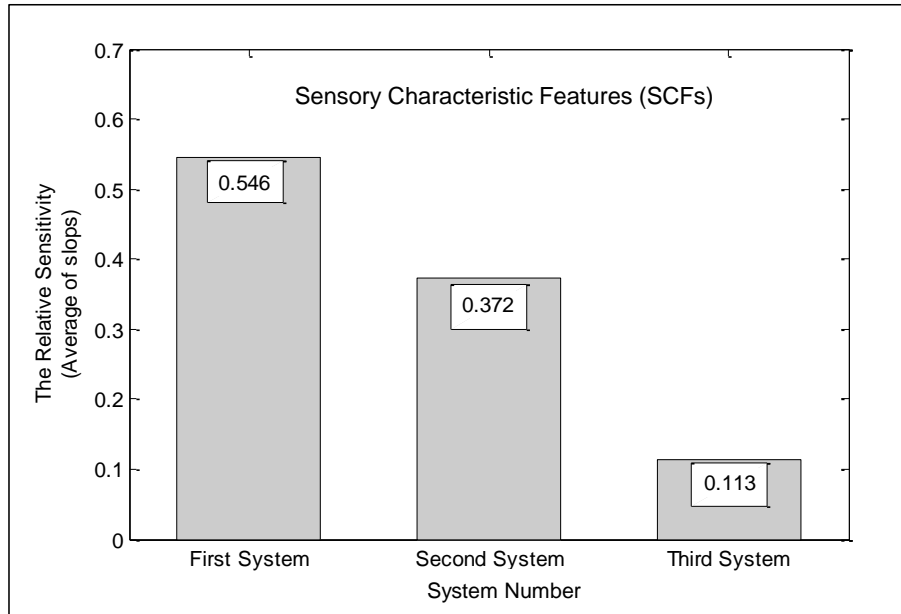


Figure 8.23: Comparison between the systems sensitivity of tool with rubber sleeve.

The first system which contains the most sensitive 10 features is shown in Table 8.6 for both types of tools (normal and with rubber sleeve). In addition, Table 8.7 shows the next 10 features and Table 8.8 shows the least sensitive 10 feature to detect fixturing quality and tool wear.

The first system is found to have relative sensitivity (LR average of 0.540, 0.546) which are much more than the average sensitivity of the second. In addition, the third system is found to have the lowest sensitivity for the detection of the fixturing stability and tool wear.

Table 8.6: First system with the SCFs sensitivity (LR) slope for the both tools.

Tool without sleeve			Tool with rubber sleeve		
Sensory Signal	Signal Processing method	Sensitivity (LR slope)	Sensory Signal	Signal Processing method	Sensitivity (LR slope)
Fy	Minimum	0.701	Fy	Average	0.589
Fy	Average	0.651	Fy	Minimum	0.577
Fx	Average	0.638	Fy	Maximum	0.567
Fy	Range	0.611	Mic	Power	0.560
Fy	Std	0.528	Strain	Std	0.553
Fz	Kurtosis	0.490	Mic	Std	0.551
Fy	Max	0.451	Vwy	Kurtosis	0.548
Fz	Range	0.451	Strain	Skew	0.543
AERMS	Max	0.447	Mic	Kurtosis	0.492
AERMS	Std	0.423	Fx	Average	0.473
Average		0.540	Average		0.546

Table 8.7: Second system with the SCFs sensitivity (LR) slope for both tools.

Tool without sleeve			Tool with rubber sleeve		
Sensory Signal	Signal Processing method	Sensitivity (LR slope)	Sensory Signal	Signal Processing method	Sensitivity (LR slope)
Strain	Kurtosis	0.423	Mic	Range	0.455
Fx	Minimum	0.416	AE	Average	0.454
AERMS	Range	0.415	Strain	Range	0.445
Fz	Maximum	0.406	Mic	Maximum	0.404
AERMS	Average	0.385	Mic	Minimum	0.398
Fx	Range	0.379	Strain	Maximum	0.383
AERMS	Minimum	0.373	Strain	Kurtosis	0.304
AE	Std	0.365	AERMS	Minimum	0.299
AE	Skew	0.362	Mic	Skew	0.294
Vwy	Std	0.325	Strain	Average	0.283
Average		0.385	Average		0.372

Table 8.8: Third system with the SCFs sensitivity (LR) slope for the both tools.

Tool without sleeve			Tool with rubber sleeve		
Sensory Signal	Signal Processing method	Sensitivity (LR slope)	Sensory Signal	Signal Processing method	Sensitivity (LR slope)
Mic	Skew	0.147	AERMS	Kurtosis	0.140
Mic	Average	0.136	Fx	Skew	0.132
AE	Kurtosis	0.131	Fy	Kurtosis	0.126
Fz	Average	0.129	Vwy	1	0.113
Fz	Power	0.124	Vwy	Average	0.111
Fx	Kurtosis	0.121	Vwy	Minimum	0.110
Fx	Skew	0.111	Fz	Minimum	0.108
Mic	Std	0.082	Vwy	Range	0.102
Mic	Maximum	0.070	AERMS	Average	0.096
Strain	Maximum	0.061	Fx	Minimum	0.082
Average		0.111	Average		0.113

As can be noticed from the above tables, the first system has the highest sensitivity, for example, the force (Fy) and minimum have the highest sensitivity (0.701) for the tool without sleeve, while the force (Fy) and average have the highest sensitivity (0.589) for the tool with rubber sleeve. The second system has a medium to high level of sensitivity and third system has the lowest sensitivity. For example, strain sensor and maximum have the lowest SCFs (0.061) for normal tool, also the force (Fx) and minimum for the other tool in the third system. Looking at the above tables,

it can be seen that the first 16 SCFs are almost the same but then the sensitivity of the other SCFs drops considerably. Therefore, the ASM matrix is found very useful in predicting the sensitivity of the SCFs. The sensitivity of the SCFs is proven to be measurable and there is a difference between the type of the sensor to detect the changes in the fixturing quality (fixturing type and material). The details of the first few SCFs structure can be used to optimise system cost without significantly affecting system performance. It is important to notice that the statement of high sensitivity means high information is based on the visual inspection of each feature and the way it behaves during the fault's development.

Therefore, a statement can be made that the average sensitivity of a system is a reflection of the expected behaviour of the system. The proof of this statement will be described in the next chapters using neural networks and Taylor's Equation Induced Pattern (TIP) classification systems.

8.4.2 Selection of Principal Component Features (PCFs)

For more reliable decision, and as sensory characteristic features (SCFs) have been used in the previous section, the principal component features (PCFs) are used to create a more useful classification. The classification depends on the same set of 10 PCFs. The principal component features are grouped into 3 systems, with 10 features in each. A Matlab computer program is also used to arrange the EVSM features according to the absolute principal component analysis (PCA) and arrange every 10 as a separate system. The three systems have the average sensitivity as shown in Figure 8.24 and Figure 8.25 for the tool without sleeve and tool with rubber sleeve. It can be detected that the first system has the most sensitivity features for fixturing system stability and tool wear detection compared to the other systems.

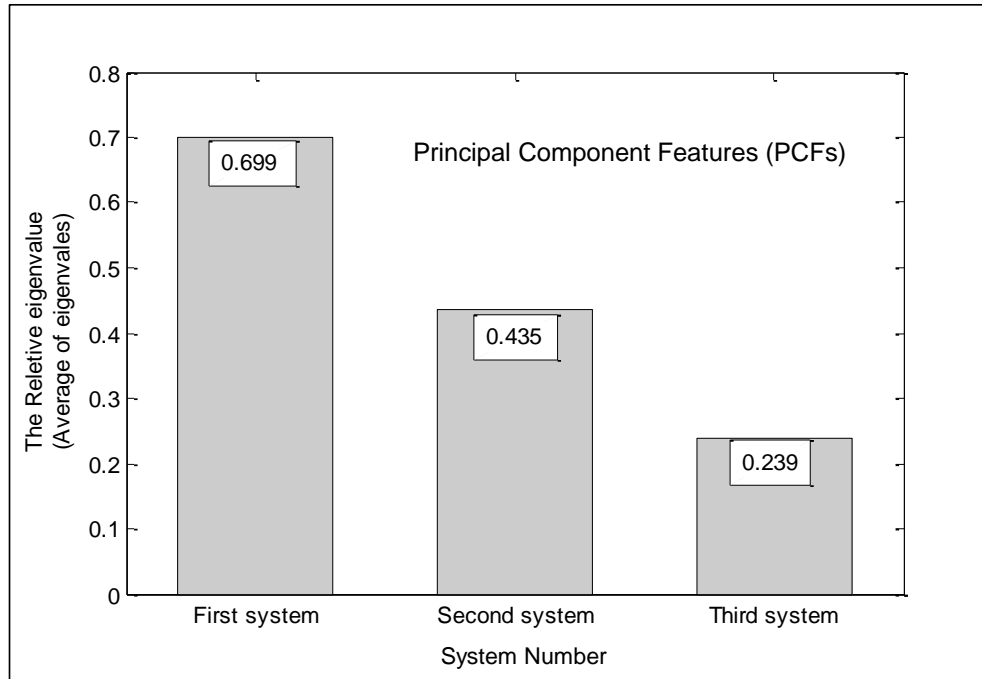


Figure 8.24: Comparison between the systems eigenvalue of tool without sleeve.

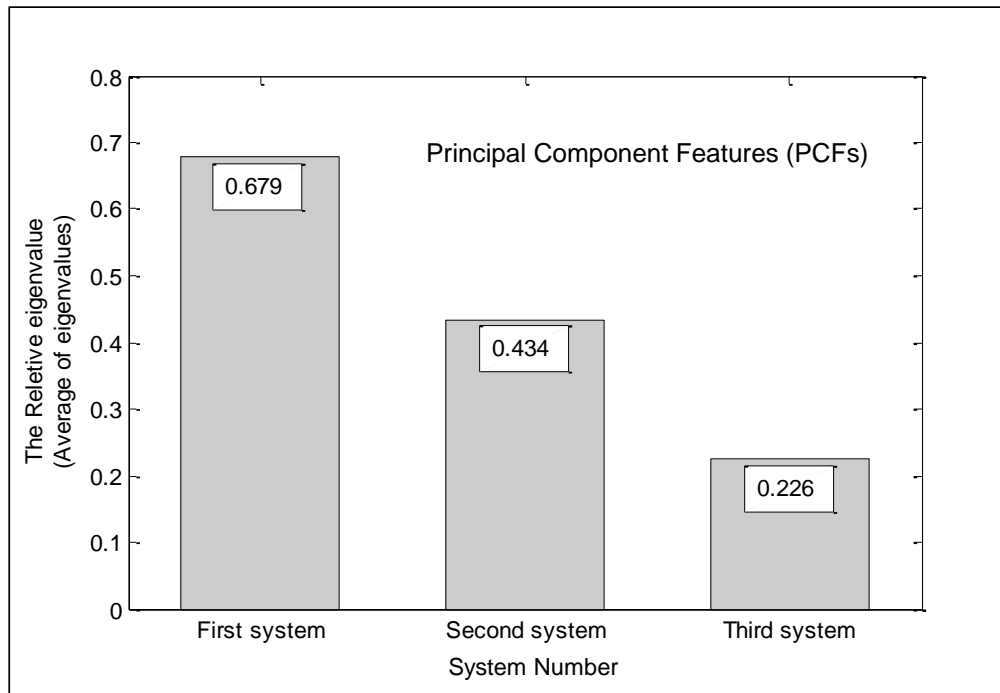


Figure 8.25: Comparison between the systems eigenvalue of tool with rubber sleeve.

The below Table 8.9 is shown the first system which contains the most sensitive 10 features for both types of tools (without and with rubber sleeve).

In addition, Table 8.10 shows the next 10 features and Table 8.11 shows the least sensitive 10 feature to detect the abnormalities of fixturing quality and tool. For both tools, the first system is found to have relative eigenvalues (Eigenvalue average of 0.699, 0.679) which are much more than the average sensitivity of the second. In addition, the third system is found to have the lowest sensitivity for the detection of the fixturing stability and tool wear.

Table 8.9: First system with the PCFs eigenvalue (PCA) for the both tools.

Tool without sleeve			Tool with rubber sleeve		
Sensory Signal	Principal Component method	Eigenvalue (PCA)	Sensory Signal	Principal Component method	Eigenvalue (PCA)
Fy	PC2	0.872	Fy	PC2	0.850
Fx	PC7	0.781	Mic	PC5	0.842
Fx	PC5	0.768	Fx	PC6	0.840
Mic	PC8	0.730	Mic	PC2	0.690
Fx	PC2	0.704	AERMS	PC2	0.669
Fx	PC6	0.693	Mic	PC8	0.644
Mic	PC3	0.651	AERMS	PC8	0.580
Fx	PC4	0.611	Mic	PC3	0.575
Mic	PC5	0.604	AERMS	PC3	0.577
Fx	PC8	0.579	Fx	PC4	0.530
Average		0.699	Average		0.679

Table 8.10: Second system with the PCFs eigenvalue (PCA) for both tools.

Tool without sleeve			Tool with rubber sleeve		
Sensory Signal	Principal Component method	Eigenvalue (PCA)	Sensory Signal	Principal Component method	Eigenvalue (PCA)
Fx	PC3	0.563	Mic	PC4	0.496
Mic	PC7	0.524	Fy	PC4	0.490
Fy	PC4	0.423	Fx	PC4	0.465
Fx	PC1	0.412	Fy	PC7	0.443
Mic	PC1	0.411	Fx	PC3	0.423
AERMS	PC1	0.410	Fy	PC1	0.423
AE	PC1	0.407	Mic	PC1	0.423
Vwy	PC1	0.405	AERMS	PC1	0.402
Strain	PC1	0.404	AE	PC1	0.398
Fy	PC6	0.391	AE	PC3	0.385
Average		0.435	Average		0.434

Table 8.11: Third system with the PCFs eigenvalue (PCA) for the both tools.

Tool without sleeve			Tool with rubber sleeve		
Sensory Signal	Principal Component method	Eigenvalue (PCA)	Sensory Signal	Principal Component method	Eigenvalue (PCA)
Mic	PC4	0.381	Fz	PC1	0.379
Fy	PC1	0.318	AERMS	PC5	0.336
AERMS	PC4	0.300	Mic	PC6	0.306
Fy	PC3	0.298	Vwy	PC5	0.268
AE	PC4	0.270	Fy	PC6	0.268
AE	PC3	0.212	Fy	PC8	0.217
Strain	PC4	0.182	Mic	PC7	0.154
Fz	PC3	0.150	Fz	PC8	0.137
Vwy	PC6	0.142	Fz	PC7	0.108
AE	PC5	0.138	AE	PC4	0.093
Average		0.239	Average		0.226

8.5 System Cost and Utilisation

The main target for the industrial approach, is implementing the project with higher performance and reduced cost possible. The ASPSF approach, adding to their ability to select the more sensitive sensor, it is could be used to minimise the cost of the condition monitoring system. According to the number and type of used sensors, the cost of the monitoring system can be easily calculated. It is vital to reduce the cost of the system by eliminating sensors which do not significantly contribute to the selected SCFs. This is achieved by removing their SCFs from the system and replacing them by SCFs which come next on the rank from sensors already in the system. This cost reduction is possible without having to significantly reduce the overall sensitivity of the system (i.e. the new SCFs should still have relatively high sensitivity). The contribution of a sensor in a system is defined as the sensor utilisation (U). The U for a sensor is defined as shown in equation 8.5:

$$U = \frac{S}{T \times P} \times 100 \quad (8.5)$$

S: number of SCFs used from the sensor.

T: total number of features in the system (10 in this case)

P: number of signals produced by the sensor (e.g. 3 for the 3-components force dynamometer, 1 for the strain, 1 for Vibration, 2 for acoustic emission, 1 for sound).

The overall sensor utilisation average factor for a system (UA) is defined as the average value of the sensor utilisation (U) of all the sensors used in the system. When removing the least used sensors in the system, it has been found that the sensor utilisation (U) factor is useful in minimising the cost of the system. The variable supposed cost of each system is calculated and compared to optimise the performance of the system related to its cost. The cost reduction process is discussed in Chapter 6, section 6.4.1. It explains and evaluates the cost reduction process with the support of the fixturing quality and tool wear experimental work. Figure 8.26 shows the sensor set-up for the experimental work in this chapter. In this work, cost means the supposed variable cost of the monitoring system since the objective is to compare systems.

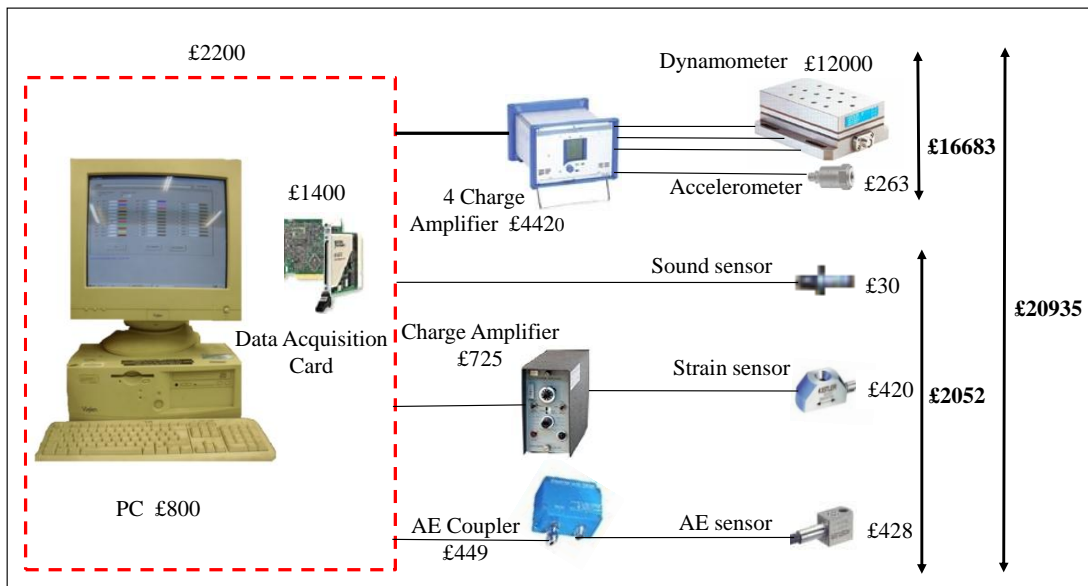


Figure 8.26: The sensor setup used to calculate the cost of the system (prices are based on quotation).

8.5.1 System Optimisation

8.5.1.1 Linear Regression (LR) method

From Tables 8.6 and 8.7, it can be observed that there is no significant difference in the average sensitivity for both systems for the tools (without and with rubber sleeves). For the tool without sleeve, the cost of the first and second systems is relatively different (£19497, £20905). But, it is still can be optimised by increasing the system utilisation by replacing the sensory characteristic features of the AE

sensor from the first system with the forces sensory signals from the second system to reduce the cost and still have the sensitivity level.

Table 8.12: Sensors utilisation for the tool without sleeve using LR.

Sensor	U 1 st system	U 2 nd system	Optimised System
Dynamometer	27%	10%	33.3%
Strain	-----	10%	-----
Vwy	-----	10%	-----
AE	10%	25%	-----
UA Average Utilisation	18.5%	13.75%	33.3%
System Cost	£19497	£20905	£18620
Average Sensitivity	0.540	0.385	0.534

As shown in Table 8.12, the overall average utilisation has increased in the first system from 18.5% up to 33.3% and from 13.75% up to 33.3% in the second system and the cost is reduced by 11% from £20935 to £18620. In addition, the average sensitivity of the system did not significantly change as can be seen in Table 8.13. In fact the average sensitivity has increased to 0.534 compared with the second system.

Table 8.13: The optimised system (1st and 2nd system) for the tool without sleeve using LR.

Tool without sleeve		
Sensory Signal	Signal Processing method	Sensitivity (LR slope)
Fy	Minimum	0.701
Fy	Average	0.651
Fx	Average	0.638
Fy	Range	0.611
Fy	Std	0.528
Fz	Kurtosis	0.490
Fy	Max	0.451
Fz	Range	0.451
Fx	Minimum	0.416
Fz	Maximum	0.406
Average		0.534

For the tool with rubber sleeve, there is significant difference between the cost of first and second systems which are (£20058, £4252). But it is still can be optimised

by increasing the system utilisation by replacing the sensory characteristic features of the strain and accelerometer sensors from the first system with the sound sensory signals from the second system to reduce the cost and still have the sensitivity level.

Table 8.14: Sensors utilisation for the tool with rubber sleeve using LR.

Sensor	U 1 st system	U 2 nd system	Optimised System
Dynamometer	13.33%	-----	13.33%
Strain	20%	40%	-----
Vwy	10%	-----	-----
AE	-----	10%	-----
Mic	30%	40%	60 %
UA Average Utilisation	18.33%	30%	36.66 %
System Cost	£20058	£4252	£18650
Average Sensitivity	0.546	0.372	0.507

As shown in Table 8.14, the overall average utilisation has increased in the first system from 25% up to 50% and from 33.33% up to 50 % in the second system and the cost is reduced by 10.9 % from £20935 to £18650. In addition, the average sensitivity of the system did not significantly change as can be seen in Table 8.15. In fact the average sensitivity has increased to 0.507 compared with the second system.

Table 8.15: The optimised system (1st and 2nd system) for the tool with rubber sleeve using LR.

Tool with rubber sleeve		
Sensory Signal	Signal Processing method	Sensitivity (LR slope)
Fy	Average	0.589
Fy	Minimum	0.577
Fy	Maximum	0.567
Mic	Power	0.560
Mic	Std	0.551
Mic	Kurtosis	0.492
Fx	Average	0.473
Mic	Range	0.455
Mic	Maximum	0.404
Mic	Minimum	0.398
Average		0.507

From Tables 8.13, 8.15, it can be seen that the average optimized sensitivity of the monitoring system for tool without sleeve is 0.534 and 0.507 for tool with rubber. The cost of the system is reduced from £20935 to £18620 for the normal tool and from £20935 to £18650 for tool with rubber sleeve. This gives an indicator that the sensitive and the cost of the monitoring system could be changed according to type of the fixturing system.

9.5.1.2 Principal Component Analysis (PCA) method

From Tables 8.9 and 8.10, it can be noticed that there is no significant difference in the average sensitivity for both systems for the tools (without and with rubber sleeves).

For the tool without sleeve, the cost of first and second systems is relatively different (£18650, £20935). But it is still can be optimised by increasing the system utilisation by replacing the principal component features of the sound sensor from the first system with the forces sensory signals from the second system to reduce the cost and still have the eigenvalue level.

Table 8.16: Sensors utilisation for the tool without sleeve using PCA.

Sensor	U 1 st system	U 2 nd system	Optimised System
Dynamometer	23.3%	13.3%	33.3%
Strain	-----	10%	-----
Vwy	-----	10%	-----
AE	-----	10%	-----
Mic	30%	20%	
UA Average Utilisation	26.6%	12.66%	33.3%
System Cost	£18650	£20935	£18620
Average Eigenvalue	0.699	0.435	0.641

As shown in Table 8.16, the overall average utilisation has increased in the first system from 26.6 % up to 33.3% and from 12.66% up to 33.3% in the second system and the cost is reduced by 11% from £20935 to £18620. In addition, the average eigenvalue of the system did not significantly change as can be seen in Table 8.17. In fact the average eigenvalue has increased to 0.641 compared with the second system.

Table 8.17: The optimised system (1st and 2nd system) for the tool without sleeve using PCA.

Tool without sleeve		
Sensory Signal	Principal Component method	Eigenvalue (PCA)
Fy	PC2	0.872
Fx	PC7	0.781
Fx	PC5	0.768
Fx	PC2	0.704
Fx	PC6	0.693
Fx	PC4	0.611
Fx	PC8	0.579
Fx	PC3	0.563
Fy	PC4	0.423
Fx	PC1	0.412
Average		0.641

For the tool with rubber sleeve, the cost of both systems is the same (£19795). However, it is still can be optimised by increasing the system utilisation by replacing the principal component features of the AE sensor from the first system with the sound and force sensory signals from the second system to reduce the cost and still keep the reliable eigenvalue level.

Table 8.18: Sensors utilisation for the tool with rubber sleeve using PCA.

Sensor	U 1st system	U 2nd system	Optimised System
Dynamometer	10%	16.66%	16.66%
Strain	-----	-----	-----
Vwy	-----	-----	-----
AE	15%	15%	-----
Mic	40%	20%	50%
UA Average Utilisation	21.66%	17.22%	33.33%
System Cost	£19795	£19795	£18650
Average Eigenvalue	0.679	0.434	0.642

As illustrated in Table 8.18, the overall average utilisation has increased in the first system from 21.66% up to 33.33% and from 17.22% up to 33.33 % in the second system and the cost is reduced by 10.9% from £20935 to £18650. In addition, the

average eigenvalues of the system did not significantly change as can be seen in Table 8.19. In fact the average sensitivity has increased to 0.642 compared with the second system.

Table 8.19: The optimised system (1st and 2nd system) for the tool with rubber sleeve using PCA.

Tool with rubber sleeve		
Sensory Signal	Principal Component method	Eigenvalue (PCA)
Fy	PC2	0.850
Mic	PC5	0.842
Fx	PC6	0.840
Mic	PC2	0.690
Mic	PC8	0.644
Mic	PC3	0.575
Fx	PC4	0.530
Mic	PC4	0.496
Fy	PC4	0.490
Fx	PC4	0.465
Average		0.642

8.5.1.3 System optimisation correlation using LR slope and PCA

In the previous sections, the sensory system optimisation is implemented using different methods, namely, Linear Regression (LR) and Principal Component Analysis (PCA). However, it can be seen that there is significant similarity between two methods to reduce the cost of the monitoring system to detect the changes of the fixturing stability or tool wear occurred.

From Tables (8.12, 8.14, 8.16 and 8.18), it can be observed that the selected sensor for the tool without sleeve is dynamometer in both used methods (LR slope and PCA), whereas, the dynamometer and sound sensors are the selected sensors for the tool with rubber sleeve. The sensor utilisation average (UA) of optimised system are 33.3% which them same in both methods for the tool with and without sleeve, but the UA for the tool without sleeve are slightly different (i.e. 36.66% and 33.3%) due to increase the number of feature of the sound sensor as shown in Table 8.20. For both used methods, The cost of the optimised systems are same which are £18620 for the normal tool, and £18650 for the tool with rubber sleeve with reduced cost ratio 11% and 10.9 % respectively.

Table 8.20: Comparison between the optimised systems from LR slope and PCA.

Method	Variable	Linear Regression (LR)	Principal Component Analysis (PCA)
Tool without sleeve	Selected sensor	Dynamometer	Dynamometer
	UA of optimised system	33.3%	33.3%
	Optimised System Cost	£18620	£18620
	Reduced cost ratio	11 %	11 %
	Optimised System Sensitivity	0.534	0.641
Tool with rubber sleeve	Selected sensor	Dynamometer Mic	Dynamometer Mic
	UA of optimised system	36.66 %	33.3%
	Optimised System Cost	£18650	£18650
	Reduced cost ratio	10.9 %	10.9 %
	Optimised System Sensitivity	0.507	0.642

8.5.2 System Evaluation

8.5.2.1 Linear Regression (LR slope) method

The ASM matrix could be used to evaluate the effectiveness of a sensor or signal processing method based on the sensitivity of every sensor and signal processing method to the fault which is embedded in the ASM matrix.

The average sensitivity of all the sensory characteristic features, for a Signal Processing method SPk, achieved using all the sensory signals can be used as an indication of how relatively the signal processing method is valuable. The average value of the kth column of the ASM matrix for a signal processing SPk is the average sensitivity of the kth signal processing method and can be defined as [156]:

$$A_{spk} = \frac{\sum_{i=1}^n d_{ik}}{n} \quad (8.6)$$

Where n is the number of rows in the ASM.

In addition, the average sensitivity of the k th signal (A_s) can represent the general sensitivity of a signal to the failure and can be defined as:

$$A_{sk} = \frac{\sum_{i=1}^m d_{jk}}{m} \quad (8.7)$$

Where m is the number or columns in the ASM.

For the ASM matrix, the average of the summation of sensitivity coefficients (A_c) can provide an evaluation of the condition monitoring system sensitivity in the detection of the failure under investigation. And can be defined as:

$$A_c = \frac{\sum_{i=1}^n \sum_{j=1}^m d_{ij}}{n \times m} \quad (8.8)$$

The A_s values for the sensory signals used in the system for both tools (normal and with rubber sleeve) are shown in Figure 8.27 and the A_{sp} values for the signal processing methods used in the system are shown in Figure 8.28. As can be noticed from the figures, the results reflect what is found in the optimum system where the force sensor (F_y) is the most sensitive sensor for normal tool (tool without sleeve), meanwhile the sound sensor (Mic) is more sensitive for the tool with rubber sleeve to detect fixturing stability and tool wear.

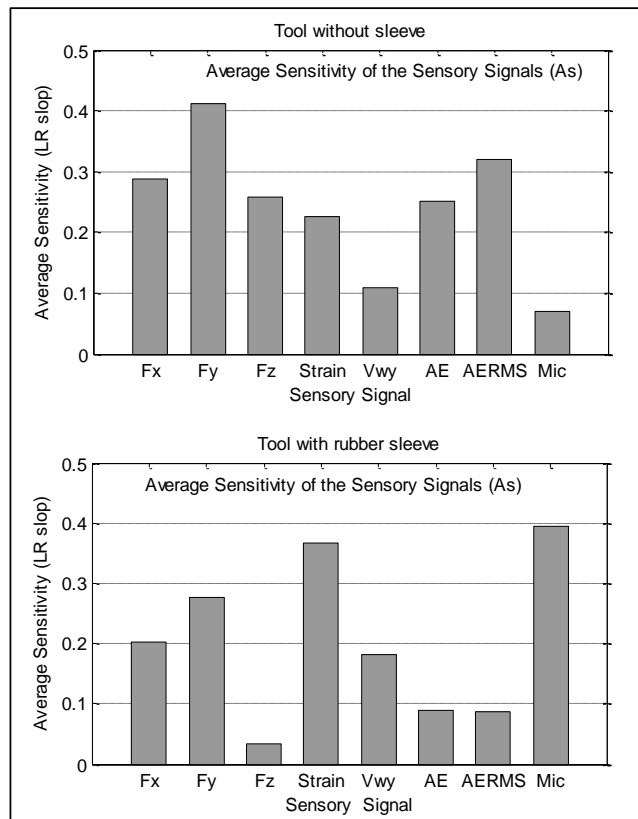


Figure 8.27 : As values for the sensory signals of both tools.

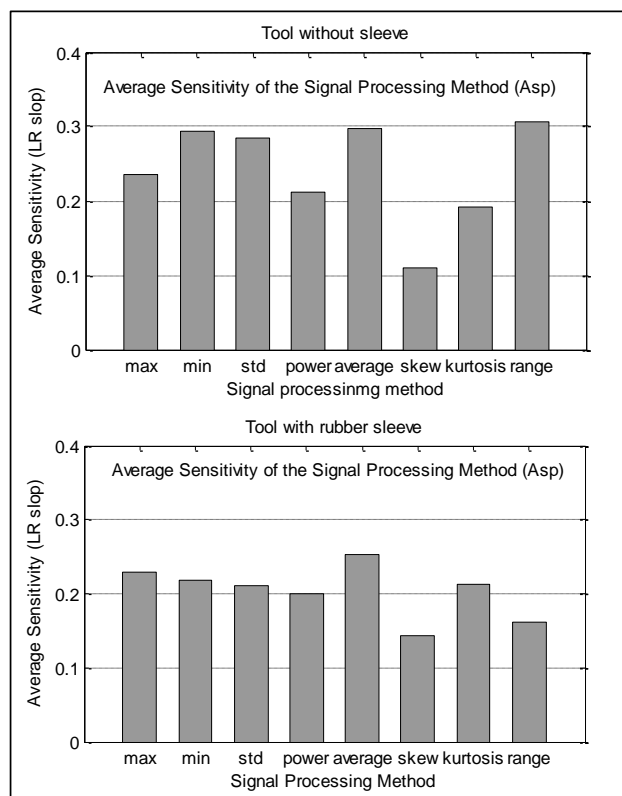


Figure 8.28: Asp values for the signal processing methods of both tools.

The Ac factor of this system is found to be (0.20) for the normal tool and (0.24) for the tool with rubber sleeve. However, to find the effectiveness of the selection of the utilised sensors and signal processing methods, the evaluated values can be compared with other systems. The high Ac value mean high sensitivity level, meaning high information and low Ac, means low sensitivity value and less information. But a low Ac could include features with high sensitivity.

8.5.2.2 Principal Component Analysis (PCA) method

As the ASM matrix which is structured from the sensor and signal processing method is used to evaluate the performance of the sensor in the previous section, the eigenvalue sensory matrix (EVSM) which is also structured from the sensor and principal component and used to assess the effectiveness of same sensory system using principal component analysis.

The average eigenvalue of all the sensory principal component, for a Principal component method PCK, obtained using all the sensory signals (Aev) can be also used as an indication of how relatively the principal component method is applicable as signal processing method. The average value of the *kth* column of the EVSM matrix for a principal component PCK is the average sensitivity of the *kth* principal component method and can be calculated as [169]:

$$A_{pck} = \frac{\sum_{i=1}^n EV_{ik}}{n} \quad (8.9)$$

Where *EV* is the eigenvalue for each sensor, *n* is number of the row in EVSM matrix. Moreover, the average eigenvalue of the *kth* signal (Aev) can characterise the general eigenvalue of a signal to the abnormal and can be calculated as:

$$A_{evk} = \frac{\sum_{j=1}^m EV_{jk}}{m} \quad (8.10)$$

Where *m* is the number or columns in the EVSM matrix.

For the EVSM matrix, the average of the summation of eigenvalue coefficients (E_c) can obtain an evaluation of the condition monitoring system performance in the detection of the abnormal under analysis. And can be defined as:

$$E_c = \frac{\sum_{i=1}^n \sum_{j=1}^m EV_{ij}}{n \times m} \quad (8.11)$$

The Aev values for the sensory signals used in the system for both tools (normal and with rubber sleeve) are shown in Figure 8.29 and the Apc values for the principal component methods used in the system are shown in Figure 8.30. As can be noticed from the figures, the results reflect what is found in the optimum system where the force sensor (Fx) is the most sensitive sensor for normal tool (tool without sleeve), meanwhile the sound sensor (Mic) is more sensitive for the tool with rubber sleeve to detect fixturing stability and tool wear.

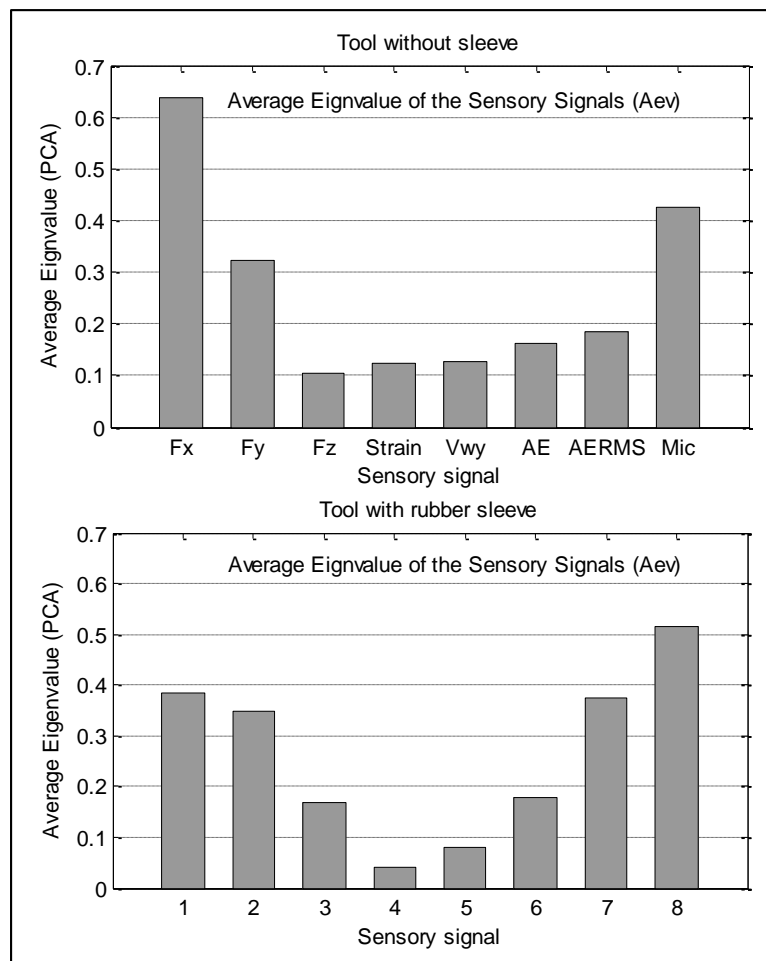


Figure 8.29: Aev values for the sensory signals of both tools.

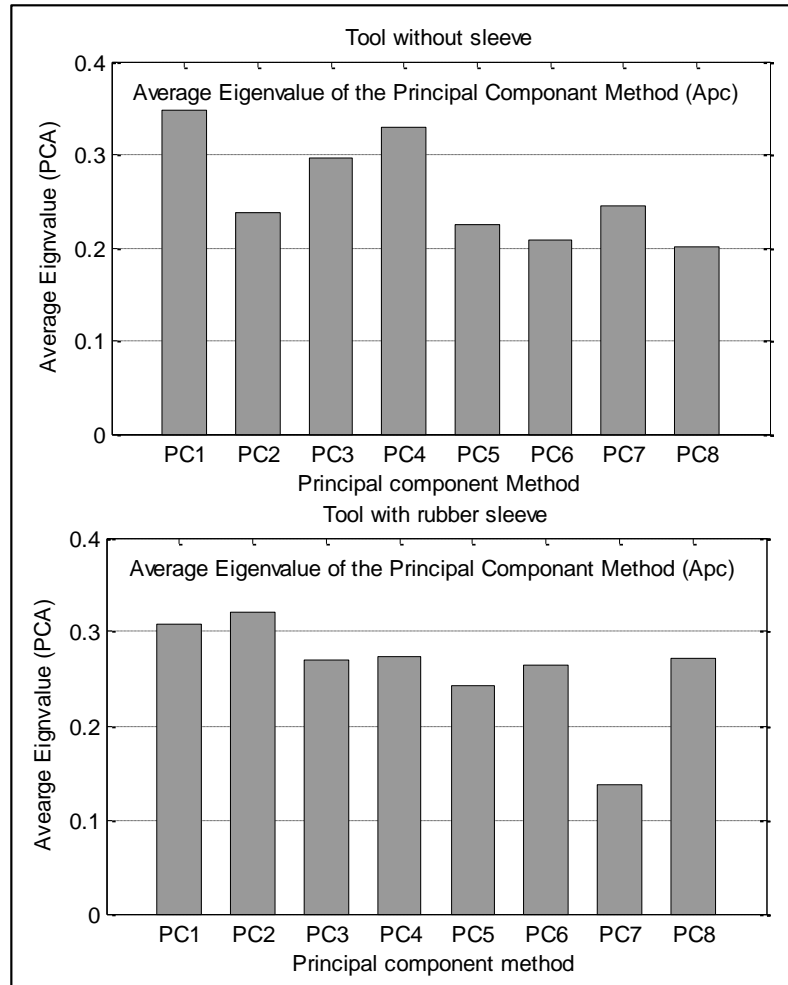


Figure 8.30: Apc values for the principal component methods of both tools.

The eigenvalue coefficients (E_c) of this system is found to be (0.26) for the normal tool and (0.27) for the tool with rubber sleeve. However, the effectiveness of the selection of the utilised sensors and principal component methods, the evaluated values can be compared with sensory coefficient (A_c) resulted by using signal processing methods.

8.5.2.3 Comparison between LR slope and PCA methods

Figure 8.31 shows the values of the A_c factor and the E_c factor for both tools (normal and tool with rubber sleeve). It can be seen that there is a difference between the factors in the value as for normal tool and tool with rubber sleeve as they are (0.20, 0.24) and (0.26, 0.27) for the A_c an E_c for both tools respectively. The more significant findings to emerge from this discussion are that:

- 1- Linear Regression method and Principal component together could be provided similar indication with regard to determine which sensor has a higher sensitivity.
- 2- Both methods indicate that the automated monitoring system has ability to define the changes in the fixturing system; therefore it could be used to detect the abnormalities or the changes of the machine setup during the machining process.

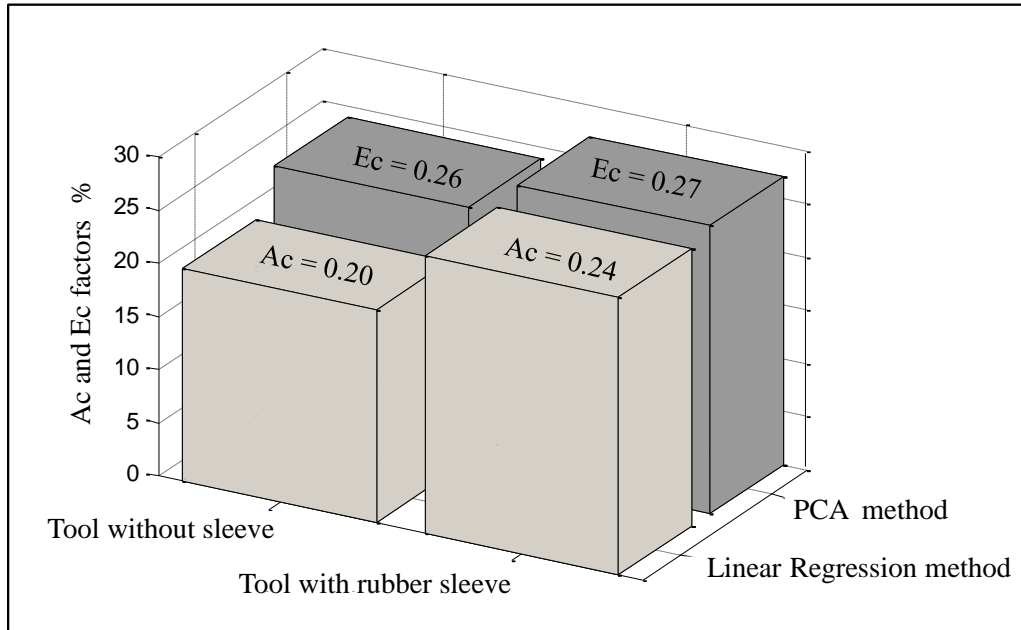


Figure 8.31: Comparison between Ac and Ec of both tools.

8.6 Approach to measure surface roughness

8.6.1 Proposed Approach

Generally all surfaces have their own characteristics, which are referred to as surface texture. Surface texture is the pattern of the surface which deviates from a nominal surface. The deviations may be repetitive or random and may result from roughness, flaws and waviness. Therefore, the surface roughness is defined as a closely spaced, irregular deviation on a scale smaller than waviness. Figure 8.32 shows the standard terminology and symbols to describe surface roughness. In machining, surface roughness is generally specified mathematically in terms of the arithmetic average deviation from the mean using Eq. (8.12) [203].

$$Ra = \frac{1}{L} \int_0^L |Y(x)| dx \quad (8.12)$$

Where L is the sampling length and Y is the ordinate of the profile curve. In other words, R_a is the area between the roughness profile and its mean line, or the integral of the absolute profile height over the evaluation length which needs to be optimised. The spindle-tool system including collet and chuck holder modelled as a cantilever beam was assumed to be the main vibration to determine surface roughness. Then the relationship between tool motion and force waveform could express as [78]:

$$r_{\text{tool}} = C \times r_{\text{force}} \quad (8.13)$$

Where r_{tool} is displacement of tool, C is coefficient to be estimated from using the experimental data, and r_{force} is displacement of cutting force signal.

Surface roughness considered in this research is R_a , which is calculated from cutting force by equation 8.13:

$$Ra_{\text{workpiece}} = C \times Ra_{\text{force}} \quad (8.14)$$

Where Ra_{force} is a centreline average value directly calculated from r_{force}

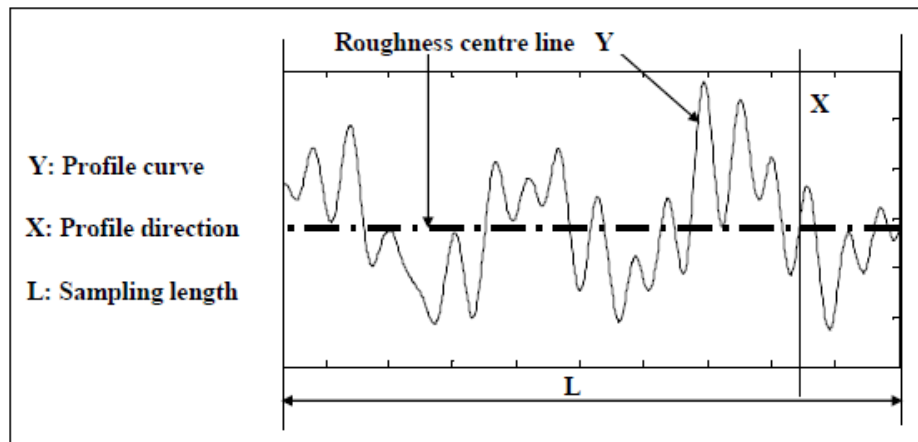


Figure 8.32: Surface roughness profile.

In the current research, as a novel investigation, the relation pattern of forces signals will be used to measure the surface roughness of the workpiece using equation 8.12. The real surface roughness of the machined surface is measured using surface tester as illustrated in Figure 8.33. By using the equation 8.13, the value of the constant (C) can be calculated, this leads to predict the surface roughness for the future work in the machining process and helps to avoid using the manual measurement by using the equation 8.14.

8.6.2 Implementation of the proposed Approach

The experimental work of the condition monitoring system of this study is performed on a milling CNC machine type (DENFORD) using Aluminium workpiece. The force signals are monitored using 3-component Dynamometer (Kistler 9257A) and the workpiece is fixed on the dynamometer. The force dynamometer is connected to a 4-channel charge amplifier (Kistler 5070A). All the wires and cables of the sensors are connected to a National instrument connection box (SCB-100). The signals are monitored using data acquisition card NI PCI-6071E from National Instrument using special data acquisition software written using the National Instrument CVI programming package. A Mitutoya (SJ-210) apparatus is used for the surface roughness measurements. The average value (R_a) was recorded as the value of surface roughness.

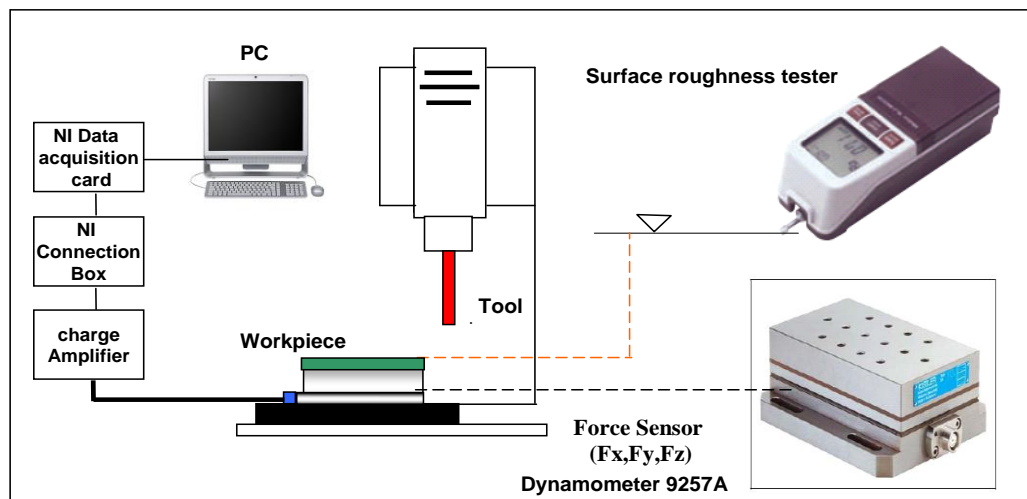


Figure 8 33: Schematic diagram of experimental setup.

The shank of the tool is covered by a rubber sleeve to emulate a fixturing system with low rigidity. The tests start with a fresh tool and finish with completely worn tool. The raw signals for the tools are collected from the sensors to monitor 45 machining samples for each type of tools.

To verify prediction models, cutting tests using 45 cutting tests are conducted. Step cutting is also performed using same end mill tools. Axial depth of cut is 0.22 mm and feed rate of cut is 250mm/min. Detailed cutting conditions are listed in Table 8.1. Surface roughness values have been measured by using stylus type profilometer (SJ-210) after each cut. Measuring position has been at the centre line of machined

surface. Surface roughness from the measured cutting forces is calculated on PC using software after targeted area was machined. Cutting forces have been measured using force sensor (Dynamometer Kistler 9257A). The testing planning has been divided into two phases. The first phase is a preparation in which sample data are collected so the mathematical surface roughness can be computed. In the second step, the experimental surface roughness measurements are collected in the z-axis. From cutting tests which is started by fresh tool and finished with worn tool, coefficient C of equation 8.13 is ($0.733 \pm 0.002 \mu\text{m/N}$) for tool without sleeve and ($0.625 \pm 0.002 \mu\text{m/N}$) for tool with rubber sleeve. The statistic methods and roughness quantity are used such as the average surface roughness (mean of Ra). Figures (8.34, 8.35) have shown that there are statistical parameters qualify between the patterns of the curves for surface roughness of workpiece using surface apparatus (SJ-210) for the tool without sleeve and the tool with rubber sleeve, and mathematical surface roughness using cutting forces signals. Where the average of each five tests has been computed gradually to nine groups as shown in Figures 8.36 and 8.37. It can be noticed that the values of both real and modelled surface roughness have been increased when used tool with rubber sleeve. This finding provides an indicator for the ability of this approach to detect the changes of the quality of the fixturing system.



Figure 8.34: surface roughness of forces and workpiece for the tool without sleeve.

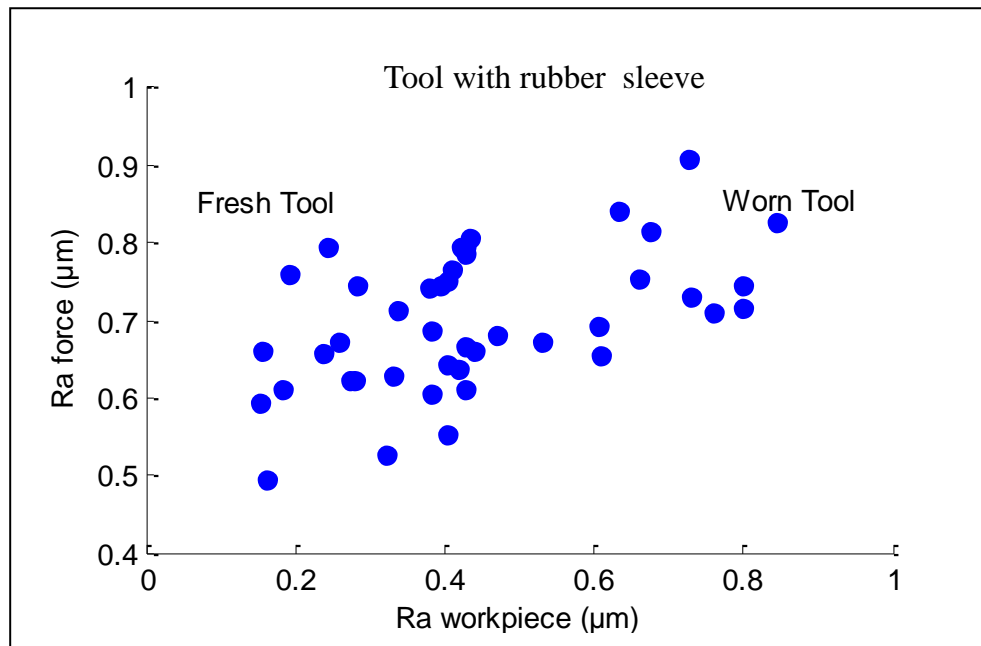


Figure 8.35: surface roughness of forces and workpiece for the tool with rubber sleeve.

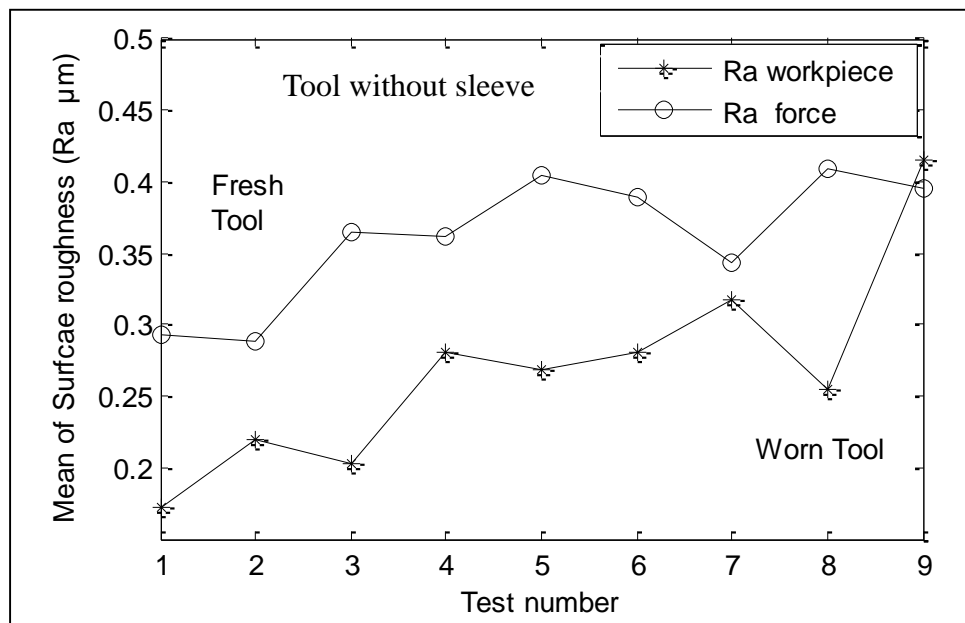


Figure 8.36: Mean of the surface roughness for the tool without sleeve.

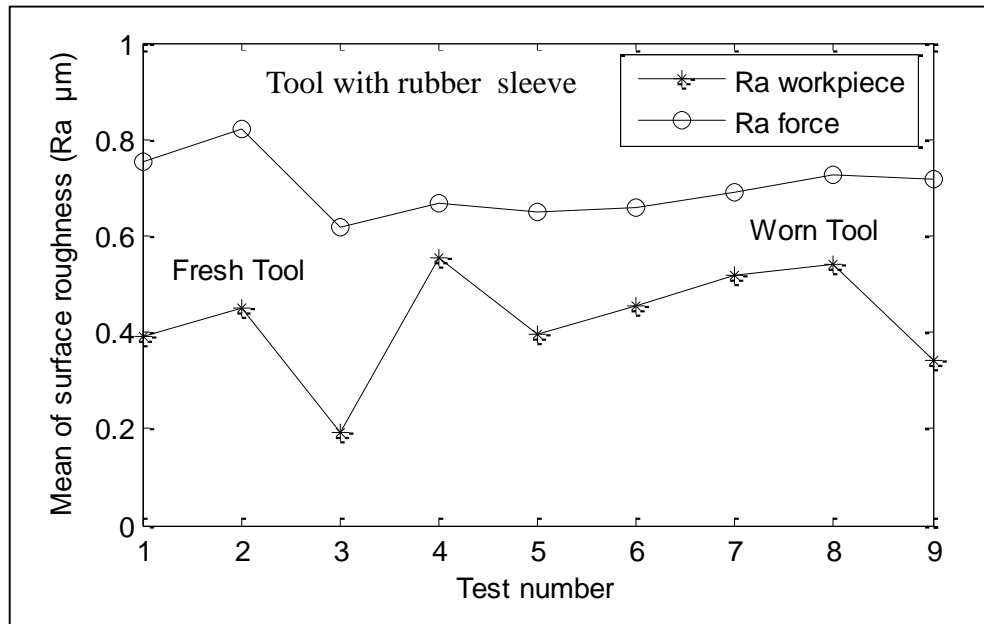


Figure 8.37: Mean of the surface roughness for the tool with rubber sleeve.

This study has investigated a metal cutting surface quality control procedure that takes advantage of the known change pattern of surface roughness. This procedure is performed on statistical analysis of surface roughness measurement and will directly respond to the features of the surface roughness curve. A set of actual data collected from metal cutting process is studied. The data are measurement of the surface roughness of a practicable workpiece. First, mathematical model has been found to describe the behaviour of surface roughness. Then a surface roughness is measured for the same area of machined surface which the data of cutting forces are used to create this mathematical model. This study has proven that the accurate resulting value for the prediction performance measure could be obtained from a predicted mathematical model and the testing samples by using the available experimental data.

8.7 Conclusion

This chapter described the practical details of the ASPSF approach. The ASPSF approach for eight sensory signals is explained using an experimental machining test to monitor a fixturing system stability and gradual tool wear in milling process. The implemented ASPSF approach utilises two matrixes, named the Association Matrix (ASM), and Eigenvalue Sensory Matrix (EVSM) to compare the sensitivity of the

features and eigenvalue of the principal component to the fault under investigation. In addition to evaluate the overall monitoring system using the average sensitivity and eigenvalue of sensors, and signal processing methods and principal component methods. The Linear regression (LR) analysis and Principal Component Analysis (PCA) are used to find out the most sensitive features to detect fixturing setup and cutting tool wear. Two types of the fixturing setup have been used to hold the cutting tools, tool without sleeve and tool with rubber sleeve. The SCFs of LR method are visually examined and examples of high-sensitivity and low sensitivity SCFs are presented, similarly, the PCFs obtained from the PCA method are described and the images of EVSM matrix are utilised. Sensory utilisation is implemented within the ASPSF approach to reduce the cost of the system without affecting the sensitivity of the system. The ASPSF approach is found useful in selecting the most sensitive sensors either by using linear regression method or principal component analysis method which they both emerged a reliable correlation to design a condition monitoring system for milling process.

On the other hand, the proposed approach to predict the surface roughness of the machined surface using the response of the force sensor presented valuable results to avoid the manual measurements.

Chapter 9 The Applications of ASPSF Approach Using Pattern Recognition Systems

9.1 Introduction

In order to implement the ASPSF approach with different applications, in this chapter, different groups of multi-sensor fusion models have been presented. The chapter provides more experimental work to verify the capability of the applied ASPSF approach in developing and designing a sensor fusion model of a condition monitoring system for milling process by selecting the most sensitive sensors and signal processing methods using pattern recognition systems. It describes the same achieved methodology in the previous chapter for the following investigations:

- **Taylor's Equation Induced Pattern (TIP) Investigation:** The chosen process parameters monitored are force (dynamometer), acoustic emission (AE), sound, accelerometers, strain, power, eddy current sensors using different types of constant functions. These methods are applied for finding the relation between the suggested patterns of the constant function with those resulted from the sensory signals.
- **Back Propagation Neural Network Investigation:** This process complement the previous investigation by training the data according to the obtained target. Both investigations represent the same methodology and experimental work to detect fixturing setup and tool wear and provide diagnostic and prognostic information.
- **Surface Roughness Investigation:** As the surface roughness is a reliable indicator to the quality of the machined surface, therefore it is employed in this chapter to reflect the effect of the machining quality on the sensitivity of the monitoring system.

This chapter also seeks to confirm the methodology and the technique applied in Chapter 8 for the milling process with different multi-sensors using different pattern recognition systems. The main assumption to be tested is that linear regression and principal component analysis methods are capable of detecting the sensitivity of the SCFs and sensory signals.

9.2 Data Analysis

The experimental work is conducted to examine the behaviour of the signals for different fixturing types and material and to monitor tools status (fresh and worn), and

also to find the most sensitive sensory characteristic features to fixturing and tool failures. As illustrated in Figure 10.1, the experimental work of the condition monitoring system of this study is performed on a milling CNC machine type (DENFORD). Several sensory signals are used in this study including cutting forces (F_x , F_y and F_z), strain, accelerometers (V_{wx} , V_{wy} , V_{sx} , V_{sy} and V_{sz}), Acoustic Emission sensor (AE), eddy current sensors (E_{dx} , E_{dy}), power sensor (Pwr), and microphone (Mic) for measuring sound. The force signals are monitored using 3-component dynamometer (Kistler 9257A) and the work piece is fixed on the dynamometer. The dynamic and quasistatic force signals are monitored using a strain sensor (Kistler 9232A). The AE sensor (Kistler 8152b111) is attached to the workpiece to monitor AE signals transmitted during machining and connected to AE coupler (Kistler 5125B). The accelerometers (B&K4366) are mounted on the moveable table of machine and connected to charge amplifier (Kistler 5001). The other accelerometers (Kistler 8704B) are attached to the machine spindle and connected to coupler (Kistler 5134B). Sound signals are collected using a microphone (EM400) placed in the direct vicinity of the workpiece. Eddy current sensors (IC12-02) are connected to power supply (PDA- 3502 A) with 12 volts. Power sensor (IP-151) is connected directly to the data acquisition card. All the wires and cables of the sensors are connected to a National instrument connection box (SCB-100). The signals are monitored using data acquisition card NI PCI-6071E from National Instrument using special data acquisition software written using the National Instrument (Lab windows/ CVI) programming package. Mitutoya apparatus (SJ-210) is used for the surface roughness measurements. The experimental work is performed on milling machine using Aluminium workpiece. The milling process is carried out at the conditions as shown in the Table 9.1.

Table 9.1: The machining parameters of the milling process.

Machining conditions	Specifications
Feed rate	215 mm/min
Depth of cut	0.36 mm
Coolant type	No coolant (Dry)
Spindle speed	2860 RPM
Diameter of tool	3mm/ 6mm shank
Material of tool	HSS (End mill HSS)
Type of tool	End mill Tool(4 Flutes, Uncoated)

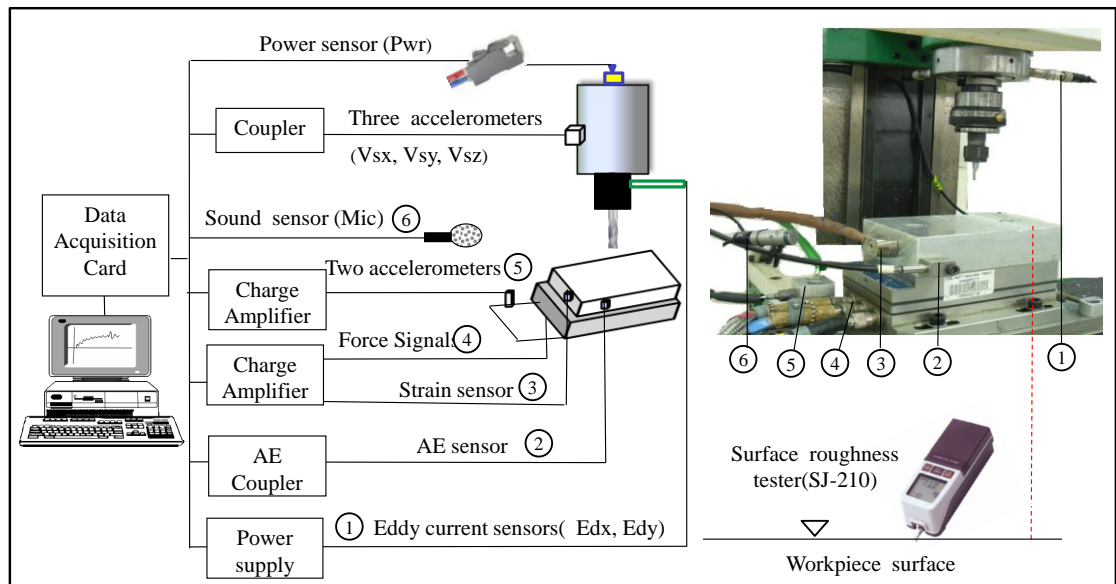


Figure 9.1: Schematic diagram of experimental setup for the monitoring system.

To emulate a fixturing system with low rigidity, the shank of the tool is covered by three different elastic materials namely rubber, copper and aluminium with thickness of 1mm as shown in Figure 9.2 where the tests start with a fresh tool and finished with completely worn tool.

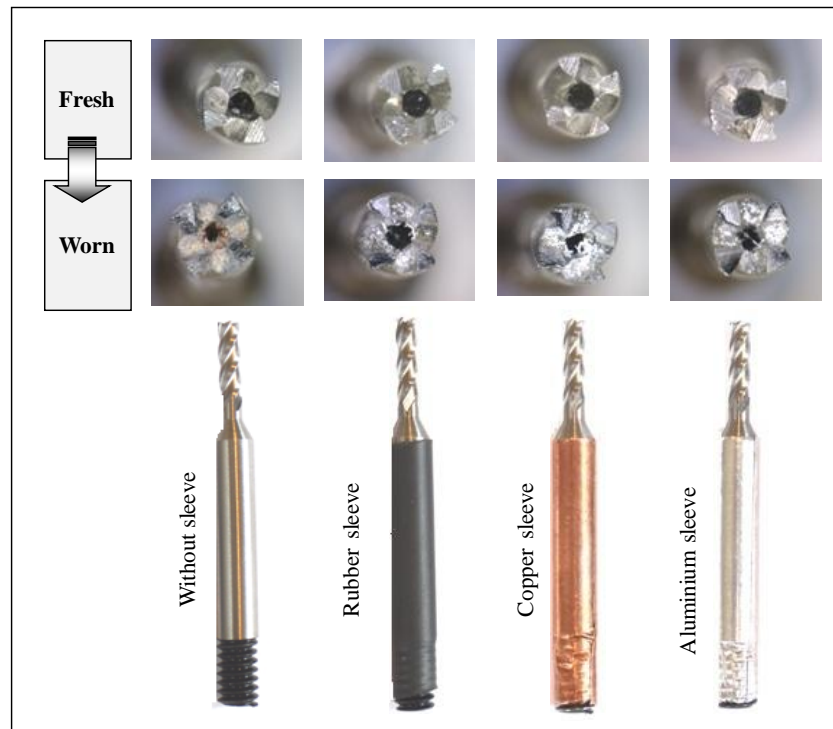


Figure 9.2: The two states of the milling tool (fresh and worn tool).

9.2.1 Signals Simplifications

One of the complex machining processes is milling, and it is assumed complex sensory signals presented as a function of time as shown in Figure 9.3 and Figure 9.4. It is assumed that the process starts with a healthy condition (fresh tool), and gradually or suddenly the state of the process changes with an introduced fault (worn tool). It is relatively clear these machining signals have been found difficult to predict the most sensitive signals to fixturing rigidity and tool wear directly from the unprocessed data.

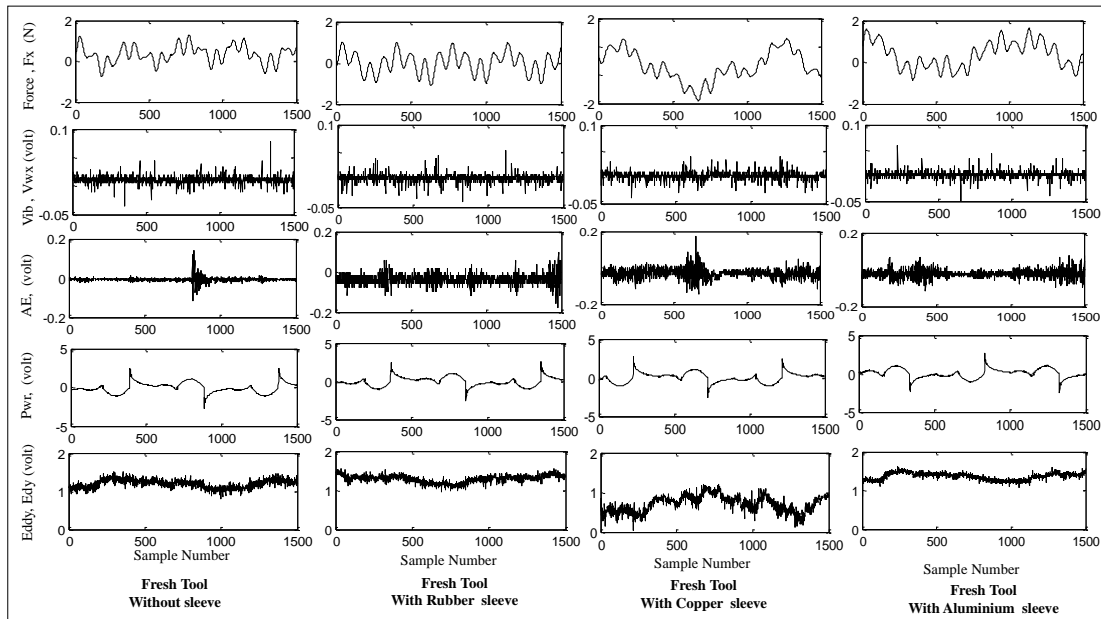


Figure 9.3: Example of the raw signals of the milling process for fresh tool.

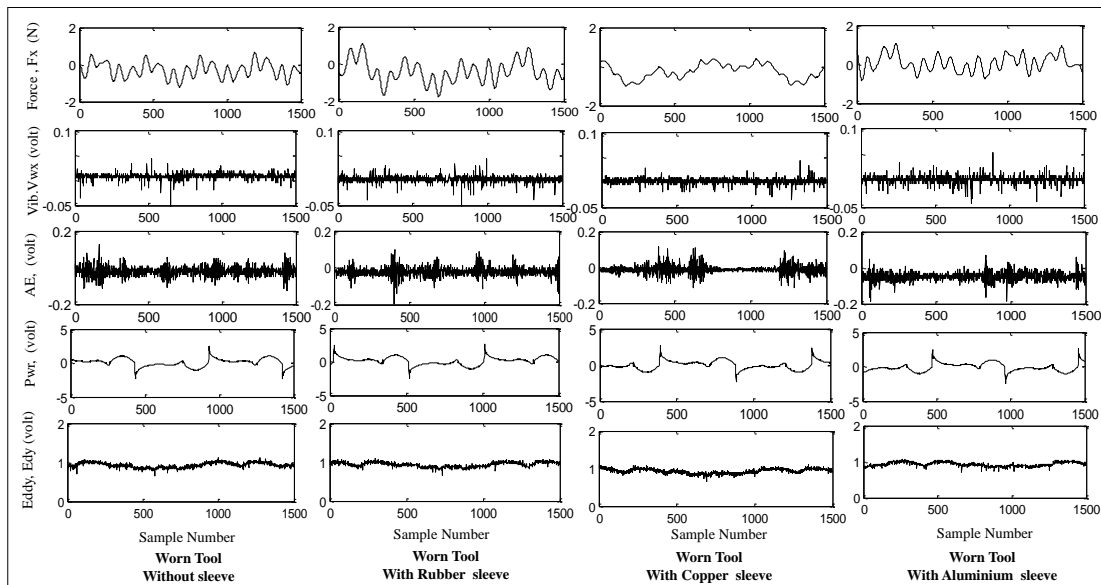


Figure 9.4: Example of the raw signals of the milling process for worn tool.

It can be observed from Figures 9.3 and 9.4 that the vibration level of some signals has increased for the worn tool, as in the cutting forces signals. In addition, the level of some sensory signals has changed such as the acoustic emission (AE) signal. It may be difficult to assess the state of the process from the produced signal, therefore the first step is to transfer signals from its complex form into a group of simplified sensory signals denoted Sensory Characteristic Features (SCFs). For example, if a milling process sensory signal can be transformed into a group of SCFs with relatively simple nature with less variation, then it is expected to be much easier to retrieve the necessary information which presents the state of the process based on the change in the level of the extracted SCFs.

9.2.1.1 Linear Regression (LR) method

The raw signals are processed using several time domain signal processing methods to extract the Sensory Characteristic Features (SCFs). The signal processing methods used are maximum (max), minimum (min), standard deviations (std), the average (μ), the range, the skewness (skew), kurtosis value (K) and power as explained in Chapter 7. The 8 signal processing methods are used to process the 15 sensory signals to construct an Association Matrix ASM of (8×15) which allows the investigation of 120 sensory characteristic features (SCFs) for the design of the monitoring system. The SCFs are arranged according to their sensitivities to tool status based on the absolute slope of the linear regression method as shown in Figures 9.5- 9.8.

Figure 9.5 presents examples of high and low-sensitivity SCFs to tool wear for three tools without sleeve. However, Figures 9.6, 9.7 and 9.8 present different examples of the sensitivity SCFs when used cutting tools with rubber sleeve, copper and aluminium sleeves respectively.

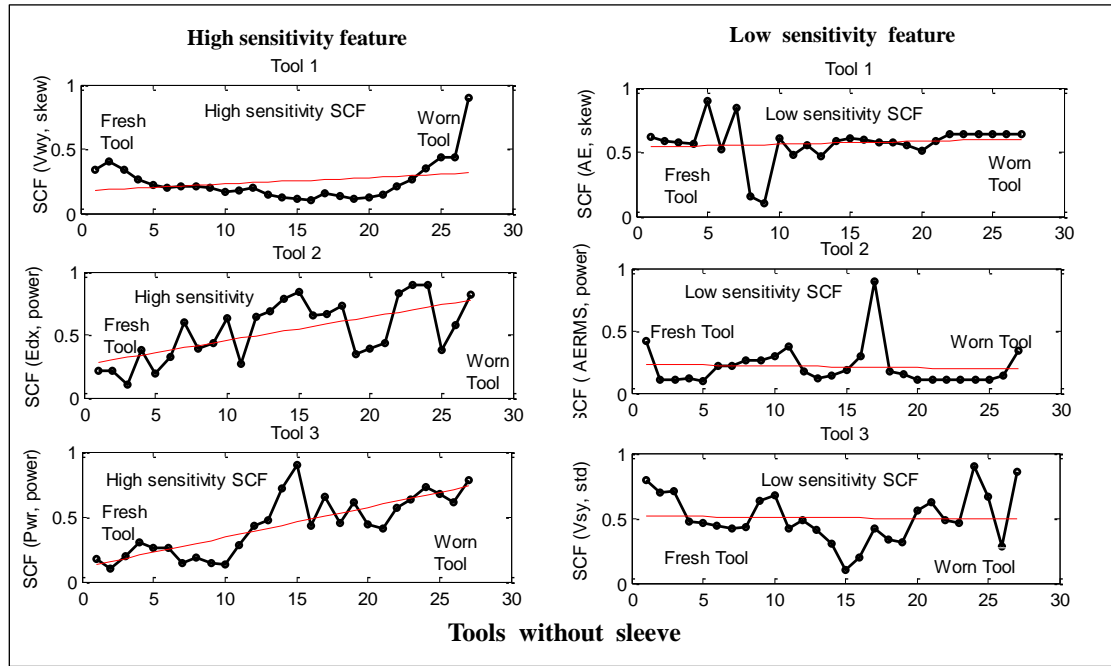


Figure 9.5: Example of high and low sensitivity SCF for the tools without sleeve.

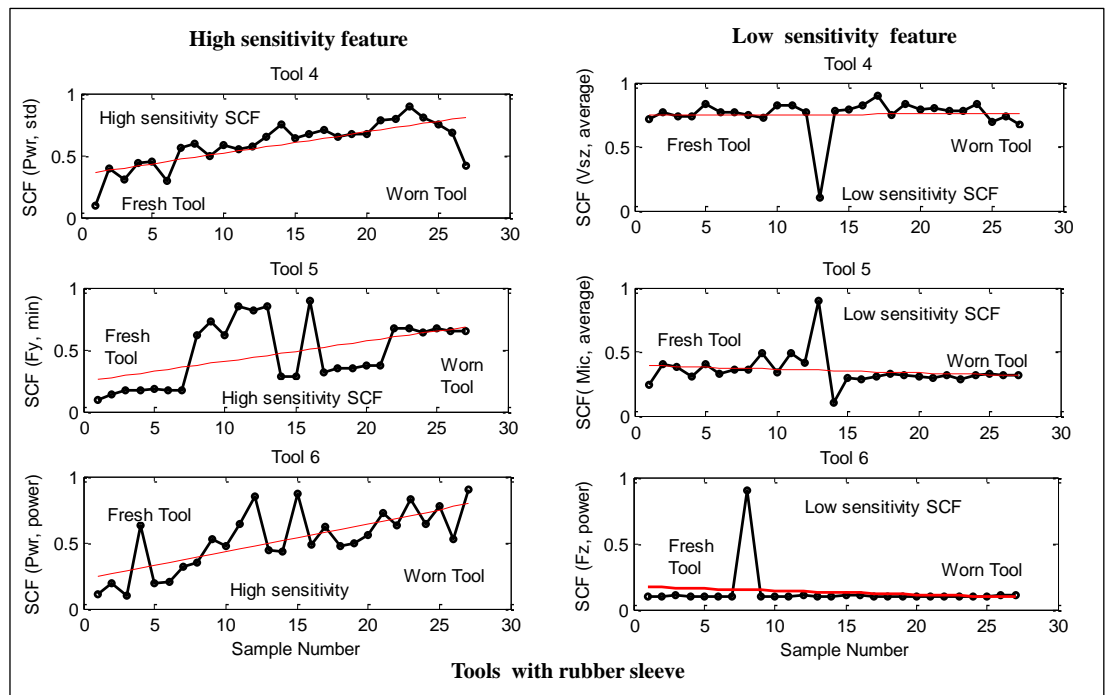


Figure 9.6: Example of high and low sensitivity SCF for the tools with rubber sleeve.

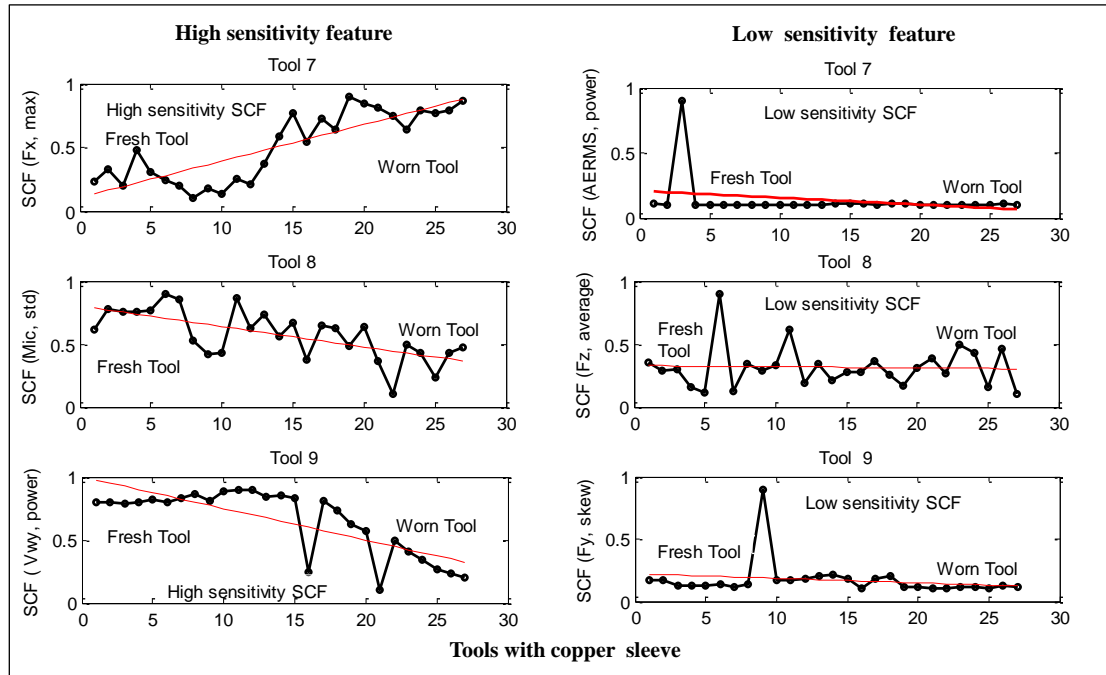


Figure 9.7: Example of high and low sensitivity SCF for the tools with copper sleeve.

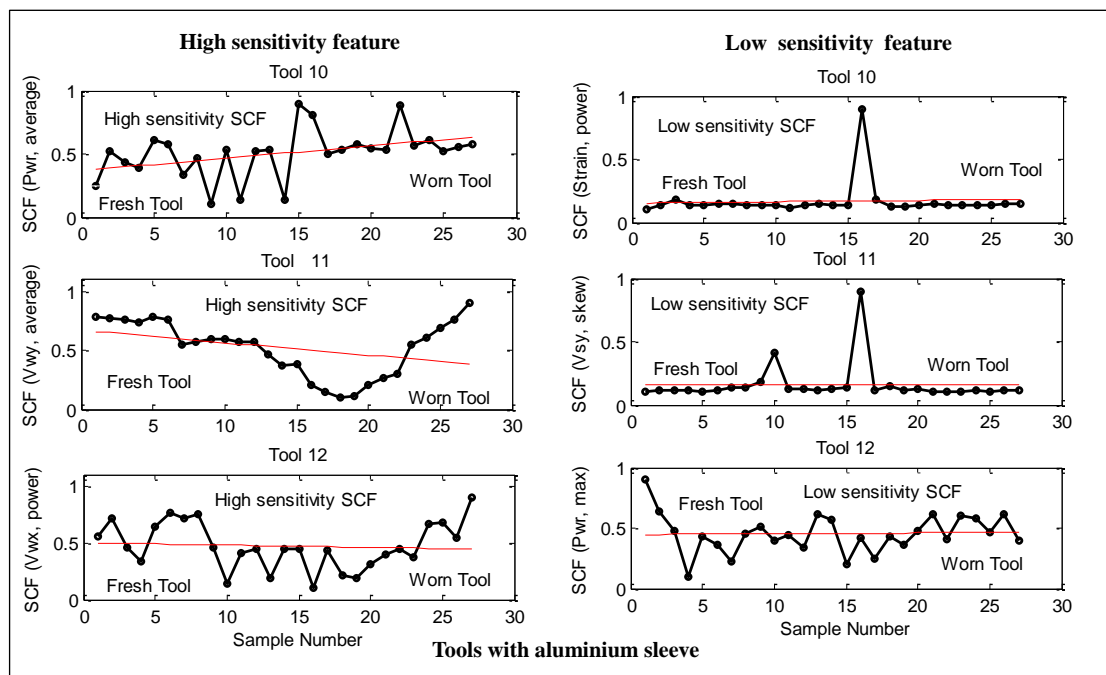


Figure 9.8: Example of high and low sensitivity SCF for the tools with aluminium sleeves.

The SCFs are visually inspected and it has been found that SCFs with high absolute slope show higher sensitivity to the fault. Table 9.2 presents example of the highest

and lowest sensitive SCFs for this particular tool wear test where sensitivity values are the linear regression slope of the normalised features. Notice that the above figures indicate that the change in the characteristic of the fixturing system has caused change in the most sensitive sensors and signal processing systems that can be used to detect tool wear. For example, with normal fixturing system, eddy current signals (Edy) and force (Fx) are found to be the most sensitive to detect tool wear. However, with the rubber sleeve system, eddy current (Edx) and force signals are found to be the most sensitive signals to detect tool wear. Differently, with holding by copper sleeve, force and power signals are indicated more performance to sense the tool conditions. Similarly, with clamping by the aluminium sleeve, power and force signals have effectively stated the tool wear.

Table 9.2: The Associated matrix of the system for tool 1 without sleeve.

Tool 1	Signal Processing Methods							
Sensor	max	min	std	power	average	skew	kurtosis	range
Fx	0.844	0.742	0.158	0.408	0.805	0.416	0.216	0.100
Fy	0.761	0.754	0.437	0.943	0.777	0.075	0.379	0.106
Fz	0.503	0.614	0.022	0.047	0.507	0.696	0.332	0.288
Strain	0.661	0.672	0.689	0.542	0.385	0.603	0.351	0.687
Vwy	0.532	0.517	0.555	0.535	0.533	0.570	0.348	0.440
AE	0.952	0.974	0.923	0.892	0.532	0.136	0.498	0.966
AERMS	0.926	0.725	0.702	0.929	0.919	0.165	0.344	0.727
Mic	0.943	0.645	0.770	0.921	0.922	0.904	0.008	0.726
Vsx	0.843	0.559	0.741	0.920	0.892	0.082	0.504	0.482
Vsy	0.162	0.399	0.725	0.930	0.875	0.256	0.262	0.367
Vsz	0.452	0.343	0.515	0.713	0.740	0.084	0.076	0.006
Vwx	0.436	0.478	0.467	0.877	0.880	0.756	0.486	0.004
Pwr	0.091	0.742	0.853	0.991	0.325	0.226	0.150	0.591
Edx	0.299	0.437	0.129	0.821	0.821	0.762	0.368	0.340
Edy	0.998	1.195	1.146	1.194	1.193	1.075	1.071	1.107

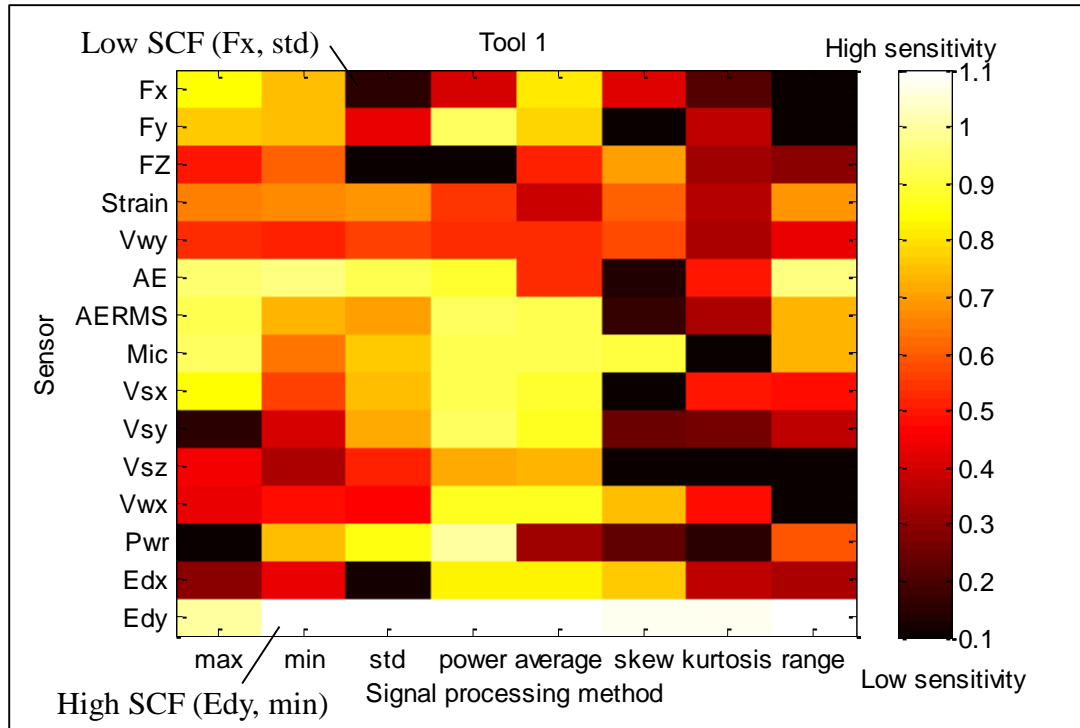


Figure 9.9: A graphical presentation of the sensitivity for tool 1 without sleeve.

Figure 9.9 presents images of the Association Matrix (ASM) which includes the sensitivity of a few SCFs implemented in this monitoring system. The ASM presents for each sensor and signal processing method (SCF) the sensitivity to detect the machining faults, where high sensitivity indicates high capability to detect the fault. The numbers with small value in Table 9.2 is shown in black in the image in Figure 9.9. This mean low sensitivity, numbers with medium values are shown in red which means medium sensitivity, and numbers with high values are shown in yellow which means high sensitivity. The associated matrixes, tables and images, for the tools are described in Appendix B.

9.2.1.2 Principal Component Analysis (PCA) method

The fourth step is implemented by calculating the eigenvectors and eigenvalues for the PCA matrix since it is square. The concept of the eigenvector and eigenvalue is defined in chapter 7. This gives the components in order of significance. To be precise, if you originally have n variables in the row data, and so you calculate n eigenvectors and eigenvalues. Eigenvector determine the location of the variables on the n - variables space, meanwhile the eigenvalues evaluate the distance between the

variable and the mean zone. In general, once eigenvectors are found from the covariance matrix, the next step is to order them by eigenvalue, highest to lowest. That is meaning the eigenvector with the largest eigenvalue was the one that pointed as the most significant relationship between the data variables.

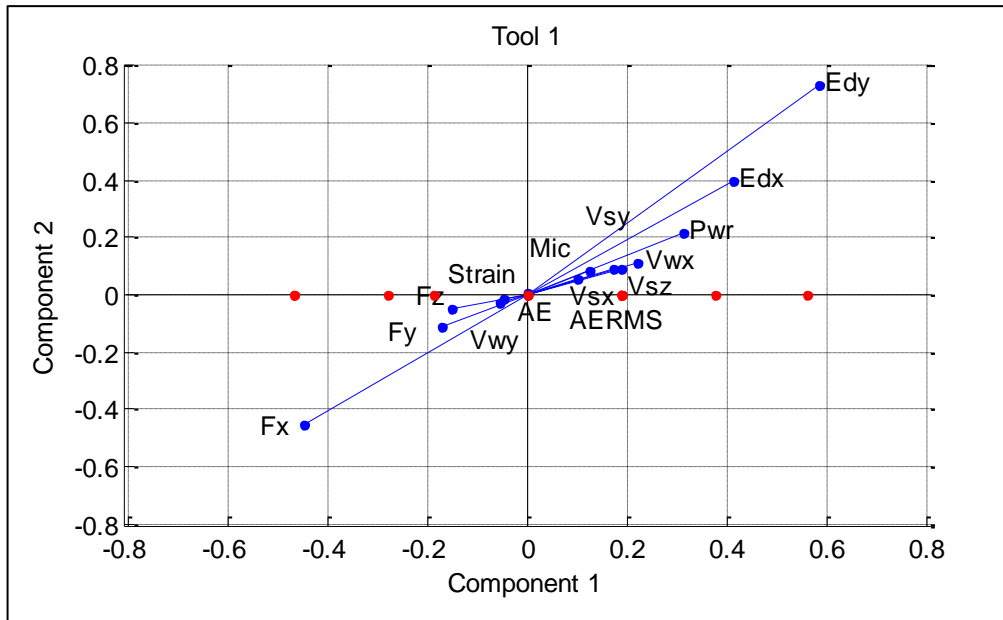


Figure 9.10: A plot of the principle components according to eigenvalue of variables in the covariance matrix for tool 1 without sleeve.

Figure 9.10 shows the application of the above procedure in this research, and visually clear that the eddy current sensor in y-axis (Edy) has the maximum eigenvalue for tool 1, that is indicated it as a most sensitive to the changes of the machining process for the tool without sleeve, meanwhile the dynamometer, force sensor in x axis (Fx), and eddy current sensor in x axis (Edx) are second and third more sensitive sensors for detecting the tool and fixturing conditions.

The principal components for the all sensors used in the test are arranged to create Eigenvalue Sensory matrix (EVSM). The EVSM is similar with that one constructed in the linear regression. The EVSM for tool 1 without sleeve is showing in Table 9.3 and graphically presented in Figure 9.11. It can be noticed that the feature PCF(Edy, PC1) is the most sensitive; it is constructed from the combination of the Edy sensor with the first principal component. The EVSM for the other tools (2-12) are described in Appendix C.

Table 9.3: The Eigenvalue Sensory Matrix (EVSM) of the system for tool 1 without sleeve.

	Principal component Analysis														
Sensor	PC1	PC2	PC3	PC4	PC5	PC6	PC7	PC8	PC9	PC10	PC11	PC12	PC13	PC14	PC15
Fx	0.36	0.40	0.47	0.11	0.29	0.66	0.46	0.38	0.53	0.52	0.44	0.55	0.42	0.50	0.37
Fy	0.35	0.38	0.42	0.10	0.13	0.24	0.29	0.28	0.34	0.49	0.22	0.44	0.19	0.14	0.33
Fz	0.32	0.23	0.27	0.05	0.10	0.12	0.14	0.21	0.20	0.43	0.16	0.26	0.14	0.11	0.23
Strain	0.23	0.18	0.22	0.04	0.04	0.10	0.07	0.19	0.17	0.40	0.12	0.15	0.07	0.05	0.21
Vvy	0.09	0.15	0.18	0.03	0.00	0.06	0.06	0.16	0.06	0.19	0.12	0.11	0.05	0.04	0.08
AE	0.06	0.14	0.17	0.02	0.02	0.05	0.03	0.07	0.04	0.19	0.06	0.07	0.03	0.02	0.05
AERMS	0.02	0.02	0.12	0.00	0.03	0.05	0.03	0.00	0.01	0.14	0.05	0.04	0.01	0.00	0.01
Mic	0.03	0.02	0.08	0.02	0.03	0.05	0.02	0.03	0.01	0.10	0.04	0.02	0.03	0.01	0.01
Vsx	0.14	0.04	0.02	0.05	0.06	0.12	0.04	0.04	0.01	0.09	0.01	0.02	0.08	0.02	0.09
Vsy	0.15	0.22	0.03	0.08	0.06	0.13	0.10	0.08	0.05	0.08	0.05	0.02	0.10	0.22	0.15
Vsz	0.31	0.29	0.13	0.08	0.06	0.14	0.23	0.11	0.19	0.08	0.08	0.06	0.13	0.27	0.22
Vwx	0.31	0.31	0.17	0.17	0.12	0.16	0.24	0.30	0.27	0.01	0.18	0.07	0.26	0.28	0.27
Pwr	0.33	0.32	0.26	0.18	0.21	0.17	0.29	0.34	0.32	0.02	0.31	0.19	0.37	0.39	0.32
Edx	0.34	0.34	0.28	0.39	0.21	0.19	0.37	0.34	0.37	0.07	0.39	0.36	0.42	0.41	0.40
Edy	0.88	0.35	0.45	0.86	0.36	0.58	0.58	0.57	0.42	0.13	0.64	0.47	0.59	0.44	0.49

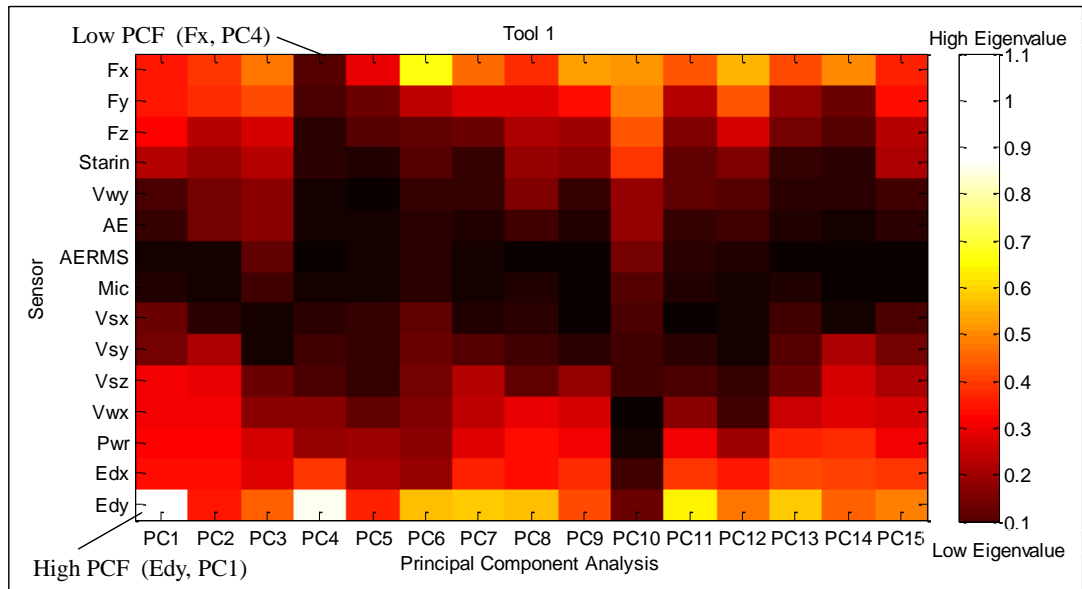


Figure 9.11: A graphical presentation of the EVSM for tool 1 without sleeve.

9.2.1.3 Correlation between LR and PCA methods

By using the same steps in the previous chapter (section 8.3.3) to calculate the correlation coefficient between the sensitivity using linear regression and the

eigenvalue using principal component analysis, the following figures show these relationships for different tools with and without sleeves.

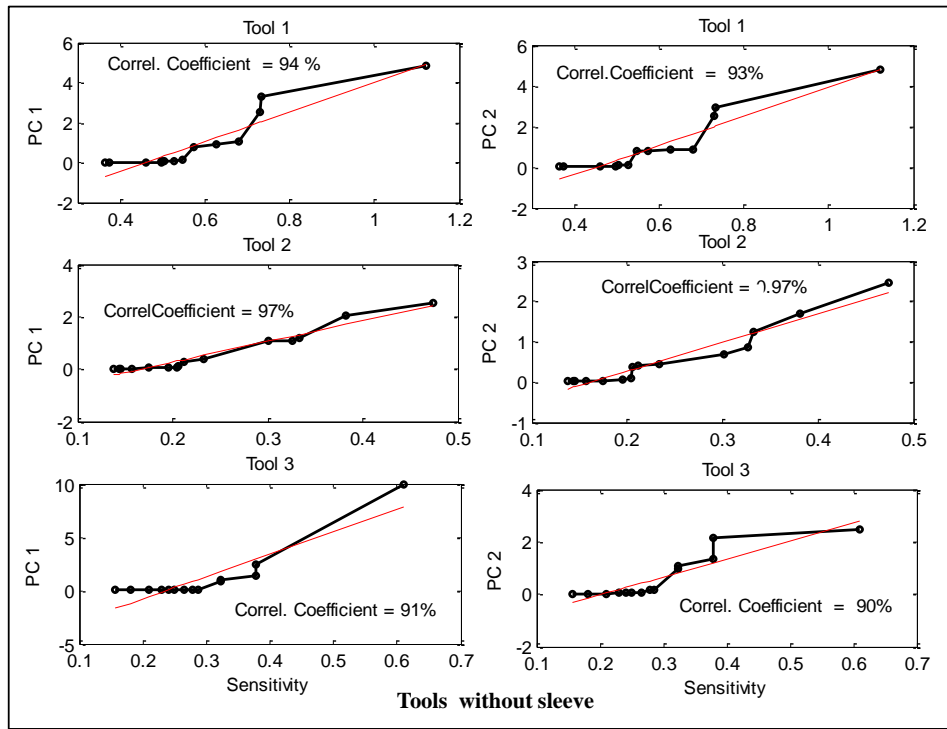


Figure 9.12: The correlation coefficient between PCA and linear regression sensitivity for tools without sleeves.

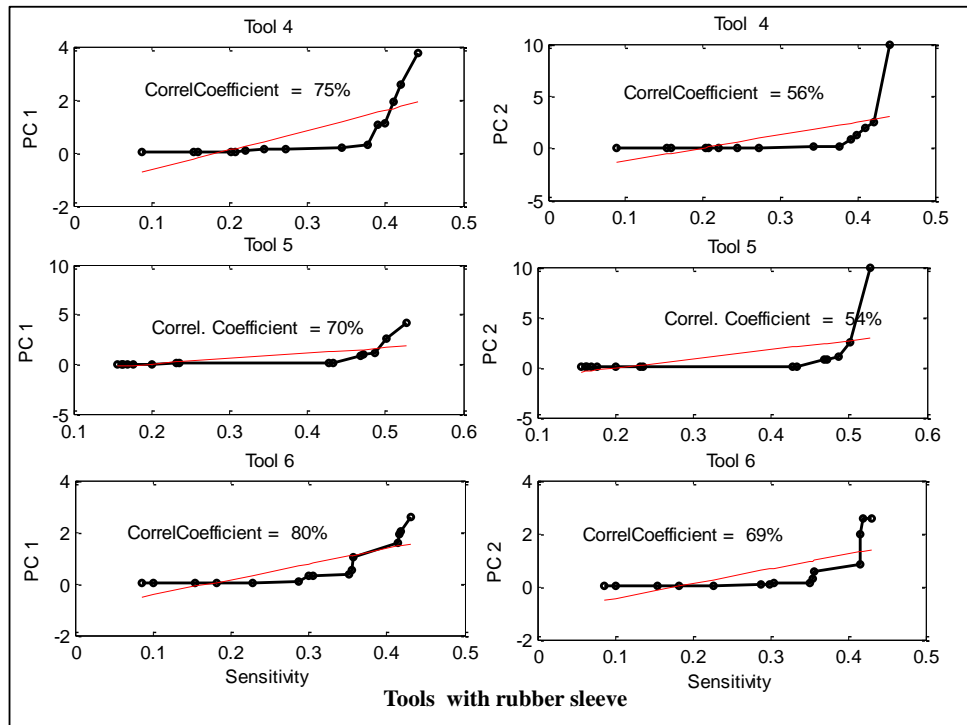


Figure 9.13: The correlation coefficient between PCA and linear regression sensitivity for tools with rubber sleeves.

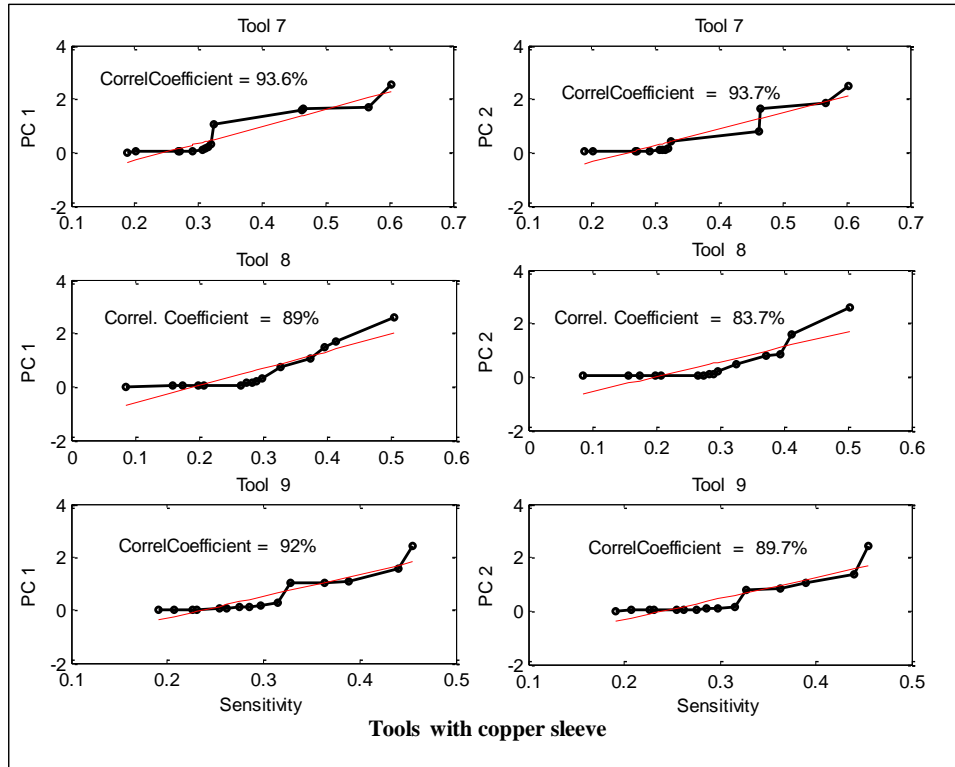


Figure 9.14: The correlation coefficient between PCA and linear regression sensitivity for tools with copper sleeves.

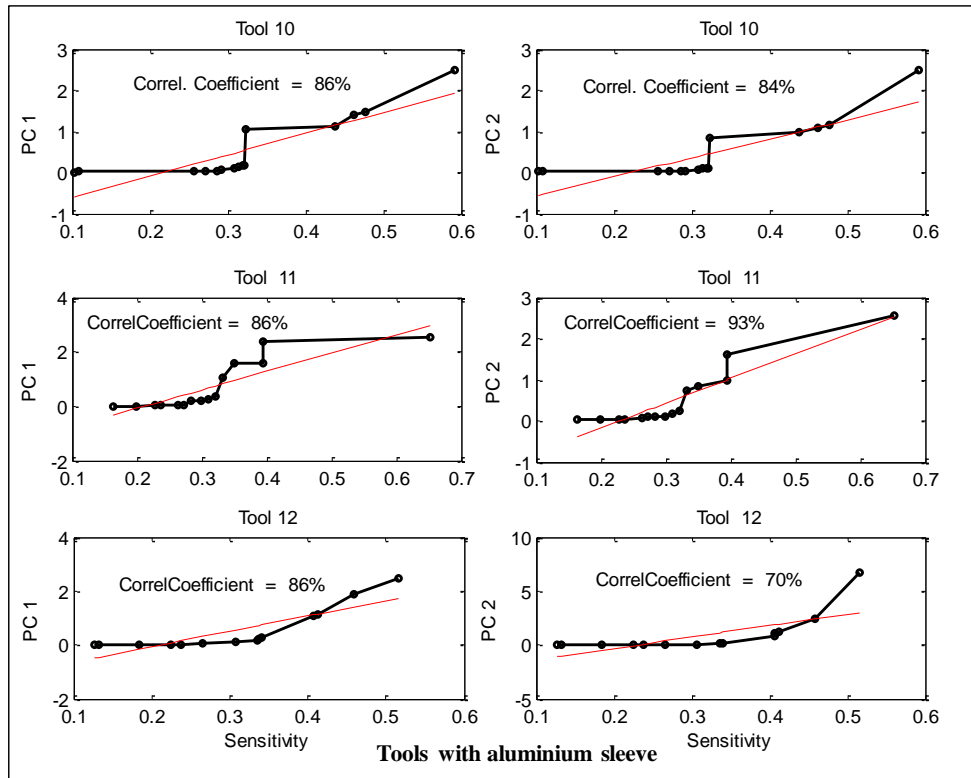


Figure 9.15: The correlation coefficient between PCA and Linear regression sensitivity methods for tools with aluminium sleeves.

Figures 9.12- 9.15 show the correlation coefficient between the sensitivity using linear regression and the sensitivity using the PCA for tools without sleeve, tools with rubber sleeve, tools with copper sleeve and tools with aluminium sleeve respectively. In the Figure 9.12, which plotted the relationship for the three tools without sleeve been used. For those tools, the correlation coefficient between the mean sensitivity and first principal component (PC1) is 94%, 97% and 91%. Meanwhile it is 93%, 97% and 90% between the sensitivity and second principal components (PC2). The correlation coefficient for the three tools with rubber sleeve it is much lower than for the tool without sleeve, where it is (75%, 70% and 80%) for sensitivity and PC1, whereas the relationship between sensitivity and PC2, they are 56%, 54% and 69% as shown in Figure 9.13. Figure 9.14 shows the correlation for the three tools with copper sleeve as (93.6%, 89% and 92%), while the values of correlation coefficient are (93.7%, 83.7% and 89.7%) for the relation between sensitivity and PC2. For the three tools with aluminium sleeve, the correlation coefficient is (86%); however it is (84%, 93% and 70%) between sensitivity and PC2 as shown in Figure 9.15.

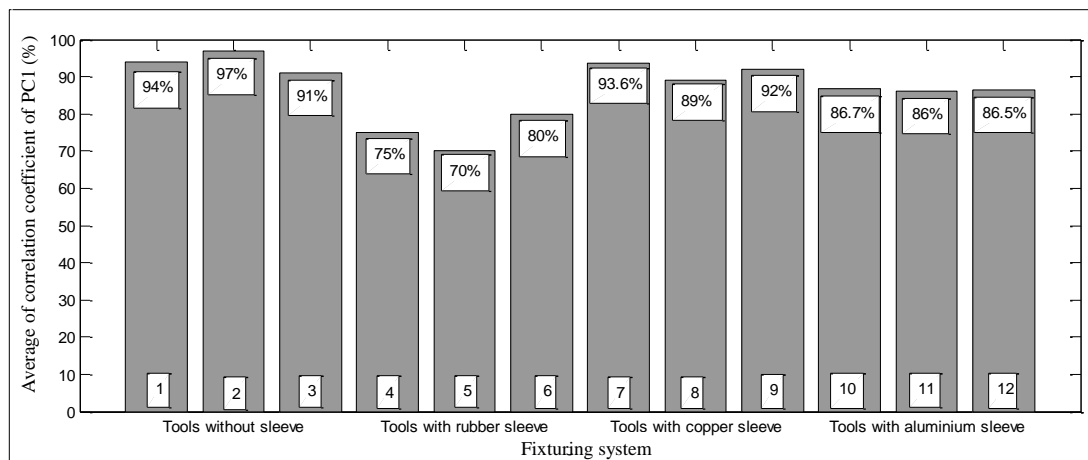


Figure 9.16: The relation between the correlation coefficient of PC1 and fixturing systems.

Figure 9.16 shows the concluding relationships between the correlation coefficient of PC1 and the fixturing materials (all the types of tools with and without sleeve), where the bar chart proves the aforementioned findings as the correlation decreased with the used material less rigidity (less modulus of elasticity) as the maximum correlation for the tools without sleeve, following by the tools with copper sleeve, tools with aluminium sleeve and finally tools rubber sleeve respectively. Figure 9.17 presents similar results for the correlations of PC2.

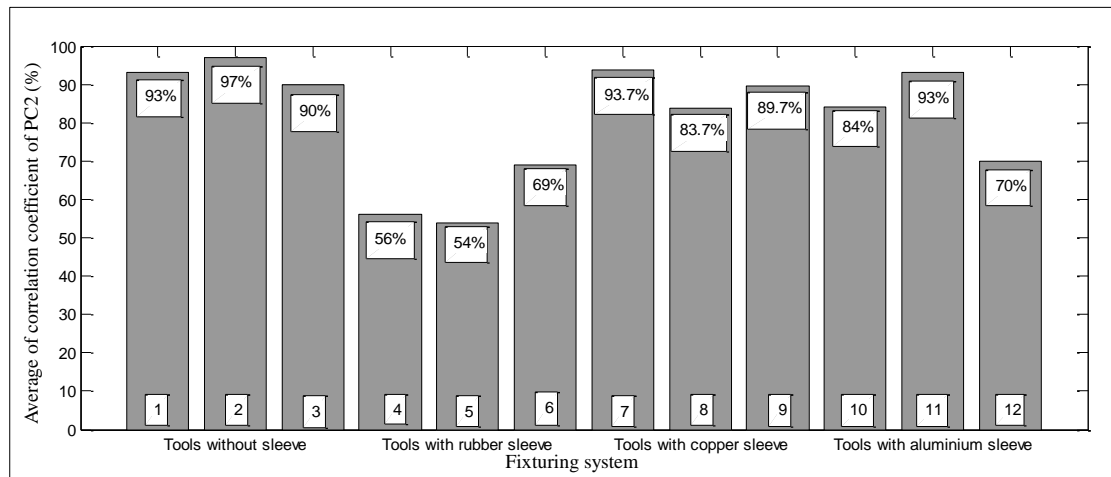


Figure 9.17: The relation between the correlation coefficient of PC2 and fixturing materials.

From the analysis and above figures, it is can be concluded that the fixturing type and material could play a significant role in the result of sensitivity level. In addition, the fixturing type and material could affect the eigenvalues of principal component analysis where there is less sensitivity and correlation coefficient of the tools with rubber sleeve. Whereas, it can be noticed that tools with normal fixturing (tools without sleeve) produce better sensitivity and high correlation coefficient.

The finding of the above discussion that:

- 1- There is significant relationship between the sensitivity using linear regression and those using principal component.
- 2- The second finding is stated that the change of the fixturing material leads to change the sensitivity of the sensory feature. This finding indicates the ability of the fixturing setup to effect on the design of monitoring system.

9.3 Data Training

9.3.1 Linear Regression (LR) method

The data have been collected online from the machining process using the monitoring sensor and signal condition equipment. As the sensor and signal processing method with higher sensitivity are applied to determine the most sensitive of sensory characteristic feature (SCF) using the linear regression slope, the following step is to create a matrix to account the feature data of this sensor arranged from higher to lower

sensitivity values. First twenty SCF of the first tool (Tool with sleeve) are selected as a training data where the first twenty SCF of the other tools are used for testing. Each feature is structured from 27 tests, on the other ward from the first test till last test as the tool status is changed from fresh to worn tool.

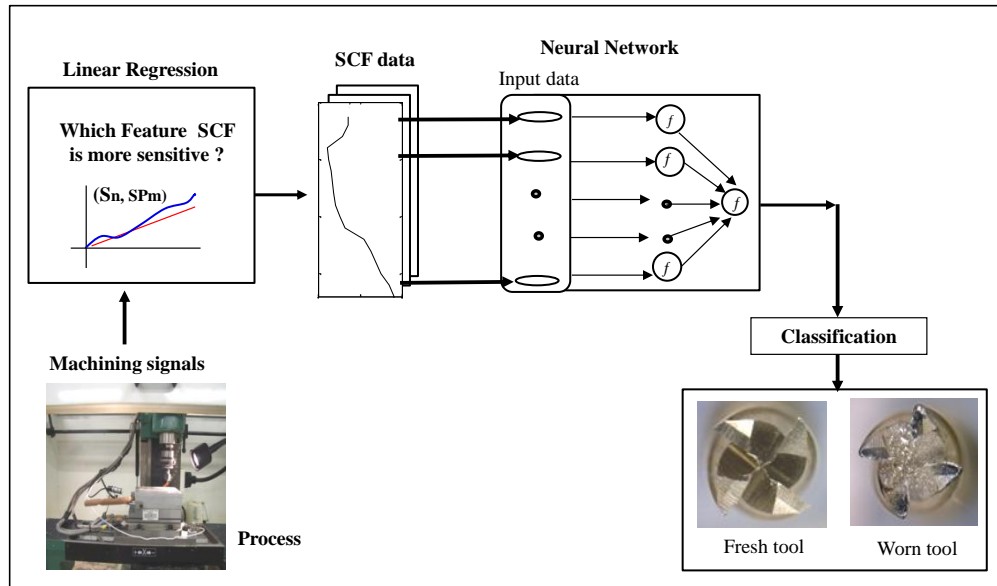


Figure 9.18: The application of Neural Network for SCF data.

Figure 9.18 shows the practical steps of the implementation the neural network for the training data. By using back propagation neural network, it can be classified the tool condition. The training error values between the used tool (first tool without sleeve) and the other tools are measured in neural network.

Figure 9.19 provides examples from the input data to the neural network, where the first twenty features are entered. The SCF of maximum point of the sound signal got high sensitivity according the linear regression slope. Similarly, the minimum point of the accelerometer (V_{sx}), and the maximum point of AE signal from the fresh tool to worn tool.

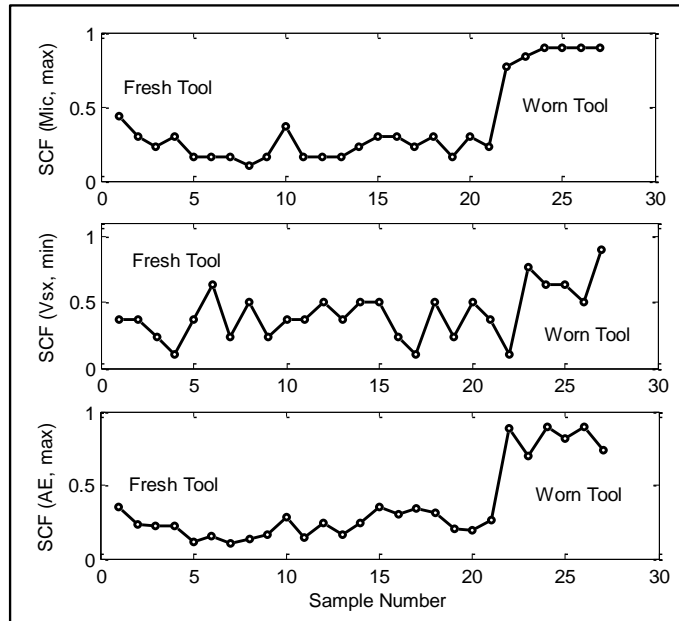


Figure 9.19: Example of the SCF data for input training data.

As the back propagation training algorithm is one of the supervised neural network method, therefore it can be determined the target for output data and it is assumed as ideal target. Moreover, the trained network can be simulated to obtain its response to the inputs in the training set, consequently the difference between the simulated data and the ideal target it is represented the training error as in the following equation:

$$\text{Training error} = \text{Simulated data} - \text{Ideal target} \quad (9.1)$$

Figure 9.20 presents the mean training error percentage for used tools in the experimental test using Back Propagation (BP) as a supervised neural network. The mean error of the tools without sleeve is 1.15 %; meanwhile it is 2.07% for the tools with rubber sleeve. The error values are relatively high for both tools with copper sleeve and tools with aluminium sleeve as they are (1.46 %, 1.84%) respectively.

Similary, Figure 9.21 shows the percentaing of training errors for used tools using un supervised neural network, namely Learning Vector Quantisation (LVQ). The error ratios are less than those obtained from data training using the BP. However, they take the similer patern as the ratio is 0.56% for the tool without sleeve and then it raised to 0.84% for tool with rubber sleeve. Meanwhile, it is 0.79%, 0.82% for the tool with copper and aluminium sleeves respectively.

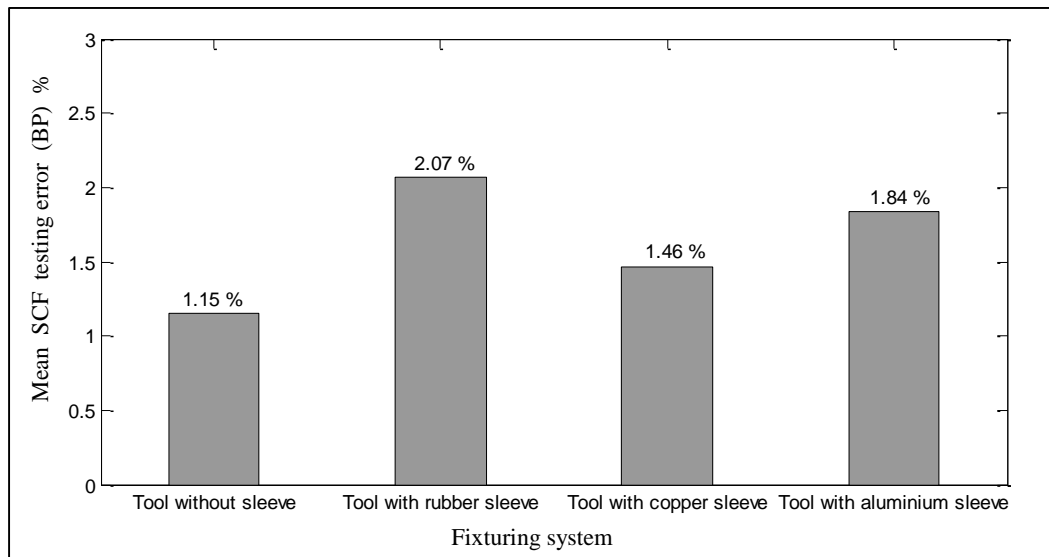


Figure 9.20: SCF testing error ratio using BP neural network for tools with different fixturing systems.

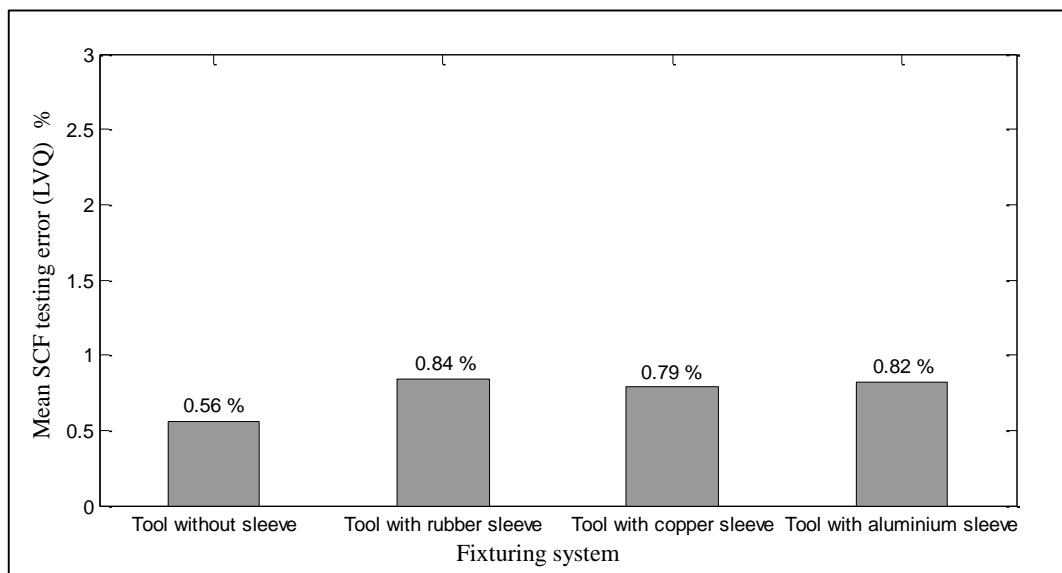


Figure 9.21: SCF testing error ratio using LVQ neural network for tools with different fixturing materials.

9.3.2 Principal Component Analysis (PCA) method

The data have been collected from the machining process using the monitoring sensor and signal condition equipment. As the sensor with higher sensitivity has been determined using the principal component analysis, the next step has also created a matrix to account the sensory data for each one of the sensitive sensors from the first test till 27th test as a tool become completely worn. The data of the first tool is

considered as a training data and the sensory data of the machining rest tools are used for testing.

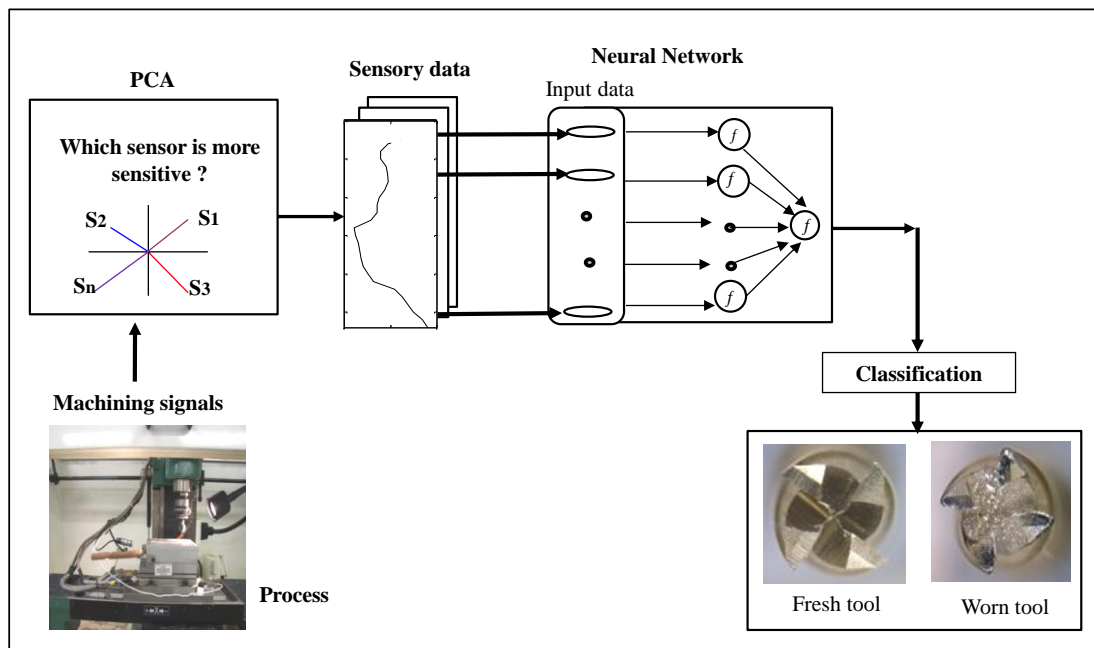


Figure 9.22: The application of Neural Network for PCA data.

Figure 9.22 shows the practical steps of application the neural network for obtained data based on the principle component analysis. It presents that the PCA has ability to state the level of effectiveness as regards the sensor with higher eigenvalue. Consequently, the data of the those sensor are supplied to neural network as training data, therefore the network later could classify the status of the tool as “0” when the tool is fresh(normal) or “1” for the worn tool. Then, the value of training error could be calculated from the difference between the simulated target and ideal target. Figure 9.23 illustrates examples of the input data to the neural network. It can be seen that according to the principal component that the eddy current sensor got the higher eigenvalue and this means that it more sensitive to the changes through milling process, the data of sensory characteristic features for eddy current sensor will be entered as input data (i.e. SCF(Edy, max), SCF(Edy, min), SCF(Edy, std),.....). Where SCF of this sensor are used for training from the fresh tool till the tool will be out of machining.

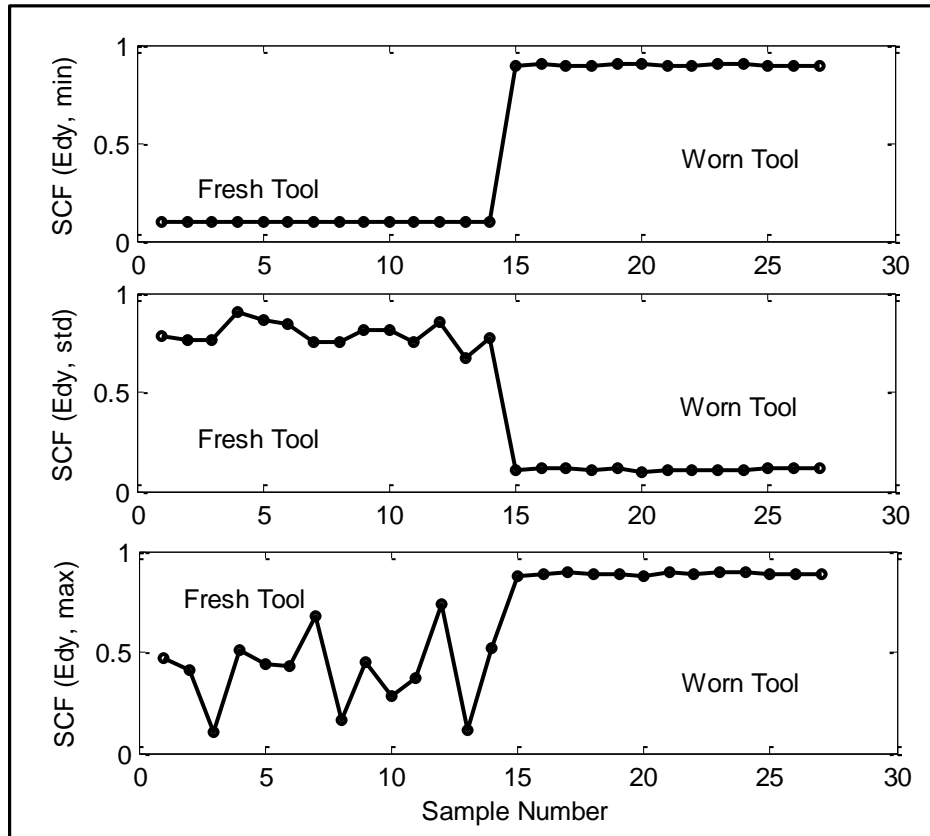


Figure 9.23: Example of the SCF data of most sensitive sensor.

As the aforementioned input data used for training in the neural network, then it is possible to calculate the training error by using the same equation 9.1. Figure 9.24 shows the mean training error for the data of the implemented tools according to the classification of the PCA to determine which sensor gets the more sensitive during the machining process. The training error value is 1.27% for the tools without sleeve, 2.25% for the tools with rubber sleeve, and 2.1%, 2.41% for tools with copper sleeve and tools with aluminium sleeve respectively. It is clear that the error percentages for the tools with sleeve higher than those for tools without sleeve. Figure 9.25 presents the error percentages of the data training using LVQ neural network where they are 0.55%, 1.16%, 0.65% and 1.1% for the tools without sleeve and tools with rubber, copper and aluminium sleeves respectively. The values of these errors lower than those resulted by using BP neural network. This could be provided an indicator to the ability to classify the fixturing as perfect or imperfect from the result of training in neural network.

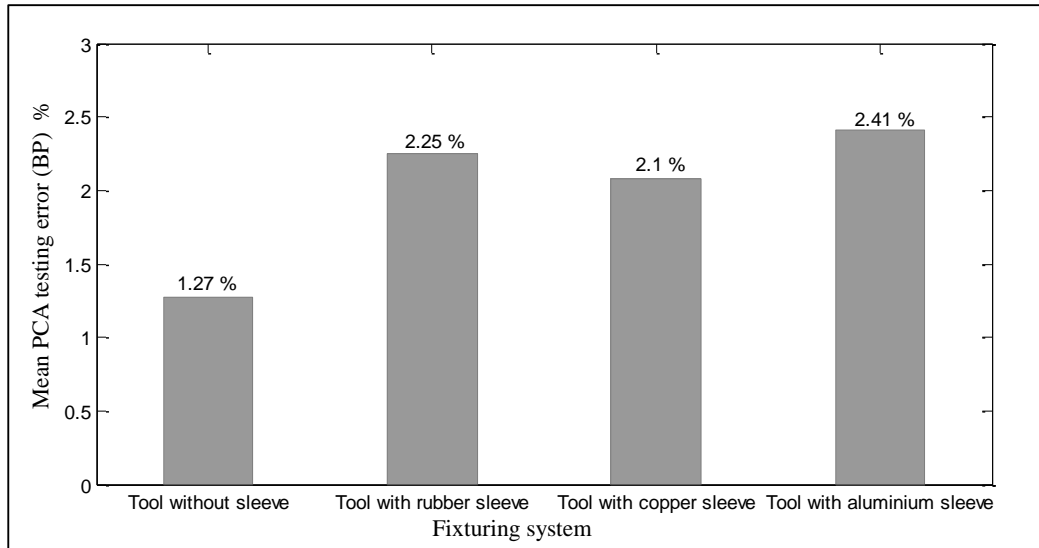


Figure 9.24: PCA testing error ratio using BP neural network for tools with different fixturing systems.

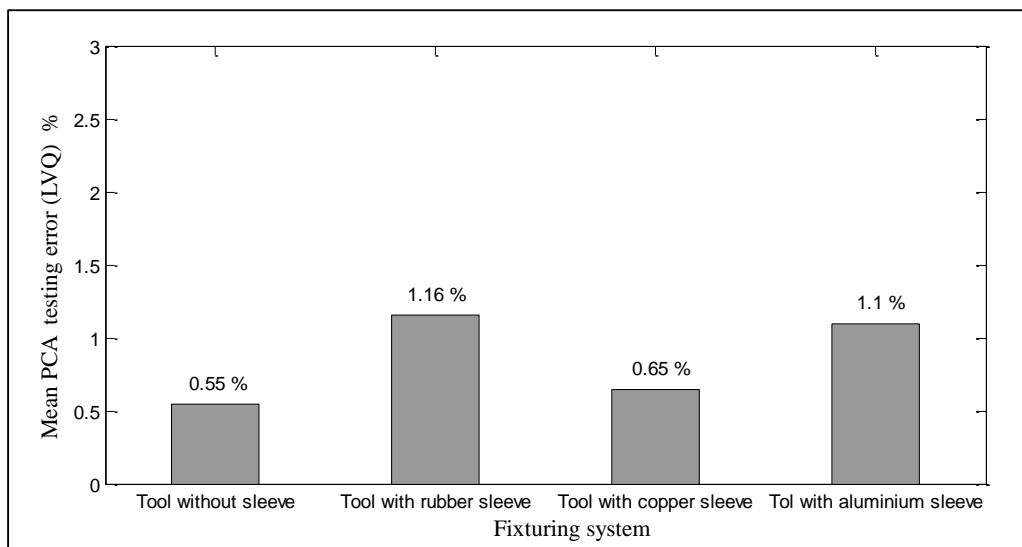


Figure 9.25: PCA testing error ratio using LVQ neural network for tools with different fixturing materials.

9.3.3 The Training Error Evaluation

It would be interesting to compare the results of mean training error depend on the training data from linear regression method and principal component analysis. Figure 9.26 has been combined the errors results from Figure 9.20, and Figure 9.24, and combined the Figures 9.21 and Figure 9.25 to show the correlation coefficient relation between the signal simplification methods using different neural networks. The

correlation coefficient is 85.5% between the LR and PCA using supervised Back propagation network (BP), whereas it is 78% between them using unsupervised learning vector quantisation (LVQ) neural networks. Generally, it can be seen that the values of errors from the training data using linear regression is lower than those obtained from the principal component analysis in both used neural network. The amount of errors using BP neural network is higher than training errors by using LVQ network. However, the patterns of training error for both methods are consistent where they started with lower error values for the tools without sleeve and then they rose for the rest tools without sleeve. One of the more significant findings to emerge from this discussion is that the training errors depend on the linear regression is less than other method, also the ability of the neural network to define the machine setup stability. Taken together, these findings support the reliability of the proposed monitoring system to detect the changes in the fixturing set up.

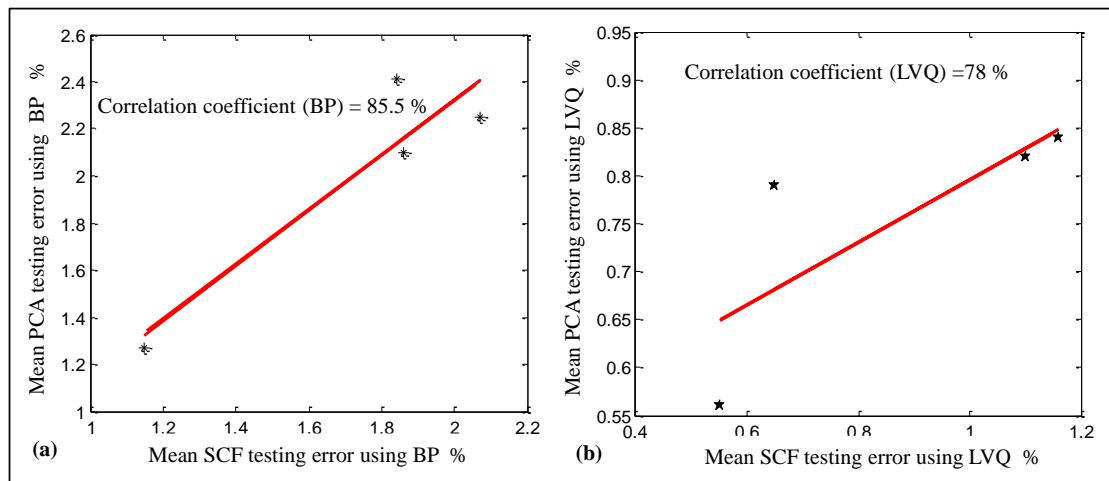


Figure 9.26: correlation coefficient between training errors of LR and PCA (a) using BP neural network, (b) using LVQ neural network.

9.4 System Cost and Utilisation

The same method used in Chapter 8 to calculate the cost of the system is used here again. Figure 9.27 shows the sensor set-up for the experimental work in this section.

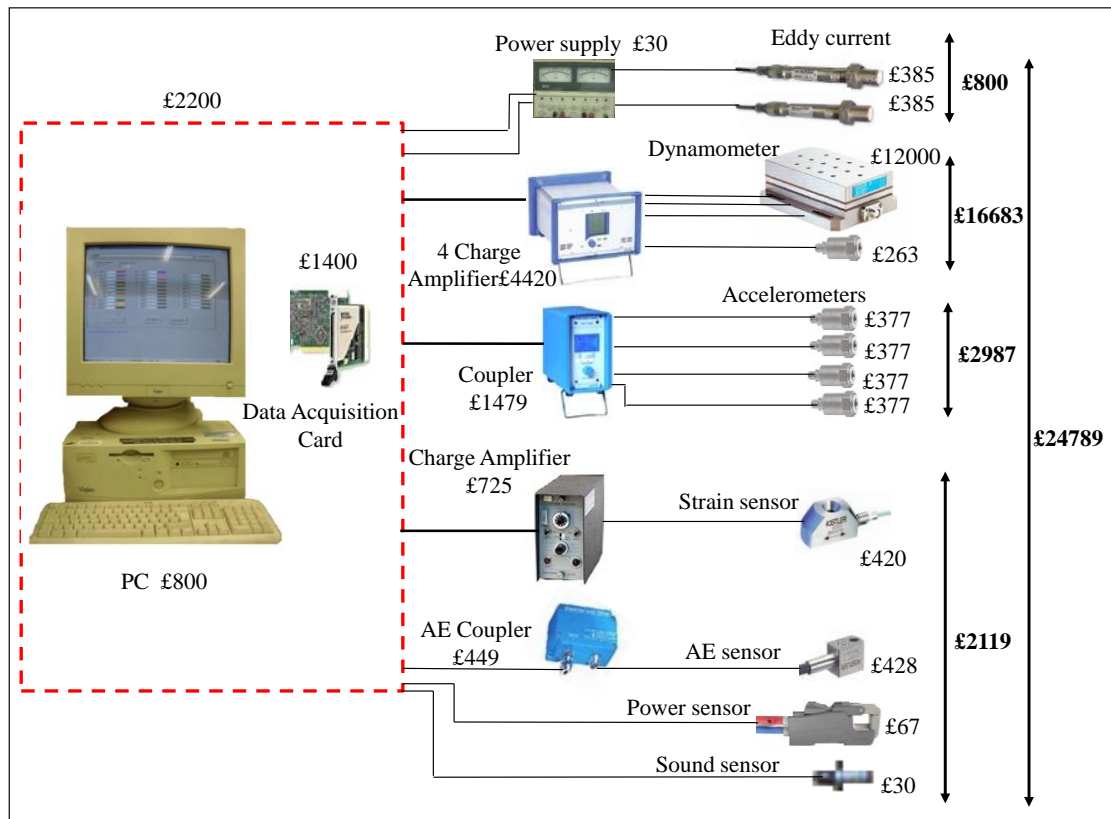


Figure 9.27: The sensor setup used to calculate the cost of the system (prices are based on quotation).

9.4.1 Selection of Sensory Features

9.4.1.1 Selection of Sensory Characteristic Feature (SCFs)

By using the linear regression method to develop the designed system, and as the 12 tools need to be analysed clearly, therefore they are classified to four groups as each three tools use the same type of sleeve and are been grouped together.

The same method for the SCF classification which is used in the chapter 8, section 8.4.1, the three systems have the average sensitivity as shown in Figure 9.28 for the tool 1 without sleeve. It can be observed that the first system has the most sensitivity features for fixturing system stability and tool wear detection compared to the other systems. The SCF classification for the other tools (2-12) is described in Appendix D.

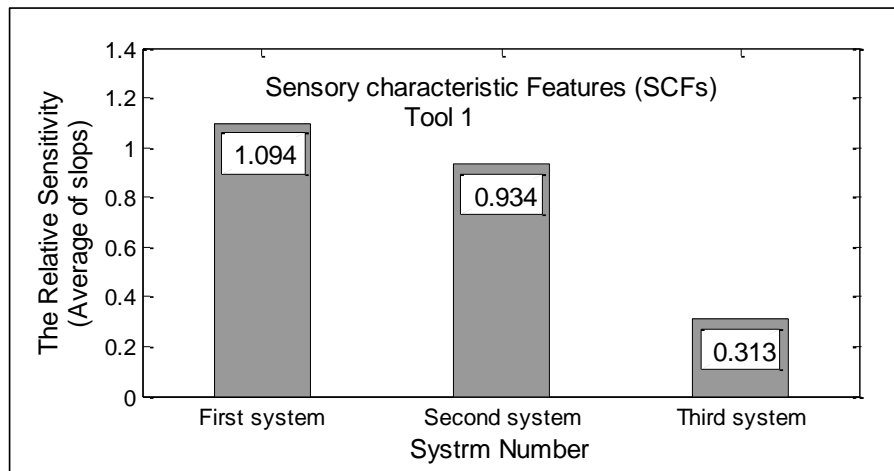


Figure 9.28: Comparison between the systems sensitivity for tool 1 without sleeve.

Table 9.4: First system with the SCFs sensitivity (LR) slope for the tool 1 without sleeve.

Tool 1 without sleeve		
Sensory Signal	SP method	Sensitivity
Edy	min	1.195
Edy	average	1.194
Edy	power	1.193
Edy	std	1.145
Edy	range	1.106
Edy	skew	1.075
Edy	kurtosis	1.071
Edy	max	0.998
Pwr	power	0.991
AE	min	0.974
Average		1.094

Table 9.5: Second system with the SCFs sensitivity (LR slope) for the tool 1 without sleeve.

Tool 1 without sleeve		
Sensory Signal	SP method	Sensitivity
AE	range	0.965
AE	max	0.951
Mic	max	0.943
Fy	power	0.942
Vsy	power	0.929
AERMS	power	0.928
AERMS	max	0.926
AE	std	0.922
Mic	average	0.921
Mic	power	0.920
Average		0.934

Table 9.6: Third system with the SCFs sensitivity (LR slope) for the tool 1 without sleeve.

Tool 1 without sleeve		
Sensory Signal	SP method	Sensitivity
Vwy	kurtosis	0.348
AERMS	kurtosis	0.343
Vsz	min	0.342
Edx	range	0.340
Fz	kurtosis	0.331
Pwr	average	0.324
Edx	max	0.298
Fz	range	0.288
Vsy	kurtosis	0.262
Vsy	skew	0.255
Average		0.313

9.4.1.2 Selection of Principal Component Feature (PCFs) Method

The same method in the section chapter 8, section 8.4.2, for PCF classification is used here for sorting the 12 tools which are implemented the experiment work. In the following subsections, the classification process for the tool 1 without sleeve, more details about the other tools are described in Appendix E.

The three systems have the average sensitivity as shown in Figure 9.29 for the tool 1 without sleeve. It can be observed that the first system has the most sensitivity features for fixturing system stability and tool wear detection compared to the other systems.

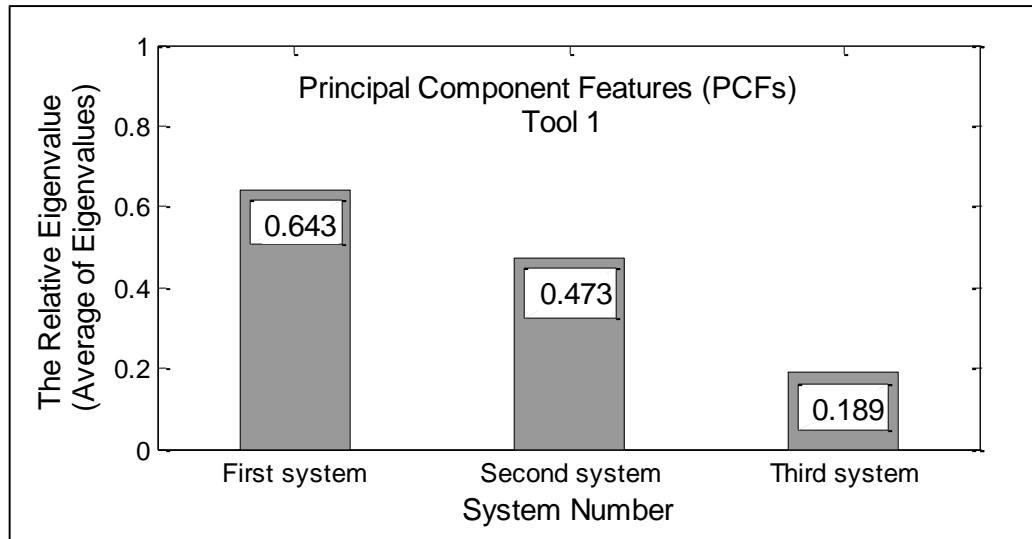


Figure 9.29: Comparison between the systems eigenvalue of tool 1 without sleeve.

Table 9.7: First system with the PCFs eigenvalue (PCA) for the tool 1 without sleeve.

Tool 1 without sleeve		
Sensory Signal	PC method	Eigenvalue
Edy	PC1	0.879
Edy	PC4	0.862
Fx	PC10	0.664
Edy	PC8	0.638
Edy	PC15	0.586
Edy	PC2	0.580
Edy	PC9	0.576
Edy	PC4	0.569
Fx	PC4	0.550
Fx	PC3	0.529
Average		0.643

Table 9.8: Second system with the PCFs eigenvalue (PCA) for the tool 1 without sleeve.

Tools 1 without sleeve		
Sensory Signal	PC method	Eigen-Value
Fx	PC3	0.516
Fx	PC 6	0.504
Fy	PC 10	0.494
Edy	PC 14	0.492
Fx	PC 6	0.474
Edy	PC 1	0.471
Fx	PC 12	0.458
Edy	PC 9	0.447
Edy	PC 13	0.442
Fx	PC 3	0.437
Average		0.473

Table 9.9: Third system with the PCFs eigenvalue (PCA) for the tool 1 without sleeve.

Tools 1 without sleeve		
Sensory Signal	PC method	Eigen-value
Pwr	PC13	0.194
Vsz	PC 9	0.193
Vwy	PC 12	0.193
Fy	PC 4	0.193
Strain	PC 6	0.193
AE	PC 8	0.193
Edx	PC 8	0.189
Strain	PC 4	0.184
Pwr	PC 8	0.181
Vwy	PC 4	0.178
Average		0.189

9.4.2 System Optimisation

9.4.2.1 Linear Regression slope (LR slope) Method

From Tables 9.4 and 10.5, it can be observed that there is no significant difference in the average sensitivity for both systems for the tool 1 without sleeve. More details about the other tools (2-12) are described in Appendix F.

The cost of first and second systems is significant different (£10146, £22138). But it is still can be optimised by increasing the system utilisation by replacing the sensory characteristic features of the *power* sensor from the first system with the *AE* sensory signals from the second system to reduce the cost and still have the sensitivity level. For the tool 2, the difference in the cost between the first and second systems is slight but for tool 3 it is too high.

Table 9.10: Sensors utilisation for the tool 1 without sleeve using LR.

Tool 1			
Sensor	U 1st system	U 2nd system	Optimised System
Dynamometer	-----	3.33%	-----
AE	5 %	25%	10%
Mic	-----	30%	-----
Vsy	-----	10%	-----
Pwr	10%	-----	-----
Edy	80%	-----	80%
UA Average Utilisation	31.66%	17%	45%
System Cost	£10146	£22138	£10116
Average Sensitivity	1.094	0.934	1.091

As shown in Table 9.10, the overall average utilisation has increased in the first system from 31.66% up to 45% and from 17% up to 45% in the second system and the cost is reduced by 59 % from £24789 to £10116. In fact the average sensitivity has increased to 1.091 compared with the second system of tool 1 as can be seen in Table 9.11.

Table 9.11: The optimised system (1st and 2nd system) for the tool 1 without sleeve using LR.

Tool 1 without sleeve		
Sensory Signal	SP method	Sens-itivity
Edy	min	1.195
Edy	average	1.194
Edy	power	1.193
Edy	std	1.145
Edy	range	1.106
Edy	skew	1.075
Edy	kurtosis	1.071
Edy	max	0.998
AE	min	0.974
AE	range	0.965
Average		1.091

9.4.2.2 Principal Component Analysis (PCA) Method

From Tables 9.7 and 9.8, it can be observed that there is no significant difference in the average sensitivity for both systems for the the tool 1 without sleeve. The details about the other tools (2-12) are described in Appendix G.

For the tool 1, for example, the cost of both systems is the same (£19035). But it is still can be optimised by increasing the system utilisation by replacing the sensory characteristic features of the eddy current sensor(Edx) from the first system with the forces sensory signals from the second system to reduce the cost and still have the sensitivity level.

Table 9.12: Sensors utilisation for the tool 1 without sleeve using PCA.

Tool 1 without sleeve			
Sensor	U 1st system	U 2nd system	Optimised System
Dynamometer	10%	20%	6.66%
Edy	70%	40%	80%
UA Average Utilisation	40%	30%	43.33%
System Cost	£19035	£19035	£19035
Average Eigenvalue	0.643	0.473	0.640

As shown in Table 9.12, the overall average utilisation has increased in the first system from 40 % up to 43.33% and from 30% up to 43.33% in the second system and the cost is reduced by 23 % from £24789 to £19035. In fact the average sensitivity has increased to 0.640 compared with the second system of the tool 1 as can be seen in Table 9.13.

Table 9.13: The optimised system (1st and 2nd system) for the tool 1 without sleeve using PCA.

Tools 1 without sleeve		
Sensory Signal	PC method	Eigen-value
Edy	PC1	0.879
Edy	PC4	0.862
Fx	PC10	0.664
Edy	PC8	0.638
Edy	PC15	0.586
Edy	PC2	0.580
Edy	PC9	0.576
Edy	PC4	0.569
Fx	PC4	0.550
Edy	PC14	0.492
Average		0.640

9.4.2.3 System Optimisation Correlation Using LR and PCA methods

In the previous sections, the sensory system optimisation is implemented using different methods, namely, Linear Regression (LR) and Principal Component Analysis (PCA). However, it can be seen that there is significant similarity between two methods to reduce the cost of the monitoring system and to detect the changes of the fixturing stability or tool wear occurred. From the above tables, it can be observed that the selected sensor for the tools without sleeve is Eddy current (Edy) in both used methods (i.e. LR and PCA), whereas, the AE and dynamometer sensors are the second selected sensors for those tools as the cost of the dynamometer is £12000 and the AE is £428. This reason creates a significant difference between the optimised system costs. The sensor utilisation average (UA) of optimised system for the tool without sleeve is 45% using LR method, but the UA for those tools is slightly different (i.e. 43.33%) due to increase the number of feature of the dynamometer sensor using PCA method as shown in Table 9.14.

Table 9.14: Comparison between the optimised systems from LR slope and PCA for tools with different fixturing systems.

Method	Variable	Linear Regression (LR)	Principal Component PCA)
Tool without sleeve	Selected sensor	Eddy current (Edy) AE	Eddy current (Edy) Dynamometer
	UA of optimised system	45%	43.33%
	Optimised System Cost	£10116	£19035
	Reduced cost ratio	59 %	23 %
	Optimised System Sensitivity	1.091	0.640
Tool with rubber sleeve	Selected sensor	Dynamometer Eddy current (Edx) Power	Dynamometer Eddy current (Edy)
	UA of optimised system	24.44%	40%
	Optimised System Cost	£21755	£19035
	Reduced cost ratio	12 %	23 %
	Optimised System Sensitivity	0.651	0.611
Tool with copper sleeve	Selected sensor	Dynamometer Power	Dynamometer Eddy current (Edy)
	UA of optimised system	33.33%	36.66%
	Optimised System Cost	£18620	£19035
	Reduced cost ratio	24.8 %	23%
	Optimised System Sensitivity	0.792	0.669
Tool with aluminium sleeve	Selected sensor	Dynamometer Microphone Power	Dynamometer Eddy current (Edy)
	UA of optimised system	22.22%	36.66%
	Optimised System Cost	£18717	£19035
	Reduced cost ratio	24%	23%
	Optimised System Sensitivity	0.685	0.695

The cost of the optimised systems is same (i.e. £19035) for all the tools using the PCA method, however this cost is different for the tools using the LR method. For the tools with different fixturing materials (rubber, copper and aluminium sleeves), it can be observed that both LR and PCA methods are presented that the dynamometer, eddy current and power are the most sensitive sensors due to the fact that they have been presented with a high ability to detect the change of machining characteristics. It is also clearly noticed that the sensitivity of the sensory system is changed according to the change in the fixturing quality. In details, the values of optimised system sensitivity are (0.651, 0.611) for the tool with rubber sleeve using LR and PCA methods respectively, however, they are (0.792, 0.669) and (0.685, 0.695) for the tools with copper and aluminium sleeves.

9.4.3 System Evaluation

9.4.3.1 Linear Regression slope (LR slope) Method

Same methods which are used to calculate the average sensitivity of the sensory signals and signal processing methods using linear regression (LR) in chapter 8, section 8.5.2.1, here it will be applied for the signals for testing tool 1 without sleeve as in the next sections. More details about the testing other 11 tools are described in Appendix H.

Figure 9.30 shows the average sensitivity (A_s) for the tool 1 without sleeve, as it is clear that the eddy current sensor (Edy) is the more sensitive, and the acoustic emission (AE) and microphone sensors are the following higher sensitivity for this tool.

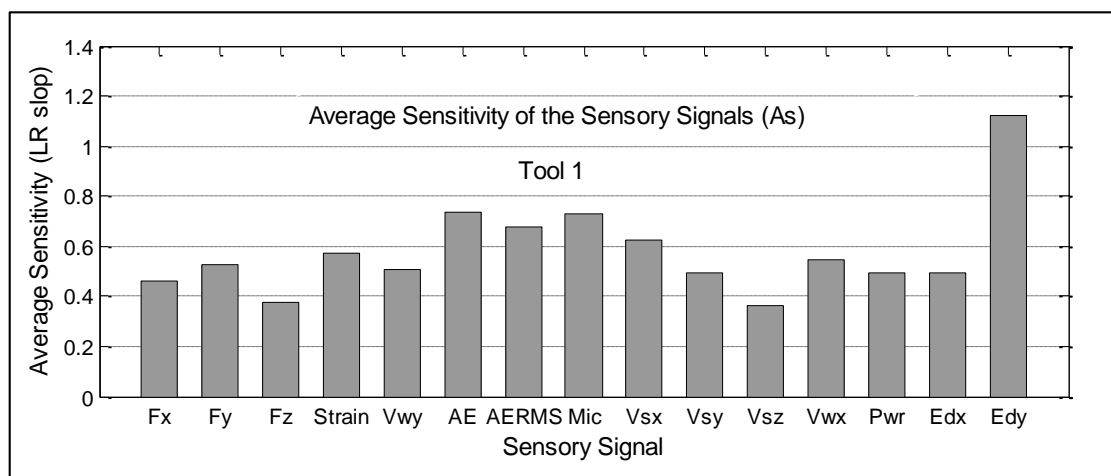


Figure 9.30: A_s values for the sensory signals of tool 1 without sleeve.

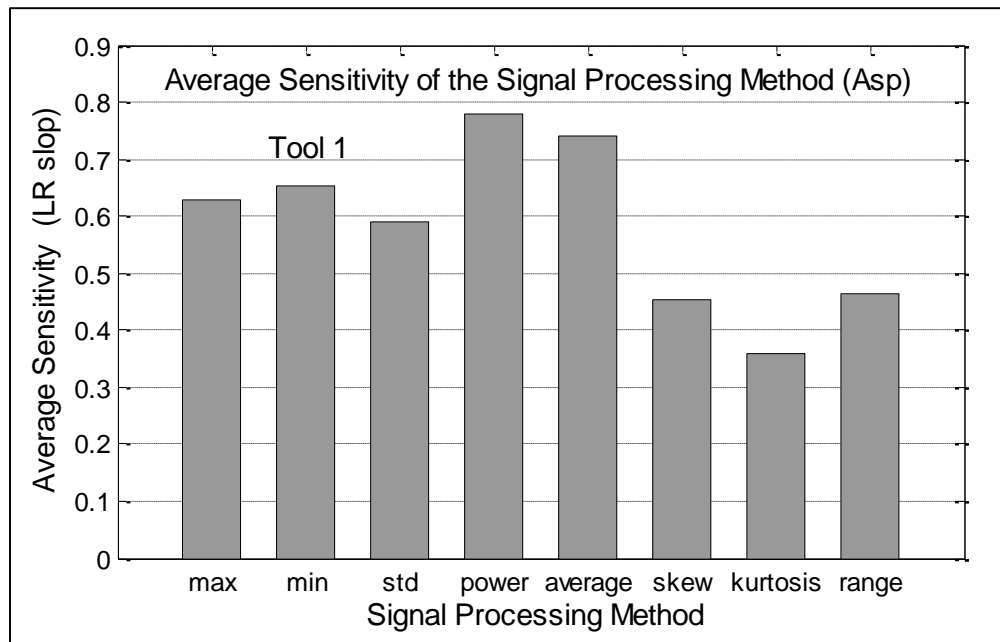


Figure 9.31: Asp values for the signal processing methods of tool 1 without sleeve.

Figure 9.31 shows the average of the sensitivity of the signal processing methods (Asp) for the tool 1 without sleeve. It presents that the power as a signal processing method take the higher rank as most sensitive method for the tool 1 without sleeve. Following this, the average and minimum signal processing methods are the more sensitive methods.

Same method in the chapter 8, section 8.5.2.1, here the average of the summation of sensitivity coefficients (A_c) of those systems is found to be (0.58) for the tool 1 without sleeve. However, to find the effectiveness of the selection of the utilised sensors and signal processing methods, the evaluated values can be compared with other systems.

9.4.3.2 Principal Component Analysis (PCA) Method

Same methods which are used to calculate the average eigenvalue of the sensory signals and signal processing methods using Principal Component Analysis (PCA) in chapter 8, section 8.5.2.2, here it will be applied for the signals for testing tool 1 without sleeve, however, more details for testing 11 tools in the Appendix I.

Figure 9.32 shows the average eigenvalue (Aev) for the tool 1 without sleeve, as it is clear that the eddy current (Edy) sensor is the most sensitive to detect the tool wear and fixturing quality. Force sensor (Fx) is also the higher sensitivity.

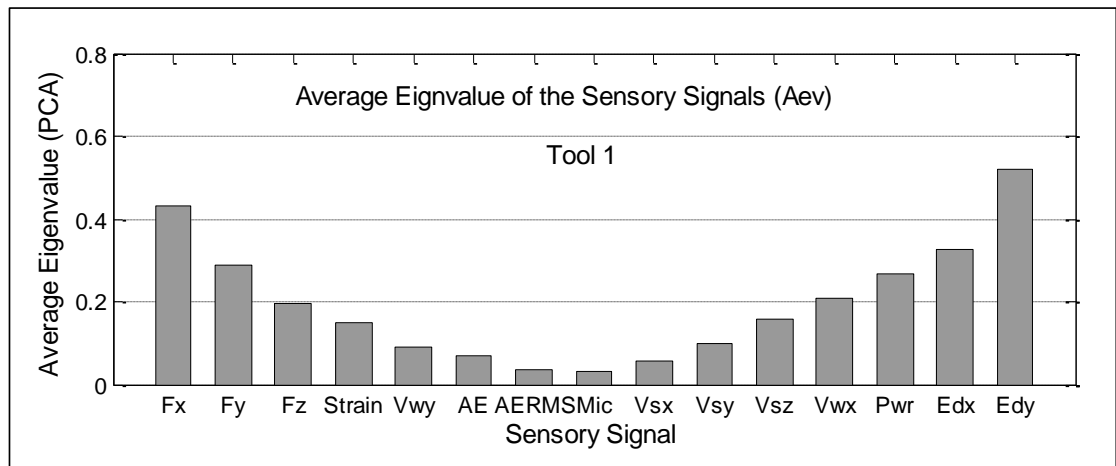


Figure 9.32: Aev values for the sensory signals of tool 1 without sleeve.

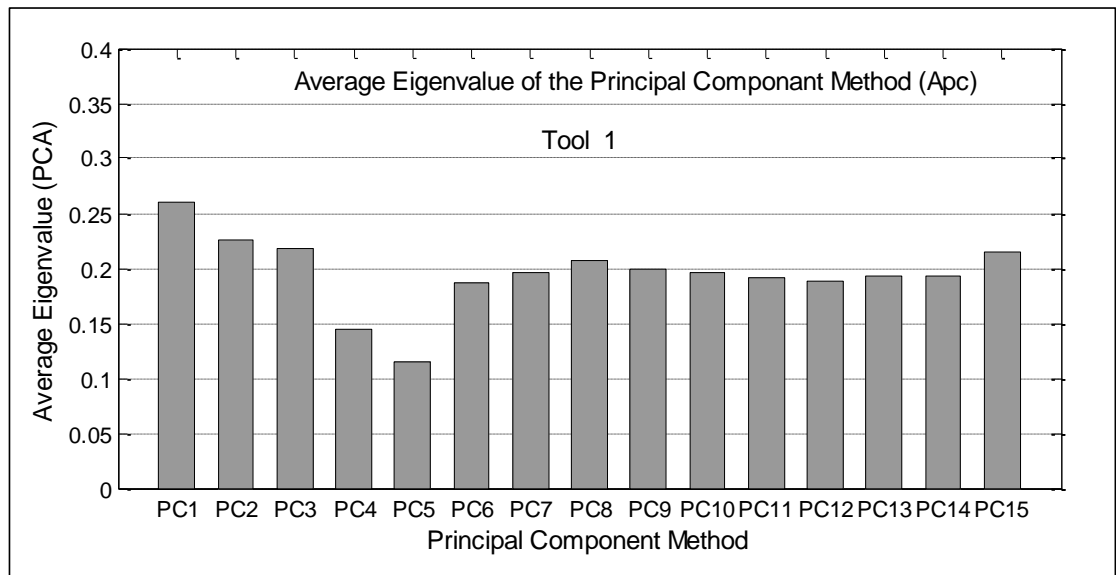


Figure 9.33: Apc values for the principal component methods of tool 1 without sleeve

The average of the eigenvalue of the principal component methods (Apc) for the tool 1 without sleeve as shown in Figure 9.33. It presents the first principal component (PC1) as a most sensitive method for tool 1 without sleeve, however the second and third principal components (PC2 and PC3) are also more sensitive methods for this tool.

The same method in the chapter 8, section 8.5.2.2, here the average of the summation of eigenvalue coefficients (E_c) of those systems is found to be (0.19) for the tool 1 without sleeve.

9.4.3.3 Comparison between LR and PCA methods

Figure 9.34 shows the values of the A_c factor and the E_c factor for 12 tools (normal and tools with rubber, copper and aluminium sleeve). It can be seen that there is a

difference between the factors in the value as for normal tools, for example, the average of the sensitivity coefficients (A_c) for three tools without sleeve is (0.58, 0.32 and 0.28) , however the average of the eigenvalue coefficients (E_c) for those tools is (0.19,0.20 and 0.18) respectively. This comparison for other tools is shown in the Figure 10.44. The more significant findings to emerge from this discussion are that:

- 1- Both linear regression (LR) and principal component method (PCA) could be provided similar indication with regard to determine which sensor has a higher sensitivity.
- 2- Those methods indicate that the ability of the suggested monitoring system to detect the changes in the fixturing system, therefore it could be used to monitor the faults or the changes of the machine setup during the manufacturing operation.

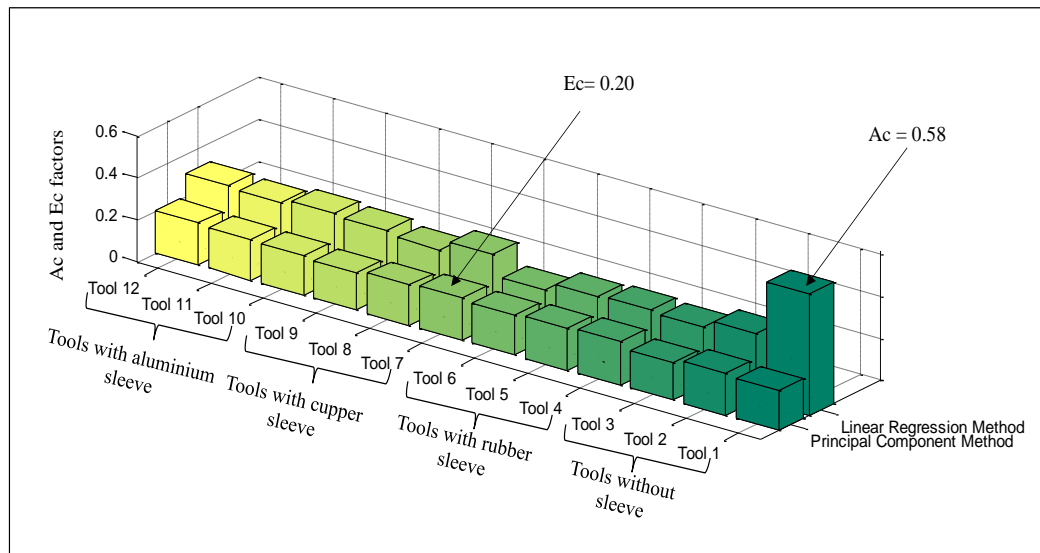


Figure 9.34: Comparison between A_c and E_c of both tools.

9.5 Pattern Recognition

As discussed in the previous sections that approved the ability of the sensitivity measuring methods to define the more sensitive features, that is will lead the investigation to the next stage of the monitoring system which is the pattern recognition. In general, therefore, it seems that is important to classify the status of the tool from fresh to worn then making the decision. The most important limitation lies in the fact that when to spot that the fresh stage has been finished and the tool raised to semi-worn or completely worn. It can therefore be assumed that the tool status has

taken different start or end points. On the other ward, the fresh stage may be finished at point n_{ij} , meanwhile the semi-worn finished before or after point n_{ij} and so on. In this research, Taylor's Equation Induced Pattern (TIP) has been proposed to deal with this obstacle, as the patterns of constant functions and the experimental sensory feature could be used as shown in Figures 9.35- 9.37. These patterns are considered as templates to divide the target of neural network. Here, Back Propagation (BP) Neural Network will be implemented the data training and testing since it is supervised method and definitely needs to determine the target in advance.

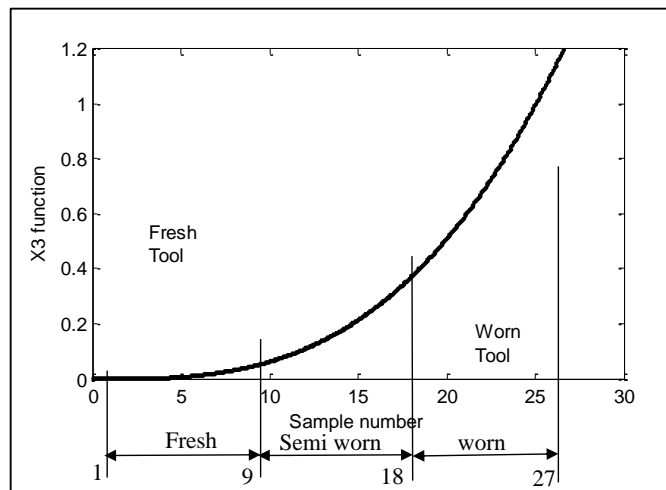


Figure 9.35: The BP neural target division according to the X3 function.

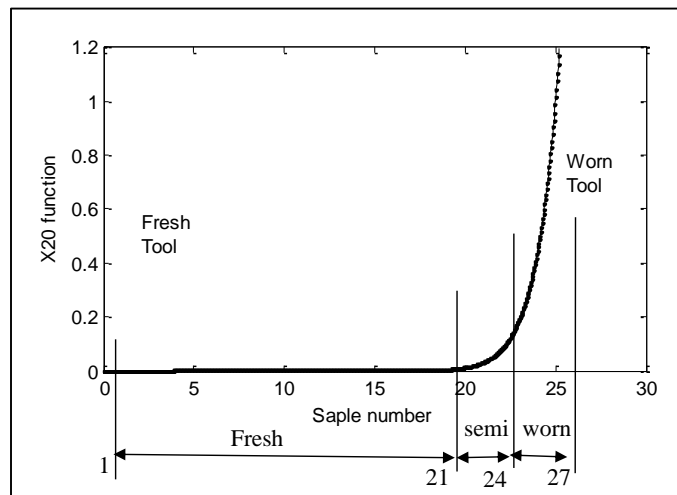


Figure 9.36: The BP neural target division according to the X20 function.

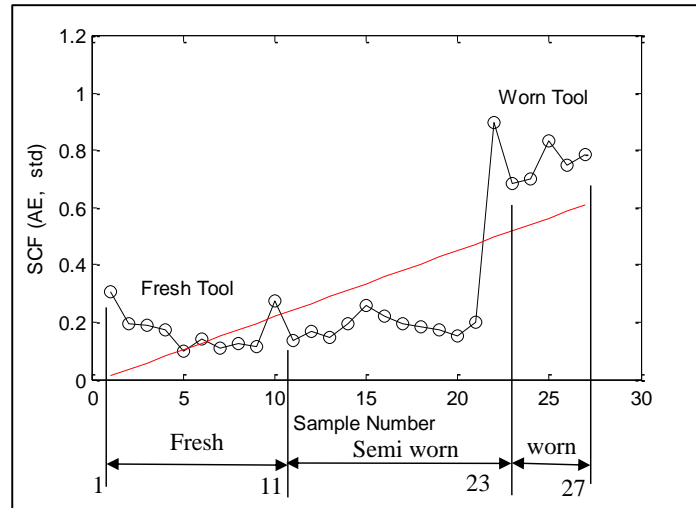


Figure 9.37: The BP neural target division according to the experimental feature (Experimental).

Figure 9.35 shows the first constant function (X3 function) divided the 27 tests to three equal sections, meanwhile Figure 9.36 shows the second function (X20 function) divided to different sections length (21 fresh, 3 semi-worn, 3 worn). The experimental sensory feature (Experimental) divided to (11 fresh, 12semiworn, 4worn) as illustrated in Figure 9.37. Each type of the above function has been used as a suggested target for the Back Propagation (BP) Neural Network. The learning role for BP are (epochs=500; Learning rate=0.7). Following this, the feature data of the first tool used for training and the data for else tools used for testing.

The results of the training and testing for the tools used in the tests have shown that the X20 function achieves lower ratio of error in comparing with the two another methods as illustrated in Figure 9.38. The finding of this means that generally the tool still fresh and could be used as fresh tool till the test 21, and then from test 22 to 24 as a semi worn. On the other word, it can be considered a 77% of the tool life as a fresh tool and till 88% as semi worn. The remained percentage is considered as a worn. The results of the training error BP neural network are different from the tools to other depend on the quality of the fixturing system, as errors for tools without sleeve are different with those for tool with rubber sleeve , tool with copper sleeve or tool with aluminium sleeve.

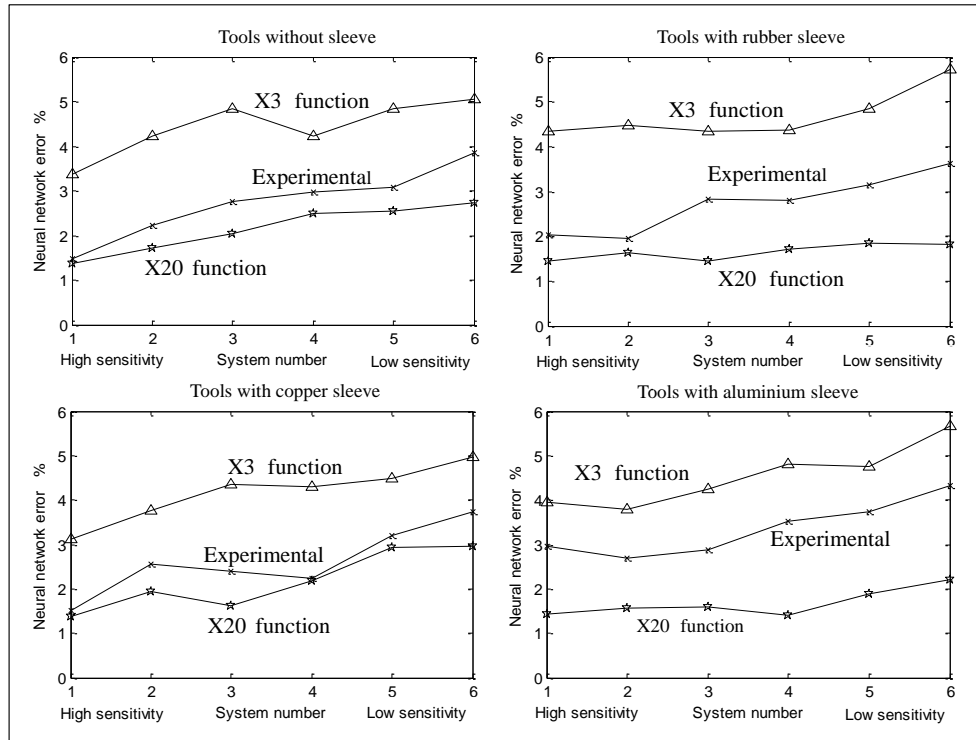


Figure 9.38: The of testing errors for all the tools using different target functions.

Consequently, according to the results as shown in the Figure 9.38 that the suggested function (X20) proves the significant ability to represent the most of the patterns of the features and provides the decision for the status of the tool condition. Furthermore, it is clearly evidenced that the type and material of the fixturing system could be considerably effect on the design of the condition monitoring system.

9.6 Surface Roughness

Surface specification can also be a good reference point in determining the quality of a production process, because the stability of the machine is affected on the feature of the operating part. In this section, the surface roughness will be measured for the machined surface, and then investigate the correlation between the sensitivity of the sensors which is increased with change the tool condition (from fresh to worn) and the roughness of the surface.

9.6.1 Roughness of Machined Surface

The surface roughness of the workpiece has been measured for each track of 27 tests with used normal fixturing and different elastic material sleeves namely rubber, copper and aluminium.

Figure 9.39 has shown the results of the surface roughness for four cases. The consequences of the patterns indicate that the values of the surface toughness when using tool without sleeve is less than those obtained when using tools with rubber, copper and aluminium sleeves which are also illustrated in the same figure using the average of surface roughness measurement for each case. The reason for these results may be the modulus of elasticity of steel (200 GPa) which is significantly more than for elastic materials (0.01- 0.1 GPa, 120 GPa and 69 GPa, [204] as rubber, copper and aluminium respectively as shown in Table 9.15. It is clear from the statistical methods that the surface roughness is increased with reduced of the modulus of elasticity for the fixturing materials.

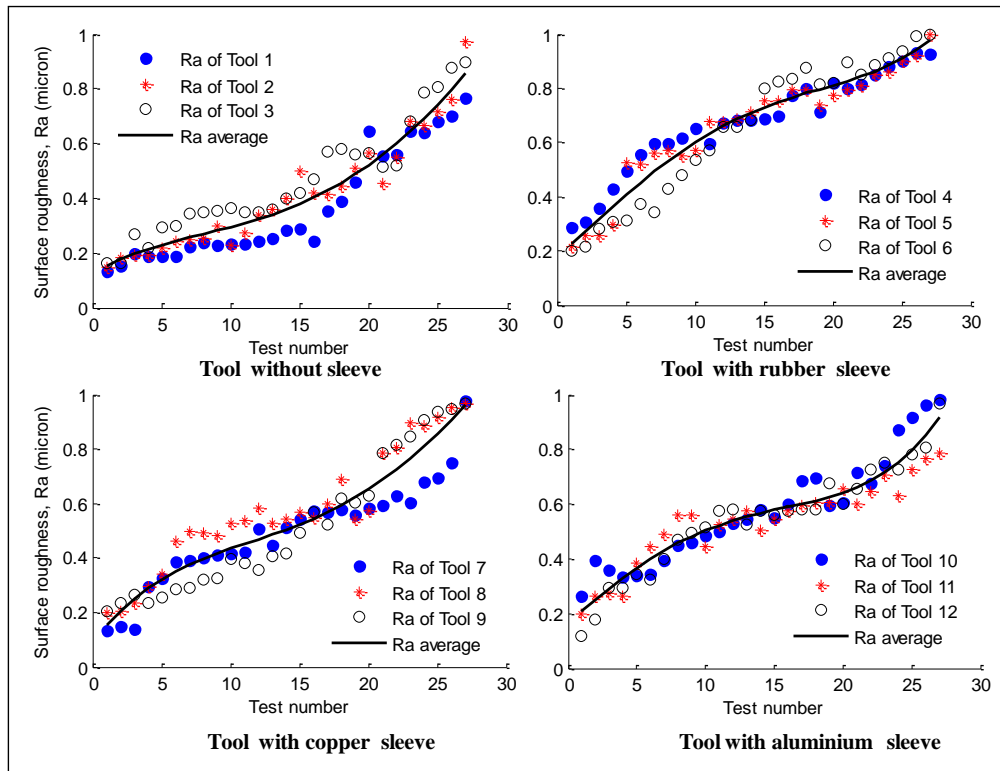


Figure 9.39: Surface roughness of workpiece for four types of fixturing materials.

Table 9.15: The modulus of elasticity (E) and average of surface roughness.

Material	Without sleeve (steel)	Rubber sleeve	Copper sleeve	Aluminum sleeve
Factor				
Modulus of elasticity E (GPa)	200	0.01-0.1	120	69
Max. Ra (µm)	0.878	0.9740	0.9713	0.9117
Min. Ra (µm)	0.148	0.2357	0.1797	0.1933
Median Ra (µm)	0.3603	0.6910	0.4907	0.5517

9.6.2 The Correlation Coefficient

The correlation coefficient is a quantity that gives the quality of a least squares fitting to the original data or to define the relation between two cases. In this research, it is used to calculate the relation between the sensor sensitivity and surface roughness values. High, medium and low correlation have been illustrated as example of correlation according to the relation between the sensor features and surface roughness for the normal tool and tool with rubber, copper and aluminium sleeves respectively as shown in Figure 9.40.

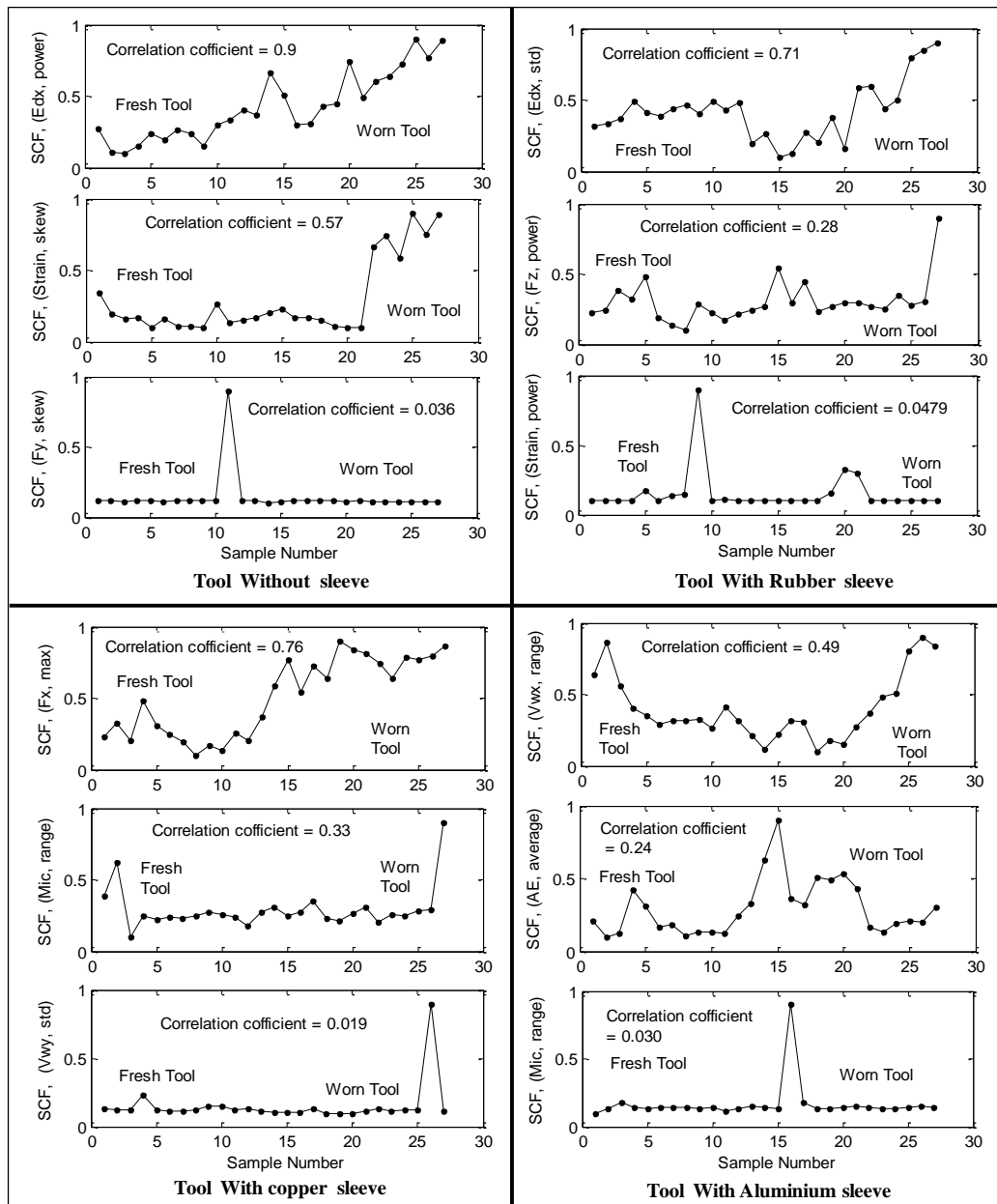


Figure 9.40: Examples of low, medium and high correlation SCF for the tools.

Examples of the values of the correlation are documented in Table 9.16, as a part of the whole results which have been created the ASM matrix as visually shown in Figure 9.41. It is clear that the correlation between two techniques to predict the tool condition (tool wear), and secondly using the correlation between the sensor characteristic features (SCF) and surface roughness, has achieved high agreement especially for SCFs with high sensitivity. Both sensitivity measures have indicated that the change of fixturing conditions has influenced surface roughness and the most sensitive features (i.e. sensor and signal processing methods) to be used to detect tool wear effectively.

Table 9.16: The most sensitivity of the sensory the system for different tools.

Tool without sleeve			Tool with rubber sleeve		
Sensor	SP	Correlation	Sensor	SP	Correlation
Edx	Power	0.9091	Edx	Std	0.7175
Edy	Min	0.8271	Fx	Range	0.4648
Mic	Max	0.7934	Vwx	Kurtosis	0.4286
Edx	Min	0.6097	AE	Skew	0.3561
Strain	Skew	0.5739	Fz	Power	0.2849
Vwx	Kurtosis	0.4741	Fz	Max	0.2428
Fx	Skew	0.3130	FY	Min	0.2087
Pwr	Min	0.2813	Edy	Max	0.1412
Fx	Kurtosis	0.1447	Vwy	Std	0.0836
Fy	Skew	0.0367	Strain	Power	0.0479
Tool with copper sleeve			Tool with aluminium sleeve		
Sensor	SP	Correlation	Sensor	SP	Correlation
Fx	Max	0.7687	Vwx	Range	0.4945
Pwr	Std	0.5129	Vwy	Range	0.4457
Fy	Kurtosis	0.4543	Fx	Std	0.3777
Fy	Max	0.4146	Fz	Power	0.2765
Mic	Range	0.3369	AE	Average	0.2473
Edy	Min	0.2698	Fx	Skew	0.2037
Vwx	Min	0.1794	Strain	Power	0.1057
Vwx	Range	0.1101	Fy	Max	0.0946
AE	Average	0.0853	Edx	Skew	0.0636
Vwy	Std	0.0191	Mic	Range	0.0304

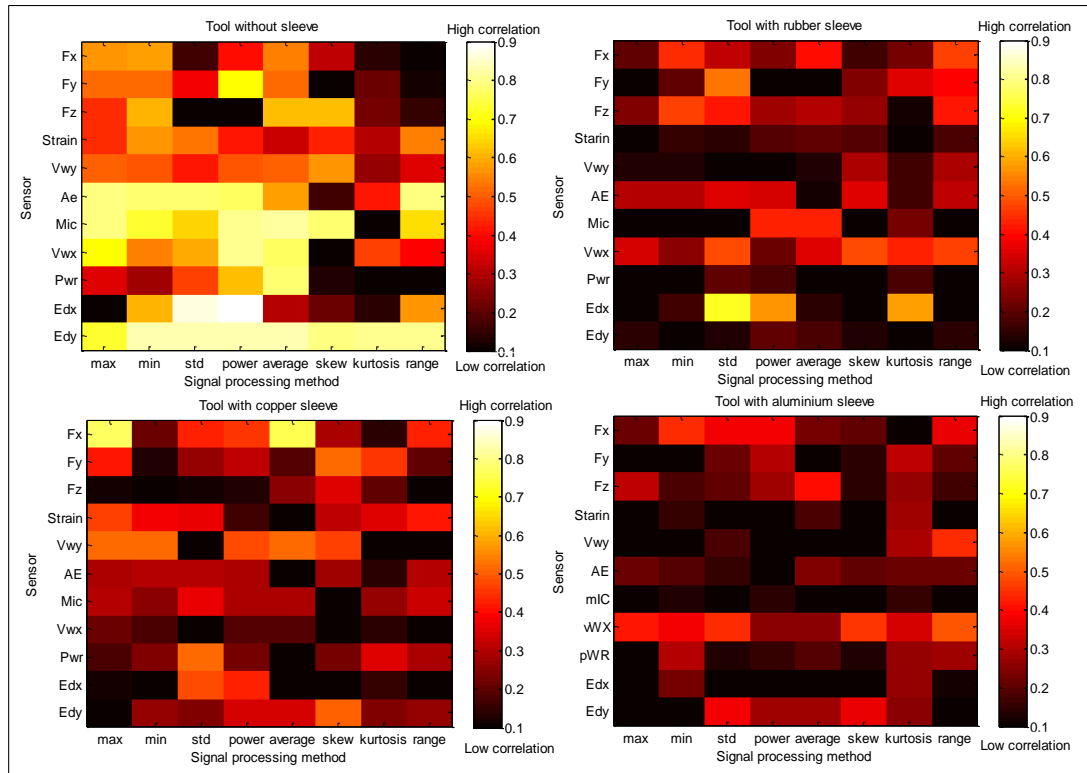


Figure 9.41: The correlation coefficient between the sensitivity SCF and surface roughness for different fixturing materials.

9.7 Conclusion

In this chapter, the ASPSF approach for multi-sensors combined with artificial neural networks (BP and LVQ), and Taylor's Equation Induced Pattern (TIP) in the experimental test, is explained using two methods of the signal simplification as linear regression and principal component analysis to monitor gradual tool wear in the milling process with regards to the change of the fixturing type and material system. The ASPSF approach utilises the Association Matrix (ASM) and Eigenvalue Sensory Matrix (EVSM) to compare the sensitivity of the feature to the fault under investigation. In addition, they evaluate the overall monitoring system using the average sensitivity of sensors and signal processing methods, also using the average of the eigenvalue of the principal component methods. The analysis of Linear Regression (LR) and Principal Component Analysis (PCA) analyses are used to find the most sensitive features to detect tool wear in milling processes. The SCFs and PCFs are visually examined and examples of low sensitivity and high sensitivity

features are presented. Sensory utilisation is implemented within the ASPSF approach to minimise the cost of the system without affecting the system sensitivity. There is a reliable relationship between the signal simplification methods (i.e. LR and PCA) either in eliminating the insensitive sensor or in reducing the monitoring system. The Taylor's Equation Induced Pattern (TIP) technique used to define the pattern recognition and make the accurate decision for the tool condition status and states the effect of the fixturing system quality on the efficiency of the monitoring system. The results show the ability of the technique to describe the tool condition and the quality of fixture could be significantly changed the monitoring system construction. Consequently, the ASPSF approach has been found useful in selecting the most sensitive sensors and signal processing methods or principal component methods to design a condition monitoring system with low experimental work and minimised cost. Furthermore, surface roughness is used as a good indicator to explain the effect of the fixturing system on the design of condition monitoring system as the findings proved that the change in fixturing quality could change the roughness of machined surface and leads to change in the sensitivity of the detecting system.

Chapter 10 The Evaluation of ASPSF Using Broken Teeth of Cutting Tool

10.1 Introduction

This chapter provides the full details for the concept of the ability of the ASPSF using different types of the sensor fusion model. It describes the implementation of the ASPSF approach to detect the changes in the machine setup and the stability of the four fixturing systems as perfect or imperfect fixturing systems. The methodology in the current chapter has been changed as the tests in the previous chapters started by using fresh tool and finished with completely worn tool. Here, fresh tool and tool with different broken teeth will be used where the transfer of the tool conditions from new to breakage may take considerable time. All these tools used will have different fixturing systems. Surface roughness as a reliable indicator to product quality will be studied and will produce a relation between the ASPSF approach and the machined surface roughness.

The current questions that could be asked include the ability of the ASPSF approach to detect the tool breakage from the collected data and provide a classification to the tool condition to avoid a future problem of the machine breakdown.

10.2 Experimental Setup

The experimental work is performed on the CNC milling machine, the signal processing equipment in the previous chapter has been employed to achieve the aim of the current investigation. The sensors used are force sensor (F_x , F_y and F_z), accelerometers attached to the machine table (V_{wx} , V_{wy}), strain, acoustic emission (AE), sound (Mic), accelerometers attached to machine spindle (V_{sx} , V_{sy} , V_{sz}), power, eddy current sensors (E_{dx} , E_{dy}). The tools used in this test are made from carbide with 3mm flute and 6 mm shank as described in the Table 10.1 for machining specification. The surface roughness has been measured manually for the machined surface using the roughness measuring device (Mitutoyo SJ-210). Figure 10.1 shows the schematic of the experiment work of the current chapter, where the whole sensory signals are collected by the sensor and the signal condition equipment, and then

transferred to the data acquisition card to process the information in the personal computer (PC).

Table 10.1: The machining parameters of the milling process.

Machining condition	Specifications
Feed rate	250 mm/min
Depth of cut	0.36 mm
Coolant type	No coolant (Dry)
Spindle speed	2490 RPM
Diameter of tool	3mm/ 6mm shank
Material of tool	Carbide (End mill carbide)
Type of tool	End mill Tool (4 Flutes, Uncoated)

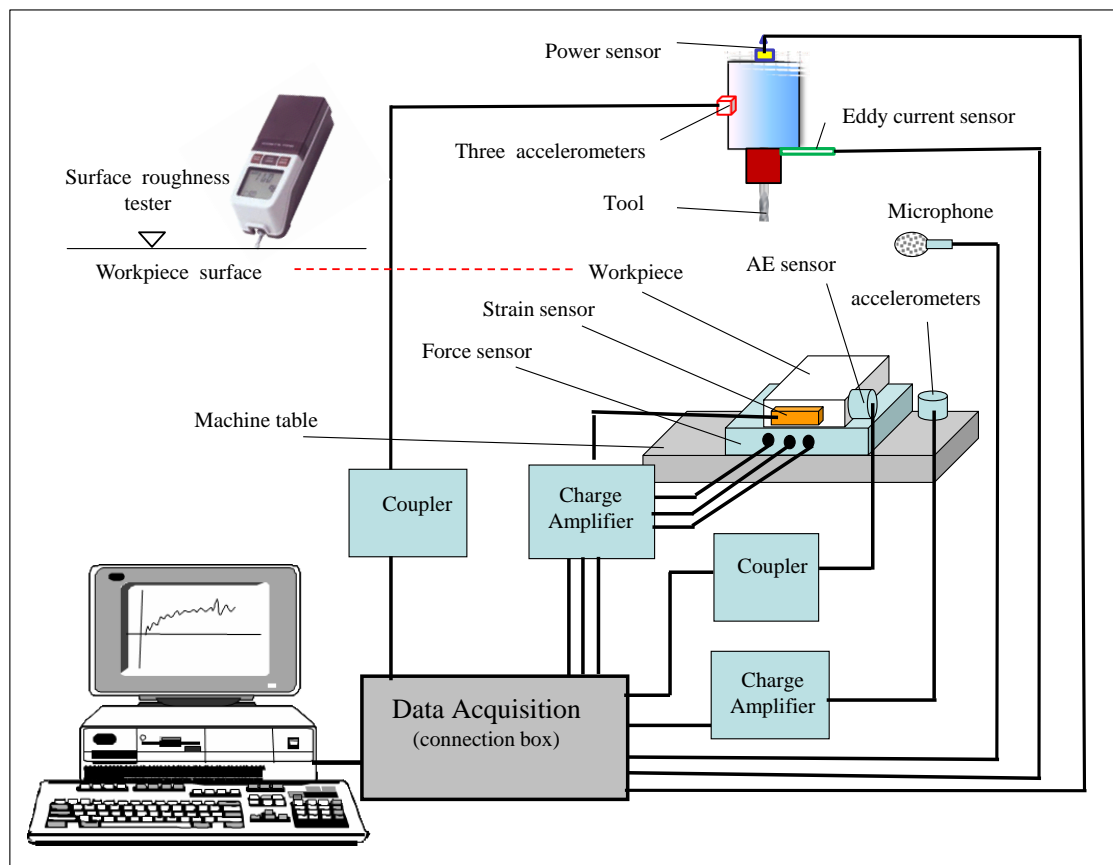


Figure 10.1: Schematic diagram of the monitoring system and surface roughness.

Different types of the sleeve will be used to cover the shank of the used tools as rubber, copper and aluminium sleeves. In the machining test, there are three types of the tool tip conditions, namely fresh, one broken tooth, two broken teeth as shown in

Figure 10.2. This is just to simulate the tool breakage and the relation between the tool condition and fixturing system quality.

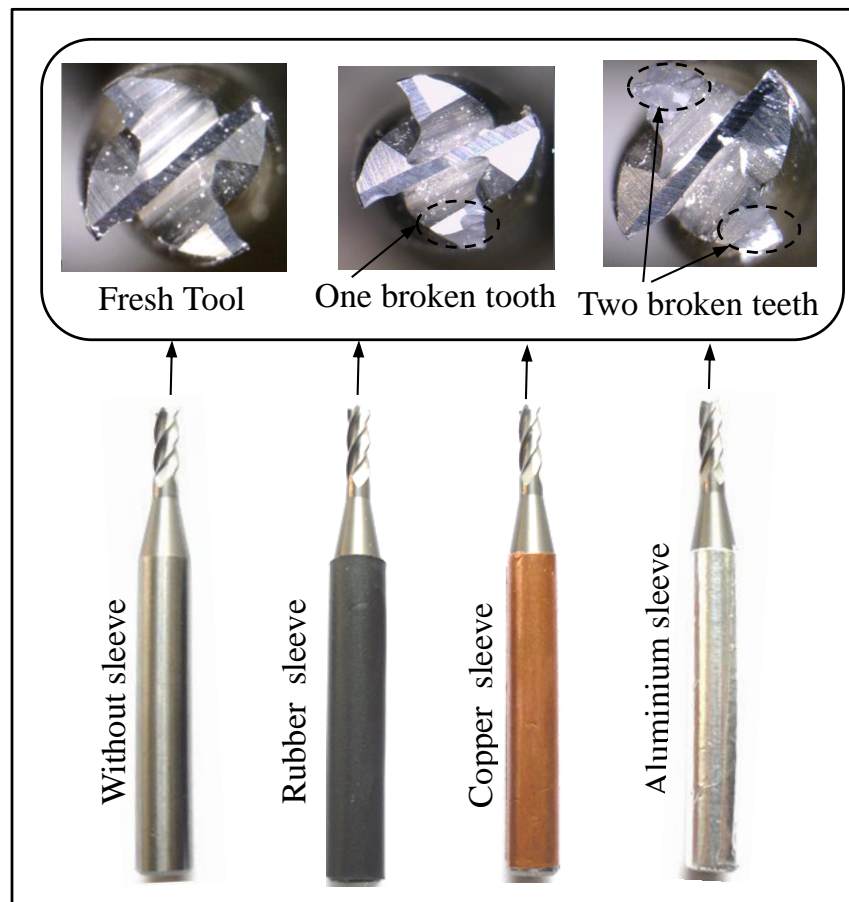


Figure 10.2: The three states of the milling tool (fresh, 1 broken tooth and 2 broken teeth) with four fixturing systems.

10.3 Signal Simplification

Since the milling is complex process and the monitoring signals which are collected from the sensor difficulty to expect what may be happened during the forward of machining, this further to the amount of the huge data and the need to make the fast decision to tackle any abnormal conditions. Therefore, signal simplification is applied on the data to emerge the useful information. Generally, it can be considered that the visual patterns could indicate to initial expression that the amplitude of the sensory signal raise up as shown in the following Figures.

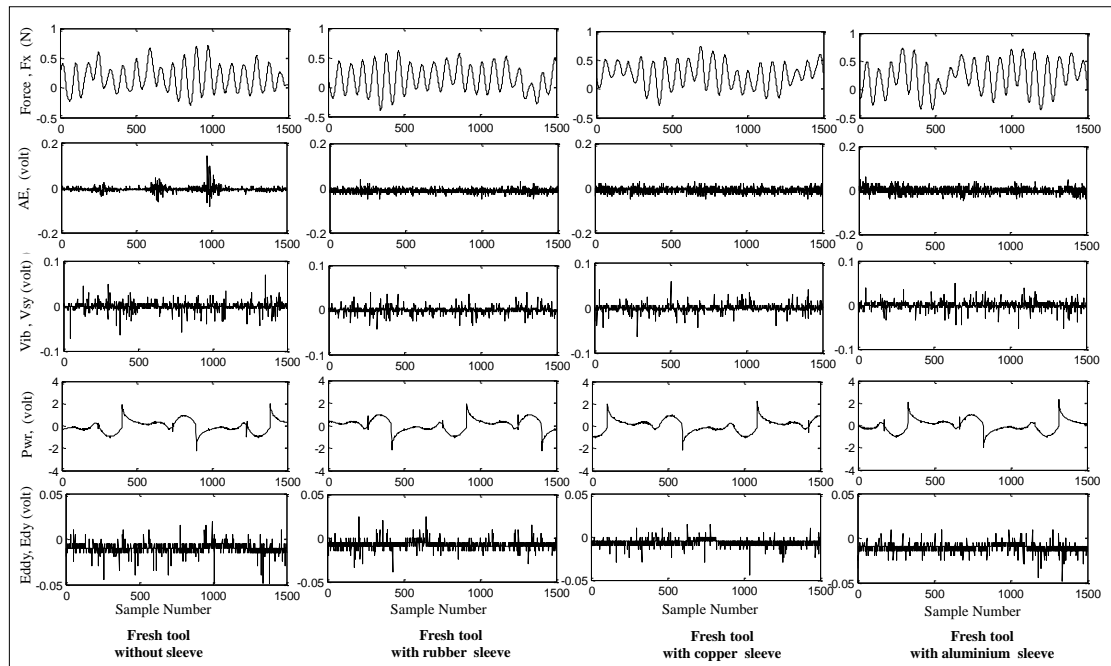


Figure 10.3: Examples of the raw signals of the machining process for fresh tools.

Figure 10.3 shows examples of the collected signal of fresh tools for different fixturing system (Tool without sleeve, tool with rubber sleeve, tool with copper sleeve and tool with aluminium sleeve). It can be seen from this figure that the amplitude and pattern of force signal (F_x) is different from system to another, same thing with regard to other signals as acoustic emission (AE) and vibration, power and Eddy current sensors.

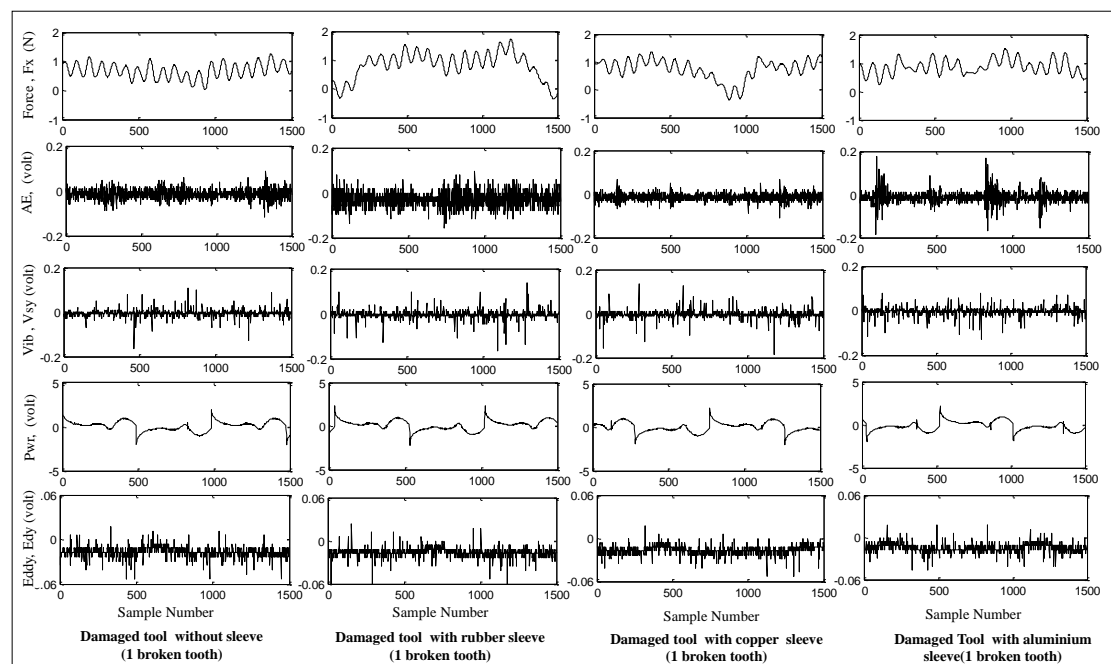


Figure 10.4: Examples of the raw signals of the machining process for tools with one broken tooth.

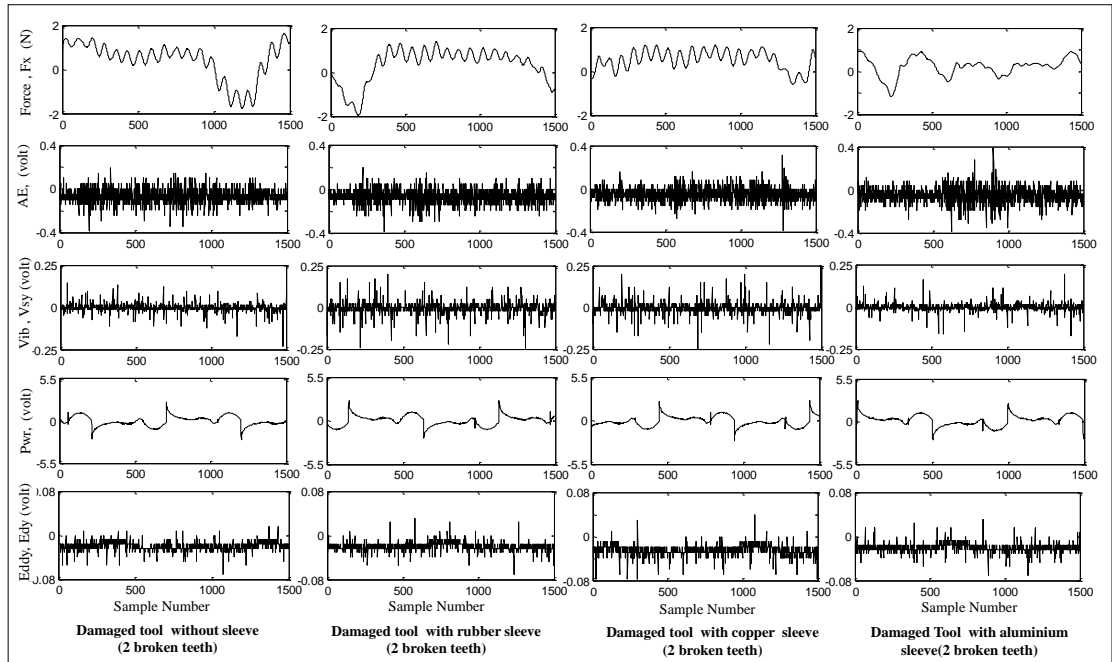


Figure 10.5: Examples of the raw signals of the machining process for tools with two broken teeth.

Following this, Figure 10.4 explains the signals of the tools with one broken tooth, it can be noticed clearly the changes in the amount of the amplitude range. As illustrated for the force sensor, it is observed that signal is sharply declined and then raised up which means at that moment there is no cutting or broken tooth. Other signals show that there are sudden changes in the signal pattern and relative rise in the amount of the signal amplitude. Gradually, Figure 10.5 shows the tools with two broken teeth, here force sensor provides that the declines in the signal are become close each to other refer to cutting down, and it can be seen that the AE sensor reflects a considerable difference in the size of the signal as it indicates that something is abnormal. Other sensors in the above examples as vibration (V_{sy}), power or eddy current visually are obtained significant changes. These findings enhance our understanding of the importance to use the simplification methods. In this chapter, a variety of the sensitivity measuring methods have been used to select the feature (SCF) which has the most sensitive to the variables of the cutting process which are as follows, this to find the best method to measure the sensitivity:

1. The Linear Regression (LR) method
2. The Range Value (RV) method
3. The Sudden Change In Value (SCIV) method
4. Correlation Coefficients (CCX3) method

5. Correlation Coefficients (CCX20) method

6. Fuzzy Logic (FL) method

10.3.1 Linear Regression (LR) Method

As explained in the previous chapters, the linear regression method is used to find the linear equation which best represents the linear relationship between two variables depend on the feature in time domain. Here, it will be used to measure the sensitivity of the sensory characteristic feature in time, frequency and time frequency domains. Therefore, the Fast Fourier transforms (FFT) and wavelet features are grouped to the statistical time domain in this analysis.

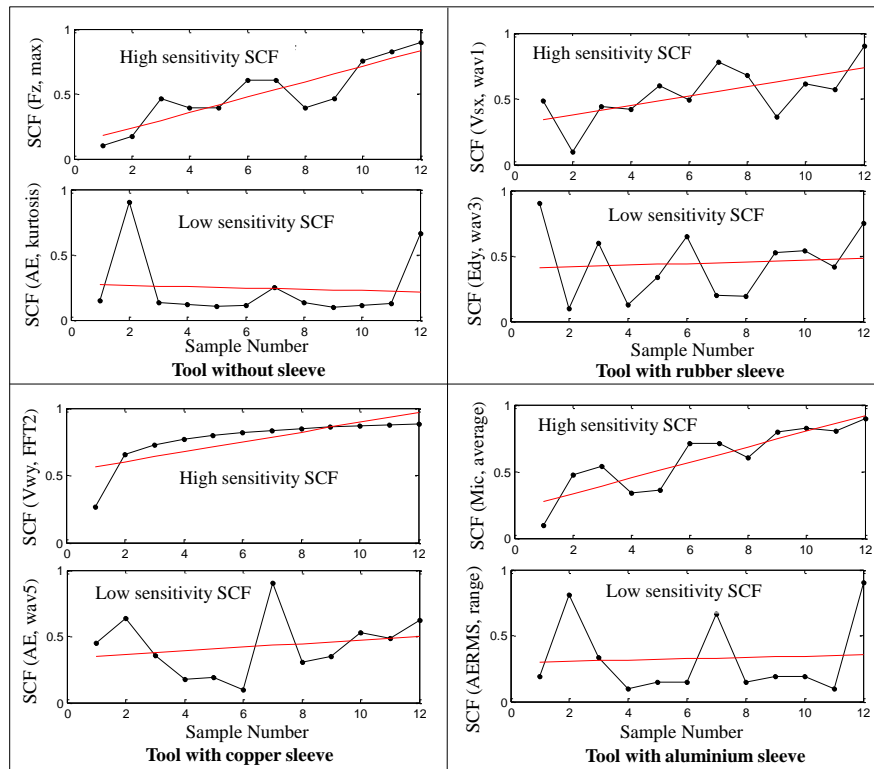


Figure 10.6: Example of the result for all the SCFs using LR method for four fresh tools with different fixturing systems.

From Figure 10.6, it can be noticed that the SCF(Fz, max) shows the high sensitivity to the changes in the condition of fresh tool without sleeve, however the SCF(AE, kurtosis) shows the low sensitivity for tool wear. The tools with different sleeves show different features, for example, the SCF(Vsx.wav1) is the most sensitive feature for tool with rubber sleeve, but the SCF(Edy, wav3) obtained low sensitivity. The different is continuous for tools with copper and aluminium sleeves. However, for all

examples which are indicated low sensitivity, it can be noticed that this method does not represent the real condition of the feature since the feature reflects that there is a raise in the pattern especially at the end of the test, but the method considered these features as low sensitive. The images of the Associated Matrix (ASM) for 15 sensors and 28 signal processing methods used in this test, which totally will create 420 features as shown in Figure 10.7. Where the high sensitivity value (lighter colour) indicates high capability of detecting the machining faults, meanwhile black colour represents low sensitivity.

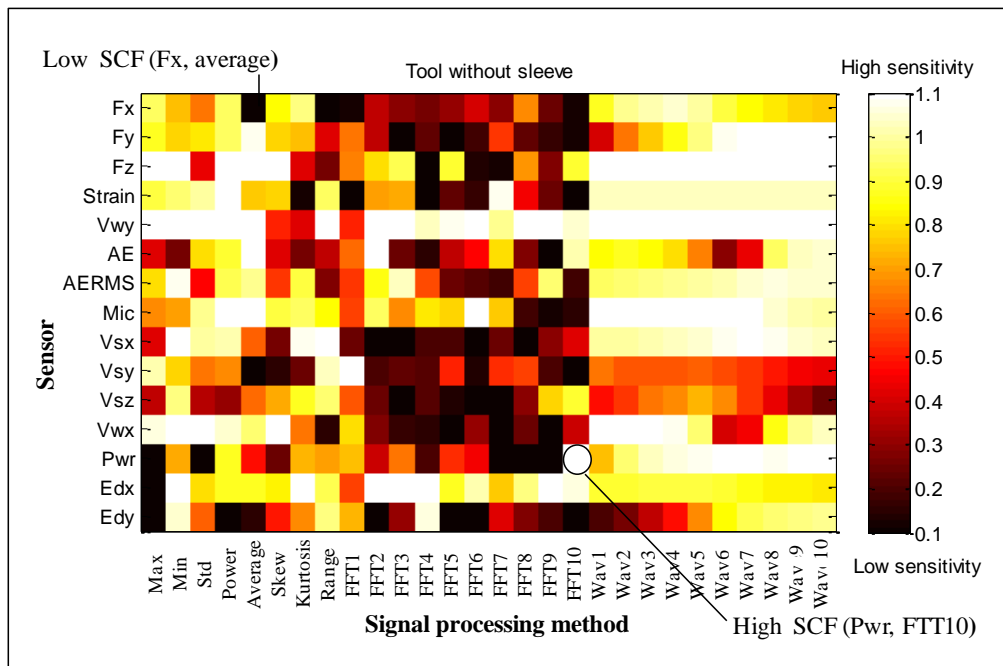


Figure 10.7: A graphical presentation of the sensitivity for fresh tool without sleeve using LR method.

As the tool breakage is difficult and complex phenomena, this encouraged us to study it in this chapter, Figure 10.8 shows the image of the associated matrix for the 420 features to define the required considerations for designing monitoring system in case of damaged tool with one tooth for four fixturing systems.

From Figure 10.8, it can be observed that the sensitivity values of the features are completely different with those of the fresh tool for all fixturing system. Since, the SCF (Mic, wav8) is taken the highest place in the rank of the most sensitive features for the tool without sleeve with one broken tooth. Meanwhile the SCF(Vwy, FTT2) is high sensitive for the tool with rubber sleeve. For the tool with copper sleeve, the SCF (Fy, std), while the high sensitive feature SCF(Fz, FFT7) for tool with aluminium sleeve. More details about the 3 tools are described in Appendix J.

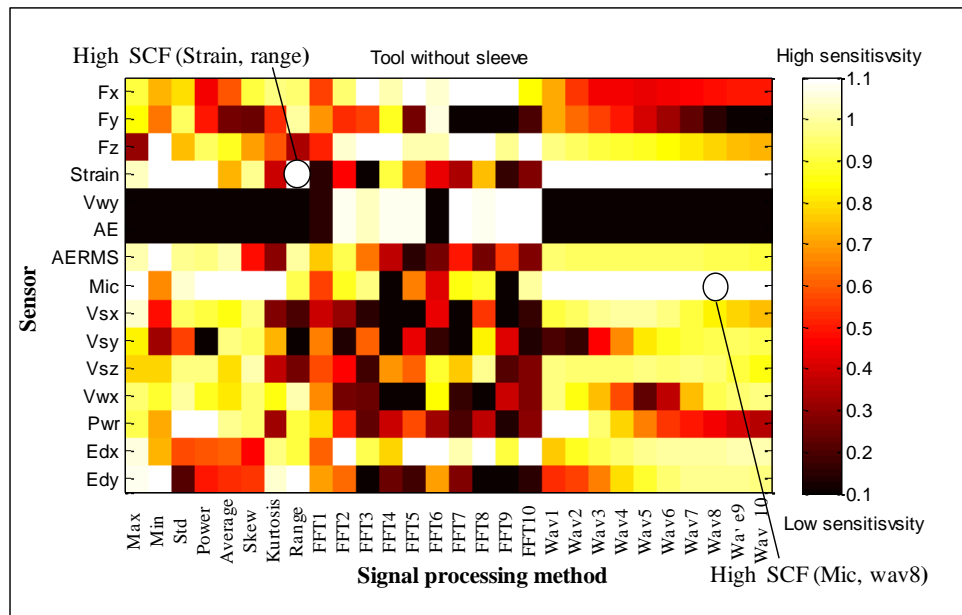


Figure 10.8: A graphical presentation of the sensitivity for tool with one broken tooth, using LR slope method.

Continuously, Figure 10.9 shows visually the associated matrix of the features for normal tool with two broken teeth. In the cutting process, it is highly expected to damage tool with two or more teeth after it's broken the first tooth due to the cutting process will not continuous. This will create a significant stress on the following tooth and may be broken it. It can be simulated this case using ready damaged tool to investigate the effect of this phenomena on the detecting system.

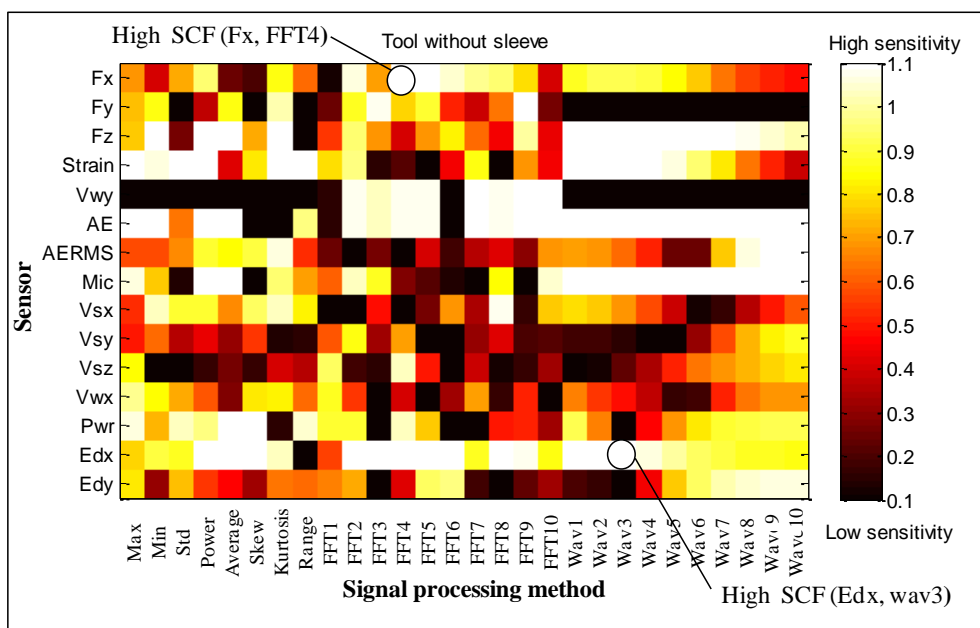


Figure 10.9: A graphical presentation of the sensitivity for tool with two broken teeth, using LR method.

Figure 10.9 shows the extreme changes between the figures either comparing with the previous ASM images or between the different fixturing systems for tool with two broken teeth. Here, the SFC(Fx, FFT4) got the great ability to detect the variable in the discrete machining process for the tool without sleeve, nevertheless, the SFC(Fz, skew) presents high efficiency to do that for the tool with rubber sleeve. The SCF (Strain, std), and SCF(Mic, power) are taken the high sensitive for tool with copper and aluminium sleeves respectively as described in Appendix J. So far this method has been applied to obtain the slope of the signal feature to contribute the sensitivity of the feature, but it is not too efficient to measure correctly all the pattern with reliable precision. The possible explanation for this limitation is due to some features show visually high sensitivity to tool wear but in this method considered as a low sensitivity.

10.3.2 Range Value (RV) Method

The range value method used to measure the absolute difference between the last point and first point of the feature. This is to explain the range in the change of the signal pattern. Figure 10.10 shows example of the feature using this method. Where the SCF(Vsx, range) is achieved the higher rank of the sensitivity, and this reflects a good indicator to the ability of this method to detect the abnormal conditions. However the second SCF(Fx, max) reflects the low sensitivity. But, visually it can be seen that this feature relatively interacts with the changes of tool status and presents an indicator to increase the cutting force at the end points of the test.

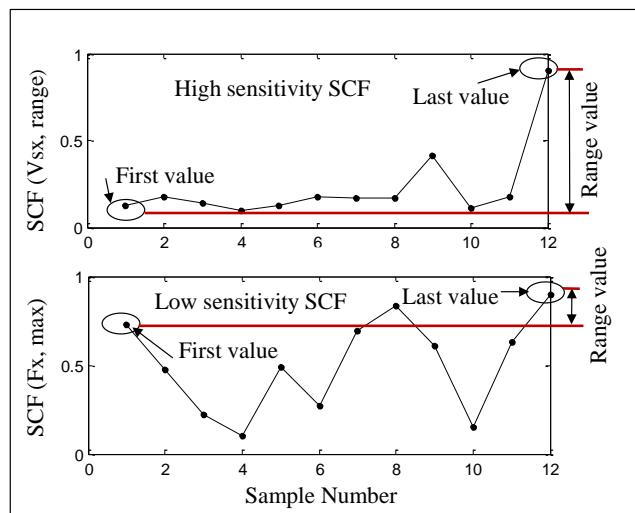


Figure 10.10: Examples of SCFs using Range Value method for fresh tool without sleeve.

From the above examples, it can be clearly noticed that this method has ignored the points in the mean path between the first and last points. This certainly will effect on the reliability of this method. However, Figure 10.11 shows the image of the associated matrix of the sensitivity according to the range value method for the fresh tools with different fixturing systems.

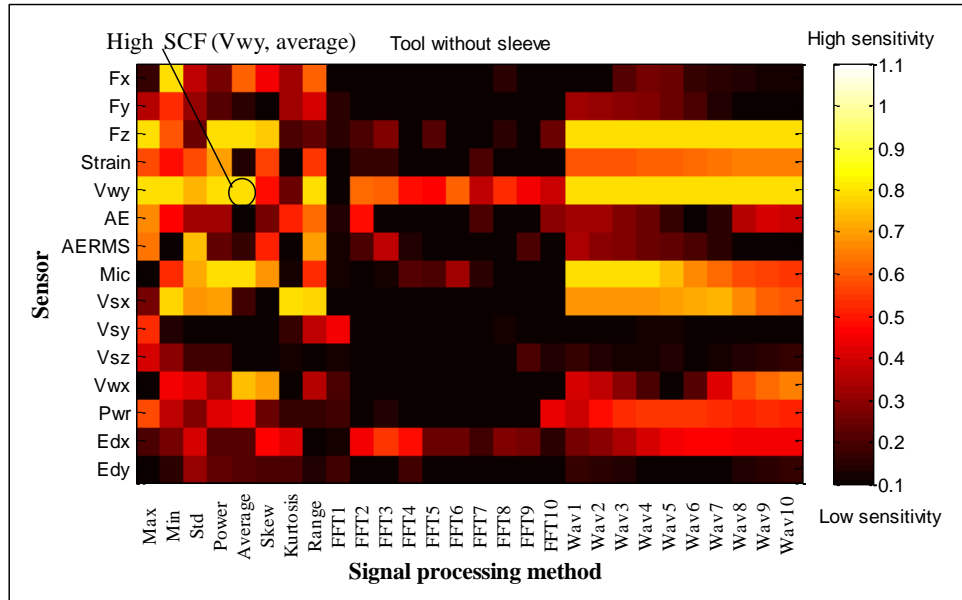


Figure 10.11: A graphical presentation of the sensitivity for fresh tool without sleeve using Range value method.

As shown in Figure 10.11, the Range Value (RV) method has been presented different examples for sensitivity of feature, where in the fresh tool without sleeve, the SCF(Vwy, average) is the most sensitive, meanwhile the SCF (AERMS, std) is taken the first feature in the sensitivity rank for fresh tool with rubber sleeve. The SCF(Fz, average) and the SCF(Vwy, range) is the best feature to detect the conditions for the fresh tools with copper and aluminium sleeve as described in Appendix K.

Following this, Figure 10.12 shows the ASM matrix for the tool with one broken teeth. For the tool without sleeve and tool with rubber sleeve, the SCF(Mic, power) and SCF(Edy, min) achieved the higher value of the range to monitor the tool status, nevertheless, for tool with copper sleeve and aluminium sleeve, the SCF(AE, FFT7) and SCF(Fx, std) are the more sensitive features.

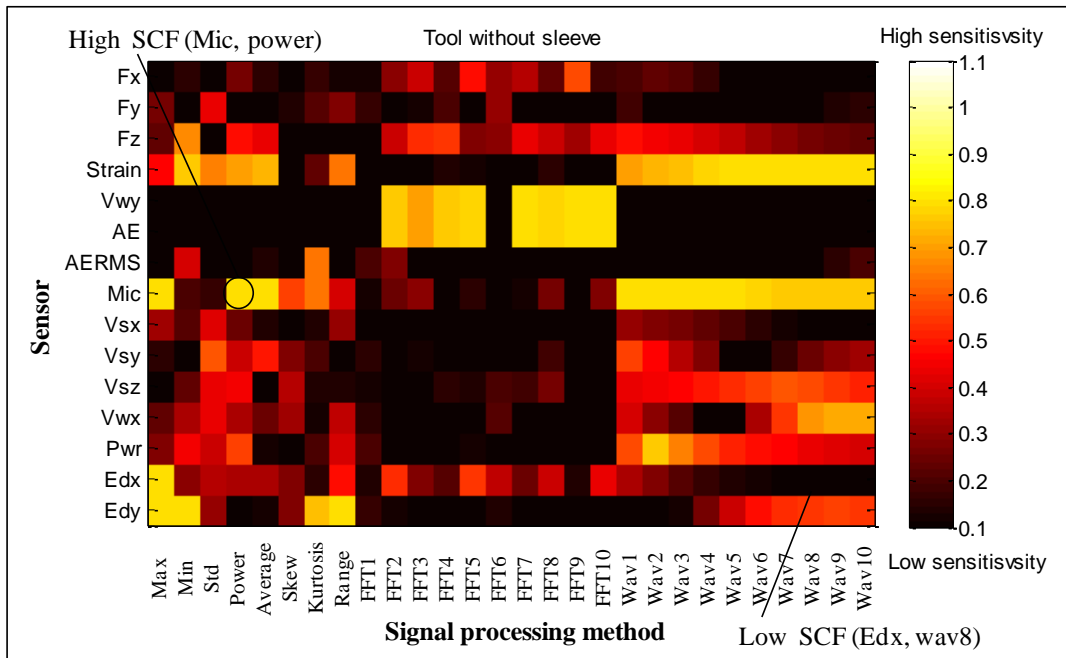


Figure 10.12: A graphical presentation of the sensitivity for tool with one broken tooth, without sleeve using Range value method.

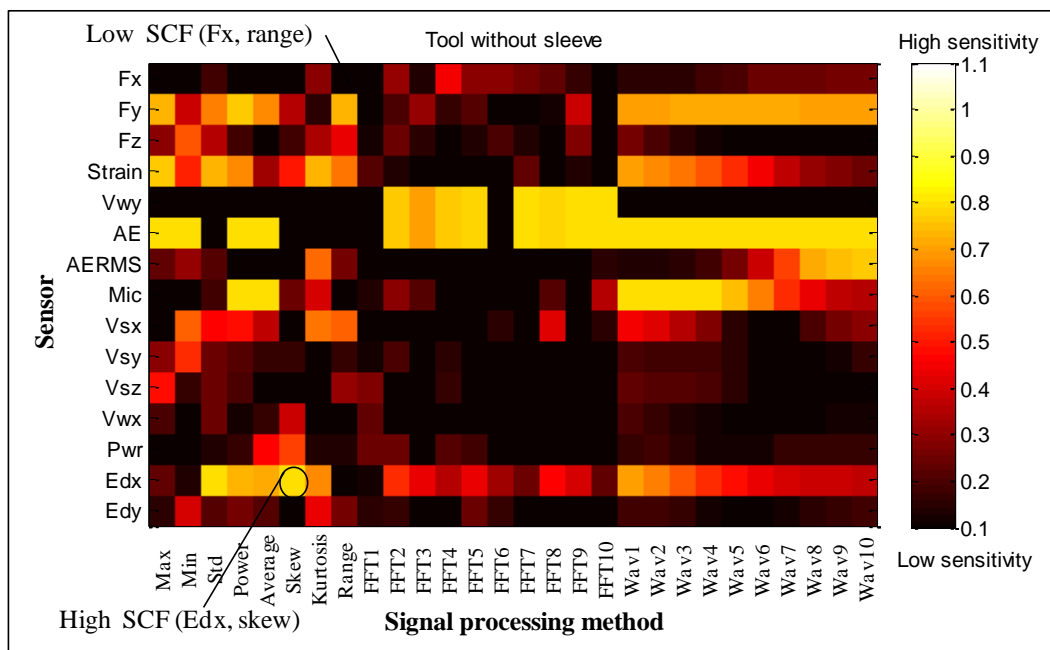


Figure 10.13: A graphical presentation of the sensitivity for tool with two broken teeth, without sleeve using Range value method.

From the above images for the tools with different types of fixturing system, it can be noticed that the values of the sensitivity are different between one system to another; also those values have been raised up when the tool condition transferred from the fresh tool to tool with one broken tooth. This situation will give an indicator that the

output of the sensors increased due to the disturbing or the abnormal cutting in the machining process. This phenomenon will become more appearance especially for the normal tool with two broken teeth as it can be seen in the Figure 10.13. More details for other three tools are described in Appendix K.

10.3.3 Sudden Change In Value (SCIV) Method

The Sudden Change In Value method used to measure the sensitivity of the sensory characteristic feature. Where this value is obtained from the absolute difference of 5% of minimum first points and 0.95% of the maximum of last points. Figure 10.14 shows examples of the feature for fresh tool.

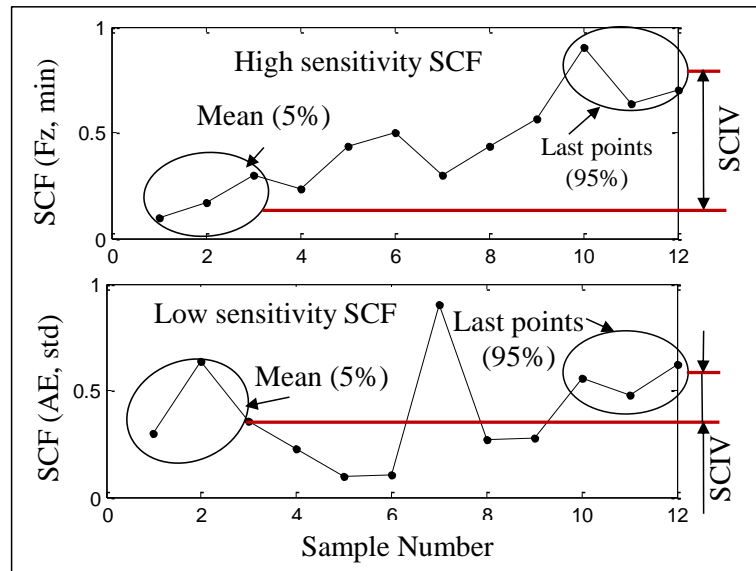


Figure 10.14: Examples of SCFs using SCIV method for fresh tool without sleeve.

Similar to the previous measuring sensitivity methods, this method has been shown that there are different values of the sensitivity. Also there is a difference between the features to detect the tool conditions. Visually, in the Figure 10.15, it can be observed that the SCF(Mic, range) got the high level in the sensitivity for the fresh tool without sleeve. However, for the fresh tools with rubber, copper and aluminium sleeves, the SCF(Vsy, wav8), SCF(Fx, average) and the SCF(Vwy, min) are the most sensitive features to monitor the tool and fixturing conditions.

One major issue in this method concerned to the lack of investigating the changes of the features for the points between the first and last points.

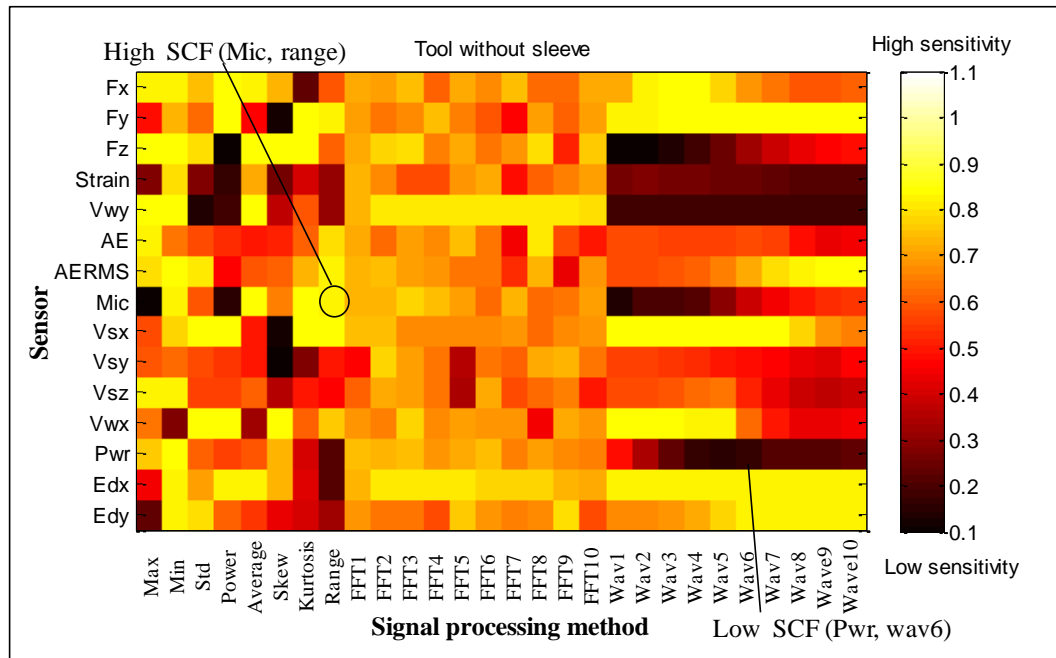


Figure 10.15: A graphical presentation of the sensitivity for fresh tool with, without sleeve using SCIV method.

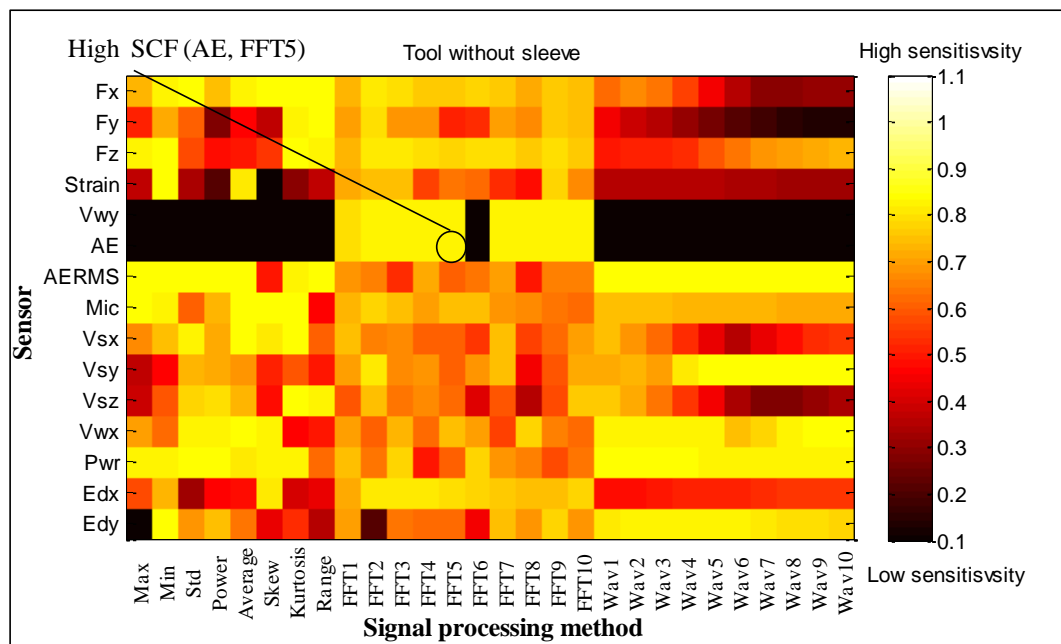


Figure 10.16: A graphical presentation of the sensitivity for tool with one broken tooth, without sleeve using SCIV method.

Continuously, from the Figure 10.16, it can be noticed that the SCF(AE, FFT5) obtained the higher sensitive for the tool wear using normal tool with one broken tooth. Meanwhile the SCF(Fx, min), SCF(Edy, wav5) and SCF(Pwr, kurtosis) represent the high sensitive features for the tools with rubber sleeve, copper or aluminium sleeve as described in Appendix L.

It can be concluded from the images for the tools with one broken tooth, that the difference between the SCIV for the feature is increased, since it can be noticed that some of the features got higher sensitivity (light colour) and other features got a less sensitivity (black colour), this behaviour indicates that when tool edge cutting the workpiece (remove the chip), the sensor surely obtained high signal, but in case of passing the broken tool edge and there is no cutting, this means that there is no considerable signal could be collected. The uncontrollable cutting in the rotating machining process will provide a high problem in the sequence of the tool over the workpiece and therefore the thickness of the chip will be changed and the tolerance of the product dimension will become imprecise.

Since the discrete cutting will increase in the tool with two broken teeth due to the cutting time-off between the teeth will increase, this phenomena will not obtain continuous signal from the sensor and certainly the sensitivity will decline to lower level as illustrated in Figure 10.17, mean while it will raise in case of cutting.

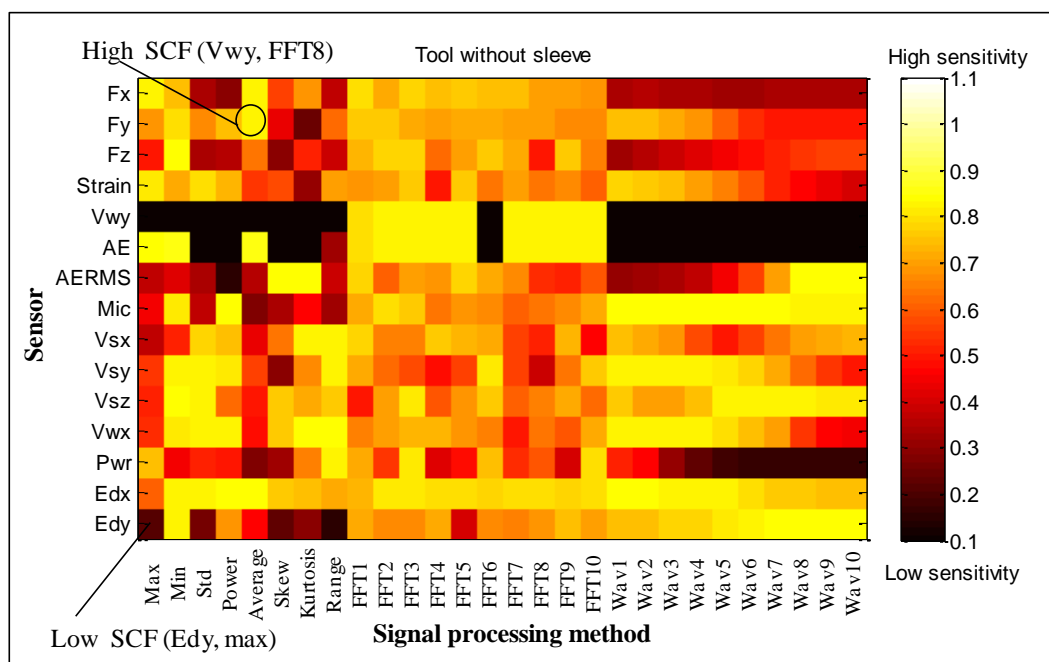


Figure 10.17: A graphical presentation of the sensitivity for tool with two broken teeth, without sleeve using SCIV method.

10.3.4 Correlation Coefficients (CCX3) and (CCX20) methods

The correlation coefficient is a quantity that gives the quality of a least squares fitting to the original data or to explain the relation between two cases. It is very important to

define the relationship between theoretical curve of the expected pattern and the experimental curve of the sensory feature. The theoretical curve of the tool wear can be plotted according to the constant function (X^3 or X^{20}). Generally, these constant functions have been built based on the Taylor's equation for the tool life. Then, the relationship will be used as a calibration to find the correlation coefficient, the first correlation coefficient (CCX3) is the correlation between the SCF pattern and X^3 function, and the second correlation coefficient (CCX20) is the correlation between the SCF pattern and X^{20} function as described in Chapter 6, section 6.6.4. Both of these coefficients will consider reliable methods for measuring the sensitivity of the feature. As the high correlation means the high sensitivity for the changes which may be occurred while the machining process, following this, the low correlation means low SCF sensitivity.

By finding the correlation coefficient between the above constant function and the pattern of the sensory feature, it is possible to assess the sensitivity of the feature as it represents the general behavior of the tool life. Figure 10.18 shows examples of the high and low sensitivity of the feature according to this concept for the fresh tool without sleeve.

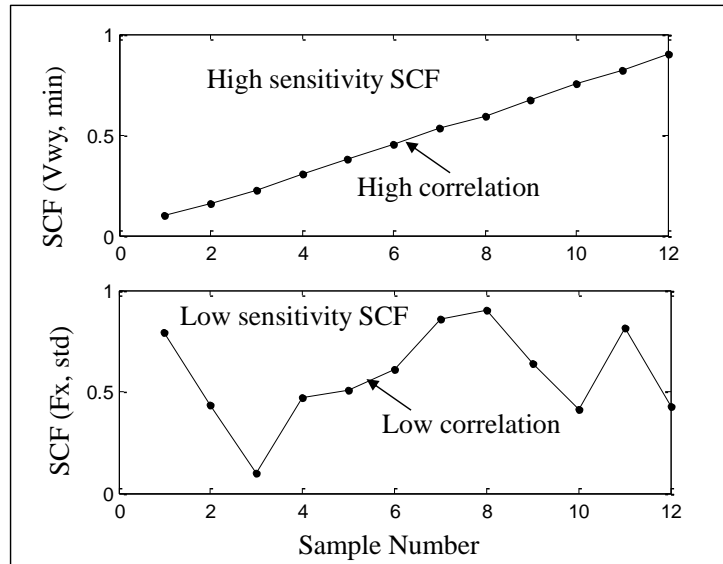


Figure 10.18: Examples of SCFs using CCX3 method for fresh tool without sleeve.

After conformational measuring of CCX3 and CCX20, it was necessary to arrange them to create the Association Matrix (ASM). Figure 10.19 shows example of the image of the sensitivity value according to the relationship between the constant function (CCX3) and the sensory feature for fresh tool without sleeve. It could be seen

that the SCF (Strain, FFT6) is the most sensitive feature for detecting the condition changes of the tool without sleeve, while the SCF (Vsz, FFT9) is high sensitive for fresh tool with rubber sleeve. Tools with copper and aluminium sleeves are obtained different sensitive features using CCX3 method as described in Appendix M. Therefore, it can be noticed that there is a clear difference among those systems. By using CCX20 method, the SCF(Vsx, Kurtosis) and the SCF(AERMS, FFT8) are the most sensitive features for fresh normal tool and tool with rubber sleeve. But, SCF(Vsx, Kurtosis) and the SCF(AERMS, FFT8) are sensitive features for fresh tools with copper and aluminium sleeves as presented in Appendix N.

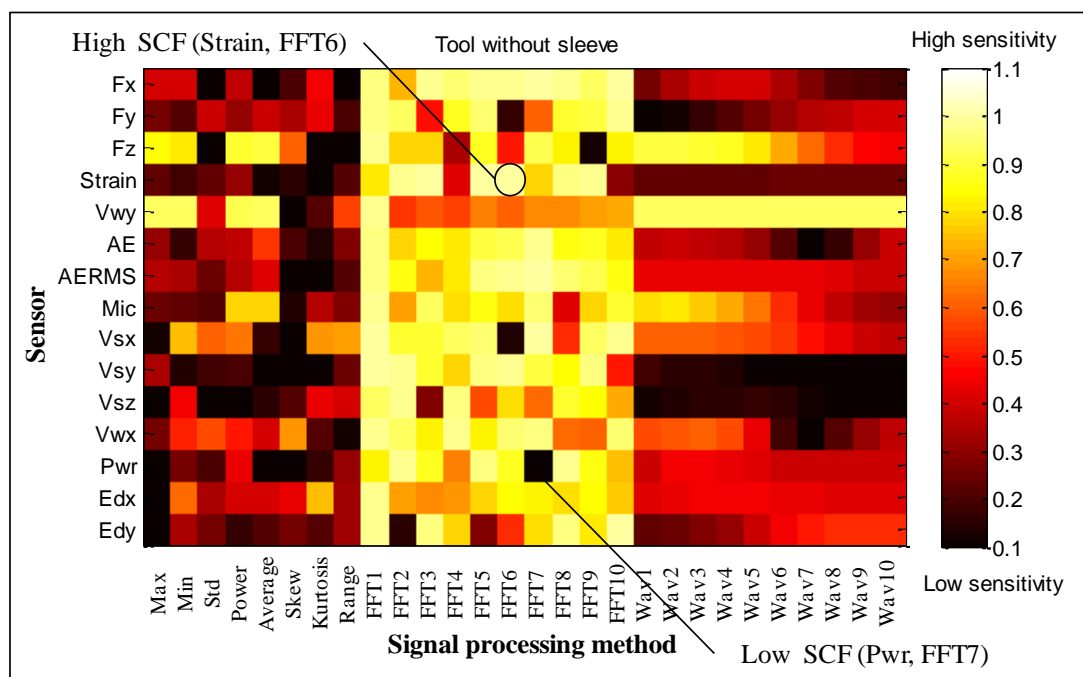


Figure 10.19: A graphical presentation of the sensitivity for fresh tool without sleeve using CCX3 method.

For all the tools with one broken tooth, it can be observed that the correlation coefficients relatively are decreased since the pattern of the feature will become unexpected and may be far or less consistent from the pattern of the constant function. Therefore, it can be seen that the most of the sensory characteristic features have been tended to take the black colour as a reflection to the low sensitive especially in the time and wavelet domains as illustrated in Figure 10.20.

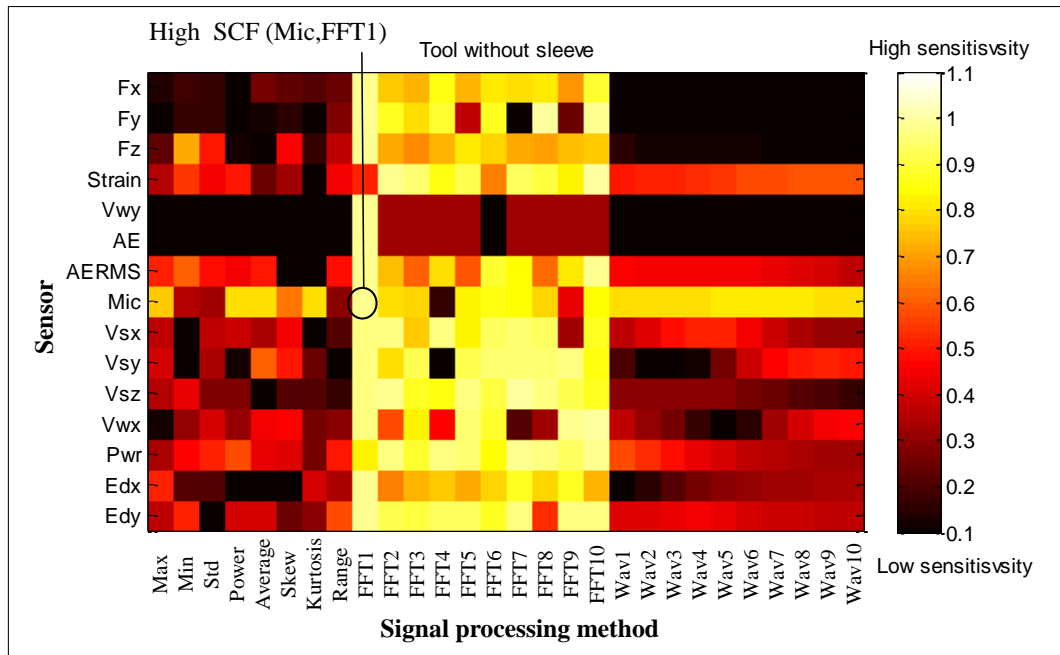


Figure 10.20: A graphical presentation of the sensitivity for tool with one broken tooth, without sleeve using CCX3 method.

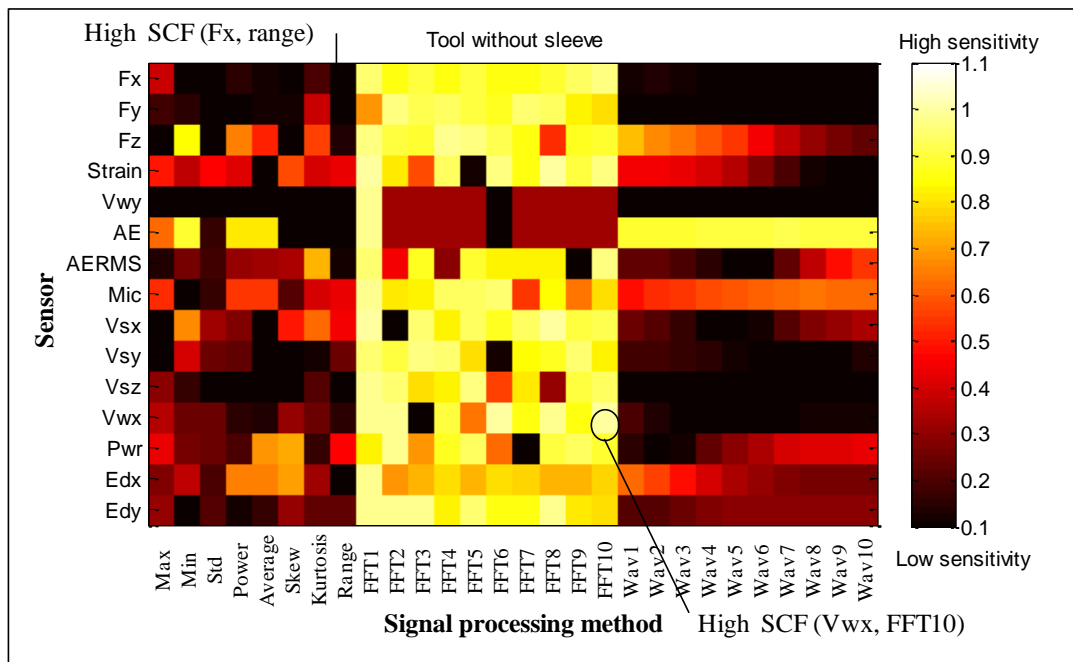


Figure 10.21: A graphical presentation of the sensitivity for tool with two broken teeth, without sleeve using CCX3 method.

Continuously, for the damaged tools with two broken teeth, low sensitivity features will become more common as vision in Figure 10.21. A possible explanation for this might be that the consistent between the pattern of the features and the constant function is significantly reduced as the two teeth breakage will directly effect on the stability of the cutting process. This fact leads to prove the ability of the suggested

monitoring system to classify the tool conditions as fresh or damaged tools. The present findings seem to be consistent with other previous methods which found that design of the monitoring system is generally affected by the type of the fixturing system.

All the five measuring methods (i.e. LR, Range Value, SCIV, CCX3 and CCX20) presented different sensitivity results, as each one of them deals with the signal feature from different view as some of these methods focused on the first and last point regardless the mean points, and other created the correlation depend on the similarity between the suggested and experimental feature patterns. However, the approach of using one method shows that these results are not statistically significant. There is, consequently, a definite need for a reasonable approach to tackle this issue.

10.3.5 Fuzzy Logic (FL) Method

As described in the aforementioned sections, that there are different methods to measure the sensitivity of the features. In the current section, a fuzzy logic has been used to characterise the sensitivity of the features when the five methods combined together. This will be implemented by a membership function (0---1) which associates with each element of universe and represents the grade of membership specify for the condition each case. As illustrated in Figure 10.22, the features obtained from each method have been interred in the fuzzy logic rules, these rules to evaluate each type of the method and then the results of the rules are combined to determine the most sensitive features.

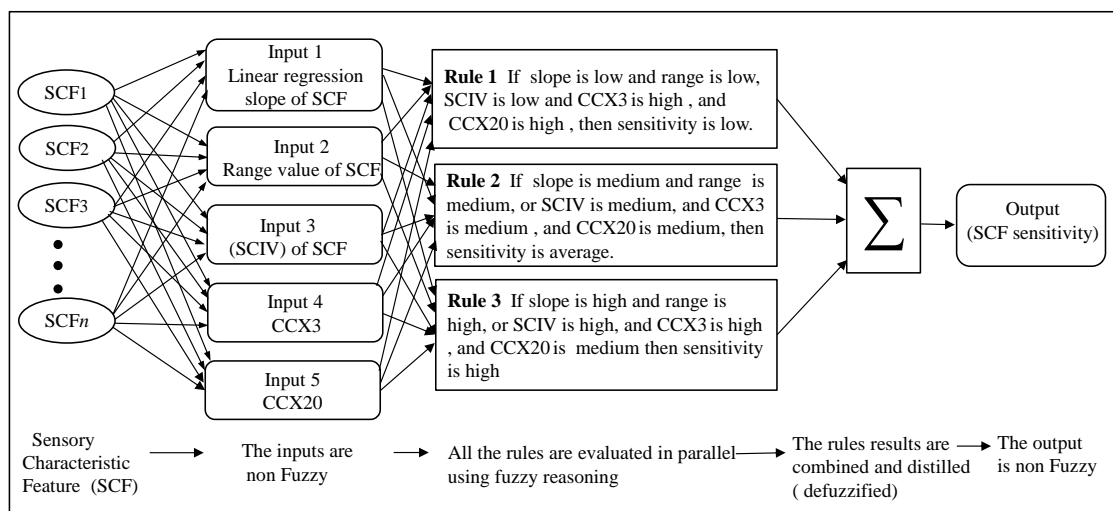


Figure 10.22: Steps of the proposed fuzzy logic approach.

For an instance, Table 10.2 shows an example of the first maximum twenty features of fresh tool without sleeve, they are arranged according to the evaluation of fuzzy logic. It is clear that the sequence of the features is significantly different with those in the previous sensitivity measurement methods (i.e. LR, Range Value, CCX3, CCX20). The association matrix (ASM) of the sensitivity according to fuzzy logic has been imaged as illustrated in Figure 10.23. The SCF(Vsx, wav2), SCF(Vwy, max) and SCF(Vsx, wav1) are the most sensitive features for the fresh tool without sleeve. Meanwhile, the SCF(Fy, min), SCF(Vwy, average) and SCF(Mic, wav6) represent the high sensitive features for the fresh tool with rubber sleeve. The most sensitive features for the fresh tool with copper sleeve are SCF(Vsz, wav4), SCF (Vsx, wav2) and SCF(Fz, kurtosis). The SCF(Edx, FFT6), SCF(Fz, FFT3) and SCF(Vsz, std) are the most sensitive features for the tool with aluminium sleeve as described in Appendix O.

Table 10.2: Example of the results of the fuzzy logic evaluation for the SCF of fresh tool without sleeve.

SCF		LR Slope	Range Value	SCIV	CCX3	CCX20	Fuzzy logic
Sensor	SP						
Vsx	wav2	1.0235	0.6923	0.8434	0.5939	0.8604	0.9999
Vwy	max	1.3375	0.8000	0.8470	0.9318	0.5679	0.9998
Vsx	wav1	0.9999	0.6821	0.8433	0.6089	0.8972	0.9997
Mic	average	1.2810	0.8000	0.8363	0.7790	0.4536	0.9996
Vsx	std	0.9985	0.6797	0.8434	0.6138	0.9026	0.9995
Vsy	FFT1	1.1312	0.4458	0.4624	0.9923	0.7361	0.9994
Fz	wav8	1.2056	0.8000	0.4410	0.5315	0.4288	0.9994
Vsx	wav8	1.0833	0.6773	0.7737	0.4288	0.5648	0.9993
Edx	kurtosis	1.2046	0.4145	0.4165	0.7486	0.4889	0.9992
Vwx	std	1.1029	0.4139	0.8377	0.5724	0.5812	0.9991
Fz	min	1.2765	0.6000	0.8456	0.8096	0.4133	0.9990
Vwx	wav1	1.1178	0.4121	0.8378	0.5821	0.5640	0.9989
Fz	wav9	1.1837	0.8000	0.4722	0.4743	0.4042	0.9986
AE	FFT2	1.1944	0.4773	0.6200	0.7751	0.3946	0.9980
Fz	wav10	1.1755	0.8000	0.4838	0.4528	0.3941	0.9979
Pwr	FFT10	1.2119	0.4418	0.6538	0.7421	0.3707	0.9950
Vwx	Wav7	1.1138	0.3678	0.8371	0.5981	0.5656	0.9945
AERMS	FFT3	1.0337	0.3715	0.7016	0.7375	0.3689	0.9929
Vsx	wav10	1.0355	0.5873	0.6549	0.3681	0.4707	0.9929
Edx	wav5	0.9043	0.4551	0.8315	0.4451	0.5655	0.9925

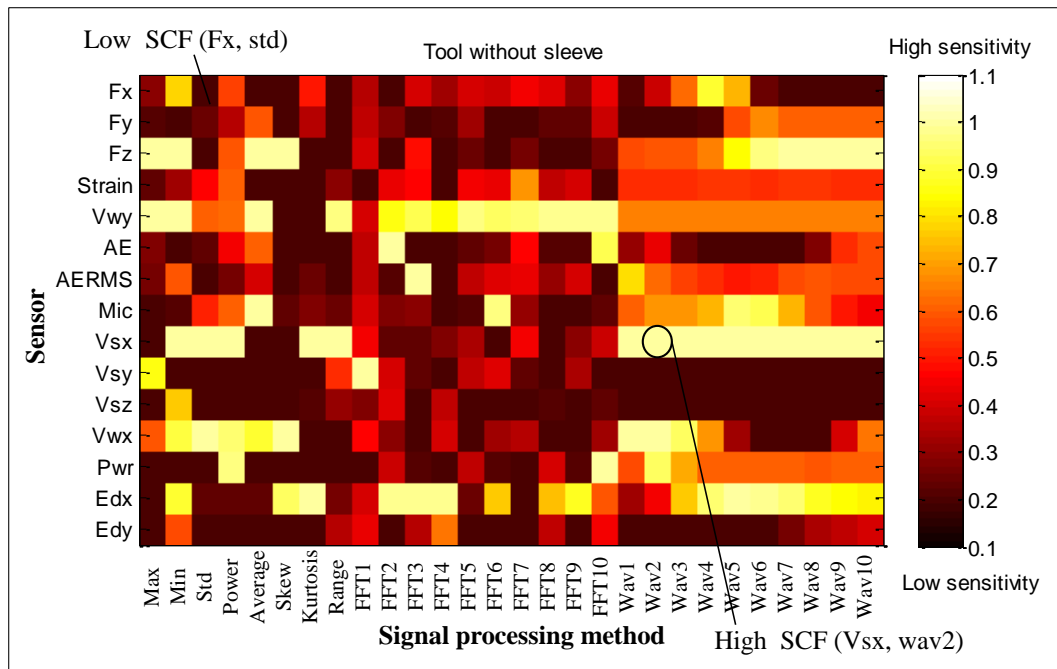


Figure 10.23: A graphical presentation of the sensitivity for fresh tool without sleeve using fuzzy method.

Similarly, the above procedures have been implemented for classifying the feature sensitivity for the tools with one broken tooth; Table 10.3 presents an example for the damaged tool without sleeve. It can be observed that the SCF (Mic, average), SCF(Mic, wav1) and SCF(Pwr, wav2) have been selected as the most sensitive features according to the evaluation of fuzzy logic. All the values of the sensitivity which are created by fuzzy logic imaged in Figure 10.24. However, the SCF(Fz, min), SCF(Fx, skew) and SCF(strain, min) are the most sensitive features for the tool with rubber sleeve. For the tool with copper sleeve, the most sensitive feature are the SCF(Fz, max), SCF(Fy, skew) and SCF(Fz, range), while the features for tool aluminium sleeve are the SCF (Vsz, std), SCF(Vsz, power) and SCF(Vsz, wav1) as described in Appendix O. It is clear that the evaluation of the fuzzy logic is different with the sequence of the each method individually.

Table 10.3: Example of the results of the fuzzy logic evaluation for the SCF of tool without sleeve with one broken tooth.

SCF		LR Slope	Range Value	SCIV	CCX3	CCX20	Fuzzy logic
Sensor	SP						
Mic	average	1.1464	0.8000	0.8488	0.7924	0.9789	0.9999
Mic	wav1	1.1505	0.7981	0.7469	0.7957	0.9789	0.9998
Pwr	wav2	1.1265	0.7643	0.8423	0.5371	0.5320	0.9997
Strain	min	1.1982	0.7704	0.8416	0.5473	0.5299	0.9997
Edx	max	1.0675	0.8000	0.5700	0.5097	0.5525	0.9996
Mic	skew	1.2119	0.5605	0.8398	0.6317	0.4847	0.9995
Vsy	average	0.9704	0.4915	0.6858	0.6100	0.8711	0.9994
Vwx	wav10	0.9715	0.7202	0.8393	0.4661	0.6304	0.9992
Pwr	wav3	0.9472	0.6564	0.8379	0.4771	0.5940	0.9987
Vwx	wav9	0.9567	0.7156	0.8393	0.4445	0.6109	0.9984
Edx	FFT10	1.1080	0.3945	0.7521	0.7809	0.3957	0.9980
Vwx	std	1.0032	0.4418	0.8250	0.4087	0.5066	0.9976
Pwr	wav1	1.1317	0.5835	0.8423	0.5702	0.3843	0.9970
Fz	FFT10	1.1293	0.4331	0.7706	0.7605	0.3812	0.9966
Edx	FFT6	1.1562	0.3730	0.7867	0.7740	0.3881	0.9954
Strain	range	1.1464	0.6456	0.3691	0.4592	0.4591	0.9947
Fx	FFT3	1.1425	0.3874	0.7954	0.7403	0.3644	0.9938
Edy	wav7	0.9765	0.5245	0.8144	0.3955	0.4744	0.9935
Fx	FFT5	1.1838	0.4798	0.7700	0.7385	0.3632	0.9935
Edx	FFT10	1.1329	0.4422	0.7829	0.7322	0.3612	0.9930

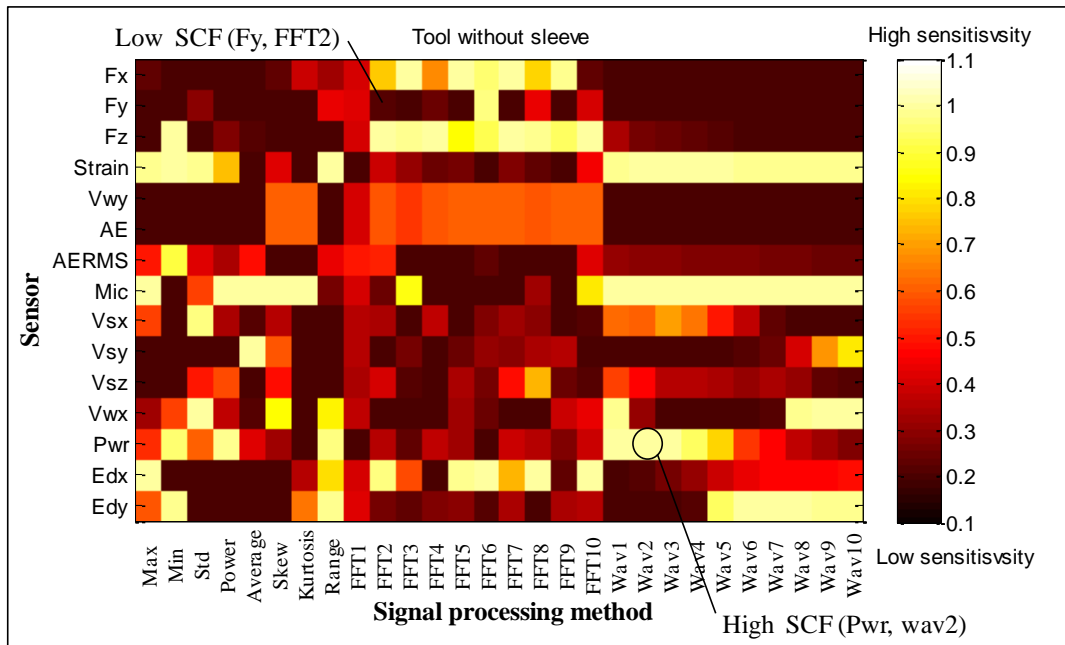


Figure 10.24: A graphical presentation of the sensitivity for normal tool with one broken tooth using fuzzy method.

Furthermore, Table 10.4 shows an example of the sensitivity values arranged according to the evaluation of fuzzy logic for the normal tool with two broken teeth, since the suggested approach has been dependent on the control of the fuzzy roles. It is observed that this method classify the sensitivity to three categories, namely, high, medium and low and take all the methods presentations in their decision, therefore it can be considered as a more reliable and accurate method to determine the most sensitive feature. Figure 10.25 shows the image of associated matrix for the normal tools with two broken teeth, where the SCF(AERMS, kurtosis), SCF(Fz, min) and SCF (Strain, wav1) are the most sensitive features. However, the SCF(Fy, wav1), SCF(Fy, wav9) and SCF(Fy, std) are the most sensitive features for tools with rubber sleeve. For the tool with copper sleeve, the most sensitive features are SCF(AERMS, skew), SCF(Vsx, range) and SCF(Vsx, std), and those for the tool with aluminium sleeve are the SCF(Fy, power), SCF(Pwr, std) and SCF(Fz, average) as described in Appendix O.

Table 10.4: Example of the results of the fuzzy logic evaluation for the SCF of tool without sleeve with two broken teeth.

SCF		LR Slope	Range	SCIV	CCX3	CCX20	Fuzzy logic
Sensor	SP						
AERMS	Kurtosis	1.0615	0.6285	0.8429	0.7256	0.8937	0.9999
Fz	min	1.3088	0.5854	0.8415	0.8465	0.4709	0.9998
Strain	wav1	1.1913	0.6962	0.7774	0.4563	0.4525	0.9997
Mic	wav4	1.1921	0.7507	0.8376	0.5954	0.4521	0.9997
Mic	wav6	1.1509	0.5282	0.8351	0.6298	0.4416	0.9996
Strain	wav3	1.1588	0.6366	0.7408	0.4344	0.4383	0.9995
Strain	min	1.2214	0.7667	0.8144	0.4971	0.4306	0.9995
Mic	Wav8	1.1285	0.4367	0.8343	0.6321	0.4295	0.9995
Mic	power	1.1752	0.8000	0.8368	0.5472	0.4256	0.9994
Strain	power	1.1192	0.6645	0.7374	0.4195	0.4940	0.9992
Vsx	FFT8	1.0743	0.4160	0.5159	0.9935	0.8106	0.9991
Strain	range	1.1496	0.6370	0.7068	0.4429	0.4111	0.9989
Strain	wav4	1.1232	0.5914	0.7042	0.4054	0.4201	0.9986
Edx	wav4	1.0549	0.5321	0.8312	0.3999	0.4073	0.9982
Fy	FFT9	1.1431	0.3850	0.6781	0.8280	0.4300	0.9971
Mic	wav9	1.1126	0.3780	0.8338	0.6284	0.4179	0.9962
AERMS	wav8	1.0614	0.7131	0.8363	0.3792	0.4184	0.9962
Strain	min	1.0548	0.5161	0.7145	0.3702	0.3715	0.9944
Edx	FFT3	1.0982	0.4341	0.8053	0.7352	0.3674	0.9944
Edx	FFT8	1.1430	0.4695	0.7909	0.7381	0.3673	0.9944

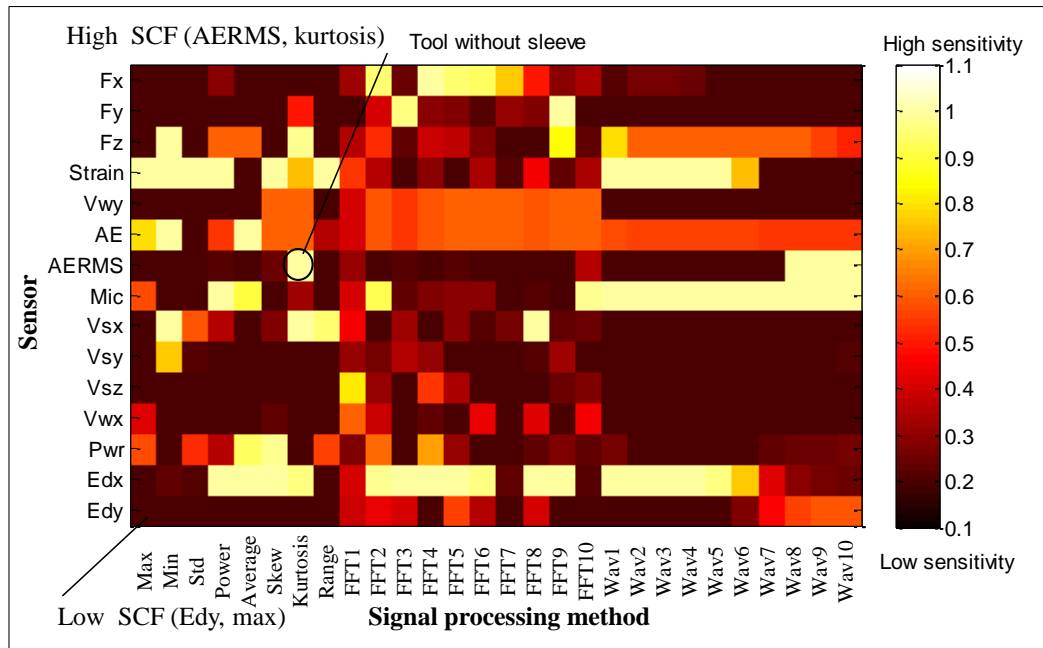


Figure 10.25: A graphical presentation of the sensitivity for tool with two broken teeth, without sleeve using SCIV method.

From the above figures, it can be concluded that there is a clear difference between the sensitive systems which are designed to detect the tool condition and to define the effect of the quality of fixturing system on the monitoring system. It seems possible that these results proved that the change of the fixturing material could affect the stability of the system, and consequently effects on the design of online monitoring system. However, an independent assessing method is important to evaluate the reliability and the precision of the fuzzy logic in comparing with the other methods.

10.3.6 LVQ Neural Network Training

However, such expositions are unsatisfactory unless they assessed by another method for verification, therefore the Learning Vector Quantization (LVQ) neural network has been used to define which method of the measuring sensitivity exist less training and testing error. LVQ has been selected as it is unsupervised neural network therefore, independently, it will create a classification for the input training data and it will test the new input data and explore the error between them. For each tool, 420 features will be divided to 12 systems, starting from higher to lower sensitivity and arranged according to different measuring sensitivity methods which are mentioned earlier (i.e. LR, Range value, correlation coefficients, Fuzzy). The data of tool without

sleeve will be used for training and the three rest tools (tool with rubber sleeve, tool with copper sleeve and tool with aluminium sleeve) will be used for testing.

Figure 10.26 shows individually the average of the training errors of SCF for tools with four types of fixturing system. These features arranged according to the used measuring sensitivity methods. It is clear that the Range Value and CCX3 methods obtained the higher ratio of training error, which provided an indicator that those methods are far from the real representative for the LR slop signals. In contrast, it can be seen that the rest four methods (LR, SCIV, CCX20 and Fuzzy logic) achieved comparatively lower errors and noticeably that the fuzzy logic is lowest one in error as shown in Figure 10.27.

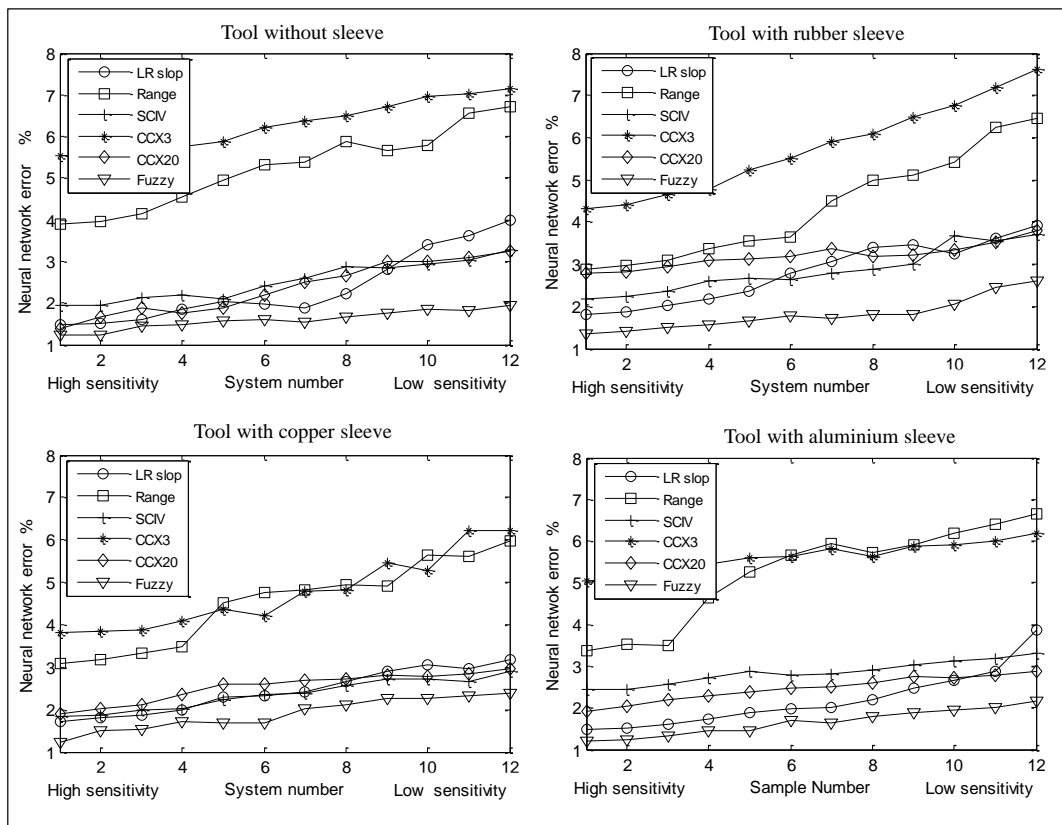


Figure 10.26: The LVQ neural network errors of sensitivity feature for fresh tools with deferent fixturing systems.

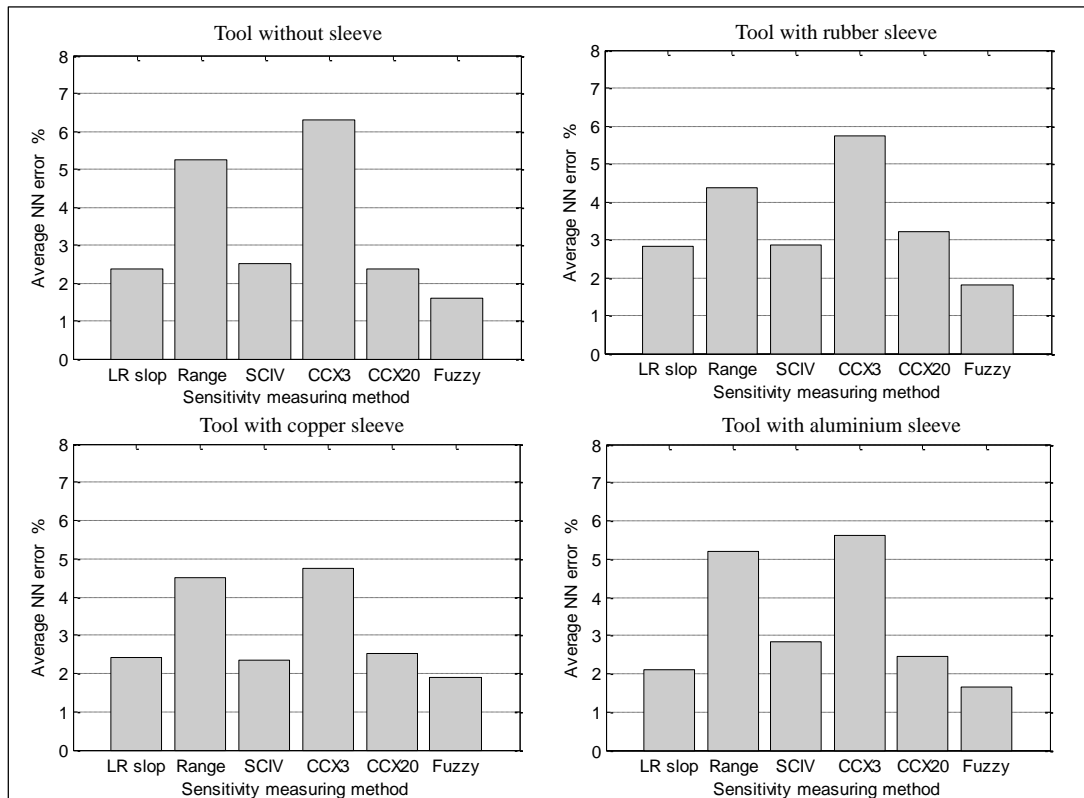


Figure 10.27: The average LVQ errors of the sensitivity measuring methods for fresh tools.

The above procedures have been applied to measure the training error of the data for the tools with one broken tooth. Similarly, the data of tool without sleeve will be used for training and the data of other tools with different sleeves for testing. Figure 10.28 shows the LVQ training errors for the tool with different fixturing system. For four types of tools, it can be observed that the fuzzy logic obtained the lower training error for all the tools. Both the Range Value and CCX3 methods produced the higher ratio of the errors, meanwhile the LR, SCIV and CCX20 methods obtained the error but more than the fuzzy logic as illustrated in Figure 10.29. Generally, it can be noticed that the error values have been raised up comparing with those of the fresh tools.

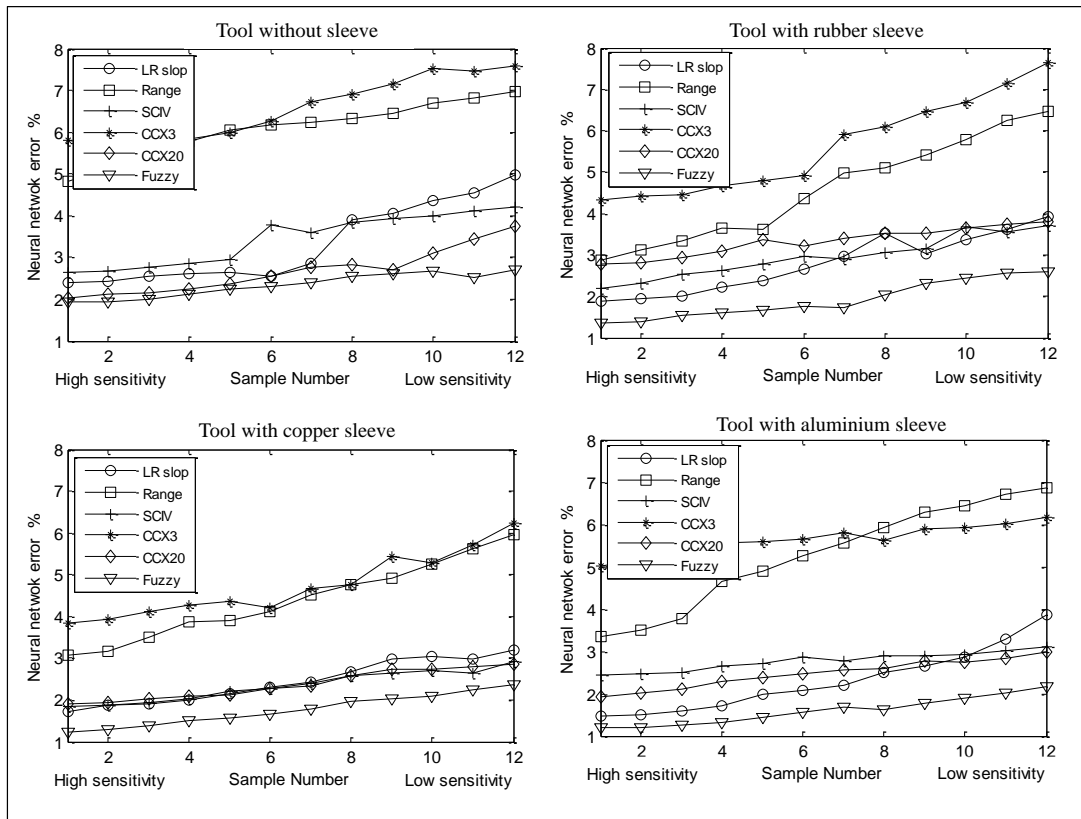


Figure 10.28: The LVQ neural network errors of sensitivity feature for tools with one broken tooth for deferent fixturing systems.

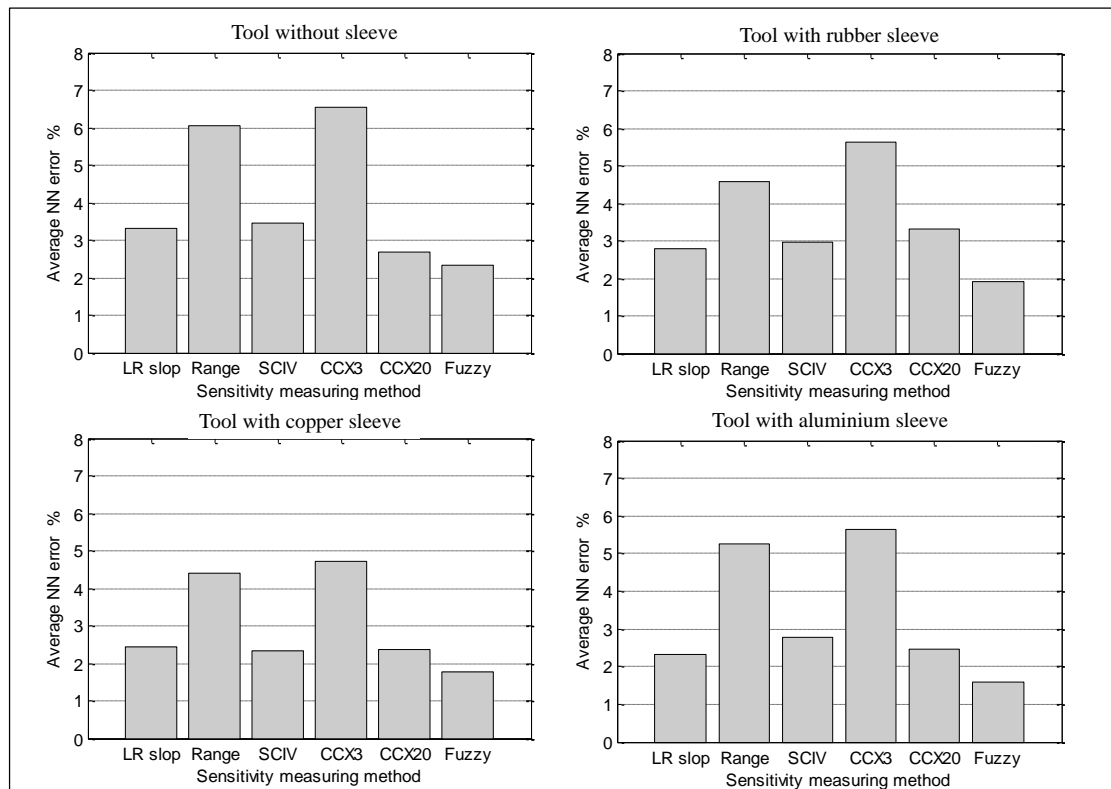


Figure 10.29: The average LVQ errors of the sensitivity measuring methods for tools with one broken tooth.

This analysis will be continued to measure the error of the LVQ training error of the tools with two broken teeth as shown in Figure 10.30. It is significantly clear that two methods (Range Value and CCX3) obtained high errors ratio.

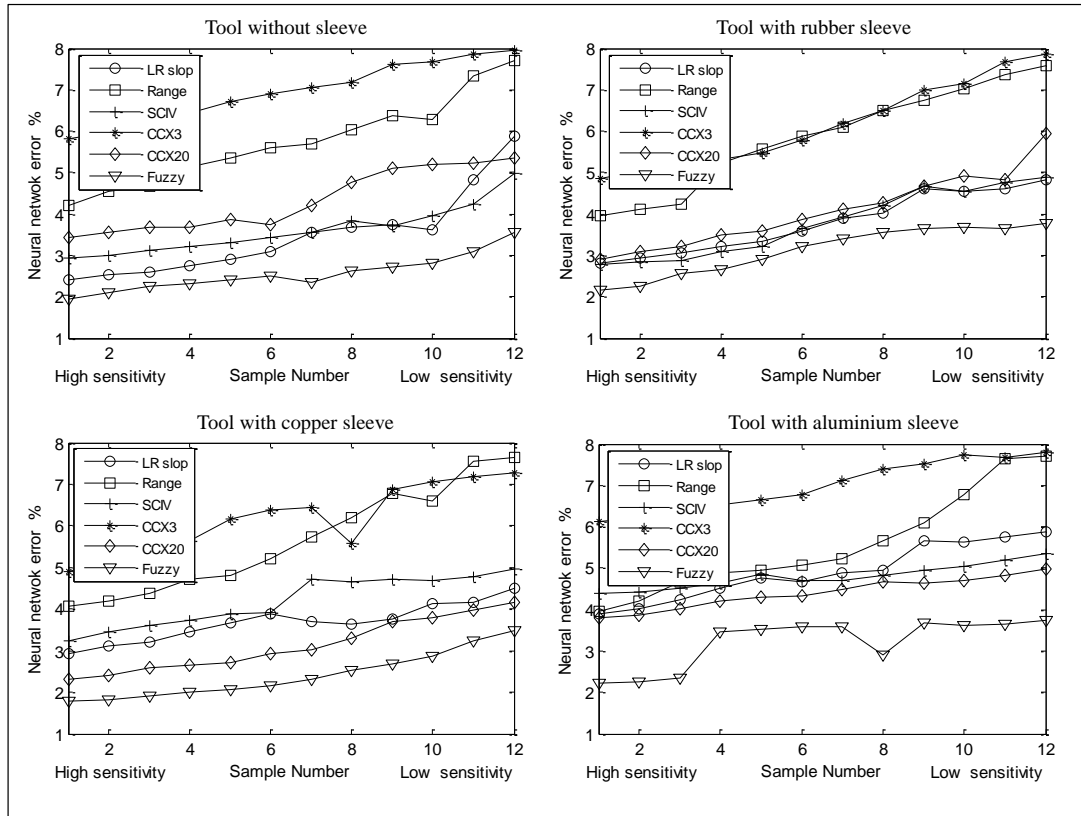


Figure 10.30: The LVQ neural network errors of sensitivity feature for tools with two broken teeth for deferent fixturing systems.

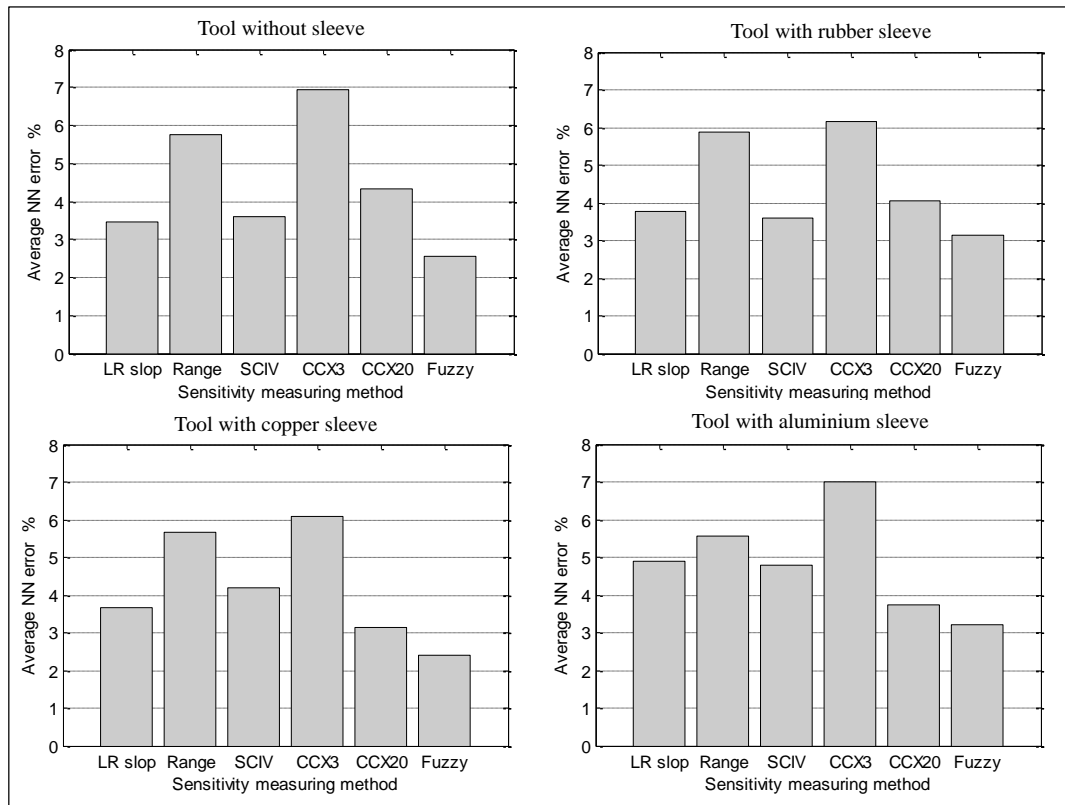


Figure 10.31: The average LVQ errors of the sensitivity measuring methods for tools with two broken teeth.

Figure 10.31 shows the average of the LVQ errors of the sensitivity measuring methods for tools with two broken teeth. It is clearly showed that fuzzy logic keeps the last place in the rank of the lower training error. But, generally it can be noticed that the error values for the tools with two broken teeth are increased in comparing with the previous tools.

The previous discussion for the training error of the LVQ neural network showed that each type of the tools either different in the tool condition (fresh, with one broken tooth and two broken teeth) or in the type of fixturing system (without sleeve, with rubber, copper and aluminium sleeve), got different values of the errors. In addition, the error ratio increasing gradually when the tool condition transferred from the new tool to the damaged tools as seen in Figure 10.32. This presents an ability to define the type of the tool condition depends on the results of the neural network training. Consequently, this presented an indicator that the results of measuring sensitivity method could be different according to the type of the fixturing system.

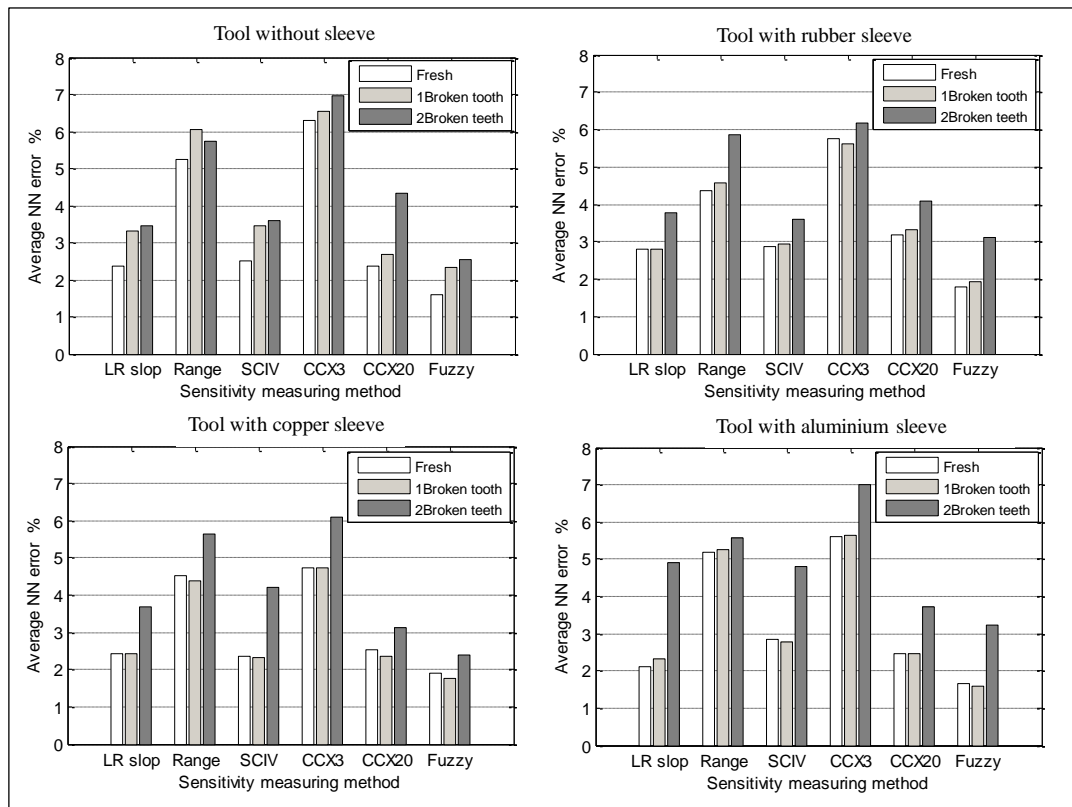


Figure 10.32: Comparison between the average LVQ errors of the sensitivity measuring methods for three tool conditions.

The present findings seem to be consistent with other results of previous chapters which found the quality of the fixturing system could affect the design of the condition monitoring system.

10.4 Pattern Recognition

10.4.1 Taylor’s Equation Induced Pattern (TIP)

As discussed in the previous section that proved the ability of the fuzzy logic to define the more sensitive features by combining different techniques as a fusion model, that will lead the investigation to the next stage of the monitoring system which is the pattern recognition. In general, therefore, it seems that is important to classify the status of the tool from fresh to worn, and then make a decision. The most important limitation lies in the fact that how to classify the tool condition after simplifying the collected signal from the sensor. A Taylor’s Equation Induced Pattern (TIP) technique used to define the pattern recognition and make the accurate decision for the tool condition status. Since, this research has been studying three stages of the tool

condition stages, fresh and tool with one broken tooth and tool with two broken teeth, logically, there is a difference among the sensory signals of those stages. Here, it will be focused on two variables for the signal, first is the amplitude of the first points which are (0.2, 0.4 and 0.6) for the first experimental pattern for fresh tool, the second and third patterns for tools with one broken tooth and two broken teeth (V_f , V_{b1} and V_{b2}) respectively. The variable is the average variance among last points which are (0.4, 0.6 and 0.8) for three stages (V_{a0} , V_{a1} and V_{a2}). These values extracted from the experimental signals as shown in Figures 10.33, 10.34 and 10.35.

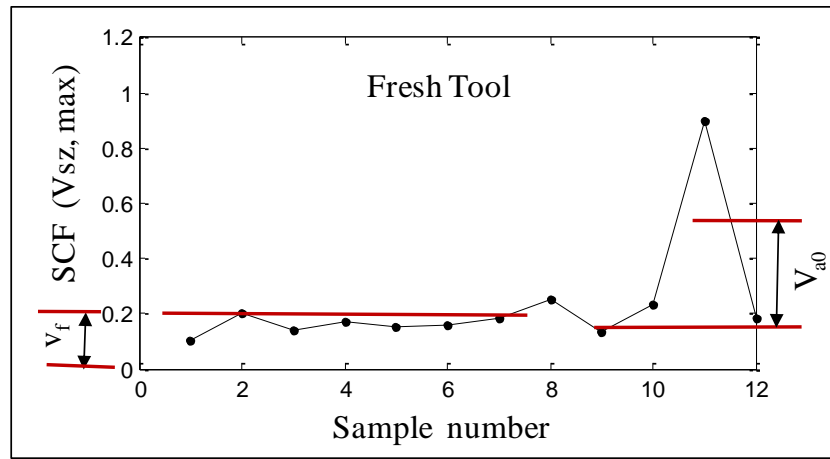


Figure 10.33: The amplitude and variance of first experimental pattern (pattern 1).

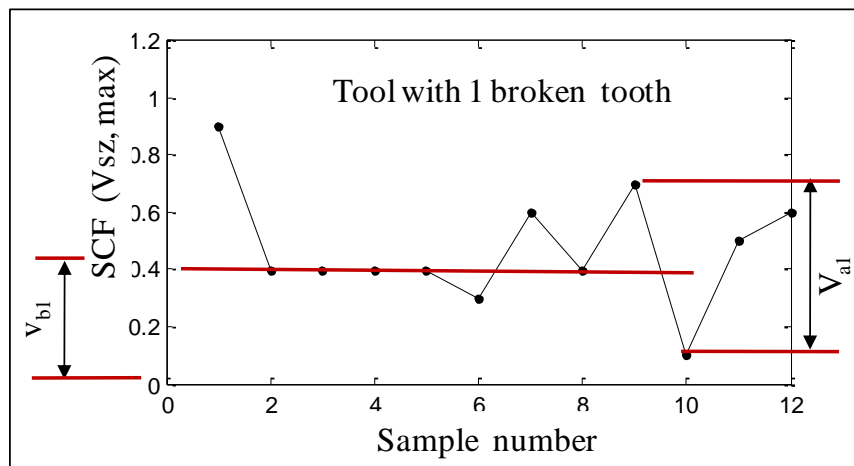


Figure 10.34: The amplitude and variance of second experimental pattern (pattern 2).

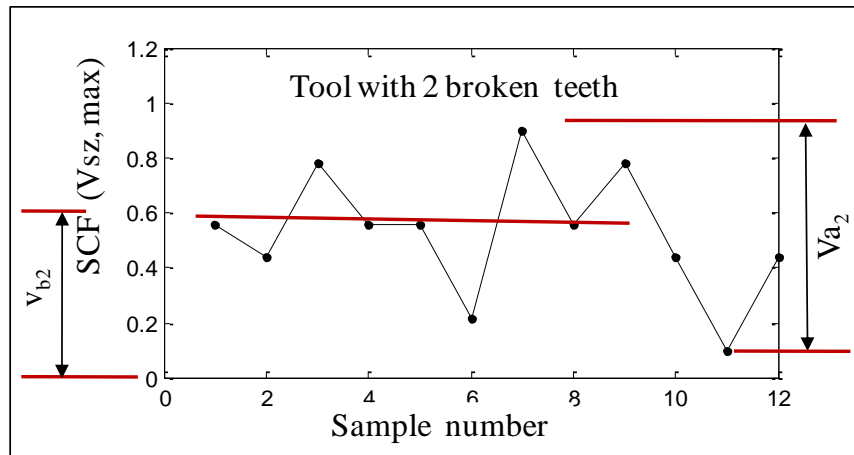


Figure 10.35: The amplitude and variance of third experimental pattern (pattern 3).

In this research, the above applicable approach has been proposed to deal with the patterns of all experimental sensory features. These patterns are considered as templates to divide the target of neural network. Here, Back Propagation (BP) Neural Network will be implemented the data training and testing because it is a supervised method and definitely needs to determine the target in advance. Since the fuzzy logic is the best method to obtain the sensitivity, therefore the sequence of the features will be taken according to the arrangement of fuzzy logic. The features of first system of sensitivity for the tool without sleeve will be used for training and the data of other tools (tool with rubber, copper and aluminium sleeves) will be used for testing. This procedure will be also applied for the damaged tools with one broken tooth and two broken teeth.

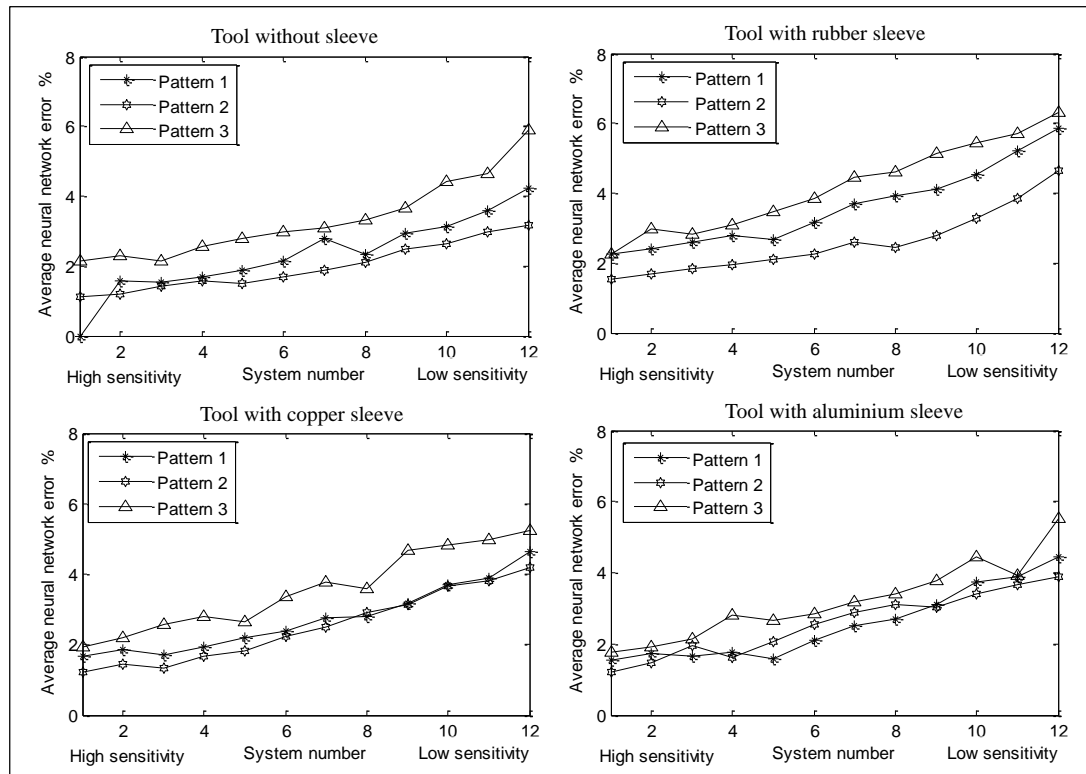


Figure 10.36: The BP neural network errors for fresh tools using different patterns.

Figure 10.36 shows the results of the training and testing of the BP neural network for the fresh tools. It can be observed that Pattern 3 has obtained the higher ratio of training error for all the used tools, this is especially very clear for the tool with rubber sleeve where the error raised to 6.32 %, while Pattern 1 presented medium errors. However, Pattern 2 is clearly provided less error which it is 4.66 %, and obtained less than this error ratio for the other tools. This indicates that Pattern 2 is the more suitable to represent the behaviour of the feature for the fresh tools with different fixturing system.

Figure 10.37 shows the error of the BP neural network for the tools with one broken tooth. Here, the tool with rubber sleeve even it is got the higher error with Pattern 3 (5.35%) but it is still less than that for fresh tool. Pattern 2 obtained 3.27% as error ratio for the mentioned tool. However, it is 2.41%, 3.18% and 3.47% for the tools without sleeve, and with copper and aluminium sleeves.

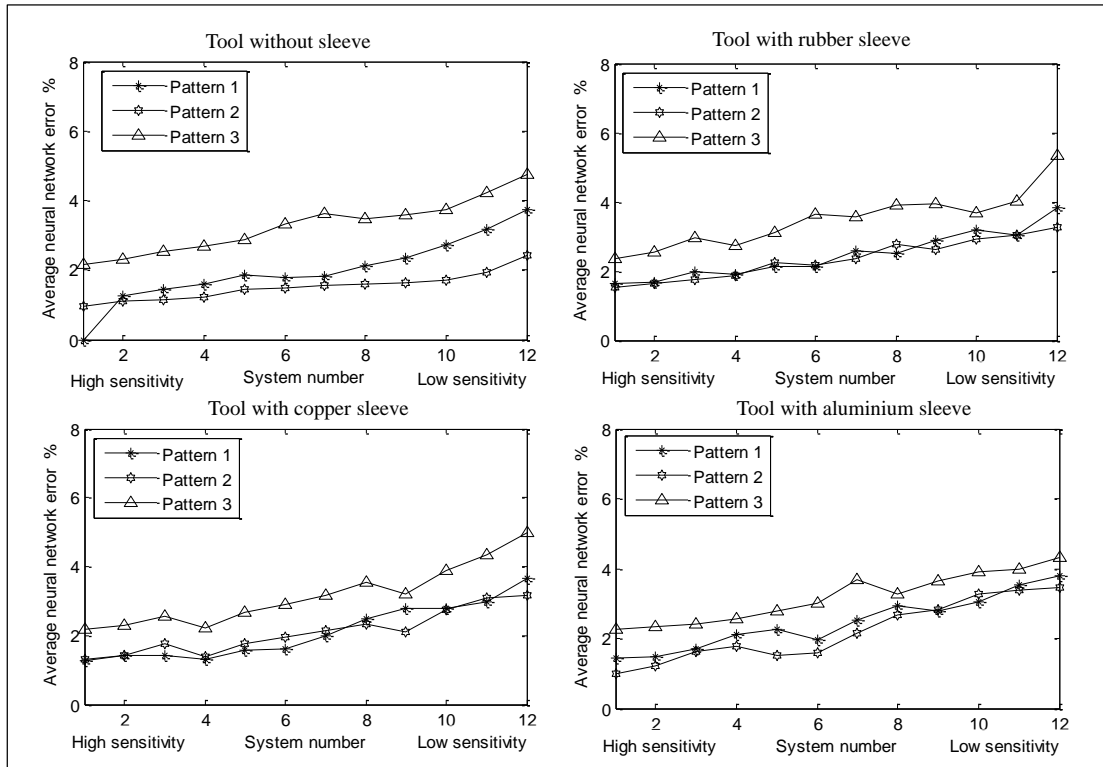


Figure 10.37: The training errors of different patterns for tools with one broken tooth.

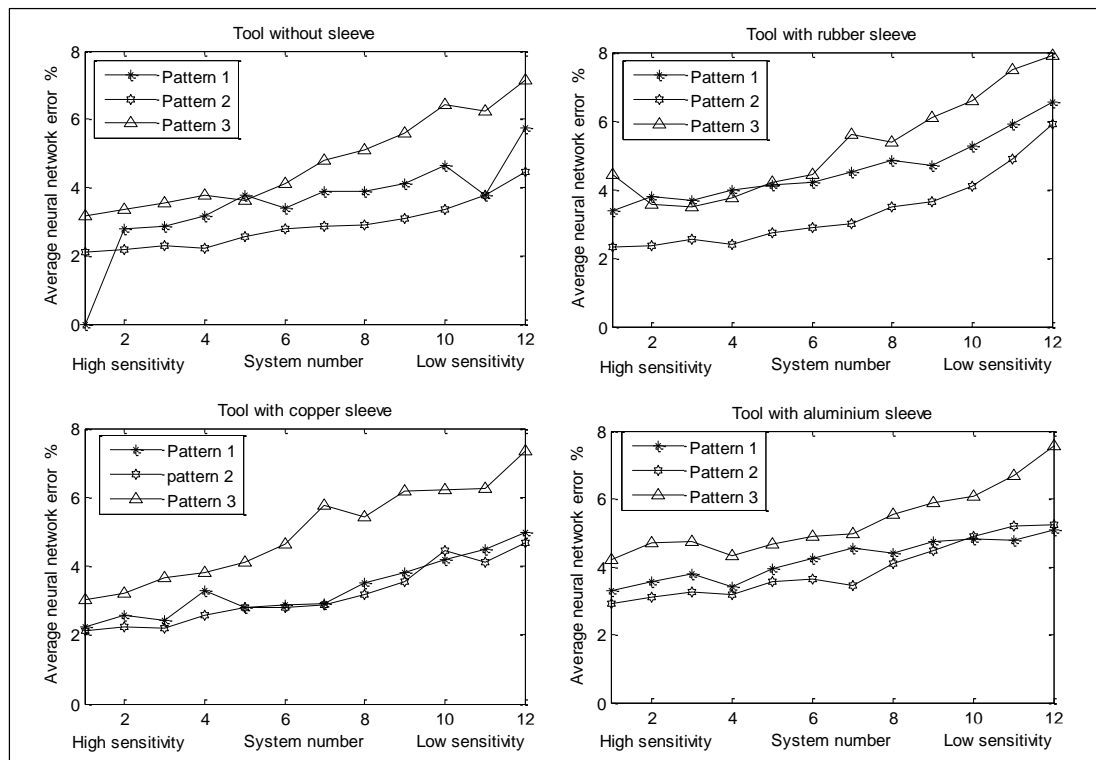


Figure 10.38: The training errors of different patterns for tools with two broken teeth.

For the tools with two broken teeth, as shown in Figure 10.38, it can be seen that the training error have been significant increased especially for the pattern 3 which obtained 7.92 % for the tool with rubber sleeve. For the same tool, pattern 2 made an error ratio by 5.89%; meanwhile pattern 1 is 6.53%. Other tools have achieved less error ratio with pattern 3 which are 7.15%, 7.35 and 7.55% respectively.

10.4.2 Comparison between the Pattern Types

From the above discussion, it can be concluded that pattern 3 has found to be achieved higher error in comparing with the other two patterns, and relatively pattern 1 keeps the middle stage for the all the tools, and clearly pattern 2 presented the lower error. Therefore, pattern 2 seems more agreement to represent the features of the fresh or damaged tools as shown in the Figure 10.39. Where in all tool conditions and for all the fixturing system, pattern 2 achieved lower errors, this provides an indicator about their reliability and ability to simulate the features of the sensory signals. One major finding of this approach is that the ability to classify the status of the tool conditions and the type of the fixturing system. Another important finding is that the capability of the ASPSF approach to define the relation between the tool conditions, fixturing system and condition monitoring system, since the effect of changing the tool condition or fixturing system could be significantly effected on the sensitivity of the sensory signal and consequently on the design of the monitoring system.

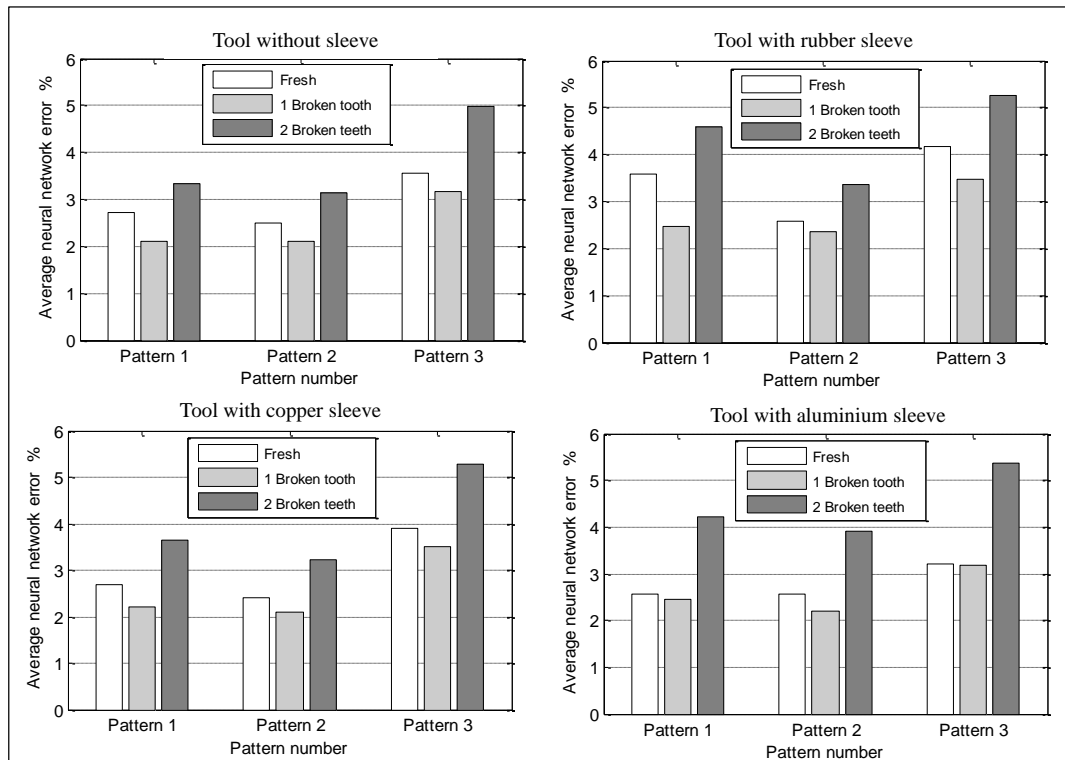


Figure 10.39: Comparison between the pattern errors for tools with different fixturing systems.

10.5 Surface Roughness

10.5.1 Roughness of Machined Surface

The surface roughness is a vital and critical factor to measure the quality of the component produced since even the dimensions of the product are agreed within the dimensional tolerances, still there are possibilities of rejecting the workpiece due to lack of surface finishing. One of the main parameter to control the surface finish is determined the mechanical properties such as tool wear, tool breakage and tool runout due to imperfect fixturing system. Therefore in this section the relationship between the surface roughness and the type of the tool condition and fixturing system will be investigated. The surface tester (type Mitotoya SJ120) has been used to measure the roughness of the workpiece by tracking the machining process on the workpiece. After each machining test by using fresh tool with different fixturing system, the measurement of the surface roughness has collected as shown in Figure 10.40. It can be observed that the surface roughness (R_a , μm) is increased with the continuously of the machining process for all tools with different types of fixturing systems. But,

visually, it is clear that the roughness values for the tool with rubber sleeve are higher than those for other tools that may be because the rubber material is lowest elastic modulus and allows to the tool to move flexibly.

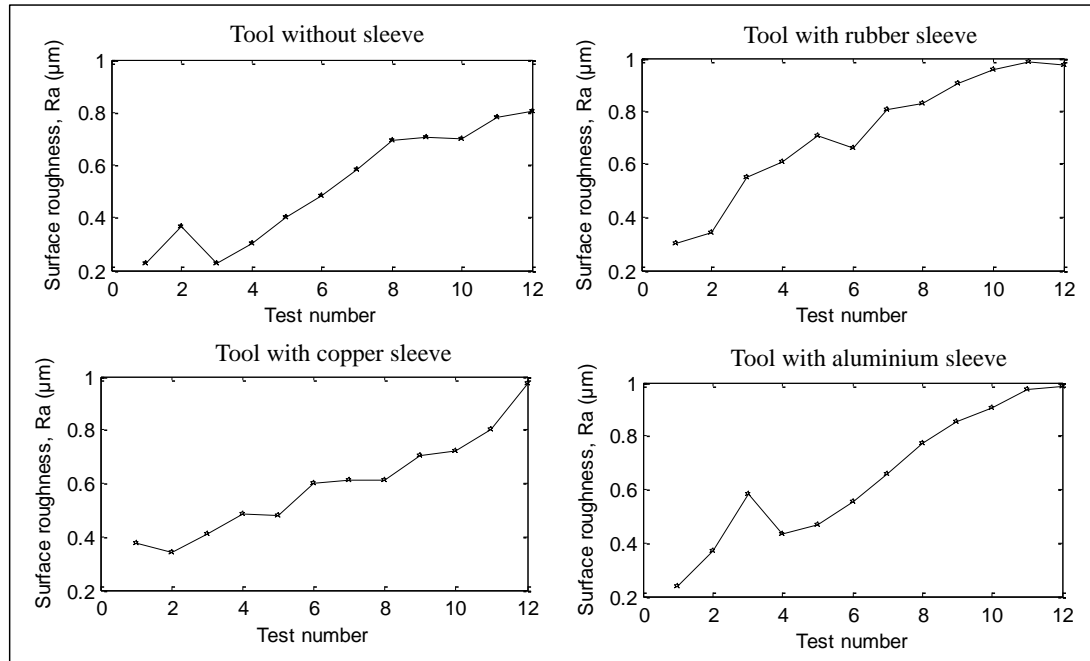


Figure 10.40: Surface roughness of workpiece for fresh tools.

The tools with one broken tooth are used in the following test with same procedures to measure the roughness of the machined surface. The result of the measurements is illustrated in Figure 10.41, where it can be noticed that the values of collected data are increased for all the types of tools with different fixturing systems. This finding reflects the effect of the tool breakage phenomena on the quality of the surface, especially for the tool with rubber sleeve as both the effect of the rubber flexibility and tool breakage have been interfaced together to create significant change in the surface roughness which increased to around $2 \mu\text{m}$.

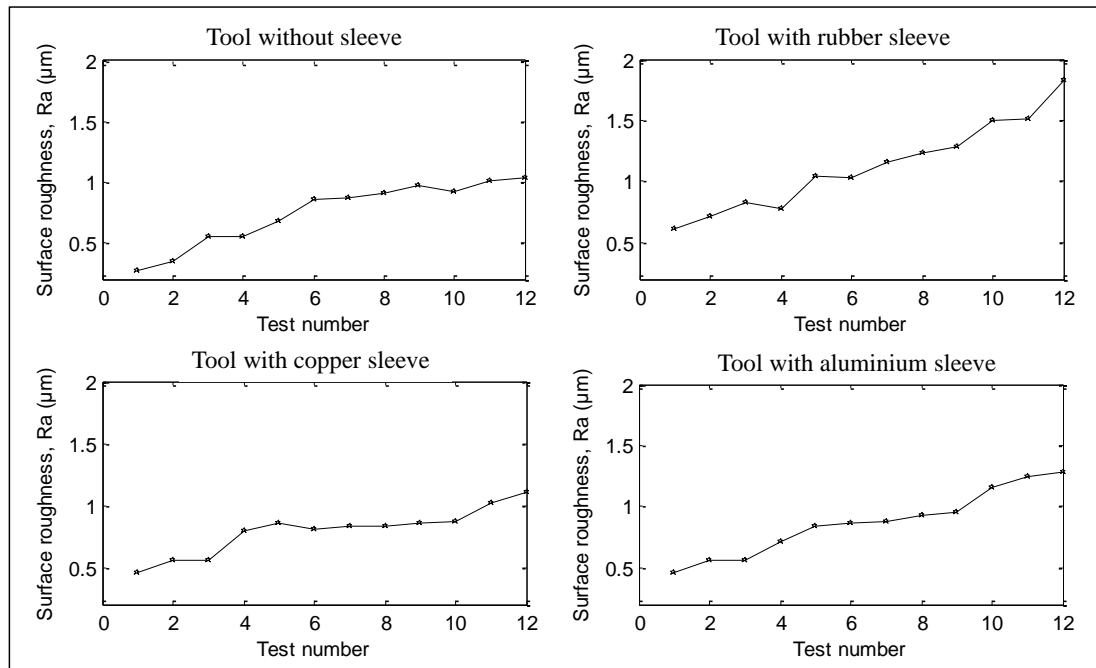


Figure 10.41: Surface roughness of workpiece for tools with one broken tooth.

The effect of increasing the number of the cutter broken teeth has been investigated in this experimental work. Figure 10.42 shows the measurement of tools with two broken teeth using tool without sleeve, tool with rubber sleeve, tool with copper sleeve and tool with aluminium sleeve. The results are agreement with our exceptions as the measurement of the roughness relatively near to 2.5 μm for the tool with rubber sleeve and around 1.5 μm for other tools.

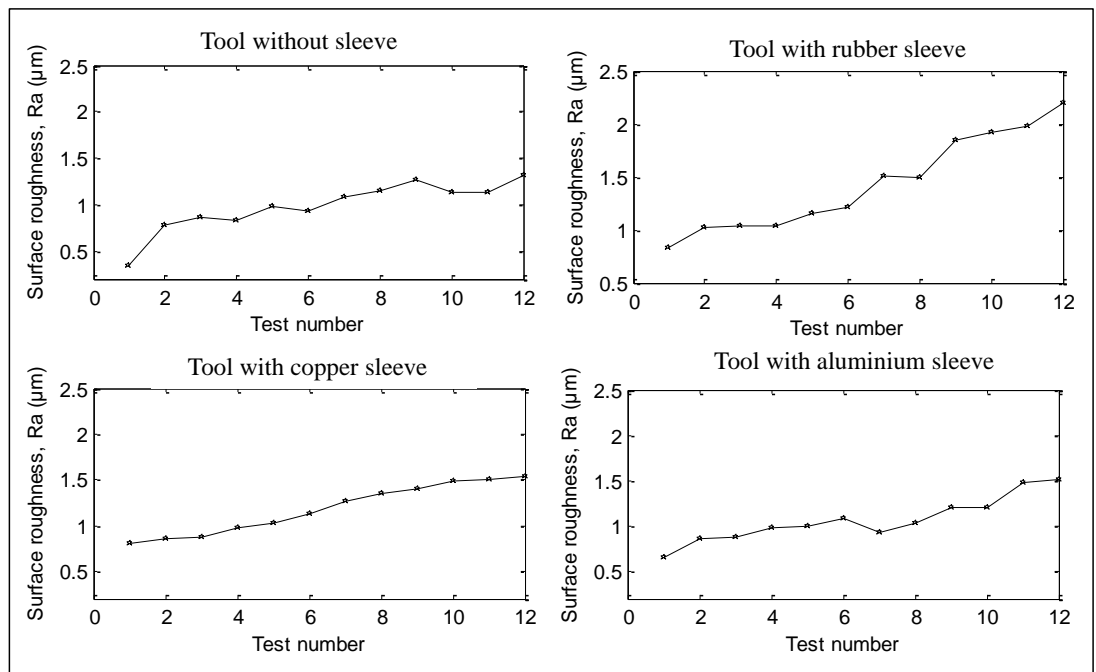


Figure 10.42: Surface roughness of workpiece for tools with two broken teeth.

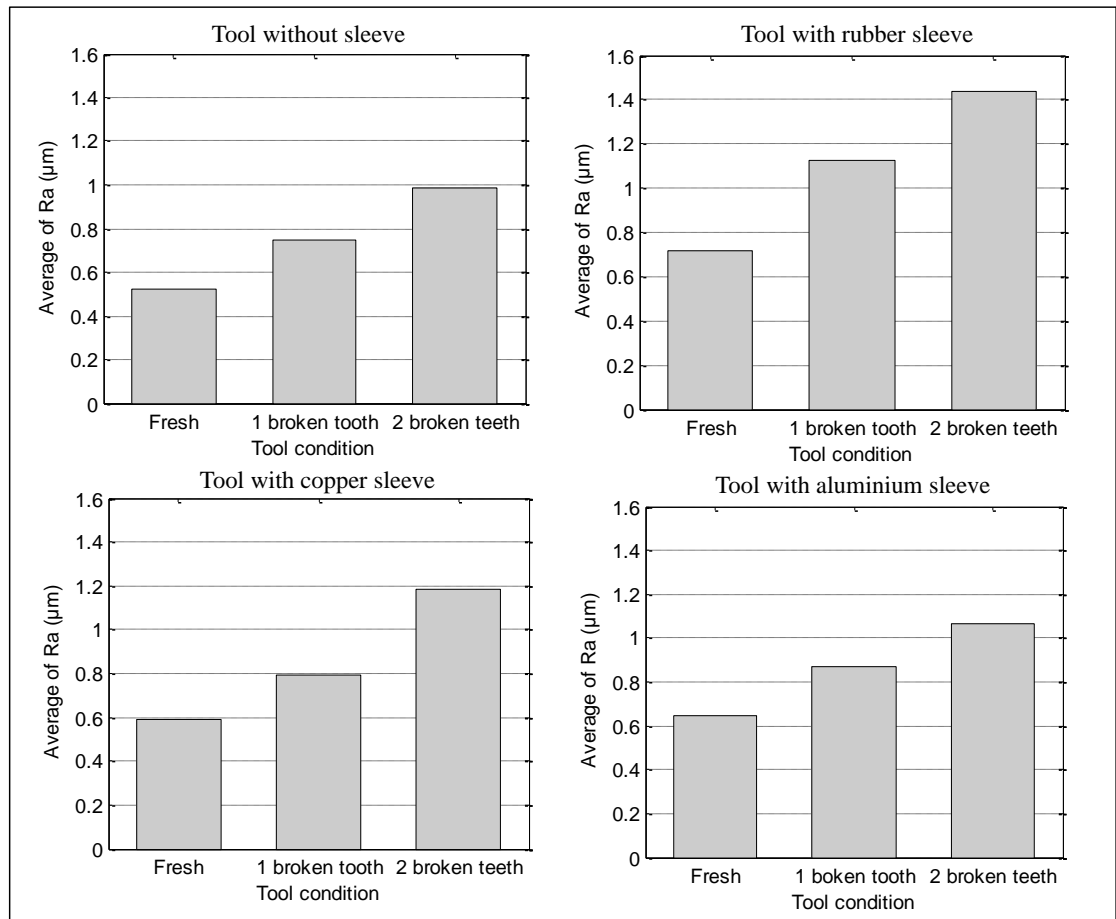


Figure 10.43: Average of surface roughness of workpiece for all tools conditions.

For exploring the results in one graph to compare between the surface roughness measurements for each fixturing system individually in different tool conditions, Figure 10.43 presents the chart of the average of roughness. It can be clearly noticed that the roughness gradually increasing with regards to change the type of the tool conditions from the fresh tool to tool with one broken tooth to tool with two broken teeth.

For conclusion, Figure 10.44 shows the relationship between the surface roughness and the type of the tool conditions, to evaluate the surface roughness of all the tools in case of fresh tool, also in the damaged tools with one and two broken teeth. It can be observed that the tools without sleeve have been obtained the lower values of the roughness measurements for three tool conditions. However, the tools with rubber sleeve produced the higher roughness meanwhile the tools with copper and aluminium sleeve produced less roughness than those for the tool with rubber sleeve. The findings of this study indicate that the tool condition and fixturing system have direct effect on the measurement of the surface roughness and consequently on the

quality of the products. This finding encourages us to investigate about the relation between the surface roughness and design of the condition monitoring system in terms of changing the condition of tool and fixturing types.

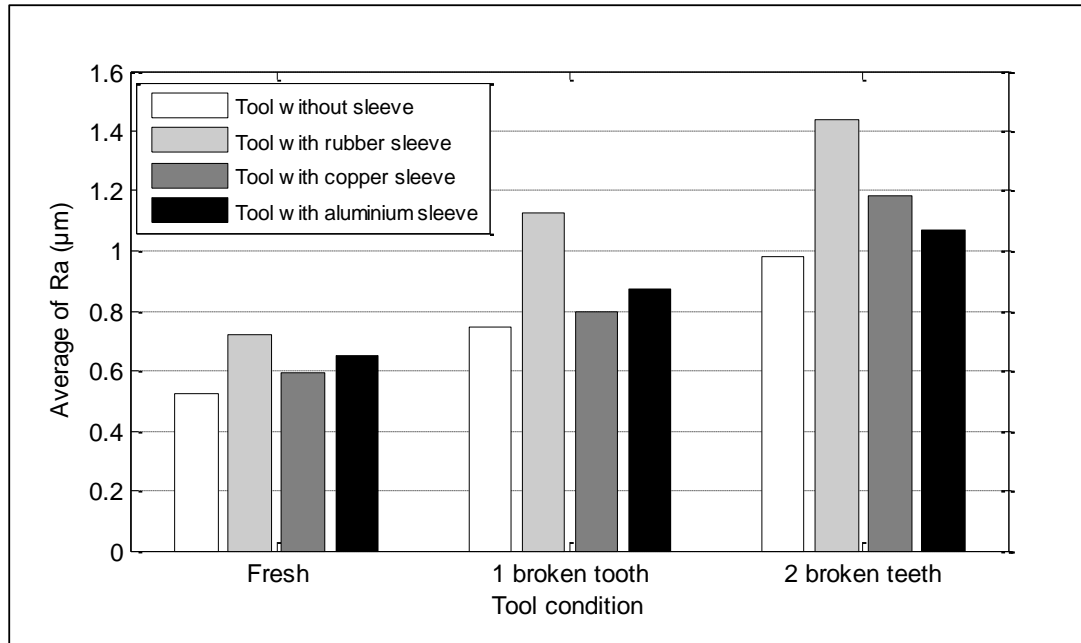


Figure 10.44: Comparison between the averages of Ra of workpiece for three tool conditions.

10.5.2 Relation between Surface Roughness and Sensitivity

As described in the previous section for the importance of the surface roughness to determine the quality of the workpiece, therefore it is important also to find a method to evaluate or control the roughness during the machining process. In this research, a suitable method is used to determine the correlation between the sensitivity of the sensory characteristic feature (SCF) and the surface roughness measurements. This correlation will explain is there any relation or its indicator to the overall change in the sensitivity or surface roughness.

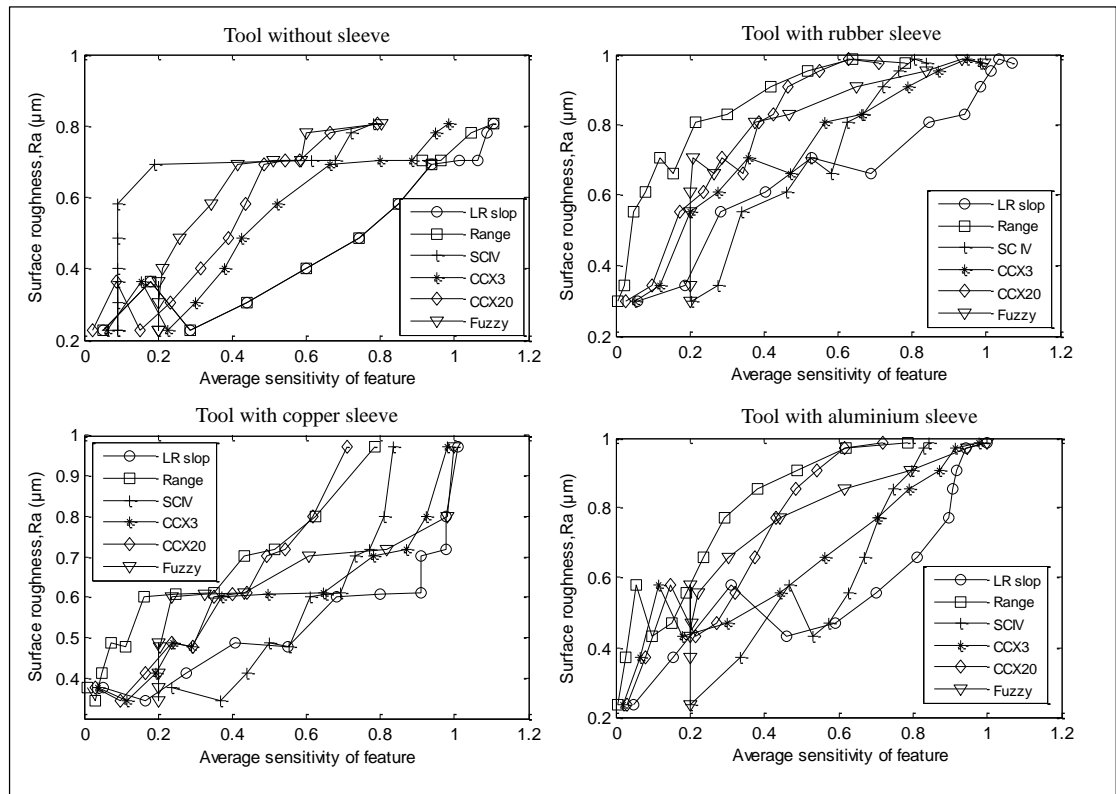


Figure 10.45: The relation between surface roughness and average of sensitivity of features of system for fresh tools.

Figure 10.45 shows the correlation between the sensitivity of the feature using different sensitivity measuring methods (i.e. LR, Range Value, SCIV, CCX3, CCX20, Fuzzy) and the surface roughness measurement of workpiece. It is visually clear that the sensitivity has a proportional increasing with the surface roughness since the change in the fixturing system for fresh tool will generate an increase in the surface roughness as explained in the previous section. This change leads to obtain sensory signals with high amplitudes, which means there is a possibility to increase the sensitivity of the feature. In addition, it can be seen that the roughness values of the tool with rubber sleeve are higher than those for other types of tools.

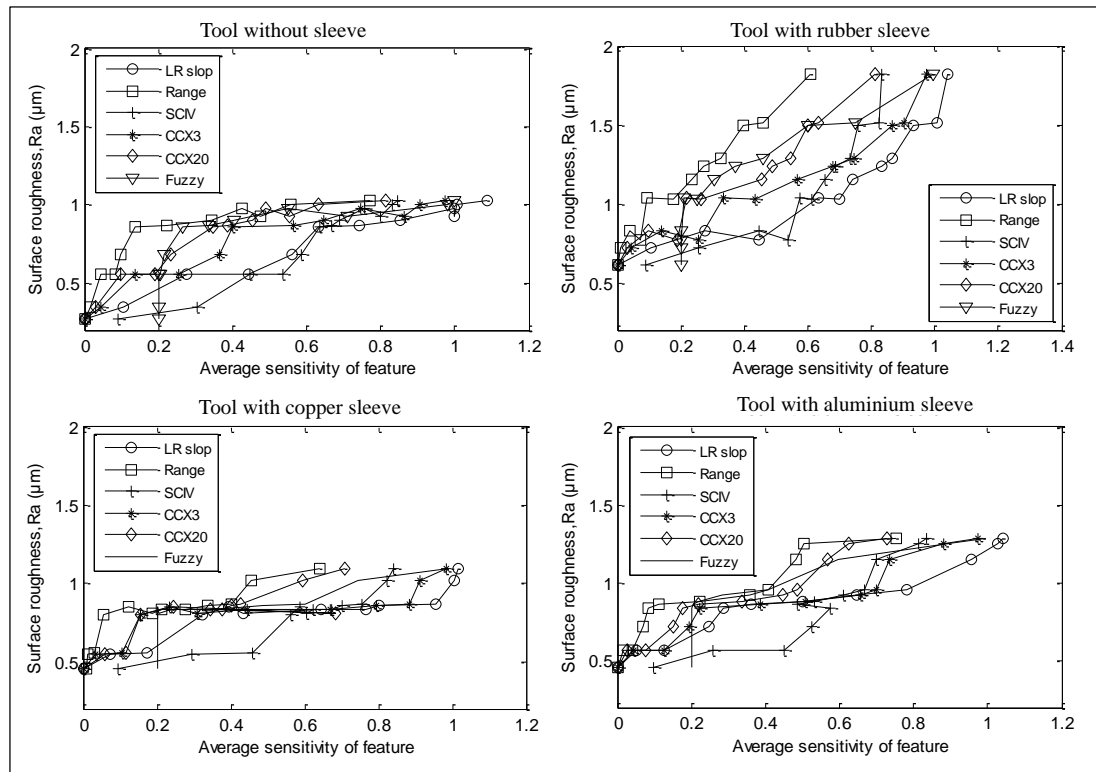


Figure 10.46: The relation between surface roughness and average of sensitivity of features of system for tools with one broken tooth.

For the tools with one broken tooth, Figure 10.46 presents the relationship for the tools with different featuring system. It can be observed that the correlation values have been increased due to increase the agreement between the rise of surface roughness and the sensitivity of feature, also, here it can be seen that the tool rubber sleeve shows the higher relation among other tools without or with copper and aluminium sleeves. A possible explanation for this might be that the response of the sensor will rise as a result to redundancy in the cutting process. The most interesting finding is that an indicator to address the status of the tool depends on the response of the sensors and consequently depends on the sensitivity of the feature.

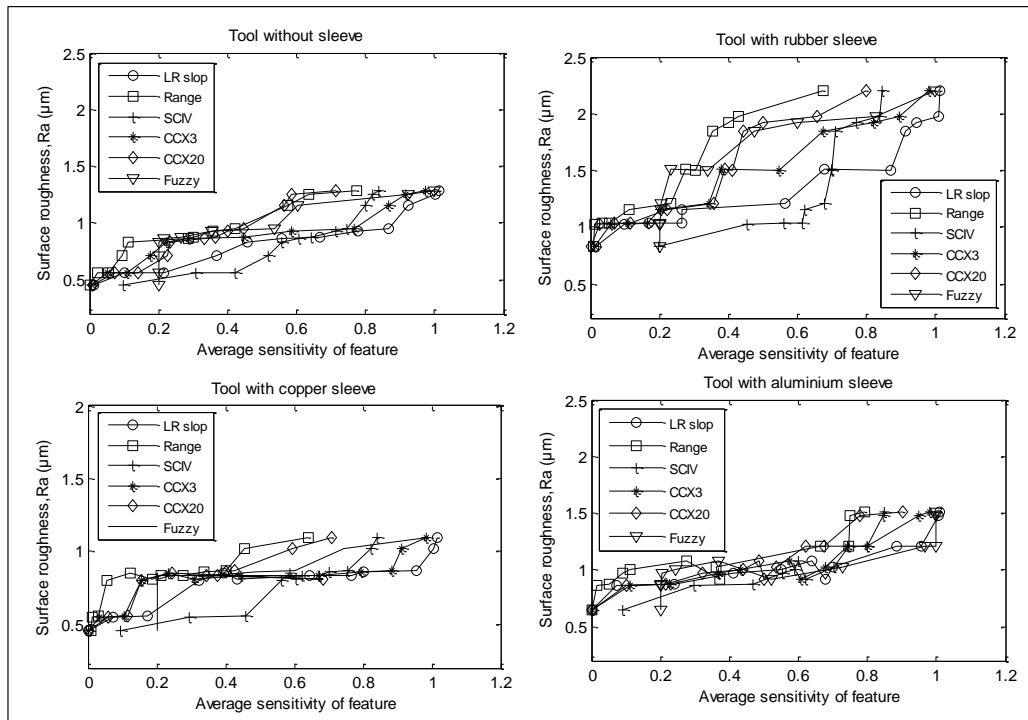


Figure 10.47: The relation between surface roughness and average of sensitivity of features of system for tools with two broken teeth.

Continuously, Figure 10.47 shows the results of correlation for the tools with two broken teeth, where the surface of roughness of the workpiece has increased as mentioned in the previous section and therefore the correlation increased as well, this phenomena obtains a gradual increasing in the consistent of two variables.

Taken together, these findings prove that the change in the tool condition or fixturing system could have a significant effect on the quality of the product; this case can be detected by using tool condition monitoring. Therefore, on the other word, it can be concluded that these changes could be effected on the design and the efficiency of monitoring system.

10.6 Conclusion

The full capability of the ASPSF approach has been approved in this chapter. It has been used to create the affordable and effective detecting system to evaluate the effect of quality of the fixturing system and tool conditions on the design of the monitoring system in the milling process. Therefore, three types of the tool conditions have been investigated, namely fresh, one broken tooth and two broken teeth, these conditions

are studied using different fixturing system , such as tool without sleeve , tool with rubber sleeve , tool with copper sleeve and tool with aluminium sleeve.

A wide range of the sensor and signal processing methods used to develop the ASPSF approach which is evaluated using different types of the measuring sensitivity application such as linear regression (LR), Range value (RV), Sudden change in Value (SCIV), Correlation coefficients (CCX3 and CCX20), and then all these methods have been utilised by fuzzy logic. The sensors are specifically chosen to cover most of the effected places in the CNC milling machine (i.e. machine table, rotating spindle and spindle case). The used sensors are dynamometer, AE, strain, accelerometers, and power, eddy current and sound sensor. The features of these sensors have constructed an associated matrix which is imaged to show visually the most sensitive feature depends on the mentioned measuring sensitivity methods. The LVQ neural network has been used to train the data of the feature and to define which method obtains the lower training error. In addition, Taylor's Equation Induced Pattern (TIP) used to define the pattern recognition of the used tools in the machining tests.

Surface roughness has been measured using roughness tester (Mitotoya SJ 120), this measurement has been used in the new investigation to state the relationship between the experimental roughness and the sensitivity of the sensory feature.

The results of the investigation in this chapter has proved the ability of the ASPSF approach to define the relationship between the tool conditions, fixturing system and the monitoring system. Since, any change in the tool condition as wear or breakage, also any change in the fixturing system (perfect or imperfect fixturing) could be effected on the efficiency of the monitoring system using fuzzy logic system or depend on the surface roughness measurements.

Chapter 11 Discussion and Conclusion

11.1 Introduction

Fixturing systems play an important part to hold a tool or workpiece during manufacturing processes. There is a limited research to focus on fixturing systems and their relationship to the design of condition monitoring systems. This has driven this research towards the development of a sensor fusion system to investigate the effect of fixturing quality on the design of condition monitoring systems. Consequently, a novel approach, termed ASPSF, (Automated Sensor and Signal Processing Selection for Fixturing) has been implemented. The approach has investigated the sensitivity of the SCFs (Sensory Characteristic Features) and their behaviour during machining faults taking into consideration fixturing quality. This Chapter presents a summary of the suggested solution, aim of the research and the contribution to knowledge. It also shows the limitations and suggestions for future research.

11.2 Suggested Solution

The sensitivity measuring methods which are used by the previous references are not sufficient to address the relationship between the fixturing systems and the design of the monitoring system. Therefore, the suggested ASPSF approach is used to solve these problems using automated sensitivity detection for the selection of sensor and signal processing methods and in identifying the effect of the fixturing system on such features.

The ASPSF approach is designed to be generic for monitoring machining systems with reduced time and cost. In addition, it provides quality information regarding the machining process and its conditions.

In the implemented experimental work, different types of fixturing systems are used to secure the cutting tool. Also, several sensory signals are used for monitoring the process. The signals of the sensory automatically transferred to a PC for processing. The ASPSF objective is to extract the SCFs obtained from the sensory signals using different signal processing methods and to find out the sensitivity of such features for different machine/fixture conditions. If a specific feature from a specific sensor

shows a high sensitivity to the fault, this simply means this SCF is useful in detecting or evaluating the condition of the fixturing system or addressing the tool faults. Therefore, the ASPSF can provide the condition monitoring designer by a methodology for continuous design and improvement of the condition monitoring system. Consequently, the designer has ability to adjust the monitoring system in normal case and recalibrate it when the change of parameters becomes significant.

This approach is considered as the author's main contribution which is established to combine previous points with the idea of developing a generic structured sensor-fusion model using the following techniques:

1. Evaluating the new ASPSF approach (Automated Sensor and Signal Processing Selection for Fixturing).
2. Further applications of the automated simplification of complex signals into simple sensory characteristic features (SCFs).
3. New automated detection techniques of sensitive SCFs and hence the associated sensors and signal processing methods. These methods include the Principal Component Analysis (PCA), Correlation Coefficients (CCX3 and CCX20), and Fuzzy Logic (FL) method. All the automated detection techniques are evaluated using LVQ neural network.
4. Testing Taylor's Equation Induced Pattern (TIP) and neural networks for defining the effect of fixturing quality on the design of the monitoring system.
5. Further evaluations of cost-reduction technique based on removing the least utilised sensors when possible.
6. Evaluating the results of the automated approach with surface roughness measurements.

Therefore, the thesis has been designed to develop an effective sensor fusion system for milling operation and to determine the effect of fixturing system on the efficiency of the monitoring system. The overall structure of the thesis is described in Figure 11.1. Chapter 1 began by laying out an introduction for the problematic dimensions of the research. The following Chapters 2, 3, 4 and 5 reported the literature concerning the research conducted in the problem domain under investigation. The methodology of this thesis and the elements of the experimental work which have been used to implement the ASPSF approach are described in Chapters 6 and 7. The application of the ASPSF in this research has been described

in Chapter 8. Following this, Chapter 9 provides a further application for the proposed approach. Chapter 10 shows a new application of the ASPSF highlighting the full advantage of the approach.

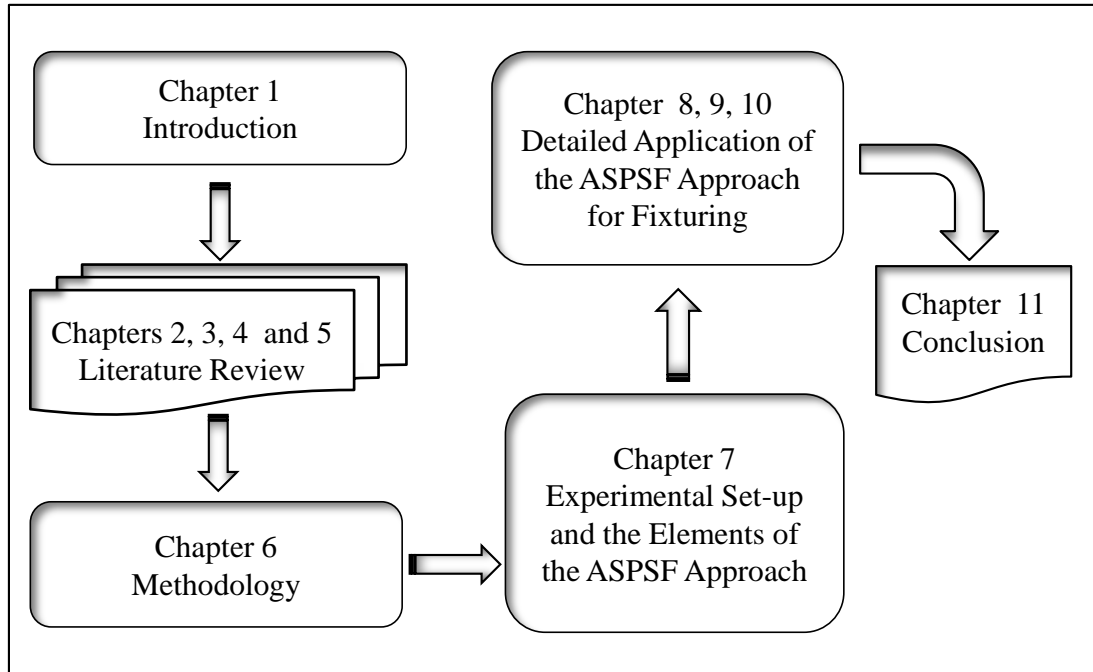


Figure 11.1: Summary of the overall thesis structure.

11.3 Research Aim and ASPSF Approach Implementation

11.3.1 Research Aim

The aim of this research is to investigate the influence of fixturing quality and its problems on the design of condition monitoring system. To address this aim, the novel ASPSF approach has been suggested.

11.3.2 ASPSF Approach Implementation

In spite of the importance of fixturing system in the machining processes to produce the best quality of machined parts, the survey of the literature review concludes that the lack of research to investigate the effect of the fixture on the condition monitoring system. Therefore, this investigation identified this gap in knowledge and addresses these limitations by creating and designing an automated monitoring

system that can detect the faults or the abnormalities in tool conditions and the fixturing system. Significant research has been performed concerning the development of reliable TCM. However, several factors have obstructed advances in the development of TCM including unsuitable choice of sensor signals and their utilisation. However, the previous reference [19] has presented the ASPS approach to select the sensors and signal processing techniques for monitoring the tool conditions. The ASPS approach has been modified and improved to be used in this research.

The ASPSF approach has been used to cover faults in tool conditions such as tool wear and breakage. It also investigates the effect of the material and type of fixturing system by using different sleeves made from different elastic materials (rubber, copper and aluminium). These sleeves individually shrink to the shank of the tool to emulate the stability of the fixturing system as the normal tool namely tool without sleeve, abnormal tools which have rubber, copper or aluminium sleeves. A wide range of different sensors has been used, attached to the most suitable position in the machine as the workpiece, tool holder, spindle and machine electric supply. These sensors are the force dynamometer, acoustic emission, strain, accelerometers, sound, eddy current and power sensor.

Many signal processing methods are applied in this thesis including maximum, minimum, standard deviation, power, average, skew value, kurtosis value, range, Fourier transformation and wavelet analysis. More details about the sensors and signal processing methods are described in Chapters 8, 9 and 10. The ASPSF approach for fixturing system is built based on the modification of the ASPS approach. However significant modifications are applied to investigate the tool and the fixturing quality problem as illustrated in the Figure 11.2.

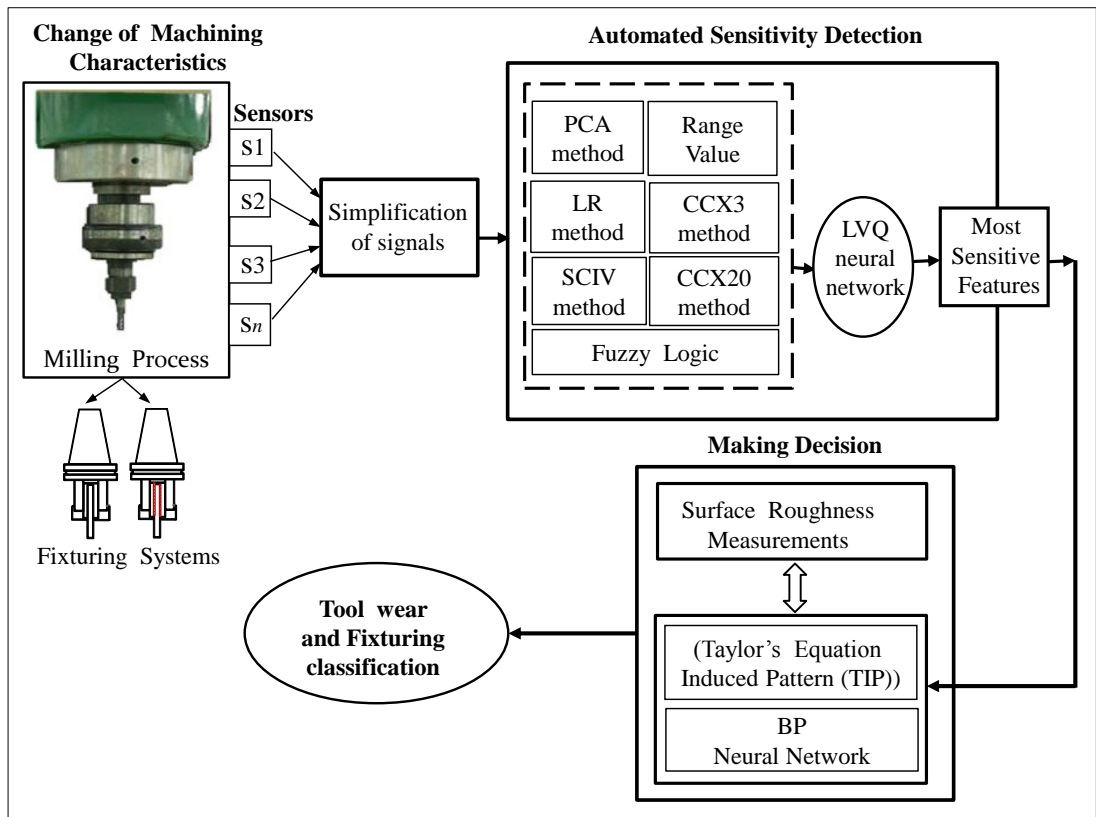


Figure 11.2: Graphic illustration of the suggested ASPSF approach.

The proposed ASPSF approach included the following steps:

Signal simplification

The approach utilises a wide range of sensory signals processed by a wide range of signal processing methods to extract the information in the signals as SCFs. These methods successfully applied in this research with different domains to create the Sensory Characteristic Features (SCFs). The SCFs are arranged together to build the Sensory Feature Matrix (SFM) which provides the features in an organised 3D matrix and in order to address the rank of the sensor sensitivity. In comparison to references [19, 20], this research has included newly used sensors as eddy current, power, and accelerometers attached to the spindle case.

Automated sensitivity measuring method

Automated sensitivity detection uses several types of analytical method such as the Principal Component Analysis (PCA) in order to evaluate the linear regression method as described in Chapter 8. The same techniques have been used in further applications as presented in Chapter 9. Moreover, Fuzzy logic has been implemented

to evaluate several sensitivity measuring methods including linear Regression, Range Value, Sudden Change In Value, Correlation Coefficient (CCX3) and Correlation Coefficient (CCX20) as explained in Chapter 10. The LVQ neural network has been used to measure the training error for each method and define the most accurate option. Consequently, this method will be used to define the most sensitive SCF.

Selection of the Sensory Characteristic Features (SCF)

The performance of the extracted SCFs is investigated against the tool faults and fixturing characteristics. The feature (SCF) which is produced from the sensor and signal processing method is arranged according to the value of the sensitivity. The total number of SCFs used in Chapters 8 is 64 features which resulted from 8 sensors and 8 signal processing method. In Chapter 9, 120 features are constructed from 15 sensors and 8 signal processing (SP) methods. However, 420 features are built from 15 sensors and 28 of SP methods in Chapter 10. These features are divided into different groups (systems) to evaluate their performance.

Cost Reduction and Evaluation

One of the main aims of the ASPSF approach is to reduce the cost of the designed monitoring system by eliminating the insensitive features. The procedures of the cost reduction have been applied for the experimental work and it has proved the ability of the ASPSF approach to change cost to a reasonable level. This can be implemented by exchanging some of SCFs by others without significantly reducing the sensitive of the system.

Another process follows that which is the evaluation to the system by measuring the sensitivity coefficients (A_c) and Eigenvalue coefficients (E_c) which are resulted from the averages of the associated matrix and eigenvalue matrix as explained in the section 8.5.2 of Chapter 8. The results prove the capability of ASPSF approach to evaluate the overall sensitivity of the monitoring system.

Surface Roughness

Chapters 9 and 10 have shown that there is a relationship between surface roughness (R_a) and the design of the condition monitoring system to address and evaluation that.

11.4 Results and Discussion

The suggested ASPSF approach has been applied to a milling process. The methodology involves the application of several techniques and developments to design the condition monitoring system in order to detect the faults of fixturing system and the tool. The main key developments and findings of this thesis are:

Chapter 8: The shank of the cutting tool (Carbide tool 3/3 mm) is covered by a rubber sleeve to emulate a fixturing system with low rigidity. A group of sensors, namely acoustic emission, force, strain, vibration and sound, are used to design the tool wear monitoring system. The tests start with a fresh tool and finish with a completely worn tool. The Linear regression (LR) method has been successfully applied to measure the sensitivity of the feature (SCF). The Principal Component Analysis (PCA) method has been utilised to evaluate the LR method. A novel approach has been successfully implemented to predict the surface roughness (Ra value) based on the cutting force signal as described in section 8.6.

The main findings are:

1. A significant relationship between Linear Regression method and Principal Component Analysis method to find out the most sensitive features required to detect fixturing set-up and cutting tool wear has been found. The correlation coefficient between the two methods is 88% with a normal tool and 75% when using a tool with rubber sleeve. This indicates that the fixturing quality affects the sensitivity of the monitoring system.
2. The ability of the automated detection methods to define the most sensitive Sensory Characteristic Features (SCFs). The features (SCFs) are obtained from the sensors and associated signal processing methods. The linear regression method has proved that the features SCF(Fy, min) and the SCF(Fy, average) are the most sensitive features for normal tool and tool with rubber sleeve. However, the principal component analysis method confirmed that the feature PCF(Fy, PC2) is the most sensitive feature in both cases.
3. The capability of the ASPSF approach to recognise the changes in the fixturing system, and then detect the tool wear. Therefore it could be used to detect the abnormalities or the changes of the machine set-up during the machining

process. Also, the ability of the ASPSF approved to reduce the cost of monitoring system by 11% without significantly reducing the performance.

4. The ability to predict the surface roughness using the signals generated by the cutting forces. A close relationship between the machined surface roughness and roughness predicted using the force signals has been found.

Chapter 9: The application of the ASPSF has been successfully resulted in this chapter. The shank of the tools (High Speed Steel (HSS 3/6 mm) are covered individually by a rubber sleeve, copper sleeve and aluminium sleeve to emulate a fixturing system with different quality and flexibility. Further sensors have been also performed in the experimental work namely eddy current, power and accelerometers attached to the spindle case. This application has provided further evidence to support the capability of the ASPSF to monitor the abnormalities of the tool conditions and has presented a good agreement between the two measuring sensitivity methods (i.e. LR and PCA). For pattern recognition of the sensory signal, a novel method (Taylor's Equation Induced Pattern (TIP)) has been implemented to detect the pattern of the sensory features (SCFs) under the variability of fixturing and tool conditions. Successfully, the back propagation neural network has evaluated the capability of the monitoring systems. Surface roughness measured using roughness tester (Mitotoya SJ 120), these measurements have been used in the new investigation to evaluate the relationship between the experimental roughness and the sensitivity of the sensory feature.

The results of Chapter 9 indicated:

1. The relationship between Linear Regression and Principal Component Analysis methods has been found to be significant to determine the most sensitive features to detect fixturing quality and cutting tool condition.

The correlation coefficient between the two methods is around 94% with normal tools and 75% for tools with rubber sleeve. Also, it is around 93.6 %, 86 % for tools with copper, aluminium sleeves respectively.

2. The linear regression method demonstrated that the sensory features SCF(E_{dy}, min) and the SCF(P_{wr}, std) are the most sensitive features for normal tool and tool with rubber sleeve. Also, the features SCF(F_x, max) and SCF(Mic, max) are the most sensitive features for tools with copper and aluminium sleeves

respectively. However, the PCA method has presented that the features PCF(Edy, PC1) and PCF(Fx, PC2) are the most sensitive features for normal tool and tool with rubber sleeve. Whilst, the features PCF(Fx, PC7) and PCF(Fx, PC11) provide better sensitivity features for tools with copper and aluminium sleeves.

3. Based on Taylor's Equation Induced Pattern (TIP) which used to define the pattern recognition accuracy, the ASPSF has the capability to determine the effect of the quality of the fixturing system on the capability of the monitoring system. Also, the ability of the ASPSF to reduce the cost of the monitoring system to 23% without significantly reducing its capability.
4. Surface roughness measurements are used to evaluate the effect of the fixturing system on the design of condition monitoring system. The findings have proved that the change in fixturing quality could cause significant change in the roughness of a machined surface and lead to a change in the sensitivity of the monitoring system. The correlation coefficient between the surface roughness and the sensitivity is 90%, 71%, 76% and 49% with normal tools and the tools with rubber, copper and aluminium sleeves respectively.

Chapter 10: Another important condition of the tool is investigated, which is the tool breakage. This case has been simulated experimentally using fresh tool, tool with one broken tooth and tool with two broken teeth. The Carbide tools (3/6mm) are used with the same fixturing systems as in Chapter 9. Several of the automated measuring sensitivity methods have been applied to implement the ASPSF approach, including the Linear Regression (LR), Sudden Change In Value (SCIV), Range Value (RV), Correlation coefficient (CCX3) and Correlation coefficient (CCX20).

These methods have obtained different results for the sensitivity. Therefore, fuzzy logic method has been successfully applied to control and combine these results to find the most sensitive features (SCFs). The LVQ neural network has been used to evaluate all the measuring sensitivity methods. It has proved that fuzzy logic is the most suitable method among the sensitivity methods. Taylor's Equation Induced Pattern (TIP) is used to define the pattern recognition of the sensory feature for monitoring tool conditions.

The key findings are:

1. Fuzzy logic has been used to characterise the sensitivity of the features when different five methods are combined together. The fusion of different sensitivity measures using fuzzy logic has been found very reliable to select the most sensitive SCFs. The LVQ neural network has presented that the lowest training error is achieved by fuzzy logic within 1.5% for the fresh tool, 2% for tool with one broken tooth and 3% for tool with two broken teeth. However, the highest training error is achieved by correlation coefficient (CCX3) method with 5% for fresh tool, 5.5% and 6% tools with one and two broken teeth. For more details, see the section 10.3.
2. The most sensitive features according to the evaluation of the fuzzy logic are described in Table 11.1. It can be observed that the SCF(V_{sx} , wav2) is the most sensitive feature for a fresh tool without sleeve. The SCF(F_y , min) is the most sensitive feature for a fresh tool with rubber sleeve. However, the features SCF(V_{sz} , wav4) and SCF(E_{dx} , FFT6) are the most sensitive features for fresh tools with copper and aluminium sleeves, and so on for other features.

The force and vibration sensors are the most sensitive sensors and the wavelet and standard deviation are the most sensitive signal processing methods. This indicates that the sensitivity of the monitoring system is significantly dependent on the fixturing quality and tool condition.

Table 11.1: The most sensitive sensor (S) and signal processing (SP) in the different machining conditions using fuzzy logic.

Tool condition Fixturing type	Fresh Tool		Tool with 1 broken tooth		Tool with 2 broken teeth	
	S	SP	S	SP	S	SP
Tool without sleeve (Normal Tool)	Vibration (Vsx)	Wavelet2	Sound	average	Acoustic Emission (AERMS)	Kurtosis
	Vibration (Vwy)	maximum	Sound	Wavelet1	Force (Fz)	minimum
	Vibration (Vsx)	Wavelet1	Power	Wavelet2	Strain	Wavelet1
Tool with rubber sleeve	Force (Fy)	minimum	Force (Fz)	minimum	Force (Fy)	Wavelet1
	Vibration (Vwy)	average	Force (Fx)	skew	Force (Fy)	Wavelet9
	Sound	Wavelet6	strain	minimum	Force (Fy)	Standard deviation
Tool with copper sleeve	Vibration (Vsz)	Wavelet4	Force (Fz)	maximum	Acoustic Emission (AERMS)	skew
	Vibration (Vsx)	Wavelet2	Force (Fy)	skew	Vibration (Vsx)	range
	Force (Fz)	Kurtosis	Force (Fz)	range	Vibration (Vsx)	Standard deviation
Tool with aluminium sleeve	Eddy current (Edx)	FFT6	Vibration (Vsz)	Standard deviation	Force (Fy)	power
	Force (Fz)	FFT3	Vibration (Vsz)	power	Power	Standard deviation
	Vibration (Vsz)	Standard deviation	Vibration (Vsz)	Wavelet1	Force (Fz)	average

3. The full capability of the ASPSF approach has been demonstrated in this chapter. The general results have proved that the tool condition and the type of the fixturing system could affect the sensitivity of the sensory signal and consequently affect the design of the condition monitoring system as described in section 10.4 of Chapter 10. Surface roughness measurement has also proved the ability of the ASPSF approach by outlining the significant relationship between

surface roughness and the sensitivity of the SCFs under the variability of tool and fixturing conditions. For more details, see the section 10.5 of Chapter 10.

The present findings seem to be consistent with other results of previous chapters which found that the quality of the fixturing system could influence the design of the condition monitoring system.

11.5 Contribution to knowledge

The main contribution and novelty of this work is the investigation into the effect of tool fixturing quality on the design of condition monitoring system using sensor fusion model. This contribution has addressed the limitations and gaps in knowledge identified in the literature review. The research examined the use of a combination of sensors which are used to detect the status of the tool condition in terms of changing the fixturing system. The real measurements of the surface roughness of the machined surface have been employed in this research to reflect the relationship between the quality of the surface finish and the sensitivity of the monitoring system. Further to the main contribution, there are several conceptual and technical contributions as follows:

11.5.1 Conceptual Contribution

In addition, the research included the following contributions:

1. Testing the effect of fixturing quality on the design of condition monitoring systems to detect tool wear. The ASPSF approach has investigated the difference in the system's behaviour and the changes in the condition monitoring system when the tool is not rigidly fastened to the fixture which is emulated using different materials with different modulus of elasticity.
2. The ASPSF approach highly focused on the fixturing system as an important part in the machining process which is used to secure the cutting tool. This research concentrated on the complex phenomena to define the relationship between the tool conditions, fixturing system and design of the monitoring system.
3. The ASPSF is generic and it could be applied for studying other issues related to the milling process or the stability of the machine. For example, it could be used to investigate other types of fixturing systems, or using different cutting tools.

4. The ASPSF approach has been developed based on the ASPS approach [19] with significant modification and the addition of different application.
5. The proposed approach is fully automated and provides the flexibility, simplification and possibility of applying the model of condition monitoring for milling processes with decision making process into real industrial environment.

11.5.2 Technical Contribution

There are mainly different technical contributions have been presented in the thesis:

1. This study adapted several signal simplification methods in order to extract useful information from the collected data. The wide range of the new sensors and signals enable the system to be more effective and more accurate.
2. The new automated sensitivity measuring method has been used to implement and evaluate the ASPSF by using Principal Component Analysis (PCA). This method depends on calculating the eigenvalue or the distance between the position of the sensor and the mean of the data coordinate, the amount of this value will determine the effect of the variable (or the sensor) on the whole data, this function is employed to find the most sensitive sensor.
3. More evaluations are applied to reduce the cost of the suggested system and to keep the high performance and reliability of the evaluated system.
4. In order to detect the change of the fixturing systems on the detecting system, four types of fixturing system have been implemented in the experimental work represented by using tool without sleeve, and tools with elastic materials such as tool with rubber sleeve, tool with copper sleeve and tool with aluminium sleeve.
5. To compare the efficiency of the used sensitivity measuring system, five methods are investigated, and then evaluated using fuzzy logic. The methods are:
 - a. Linear Regression (LR) method.
 - b. Range Value (RV) method.
 - c. Sudden Change In Value (SCIV) method.
 - d. Correlation Coefficient (CCX3) method.
 - e. Correlation Coefficient (CCX20) method.
6. A new sensor which is considered as one of the sensitive sensor (Eddy current sensor) to monitor the vibration of the spindle. This sensor has been carefully

attached to the spindle case using the fixture without effect on the design of the machine.

7. Several sensors are used with the eddy current sensor to achieve the aim of the proposed approach namely, the force dynamometer, strain, acoustic emission, accelerometer, sound and power sensor. These sensors dealt with the most of milling machine problems.

8. For data analysis, an unsupervised neural network, Learning Vector Quantisation (LVQ) is implemented to explore the relation between the investigated variables or to be used as a reliable classifier for the sensory sensitivity methods.

9. A new technique, Taylor's Equation Induced Pattern (TIP), has been suggested and successfully applied to represent the pattern of the signal and to detect the moment of changing the tool conditions. This technique is also supported by using a supervised neural network, as a back propagation neural network.

10. Surface roughness has been measured and compared with the sensitivity of the monitoring system for further evaluation and analysis.

11.6 Limitation and suggestion for future work

The author identifies the following limitations and suggestions of this research and future studies.

1. In the current research, it is focused on one type of the fixturing system, the collet, in the future work, other types (i.e. Hydraulic collet and Jaw chuck) of the fixturing system may be used to study the effect of the difference of fixturing system on the monitoring system.
2. Different sensors and signal processing methods could be used to assess the proposed approach; this may influence the trend of the results.

11.7 Final Conclusion

Recently, more attention has been directed towards improving sensor fusion techniques to detect or predict faults in manufacturing processes. There has been limited research focusing on fixturing systems and their relationship to the design of condition monitoring systems. The identification of this gap in knowledge combined

with the recent developments improving sensor fusion techniques have led this thesis to investigate the effect of fixturing quality on the design of condition monitoring systems to detect tool wear. Importantly, the thesis focusses on the difference in the system's behaviour and the changes in the condition monitoring system when the cutting tool is not rigidly fastened to the collet, which is emulated using elastic materials (e.g. rubber sleeve). A group of sensors, namely acoustic emission, force, eddy current, strain, power, vibration and sound, have been utilised to design the condition monitoring system. This has led to the development of a novel approach, termed ASPSF, (Automated Sensor and Signal Processing Selection for Fixturing) addressing the effect of the tool holding device (collet) on the monitoring system together with an assessment of the most sensitive sensors and signal processing method to detect tool wear.

The results prove that the change in the fixturing quality has caused variation in the dynamics of the system and demonstrated significant effect on most sensitive sensors and signal processing methods for the detection of tool condition. Therefore, this thesis has proved that minor changes in the setup of the machining operation could have significant influence on the condition monitoring system, subsequently this requires redesign the monitoring system.

References

- [1] Al-Habaibeh A, Gindy N and Parkin R M ., (2003), Experimental design and investigation of a pin-type reconfigurable clamping system for manufacturing aerospace components, *Proceedings of the Institution of Mechanical Engineers, Part B: Journal of Engineering Manufacture*, Vol. 217, No. 12, pp. 1771-1777.
- [2] Chung T. and A. Geddam, (2003), A multi-sensor approach to the monitoring of end milling operations, *Journal of Materials Processing Technology*, Vol. 139, Issues 1-3, pp. 15-20.
- [3] Liao J.G. and S.J. Hu, (2000), Flexible multibody dynamics based fixture-workpiece analysis model for fixturing stability, *International Journal of Machine Tools and Manufacture*, Vol. 40, pp. 343–362.
- [4] Rodolfo Haber, Jose E. Jimenez, C. Ronei Peres and Jose R. Alique, (2004), An investigation of tool-wear monitoring in a high-speed machining process, *Sensors and Actuators A: Physical*, Vol. 116, Issue 3, pp.539-545.
- [5] Anand Raghu and Shreyes N. Melkote, (2004), Analysis of the effects of fixture clamping sequence on part location errors, *International Journal of Machine Tools and Manufacture*, Vol. 44, Issue 4, pp. 373-382.
- [6] Jedrzejewski J., Modrzycki W., (1997), Intelligent supervision of thermal deformations in high precision machine tools, *Proc. 32nd Int. MATADOR Conf*, Manchester, pp. 457- 462, UK.
- [7] Ramesh R., Mannan M. A. and Poo A. N., (2000), Error compensation in machine tools-a review: Part I: geometric, cutting-force induced and fixture-dependent errors, *International Journal of Machine Tools and Manufacture*, Vol. 40, Issue 9, pp. 1235-1256.
- [8] Thomas Nikolaou, (2011), Modelling and Design Methodology for Fully-Active Fixtures, PhD thesis, Nottingham University, UK.
- [9] Govender, Evandarin, (2001), an intelligent deflection prediction system for machining of flexible components, PhD Thesis, Nottingham University, UK.
- [10] CNC Router Technology-Technical Section Catalog-spindles, [Online, accessed on 26/6/2009].
www.technocnc.co.uk/cncpages/HTML/Tech_Section_7.html
- [11] Uriarte L., Herrero A., Zatarain M., Santiso G., Lopéz de Lacalle, Lamikiz A. , Albizuri J., (2007), Error budget and stiffness chain assessment in a micromilling machine equipped with tools less than 0.3 mm in diameter, *Precision Engineering*, Vol. 31, Issue 1, pp. 1-12.
- [12] Robert b.Ruce, Thompson P. C. Krishnamachary, (2008), Annual Student Light Fixture Design Competition 2007,[Online].

- www.i-m-a-d-e.org/robert-bruce-thompson-annual-student-light-fixture-design-competition.
- [13] Yeh J.H. and Liou F.W., (2000), Clamping Fault Detection in a Fixturing System, *Journal of Manufacturing Processes*, Vol. 2, Issue 3, pp. 194-202.
- [14] Teti R., Jemielniak K., Donnell G., Dornfeld D., (2010), advanced monitoring of machining operations, *CIRP Annals - Manufacturing Technology*, Vol. 59, Issue 2, pp. 717-739.
- [15] Brophy B., Kelly K. and Byrne G., (2002), AI-based condition monitoring of the drilling process, *Journal of Materials Processing Technology*, Vol. 124, Issue 3, pp. 305-310
- [16] Montronix Inc., (2003), Process Monitoring to Improve Machine Tool Performance, *Research and data for Status Report* , Vol.95, Issue 2.
- [17] Al-Habaibeh A., Zorriassatine F. and Gindy N., (2002), Comprehensive experimental evaluation of a systematic approach for cost effective and rapid design of condition monitoring systems using Taguchi's method, *Journal of Materials Processing Technology*, Vol.124, Issue 3, pp. 372-383.
- [18] Al-Habaibeh A., Cai R., Jackson M.R., Parkin R.M., (2004), Modern development in sensor technology and its applications in condition monitoring, *7th International Conference on Monitoring and Automatic Supervision in Manufacturing*, Zakopane, 19-21August. Poland.
citeseerx.ist.psu.edu/viewdoc/download?doi=10.1.1.200.1142
- [19] Al-Habaibeh A, (2000), Rapid Design of Condition Monitoring Systems, PhD thesis, University of Nottingham, UK.
- [20] Al-Azmi Abdulrahman F., (2008), The Design of an effective sensor fusion model for condition monitoring system of turning processes, PhD Thesis, Nottingham Trent University, UK.
- [21] Nee A. Y. C., Bhattacharyya N. and Poo A. N., (1987), Applying AI in jigs and fixtures design, *Robotics and Computer-Integrated Manufacturing*, Vol. 3, Issue 2, pp. 195-200.
- [22] Z.M. Bi and Zhang W.J., (2001), Flexible fixture design and automation: Review, issues and future direction, *International Journal of Production Research*, Vol. 39, Issue13, pp. 2867–2894.
- [23] Hargrove S.K., Kusiak, A. (1994), Computer-aided fixture design: a review., *International Journal of Production Research*, Vol.32, Issue 4, pp. 733-753.
- [24] Hou, J.L., Trappey, A.J.C. (2001), Computer-aided fixture design system for Comprehensive modular fixtures, *International Journal of Production Research*, Vol.39, Issue 16, pp.3703-3725.

- [25] Gaoliang Peng, Gongdong Wang, Wenjian Liu and Haiquan Yu, (2010), A desktop virtual reality-based interactive modular fixture configuration design system, *Computer-Aided Design*, Vol.42, pp.432-444.
<http://dx.doi.org/10.1016/j.cad.2009.02.003>.
- [26] Qiang Li, (2008), Virtual Reality for Fixture Design and Assembly, PhD thesis, Nottingham University, UK.
- [27] McIlwraith A H, (2005), Collets and friction, *Measurement Science and Technology*, Vol.16, pp.1442–1448, [Online, Accessed on 9/9/2009].
www.iop.org/EJ/article/0957-0233/16/7/006/mst5_7_006.pdf.
- [28] Daniel P. Soroka, (2004), Work holding Collets and Factors That Affect Grip Force, *Article from: Production Machining, Contributed by: Daniel Soroka, Hardinge Workholding Division* [Online, Accessed on 18/8/2009].
www.productionmachining.com › Articles.
- [29] Jim Destefani, (2002), Holding the precision line, *Sme.org/manufacturing engineering*, Vol.57, Issue5, [Online, Accessed on 10/9/2009].
www.tmsmith.com/Holding_the_Precision_Line.pdf
- [30] Hynek P, Jackson MR, Brown N, Parkin RM, (2004), Improving Wood Surface Form by Modification of the Rotary Machining Process, *Proceedings of the Institution of Mechanical Engineers, Part B: Journal of Engineering Manufacture*, 218(8), pp.875-887, ISSN: 0954-4054.
<http://pib.sagepub.com/content/218/8/875.full.pdf+html>.
- [31] Woo-Cheol Shin, Seung-Kook Ro, Hyung-Wook Park and Jong-Kweon Park, (2009), Development of a micro/meso-tool clamp using a shape memory alloy for applications in micro-spindle units, *Int. Journal of machine tool and Manufacture*, Vol.16, pp. 579-585 .
- [32] Huntera R., J. Riosb, J.M. Pereza, A. Vizana, (2006), A functional approach for the formalization of the fixture design process, *International Journal of Machine Tools and Manufacture*, Vol. 46, Issue 6, pp. 683-697.
- [33] www.spindlesworld.com/spindle-collet.html
- [34] Mehdi Namazi, Yusuf Altintas, Taro Abe, Niml Rajapakse, (2007), Modeling and identification of tool holder spindle interface dynamics, *International Journal of Machine Tools and Manufacture*, Vol. 47, Issue 9, pp. 1333-1341.
- [35] www.its.fvtc.edu/machshop3/basicmill/Toolhold.htm
- [36] www.technocnc.co.uk/cncpages/HTML/Tech_Section_7.html
- [37] Paris H., Brissaud, D., (2005), Process planning strategy based on fixturing indicator evaluation, *The International Journal of Advanced Manufacturing Technology*, Vol.25, Issue9, pp.913-922.

- [38] Michael Minton, Michael Sullivan, (2002), When to Use A Collet Chuck, *Article from: Modern Machine Shop, Contributed by: Michael Minton and Michael Sullivan, ATS Systems*. Posted on: 5/15/2002.
- [39] Yeh J.H. and Liou F.W., (2000), Clamping Fault Detection in a Fixturing System, *Journal of Manufacturing Processes*, Vol. 2, Issue 3, pp. 194-202.
- [40] Edward C. De Meter, Wei Xie, Shabbir Choudhuri, Subramanian Vallapuzha and Martin W. Trethewey, (2001), A model to predict minimum required clamp pre-loads in light of fixture-workpiece compliance, *International Journal of Machine Tools and Manufacture*, Vol. 41, No. 7, pp. 1031-1054.
- [41] Sanchez H.T., Estrems M., Faura F., (2006), Fixturing analysis methods for calculating the contact load distribution and the valid clamping regions in machining processes, *The International Journal of Advanced Manufacturing Technology*, Vol.29, Issue 5, pp.426-435.
- [42] Salisbury J.K. and Roth B., (1983), Kinematic and Force Analysis of Articulated Mechanical Hands, *ASME Journal of Mechanisms, Transmissions and Automation in Design*, Vol. 105, pp. 34-41.
- [43] Menassa R.J. and DeVries W.R., (1989), Locating Point Synthesis in Fixture Design), *Annals of the CIRP*, Vol. 38, pp. 165-169.
- [44] Asada H. and A., (1985), Kinematic Analysis of Work Part Fixturing for Flexible Assembly with Automatically Reconfigurable Fixtures, *IEEE Journal of Robotics and Automation RA-1*, Vol, 2, pp. 86-94.
- [45] Tsutsumi M., (1989), Chucking force distribution of collet chuck holders for machining centres, *Journal of Mechanical Working Technology*, Vol.20, pp. 491-501.
- [46] Wang Y.F., Wong Y.S. and Fuh J.Y.H., (1999), Off-line modelling and planning of optimal clamping forces for an intelligent fixturing system, *International Journal of Machine Tools and Manufacture*, Vol. 39, pp. 253-271.
- [47] Lee S.H. and Cutkosky M.R., (1991), Fixture planning with friction, *ASME Journal of Engineering for Industry*, Vol.113, pp. 320-327.
- [48] Haruhiko Asada and Masaya Kitagawa, (1989), Kinematic analysis and planning for form closure grasps by robotic hands) *Robotics and Computer-Integrated Manufacturing*, Vol. 5, Issue 4, pp. 293-299.
- [49] Ibrahim M. Deiaband Mohamed A. Elbestawi, (2005), Experimental determination of the friction coefficient on the workpiece-fixture contact surface in workholding applications, *International Journal of Machine Tools and Manufacture*, Vol. 45, Issue 6, pp. 705-712.

- [50] Haiyan Deng and Shreyes N. Melkote, (2006), Determination of minimum clamping forces for dynamically stable fixturing, *International Journal of Machine Tools and Manufacture*, Vol. 46, Issues 7-8, pp. 847-857
- [51] Xavier F. Brun and Shreyes N. Melkote, (2008), Modelling and experimental verification of partial slip for multiple frictional contact problems, *Journal of Wear*, Vol. 265, Issues 1-2, pp. 34-41.
- [52] Necmettin Kaya, (2006), Machining fixture locating and clamping position optimization using genetic algorithms, *Computers in Industry*, Vol. 57, pp. 112-120 .
- [53] Pham D.T. and Yeo S.H., (1991), Strategies for gripper design and selection in robotic assembly, *International Journal of Production Research*, Vol. 29, Issue 2, pp. 303–316.
- [54] Choi Ho and Muammer Koc, (2006), Design and feasibility tests of a flexible gripper based on inflatable rubber pockets, *International Journal of Machine Tools and Manufacture*, Vol. 46, Issues 12-13, pp. 1350-1361.
- [55] Gracia L.A., Liarte E., Pelegay J.L. and Calvo B., (2010), Finite element simulation of the hysteretic behaviour of an industrial rubber. Application to design of rubber components, *Finite Elements in Analysis and Design*, Vol. 46, Issue 4, pp. 357-368
- [56] Zhang S.W., (1998), State-of-the-art of polymer tribology, *Tribology International*, Vol. 31, Issues 1-3, pp.49–60.
- [57] Bielsa J.M., Canales M., Martínez. and Jiménez M.A, (2010), Application of finite element simulations for data reduction of experimental friction tests on rubber–metal contacts, *Tribology International*, Vol, 43, Issue 4, pp. 785-795 .
- [58] Yung-Chang Yen, Jörg Söhner, Blaine Lilly and Taylan Altan, (2004), Estimation of tool wear in orthogonal cutting using the finite element analysis, *Journal of Materials Processing Technology*, Vol. 146, Issue 1, pp.82-91.
- [59] <http://uhv.cheme.cmu.edu/procedures/machining/CH8.PDF>
- [60] Melin Tool company, (End Mill Training - End Mill Design Criteria and Technical Features).
<http://www.endmill.com/pages/training/design.html>.
- [61] Morris T.J., (1997), The real accuracy of machine tools, *Proc. 3rd Int. Conf. on Laser Metrology and Machine Performance - LAMDAMAP*, pp. 113–122.
- [62] Evans C.J. and Kocken R.J, (1996), Self-calibration: reversal, redundancy, error separation and absolute testing, *Annals of the CIRP*, Vol. 45, Issue 2 ,pp. 617–632.

- [63] Ramesh R., Mannan M. A. and Poo A. N., (2000), Error compensation in machine tools -a review: Part I: geometric, cutting-force induced and fixture-dependent errors, *International Journal of Machine Tools and Manufacture*, Vol. 40, Issue 9, pp. 1235-1256.
- [64] Huseyin M. Ertunc, Kenneth A. Loparo, Hasan Ocak, (2001), Tool wear condition monitoring in drilling operations using hidden Markov models (HMMs), *International Journal of Machine Tools and Manufacture*, Vol. 41, Issue 9, pp. 1363–1384
- [65] Cho SS, Komvopoulos K ,Cutting force variation due to wear of multi-layer ceramic coated tools, *ASME J Tribology*, 120:75–81. doi:10.1115/1.2834193.
- [66] Rahman M, Wang ZG, Wong S, (2006), A review on high-speed machining of titanium alloys, *JSME Int J C*, Vol. 49, Issue 1, pp.11–20.
- [67] Dahu Zhu, Xiaoming Zhang, Han Ding, (2013), Tool wear characteristics in machining of nickel-based superalloys, *International Journal of Machine Tools and Manufacture*, Vol. 64, pp. 60-77.
- [68] Dimla E. DimlaSnr, (2000), Sensor signals for tool-wear monitoring in metal cutting operations-a review of methods, *International Journal of Machine Tools and Manufacture*, Vol. 40, Issue 8, pp. 1073-1098.
- [69] Alauddin M., M.A. El, (1997), Tool life model for end milling steel (190 BHN), *Journal of Materials Processing Technology*, Vol. 68, Issue 1, pp. 50-59.
- [70] Marksberry P.W., Jawahir I.S., (2008), A comprehensive tool-wear/tool-life performance model in the evaluation of NDM (near dry machining) for sustainable manufacturing, *International Journal of Machine Tools and Manufacture*, Vol. 48, Issues 7–8, pp. 878-886.
- [71] <http://web.iitd.ac.in/~suniljha/MEL120/Tool%20Life2012.pdf>
- [72] Farhad Nabhani, (2001), Wear mechanisms of Ultra-hard Cutting Tool Materials), *Journal of Materials Processing Technology*, Vol.115, Issue 3, PP. 402-412.
- [73] Oguz Colak, Cahit Kurbanoglu, and M. Cengiz Kayacan, (2007), Milling surface roughness prediction using evolutionary programming methods, *Materials and Design*, Vol. 28, Issue 2, pp. 657-666.
- [74] Rosales A., Vizán A. and Diez E., (2010), Prediction of Surface Roughness by Registering Cutting Forces in the Face Milling Process, *European Journal of Scientific Research*, Vol.41, No.2, pp.228-237.
<http://www.eurojournals.com/ejsr>.
- [75] Geoffrey Boothroyd, (1975), Fundamentals of metal machining and machine tools, *McGraw-Hill Book Company*, Washington, USA.

- [76] Benardos P. G., Vosnaikos G. C, (2003), Predicting surface roughness in machining: a review, *International Journal of Machine Tools and Manufacture*, Vol. 43, pp. 833–844.
- [77] Hun-Keun Chang, Jin-Hyun Kim, Hae Kim, Dong Young Jang and Dong Chul Han, (2007), In-process surface roughness prediction using displacement signals from spindle motion, *International Journal of Machine Tools and Manufacture*, Vol. 47, Issue 6, pp. 1021-1026.
- [78] Chen J.C., Huang L.H., A.X. and Lee S., (1999), Analysis of an effective sensing location for an in-process surface recognition system in turning operations, *Journal of Industry Technology*, Vol.15, No. 3.
<http://atmae.org/jit/Articles/chen0499.pdf>
- [79] Kai Yang, Angus Jeang, (1994), Statistical surface roughness checking procedures based on a cutting tool wear model, *Journal of Manufacturing Systems*, Vol.13, Issue 1, pp. 1-8.
- [80] Habeeba H.H., Abou-El-Hosseinb A., Mohammada B. and Kadirgamaa K., (2008), Effect of tool holder geometry and cutting condition when milling nickel-based alloy 242, *Journal of Materials Processing Technology*, Vol. 201, Issues 1-3, pp. 483-485.
- [81] Al-Habaibeh A. and Gindy N, (2000), A new approach for Systematic Design of condition monitoring systems for milling Processes, *Journal of Materials Processing Technology*, Vol. 107, Issues1-3, pp. 243-251.
- [82] <http://www.coromant.sandvik.com>.
- [83] Oliveira dilson Jose de and Anselmo Eduardo Diniz, (2009), Tool life and tool wear in the semi-finish milling of inclined surfaces, *Journal of Materials Processing Technology*, Vol. 209, Issue 14, pp. 5448-5455.
- [84] Rakowski Leo, (2003), Monitoring Improves Machine Up Time And Shop Efficiency, *Production Machining, Brankamp process automation*. Inc.
<http://www.productionmachining.com/articles/monitoring-improves-machine-up-time-and-shop-efficiency>.
- [85] Jemielniak K, (1999), Commercial tool condition monitoring systems, *International Journal of Advanced Manufacturing Technology*, Vol. 15, pp. 711–721.
- [86] Salgado D.R., and Alonso F.J., (2007), An approach based on current and sound signals for in-process tool wear monitoring, *International Journal of Machine Tools and Manufacture*, Vol.47, Issue 14, pp. 2140-2152.
- [87] Mathieu Ritou, Sebastien Garnier, Benoit Furet, Jean-Yves Hascoet, (2006), A new versatile in-process monitoring system for milling, *International Journal of Machine Tools and Manufacture*, Vol. 46, Issue 15, pp. 2026-2035.

- [88] Byrne G., Dornfeld D., Inasaki I., Ketteler G., Konig W. and Teti R., (1995), Tool condition monitoring (TCM)-the status of research and industrial application, *Annals of CIRP*, Vol.44, Issue 2, pp. 541–567.
- [89] James Griffin, (2007), Pattern recognition of micro and macro grinding phenomenon with a generic strategy to machine process monitoring, PhD thesis, University of Nottingham , UK.
- [90] Martin K.F., (1994), A review by discussion of condition monitoring and fault diagnosis in machine tools, *Int. J. Mach. Tools Manufact.*, Vol.34, Issue 4, pp. 527–551.
- [91] Kistler Instruments Ltd, Rotating cutting force dynamometer 9123B, Whiteoaks, The Grove Hartley Wintney, Hants, UK.
- [92] Bertok P., Takata S., Matsushima J., Ootsuka J. and Sata T., (1983), A system for monitoring the machining operation by referring to a predicted cutting torque pattern, *CIRP Annals- Manufacturing Technology*, Vol. 32, Issue 1, pp. 439–443.
- [93] Zizka J., (1996), Tool wear and chatter monitoring, *Condition Monitoring and Diagnostic Engineering Management COMADEM 96 Conference*, pp. 377–387.
- [94] Jackobsen M.L, Carolan T.A, Barton J.S., Jones J.D.C, Reuben R.L, (1997), Optical probing of Acoustic Emission from a rotating tool, *8th Sensors and their application Conference*, Inst. of Physics, Glasgow, pp. 109–114.
- [95] Lee J.M, Choi D.K. and Chu C.N, (1995), Real time tool breakage monitoring for NC milling process, *Ann. CIRP*, Vol. 44, Issue 1, pp. 59–62.
- [96] Grosvenor R.I., Johns C., Prickett P.W., (1996), Machine tool axis signals for condition monitoring, *Condition Monitoring and Diagnostic Engineering Management COMADEM 96 Conference Proceedings*, pp. 665-674.
- [97] Kim J. and Choi I., (1996), Development of a tool failure detection system using multi-sensors, *Int. J. Mach. Tools Manufact.*, Vol. 36, Issue 8, pp. 861-870.
- [98] Koenigsberger F. and Sabberwal A.J.P., (1961), An investigation into the cutting force pulsations during milling operations, *Journal of Machine Tool Design and Research*, Vol. 1, Issue 1 , pp. 15–33.
- [99] Lombardo A., Masnata A. and Settineri L., (1997), In process tool failure detection by means of AR models, *Journal of Adv. Manufact. Tech.*, Vol. 13, pp. 86–94.
- [100] Dargie Walteneagus, (2009), Analysis of Time and Frequency Domain Features of Accelerometer Measurements, *Proceedings of 18th International Conference on Computer Communications and Networks(ICCCN2009)*,

- Germany.
<http://ieeexplore.ieee.org/stamp/stamp.jsp?tp=&arnumber=5235366>
- [101] Sifuzzaman M., Islam M.R. and Ali M.Z., (2009), Application of Wavelet Transform and its Advantages Compared to Fourier Transform, *Journal of Physical Sciences*, Vol. 13, ISSN: 0972-8791, pp.121-134.
<http://vidyasagar.ac.in/journal/math/vol13/art11.pdf>
- [102] Li A.U. and Elbestawi M.A., (1996), Fuzzy clustering for automated tool condition monitoring in machining. *J. Mech. Systems and Signal Processing*, Vol. 10, Issue 5, pp. 533–550.
- [103] Al-Habaibeh A., Al-Azmi A., Radwan N. and Yang Song, (2010), The Application of Force and Acoustic Emission Sensors for Detecting Tool Damage in Turning Processes, *Key Engineering Materials*, Vols. 419-420, pp. 381-384.
- [104] Ertunc H. M. and Loparo K. A., (2001), A decision fusion algorithm for tool wear condition monitoring in drilling, *Journal of machine tools and Manufacture*, Vol.6, pp. 1347-1362.
- [105] Kegg R.L. (1984), On-line machine and process diagnostics, *Annals of the CIRP*, Vol.2, pp.469–473.
- [106] Kurada S. and C. Bradley, (1997), A review of machine vision for tool condition monitoring, *Computers in Industry*, Vol. 34, pp. 55–72.
- [107] Li H.Z., Zeng H. and Chen X.Q.,(2006), An experimental study of tool wear and cutting force variation in the end milling of Inconel 718 with coated carbide inserts, *Journal of Materials Processing Technology*, Vol. 180, Issues 1-3, pp. 296-304 .
- [108] Cuneyt Aliustaoglu, Metin Ertunc H. and Hasan Ocak,(2009),Tool wear condition monitoring using a sensor fusion model based on fuzzy inference system, *Mechanical Systems and Signal Processing*, Vol. 23, Issue 2, pp. 539-546.
- [109] Christer A.H., Wang W., (1995), A simple condition monitoring model for a direct monitoring process, *European Journal of Operational Research*, Vol. 82, Issue 2, pp. 258-269.
- [110] Uehara K., (1973), New Attempts for Short Time Tool-Life Testing, *Ann. CIRP*, Vol. 22, pp 23-24.
- [111] Smith G.T, (1993), Trends in Tool Condition Monitoring Techniques-Wear and Cutting Forces-on Turning Centres, *Condition Monitoring and Diagnostic Engineering Management*, pp 314-324.
- [112] Kouros Tatar, Per Gren, (2008), Measurement of milling tool vibrations during cutting using laser vibrometry , *International Journal of Machine*

- Tools and Manufacture*, Vol. 48, Issues 3–4, pp. 380-387.
- [113] Rothberg Steve J., Halkon Ben J., Tirabassi Mario, Pusey Chris, (2012), Radial vibration measurements directly from rotors using laser vibrometry: The effects of surface roughness instrument misalignments and pseudo-vibration, *Mechanical Systems and Signal Processing*, Vol. 33, pp. 109-131.
- [114] Lunde G., Anderson P.B, (1970), A study of the wear processes on cemented carbide cutting tool by a radioactive tracer technique, *International Journal of Machine Tool Design and Research*, Vol. 10, Issue 1, pp. 79-93.
- [115] Kurada S., Bradley C, (1997), A review of machine vision sensors for tool condition monitoring, *Computers in Industry*, Vol. 34, Issue 1, pp. 55-72.
- [116] Proximity Sensors - Engineers' Handbook
www.engineershandbook.com/Components/proximitysensors.htm
- [117] Kerrigan K., Thil J., Hewison R., O'Donnell, G.E., (2012), An Integrated Telemetric Thermocouple Sensor for Process Monitoring of CFRP Milling Operations, *Procedia CIRP*, Vol. 1, pp. 449-454.
- [118] Brudek1 G., Wulfsberg1 J.P, (2005), Monitoring of Micro Machining Operations, University of the Federal Armed Forces Hamburg, Laboratory of Production Engineering, Hamburg, Germany.
www.mikromaschinenbau.com/Brudek_Monitoringof_Micro_Machining_Operations.pdf.
- [119] Süleyman Yıldız, Faruk Ünsaçar, Hacı Sağlam, Hakan Işık, (2007), Design, development and testing of a four-component milling dynamometer for the measurement of cutting force and torque, *Mechanical Systems and Signal Processing*, Vol. 21, Issue 3, pp. 1499-1511.
- [120] Kious M., Ouahabi A, Boudraa M, Serra R, Cheknane A., (2010), Detection process approach of tool wear in high speed milling, *Measurement*, Vol. 43, Issue 10, pp. 1439-1446.
- [121] Transchel R., Stirnimann J., Blattner M., Bill B., Thiel R., Kuster F., Wegener K., (2012), Effective Dynamometer for Measuring High Dynamic Process Force Signals in Micro Machining Operations, *Procedia CIRP*, Vol. 1, pp. 558-562.
- [122] Cus F., Milfelner M. and Balic, (2006), An intelligent system for monitoring and optimization of ball-end milling process, *Journal of Materials Processing Technology*, Vol. 175, Issues 1-3, pp. 90-97.
- [123] Alonso F.J., Salgado D.R, (2008), Analysis of the structure of vibration signals for tool wear detection *Mechanical Systems and Signal Processing*, Vol. 22, Issue 3, pp. 735-748.

- [124] Bovic Kilundu, Pierre Dehombreux and Xavier Chimentin, (2011), Tool wear monitoring by machine learning techniques and singular spectrum analysis, *Mechanical Systems and Signal Processing*, Vol. 25, Issue 1, pp. 400-415.
- [125] Burke L.I., Rangwala S, (1990), Tool condition monitoring in metal cutting: a neural network approach, *Journal of Intelligent Manufacturing*, Vol. 2, pp. 269–280.
- [126] Park S.S., and Malekian M., (2009), Mechanistic modeling and accurate measurement of micro end milling forces, *CIRP Annals - Manufacturing Technology*, Vol. 58, Issue 1, pp. 49-52.
- [127] Jesus R.R.D., Gilberto H., Ivan T., Carlos J.J, (2003), Driver current analysis for sensorless tool breakage monitoring of CNC milling machines, *International Journal of Machine Tools and Manufacture*, Vol.43. , pp. 1529–1534.
- [128] Shao H., Wang H.L., Zhao X.M., (2004), A cutting power model for tool wear mentoring in milling, *International Journal of Machine Tools and Manufacture*, Vol. 44 pp. 1503–1509.
- [129] X.L. Li, Ouyang G.X., Liang Z.H,(2008), Complexity measure of motor current signals for tool flute breakage detection in end milling, *International Journal of Machine Tools and Manufacture*, Vol. 48, pp.371–379.
- [130] Hua Shao, Xinha Shi, Lin Li, (2011), Power signal separation in milling process based on wavelet transform and independent component analysis, *International Journal of Machine Tools and Manufacture*, Vol. 51, Issue 9, pp.701-710.
- [131] Peng Z.K., Jackson MR, L.Z. Guo, R.M. Parkin, G. Meng, (2010), Effects of bearing clearance on the chatter stability of milling process, *Nonlinear Analysis: Real World Applications*, Vol. 11, Issue 5, pp. 3577-3589.
- [132] Dahu Zhu, Xiaoming Zhang, Han Ding, (2013), Tool wear characteristics in machining of nickel-based superalloys, *International Journal of Machine Tools and Manufacture*, Vol. 64, pp. 60-77.
- [133] Dornfeld D., (1990), Neural Network Sensor Fusion for Tool Condition Monitoring, *Annals CIRP*, Vol. 39, (1), pp. 101-105.
- [134] Wang, Z. and D.A. Dornfeld, (1992), In-Process Tool Wear Monitoring Using Neural Networks, *Japan/USA Symposium on Flexible Automation Part 1(of 2)*, San Francisco, pp. 263-270.
- [135] Charniya Nadir N., Dudul Sanjay V., (2011), Classification of material type and its surface properties using digital signal processing techniques and neural networks, *Applied Soft Computing*, Vol. 11, Issue 1, pp. 1108-1116

- [136] Chen, S.L. and Jen, Y.W., (2000), Data Fusion Neural Network for Tool Condition Monitoring in CNC Milling Machining, *International Journal of Machine Tools and Manufacture*, Vol. 40, pp 381-400.
- [137] Sultan Binsaeid, Shihab, Sohyung Cho, Arzu Onar, (2009), Machine ensemble approach for simultaneous detection of transient and gradual abnormalities in end milling using multisensor fusion, *Journal of Materials Processing Technology*, Vol. 209, Issue 10, pp. 4728-4738.
- [138] Chung K.T., Geddam A., (2003) , A multi-sensor approach to the monitoring of end milling operations, *Journal of Materials Processing Technology*, Vol. 139, Issues 1–3, pp.15-20.
- [139] Rehorn A.G., Jiang J. and P.E. Orban, (2005), State-of-the-art methods and results in tool condition monitoring: a review, *International Journal of Advance Manufacturing Technology*, Vol. 26, pp. 693–710.
- [140] Norman P., A. Kaplan, M. Rantatalo and I. Svenningsson, (2007) ,Study of a platform for monitoring machining of aluminium and steel, *Measurement Science & Technology*, Vol. 18, pp. 1155–1166.
- [141] Tomas Kalvoda and Yean-Ren Hwang, (2010), A cutter tool monitoring in machining process using Hilbert–Huang transform, *International Journal of Machine Tools and Manufacture*, Vol. 50, Issue 5, pp. 495-501.
- [142] Kunpeng Zhu, Yoke San Wong, Geok Soon Hong, (2009), Wavelet analysis of sensor signals for tool condition monitoring: A review and some new results, *Int. Journal of Machine Tools and Manufacture*, Vol. 49, Issues 7–8, pp. 537-553.
- [143] Tansel I. Nur, (1995), Detection of tool failure in end milling with wavelet transformations and neural networks (WTNN), *Int. Journal of Machine Tools Manufacturer*, Vol.35, Issue 4, pp. 1137–1147.
- [144] Xiaoli Li, Shen Dong, Zhejun Yuan, (1999), Discrete wavelet transform for tool breakage monitoring, *International Journal of Machine Tools and manufacture*, Vol. 39, Issue 12, pp. 1935-1944.
- [145] Chung-Jen, Yu-Tsun Hsu, (2002), Vibration analysis of an inhomogeneous string for damage detection by wavlet transform, *International Journal of Mechanical Sciences*, Vol. 44, Issue 4, pp. 745-754.
- [146] Sanjit Moshat, Saurav Datta, Asish Bandyopadhyay and Pradip Kumar Pal, (2010), Optimization of CNC end milling process parameters using PCA-based Taguchi method, *International Journal of Engineering, Science and Technology*, Vol. 2, No. 1, pp. 92-102
- [147] Jiang Wanlu, Meng Yuru, Zang Sheng, (2011), Kernel principal component analysis fault diagnosis method based on sound signal processing and its

- application in hydraulic pump, *2011 International Conference of Fluid Power and Mechatronics (FPM)*, pp.17-20.
- [148] Weiyuan Shi, Wei Zhang, (2010), Research on Signal Processing Method in Complex Textile Machinery System Based on Principal Component Analysis and Wavelet Analysis, *2010 International Conference on Intelligent Computation Technology and Automation*, Vol.3, pp. 108– 111, China.
- [149] Correa M., Bielza C., Pamies-Teixeira J., (2009), Comparison of Bayesian networks and artificial neural networks for quality detection in a machining process, *Expert Systems with Applications*, Vol. 36, Issue 3, pp. 7270-7279
- [150] Rao B.K.N., Hope A. D., 1996), On-line tool wear classification using fuzzy based reasoning, *Condition Monitoring and Diagnostic Engineering Management COMADEM 96 Conference Proceedings*, pp. 355–366.
- [151] Sadettin Orhan, Ali Osman Er, Necip Camuşcu and Ersan Asla, (2007), Tool wear evaluation by vibration analysis during end milling of AISI D3 cold work tool steel with 35 HRC hardness, *NDT & E International*, Vol. 40, Issue 2, pp.121-126 .
- [152] Dimla D.E., P.M. Lister and Leighton N.J., (1997) ,Neural network solutions to the tool condition monitoring problem in metal cutting-a critical review. *Int. J. Mach. Tools Manufact*, Vol. 37 , Issue 9 , pp. 1219-1241.
- [153] Dohyun Kim, Doyoung Jeon, (2011), Fuzzy-logic control of cutting forces in CNC milling processes using motor currents as indirect force sensors, *Precision Engineering*, Vol. 35, Issue 1, pp. 143-152.
- [154] Suleyman Yaldiz, Faruk Unsacar, Haci Saglam, (2006), Comparison of experimental results obtained by designed dynamometer to fuzzy model for predicting cutting forces in turning, *Materials & Design*, Vol. 27, Issue 10, pp. 1139-1147.
- [155] Cuneyt Aliustaoglu, H. Metin Ertunc, Hasan Ocak, (2009), Tool wear condition monitoring using a sensor fusion model based on fuzzy inference system, *Mechanical Systems and Signal Processing*, Vol. 23, Issue 2, pp.539-546.
- [156] Mohammad Malekian, Simon S. Park and Martin B. Jun, (2009), Tool wear monitoring of micro-milling operations, *Journal of Materials Processing Technology*, Vol. 209, Issue 10, pp. 4903-4914.
- [157] Abbas Jabbar, (2001), Design and Performance Evaluation of Technically Guided Fixture for gripping Cylindrical Parts using Computer modelling, MSc thesis, University of Technology, Baghdad, Iraq.

- [158] Preben Hansen, (2001), Solid contact, the advantages of dual and triple contact dual and triple contact toolholding systems for high speed machining, Vol. 53, No. 7. www.ctemag.com/pdf/2001/0107-solid.pdf
- [159] Reha Haymanali, Edward C. De Meter, Martin W. Trerhewey, (2000), Development of a compliance tester for assessing and reducing the static compliance of fixture-workpiece, *Journal of manufacturing Systems*, Vol. 19, Issue 2, pp. 108-120.
- [160] <http://www.newmantools.com/jacobs/collets.htm>.
- [161] Sun Ji-wen, Li-feng Xi, Er-shun Pan, Shi-chang Du and Tang-bin Xia, (2009), Design for diagnosability of multistation manufacturing systems based on sensor allocation optimization, *Computers in Industry*, Vol. 60, Issue 7, pp. 501-509.
- [162] Möhring H.-C., Litwinski K.M. and Gümme O, (2010), Process monitoring with sensory machine tool components, *CIRP Annals - Manufacturing Technology*, Vol. 59, Issue 1, pp. 383-386 .
- [163] Banardos P.G. and Vosniakos G.C, (2002), Prediction of surface roughness in CNC face milling using neural networks and Taguchi's design of experiments, *Robotics and Computer-Integrated Manufacturing*, Vol. 18, Issues 5-6, pp.343-354.
- [164] Ertekin Y.M., Kwon Y. and Tseng T. L., (2003), Identification of common sensory features for the control of CNC milling operations under varying cutting conditions, *International Journal of Machine Tools and Manufacture*, Vol, 43, Issue 9, pp. 897–904.
- [165] Lou S. M., Chen C.J., Li M.C., (1998), Surface roughness prediction technique for CNC end-milling, *Journal Industrail Technology*, Vol. 15, Issue 1, pp.1-6.
- [166] Alauddin M., El Baradie M. A., Hashmi M. S. J., (1996), Optimization of surface finish in end milling Inconel 718, *Journal of Materials Processing Technology*, Vol. 56, Issues 1-4, pp. 54-65.
- [167] Dae Kyun Baek, Tae Jo Ko, Hee Sool Kim, (1997), A dynamic surface roughness model for face milling, *Precision Engineering*, Vol. 2, pp. 171-178.
- [168] Cemal Cakir M., Cihat Ensarioglu, Ilker Demirayak, (2009), Mathematical modeling of surface roughness for evaluating the effects of cutting parameters and coating material, Original Research Article, *Journal of Materials Processing Technology*, Vol. 209, Issue 1, pp.102-109.
- [169] Lee B.Y. and Y.S. Tarng, (2001), Surface roughness inspection by computer vision in turning operations, *Inter. Journal Machine Tools Manufacture*, Vol.41, pp. 1251–1263.

- [170] Wang M.Y. and Chang H.-Y., (2004), Experimental study of surface roughness in slot end milling AL2014-T6, *International Journal of Machine Tools and Manufacture*, Vol.44, Issue1, pp.51–57.
- [171] Baek D.K., T.J. Ko and Kim H.S., (2001), Optimization of feedrate in a face milling operation using a surface roughness model, *Int. Journal of Machine Tools and Manufacture*, Vol. 41, Issue 3, pp.451-462.
- [172] Lee K.Y., Kang M.C., Jeong Y.H., Lee D.W. and Kim J.S., (2001), Simulation of surface roughness and profile in high-speed end milling, *Journal of Materials Processing Technology*, Vol.113, Issue 1–3, pp. 410-415.
- [173] Franco P., Estrems M. and Faura F., (2004), Influence of radial and axial runouts surface roughness in face milling with round insert cutting tools, *International Journal of Machine Tools and Manufacture*, Vol. 44, Issue 15, pp.1555-1565.
- [174] Bernie P. Huang, Joseph C. Chen and Ye Li, (2008), Artificial-neural-networks-based surface roughness Pokayoke system for end-milling operations, *Neurocomputing*, Vol. 71, Issues 4-6, pp.544-549.
- [175] Franco P., Estrems M. and Fau F., (2008), A study of back cutting surface finish from tool errors and machine tool deviations, *International Journal of Machine Tools and Manufacture*, Vol.48, Issue1, pp.112-123.
- [176] Guillem Quintana, Thomas Rudolf, Joaquim Ciurana, Christian Brecher, (2011), Using kernel data in machine tools for the indirect evaluation of surface roughness in vertical milling operations, *Robotics and Computer-Integrated Manufacturing*, Vol. 27, Issue 6, pp. 1011-1018.
- [177] Al-Habaibeh A. and Gindy N., (2001), Self-Learning Algorithm for Automated Design of Condition Monitoring Systems for Milling Operations, *International Journal of Advanced Manufacturing Technology*, Vol. 18 (6), pp 448-459.
- [178] Al-Habaibeh A. and Gindy N., (2000), A New Approach for Systematic Design of Condition Monitoring Systems for Milling Processes, *Journal of Materials Processing Technology*, Vol.107, Issue1-3, pp 243-251.
- [179] Pearson K., (1901), On lines and planes of closest to systems of points in space, *Philosophical Magazine*, Vol. 2, No. 6, pp. 559-572.
<http://pbil.univ-lyon1.fr/R/pearson1901.pdf> .
- [180] Bellman R., Kalaba R., Zadeh L.A., (1966), Abstraction and pattern classification, *Journal of Mathematical Analysis and Applications*, Vol. 13 , pp. 1–7.
- [181] Lindsay I Smith, (2006), A tutorial on Principal Components Analysis.

- www.cs.otago.ac.nz/cosc453/student_tutorials/principal_components.pdf.
- [182] Zadeh L.Ahmad, (1978), A fuzzy- algorithm approach to the definition of complex or imprecise concepts, *Int. J. Man-Machine studies*, Vol.8, pp.249-291.
- [183] Sushmita Mitra, Sankar K. Pal, (2005), Fuzzy sets in pattern recognition and machine intelligence, *Fuzzy Sets and Systems*, Vol. 156 ,pp. 381–386.
- [184] James Rossiter, (2011), Multimodal Intent Recognition for Natural Human-Robotic Interaction, PhD Thesis, University of Birmingham, ,UK.
- [185] Jianli Liu, Baoqi Zuo, Xianyi Zeng, Philippe Vroman, Besoa Rabenasolo, (2010), Nonwoven uniformity identification using wavelet texture analysis and LVQ neural network, *Expert Systems with Applications*, Vol. 37, Issue 3, pp. 2241-2246.
- [186] <http://mathworld.wolfram.com/LeastSquaresFitting.html>
- [187] Franklin D Jones, Henry H Ryffel, Erik Oberg, Christopher J McCauley, Ricardo M Heald, (2004), Machinery's Handbook 27th Edition, Industrial Press, Inc., New York, USA.
http://www.sportpilot.info/sp/Machinery/27_Mach_06A.pdf
- [188] Al-Habaibeh A., Zorriassatine F., Parkin RM. and Jackson MR, (2005), Application of Infrared Technology for Quality Control of Diesel Engine GlowPlugS, *Proc ImechE, Part B, Journal of Engineering Manufacture (In Press JEM175R1)*, DOI: 10.1243/095440505X32256.
- [189] www.auto-met.com/mitutoyo/form_lit.htm
- [190] www.Kistler.com.
- [191] Ravindra H.V., Srinivasa Y.G. and Krishnamurthy R., (1993), Modelling of tool wear based on cutting forces in turning, *Wear* , Vol.169, Issue 1, pp. 25–32.
- [192] Tansel I, Trujillo M, Nedbouyan A, Velez C, Bao Wei-Yu, Arkan T.T, B Tansel, (1998), Micro-end-milling-III. Wear estimation and tool breakage detection using acoustic emission signals, *International Journal of Machine Tools and Manufacture*, Vol. 38, Issue 12, pp. 1449-1466.
- [193] Weller E.J., Schrier H.M. and Weichbrodt B., (1969), What Sound Can Be Expected from a Worn Tool, *Journal of Engineering Industry*, Vol. 91, Issue 3, pp 525-534.
- [194] www.lionprecision.com/inductive-sensors/index.htm.
- [195] www.waycon.de/eddycurrentprobe.html.

- [196] Alonso F.J. and Salgado D.R., (2005), Application of Singular Spectrum Analysis to Tool Wear Detection Using Sound Signals, *Proceedings of the IMechE Journal of Engineering Manufacture*, Vol.219, Issue 9, pp. 703–710.
- [197] Silva, R.G., Baker, K.J. and Wilcox, S.J., (2000), The Adaptability of a Tool Wear Monitoring System under Changing Cutting Conditions, *Mechanical Systems and Signal Processing*, Vol. 14, Issue 2, pp. 287-298.
- [198] Teti R., Jemielniak K., O'Donnell G. and Dornfeld D., (2010), Advanced monitoring of machining operations, *CIRP Annals- Manufacturing Technology*, Vol. 59, Issue 2, pp. 717-739.
- [199] Al-Habaibeh A., Powell N.P. and Gindy N.N.Z., (1999), Comprehensive Process and Machine Condition Monitoring Strategy for the Variax Hexacenter, *Computational intelligence for modelling, control and automation: Neural networks & advanced control strategies*, Vienna, pp. 249-254.
- [200] Bishop C.M., (1995), Neural Networks for Pattern Recognition, *Clarendon Press*, Oxford, UK.
- [201] Songmene V., Khettabi R., Zaghbani I., Kouam J., and Djebara A., (2011), Machining and Machinability of Aluminium Alloys, *Theory and Applications*, online, accessed on 4/11/2011.
http://cdn.intechopen.com/pdfs/13408/InTech-machiningand_machinability_of_aluminium-alloys.pdf.
- [202] Michael Negnevitsky, (2002), Artificial Intelligence: A Guide To Intelligent Systems, Book, Pearson Education limited, British Libraray ISBN 0201-71159-1.
- [203] Sabberwal A.J.P., Fleischer P., (1964), The effect of material and geometry on the wear characteristics of cutting tools during facemilling, *International Journal of Machine Tool Design and Research*, Vol. 4, Issue 1, pp. 47-71.
- [204] Hearn E.J., (1988), Mechanics of Materials, Book, 2nd Edition, city of Birmingham polytechnic, Pergamon Press, Vol. 1, pp. 429.

Appendices

Appendix A: Certificate of Participation in the First Iraqi Conference and won the first prize for the best research.....	2
Appendix B: Signals Simplifications (For Chapter 9/ section 9.2.1.1 Linear regression (LR) method).....	3
Appendix C: Signals Simplifications (For Chapter 9/ section 9.2.1.2 Principal Component Analysis (PCA)).....	14
Appendix D: System Cost and Utilisation (For Chapter 9/ 9.4.1.1 Selection of Sensory Features	31
Appendix E: System Cost and Utilisation (For Chapter 9/ 9.4.1.2 Selection of Principal Component Feature (PCFs) Method.....	40
Appendix F: System Optimisation (For Chapter 9/ 9.4.2.1 Linear Regression (LR) Method.....	49
Appendix G: System Optimisation (Chapter 9/ 9.4.2.2 Principal Component Analysis (PCA) Method.....	58
Appendix H: System Evaluation (For Chapter 9/ 9.4.3.1 Linear Regression (LR) Method.....	66
Appendix I: System Evaluation (For Chapter 9/ 9.4.3.2 Principal Component Analysis (PCA) Method.....	73
Appendix J: Signal simplification (Chapter 10/ 10.3.1 Linear Regression (LR) method.....	79
Appendix K: Signal simplification (For Chapter 10/ 10.3.2 Range Value (RV) method.....	83
Appendix L: Signal simplification (For Chapter 10/ 10.3.3 Sudden Change In Value (SCIV) method.....	89
Appendix M: Signal simplification (For Chapter 10/ 10.3.4 Correlation coefficient (CCX3) method.....	94
Appendix N: Signal simplification (For Chapter 10/ 10.5.5 Correlation coefficient (CCX20) method.....	99
Appendix O: Signal Simplification (For Chapter 10/10.3.6 Fuzzy Logic (FL) method..	105

Appendix A: Certificate of Participation in the First Iraqi Conference at University College London (2011) and won the first prize for the best research in the conference.



Appendix B: Signals Simplifications (For Chapter 9)

9.2.1.1 Linear Regression (LR) method

Table B.1: The Associated matrix of the system for tool 2 without sleeve.

Tool 2	Signal Processing Methods							
Sensor	max	min	std	power	average	skew	kurtosis	range
Fx	0.026	0.348	0.108	0.152	0.320	0.066	0.133	0.200
Fy	0.003	0.568	0.739	0.505	0.498	0.794	0.456	0.660
Fz	0.088	0.307	0.049	0.079	0.099	0.051	0.370	0.272
Strain	0.273	0.220	0.443	0.149	0.161	0.025	0.016	0.000
Vwy	0.502	0.499	0.229	0.485	0.501	0.526	0.262	0.421
AE	0.067	0.166	0.129	0.191	0.211	0.017	0.364	0.110
AERMS	0.087	0.410	0.215	0.086	0.221	0.240	0.418	0.183
Mic	0.077	0.467	0.046	0.244	0.246	0.022	0.075	0.427
Vsx	0.182	0.019	0.201	0.243	0.200	0.294	0.112	0.168
Vsy	0.421	0.433	0.795	0.809	0.151	0.052	0.438	0.650
Vsz	0.775	0.247	0.625	0.414	0.207	0.484	0.280	0.430
Vwx	0.115	0.127	0.414	0.514	0.352	0.186	0.081	0.091
Pwr	0.560	0.349	0.666	0.738	0.353	0.325	0.333	0.574
Edx	0.076	0.373	0.016	0.826	0.825	0.788	0.507	0.358
Edy	0.715	0.000	0.671	0.559	0.592	0.671	0.085	0.715

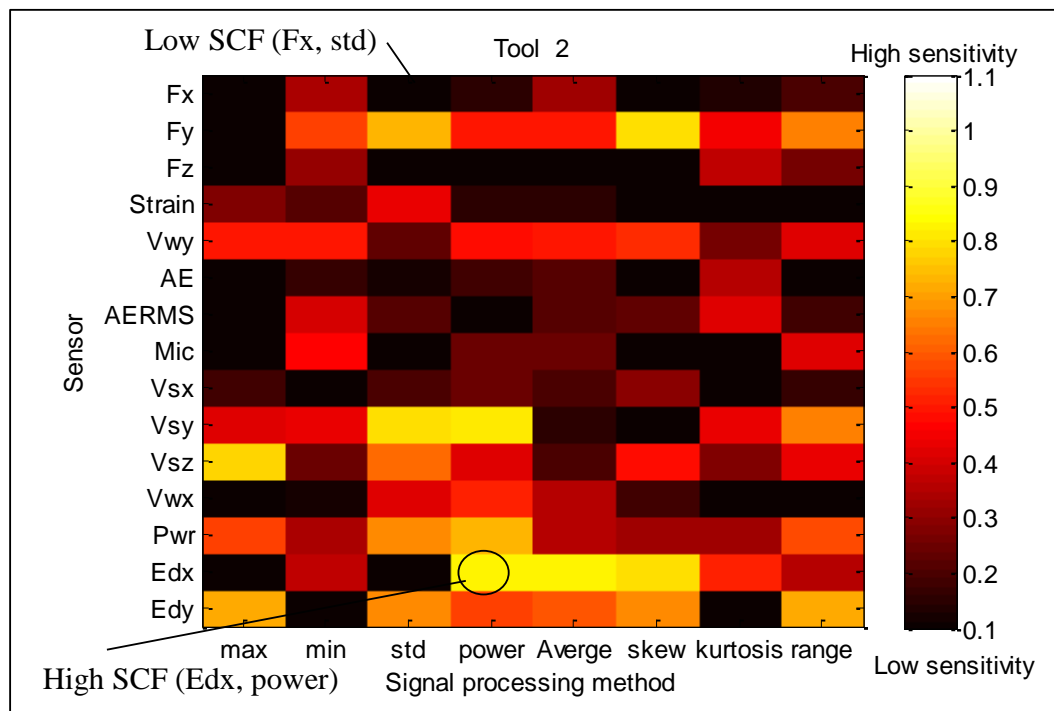


Figure B.1: A graphical presentation of the sensitivity for tool 2 without sleeve.

Table B.2: The Associated matrix of the system for tool 3 without sleeve.

Tool 3 Sensor	Signal Processing Methods							
	max	min	std	power	average	skew	kurtosis	range
Fx	0.358	0.125	0.039	0.004	0.523	0.326	0.164	0.147
Fy	0.054	0.193	0.143	0.134	0.158	0.166	0.236	0.170
Fz	0.060	0.326	0.243	0.288	0.436	0.366	0.026	0.252
Strain	0.028	0.647	0.327	0.370	0.381	0.293	0.444	0.535
Vwy	0.578	0.580	0.094	0.596	0.576	0.383	0.142	0.074
AE	0.022	0.079	0.463	0.378	0.094	0.473	0.124	0.045
AERMS	0.301	0.229	0.203	0.375	0.397	0.345	0.037	0.241
Mic	0.200	0.253	0.386	0.584	0.587	0.373	0.159	0.045
Vsx	0.429	0.042	0.158	0.224	0.170	0.104	0.054	0.264
Vsy	0.536	0.399	0.056	0.028	0.108	0.230	0.264	0.220
Vsz	0.524	0.047	0.181	0.025	0.509	0.574	0.119	0.309
Vwx	0.166	0.219	0.432	0.380	0.216	0.462	0.202	0.153
Pwr	0.520	0.707	0.910	0.924	0.317	0.447	0.255	0.798
Edx	0.427	0.010	0.211	0.268	0.270	0.167	0.215	0.352
Edy	0.171	0.000	0.501	0.488	0.480	0.499	0.271	0.171

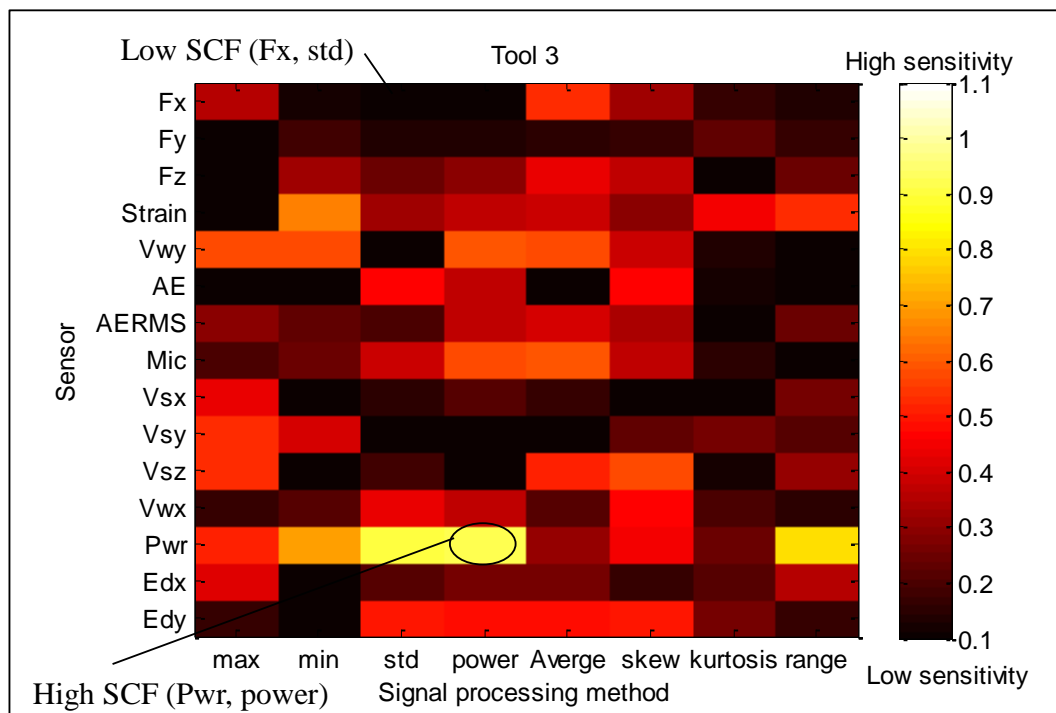


Figure B.2: A graphical presentation of the sensitivity for tool 3 without sleeve.

Table B.3: The Associated matrix of the system for tool 4 with rubber sleeve.

Tool 4	Signal Processing Methods							
Sensor	max	min	std	power	average	skew	kurtosis	range
Fx	0.247	0.623	0.331	0.211	0.636	0.163	0.325	0.587
Fy	0.002	0.214	0.404	0.023	0.045	0.240	0.356	0.339
Fz	0.368	0.542	0.576	0.342	0.397	0.321	0.270	0.548
Strain	0.061	0.265	0.208	0.255	0.289	0.269	0.122	0.299
Vwy	0.084	0.082	0.155	0.042	0.082	0.245	0.170	0.409
AE	0.395	0.510	0.534	0.484	0.115	0.463	0.256	0.437
AERMS	0.542	0.535	0.448	0.518	0.530	0.010	0.234	0.467
Mic	0.098	0.065	0.128	0.497	0.500	0.013	0.229	0.130
Vsx	0.359	0.444	0.524	0.297	0.427	0.536	0.432	0.514
Vsy	0.415	0.198	0.315	0.356	0.100	0.052	0.384	0.355
Vsz	0.105	0.014	0.104	0.067	0.035	0.092	0.196	0.095
Vwx	0.489	0.301	0.188	0.217	0.216	0.026	0.339	0.183
Pwr	0.069	0.215	0.776	0.728	0.151	0.118	0.578	0.115
Edx	0.770	0.190	0.070	0.244	0.242	0.262	0.575	0.665
Edy	0.192	0.000	0.151	0.221	0.202	0.151	0.118	0.192

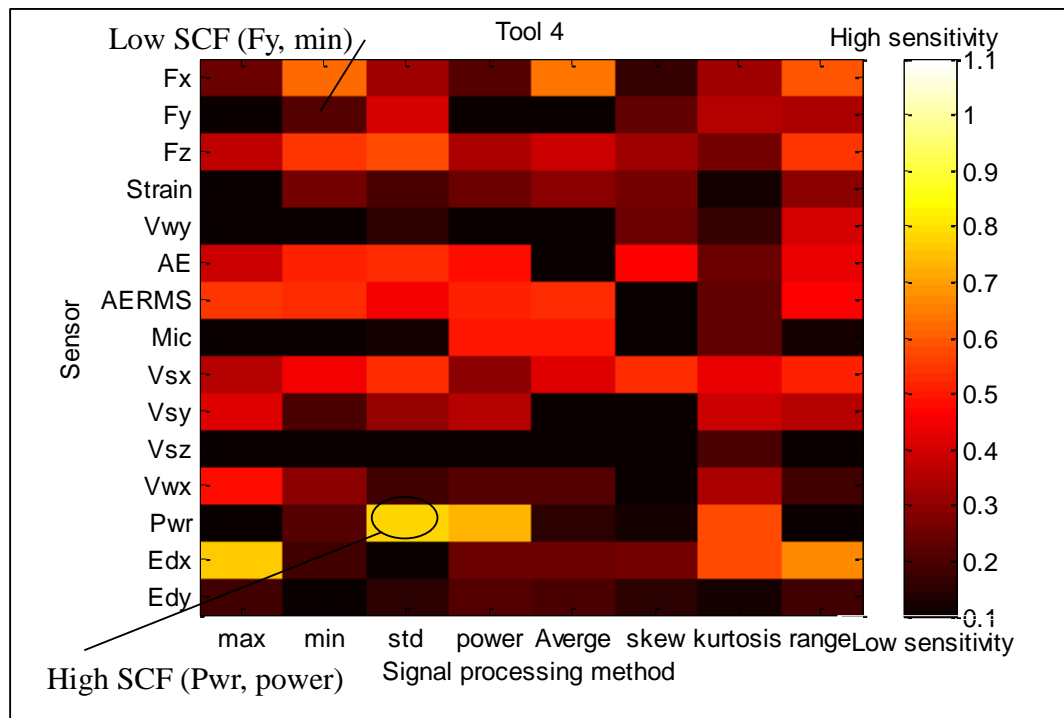


Figure B.3: A graphical presentation of the sensitivity for tool 4 with rubber sleeve.

Table B.4: The Associated matrix of the system for tool 5 with rubber sleeve.

Tool 5	Signal Processing Methods							
Sensor	max	min	std	power	average	skew	kurtosis	range
Fx	0.102	0.679	0.540	0.496	0.275	0.403	0.262	0.402
Fy	0.014	0.751	0.361	0.229	0.078	0.617	0.722	0.529
Fz	0.238	0.628	0.267	0.192	0.021	0.645	0.246	0.368
Strain	0.150	0.131	0.519	0.017	0.124	0.296	0.788	0.092
Vwy	0.667	0.673	0.260	0.810	0.671	0.235	0.305	0.415
AE	0.181	0.193	0.190	0.058	0.050	0.280	0.525	0.187
AERMS	0.268	0.462	0.234	0.095	0.333	0.112	0.431	0.254
Mic	0.247	0.252	0.219	0.168	0.167	0.212	0.002	0.328
Vsx	0.647	0.090	0.300	0.376	0.301	0.142	0.088	0.367
Vsy	0.146	0.467	0.336	0.020	0.262	0.221	0.337	0.476
Vsz	0.629	0.345	0.264	0.114	0.250	0.267	0.487	0.626
Vwx	0.014	0.139	0.281	0.082	0.184	0.372	0.054	0.134
Pwr	0.427	0.054	0.338	0.438	0.215	0.322	0.264	0.317
Edx	0.234	0.268	0.072	0.267	0.268	0.227	0.004	0.047
Edy	0.030	0.044	0.013	0.059	0.046	0.384	0.056	0.049

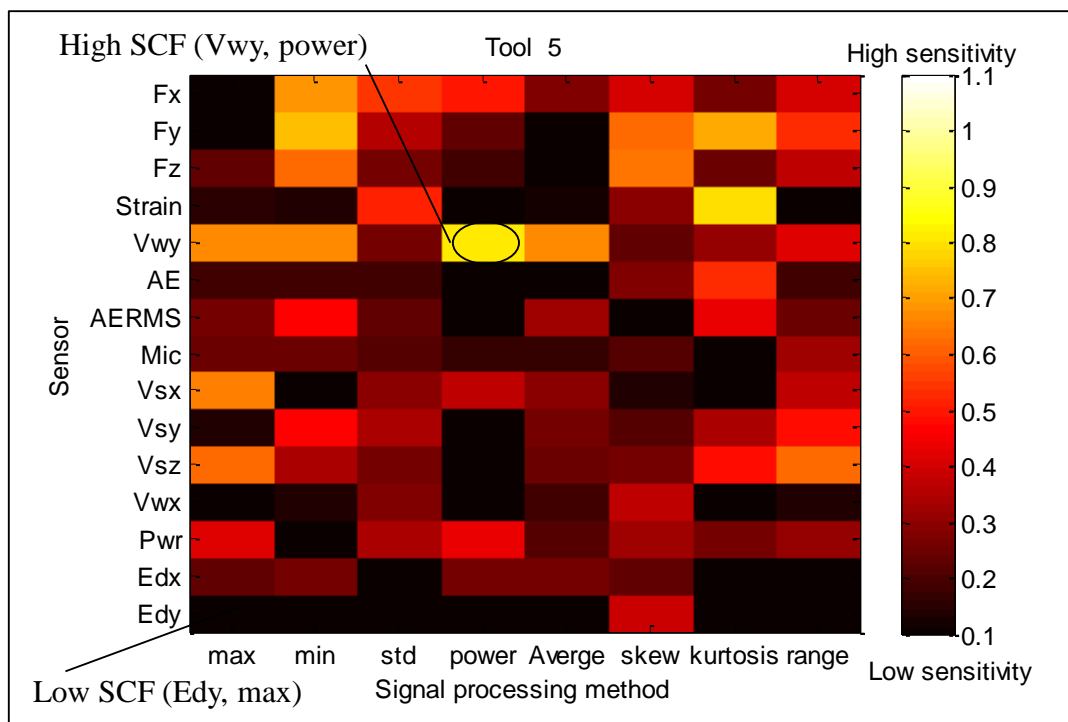


Figure B.4 : A graphical presentation of the sensitivity for tool 5 with rubber sleeve.

Table B.5: The Associated matrix of the system for tool 6 with rubber sleeve.

Tool 6	Signal Processing Methods							
Sensor	max	min	std	power	average	skew	kurtosis	range
Fx	0.296	0.345	0.212	0.203	0.359	0.291	0.579	0.325
Fy	0.160	0.170	0.159	0.160	0.306	0.101	0.174	0.166
Fz	0.164	0.168	0.166	0.166	0.137	0.009	0.168	0.167
Strain	0.159	0.166	0.167	0.166	0.037	0.148	0.155	0.165
Vwy	0.149	0.174	0.166	0.328	0.331	0.166	0.169	0.166
AE	0.286	0.654	0.525	0.267	0.261	0.474	0.183	0.406
AERMS	0.039	0.455	0.043	0.227	0.396	0.455	0.184	0.066
Mic	0.421	0.049	0.288	0.212	0.215	0.304	0.543	0.379
Vsx	0.146	0.299	0.486	0.229	0.192	0.130	0.010	0.067
Vsy	0.190	0.098	0.138	0.249	0.336	0.317	0.244	0.118
Vsz	0.077	0.093	0.410	0.393	0.036	0.016	0.072	0.006
Vwx	0.118	0.287	0.108	0.069	0.082	0.132	0.246	0.210
Pwr	0.219	0.470	0.848	0.880	0.448	0.430	0.251	0.248
Edx	0.364	0.345	0.336	0.322	0.320	0.312	0.315	0.351
Edy	0.262	0.013	0.139	0.225	0.201	0.241	0.311	0.246

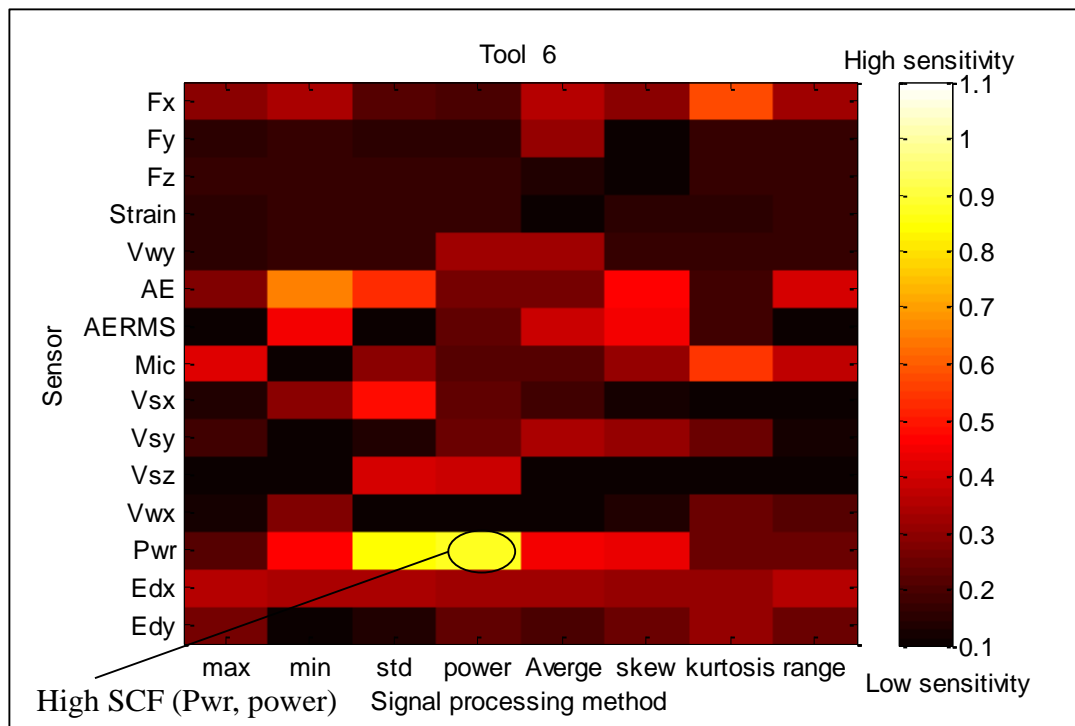


Figure B.5: A graphical presentation of the sensitivity for tool 6 with rubber sleeve.

Table B.6: Associated matrix of the system for tool 7 with copper sleeve.

Tool 7	Signal Processing Methods							
Sensor	max	min	std	power	average	skew	kurtosis	range
Fx	1.024	0.182	0.704	0.684	0.863	0.288	0.138	0.662
Fy	0.578	0.058	0.585	0.506	0.177	0.669	0.640	0.499
Fz	0.307	0.079	0.311	0.255	0.393	0.468	0.289	0.216
Strain	0.427	0.342	0.356	0.204	0.075	0.374	0.313	0.388
Vwy	0.506	0.512	0.106	0.486	0.509	0.395	0.050	0.021
AE	0.298	0.300	0.302	0.302	0.093	0.275	0.297	0.299
AERMS	0.290	0.245	0.368	0.298	0.286	0.020	0.495	0.321
Mic	0.281	0.269	0.119	0.148	0.155	0.157	0.193	0.175
Vsx	0.591	0.009	0.681	0.188	0.088	0.110	0.413	0.469
Vsy	0.231	0.288	0.676	0.241	0.072	0.186	0.390	0.363
Vsz	0.565	0.500	0.604	0.242	0.098	0.195	0.706	0.796
Vwx	0.135	0.047	0.513	0.468	0.087	0.122	0.204	0.038
Pwr	0.815	0.738	0.795	0.855	0.300	0.254	0.294	0.779
Edx	0.059	0.256	0.237	0.314	0.314	0.485	0.225	0.258
Edy	0.386	0.276	0.262	0.392	0.406	0.198	0.313	0.281

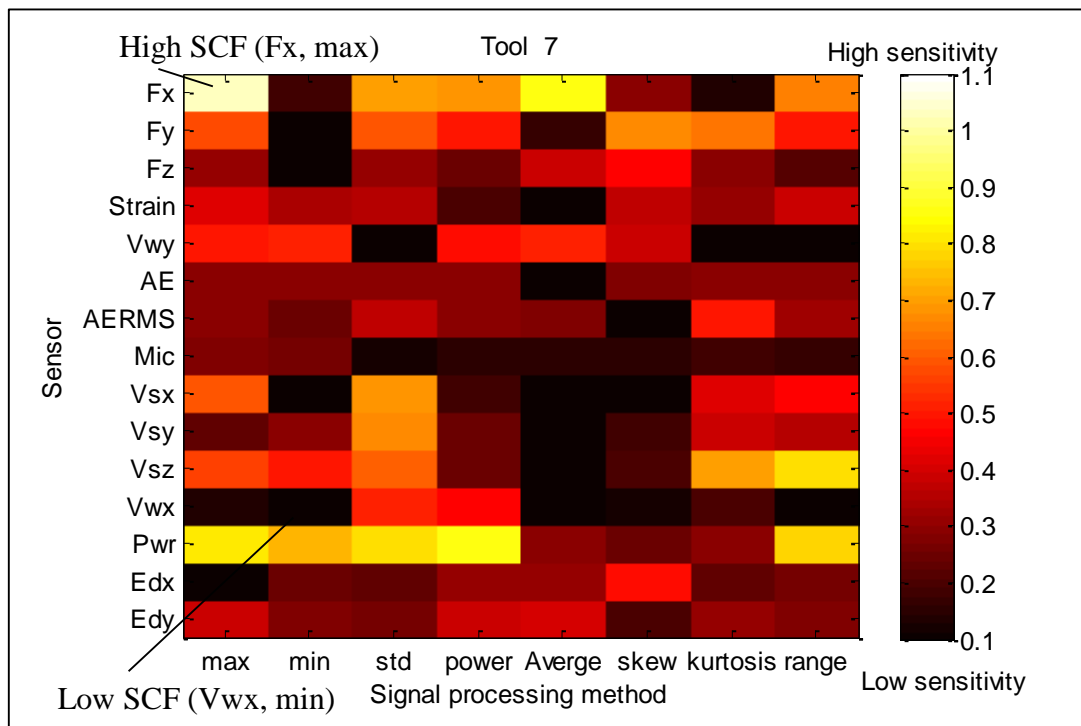


Figure B.6: A graphical presentation of the sensitivity for tool 7 with copper sleeve.

Table B.7: The Associated matrix of the system for tool 8 with copper sleeve.

Tool 8	Signal Processing Methods							
Sensor	max	min	std	power	average	skew	kurtosis	range
Fx	0.046	0.065	0.047	0.054	0.087	0.142	0.063	0.179
Fy	0.447	0.554	0.248	0.253	0.445	0.162	0.187	0.140
Fz	0.035	0.033	0.085	0.143	0.054	0.343	0.057	0.051
Strain	0.110	0.358	0.316	0.391	0.340	0.201	0.257	0.328
Vwy	0.235	0.231	0.173	0.146	0.233	0.223	0.371	0.207
AE	0.426	0.534	0.574	0.501	0.184	0.345	0.228	0.529
AERMS	0.621	0.324	0.424	0.419	0.437	0.132	0.477	0.514
Mic	0.435	0.063	0.751	0.296	0.301	0.790	0.119	0.572
Vsx	0.286	0.339	0.601	0.085	0.257	0.516	0.319	0.455
Vsy	0.199	0.310	0.330	0.467	0.264	0.027	0.417	0.385
Vsz	0.260	0.552	0.371	0.041	0.194	0.303	0.585	0.531
Vwx	0.225	0.086	0.282	0.060	0.291	0.336	0.143	0.033
Pwr	0.076	0.724	0.692	0.581	0.323	0.393	0.091	0.565
Edx	0.191	0.172	0.055	0.140	0.140	0.141	0.346	0.053
Edy	0.261	0.302	0.366	0.265	0.328	0.752	0.248	0.290

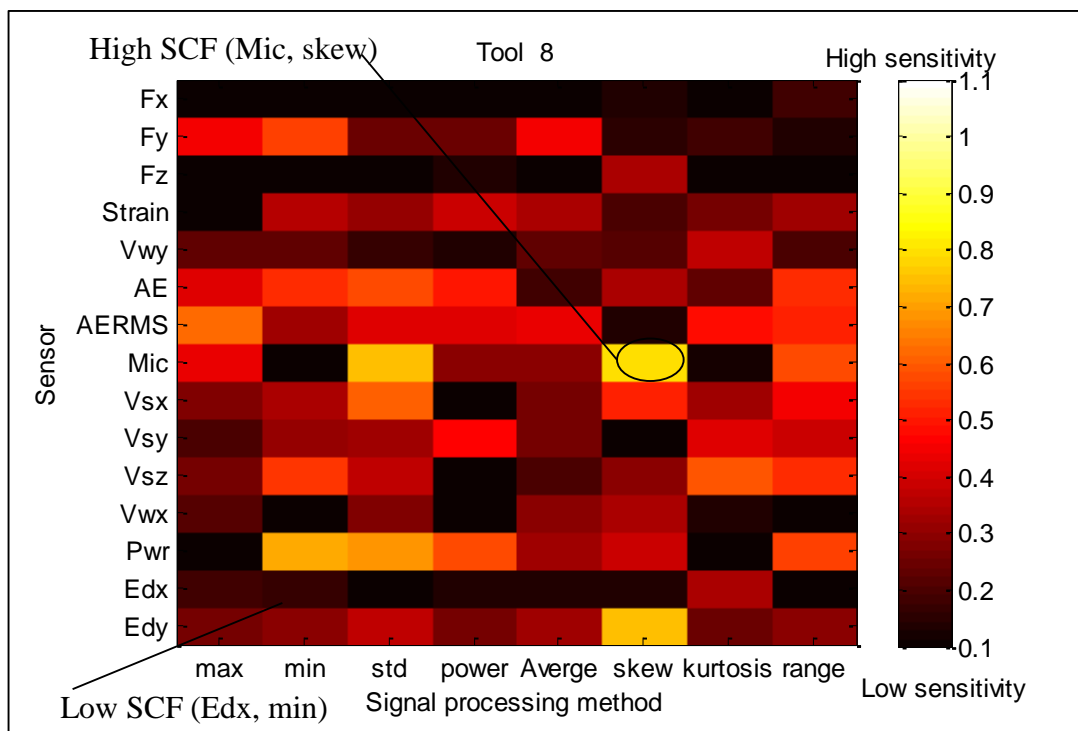


Figure B.7: A graphical presentation of the sensitivity for tool 8 with copper sleeve.

Table B.8: The Associated matrix of the system for tool 9 with copper sleeve.

Tool 9	Signal Processing Methods							
Sensor	max	min	std	power	average	skew	kurtosis	Range
Fx	0.230	0.346	0.039	0.140	0.424	0.292	0.063	0.057
Fy	0.545	0.647	0.209	0.577	0.670	0.209	0.042	0.260
Fz	0.439	0.380	0.166	0.125	0.708	0.129	0.472	0.150
Strain	0.201	0.356	0.128	0.263	0.249	0.005	0.298	0.315
Vwy	0.941	0.913	0.221	0.962	0.928	0.640	0.299	0.308
AE	0.283	0.386	0.247	0.168	0.268	0.302	0.400	0.332
AERMS	0.320	0.385	0.272	0.362	0.382	0.064	0.429	0.271
Mic	0.360	0.278	0.315	0.193	0.210	0.313	0.293	0.301
Vsx	0.278	0.337	0.218	0.347	0.925	0.412	0.306	0.332
Vsy	0.280	0.129	0.086	0.176	0.266	0.473	0.268	0.213
Vsz	0.208	0.360	0.045	0.048	0.041	0.032	0.301	0.268
Vwx	0.136	0.450	0.204	0.199	0.072	0.197	0.534	0.391
Pwr	0.260	0.409	0.531	0.595	0.232	0.184	0.247	0.337
Edx	0.072	0.348	0.249	0.316	0.316	0.282	0.287	0.236
Edy	0.198	0.312	0.374	0.380	0.390	0.407	0.299	0.305

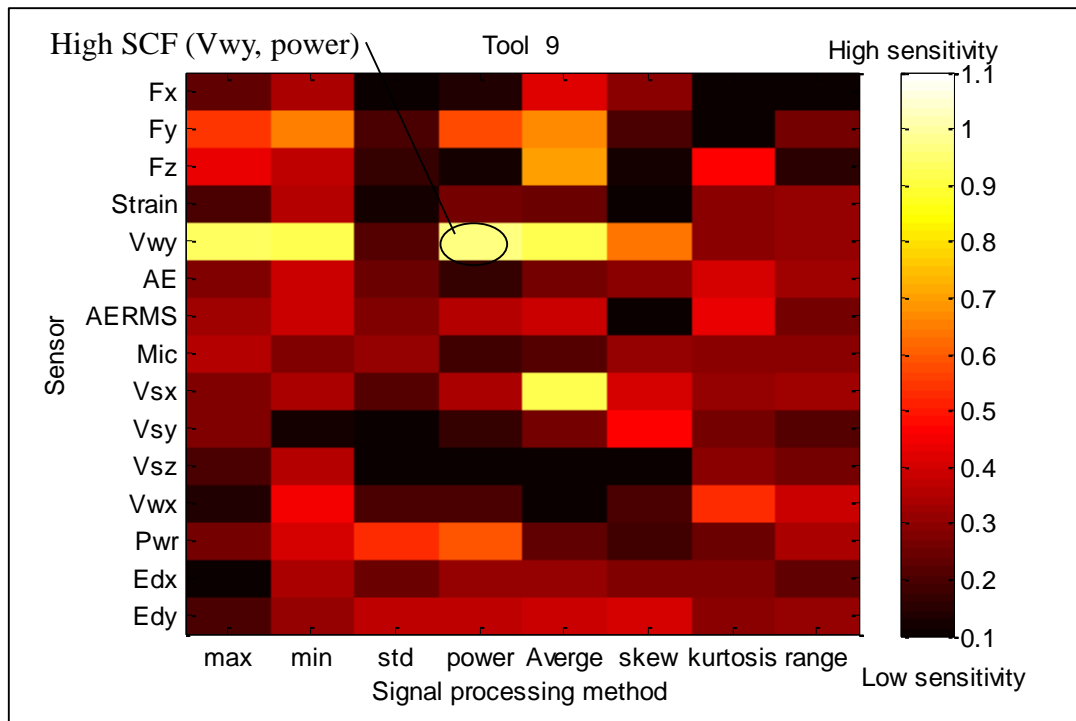


Figure B.8: A graphical presentation of the sensitivity for tool 9 with copper sleeve.

Table B.9: Associated matrix of the system for tool 10 with aluminium sleeve.

Tool 10	Signal Processing Methods							
	max	min	std	power	average	skew	kurtosis	Range
Fx	0.349	0.703	0.603	0.615	0.325	0.273	0.085	0.548
Fy	0.238	0.147	0.465	0.617	0.099	0.096	0.552	0.375
Fz	0.377	0.287	0.158	0.285	0.590	0.094	0.357	0.144
Strain	0.060	0.123	0.011	0.067	0.142	0.018	0.334	0.067
Vwy	0.248	0.271	0.235	0.235	0.268	0.188	0.407	0.707
AE	0.334	0.273	0.203	0.013	0.468	0.274	0.283	0.315
AERMS	0.071	0.175	0.007	0.175	0.134	0.036	0.250	0.016
Mic	0.816	0.591	0.528	0.492	0.493	0.537	0.519	0.753
Vsx	0.489	0.531	0.289	0.251	0.414	0.446	0.694	0.696
Vsy	0.039	0.435	0.417	0.452	0.373	0.173	0.251	0.373
Vsz	0.255	0.226	0.487	0.098	0.402	0.444	0.117	0.307
Vwx	0.008	0.514	0.200	0.108	0.220	0.231	0.446	0.332
Pwr	0.260	0.308	0.798	0.763	0.512	0.471	0.145	0.438
Edx	0.041	0.079	0.675	0.418	0.412	0.582	0.348	0.017
Edy	0.056	0.536	0.551	0.028	0.165	0.218	0.364	0.546

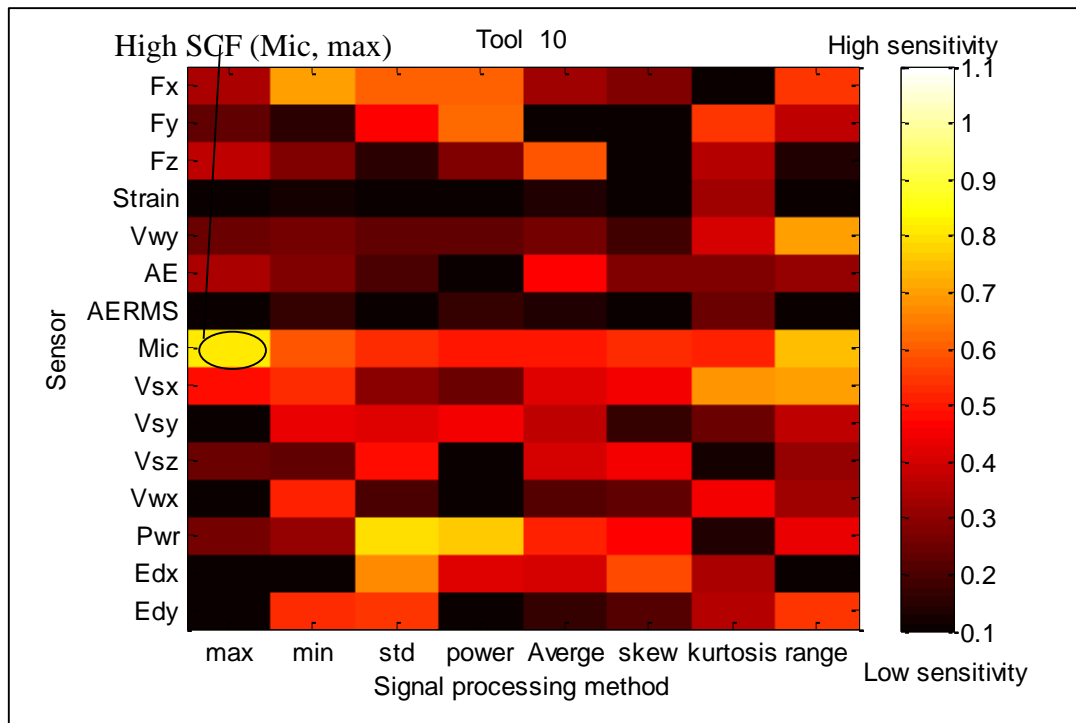


Figure B.9: A graphical presentation of the sensitivity for tool 10 with aluminium sleeve.

Table B.10: The Associated matrix of the system for tool 11 with aluminium sleeve.

Tool 11	Signal Processing Methods							
Sensor	max	min	std	power	average	skew	kurtosis	Range
Fx	0.642	0.151	0.099	0.272	0.475	0.466	0.094	0.180
Fy	0.027	0.127	0.319	0.522	0.054	0.557	0.374	0.306
Fz	0.166	0.366	0.364	0.360	0.011	0.069	0.610	0.258
Strain	0.201	0.047	0.288	0.128	0.117	0.307	0.622	0.136
Vwy	0.549	0.537	0.470	0.554	0.544	0.598	0.018	0.247
AE	0.367	0.374	0.343	0.211	0.513	0.332	0.598	0.374
AERMS	0.327	0.103	0.307	0.091	0.182	0.074	0.246	0.324
Mic	0.500	0.472	0.500	0.532	0.528	0.532	0.419	0.157
Vsx	0.562	0.438	0.072	0.260	0.275	0.175	0.155	0.160
Vsy	0.153	0.349	0.230	0.324	0.556	0.008	0.299	0.118
Vsz	0.472	0.105	0.245	0.498	0.562	0.500	0.209	0.314
Vwx	0.451	0.127	0.287	0.065	0.441	0.508	0.336	0.405
Pwr	0.084	0.356	0.028	0.092	0.453	0.232	0.165	0.119
Edx	0.095	0.466	0.050	0.357	0.360	0.239	0.451	0.502
Edy	0.040	0.188	0.256	0.430	0.433	0.184	0.101	0.182

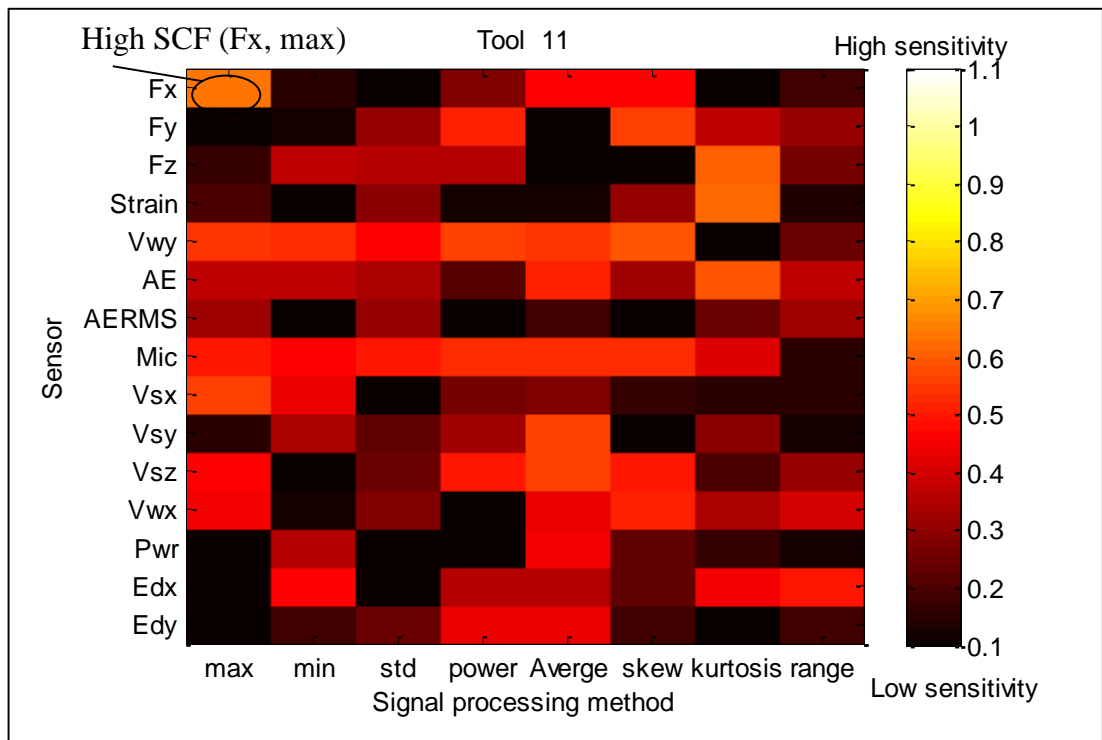


Figure B.10: A graphical presentation of the sensitivity for tool 11 with aluminium sleeve.

Table B.11: The Associated matrix of the system for tool 12 with aluminium sleeve.

Tool 12	Signal Processing Methods							
Sensor	max	min	std	power	average	skew	kurtosis	Range
Fx	0.308	0.353	0.061	0.025	0.379	0.327	0.339	0.009
Fy	0.401	0.408	0.184	0.507	0.472	0.363	0.089	0.268
Fz	0.453	0.546	0.533	0.480	0.453	0.137	0.229	0.470
Strain	0.273	0.011	0.236	0.058	0.281	0.277	0.153	0.190
Vwy	0.198	0.198	0.011	0.114	0.195	0.280	0.005	0.056
AE	0.536	0.561	0.554	0.557	0.347	0.603	0.413	0.550
AERMS	0.515	0.397	0.573	0.526	0.497	0.006	0.125	0.611
Mic	0.286	0.281	0.654	0.519	0.519	0.627	0.295	0.070
Vsx	0.367	0.139	0.183	0.389	0.423	0.368	0.484	0.373
Vsy	0.481	0.288	0.083	0.359	0.439	0.519	0.035	0.479
Vsz	0.620	0.028	0.449	0.005	0.405	0.466	0.066	0.421
Vwx	0.161	0.228	0.340	0.116	0.351	0.510	0.176	0.239
Pwr	0.038	0.041	0.299	0.317	0.177	0.134	0.002	0.002
Edx	0.030	0.337	0.255	0.330	0.333	0.158	0.154	0.304
Edy	0.618	0.729	0.079	0.661	0.667	0.110	0.540	0.260

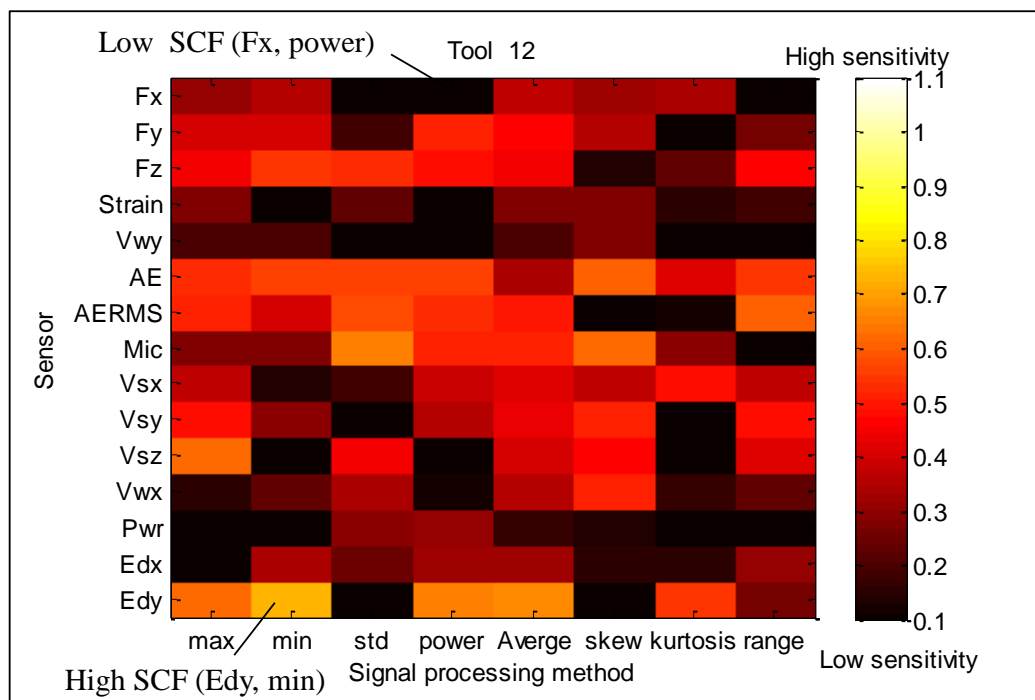


Figure B.11 : A graphical presentation of the sensitivity for tool 12 with aluminium sleeve.

Appendix C: Signals Simplifications (For Chapter 9)

9.2.1.2 Principal Component Analysis (PCA) method

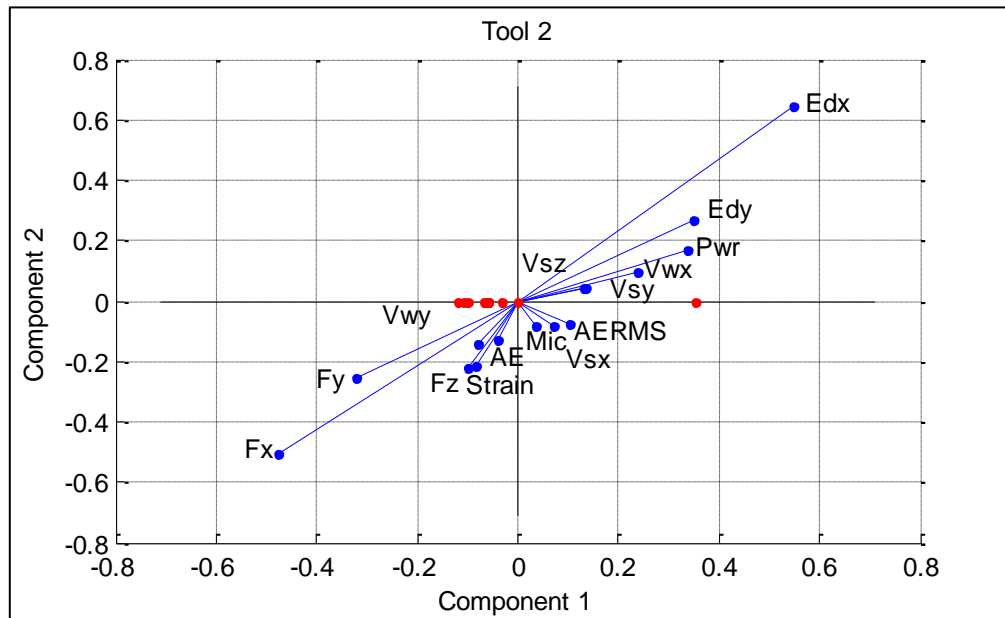


Figure C.1: A plot of the principle components according to eigenvalue of variables in the covariance matrix for tool 2 without sleeve.

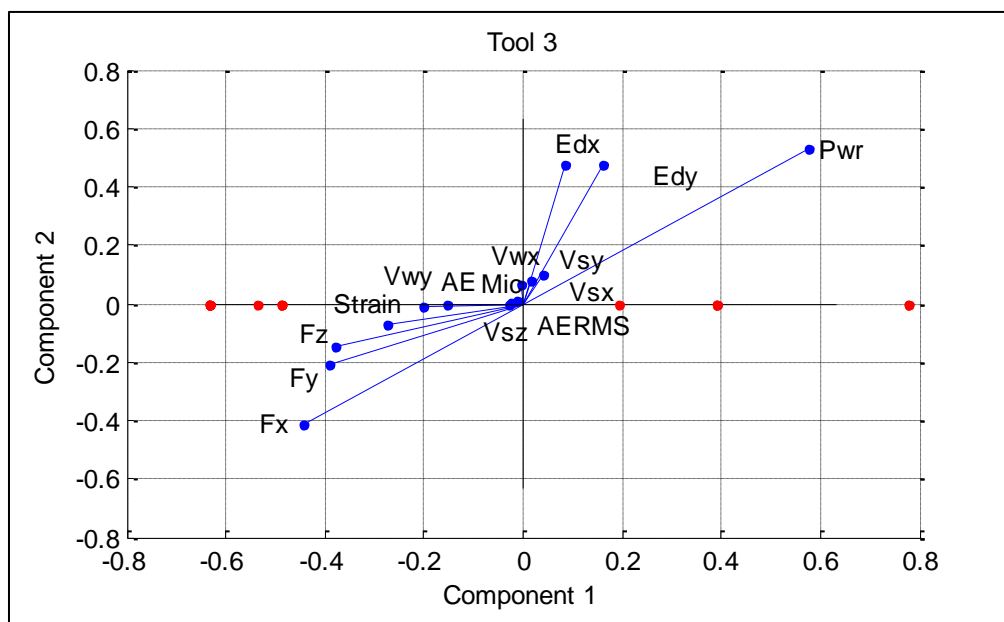


Figure C.2: A plot of the principle components according to eigenvalue of variables in the covariance matrix for tool 3 without sleeve.

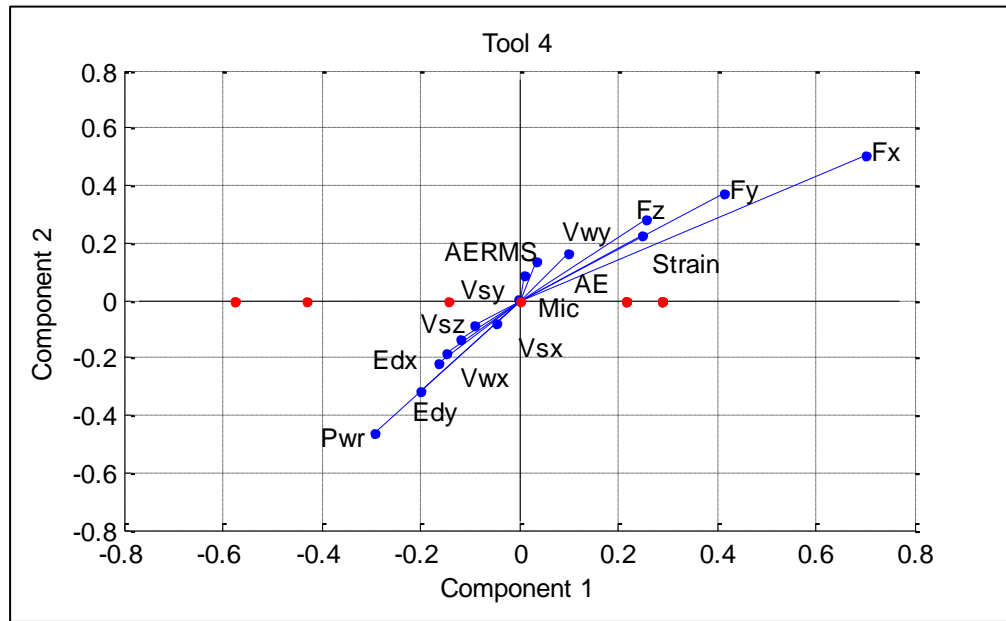


Figure C.3: A plot of the principle components according to eigenvalue of variables in the covariance matrix for tool 4 with rubber sleeve.

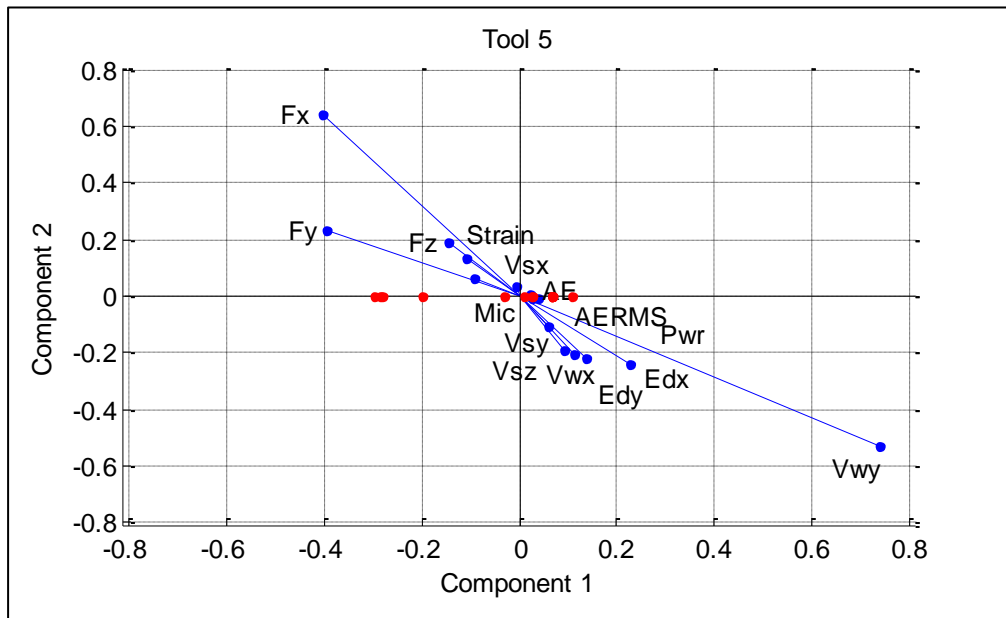


Figure C.4: A plot of the principle components according to eigenvalue of variables in the covariance matrix for tool 5 with rubber sleeve.

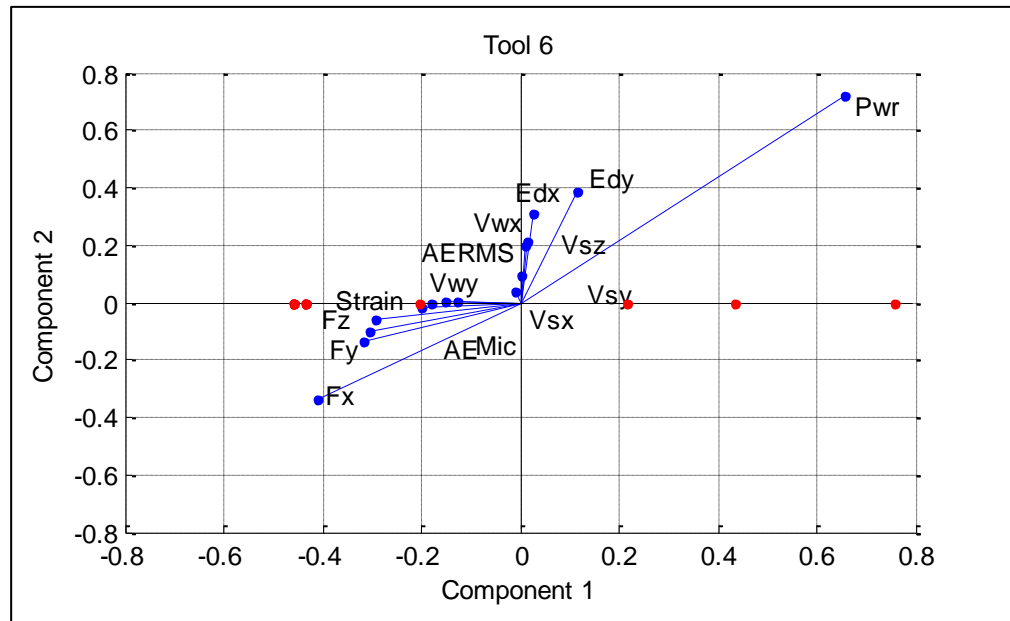


Figure C.5: A plot of the principle components according to eigenvalue of variables in the covariance matrix for tool 6 with rubber sleeve.

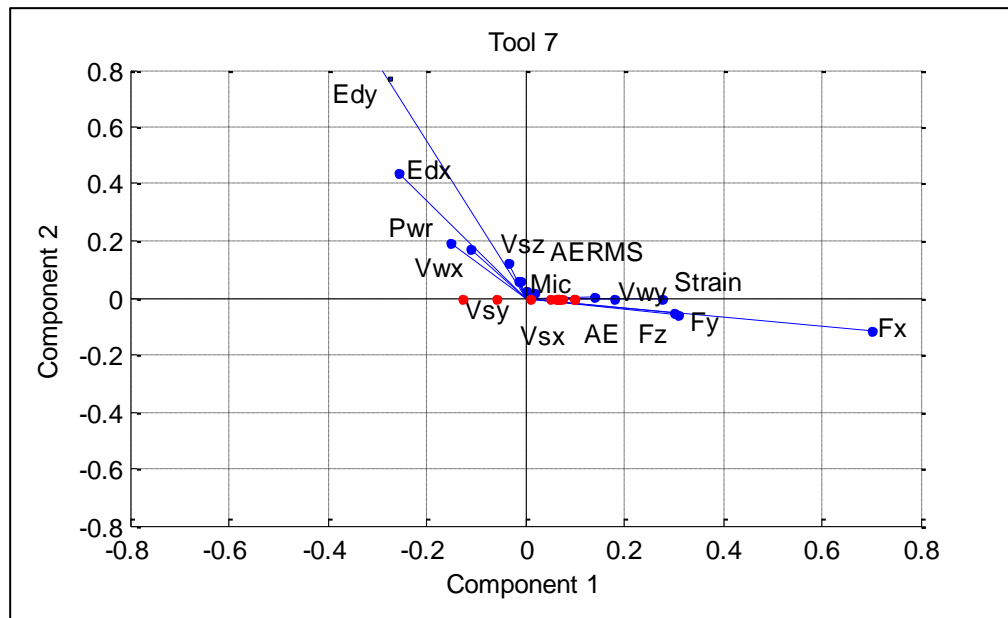


Figure C.6: A plot of the principle components according to eigenvalue of variables in the covariance matrix for tool 7 with copper sleeve.

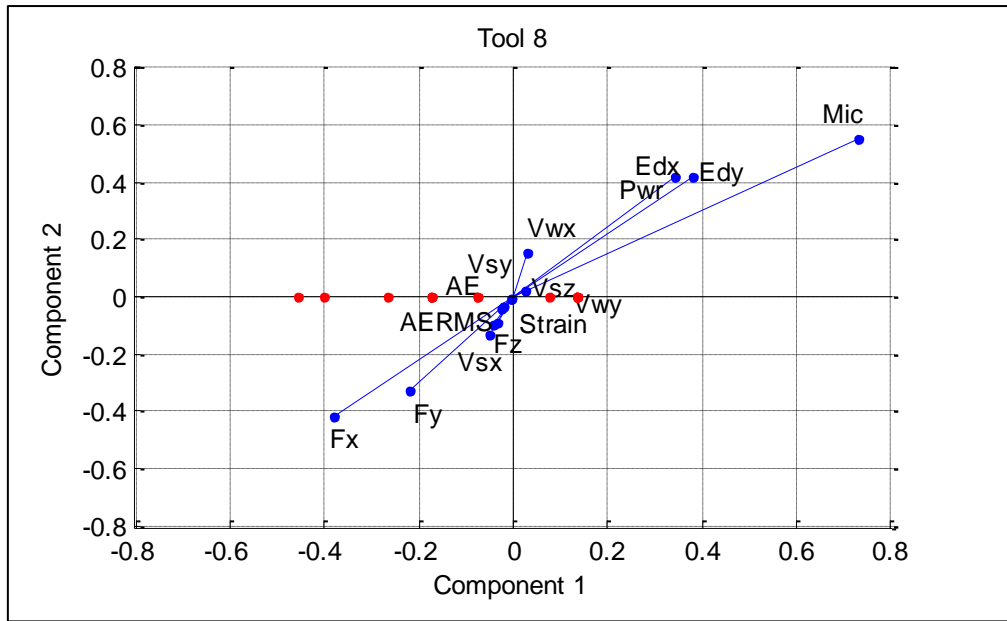


Figure C.7: A plot of the principle components according to eigenvalue of variables in the covariance matrix for tool 8 with copper sleeve.

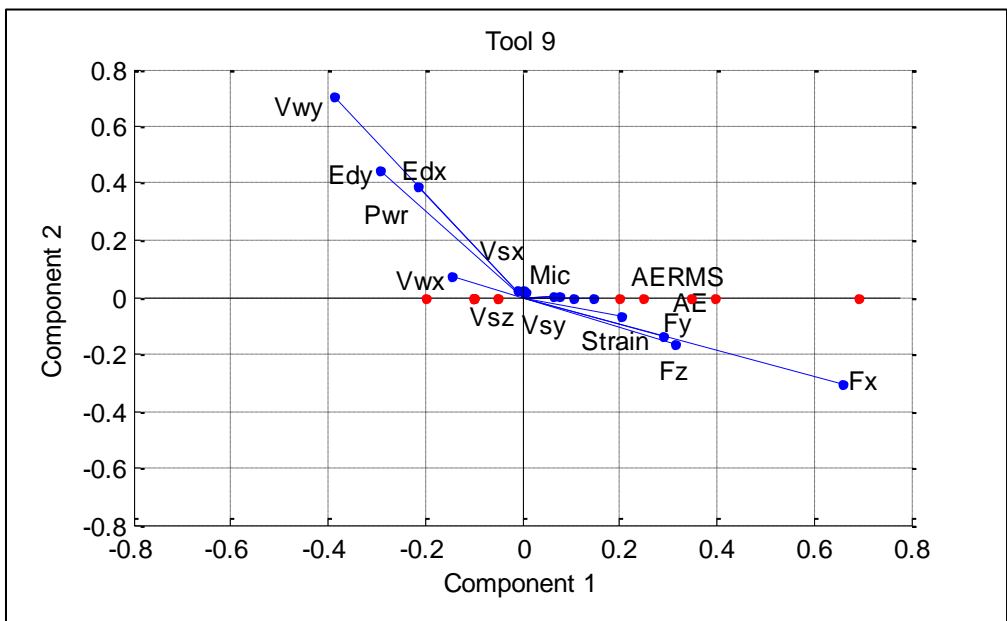


Figure C.8: A plot of the principle components according to eigenvalue of variables in the covariance matrix for tool 9 with copper sleeve.

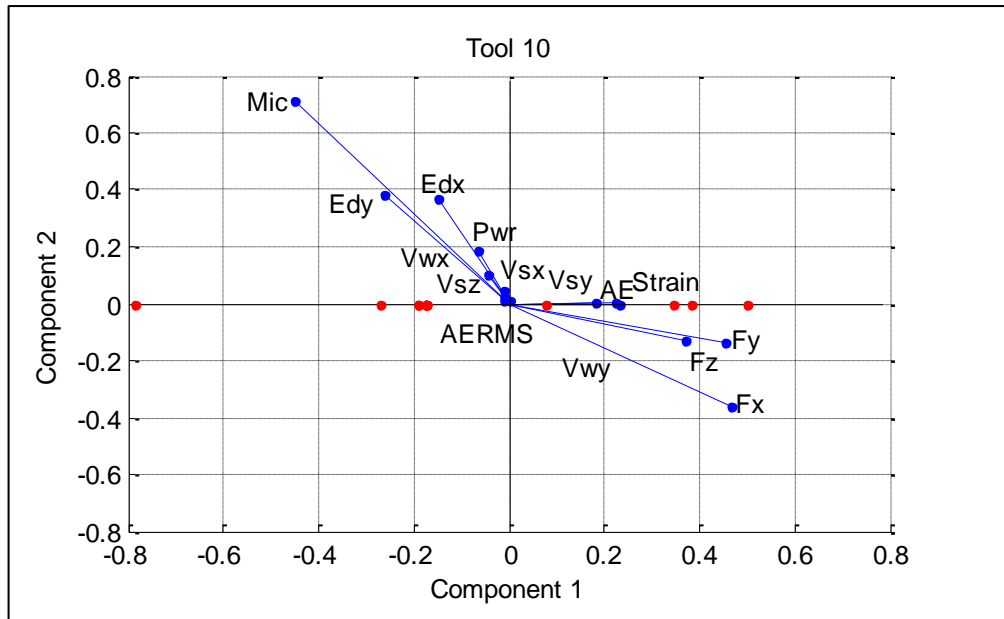


Figure C.9: A plot of the principle components according to eigenvalue of variables in the covariance matrix for tool 10 with aluminium sleeve.

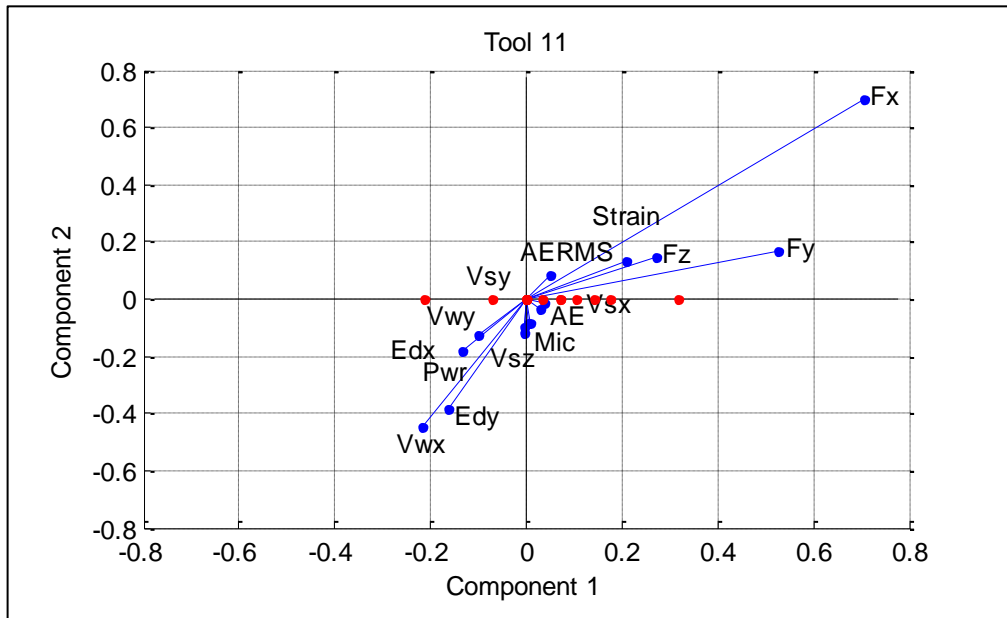


Figure C.10: A plot of the principle components according to eigenvalue of variables in the covariance matrix for tool 11 with aluminium sleeve.

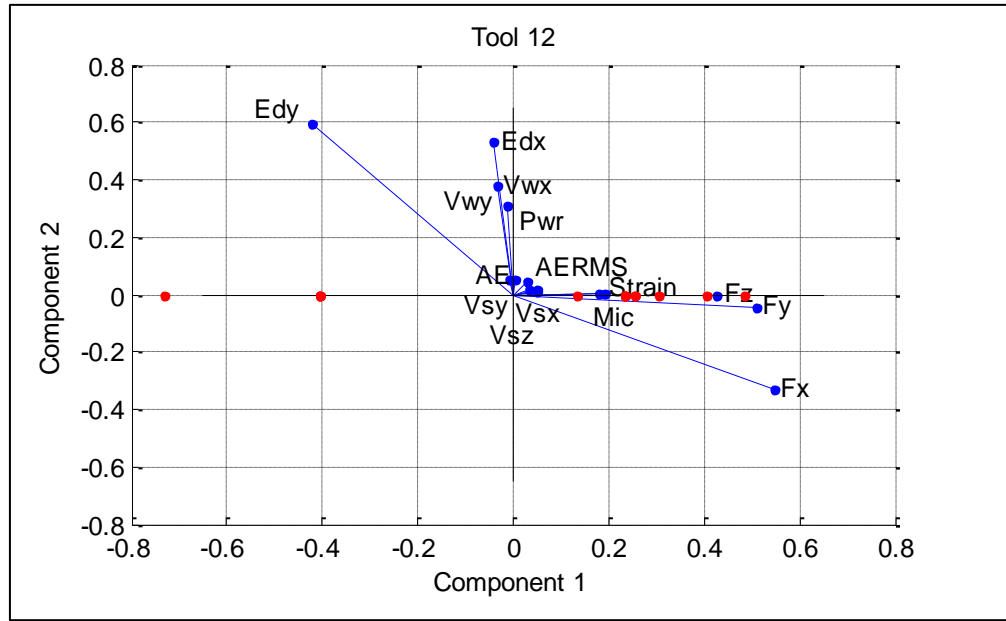


Figure C.11: A plot of the principle components according to eigenvalue of variables in the covariance matrix for tool 12 with aluminium sleeve.

Table C.1: The Eigenvalue Sensory Matrix (EVSM) of the system for tool 2 without sleeve.

	Principal Component Analysis														
Sensor	PC1	PC2	PC3	PC4	PC5	PC6	PC7	PC8	PC9	PC10	PC11	PC12	PC13	PC14	PC15
Fx	0.27	0.57	0.44	0.27	0.15	0.40	0.46	0.56	0.53	0.51	0.21	0.58	0.52	0.53	0.35
Fy	0.27	0.28	0.43	0.23	0.12	0.39	0.38	0.12	0.12	0.36	0.15	0.40	0.10	0.44	0.09
Fz	0.27	0.25	0.34	0.20	0.10	0.30	0.27	0.07	0.11	0.24	0.13	0.17	0.01	0.25	0.03
Strain	0.27	0.18	0.30	0.12	0.08	0.20	0.22	0.03	0.07	0.13	0.07	0.10	0.01	0.23	0.01
Vwy	0.26	0.15	0.09	0.11	0.08	0.19	0.08	0.03	0.03	0.10	0.02	0.10	0.02	0.19	0.01
AE	0.25	0.03	0.03	0.10	0.00	0.12	0.05	0.01	0.01	0.00	0.01	0.10	0.04	0.17	0.02
AERMS	0.25	0.05	0.04	0.07	0.01	0.12	0.03	0.02	0.02	0.01	0.00	0.07	0.08	0.02	0.03
Mic	0.22	0.06	0.09	0.05	0.05	0.04	0.01	0.03	0.06	0.10	0.08	0.04	0.12	0.02	0.07
Vsx	0.22	0.10	0.09	0.02	0.14	0.04	0.02	0.06	0.11	0.12	0.11	0.03	0.18	0.07	0.08
Vsy	0.26	0.19	0.21	0.06	0.16	0.05	0.06	0.09	0.19	0.15	0.11	0.02	0.25	0.11	0.08
Vsz	0.26	0.20	0.22	0.08	0.25	0.06	0.11	0.11	0.27	0.24	0.13	0.01	0.28	0.15	0.12
Vwx	0.27	0.22	0.22	0.08	0.26	0.13	0.15	0.18	0.27	0.24	0.25	0.14	0.29	0.18	0.15
Pwr	0.27	0.22	0.25	0.09	0.36	0.19	0.24	0.21	0.31	0.27	0.28	0.32	0.30	0.21	0.19
Edx	0.87	0.32	0.30	0.16	0.38	0.39	0.44	0.41	0.33	0.34	0.33	0.34	0.41	0.26	0.56
Edy	0.27	0.44	0.31	0.24	0.70	0.53	0.47	0.63	0.53	0.42	0.78	0.44	0.42	0.41	0.68

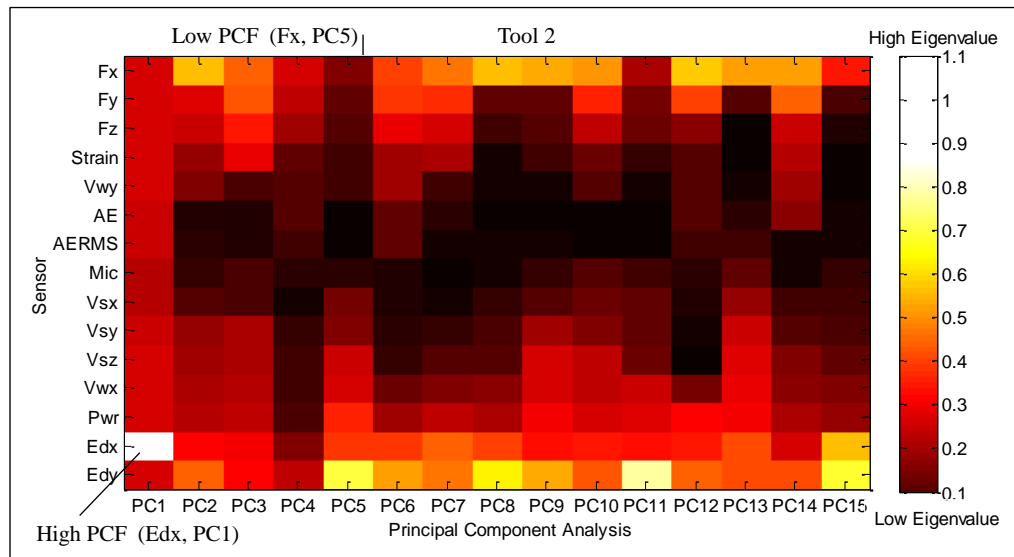


Figure C.12: A graphical presentation of the EVSM for tool 2 without sleeve.

Table C.2: The Eigenvalue Sensory Matrix (EVSM) of the system for tool 3 without sleeve.

Sensor	Principal component Analysis														
	PC1	PC2	PC3	PC4	PC5	PC6	PC7	PC8	PC9	PC10	PC11	PC12	PC13	PC14	PC15
Fx	0.33	0.41	0.46	0.15	0.26	0.22	0.30	0.70	0.60	0.69	0.46	0.61	0.59	0.67	0.80
Fy	0.32	0.40	0.46	0.15	0.19	0.15	0.05	0.30	0.46	0.45	0.44	0.33	0.43	0.07	0.26
Fz	0.32	0.38	0.19	0.13	0.17	0.12	0.03	0.22	0.34	0.28	0.27	0.32	0.23	0.02	0.24
Strain	0.31	0.20	0.15	0.12	0.17	0.11	0.01	0.20	0.23	0.15	0.11	0.30	0.17	0.01	0.23
Vwy	0.30	0.18	0.15	0.10	0.16	0.07	0.00	0.19	0.08	0.11	0.09	0.17	0.12	0.00	0.14
AE	0.29	0.14	0.05	0.07	0.10	0.01	0.02	0.18	0.04	0.05	0.00	0.11	0.11	0.01	0.10
AERMS	0.23	0.10	0.04	0.06	0.03	0.00	0.03	0.17	0.02	0.04	0.02	0.01	0.07	0.04	0.00
Mic	0.19	0.02	0.04	0.02	0.00	0.00	0.05	0.12	0.00	0.00	0.05	0.00	0.03	0.06	0.00
Vsx	0.15	0.05	0.04	0.02	0.00	0.14	0.11	0.10	0.01	0.03	0.07	0.01	0.01	0.07	0.02
Vsy	0.13	0.11	0.08	0.02	0.01	0.14	0.14	0.09	0.02	0.05	0.09	0.03	0.00	0.11	0.03
Vsz	0.03	0.17	0.08	0.06	0.05	0.15	0.31	0.01	0.04	0.05	0.09	0.04	0.07	0.18	0.04
Vwx	0.16	0.23	0.15	0.10	0.12	0.17	0.32	0.00	0.17	0.06	0.16	0.07	0.13	0.20	0.11
Pwr	0.25	0.93	0.23	0.11	0.13	0.17	0.37	0.08	0.19	0.13	0.24	0.20	0.16	0.26	0.12
Edx	0.31	0.34	0.86	0.11	0.17	0.19	0.42	0.19	0.23	0.23	0.27	0.23	0.21	0.31	0.22
Edy	0.32	0.40	0.50	0.23	0.86	0.39	0.60	0.40	0.35	0.37	0.57	0.43	0.52	0.54	0.29

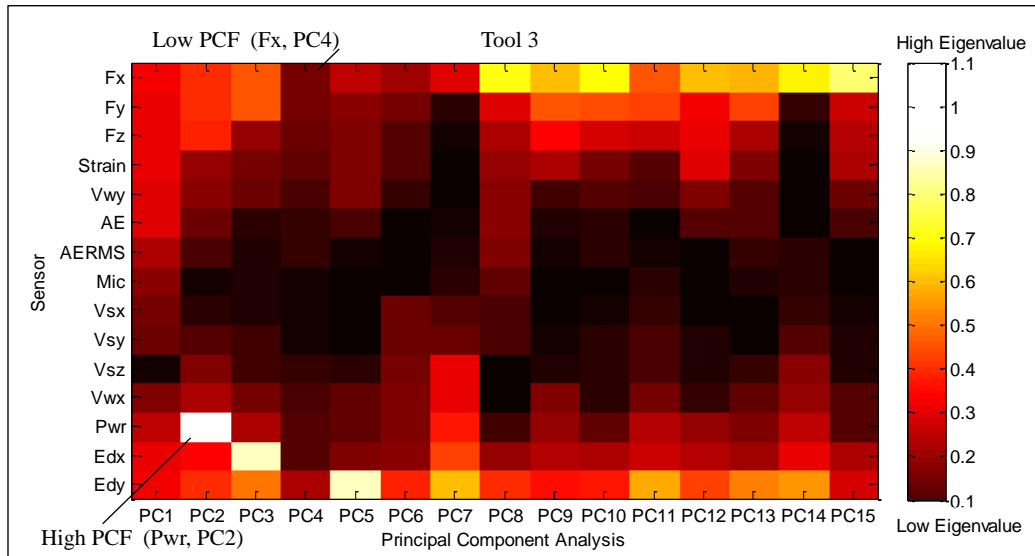


Figure C.13: A graphical presentation of the EVSM for tool 3 without sleeve.

Table C.3: The Eigenvalue Sensory Matrix (EVSM) of the system for tool 4 with rubber sleeve.

Sensor	Principal component Analysis														
	PC1	PC2	PC3	PC4	PC5	PC6	PC7	PC8	PC9	PC 10	PC 11	PC 12	PC 13	PC 14	PC 15
Fx	0.32	0.80	0.44	0.29	0.35	0.53	0.28	0.37	0.27	0.60	0.29	0.47	0.69	0.36	0.47
Fy	0.31	0.45	0.35	0.09	0.27	0.45	0.27	0.37	0.24	0.33	0.18	0.47	0.35	0.31	0.26
Fz	0.31	0.36	0.31	0.01	0.20	0.28	0.16	0.34	0.20	0.26	0.13	0.39	0.34	0.31	0.26
Strain	0.26	0.31	0.15	0.04	0.07	0.17	0.13	0.28	0.16	0.20	0.05	0.27	0.23	0.25	0.13
Vwy	0.24	0.22	0.07	0.04	0.06	0.09	0.09	0.25	0.10	0.19	0.05	0.23	0.07	0.14	0.11
AE	0.06	0.20	0.05	0.04	0.00	0.00	0.04	0.20	0.08	0.16	0.01	0.08	0.05	0.14	0.06
AERMS	0.01	0.13	0.03	0.10	0.01	0.00	0.02	0.19	0.01	0.14	0.06	0.02	0.01	0.13	0.05
Mic	0.12	0.10	0.02	0.11	0.02	0.03	0.03	0.00	0.07	0.13	0.14	0.04	0.05	0.09	0.01
Vsx	0.17	0.06	0.05	0.12	0.07	0.06	0.07	0.08	0.10	0.11	0.17	0.04	0.07	0.08	0.05
Vsy	0.24	0.03	0.11	0.14	0.09	0.09	0.09	0.12	0.14	0.08	0.20	0.14	0.10	0.15	0.10
Vsz	0.25	0.03	0.11	0.15	0.17	0.10	0.12	0.15	0.25	0.02	0.22	0.15	0.12	0.16	0.14
Vwx	0.30	0.12	0.22	0.17	0.25	0.15	0.21	0.16	0.27	0.04	0.35	0.21	0.18	0.18	0.19
Pwr	0.30	0.16	0.26	0.17	0.30	0.18	0.26	0.23	0.28	0.13	0.36	0.22	0.19	0.20	0.29
Edx	0.32	0.19	0.39	0.32	0.36	0.24	0.39	0.33	0.47	0.14	0.40	0.23	0.20	0.39	0.40
Edy	0.32	0.35	0.48	0.47	0.64	0.50	0.69	0.38	0.54	0.49	0.56	0.29	0.31	0.52	0.54

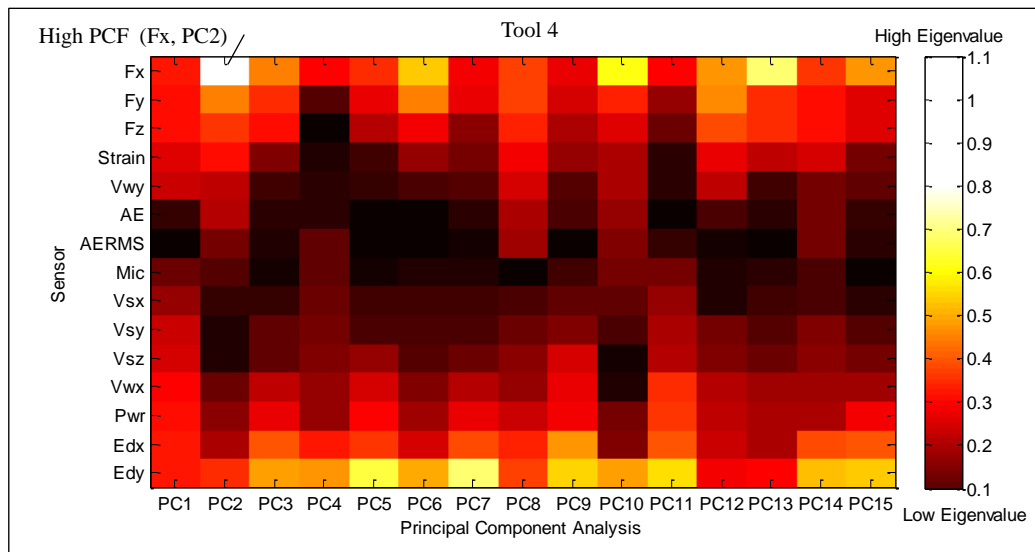


Figure C.14: A graphical presentation of the EVSM for tool 4 with rubber sleeve.

Table C.4: The Eigenvalue Sensory Matrix (EVSM) of the system for tool 5 with rubber sleeve.

	Principal component Analysis														
Sensor	PC1	PC2	PC3	PC4	PC5	PC6	PC7	PC8	PC9	PC 10	PC 11	PC 12	PC 13	PC 14	PC 15
Fx	0.31	0.52	0.41	0.25	0.71	0.83	0.59	0.44	0.49	0.67	0.50	0.42	0.21	0.12	0.45
Fy	0.30	0.50	0.28	0.17	0.22	0.18	0.37	0.16	0.30	0.38	0.13	0.11	0.13	0.09	0.35
Fz	0.30	0.34	0.24	0.15	0.18	0.16	0.32	0.15	0.22	0.30	0.12	0.10	0.12	0.09	0.20
Strain	0.30	0.08	0.22	0.08	0.12	0.15	0.22	0.08	0.15	0.25	0.07	0.07	0.09	0.06	0.20
Vwy	0.21	0.88	0.18	0.01	0.03	0.14	0.20	0.05	0.14	0.14	0.01	0.06	0.02	0.03	0.10
AE	0.01	0.03	0.17	0.06	0.00	0.14	0.16	0.05	0.13	0.13	0.00	0.06	0.02	0.02	0.10
AERMS	0.00	0.01	0.16	0.10	0.01	0.13	0.09	0.03	0.08	0.05	0.00	0.03	0.06	0.01	0.09
Mic	0.01	0.03	0.06	0.10	0.03	0.11	0.05	0.02	0.06	0.01	0.10	0.00	0.07	0.01	0.02
Vsx	0.21	0.04	0.02	0.17	0.03	0.08	0.02	0.01	0.04	0.03	0.11	0.02	0.10	0.05	0.03
Vsy	0.30	0.08	0.00	0.18	0.07	0.04	0.06	0.08	0.13	0.03	0.20	0.04	0.11	0.05	0.05
Vsz	0.30	0.08	0.07	0.20	0.08	0.04	0.10	0.08	0.18	0.05	0.31	0.05	0.13	0.07	0.05
Vwx	0.30	0.09	0.14	0.22	0.09	0.05	0.12	0.08	0.20	0.07	0.33	0.08	0.13	0.08	0.09
Pwr	0.30	0.12	0.19	0.44	0.17	0.07	0.15	0.11	0.20	0.13	0.34	0.47	0.24	0.21	0.13
Edx	0.31	0.26	0.34	0.44	0.41	0.12	0.25	0.16	0.37	0.25	0.37	0.48	0.59	0.61	0.48
Edy	0.31	0.51	0.62	0.56	0.43	0.22	0.42	0.05	0.54	0.36	0.44	0.57	0.67	0.73	0.55

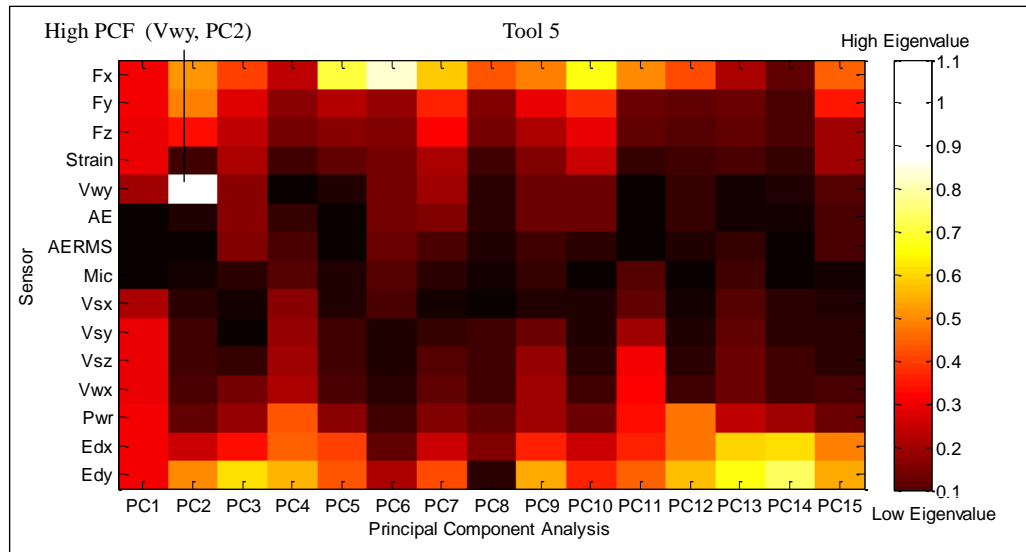


Figure C.15: A graphical presentation of the EVSM for tool 5 with rubber sleeve.

Table C.5: The Eigenvalue Sensory Matrix (EVSM) of the system for tool 6 with rubber sleeve.

Sensor	Principal Component Analysis														
	PC1	PC2	PC3	PC4	PC5	PC6	PC7	PC8	PC9	PC 10	PC 11	PC 12	PC 13	PC 14	PC 15
Fx	0.33	0.46	0.53	0.20	0.14	0.29	0.71	0.39	0.49	0.37	0.38	0.60	0.45	0.73	0.44
Fy	0.33	0.45	0.49	0.20	0.07	0.18	0.40	0.34	0.39	0.33	0.34	0.51	0.32	0.32	0.26
Fz	0.32	0.29	0.27	0.18	0.06	0.16	0.27	0.27	0.35	0.32	0.21	0.19	0.31	0.30	0.17
Strain	0.32	0.22	0.21	0.08	0.06	0.08	0.18	0.20	0.31	0.22	0.20	0.19	0.12	0.27	0.03
Vwy	0.29	0.18	0.20	0.07	0.04	0.08	0.18	0.17	0.29	0.21	0.18	0.16	0.11	0.20	0.00
AE	0.12	0.06	0.14	0.02	0.02	0.04	0.18	0.16	0.13	0.19	0.06	0.12	0.04	0.16	0.04
AERMS	0.10	0.02	0.14	0.02	0.00	0.04	0.17	0.06	0.07	0.00	0.00	0.06	0.00	0.13	0.05
Mic	0.07	0.00	0.13	0.00	0.07	0.00	0.15	0.04	0.01	0.00	0.01	0.05	0.02	0.12	0.08
Vsx	0.00	0.04	0.12	0.02	0.07	0.05	0.00	0.00	0.00	0.06	0.07	0.00	0.07	0.05	0.09
Vsy	0.00	0.15	0.09	0.04	0.09	0.06	0.01	0.00	0.07	0.07	0.09	0.10	0.07	0.02	0.09
Vsz	0.13	0.16	0.01	0.05	0.10	0.07	0.03	0.01	0.10	0.09	0.12	0.10	0.10	0.00	0.25
Vwx	0.32	0.17	0.05	0.12	0.18	0.22	0.03	0.03	0.10	0.09	0.13	0.10	0.24	0.06	0.27
Pwr	0.33	0.88	0.24	0.19	0.22	0.24	0.09	0.22	0.12	0.40	0.28	0.15	0.35	0.07	0.30
Edx	0.33	0.33	0.24	0.25	0.29	0.27	0.14	0.30	0.35	0.40	0.34	0.31	0.39	0.16	0.44
Edy	0.34	0.44	0.36	0.87	0.20	0.81	0.30	0.65	0.36	0.43	0.63	0.34	0.48	0.26	0.51

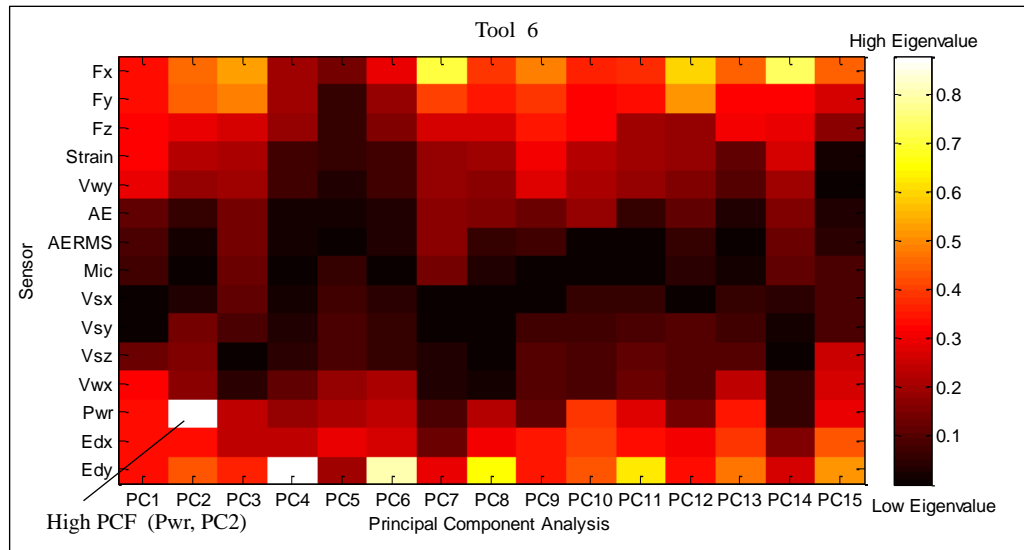


Figure C.16: A graphical presentation of the EVSM for tool 6 with rubber sleeve.

Table C.6: The Eigenvalue Sensory Matrix(EVSM) of the system for tool 7 with copper sleeve.

	Principal component Analysis														
Sensor	PC1	PC2	PC3	PC4	PC5	PC6	PC7	PC8	PC9	PC10	PC11	PC12	PC13	PC14	PC15
Fx	0.31	0.82	0.38	0.50	0.22	0.78	0.64	0.28	0.39	0.45	0.47	0.49	0.57	0.39	0.54
Fy	0.30	0.49	0.37	0.27	0.20	0.13	0.43	0.07	0.30	0.11	0.41	0.47	0.25	0.18	0.45
Fz	0.30	0.25	0.27	0.26	0.16	0.10	0.25	0.02	0.23	0.10	0.31	0.26	0.25	0.16	0.43
Strain	0.29	0.16	0.26	0.06	0.14	0.03	0.23	0.01	0.20	0.05	0.19	0.21	0.16	0.13	0.20
Vwy	0.29	0.12	0.23	0.04	0.10	0.02	0.20	0.00	0.18	0.03	0.18	0.17	0.14	0.13	0.20
AE	0.28	0.12	0.22	0.01	0.06	0.01	0.11	0.02	0.17	0.05	0.14	0.13	0.10	0.06	0.15
AERMS	0.26	0.10	0.13	0.02	0.06	0.01	0.10	0.02	0.17	0.06	0.08	0.13	0.06	0.04	0.15
Mic	0.24	0.10	0.06	0.04	0.01	0.01	0.06	0.05	0.08	0.06	0.05	0.12	0.06	0.01	0.00
Vsx	0.22	0.02	0.01	0.06	0.01	0.02	0.01	0.07	0.01	0.21	0.01	0.00	0.03	0.00	0.04
Vsy	0.21	0.04	0.01	0.07	0.10	0.05	0.11	0.15	0.14	0.22	0.06	0.03	0.03	0.05	0.04
Vsz	0.13	0.15	0.25	0.13	0.17	0.06	0.12	0.20	0.17	0.30	0.14	0.07	0.13	0.11	0.05
Vwx	0.05	0.19	0.29	0.14	0.18	0.06	0.12	0.26	0.19	0.34	0.19	0.07	0.17	0.14	0.08
Pwr	0.27	0.24	0.32	0.15	0.21	0.11	0.14	0.37	0.24	0.34	0.22	0.18	0.34	0.19	0.13
Edx	0.28	0.35	0.32	0.18	0.32	0.13	0.27	0.38	0.43	0.40	0.33	0.19	0.40	0.26	0.18
Edy	0.30	0.36	0.33	0.27	0.80	0.56	0.30	0.71	0.49	0.43	0.46	0.53	0.41	0.79	0.38

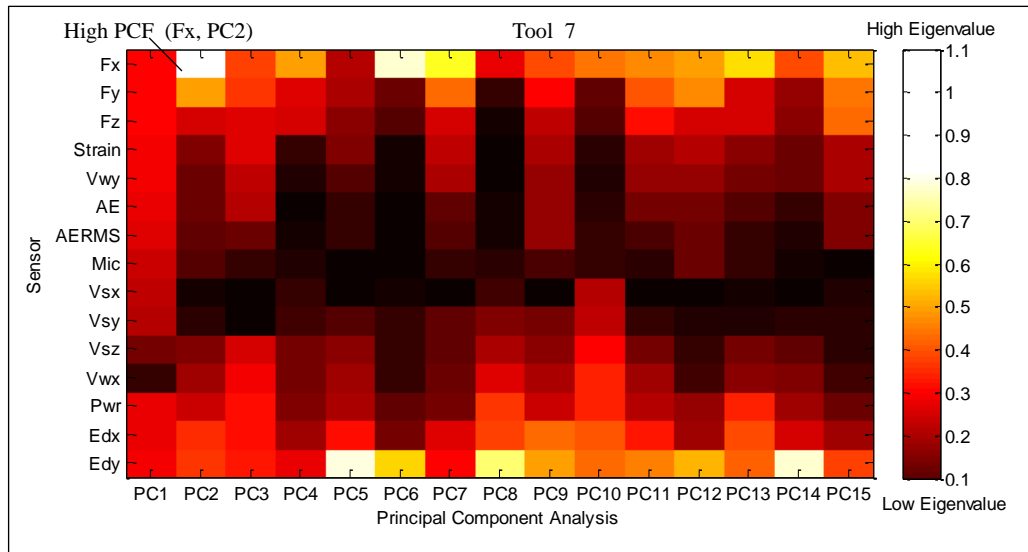


Figure C.17: A graphical presentation of the EVSM for tool 7 with copper sleeve.

Table C.7: The Eigenvalue Sensory Matrix (EVSM) of the system for tool 8 with copper sleeve.

		Principal component Analysis														
Sensor	PC1	PC2	PC3	PC4	PC5	PC6	PC7	PC8	PC9	PC10	PC11	PC12	PC13	PC14	PC15	
Fx	0.31	0.48	0.47	0.11	0.50	0.37	0.51	0.30	0.58	0.33	0.48	0.08	0.81	0.35	0.79	
Fy	0.30	0.47	0.36	0.10	0.11	0.16	0.31	0.23	0.47	0.31	0.35	0.06	0.51	0.28	0.34	
Fz	0.30	0.32	0.19	0.10	0.06	0.08	0.25	0.14	0.27	0.17	0.26	0.05	0.20	0.22	0.18	
Strain	0.30	0.26	0.16	0.06	0.02	0.06	0.23	0.11	0.19	0.15	0.22	0.01	0.14	0.20	0.14	
Vwy	0.29	0.11	0.14	0.05	0.03	0.05	0.15	0.10	0.06	0.05	0.18	0.02	0.07	0.15	0.08	
AE	0.03	0.07	0.00	0.03	0.03	0.03	0.14	0.09	0.05	0.02	0.17	0.04	0.06	0.10	0.02	
AERMS	0.02	0.05	0.04	0.03	0.03	0.03	0.14	0.08	0.04	0.00	0.08	0.08	0.05	0.07	0.02	
Mic	0.93	0.23	0.26	0.16	0.34	0.10	0.10	0.08	0.09	0.07	0.05	0.10	0.02	0.03	0.01	
Vsx	0.22	0.01	0.07	0.06	0.06	0.02	0.00	0.02	0.02	0.04	0.04	0.11	0.01	0.00	0.05	
Vsy	0.24	0.00	0.08	0.08	0.07	0.03	0.03	0.02	0.07	0.12	0.12	0.16	0.01	0.03	0.07	
Vsz	0.26	0.03	0.13	0.11	0.08	0.11	0.08	0.04	0.07	0.19	0.15	0.19	0.01	0.07	0.17	
Vwx	0.31	0.05	0.20	0.11	0.18	0.12	0.11	0.09	0.09	0.25	0.20	0.29	0.04	0.10	0.20	
Pwr	0.31	0.12	0.31	0.11	0.26	0.28	0.14	0.19	0.19	0.30	0.27	0.36	0.04	0.21	0.20	
Edx	0.31	0.32	0.36	0.21	0.42	0.39	0.23	0.58	0.28	0.47	0.39	0.52	0.06	0.37	0.21	
Edy	0.31	0.50	0.52	0.20	0.66	0.75	0.61	0.65	0.43	0.56	0.40	0.64	0.07	0.69	0.21	

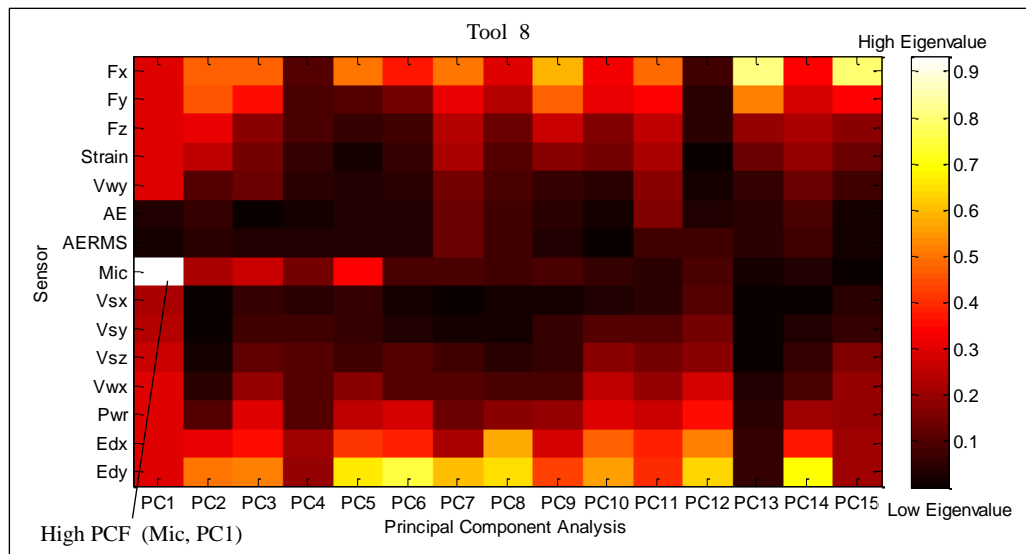


Figure C.18: A graphical presentation of the EVSM for tool 8 with copper sleeve.

Table C.8: The Eigenvalue Sensory Matrix (EVSM) of the system for tool 9 with copper sleeve.

Sensor	Principal component Analysis														
	PC1	PC2	PC3	PC4	PC5	PC6	PC7	PC8	PC9	PC10	PC11	PC12	PC13	PC14	PC15
Fx	0.90	0.56	0.23	0.21	0.30	0.30	0.74	0.65	0.62	0.79	0.34	0.32	0.70	0.87	0.65
Fy	0.29	0.55	0.21	0.20	0.26	0.23	0.31	0.42	0.38	0.36	0.25	0.30	0.25	0.22	0.50
Fz	0.29	0.24	0.20	0.17	0.22	0.20	0.28	0.37	0.34	0.08	0.19	0.25	0.25	0.21	0.29
Strain	0.28	0.13	0.17	0.16	0.16	0.19	0.19	0.31	0.31	0.04	0.12	0.19	0.18	0.17	0.11
Vwy	0.26	0.10	0.08	0.12	0.15	0.08	0.18	0.18	0.24	0.03	0.10	0.17	0.13	0.06	0.08
AE	0.08	0.08	0.06	0.11	0.14	0.04	0.11	0.13	0.23	0.02	0.05	0.16	0.08	0.03	0.07
AERMS	0.06	0.04	0.06	0.03	0.14	0.04	0.05	0.10	0.23	0.01	0.04	0.06	0.06	0.02	0.06
Mic	0.19	0.03	0.08	0.02	0.08	0.02	0.02	0.10	0.04	0.04	0.03	0.02	0.02	0.01	0.05
Vsx	0.23	0.00	0.09	0.04	0.04	0.04	0.10	0.06	0.01	0.04	0.02	0.02	0.01	0.01	0.03
Vsy	0.27	0.01	0.13	0.05	0.05	0.04	0.11	0.06	0.00	0.04	0.02	0.04	0.00	0.00	0.01
Vsz	0.28	0.01	0.24	0.06	0.08	0.05	0.12	0.03	0.00	0.12	0.00	0.08	0.01	0.00	0.01
Vwx	0.29	0.17	0.28	0.07	0.08	0.08	0.17	0.00	0.06	0.12	0.03	0.11	0.02	0.02	0.05
Pwr	0.29	0.23	0.31	0.09	0.17	0.15	0.18	0.06	0.07	0.14	0.13	0.14	0.12	0.07	0.17
Edx	0.30	0.26	0.41	0.10	0.22	0.20	0.18	0.10	0.10	0.15	0.53	0.54	0.15	0.22	0.29
Edy	0.30	0.38	0.63	0.20	0.78	0.83	0.25	0.27	0.29	0.40	0.68	0.56	0.54	0.25	0.30

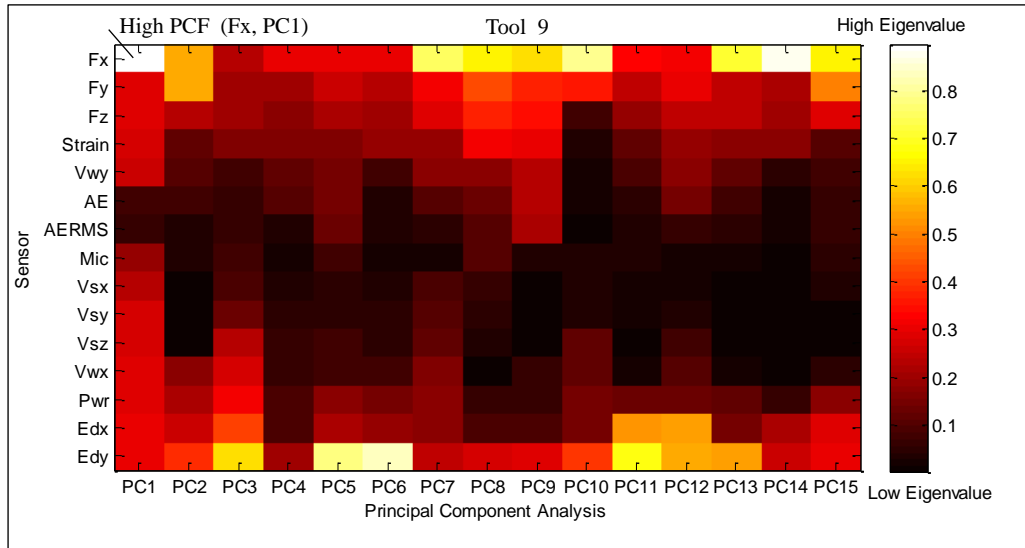


Figure C.19: A graphical presentation of the EVSM for tool 9 with copper sleeve.

Table C.9: The Eigenvalue Sensory Matrix (EVSM) of the system for tool 10 with aluminium sleeve.

	Principal component Analysis														
Sensor	PC1	PC2	PC3	PC4	PC5	PC6	PC7	PC8	PC9	PC10	PC11	PC12	PC13	PC14	PC15
Fx	0.31	0.53	0.55	0.56	0.12	0.48	0.20	0.82	0.61	0.37	0.86	0.66	0.49	0.11	0.48
Fy	0.31	0.47	0.10	0.26	0.06	0.33	0.15	0.39	0.46	0.19	0.22	0.39	0.24	0.10	0.38
Fz	0.31	0.29	0.05	0.03	0.06	0.29	0.14	0.16	0.06	0.18	0.18	0.33	0.22	0.04	0.27
Strain	0.30	0.12	0.04	0.01	0.04	0.17	0.13	0.15	0.05	0.10	0.10	0.31	0.21	0.03	0.25
Vwy	0.18	0.06	0.02	0.01	0.03	0.17	0.05	0.08	0.04	0.09	0.09	0.29	0.13	0.01	0.10
AE	0.04	0.05	0.03	0.02	0.03	0.16	0.03	0.05	0.04	0.07	0.08	0.19	0.05	0.00	0.08
AERMS	0.02	0.04	0.04	0.02	0.02	0.14	0.03	0.03	0.03	0.00	0.05	0.12	0.04	0.01	0.06
Mic	0.43	0.87	0.28	0.44	0.06	0.12	0.11	0.21	0.10	0.04	0.09	0.10	0.07	0.08	0.01
Vsx	0.25	0.03	0.12	0.05	0.07	0.06	0.04	0.02	0.00	0.07	0.04	0.01	0.01	0.04	0.01
Vsy	0.26	0.03	0.14	0.06	0.07	0.03	0.08	0.02	0.03	0.12	0.02	0.03	0.08	0.05	0.04
Vsz	0.30	0.00	0.15	0.09	0.11	0.12	0.15	0.03	0.10	0.12	0.09	0.04	0.13	0.05	0.08
Vwx	0.30	0.09	0.16	0.11	0.21	0.19	0.16	0.10	0.24	0.21	0.15	0.04	0.25	0.05	0.10
Pwr	0.31	0.10	0.29	0.20	0.33	0.21	0.19	0.10	0.29	0.27	0.16	0.07	0.29	0.20	0.13
Edx	0.31	0.42	0.45	0.37	0.43	0.29	0.21	0.11	0.35	0.52	0.20	0.15	0.43	0.51	0.23
Edy	0.31	0.44	0.55	0.64	0.44	0.53	0.78	0.29	0.37	0.59	0.24	0.23	0.49	0.82	0.62

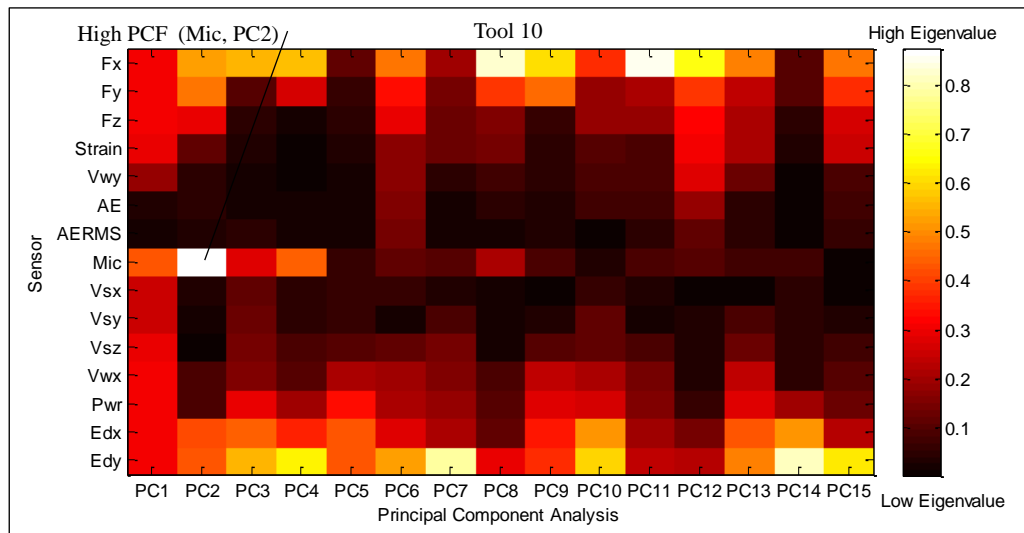


Figure C.20: A graphical presentation of the EVSM for tool 10 with aluminium sleeve.

Table C.10: The Eigenvalue Sensory Matrix (EVSM) of the system for tool 11 with aluminium sleeve.

		Principal component Analysis													
Sensor	PC1	PC2	PC3	PC4	PC5	PC6	PC7	PC8	PC9	PC10	PC11	PC12	PC13	PC14	PC15
Fx	0.81	0.40	0.56	0.60	0.34	0.45	0.35	0.59	0.79	0.29	0.30	0.48	0.31	0.29	0.74
Fy	0.29	0.23	0.43	0.19	0.13	0.15	0.31	0.27	0.23	0.17	0.22	0.40	0.26	0.19	0.27
Fz	0.29	0.16	0.13	0.18	0.09	0.12	0.11	0.22	0.16	0.13	0.13	0.39	0.16	0.16	0.18
Strain	0.29	0.11	0.12	0.15	0.06	0.08	0.11	0.17	0.13	0.04	0.09	0.38	0.14	0.12	0.12
Vwy	0.28	0.07	0.11	0.10	0.05	0.05	0.10	0.12	0.01	0.03	0.06	0.29	0.06	0.08	0.09
AE	0.25	0.02	0.10	0.09	0.03	0.03	0.07	0.06	0.01	0.03	0.00	0.27	0.05	0.04	0.07
AERMS	0.24	0.01	0.03	0.03	0.01	0.01	0.07	0.04	0.01	0.03	0.02	0.19	0.05	0.03	0.03
Mic	0.24	0.13	0.03	0.09	0.01	0.03	0.06	0.03	0.04	0.03	0.03	0.12	0.00	0.04	0.01
Vsx	0.21	0.14	0.04	0.12	0.00	0.06	0.00	0.05	0.05	0.06	0.11	0.07	0.02	0.14	0.00
Vsy	0.04	0.16	0.09	0.15	0.04	0.10	0.08	0.07	0.06	0.07	0.15	0.02	0.02	0.16	0.03
Vsz	0.15	0.19	0.10	0.17	0.07	0.15	0.10	0.09	0.08	0.08	0.18	0.01	0.07	0.24	0.08
Vwx	0.28	0.31	0.12	0.20	0.08	0.28	0.10	0.17	0.11	0.22	0.20	0.03	0.21	0.28	0.17
Pwr	0.29	0.34	0.13	0.24	0.23	0.39	0.11	0.27	0.13	0.32	0.24	0.04	0.22	0.38	0.17
Edx	0.30	0.37	0.24	0.29	0.58	0.42	0.22	0.37	0.16	0.45	0.38	0.14	0.31	0.38	0.25
Edy	0.30	0.55	0.58	0.53	0.67	0.56	0.29	0.47	0.46	0.71	0.73	0.29	0.76	0.59	0.45

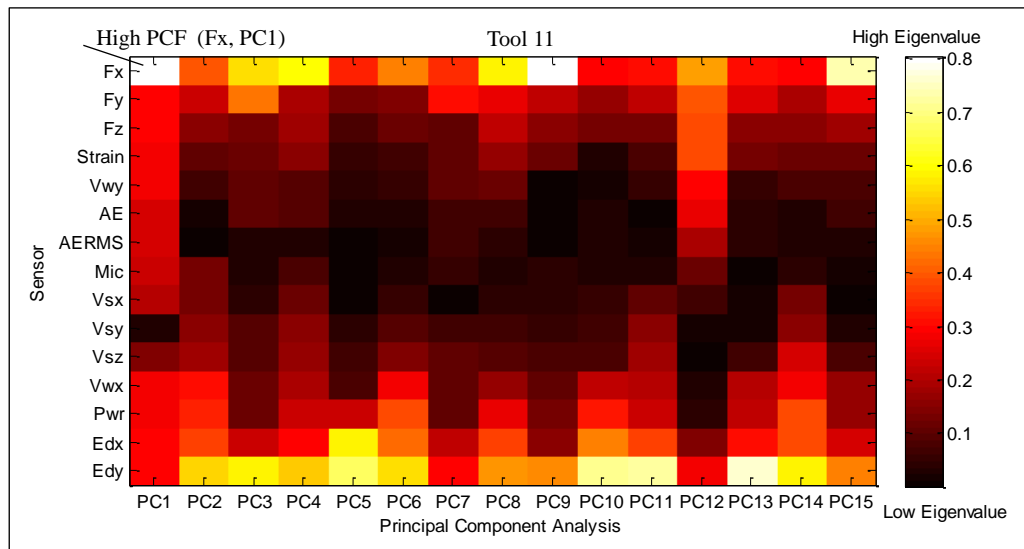


Figure C.21: A graphical presentation of the EVSM for tool 11 with aluminium sleeve.

Table C.11: The Eigenvalue Sensory Matrix (EVSM) of the system for tool 12 with aluminium sleeve.

	Principal Component Analysis														
Sensor	PC1	PC2	PC3	PC4	PC5	PC6	PC7	PC8	PC9	PC10	PC11	PC12	PC13	PC14	PC15
Fx	0.30	0.55	0.49	0.17	0.39	0.80	0.60	0.75	0.35	0.23	0.67	0.71	0.43	0.38	0.25
Fy	0.30	0.55	0.21	0.16	0.15	0.36	0.26	0.41	0.33	0.19	0.35	0.42	0.38	0.25	0.18
Fz	0.30	0.16	0.16	0.13	0.12	0.21	0.21	0.30	0.14	0.08	0.32	0.33	0.26	0.21	0.14
Strain	0.28	0.05	0.14	0.10	0.09	0.13	0.06	0.22	0.06	0.04	0.15	0.27	0.24	0.09	0.05
Vwy	0.22	0.05	0.13	0.09	0.00	0.13	0.03	0.20	0.03	0.01	0.12	0.08	0.23	0.04	0.03
AE	0.22	0.01	0.11	0.04	0.01	0.11	0.02	0.14	0.02	0.00	0.00	0.02	0.17	0.03	0.02
AERMS	0.06	0.01	0.04	0.09	0.01	0.11	0.00	0.11	0.02	0.00	0.01	0.01	0.02	0.02	0.02
Mic	0.05	0.10	0.10	0.10	0.02	0.10	0.07	0.05	0.02	0.01	0.04	0.01	0.01	0.03	0.01
Vsx	0.22	0.11	0.11	0.14	0.05	0.01	0.07	0.01	0.03	0.08	0.06	0.02	0.04	0.06	0.02
Vsy	0.24	0.12	0.11	0.14	0.09	0.01	0.11	0.03	0.09	0.12	0.10	0.04	0.14	0.07	0.07
Vsz	0.28	0.12	0.18	0.19	0.11	0.02	0.12	0.03	0.12	0.28	0.10	0.13	0.15	0.12	0.08
Vwx	0.29	0.18	0.21	0.21	0.18	0.09	0.13	0.05	0.20	0.30	0.11	0.14	0.19	0.29	0.11
Pwr	0.30	0.23	0.24	0.22	0.24	0.13	0.15	0.08	0.26	0.37	0.15	0.16	0.29	0.34	0.17
Edx	0.30	0.31	0.35	0.25	0.28	0.23	0.47	0.09	0.51	0.51	0.34	0.19	0.33	0.51	0.57
Edy	0.82	0.37	0.59	0.30	0.78	0.23	0.48	0.19	0.59	0.57	0.35	0.19	0.44	0.51	0.71

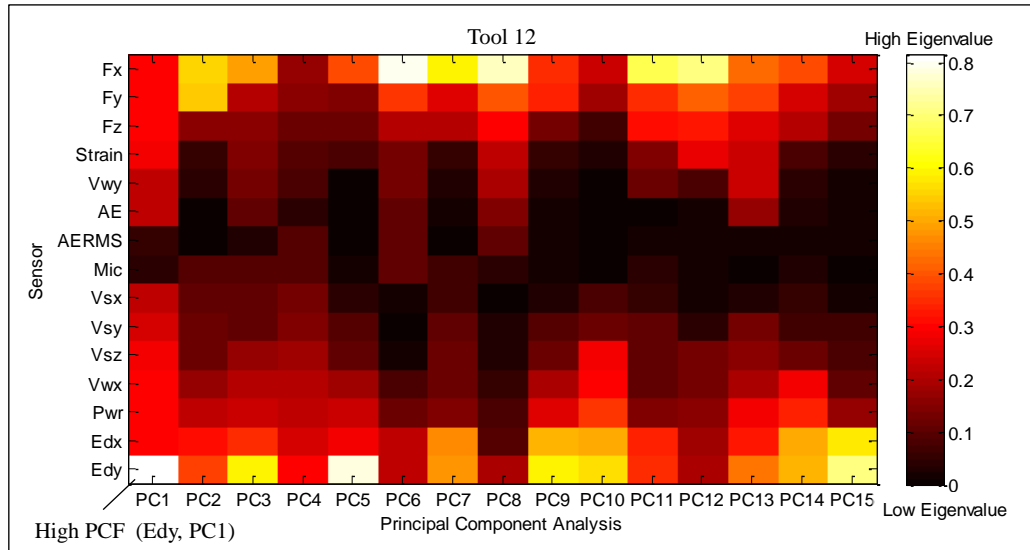


Figure C.22: A graphical presentation of the EVSM for tool 12 with aluminium sleeve.

Appendix D: System Cost and Utilisation (For Chapter 9)

9.4. 1.1 Selection of Sensory Features

1- Tool without sleeve

The same method for the SCF classification which is used in the chapter 8, section 8.4.1, the three systems have the average sensitivity as shown in Figure D.1 for the tool without sleeve. It can be observed that the first system has the most sensitivity features for fixturing system stability and tool wear detection compared to the other systems.

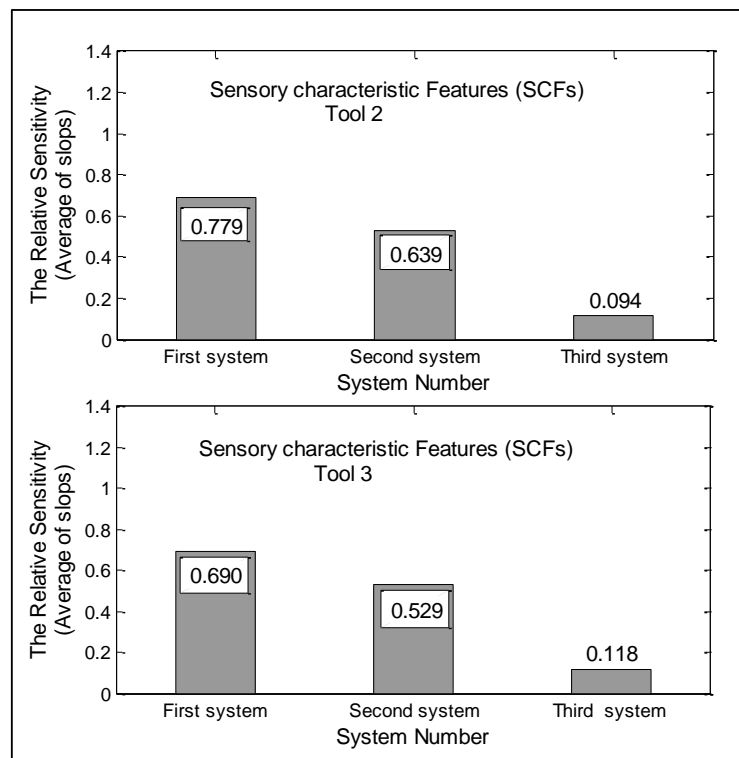


Figure D.1: Comparison between the systems sensitivity for tools without sleeve.

Table D.1: First system with the SCFs sensitivity (LR) for the tools without sleeve.

Tools without sleeve					
Tool 2			Tool 3		
Sensor Signal	SP method	Sens-itivity	Sensor Signal	SP method	Sens-itivity
Edy	power	0.826	Pwr	power	0.924
Edy	average	0.826	Pwr	std	0.909
Vsy	power	0.808	Pwr	range	0.797
Vsy	std	0.794	Pwr	min	0.707
Fy	skew	0.793	Strain	min	0.647
Edx	skew	0.787	Vwy	power	0.596
Vsz	max	0.774	Mic	average	0.586
Fy	std	0.738	Mic	power	0.583
Pwr	power	0.737	Vwy	min	0.580
Edy	max	0.714	Vwy	max	0.578
Average		0.779	Average		0.690

Table D.2: Second system with the SCFs sensitivity (LR) for the tools without sleeve.

Tools without sleeve					
Tool 2			Tool 3		
Sensory Signal	SP method	Sens-itivity	Sensory Signal	SP method	Sens-itivity
Edy	range	0.714	Vwy	average	0.575
Edy	std	0.672	Vsz	skew	0.573
Edy	skew	0.671	Vsy	max	0.536
Pwr	std	0.666	Strain	range	0.535
Fy	range	0.660	Vsz	max	0.524
Vsy	range	0.650	Fx	average	0.522
Vsz	std	0.625	Pwr	max	0.520
Edy	average	0.592	Vsz	average	0.508
Pwr	range	0.574	Edy	std	0.501
Fy	min	0.568	Edy	skew	0.499
Average		0.639	Average		0.529

Table D.3: Third system with the SCFs sensitivity (LR) for the tools without sleeve.

Tools without sleeve					
Tool 2			Tool 3		
Sensory Signal	SP method	Sens-itivity	Sensory Signal	SP method	Sens-itivity
Vsx	kurtosis	0.111	Fy	std	0.143
AE	range	0.109	Vwy	kurtosis	0.141
Fx	std	0.107	Fy	power	0.134
Fz	average	0.099	Fx	min	0.124
Vwx	range	0.090	AE	kurtosis	0.124
Fz	max	0.088	Vsz	kurtosis	0.119
AERMS	max	0.086	Vsy	average	0.107
AERMS	power	0.086	Vsx	skew	0.103
Edy	kurtosis	0.084	AE	average	0.094
Vwx	kurtosis	0.080	Vwy	std	0.093
Average		0.094	Average		0.118

2- Tool with rubber sleeve

The three systems have the average sensitivity as shown in Figure D.2 for the tool with rubber sleeve. It can be observed that the first system has the most sensitivity features for fixturing system stability and tool wear detection compared to the other systems.

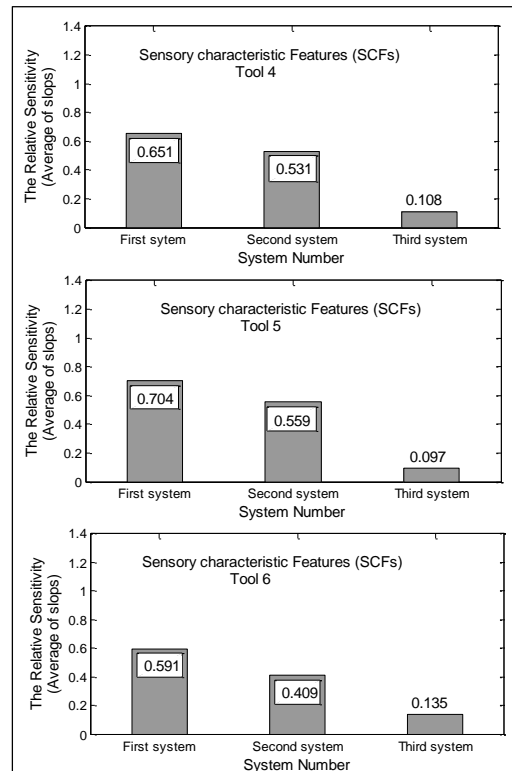


Figure D.2: Comparison between the systems sensitivity for tools with rubber.

Table D.4: First system with the SCFs sensitivity (LR) for the tools with rubber sleeve.

Tools with rubber sleeve								
Tool 4			Tool 5			Tool 6		
Sensory Signal	SP method	Sens-itivity	Sensory Signal	SP method	Sens-itivity	Sensory Signal	SP method	Sens-itivity
Pwr	std	0.776	Vwy	power	0.809	Pwr	power	0.880
Edx	max	0.769	Strain	kurtosis	0.787	Pwr	Std	0.847
Pwr	power	0.728	Fy	min	0.751	AE	Min	0.654
Edx	range	0.665	Fy	kurtosis	0.721	Fx	kurtosis	0.579
Fx	average	0.635	Fx	min	0.678	Mic	kurtosis	0.543
Fx	min	0.623	Vwy	min	0.672	AE	Std	0.524
Fx	range	0.586	Vwy	average	0.671	Vsx	Std	0.486
Pwr	kurtosis	0.577	Vwy	max	0.666	AE	Skew	0.474
Fz	std	0.576	Vsx	max	0.647	Pwr	Min	0.469
Edx	kurtosis	0.574	Fz	skew	0.645	AERMS	Min	0.455
Average		0.651	Average		0.704	Average		0.591

Table D.5: Second system with the SCFs sensitivity (LR) for the tools with rubber sleeve.

Tools with rubber sleeve								
Tool 4			Tool 5			Tool 6		
Sensory Signal	SP method	Sens-itivity	Sensory Signal	SP method	Sens-itivity	Sensory Signal	SP method	Sens-itivity
Fz	range	0.548	Vsz	max	0.628	AERMS	skew	0.454
AERMS	max	0.542	Fz	min	0.628	Pwr	average	0.447
Fz	min	0.541	Vsz	range	0.626	Pwr	skew	0.430
Vsx	skew	0.535	Fy	skew	0.617	Mic	max	0.420
AERMS	min	0.534	Fx	std	0.539	Vsz	std	0.409
AE	std	0.533	Fy	range	0.529	AE	range	0.405
AERMS	average	0.529	AE	kurtosis	0.525	Vsz	average	0.396
Vsx	std	0.524	Strain	std	0.518	Vsz	power	0.392
Vsx	power	0.517	Fx	power	0.496	Mic	range	0.379
Vsx	range	0.514	Vsz	kurtosis	0.486	Edx	max	0.363
Average		0.531	Average		0.559	Average		0.409

Table D.6: Third system with the SCFs sensitivity (LR) for the tools with rubber sleeve.

Tools with rubber sleeve								
Tool 4			Tool 5			Tool 6		
Sensory Signal	SP method	Sens-itivity	Sensory Signal	SP method	Sens-itivity	Sensory Signal	SP method	Sens-itivity
Strain	kurtosis	0.122	Strain	average	0.124	Vwy	max	0.149
Pwr	skew	0.118	Vsz	power	0.113	Strain	skew	0.147
Edy	kurtosis	0.117	AERMS	skew	0.112	Vsx	max	0.145
AE	average	0.115	Fx	max	0.102	Edy	std	0.138
Pwr	range	0.114	AERMS	power	0.094	Vsy	std	0.137
Vsz	max	0.103	Strain	range	0.091	Fz	average	0.136
Vsz	std	0.102	Vsx	min	0.089	Vwx	skew	0.132
Vsy	average	0.100	Vsx	kurtosis	0.088	Vsx	skew	0.130
Mic	max	0.097	Vwx	power	0.082	Vsy	range	0.119
Vsz	range	0.094	Fy	average	0.078	Vwx	max	0.118
Average		0.108	Average		0.097	Average		0.135

3- Tools with copper sleeve

The three systems have the average sensitivity as shown in Figure D.3 for the tool with copper sleeve. It can be observed that the first system has the most sensitivity features for fixturing system stability and tool wear detection compared to the other systems.

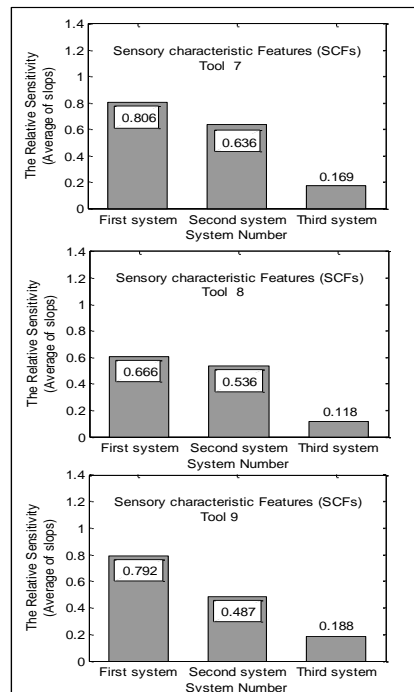


Figure D.3: Comparison between the systems sensitivity for tools with copper sleeve.

Table D.7: First system with the SCFs sensitivity (LR) for the tools with copper sleeve.

Tools with copper sleeve								
Tool 7			Tool 8			Tool 9		
Sensory Signal	SP method	Sens-itivity	Sensory Signal	SP method	Sens-itivity	Sensory Signal	SP method	Sens-itivity
Fx	max	1.023	Mic	skew	0.790	Vwy	power	0.962
Fx	average	0.862	Edy	skew	0.752	Vwy	max	0.941
Pwr	power	0.854	Mic	std	0.750	Vwy	average	0.927
Pwr	max	0.815	Pwr	min	0.724	Vsx	average	0.925
Vsz	range	0.795	Pwr	std	0.692	Vwy	min	0.912
Pwr	std	0.795	AERMS	max	0.621	Fz	average	0.707
Pwr	range	0.778	Vsx	std	0.600	Fy	average	0.670
Pwr	min	0.737	Vsz	kurtosis	0.585	Fy	min	0.647
Vsz	kurtosis	0.706	Pwr	power	0.580	Vwy	skew	0.639
Fx	std	0.703	AE	std	0.573	Pwr	power	0.594
Average		0.806	Average		0.666	Average		0.792

Table D.8: Second system with the SCFs sensitivity (LR) for the tools with copper sleeve.

Tools with copper sleeve								
Tool 7			Tool 8			Tool 9		
Sensory Signal	SP method	Sens-itivity	Sensory Signal	SP method	Sens-itivity	Sensory Signal	SP method	Sens-itivity
Fx	power	0.684	Mic	range	0.571	Fy	power	0.576
Vsx	std	0.680	Pwr	range	0.565	Fy	max	0.545
Vsy	std	0.676	Fy	min	0.554	Vwx	kurtosis	0.534
Fy	skew	0.668	Vsz	min	0.551	Pwr	std	0.530
Fx	range	0.661	AE	min	0.533	Vsy	skew	0.473
Fy	kurtosis	0.639	Vsz	range	0.531	Fz	kurtosis	0.471
Vsz	std	0.603	AE	range	0.528	Vwx	min	0.450
Vsx	max	0.591	Vsx	skew	0.516	Fz	max	0.438
Fy	std	0.584	AERMS	range	0.514	AERMS	kurtosis	0.428
Fy	max	0.577	AE	power	0.501	Fx	average	0.424
Average		0.636	Average		0.536	Average		0.487

Table D.9: Third system with the SCFs sensitivity (LR) for the tools with copper sleeve

Tools with copper sleeve								
Tool 7			Tool 8			Tool 9		
Sensory Signal	SP method	Sens-itivity	Sensory Signal	SP method	Sens-itivity	Sensory Signal	SP method	Sens-itivity
Mic	kurtosis	0.193	Edx	skew	0.141	Vwx	std	0.204
Vsx	power	0.187	Edx	power	0.140	Strain	max	0.200
Vsy	skew	0.186	Fy	range	0.139	Vwx	power	0.198
Fx	min	0.181	Edx	average	0.138	Edy	max	0.197
Fy	average	0.176	AERMS	skew	0.132	Vwx	skew	0.197
Mic	range	0.175	Mic	kurtosis	0.118	Mic	power	0.193
Mic	skew	0.156	Strain	max	0.110	Pwr	skew	0.184
Mic	average	0.155	Pwr	kurtosis	0.091	Vsy	power	0.176
Mic	power	0.148	Fx	average	0.087	AE	power	0.167
Fx	kurtosis	0.138	Vwx	min	0.085	Fz	std	0.165
Average		0.169	Average		0.118	Average		0.188

4-Tools with aluminium sleeve

The three systems have the average sensitivity as shown in Figure D.4 for the tool with aluminium sleeve. It can be observed that the first system has the most sensitivity features for fixturing system stability and tool wear detection compared to the other systems.

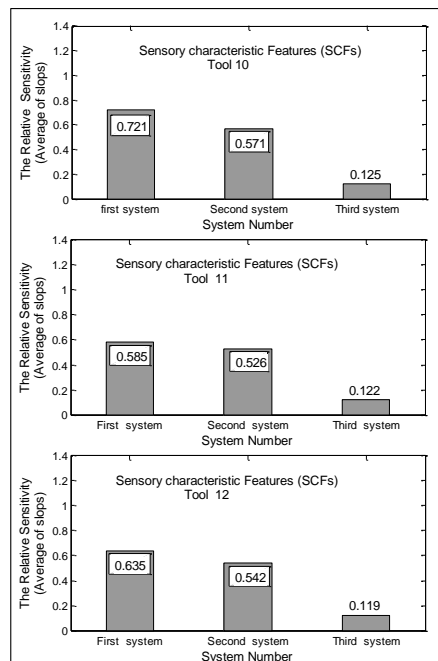


Figure D.4: Comparison between the systems sensitivity for tools with aluminium sleeve.

Table D.10: First system with the SCFs sensitivity (LR) for the tools with aluminium sleeve.

Tools with aluminium sleeve								
Tool 10			Tool 11			Tool 12		
Sensory Signal	SP method	Sens-itivity	Sensory Signal	SP method	Sens-itivity	Sensory Signal	SP method	Sens-itivity
Mic	max	0.816	Fx	max	0.642	Edy	min	0.728
Pwr	std	0.798	Strain	kurtosis	0.621	Edy	average	0.667
Pwr	power	0.763	Fz	kurtosis	0.609	Edy	power	0.660
Mic	range	0.753	Vwy	skew	0.598	Mic	std	0.653
Vwy	range	0.706	AE	kurtosis	0.597	Mic	skew	0.627
Fx	min	0.703	Vsz	average	0.562	Vsz	max	0.619
Vsx	range	0.695	Vsx	max	0.561	Edy	max	0.617
Vsy	kurtosis	0.693	Fy	skew	0.556	AERMS	range	0.611
Edx	std	0.675	Vsy	average	0.555	AE	skew	0.603
Fy	power	0.616	Vwy	power	0.554		std	0.573
Average		0.721	Average		0.585	Average		0.635

Table D.11: Second system with the SCFs sensitivity (LR) for the tools with aluminium sleeve.

Tools with aluminium sleeve								
Tool 10			Tool 11			Tool 12		
Sensory Signal	SP method	Sens-itivity	Sensory Signal	SP method	Sens-itivity	Sensory Signal	SP method	Sens-itivity
Fx	power	0.614	Vwy	max	0.549	AE	min	0.561
Fx	std	0.603	Vwy	average	0.543	AE	power	0.556
Mic	min	0.591	Vwy	min	0.536	AE	std	0.554
Fz	average	0.589	Mic	skew	0.531	AE	range	0.549
Edx	skew	0.581	Mic	power	0.531	Fz	min	0.546
Fy	kurtosis	0.551	Mic	average	0.527	Edy	kurtosis	0.540
Edy	std	0.551	Fy	power	0.521	AE	max	0.536
Fx	range	0.547	AE	average	0.513	Fz	std	0.533
Edy	range	0.546	Vwx	skew	0.508	AERMS	power	0.526
Mic	skew	0.537	Edx	range	0.502	Mic	average	0.519
Average		0.571	Average		0.526	Average		0.542

Table D.12: Third system with the SCFs sensitivity (LR) for the tools with aluminium sleeve.

Tools with aluminium sleeve								
Tool 10			Tool 11			Tool 12		
Sensory Signal	SP method	Sens-itivity	Sensory Signal	SP method	Sens-itivity	Sensory Signal	SP method	Sens-itivity
Fy	min	0.147	Fx	min	0.151	Strain	kurtosis	0.153
Pwr	kurtosis	0.145	Strain	range	0.135	Vsx	min	0.139
Fz	range	0.144	4Strain	power	0.128	Fz	skew	0.136
Strain	average	0.141	Vwx	min	0.127	Pwr	skew	0.134
AERMS	average	0.134	Fy	min	0.126	AERMS	kurtosis	0.125
Strain	min	0.122	Pwr	range	0.118	Vwx	power	0.115
Vsz	kurtosis	0.116	Vsy	range	0.118	Vwy	power	0.113
Vwx	power	0.107	Strain	average	0.116	Edy	skew	0.110
Fy	average	0.098	Vsz	min	0.104	Fy	kurtosis	0.089
Vsz	power	0.097	AERMS	min	0.102	Vsy	std	0.082
Average		0.125	Average		0.122	Average		0.119

Appendix E: System Cost and Utilisation (For Chapter 9)

9.4.1.2 Selection of Principal Component Feature (PCFs) Method

1- Tools without sleeve

The three systems have the average sensitivity as shown in Figure E.1 for the tool without sleeve. It can be observed that the first system has the most sensitivity features for fixturing system stability and tool wear detection compared to the other systems.

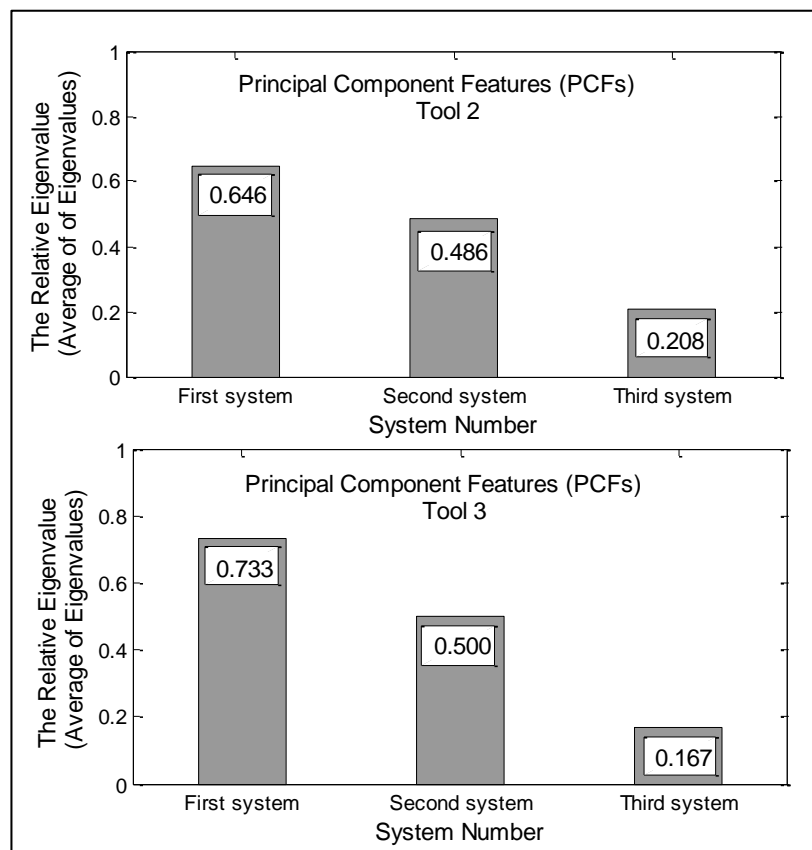


Figure E.1: Comparison between the systems eigenvalue of tools without sleeve.

Table E.1: First system with the PCFs eigenvalue (PCA) for the tools without sleeve.

Tools without sleeve					
Tool 2			Tool 3		
Sensory Signal	PC method	Eigen-value	Sensory Signal	PC method	Eigen-value
Edx	PC1	0.869	Pwr	PC 2	0.931
Edy	PC 11	0.782	Edx	PC 3	0.864
Edy	PC 15	0.698	Edy	PC 6	0.862
Edy	PC 13	0.682	Fx	PC 2	0.797
Edy	PC 7	0.631	Fx	PC 11	0.701
Fx	PC 14	0.576	Fx	PC 10	0.689
Fx	PC 10	0.569	Fx	PC 14	0.673
Fx	PC 6	0.563	Fx	PC 10	0.609
Edx	PC 14	0.560	Fx	PC 4	0.604
Edy	PC 15	0.533	Edy	PC 9	0.601
Average		0.646	Average		0.733

Table E.2: Second system with the PCFs eigenvalue (PCA) for the tools without sleeve

Tools without sleeve					
Tool 2			Tool 3		
Sensory Signal	PC method	Eigen-value	Sensory Signal	PC method	Eigen-value
Fx	PC 1	0.532	Fx	PC 14	0.585
Fx	PC 14	0.526	Edy	PC 13	0.569
Edy	PC 10	0.525	Edy	PC 5	0.539
Fx	PC 15	0.517	Edy	PC 2	0.517
Fx	PC 4	0.505	Edy	PC 11	0.501
Edy	PC 1	0.470	Fy	PC 1	0.464
Fx	PC 2	0.464	Fx	PC 4	0.464
Edx	PC 6	0.442	Fx	PC 15	0.463
Fx	PC 11	0.440	Fy	PC 15	0.456
Edy	PC 13	0.439	Fy	PC 7	0.446
Average		0.486	Average		0.500

Table E.3: Third system with the PCFs eigenvalue (PCA) for the tools without sleeve.

Tools without sleeve					
Tool 2			Tool 3		
Sensory Signal	PC method	Eigen-value	Sensory Signal	PC method	Eigen-value
Strain	PC 13	0.217	Vwx	PC 14	0.172
Vsz	PC 9	0.216	Strain	PC 3	0.171
Vwx	PC 2	0.216	Edx	PC 2	0.168
Pwr	PC 1	0.214	Fz	PC 3	0.167
Fx	PC 5	0.211	Vwy	PC 4	0.166
Vsy	PC 1	0.209	Vsz	PC 12	0.166
Pwr	PC 4	0.206	Strain	PC 11	0.166
Fz	PC 11	0.197	Vwx	PC 9	0.166
Vsz	PC 7	0.197	AERMS	PC 15	0.166
Strain	PC 2	0.196	Vwy	PC 10	0.163
Average		0.208	Average		0.167

2- Tools with rubber sleeve

The three systems have the average sensitivity as shown in Figure E.2 for the tool with rubber sleeve. It can be observed that the first system has the most sensitivity features for fixturing system stability and tool wear detection compared to the other systems.

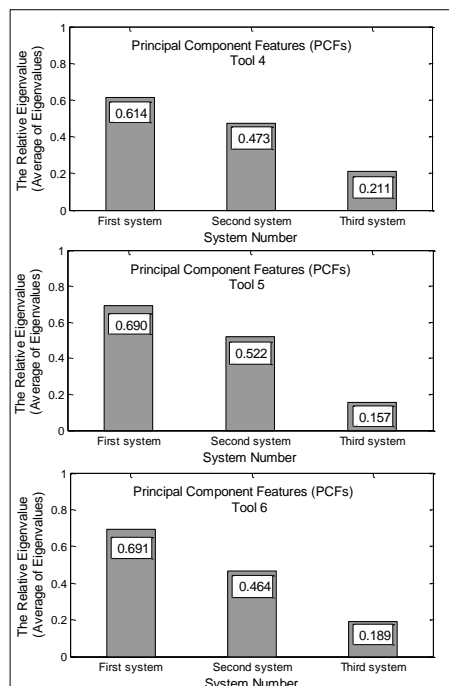


Figure E.2: Comparison between the systems eigenvalue of tool with rubber sleeve.

Table E.4: First system with the PCFs eigenvalue (PCA) for the tools with rubber sleeve.

Tools with rubber sleeve								
Tool 4			Tool 5			Tool 6		
Sensory Signal	PC method	Eigen-value	Sensory Signal	PC method	Eigen-value	Sensory Signal	PC method	Eigen-value
Fx	PC 2	0.807	Vwy	PC 2	0.881	Pwr	PC 2	0.879
Edy	PC 7	0.694	Fx	PC 6	0.833	Edy	PC 5	0.871
Fx	PC 8	0.685	Edy	PC 11	0.732	Edy	PC 1	0.810
Edy	PC 4	0.645	Fx	PC 6	0.712	Fx	PC 6	0.729
Fx	PC 9	0.607	Fx	PC 10	0.667	Fx	PC 3	0.706
Edy	PC 11	0.563	Edy	PC 9	0.666	Edy	PC 13	0.646
Edy	PC 7	0.547	Edy	PC 13	0.617	Edy	PC 6	0.626
Edy	PC 11	0.538	Edy	PC 5	0.607	Fx	PC 6	0.598
Fx	PC 7	0.535	Edy	PC 2	0.592	Fx	PC 11	0.526
Edy	PC4	0.519	Fx	PC 8	0.591	Fy	PC 4	0.512
Average		0.614	Average		0.690	Average		0.691

Table E.5: Second system with the PCFs eigenvalue (PCA) for the tools with rubber sleeve.

Tools with rubber sleeve								
Tool 4			Tool 5			Tool 6		
Sensory Signal	PC method	Eigen-value	Sensory Signal	PC method	Eigen-value	Sensory Signal	PC method	Eigen-value
Edy	PC 1	0.500	Edy	PC 6	0.570	Edy	PC 7	0.509
Edy	PC 13	0.490	Edy	PC 11	0.563	Fx	PC 1	0.493
Edy	PC 13	0.486	Edy	PC 11	0.550	Fy	PC 5	0.491
Fx	PC 6	0.479	Edy	PC 2	0.544	Edy	PC 14	0.480
Fx	PC 14	0.471	Fx	PC 14	0.520	Fx	PC 9	0.464
Fx	PC 10	0.470	Edy	PC 8	0.509	Fy	PC 11	0.447
Edx	PC 3	0.470	Fx	PC 14	0.499	Fx	PC 3	0.445
Fy	PC 9	0.467	Fy	PC 15	0.495	Fx	PC 11	0.443
Fy	PC 2	0.455	Fx	PC 5	0.486	Edx	PC 2	0.439
Fy	PC4	0.450	Edx	PC 2	0.482	Edy	PC 12	0.435
Average		0.473	Average		0.522	Average		0.464

Table E.6: Third system with the PCFs eigenvalue (PCA) for the tools with rubber sleeve.

Tools with rubber sleeve								
Tool 4			Tool 5			Tool 6		
Sensory Signal	PC method	Eigen-value	Sensory Signal	PC method	Eigen-value	Sensory Signal	PC method	Eigen-value
Vwy	PC 8	0.224	AE	PC 2	0.172	Strain	PC 2	0.201
Pwr	PC 11	0.221	Fy	PC 14	0.164	Fy	PC 11	0.196
Vwx	PC 14	0.217	AE	PC 2	0.162	Pwr	PC 3	0.195
Vsz	PC 12	0.215	AERMS	PC 11	0.159	Pwr	PC 3	0.192
Vwx	PC 4	0.212	Edx	PC 3	0.158	Fz	PC 1	0.190
AE	PC 4	0.207	Fz	PC 14	0.155	Strain	PC 7	0.187
Fz	PC 6	0.206	Pwr	PC 5	0.153	AE	PC 5	0.185
Strain	PC 6	0.204	Strain	PC 1	0.152	Vwx	PC 3	0.184
Pwr	PC 12	0.204	Fz	PC 11	0.147	Vwy	PC 2	0.182
Edx	PC 7	0.202	Fz	PC 7	0.146	Strain	PC14	0.182
Average		0.211	Average		0.157	Average		0.189

3- Tools with copper sleeve

The three systems have the average sensitivity as shown in Figure E.3 for the tool with copper sleeve. It can be observed that the first system has the most sensitivity features for fixturing system stability and tool wear detection compared to the other systems.

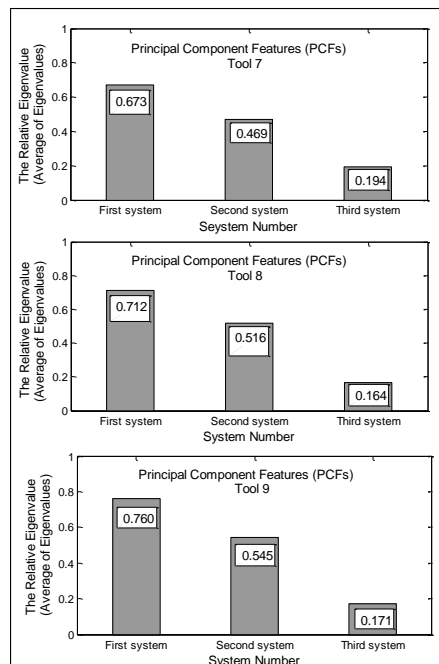


Figure E.3: Comparison between the systems eigenvalue of tools with copper sleeve.

Table E.7: First system with the PCFs eigenvalue (PCA) for the tools with copper sleeve.

Tools with copper sleeve								
Tool 7			Tool 8			Tool 9		
Sensory Signal	PC method	Eigen-value	Sensory Signal	PC method	Eigen-value	Sensory Signal	PC method	Eigen-value
Fx	PC7	0.824	Mic	PC 1	0.933	Fx	PC 1	0.897
Edy	PC 13	0.796	Fx	PC 13	0.808	Fx	PC 14	0.870
Edy	PC 8	0.785	Fx	PC 15	0.788	Edy	PC 6	0.834
Fx	PC 4	0.784	Edy	PC 8	0.752	Fx	PC 12	0.792
Edy	PC 13	0.707	Edy	PC 8	0.693	Edy	PC 15	0.776
Fx	PC 2	0.640	Edy	PC 5	0.662	Fx	PC 1	0.744
Fx	PC 1	0.572	Edy	PC 3	0.652	Fx	PC 3	0.702
Edy	PC 10	0.564	Edy	PC 9	0.641	Edy	PC 12	0.680
Fx	PC 3	0.535	Edy	PC 11	0.610	Fx	PC 2	0.654
Edy	PC 13	0.528	Fx	PC 3	0.584	Fx	PC 6	0.650
Average		0.673	Average		0.712	Average		0.760

Table E.8: Second system with the PCFs eigenvalue (PCA) for the tools with copper sleeve.

Tools with copper sleeve								
Tool 7			Tool 8			Tool 9		
Sensory Signal	PC method	Eigen-value	Sensory Signal	PC method	Eigen-value	Sensory Signal	PC method	Eigen-value
Fx	PC1	0.497	Edx	PC 9	0.575	Edy	PC 7	0.626
Fy	PC9	0.494	Edy	PC 14	0.564	Fx	PC 12	0.620
Fx	PC1	0.492	Edx	PC 1	0.524	Fx	PC 13	0.561
Edy	PC6	0.491	Edy	PC 14	0.523	Edy	PC 2	0.560
Fx	PC3	0.465	Fy	PC 5	0.514	Fy	PC 11	0.551
Fy	PC2	0.465	Fx	PC 2	0.505	Edx	PC 10	0.544
Edy	PC13	0.459	Fx	PC 8	0.500	Edy	PC 6	0.535
Fx	PC3	0.450	Edy	PC 14	0.497	Edx	PC 10	0.531
Fy	PC12	0.447	Fx	PC 11	0.484	Fy	PC 11	0.503
Fy	PC7	0.434	Fx	PC 12	0.479	Fy	PC 10	0.422
Average		0.469	Average		0.516	Average		0.545

Table E.9: Third system with the PCFs eigenvalue (PCA) for the tools with copper sleeve.

Tools with copper sleeve								
Tool 7			Tool 8			Tool 9		
Sensory Signal	PC method	Eigen-value	Sensory Signal	PC method	Eigen-value	Sensory Signal	PC method	Eigen-value
Vsz	PC5	0.199	Vwx	PC 2	0.184	Vwy	PC 2	0.175
Strain	PC 2	0.199	Vwy	PC 14	0.180	Vwy	PC 4	0.175
Vwy	PC 14	0.197	Vsz	PC 1	0.173	Pwr	PC 8	0.174
Vwy	PC 5	0.197	Fz	PC 8	0.168	Pwr	PC 9	0.174
Fy	PC 12	0.196	AE	PC 3	0.167	Fz	PC 13	0.172
Vwx	PC 9	0.194	Fy	PC 9	0.156	Vwy	PC 13	0.172
Pwr	PC 14	0.193	Fsy	PC 13	0.155	Strain	PC 15	0.171
Strain	PC 12	0.192	Strain	PC 5	0.155	Vwx	PC 5	0.170
Edx	PC 11	0.191	Vsz	PC 8	0.154	Vwx	PC 5	0.168
Vwx	PC 13	0.187	Strain	PC 13	0.152	Strain	PC 2	0.166
Average		0.194	Average		0.164	Average		0.171

4. Tools with aluminium sleeve

The three systems have the average sensitivity as shown in Figure E.4 for the tool with aluminium sleeve. It can be observed that the first system has the most sensitivity features for fixturing system stability and tool wear detection compared to the other systems.

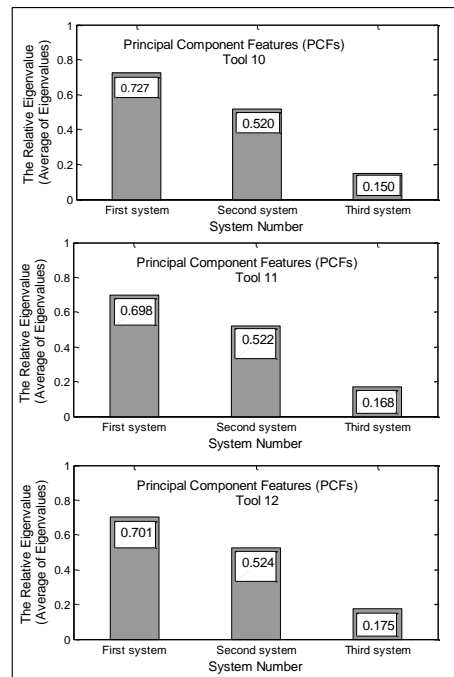


Figure E.4 : Comparison between the systems eigenvalue of tools with aluminium sleeve.

Table E.10: First system with the PCFs eigenvalue (PCA) for the tools with aluminium sleeve.

Tools with aluminium sleeve								
Tool 10			Tool 11			Tool 12		
Sensory Signal	PC method	Eigen-value	Sensory Signal	PC method	Eigen-value	Sensory Signal	PC method	Eigen-value
Mic	PC 2	0.874	Fx	PC 1	0.805	Edy	PC 1	0.816
Fx	PC 11	0.857	Fx	PC 9	0.793	Fx	PC 6	0.795
Fx	PC 8	0.822	Edy	PC 13	0.763	Edy	PC 6	0.783
Edy	PC 5	0.816	Fx	PC 15	0.735	Fx	PC 8	0.753
Edy	PC 6	0.784	Fy	PC 11	0.725	Fx	PC 13	0.707
Fx	PC 4	0.657	Fy	PC 10	0.705	Edy	PC 14	0.706
Edy	PC 8	0.642	Edy	PC 5	0.674	Fx	PC 9	0.669
Edy	PC 15	0.620	Fx	PC 4	0.597	Fx	PC 8	0.598
Fx	PC 2	0.609	Edy	PC 14	0.590	Edy	PC 9	0.592
Edy	PC 10	0.593	Fx	PC 9	0.588	Edy	PC 11	0.587
Average		0.727	Average		0.698	Average		0.701

Table E.11: Second system with the PCFs eigenvalue (PCA) for the tools with aluminium sleeve.

Tools with aluminium sleeve								
Tool 10			Tool 11			Tool 12		
Sensory Signal	PC method	Eigen-value	Sensory Signal	PC method	Eigen-value	Sensory Signal	PC method	Eigen-value
Fx	PC 7	0.562	Edy	PC 1	0.582	Edx	PC 9	0.574
Edy	PC 1	0.554	Edx	PC 7	0.581	Edy	PC 15	0.568
Fx	PC 7	0.548	Edy	PC 7	0.564	Fx	PC 5	0.549
Fx	PC 7	0.532	Fx	PC 10	0.560	Fy	PC 14	0.547
Edy	PC 8	0.527	Edy	PC 5	0.548	Edx	PC 13	0.513
Edx	PC 15	0.516	Edy	PC 12	0.531	Edy	PC 12	0.511
Edx	PC 2	0.508	Fx	PC 15	0.483	Edx	PC 7	0.508
Edy	PC 15	0.491	Edy	PC 1	0.470	Edx	PC 10	0.505
Fx	PC 10	0.490	Edy	PC 2	0.458	Fx	PC 1	0.493
Fx	PC 12	0.476	Fx	PC 5	0.448	Edy	PC 14	0.478
Average		0.520	Average		0.522	Average		0.524

Table E.12: Third system with the PCFs eigenvalue (PCA) for the tools with aluminium sleeve.

Tools with aluminium sleeve								
Tool 10			Tool 11			Tool 12		
Sensory Signal	PC method	Eigen-value	Sensory Signal	PC method	Eigen-value	Sensory Signal	PC method	Eigen-value
AE	PC 3	0.160	Fz	PC 14	0.178	Fy	PC 13	0.188
Fz	PC 9	0.159	Pwr	PC 8	0.174	Vsz	PC 12	0.188
Vwx	PC 7	0.158	Strain	PC 3	0.174	Fy	PC 13	0.181
Vsz	PC 8	0.151	Fy	PC 7	0.168	Vwx	PC 12	0.179
Fy	PC 9	0.149	Vsz	PC 1	0.168	Vsz	PC 13	0.175
Strain	PC 10	0.149	Vwx	PC 11	0.167	Vwx	PC 8	0.175
Vwx	PC 1	0.146	Vwx	PC 7	0.166	Pwr	PC 11	0.171
Edx	PC 15	0.146	Fz	PC 3	0.163	Fx	PC 7	0.167
Vsz	PC 13	0.145	Fz	PC 15	0.163	AE	PC 12	0.166
AERMS	PC 11	0.140	Vsy	PC 4	0.161	Pwr	PC 6	0.163
Average		0.150	Average		0.168	Average		0.175

Appendix F: System Optimisation (For Chapter 9)

10.4.2.1 Linear Regression (LR) Method

1- Tools without sleeve

From Tables D.1 and D.2, it can be observed that there is no significant difference in the average sensitivity for both systems for the three tools without sleeves. For the tool 2, the cost of first and second systems is different (£22894, £22509). But it is still can be optimised by increasing the system utilisation by replacing the sensory characteristic features of the power and eddy current (Edx) sensor from the first system with the Edy sensory signals from the second system to reduce the cost and still have the sensitivity level. For the tool 3, the difference in the cost between the first and second systems is too high.

Table F.1: Sensors utilisation for the tool 2 without sleeve using LR.

Tool 2			
Sensor	U 1st system	U 2nd system	Optimised System
Dynamometer	6.66%	6.66%	6.66%
Vsy	20%	10%	20%
Vsz	10%	10%	-----
Pwr	10%	20%	-----
Edx	10%	-----	-----
Edy	30%	40%	60%
UA Average Utilisation	14.44%	17.33%	28.88%
System Cost	£22894	£22509	£22065
Average Sensitivity	0.779	0.639	0.755

Table F.2: Sensors utilisation for the tool 3 without sleeve using LR.

Tool 3			
Sensor	U 1st sstem	U 2nd system	Optimised System
Dynamometer	-----	3.33%	-----
Strain	10%	10%	-----
Vwy	30%	10%	40%
Mic	20%	-----	20%
Vsy	-----	10%	-----
Vsz	-----	30%	-----
Pwr	40%	10%	40%
Edy	-----	20%	-----
UA Average Utilisation	25%	13.33%	33.33%
System Cost	£10807	£23577	£8087
Average Sensitivity	0.690	0.529	0.683

As shown in Table F.1, the overall average utilisation has increased in the first system from 14.44% up to 28.88 % and from 17.33% up to 28.88 % in the second system and the cost is reduced by 10.9 % from £24789 to £22065. In addition, for three tools without sleeve the average sensitivity of the system did not significantly change as can be seen in Table F3. In fact the average sensitivity has increased to 0.755 compared with the second system of tool 2.

Table F.3: The optimised system (1st and 2nd system) for the tools without sleeve using LR.

Tools without sleeve					
Tool 2			Tool 3		
Sensory Signal	SP method	Sens- itivity	Sensory Signal	SP method	Sens- itivity
Edy	power	0.826	Pwr	power	0.924
Edy	average	0.826	Pwr	std	0.909
Vsy	power	0.808	Pwr	range	0.797
Vsy	std	0.794	Pwr	min	0.707
Fy	skew	0.793	Vwy	power	0.596
Fy	std	0.738	Mic	average	0.586
Edy	max	0.714	Mic	power	0.583
Edy	range	0.714	Vwy	min	0.580
Edy	std	0.672	Vwy	max	0.578
Edy	skew	0.671	Vwy	average	0.575
Average		0.755	Average		0.683

2- Tools with rubber sleeve

From Tables D.4 and D.5, it can be observed that there is no significant difference in the average sensitivity for both systems for the tools with rubber sleeves. For the tool 4, the cost of first and second systems is slightly different (£21755, £22078). But it is still can be optimised by increasing the system utilisation by replacing the sensory characteristic features of the AE sensor from the first system with the forces sensory signals from the second system to reduce the cost and still have the sensitivity level.

Table F.4: Sensors utilisation for the tool 4 with rubber sleeve using LR.

Tool 4			
Sensor	U 1st system	U 2nd system	Optimised System
Dynamometer	13.33%	6.66%	13.33%
AE	-----	20%	-----
Vsx	-----	40%	-----
Pwr	30%	-----	30%
Edx	30%	-----	30%
UA Average Utilisation	24.44%	22.22%	24.44%
System Cost	£21755	£22078	£21755
Average Sensitivity	0.651	0.531	0.651

Table F.5: Sensors utilisation for the tool 5 with rubber sleeve using LR.

Tool 5			
Sensor	U 1st system	U 2nd system	Optimised System
Dynamometer	13.33%	16.66%	16.66%
Strain	10%	10%	10%
Vwy	40%	-----	40%
AE	-----	5%	-----
Vsx	10%	-----	-----
Vsz	-----	30%	-----
UA Average Utilisation	18.33%	15.41%	22.22%
System Cost	£21536	£22878	£21159
Average Sensitivity	0.704	0.559	0.703

Table F.6: Sensors utilisation for the tool 6 with rubber sleeve using LR slope.

Tool 6			
Sensor	U 1st system	U 2nd system	Optimised System
Dynamometer	3.33%	3.33%	-----
AE	20%	10%	25%
Mic	-----	20%	10%
Vsx	10%	-----	-----
Vsz	-----	30%	
Pwr	30%	20%	40%
Edx	-----	10%	
UA Average Utilisation	15.83	15.55%	25%
System Cost	£22145	£22590	£8319
Average Sensitivity	0.591	0.409	0.575

As shown in Table F.5, for the tool 5, the overall average utilisation has increased in the first system from 18.33% up to 22.22% and from 15.41% up to 22.22% in the second system and the cost is reduced by 14.6 % from £24789 to £21159. In addition, for three tools with rubber sleeve the average sensitivity of the system did not significantly change as can be seen in Table F.7. In fact the average sensitivity has increased to 0.703 compared with the second system of tool 5.

Table F.7: The optimised system (1st and 2nd system) for the tool with rubber sleeve using LR slope.

Tools with rubber sleeve								
Tool 4			Tool 5			Tool 6		
Sensory Signal	SP method	Sens- itivity	Sensory Signal	SP method	Sens- itivity	Sensory Signal	SP method	Sens- itivity
Pwr	Std	0.776	Vwy	power	0.809	Pwr	power	0.880
Edx	Max	0.769	Strain	kurtosis	0.787	Pwr	std	0.847
Pwr	power	0.728	Fy	min	0.751	AE	min	0.654
Edx	range	0.665	Fy	kurtosis	0.721	Mic	kurtosis	0.543
Fx	average	0.635	Fx	min	0.678	AE	std	0.524
Fx	Min	0.623	Vwy	min	0.672	AE	skew	0.474
Fx	range	0.586	Vwy	average	0.671	Pwr	min	0.469
Pwr	kurtosis	0.577	Vwy	max	0.666	AERMS	min	0.455
Fz	Std	0.576	Fz	skew	0.645	AERMS	skew	0.454
Edx	kurtosis	0.574	Fz	min	0.628	Pwr	average	0.447
Average		0.651	Average		0.703	Average		0.575

3- Tools with copper sleeve

From Tables D.7 and D.8, it can be observed that there is no significant difference in the average sensitivity for both systems for three tools with copper sleeves. For the tool 7, for example, the cost of first and second systems is relatively different (£22094, £23204). But it is still can be optimised by increasing the system utilisation by replacing the sensory characteristic features of the accelerometer sensor(Vsz) from the first system with the forces sensory signals from the second system to reduce the cost and still have the sensitivity level.

Table F.8: Sensors utilisation for the tool 7 with copper sleeve using LR slope.

Tool 7			
Sensor	U 1st system	U 2nd system	Optimised System
Dynamometer	10%	20%	16.66%
Vsx	-----	20%	-----
Vsy	-----	10%	-----
Vsz	20%	10%	-----
Pwr	50%	-----	50%
UA Average Utilisation	26.66%	15%	33.33%
System Cost	£22094	£23204	£18620
Average Sensitivity	0.806	0.636	0.792

Table F.9: Sensors utilisation for the tool 8 with copper sleeve using LR slope.

Tool 8			
Sensor	U 1st system	U 2nd system	Optimised System
Dynamometer	-----	3.33%	-----
AE	10%	20%	10%
Mic	20%	10%	30%
Vsx	10%	10%	-----
Vsz	10%	20%	-----
Pwr	30%	10%	40%
Edy	10%	-----	10%
UA Average Utilisation	15%	12.22%	22.5%
System Cost	£10242	£21827	£8009
Average Sensitivity	0.666	0.536	0.662

Table F.10: Sensors utilisation for the tool 9 with copper sleeve using LR slope.

Tool 9			
Sensor	U 1st system	U 2nd system	Optimised System
Dynamometer	10%	16.66%	16.66%
Vwy	50%	-----	50%
AE	-----	5%	-----
Vsx	10%	-----	-----
Vsy	-----	10%	-----
Vwx	-----	20%	-----
Pwr	10%	10%	-----
UA Average Utilisation	20%	12.33%	33.33%
System Cost	£20806	£21797	£18883
Average Sensitivity	0.792	0.487	0.752

As shown in Table F.8, the overall average utilisation has increased in the first system from 26.66% up to 33.3% and from 15% up to 33.3% in the second system and the cost is reduced by 24 % from £24789 to £18620. In addition, the average sensitivity of the system did not significantly change as can be seen in Table F.9. In

fact the average sensitivity has increased to 0.792 compared with the second system of tool 7 .

Table F.9: The optimised system (1st and 2nd system) for the tool with copper sleeve using LR.

Tools with copper sleeve								
Tool 7			Tool 8			Tool 9		
Sensory Signal	SP method	Sens-itivity	Sensory Signal	SP method	Sens-itivity	Sensory Signal	SP method	Sens-itivity
Fx	Max	1.023	Mic	skew	0.790	Vwy	power	0.962
Fx	average	0.862	Edy	skew	0.752	Vwy	max	0.941
Pwr	power	0.854	Mic	std	0.750	Vwy	average	0.927
Pwr	Max	0.815	Pwr	min	0.724	Vwy	min	0.912
Pwr	Std	0.795	Pwr	std	0.692	Fz	average	0.707
Pwr	range	0.778	AERMS	max	0.621	Fy	average	0.670
Pwr	Min	0.737	Pwr	power	0.580	Fy	min	0.647
Fx	Std	0.703	AE	std	0.573	Vwy	skew	0.639
Fx	power	0.684	Mic	range	0.571	Fy	power	0.576
Fy	Skew	0.668	Pwr	range	0.565	Fy	max	0.545
Average		0.792	Average		0.662	Average		0.752

4- Tools with aluminium sleeve

From Tables D.10 and D.11, it can be observed that there is no significant difference in the average sensitivity for both systems for the three tools with aluminium sleeve.

For the tool 10, the cost of first and second systems is relatively different (£21628, £19450). But it is still can be optimised by increasing the system utilisation by replacing the sensory characteristic features of the accelerometer sensors and eddy current (Edx) from the first system with the forces sensory signals and sound sensor from the second system to reduce the cost and still have the sensitivity level.

Table F.10: Sensors utilisation for the tool 10 with aluminium sleeve using LR.

Tool 10			
Sensor	U 1st system	U 2nd system	Optimised System
Dynamometer	10%	16.66%	16.66%
Vwy	10%	-----	-----
Mic	10%	20%	30%
Vsx	10%	-----	-----
Vsy	10%	-----	-----
Pwr	20%	-----	20%
Edx	10%	10%	-----
Edy	----	20%	-----
UA Average Utilisation	11.42%	16.66%	22.22%
System Cost	£21628	£19450	£18717
Average Sensitivity	0.721	0.571	0.685

Table F.11: Sensors utilisation for the tool 11 with aluminium sleeve using LR.

Tool 11			
Sensor	U 1st system	U 2nd system	Optimised System
Dynamometer	10%	3.33%	10%
Strain	10%	-----	-----
Vwy	20%	30%	50%
AE	5%	5%	-----
Mic	-----	30%	20%
Vsx	10%	-----	-----
Vsy	10%	-----	-----
Vsz	10%	-----	-----
Vwx	10%	-----	-----
Edx	10%	-----	-----
UA Average Utilisation	10.55%	17.08%	26.66%
System Cost	£23997	£19790	£18913
Average Sensitivity	0.585	0.526	0.571

Table F.12: Sensors utilisation for the tool 12 with aluminium sleeve using LR.

Tool 12			
Sensor	U 1st system	U 2nd system	Optimised System
Dynamometer	-----	3.33%	-----
AE	10%	30%	20%
Mic	20%	10%	20%
Vsz	20%	-----	-----
Edy	40%	10%	40%
UA Average Utilisation	22.50%	13.33%	26.66%
System Cost	£10250	£19912	£8394
Average Sensitivity	0.635	0.542	0.628

As shown in Table F.10, the overall average utilisation has increased in the first system from 11.42% up to 22.22% and from 16.66% up to 22.22% in the second system and the cost is reduced by 24.5 % from £24789 to £18717. In addition, for another tools with copper sleeve, the average sensitivity of the system did not significantly change as can be seen in Table F.13. In fact the average sensitivity has increased to 0.685 compared with the second system of the tool 10.

Table F.13: The optimised system (1st and 2nd system) for the tools with aluminium sleeve using LR.

Tools with aluminium sleeve								
Tool 10			Tool 11			Tool 12		
Sensory Signal	SP method	Sens- itivity	Sensory Signal	SP method	Sens- itivity	Sensory Signal	SP method	Sens- itivity
Mic	Max	0.816	Fx	max	0.642	Edy	min	0.728
Pwr	Std	0.798	Fz	kurtosis	0.609	Edy	average	0.667
Pwr	power	0.763	Vwy	skew	0.598	Edy	power	0.660
Mic	range	0.753	Fy	skew	0.556	Mic	std	0.653
Fx	Min	0.703	Vwy	power	0.554	Mic	skew	0.627
Fy	power	0.616	Vwy	max	0.549	Edy	max	0.617
Fx	power	0.614	Vwy	average	0.543	AERMS	range	0.611
Fx	Std	0.603	Vwy	min	0.536	AE	skew	0.603
Mic	Min	0.591	Mic	skew	0.532	AE	min	0.561
Fz	average	0.589	Mic	power	0.531	AE	power	0.556
Average		0.685	Average		0.571	Average		0.628

Appendix G: System Optimisation (Chapter 9)

9.4.2.2 Principal Component Analysis (PCA) Method

1- Tools without sleeve

From Tables E.1 and E.2, it can be observed that there is no significant difference in the average sensitivity for both systems for the three tools without sleeves. For the tool 2, for example, the cost of first and second systems is slightly different (£19420, £19035). But it is still can be optimised by increasing the system utilisation by replacing the sensory characteristic features of the eddy current sensor(Edx) from the first system with the forces sensory signals from the second system to reduce the cost and still have the sensitivity level.

Table G.1: Sensors utilisation for the tool 2 without sleeve using PCA.

Tool 2			
Sensor	U 1st system	U 2nd system	Optimised System
Dynamometer	10%	20%	13.33%
Edx	20%	10%	-----
Edy	60%	30%	60%
UA Average Utilisation	30%	20%	36.67%
System Cost	£19420	£19420	£19035
Average Eigenvalue	0.646	0.486	0.610

Table G.2: Sensors utilisation for the tool 3 without sleeve using PCA.

Tool 3			
Sensor	U 1st system	U 2nd system	Optimised System
Dynamometer	20%	20%	10%
Pwr	10%	-----	10%
Edx	10%	10%	-----
Edy	20%	40%	60%
UA Average Utilisation	15%	23.33%	26.66%
System Cost	£19487	£19420	£19035
Average Eigenvalue	0.733	0.500	0.671

As shown in Table G.1, the overall average utilisation has increased in the first system from 30% up to 36.67% and from 20% up to 36.67% in the second system and the cost is reduced by 23 % from £24789 to £19035. In addition, for another tools without sleeve, average sensitivity of the system did not significantly change as can be seen in Table G.3. In fact the average sensitivity has increased to 0.610 compared with the second system of the tool 2.

Table G.3: The optimised system (1st and 2nd system) for the tool with copper sleeve using PCA.

Tools without sleeve					
Tool 2			Tool 3		
Sensory Signal	PC method	Eigen-value	Sensory Signal	PC method	Eigen-value
Edy	PC 11	0.782	Pwr	PC 2	0.931
Edy	PC 15	0.698	Edy	PC 6	0.862
Edy	PC 13	0.682	Fx	PC 2	0.797
Edy	PC 7	0.631	Fx	PC 11	0.701
Fx	PC 14	0.576	Fx	PC 10	0.689
Fx	PC 10	0.569	Edy	PC 9	0.601
Fx	PC 6	0.563	Edy	PC 13	0.569
Edy	PC 15	0.533	Edy	PC 5	0.539
Fx	PC 1	0.532	Edy	PC 2	0.517
Fx	PC 14	0.526	Edy	PC 11	0.501
Average		0.610	Average		0.671

2- Tools with rubber sleeve

From Tables E.4 and E.5, it can be observed that there is no significant difference in the average sensitivity for both systems for the three tools with rubber sleeves. For the tool 5, for instance, the cost of first and second systems is slightly different (£19298, £19420). But it is still can be optimised by increasing the system utilisation by replacing the sensory characteristic features of the accelerometer sensor(Vwy) from the first system with the eddy current signals (Edy) from the second system to reduce the cost and still have the sensitivity level.

Table G.4: Sensors utilisation for the tool 4 with rubber sleeve using PCA.

Tool 4			
Sensor	U 1st system	U 2nd system	Optimised System
Dynamometer	13.33%	20%	10%
Edx	-----	10%	-----
Edy	60%	30%	70%
UA Average Utilisation	36.66%	20%	40%
System Cost	£19035	£19420	£19035
Average Eigenvalue	0.614	0.473	0.611

Table G.5: Sensors utilisation for the tool 5 with rubber sleeve using PCA.

Tool 5			
Sensor	U 1st system	U 2nd system	Optimised System
Dynamometer	13.33%	13.33%	13.33%
Vwy	10%	-----	-----
Edx	-----	10%	-----
Edy	50%	50%	60%
UA Average Utilisation	24.44%	24.44%	36.66%
System Cost	£19298	£19420	£19035
Average Eigenvalue	0.690	0.522	0.656

Table G.6: Sensors utilisation for the tool 6 with rubber sleeve using PCA.

Tool 6			
Sensor	U 1st system	U 2nd system	Optimised System
Dynamometer	16.66%	20%	13.33%
Pwr	10%	-----	-----
Edx	-----	10%	-----
Edy	40%	30%	60%
UA Average Utilisation	22.22%	20%	36.66%
System Cost	£19102	£19420	£19035
Average Eigenvalue	0.691	0.464	0.650

As shown in Table G.5, the overall average utilisation has increased in the first and second systems from 24.44% up to 36.66% and the cost is reduced by 23 % from £24789 to £19035. In addition, for other tools without sleeve, the average sensitivity of the system did not significantly change as can be seen in Table G.7. In fact the average sensitivity has increased to 0.656 compared with the second system of tool 5.

Table G.7: The optimised system (1st and 2nd system) for the tool with rubber sleeve using PCA.

Tools with rubber sleeve								
Tool 4			Tool 5			Tool 6		
Sensory Signal	PC method	Eigen-value	Sensory Signal	PC method	Eigen-value	Sensory Signal	PC method	Eigen-value
Fx	PC 2	0.807	Fx	PC 6	0.833	Edy	PC 5	0.871
Edy	PC 7	0.694	Edy	PC 11	0.732	Edy	PC 1	0.810
Fx	PC 8	0.685	Fx	PC 6	0.712	Fx	PC 6	0.729
Edy	PC 4	0.645	Fx	PC 10	0.667	Fx	PC 3	0.706
Fx	PC 9	0.607	Edy	PC 9	0.666	Edy	PC 13	0.646
Edy	PC 11	0.563	Edy	PC 13	0.617	Edy	PC 6	0.626
Edy	PC 7	0.547	Edy	PC 5	0.607	Fx	PC 6	0.598
Edy	PC 11	0.538	Edy	PC 2	0.592	Fx	PC 11	0.526
Edy	PC4	0.519	Fx	PC 8	0.591	Edy	PC 7	0.509
Edy	PC 1	0.500	Edy	PC 6	0.570	Edy	PC 14	0.480
Average		0.611	Average		0.659	Average		0.650

3- Tools with copper sleeve

From Tables E.7 and E.8, it can be observed that there is no significant difference in the average sensitivity for both systems for the three tools with copper sleeves.

For the tool 8, for example, the cost of first and second systems is relatively different (££19065, £19420). But it is still can be optimised by increasing the system utilisation by replacing the sensory characteristic features of the force sensor from the first system with the eddy current sensory signals from the second system to reduce the cost and still have the sensitivity level.

Table G.8: Sensors utilisation for the tool 7 with copper sleeve using PCA.

Tool 7			
Sensor	U 1st system	U 2nd system	Optimised System
Dynamometer	16.66%	26.66%	13.33%
Edy	50%	20%	60%
UA Average Utilisation	33.33%	23.33%	36.66%
System Cost	£19035	£19035	£19035
Average Eigenvalue	0.673	0.469	0.669

Table G.9: Sensors utilisation for the tool 8 with copper sleeve using PCA.

Tool 8			
Sensor	U 1st system	U 2nd system	Optimised System
Dynamometer	10%	16.66%	-----
Mic	10	-----	10
Edx	-----	20%	20%
Edy	60%	30%	70
UA Average Utilisation	26.66%	22.22%	33.33%
System Cost	£19065	£19420	£7450
Average Eigenvalue	0.712	0.516	0.660

Table G.10: Sensors utilisation for the tool 9 with copper sleeve using PCA.

Tool 9			
Sensor	U 1st system	U 2nd system	Optimised System
Dynamometer	23.33%	16.66%	20%
Edx	-----	20%	-----
Edy	30%	30	40%
UA Average Utilisation	21.66%	22.22%	30%
System Cost	£19035	19420	£19035
Average Eigenvalue	0.760	0.545	0.757

As shown in Table G.9, the overall average utilisation has increased in the first system from 26.66% up to 33.3% and from 22.2% up to 33.3% in the second system and the cost is reduced by 60% from £24789 to £7450. In addition, the average sensitivity of the system did not significantly change as can be seen in Table G.10. In fact the average sensitivity has increased to 0.660 compared with the second system of tool 8.

Table G.10: The optimised system (1st and 2nd system) for the tool with copper sleeve using PCA.

Tools without sleeve								
Tool 7			Tool 8			Tool 9		
Sensory Signal	PC method	Eigen-value	Sensory Signal	PC method	Eigen-value	Sensory Signal	PC method	Eigen-value
Fx	PC7	0.824	Mic	PC 1	0.933	Fx	PC 1	0.897
Edy	PC 13	0.796	Edy	PC 8	0.752	Fx	PC 14	0.870
Edy	PC 8	0.785	Edy	PC 8	0.693	Edy	PC 6	0.834
Fx	PC 4	0.784	Edy	PC 5	0.662	Fx	PC 12	0.792
Edy	PC 13	0.707	Edy	PC 3	0.652	Edy	PC 15	0.776
Fx	PC 2	0.640	Edy	PC 9	0.641	Fx	PC 1	0.744
Fx	PC 1	0.572	Edy	PC 11	0.610	Fx	PC 3	0.702
Edy	PC 10	0.564	Edx	PC 9	0.575	Edy	PC 12	0.680
Edy	PC 13	0.528	Edy	PC 14	0.564	Fx	PC 2	0.654
Edy	PC6	0.491	Edx	PC 1	0.524	Edy	PC 7	0.626
Average		0.669	Average		0.660	Average		0.757

4- Tools with aluminium sleeve

From Tables E.10 and E.11, it can be observed that there is no significant difference in the average sensitivity for both systems for the three tools with aluminium sleeves.

For the tool 10, for instance, the cost of first and second systems is slightly different (£19065, £19420). But it is still can be optimised by increasing the system utilisation by replacing the sensory characteristic features of the sound sensor from the first system with the eddy current sensory signals from the second system to reduce the cost and still have the sensitivity level.

Table G.11: Sensors utilisation for the tool 10 with aluminium sleeve using PCA.

Tool 10			
Sensor	U 1st system	U 2nd system	Optimised System
Dynamometer	13.33%	16.66%	13.33%
Mic	10%	-----	-----
Edx	-----	20%	-----
Edy	50%	30%	60%
UA Average Utilisation	24.44%	22.22%	36.66%
System Cost	£19065	£19420	£19035
Average Eigenvalue	0.727	0.520	0.695

Table G.12: Sensors utilisation for the tool 11 with aluminium sleeve using PCA.

Tool 11			
Sensor	U 1st system	U 2nd system	Optimised System
Dynamometer	23.33%	10%	20%
Edx	-----	10%	-----
Edy	30%	60%	40%
UA Average Utilisation	26.66%	26.66%	30%
System Cost	£19035	£19420	£19035
Average Eigenvalue	0.698	0.522	0.697

Table G.13: Sensors utilisation for the tool 12 with aluminium sleeve using PCA.

Tool 12			
Sensor	U 1st system	U 2nd system	Optimised System
Dynamometer	16.66%	10%	13.33%
Edx	-----	20%	-----
Edy	50%	30%	60%
UA Average Utilisation	33.33%	20%	36.66%
System Cost	£19035	£19420	£19035
Average Eigenvalue	0.701	0.524	0.697

As shown in Table G.11, the overall average utilisation has increased in the first system from 24.44% up to 36.66% and from 22.22% up to 36.66% in the second system and the cost is reduced by 23 % from £24789 to £19035. In addition, for another tools with aluminium sleeve, the average sensitivity of the system did not significantly change as can be seen in Table G.14. In fact the average sensitivity has increased to 0.697 compared with the second system of the tool 10.

Table G.14: The optimised system (1st and 2nd system) for the tools with aluminium sleeve using PCA.

Tools with aluminium sleeve								
Tool 10			Tool 11			Tool 12		
Sensory Signal	PC method	Eigen-value	Sensory Signal	PC method	Eigen-value	Sensory Signal	PC method	Eigen-value
Fx	PC 11	0.857	Fx	PC 1	0.805	Edy	PC 1	0.816
Fx	PC 8	0.822	Fx	PC 9	0.793	Fx	PC 6	0.795
Edy	PC 5	0.816	Edy	PC 13	0.763	Edy	PC 6	0.783
Edy	PC 6	0.784	Fx	PC 15	0.735	Fx	PC 8	0.753
Fx	PC 4	0.657	Fy	PC 11	0.725	Fx	PC 13	0.707
Edy	PC 8	0.642	Fy	PC 10	0.705	Edy	PC 14	0.706
Edy	PC 15	0.620	Edy	PC 5	0.674	Fx	PC 9	0.669
Fx	PC 2	0.609	Fx	PC 4	0.597	Edy	PC 9	0.592
Edy	PC 10	0.593	Edy	PC 14	0.590	Edy	PC 11	0.587
Edy	PC 1	0.554	Edy	PC 1	0.582	Edy	PC 15	0.568
Average		0.695	Average		0.697	Average		0.697

Appendix H: System Evaluation (For Chapter 9)

9.4.3.1 Linear Regression (LR) Method)

Same methods which are used to calculate the average sensitivity of the sensory signals and signal processing methods using Linear regression (LR) in chapter 8, section 8.5.2.1, here it will be applied for the signals for testing 12 tools as in the next sections.

1- Tools without sleeve

Figure H.1 show the average sensitivity (A_s) for the three tools without sleeve, as it is clear that the force (F_y) and Power sensors are the higher sensitivity for the tool 2 and tool 3 respectively.

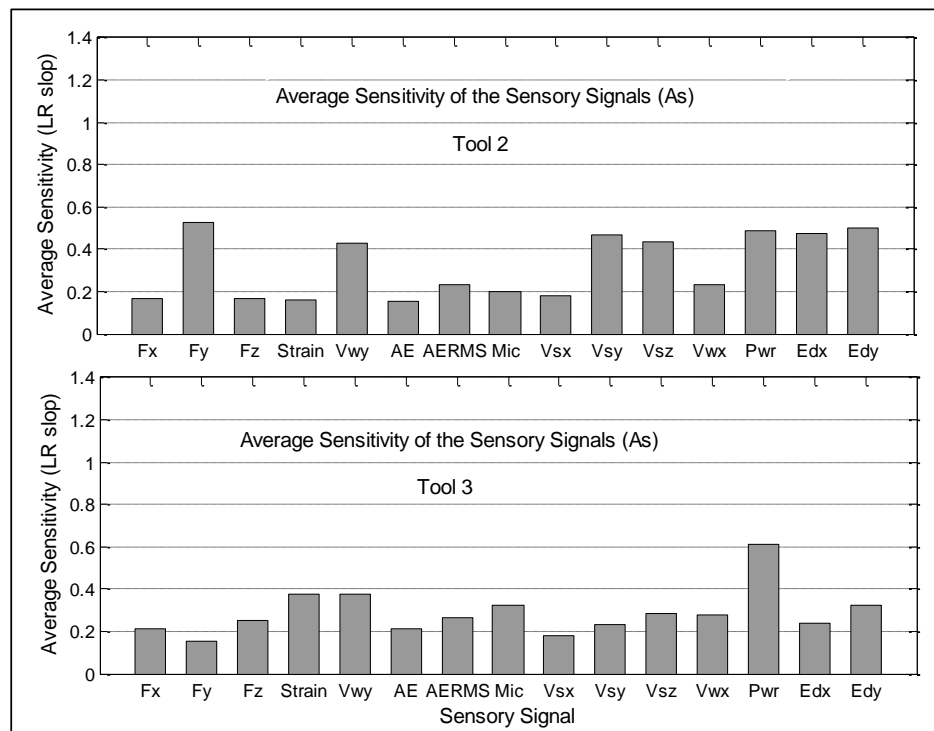


Figure H.1: A_s values for the sensory signals of tools without sleeve.

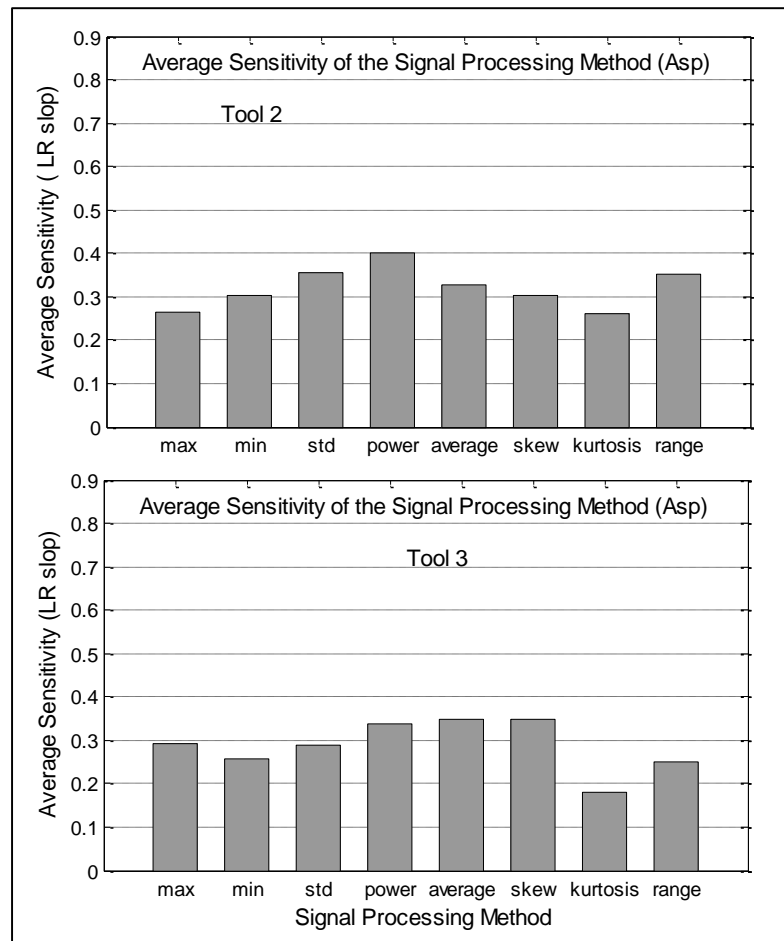


Figure H.2: Asp values for the signal processing methods of tools without sleeve.

Figure H.2 shows the average of the sensitivity of the signal processing methods (Asp) for the three tools without sleeve. It presents the power as a signal processing method take the higher rank as more sensitive method for tool 2. Meanwhile, the skewness (skew) is the more sensitive method for the tool 3.

Same method in the chapter 9, section 9.5.2.1, here the average of the summation of sensitivity coefficients (A_c) of those systems is found to be (0.58, 0.32 and 0.28) for the three tools without sleeve . However, to find the effectiveness of the selection of the utilised sensors and signal processing methods, the evaluated values can be compared with other systems.

2- Tools with rubber sleeve

Figure H.3 shows the average sensitivity (As) for the three tools with rubber sleeve, as it is clear that the accelerometer attached to spindle in x axis (V_{sx}) is the more sensitive for the tool 4, however accelerometer attached to the moveable machine

table (Vwy) and power sensor are the higher sensitivity for the tool 5 and tool 6 respectively.

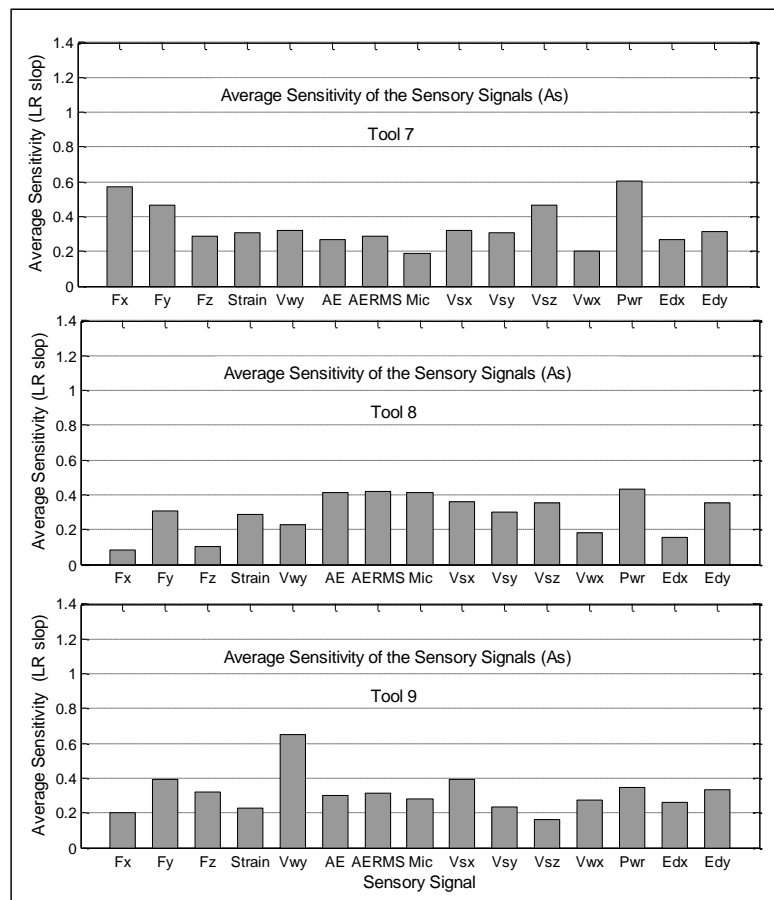


Figure H.3: As values for the sensory signals of tools with rubber sleeve.

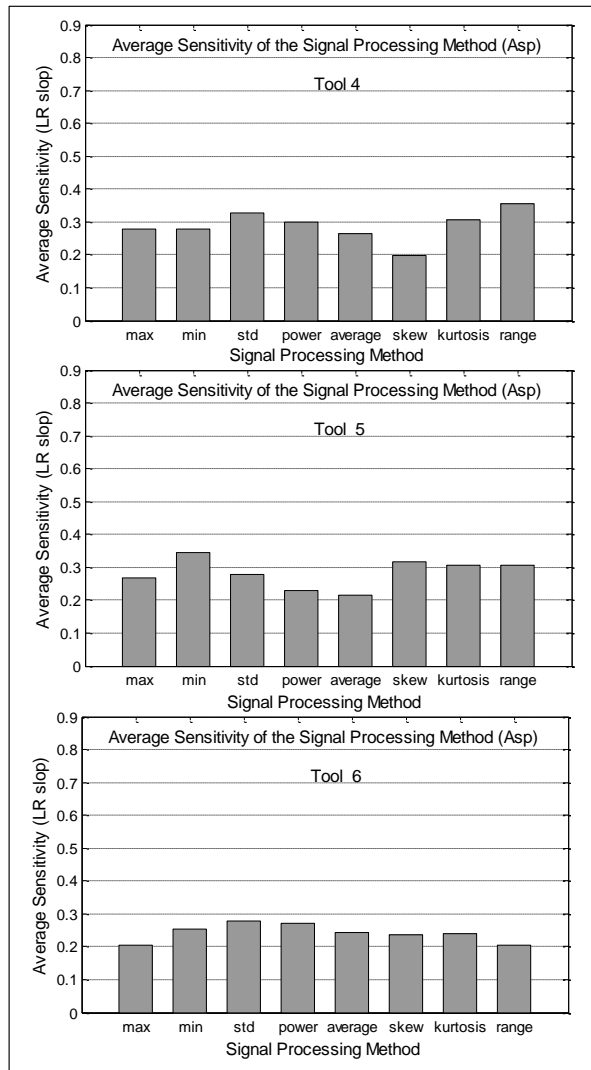


Figure H.4: Asp values for the signal processing methods of tools with rubber sleeve.

Similarly, Figure H.4 shows the average of the sensitivity of the signal processing methods (Asp) for the three tools with rubber sleeve. It presents the range as a signal processing method take the higher rank as more sensitive method for tools 4, however the minimum method (min) and standard deviation (std) for the fifth and sixth tools. The average of the summation of sensitivity coefficients (Ac) of the above systems is found to be (0.29, 0.28 and 0.24) for the three tools with rubber sleeve respectively.

3- Tools with copper sleeve

Figure H.5 shows the average sensitivity (As) for the three tools with copper sleeve, as it is clear that the power (Pwr) is the more sensitive for the tool 7, meanwhile the

acoustic emission (AE) accelerometer (Vwy) are the higher sensitivity for the tool 8 and tool 9 respectively.

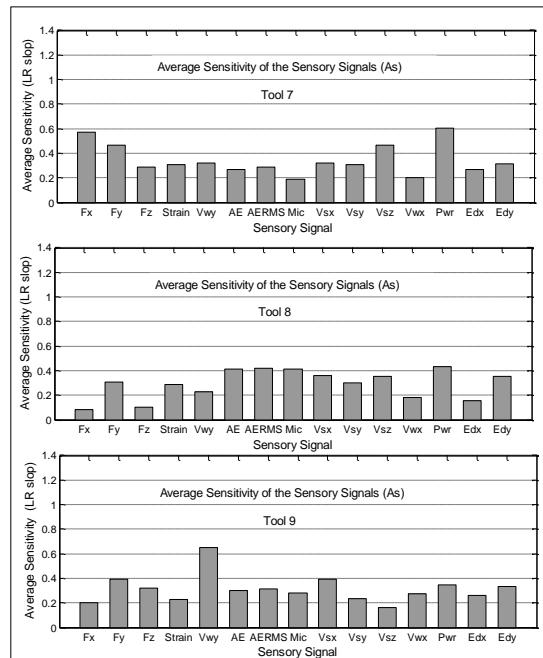


Figure H.5: As values for the sensory signals of tools with copper sleeve.

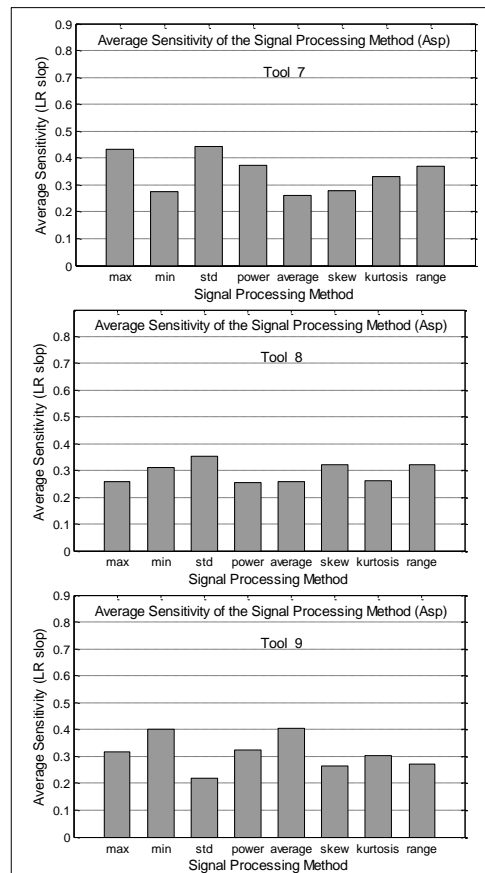


Figure H.6: Asp values for the signal processing methods of tools with copper sleeve.

The average of the sensitivity of the signal processing methods (Asp) for the three tools with copper sleeve as shown in Figure H.6. It presents the standard deviation as a signal processing method take the higher rank as more sensitive method for both tools 7 and 8 , however the average method is more sensitive for the tool 9.

The average of the summation of sensitivity coefficients (Ac) of aforementioned systems is found to be (0.34, 0.29 and 0.31) for the three tools with copper sleeve.

4- Tools with aluminium sleeve

The average sensitivity (As) for the three tools with aluminium sleeve is illustrated in Figure H.7, it shows that the sound sensor (Mic) is the more sensitive for both tools 10 and 11, whereas the AE sensor is the higher sensitivity for the tool 12.

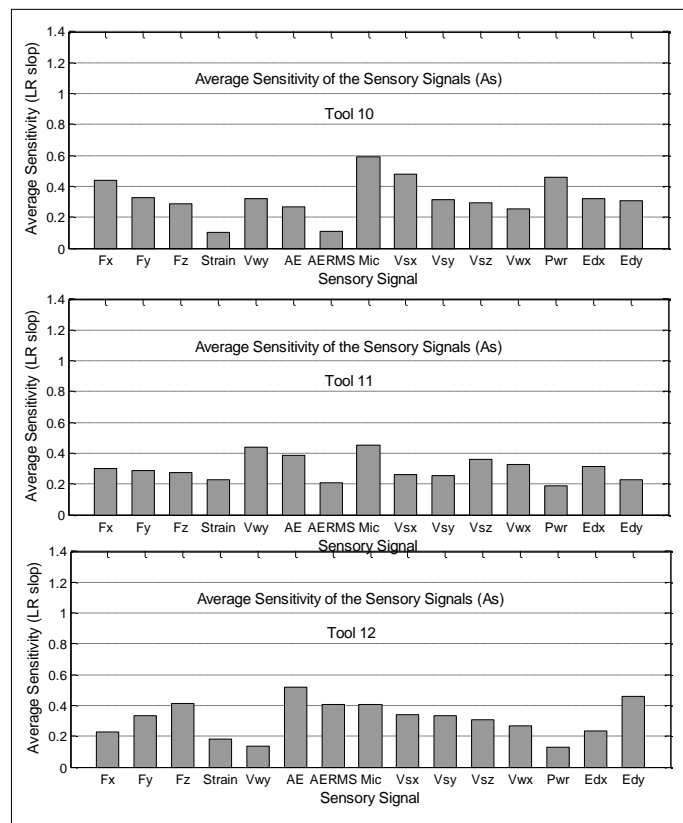


Figure H.7: As values for the sensory signals of tools with aluminium sleeve.

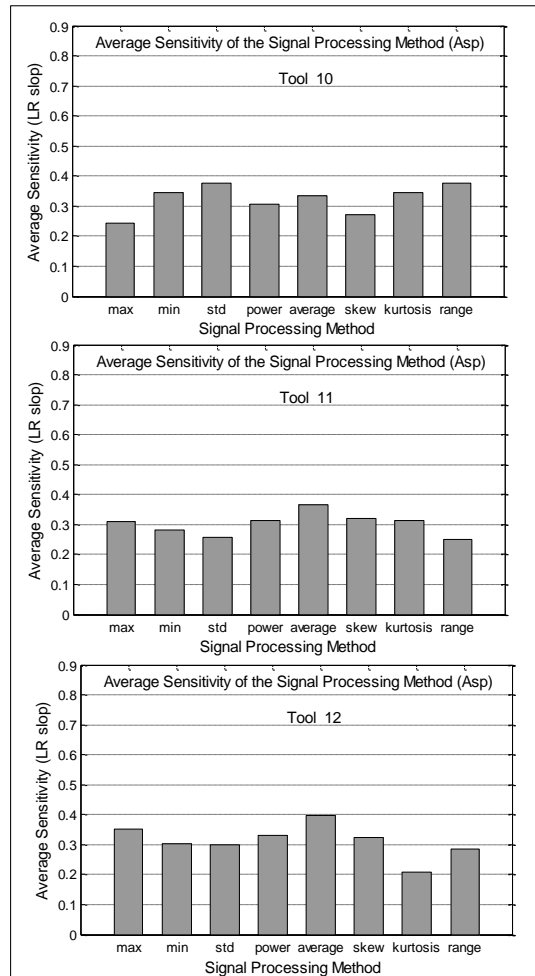


Figure H.8: Asp values for the signal processing methods of tools with aluminium sleeve.

Figure H.8 shows the average of the sensitivity of the signal processing methods (Asp) for the three tools with aluminium sleeve. It presents the standard deviation as a signal processing method take the higher rank as more sensitive method for the tool 10 , nevertheless the average method is the highest sensitive for both eleventh and twelfth tools. The average of the summation of sensitivity coefficients (Ac) of those systems is found to be (0.32, 0.30 and 0.31) for the three tools with aluminium sleeve

Appendix I: System Evaluation (For Chapter 9)

9.4.3.2 Principal Component Analysis (PCA) Method

1- Tools without sleeve

Figure I.1 shows the average eigenvalue (Aev) for the three tools without sleeve, as it is clear that the eddy current sensor is the more sensitive for both first and second tools. Force sensor (Fx) is the higher sensitivity for the third tool.

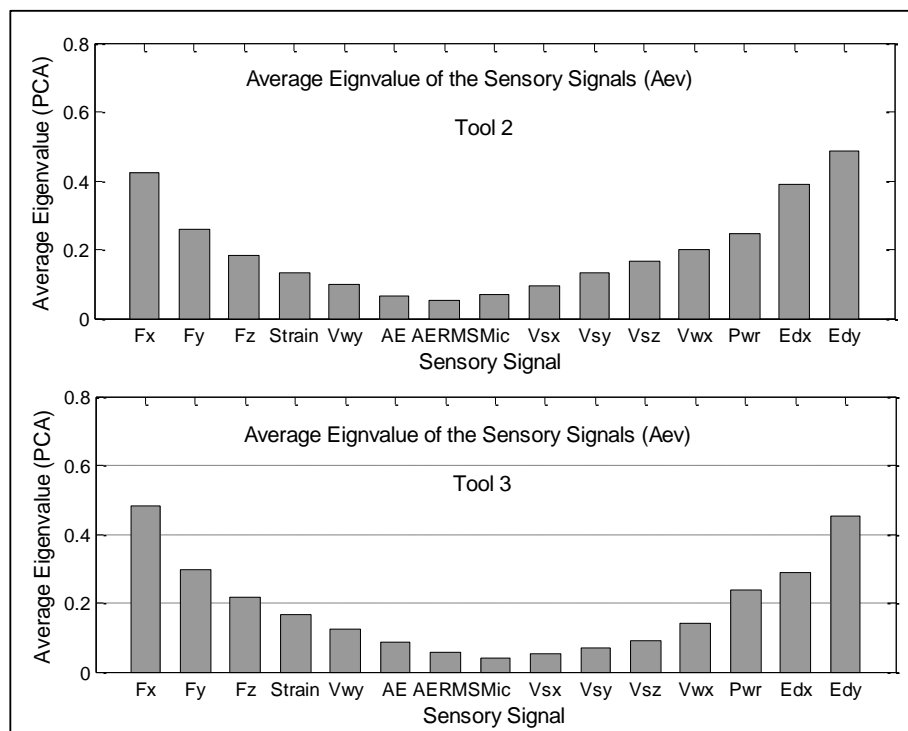


Figure I.1: Aev values for the sensory signals of tools without sleeve.

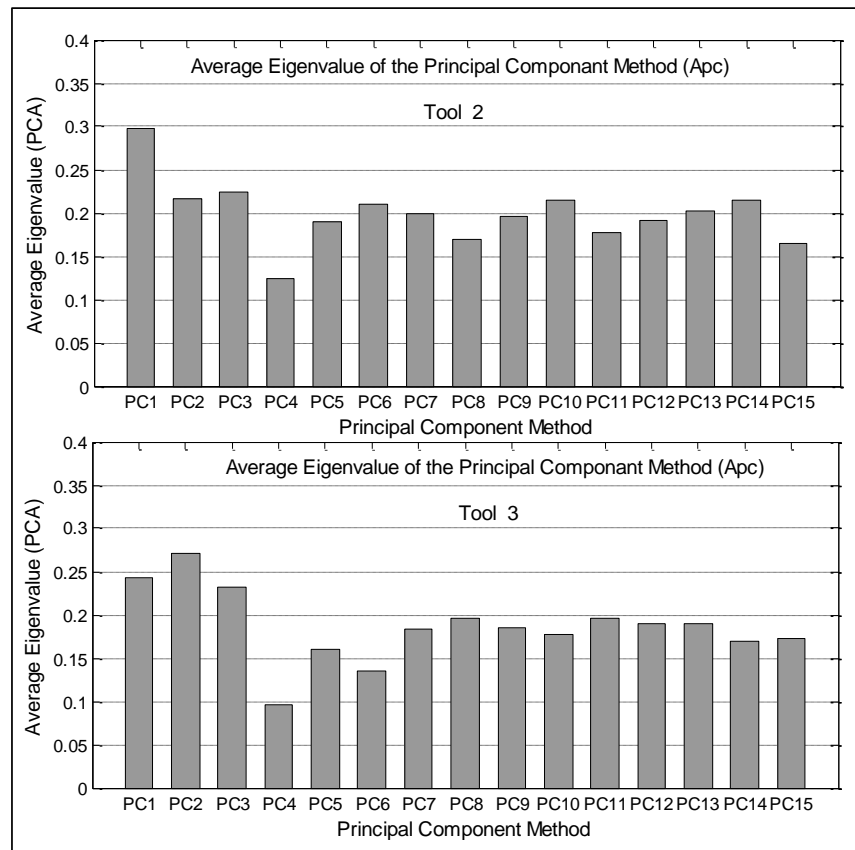


Figure I.2: Apc values for the principal component methods of tools without sleeve.

The average of the eigenvalue of the principal component methods (Apc) for the three tools with rubber sleeve as shown in Figure I.2. It presents the first principal component (PC1) as a signal method takes the higher rank as more sensitive method for tool 2 , however the second principal component (PC2) method is more sensitive for the tool 3.Same method in the chapter 9, section 9.5.2.2, here the average of the summation of eigenvalue coefficients (Ec) of those systems is found to be (0.19, 0.20 and 0.18) for the three tools without sleeve.

2- Tools with rubber sleeve

Figure I.3 shows The average eigenvalue (Aev) for the three tools with rubber sleeve, as it is clear that the eddy current sensor(Edy) attached to spindle case in y axis is the more sensitive for fourth, fifth and sixth tools.

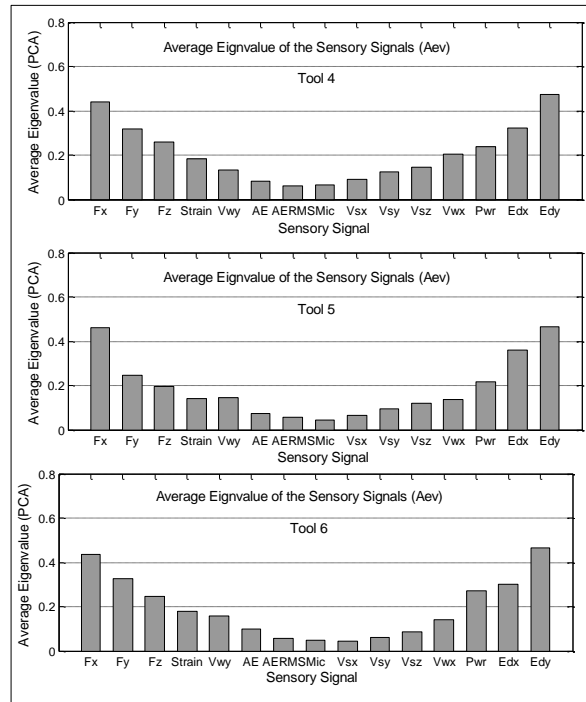


Figure I.3: Aev values for the sensory signals of tools rubber sleeve.

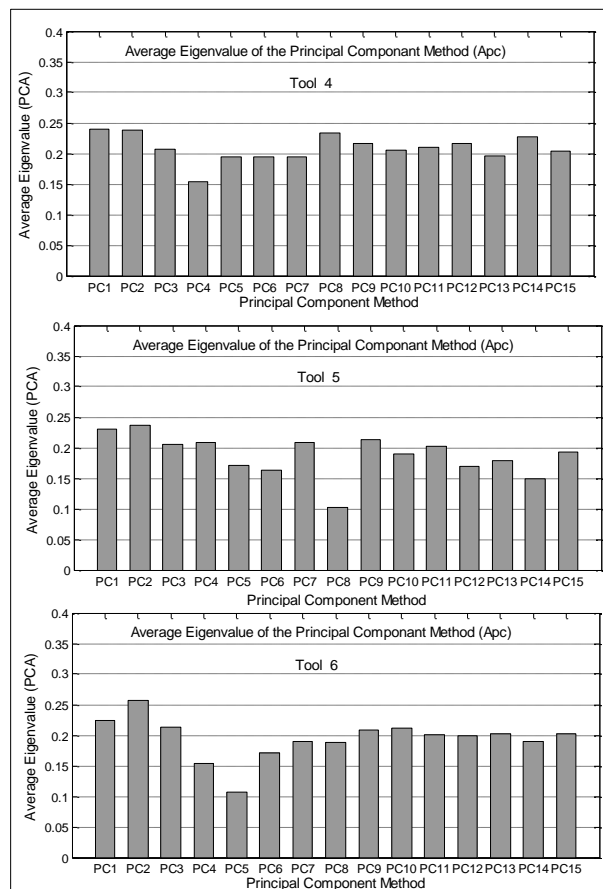


Figure I.4: Apc values for the principal component methods of tools with rubber sleeve.

Figure I.4 illustrates the average of the eigenvalue of the principal component methods (Apc) for the three tools with rubber sleeve. It presents the first principal component (PC1) as a signal method takes the higher rank as more sensitive method for both tools 4, however the second principal component (PC2) method is more sensitive for the tools 5 and 6. The average of the summation of eigenvalue coefficients (Ec) of those systems is found to be (0.21, 0.20 and 0.19) for the three tools with rubber sleeve.

3- Tools with copper sleeve

The average eigenvalue (Aev) for the three tools with copper sleeve is shown in Figure I.5. It is clear that the force sensor (Fx) is the more sensitive for both first and third tools. Eddy current (Edy) is the higher sensitivity for the second tool.

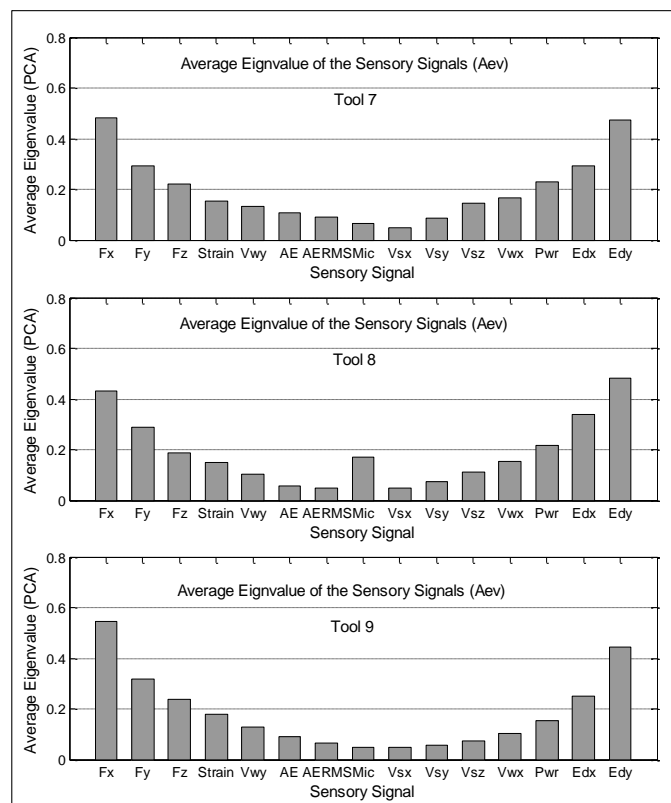


Figure I.5: Aev values for the sensory signals of tools with copper sleeve

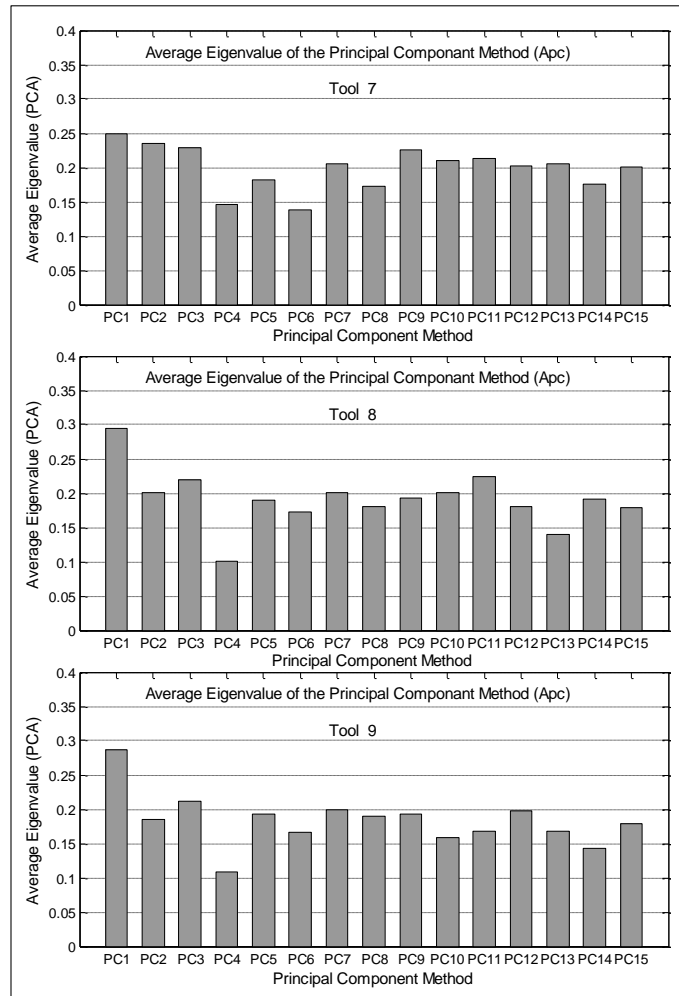


Figure I.6: Apc values for the principal component methods of tools with copper sleeve.

Similarly, Figure I.6 shows the average of the eigenvalue of the principal component methods (Apc) for the three tools with copper sleeve. It presents the first principal component (PC1) as more sensitive method for all those tools. The average of the summation of eigenvalue coefficients (Ec) of those systems is found to be (0.20, 0.19 and 0.18) for the three tools with copper sleeve.

4- Tools with aluminium sleeve

Figure I.7 shows the average eigenvalue (Aev) for the three tools with aluminium sleeve, as it is clear that the eddy current sensor (Edy) attached to spindle case in y axis is the more sensitive for those tools. However, the sound sensor (Mic) has a reasonable sensitivity for tenth tool.

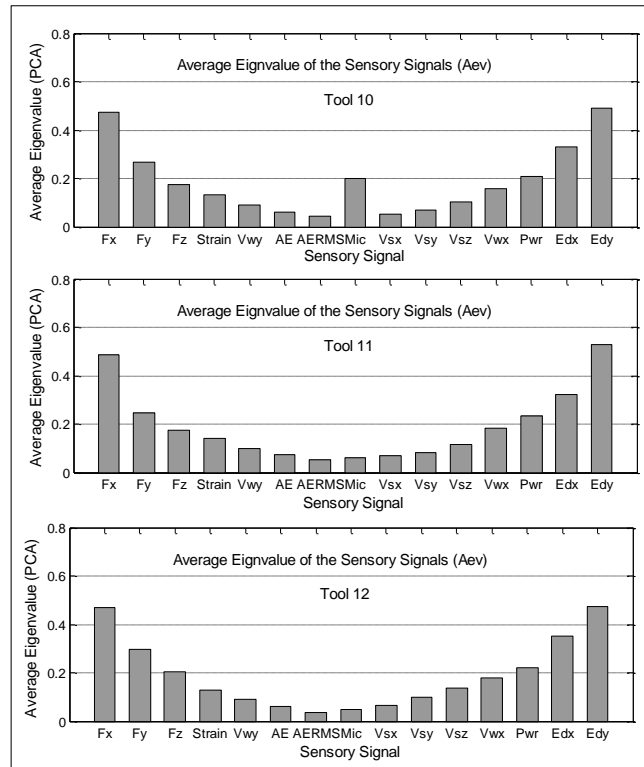


Figure I.7: Aev values for the sensory signals of tools with copper sleeve.

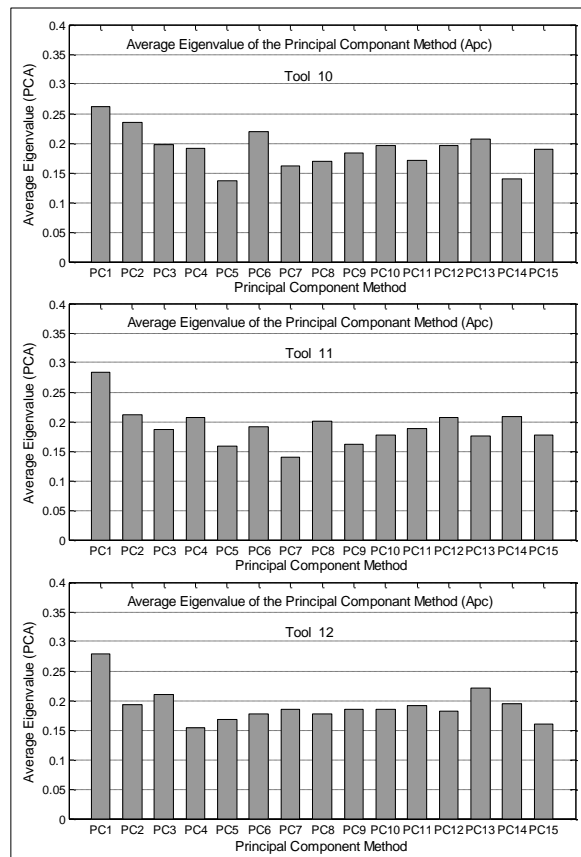


Figure I.8: Apc values for the principal component methods of tools with aluminium sleeve.

Appendix J: Signal Simplification (For Chapter 10)

10.3.1 Linear Regression (LR) method

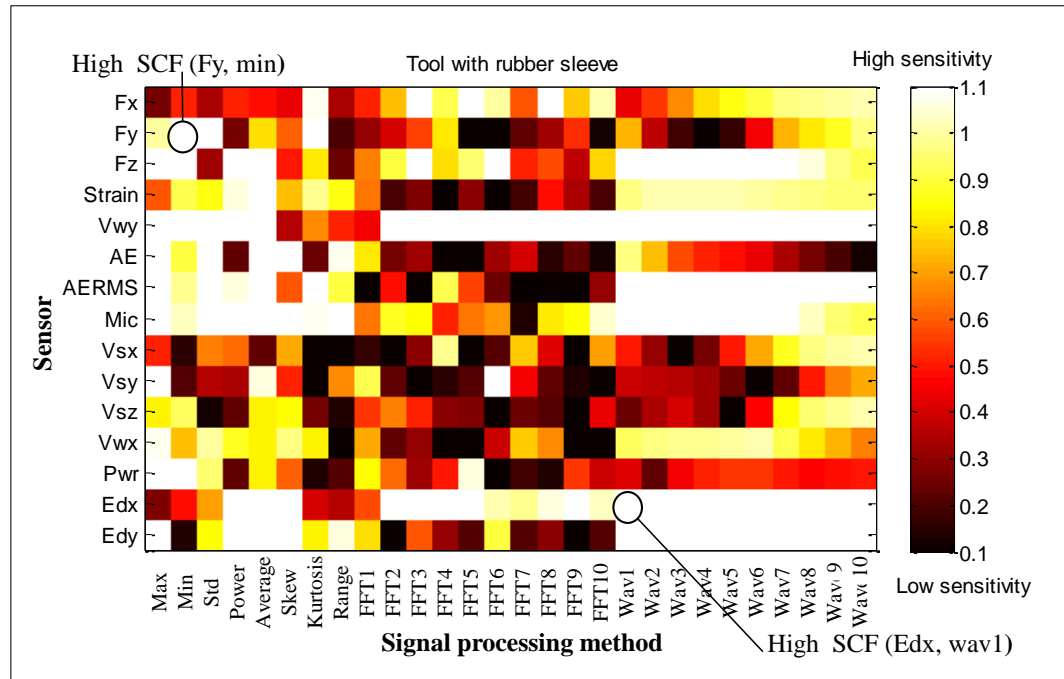


Figure J.1: A graphical presentation of the sensitivity for fresh tool with rubber sleeve using LR method.

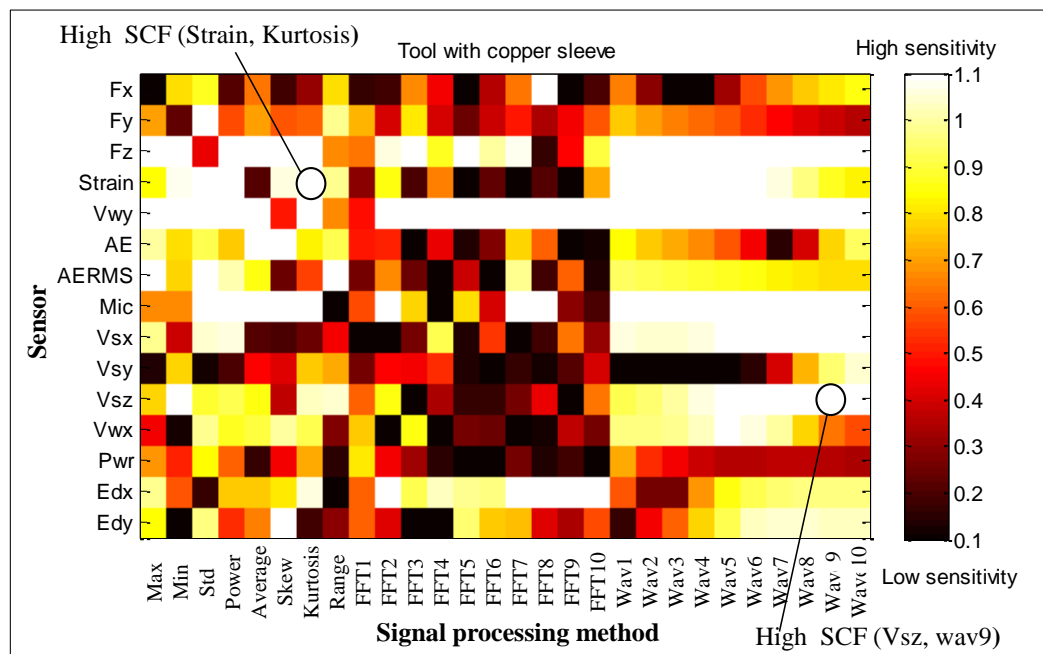


Figure J.2: A graphical presentation of the sensitivity for fresh tool with copper sleeve using LR method.

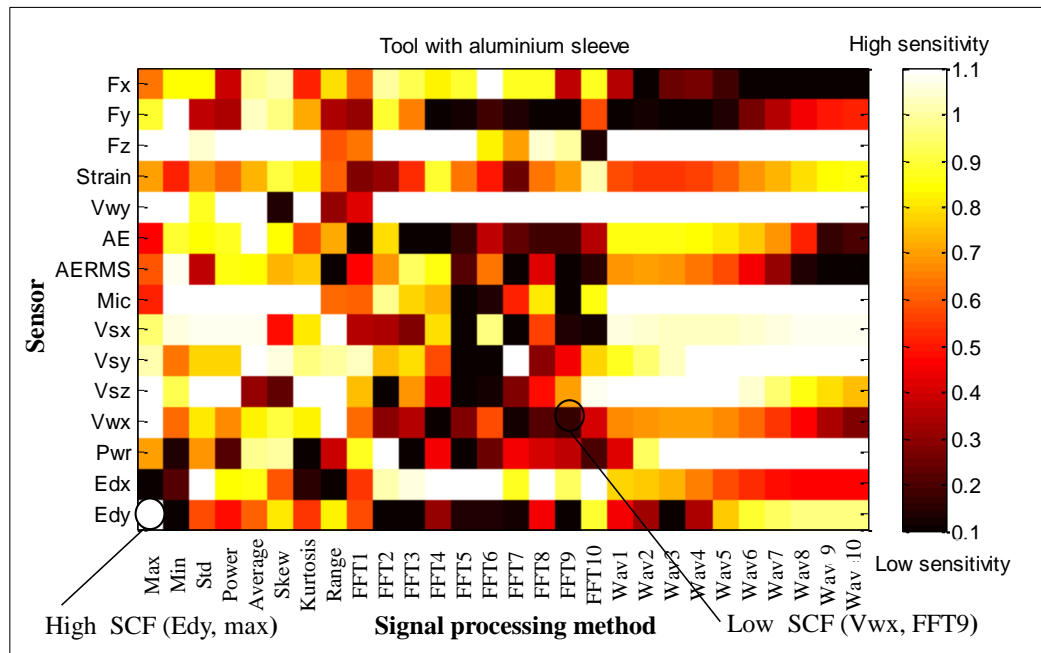


Figure J.3: A graphical presentation of the sensitivity for fresh tool with aluminium sleeve using LR method.

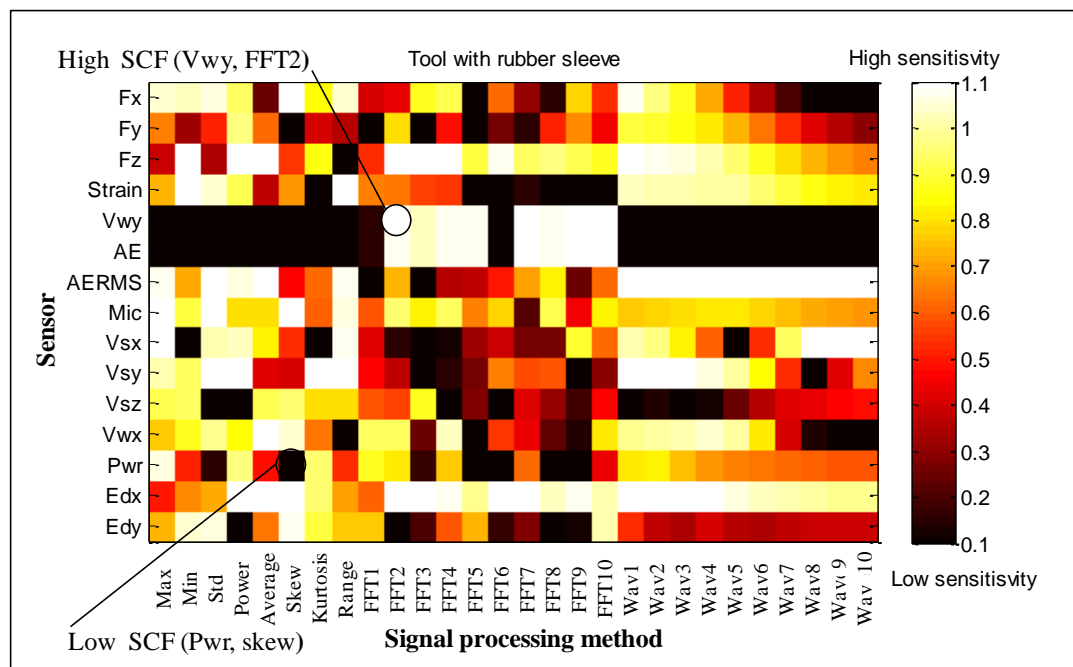


Figure J.4: A graphical presentation of the sensitivity for tool with one broken tooth, with rubber sleeve using LR method.

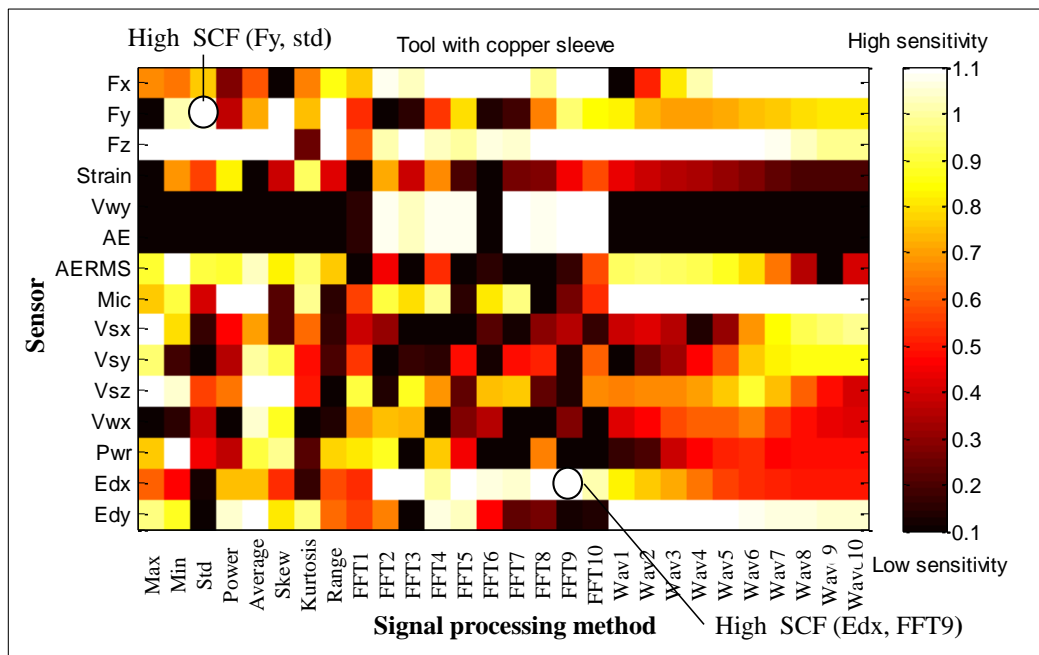


Figure J.5: A graphical presentation of the sensitivity for tool with one broken tooth, with copper sleeve using LR method.

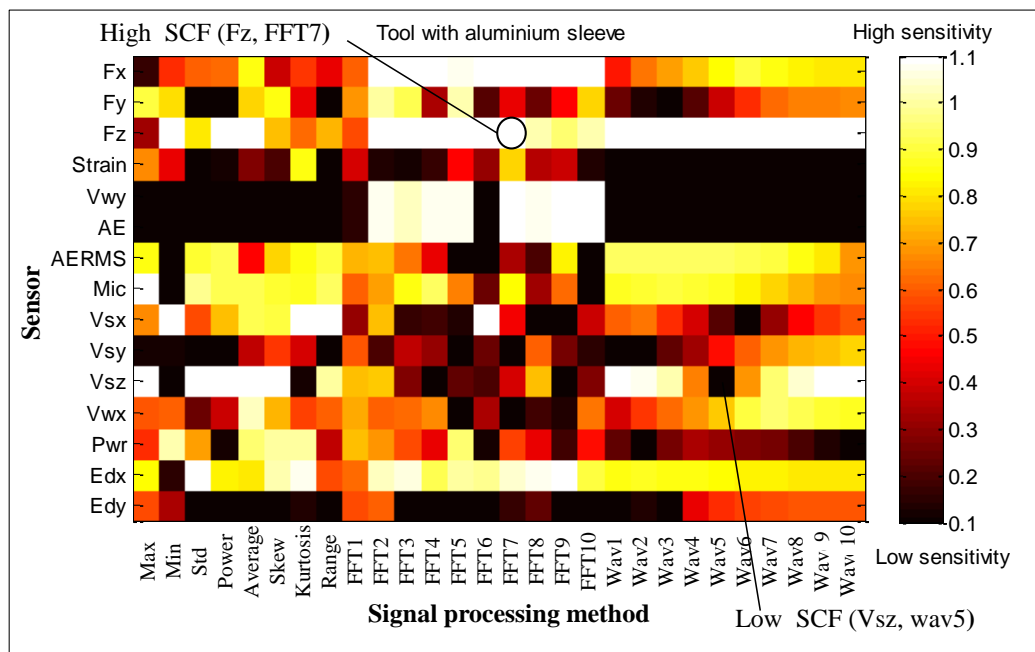


Figure J.6: A graphical presentation of the sensitivity for tool with one broken tooth, with aluminium sleeve using LR method.

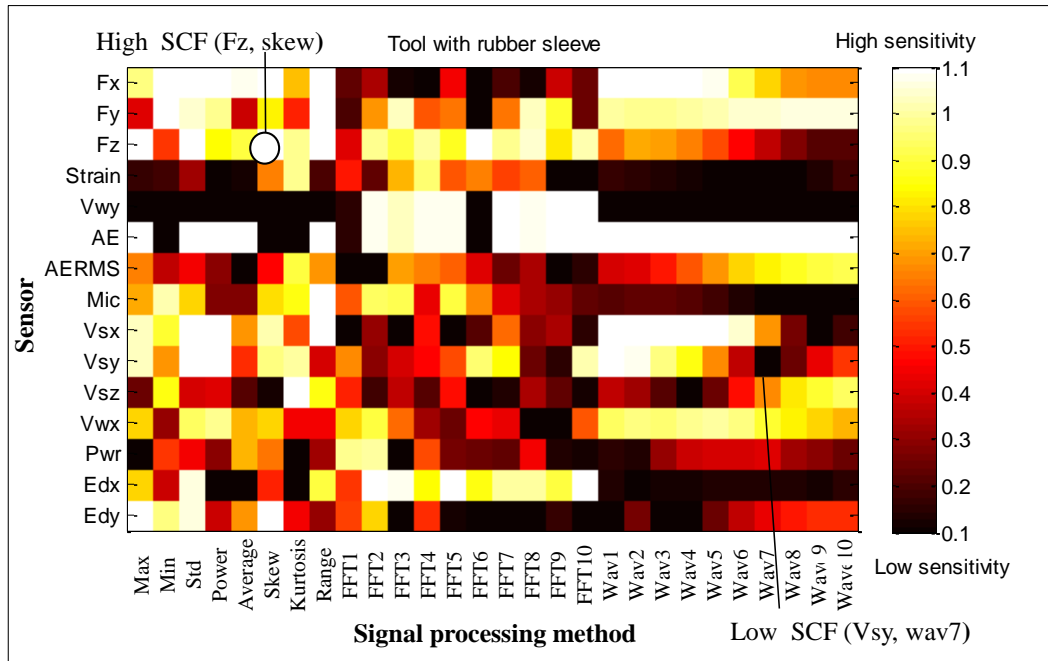


Figure J.7: A graphical presentation of the sensitivity for tool with two broken teeth, with rubber sleeve using LR method.

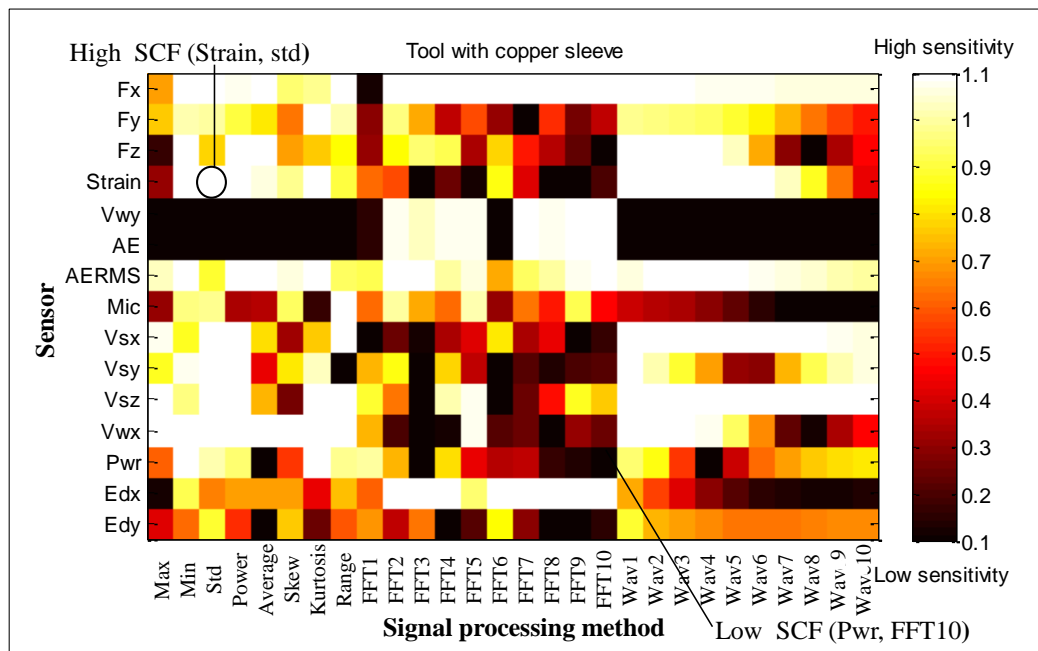


Figure J.8: A graphical presentation of the sensitivity for tool with two broken teeth, with copper sleeve using LR method.

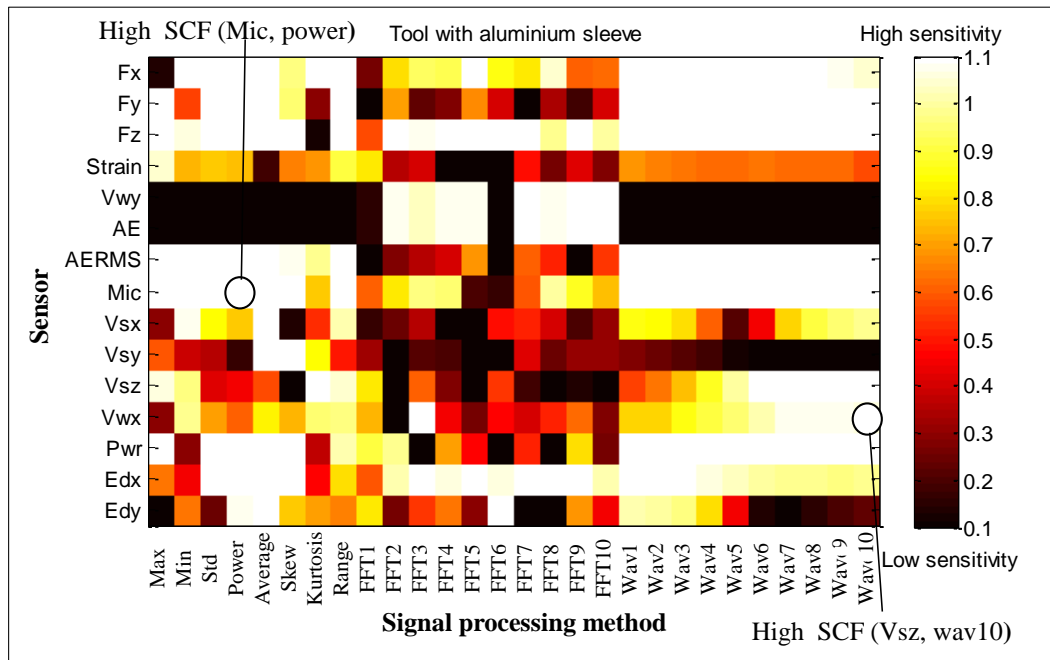


Figure J.9: A graphical presentation of the sensitivity for tool with two broken teeth, with aluminium sleeve using LR method.

Appendix K: Signal Simplification (For Chapter 10)

10.3.2 Range Value (RV) method

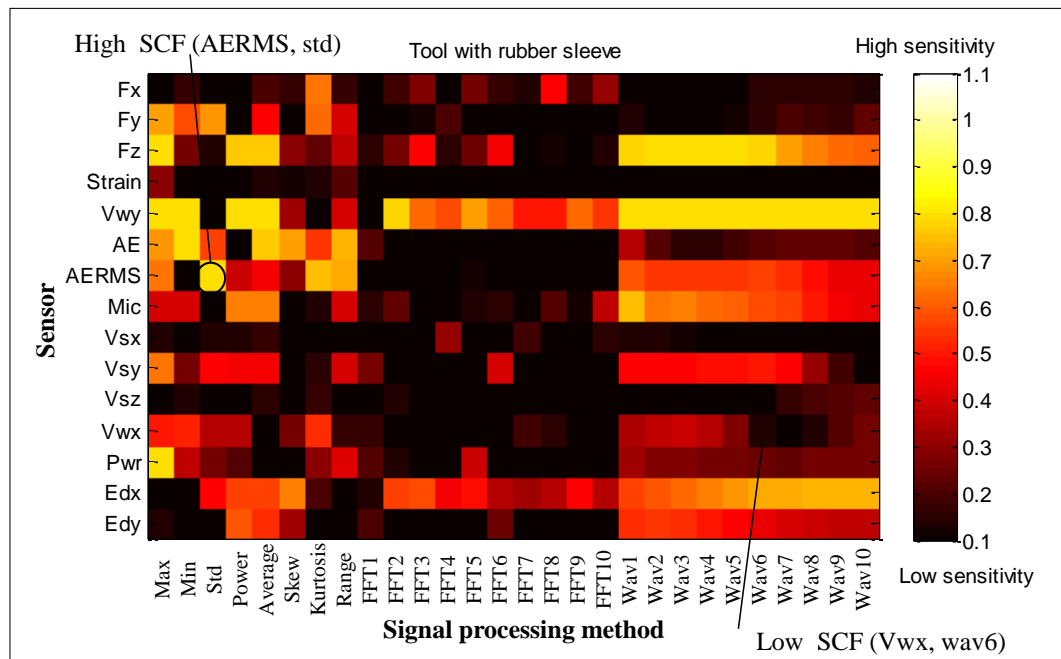


Figure K.1: A graphical presentation of the sensitivity for fresh tool with rubber sleeve using Range value method.

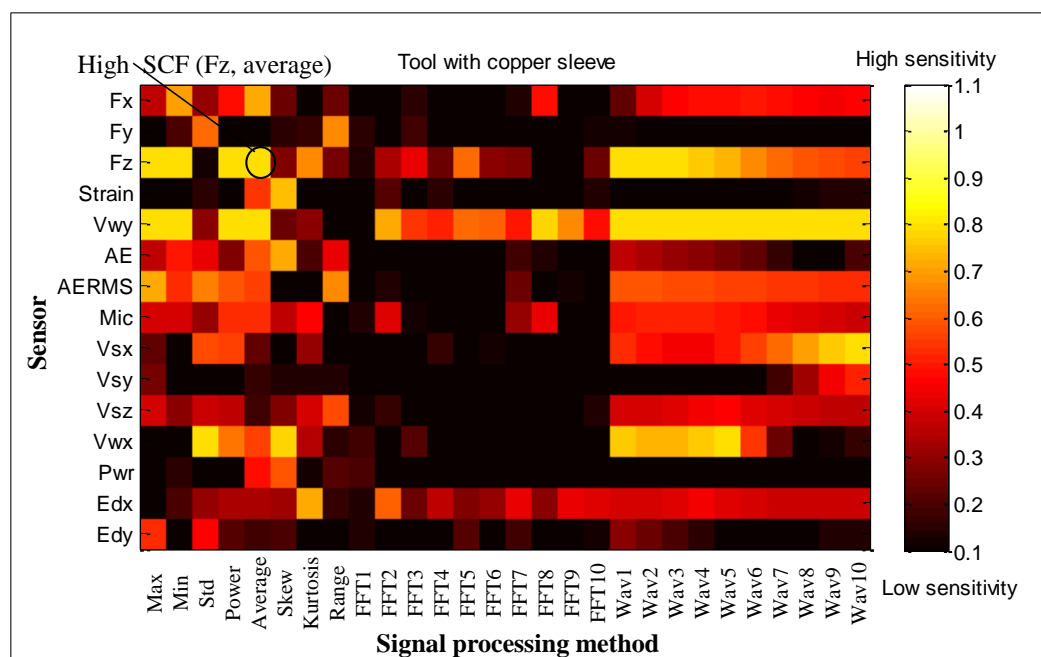


Figure K.2: A graphical presentation of the sensitivity for fresh tool with copper sleeve using Range value method.

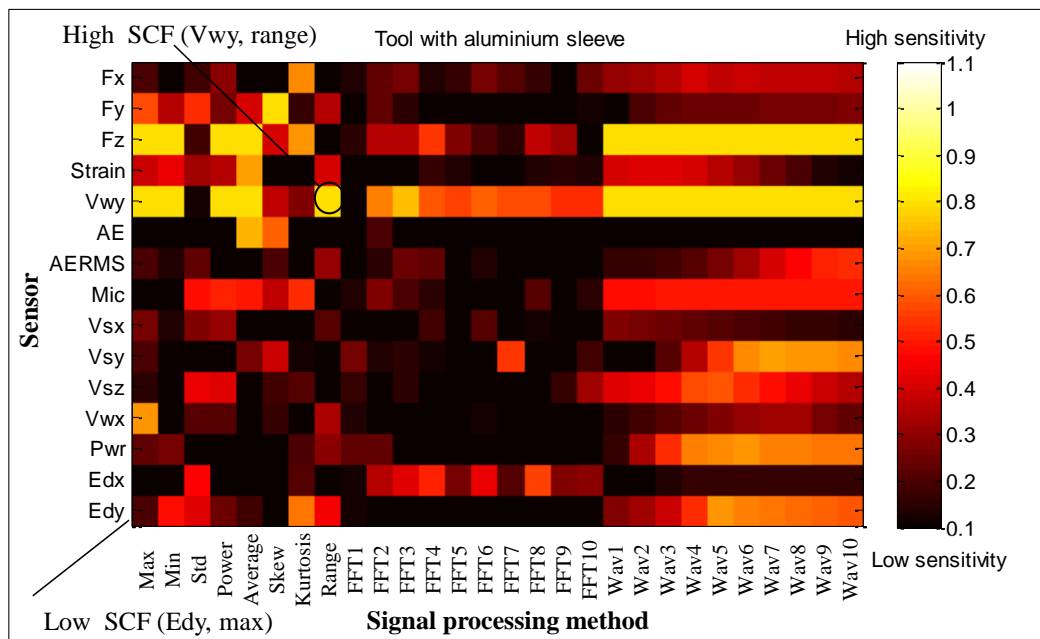


Figure K.3: A graphical presentation of the sensitivity for fresh tool with aluminium sleeve using Range value method

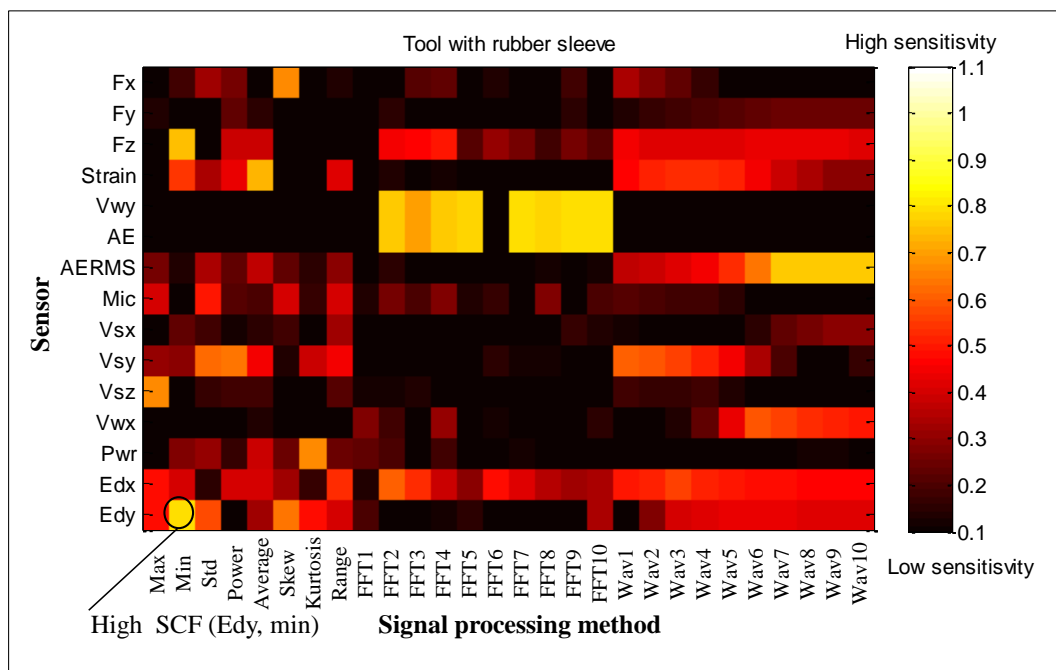


Figure K.4: A graphical presentation of the sensitivity for tool with one broken tooth, with rubber sleeve using Range value method.

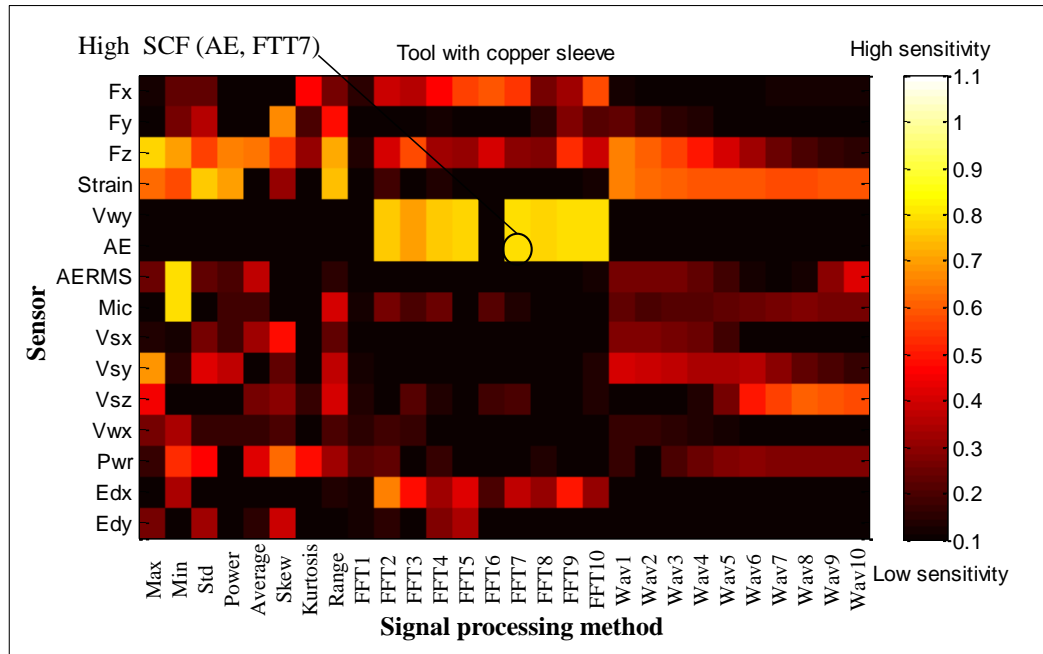


Figure K.5: A graphical presentation of the sensitivity for tool with one broken tooth, with copper sleeve using Range value method.

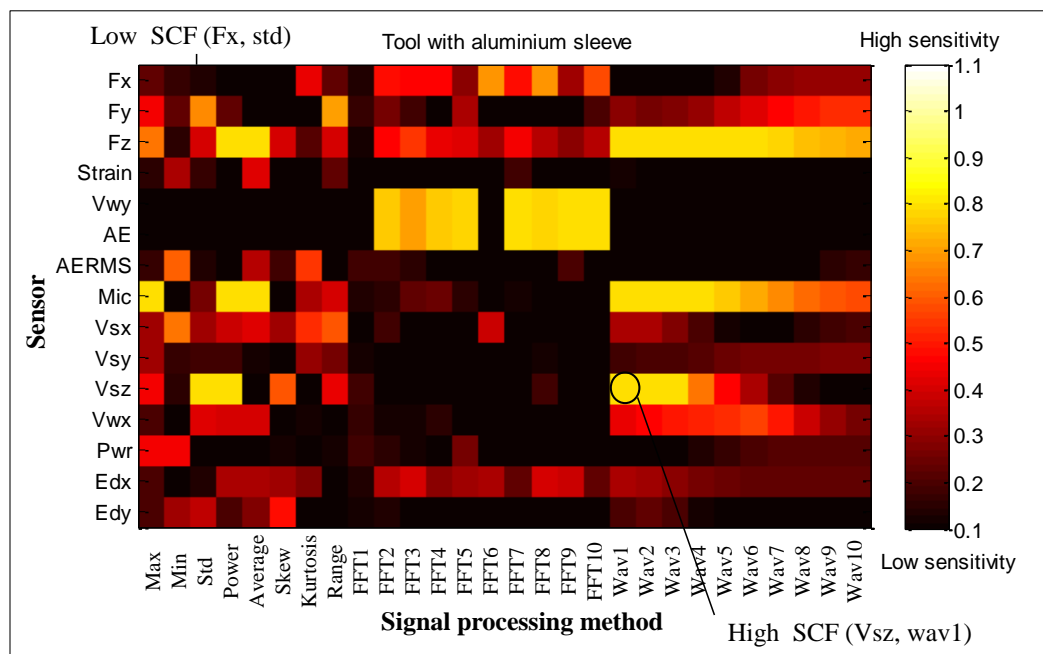


Figure K.6: A graphical presentation of the sensitivity for tool with one broken tooth, with aluminium sleeve using Range value method.

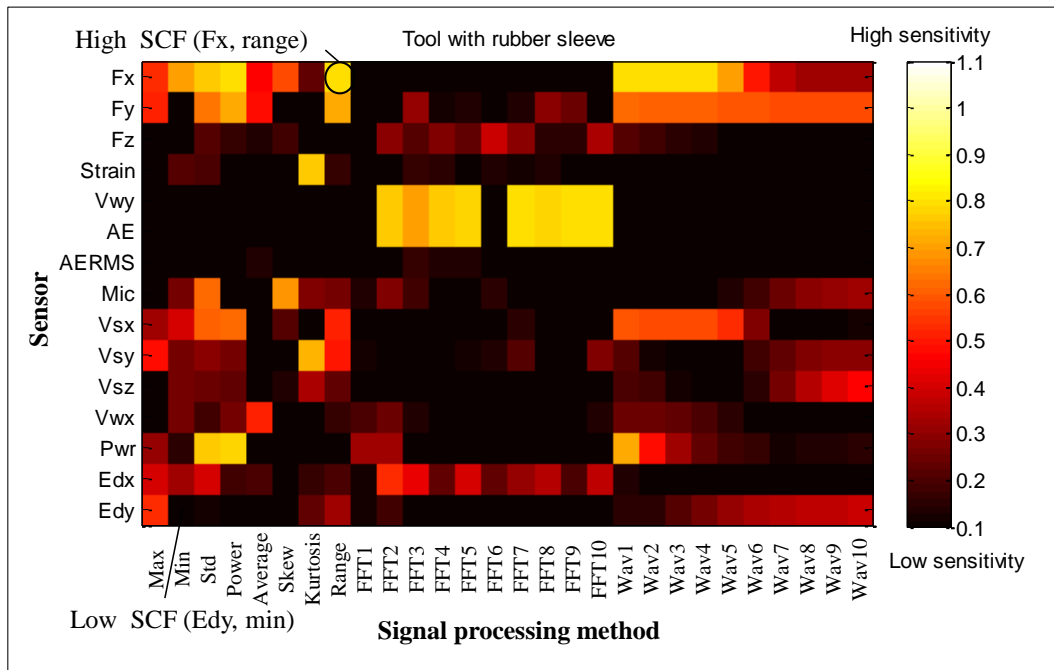


Figure K.7: A graphical presentation of the sensitivity for tool with two broken teeth, with rubber sleeve using Range value method.

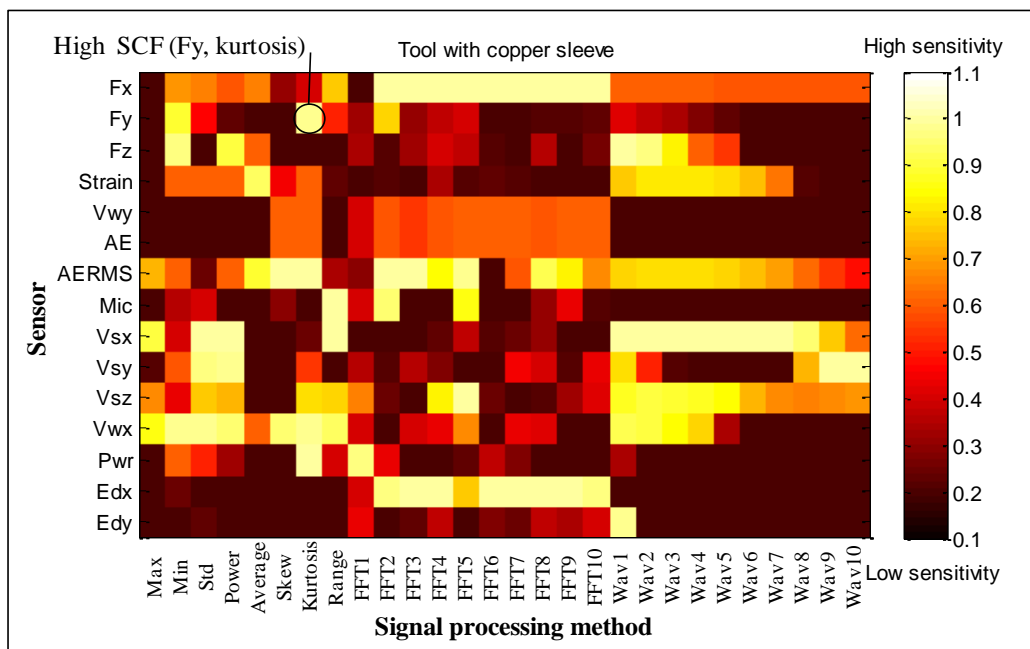


Figure K.8: A graphical presentation of the sensitivity for tool with two broken teeth, with copper sleeve using Range value method.

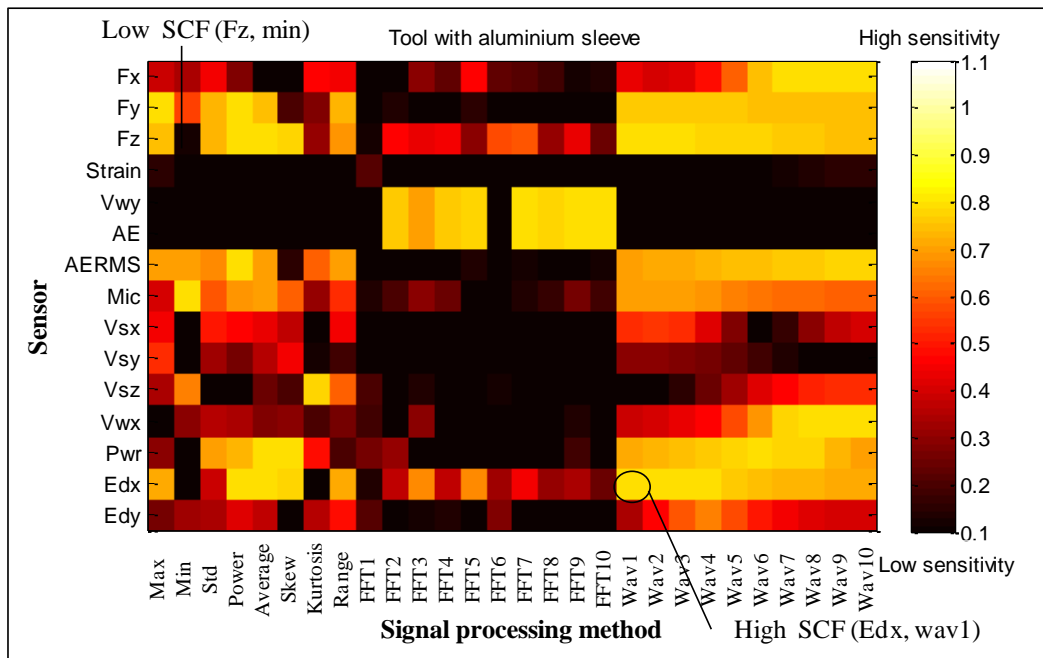


Figure K.9: A graphical presentation of the sensitivity for tool with two broken teeth, with aluminium sleeve using Range value method.

Appendix L: Signal Simplification (For Chapter 10)

10.3.3 Sudden Change In Value (SCIV) method

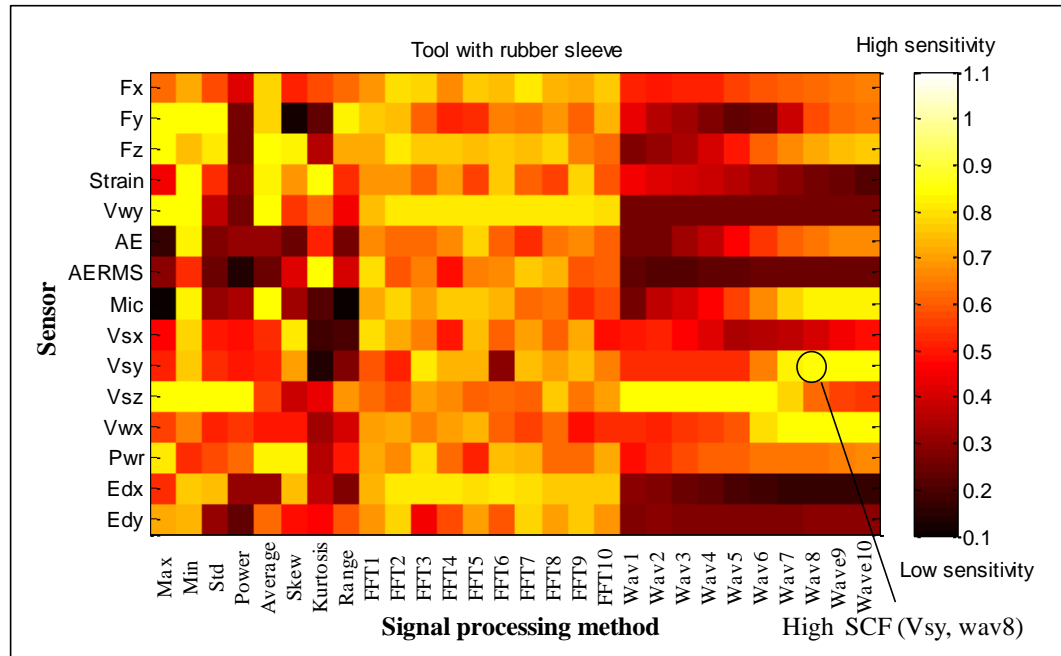


Figure L.1: A graphical presentation of the sensitivity for fresh tool with rubber sleeve using SCIV method.

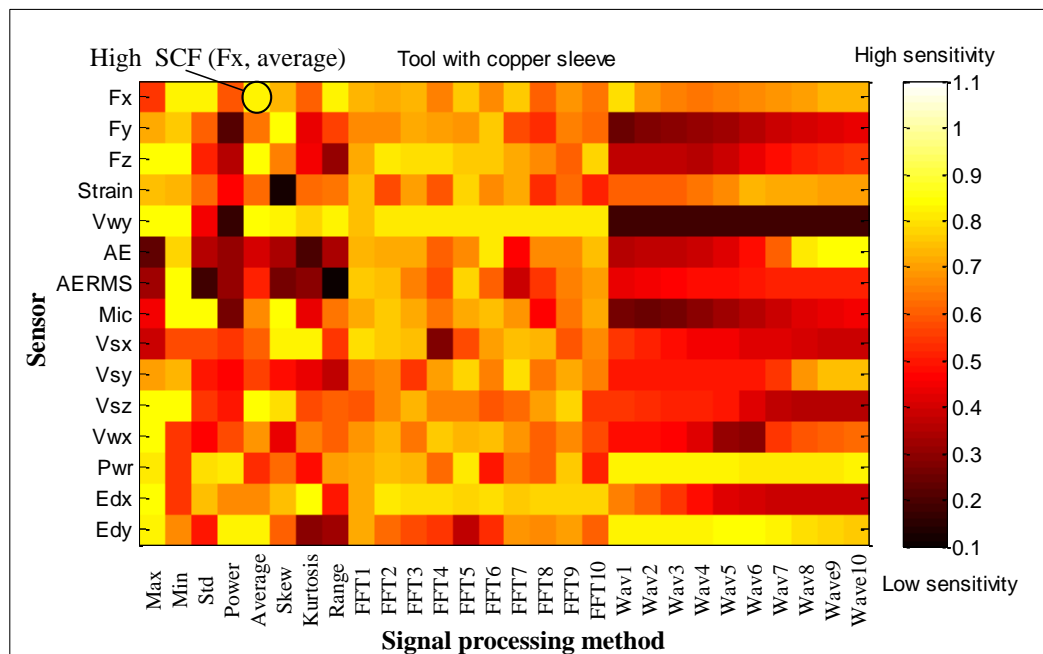


Figure L.2: A graphical presentation of the sensitivity for fresh tool with copper sleeve using SCIV method.

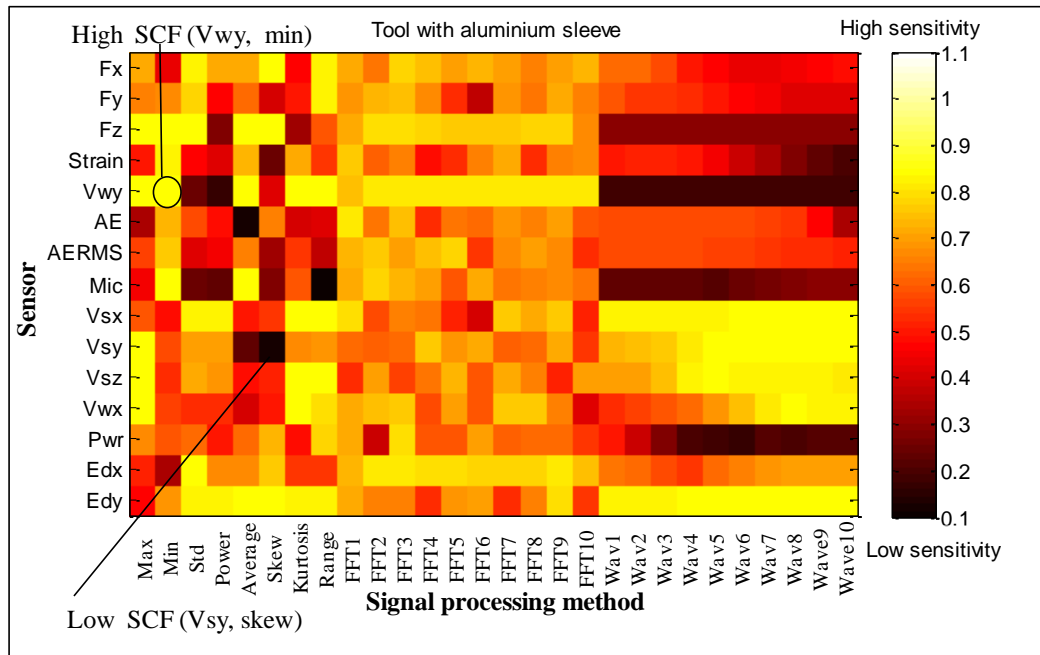


Figure L.3: A graphical presentation of the sensitivity for fresh tool with aluminium sleeve using SCIV method.

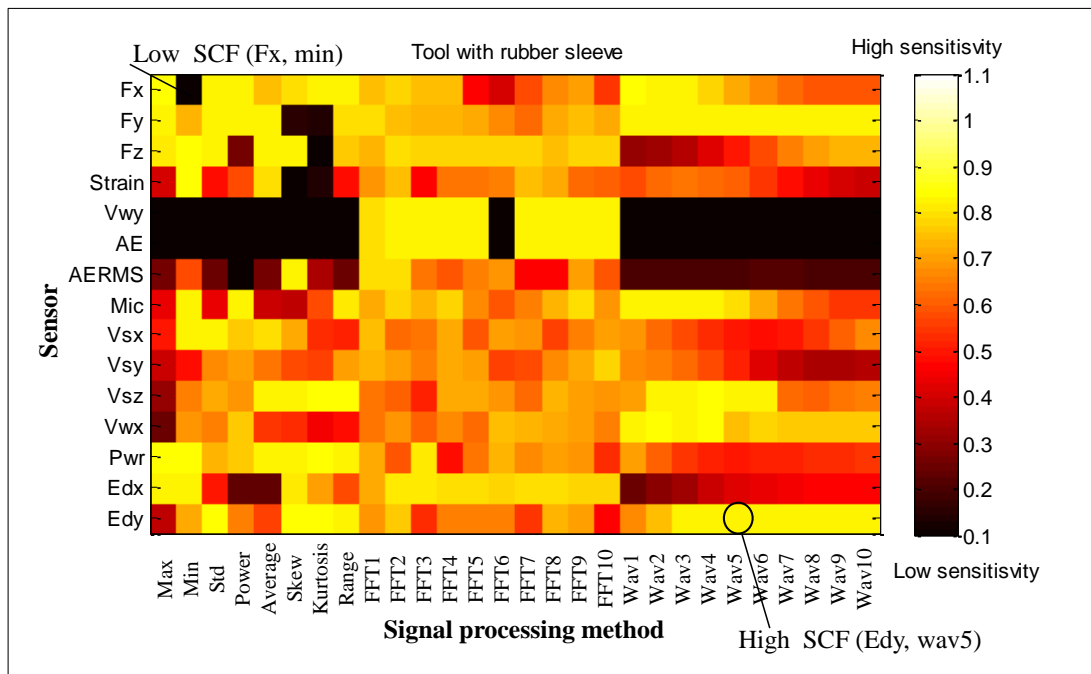


Figure L.4: A graphical presentation of the sensitivity for tool with broken one tooth, with rubber sleeve using SCIV method

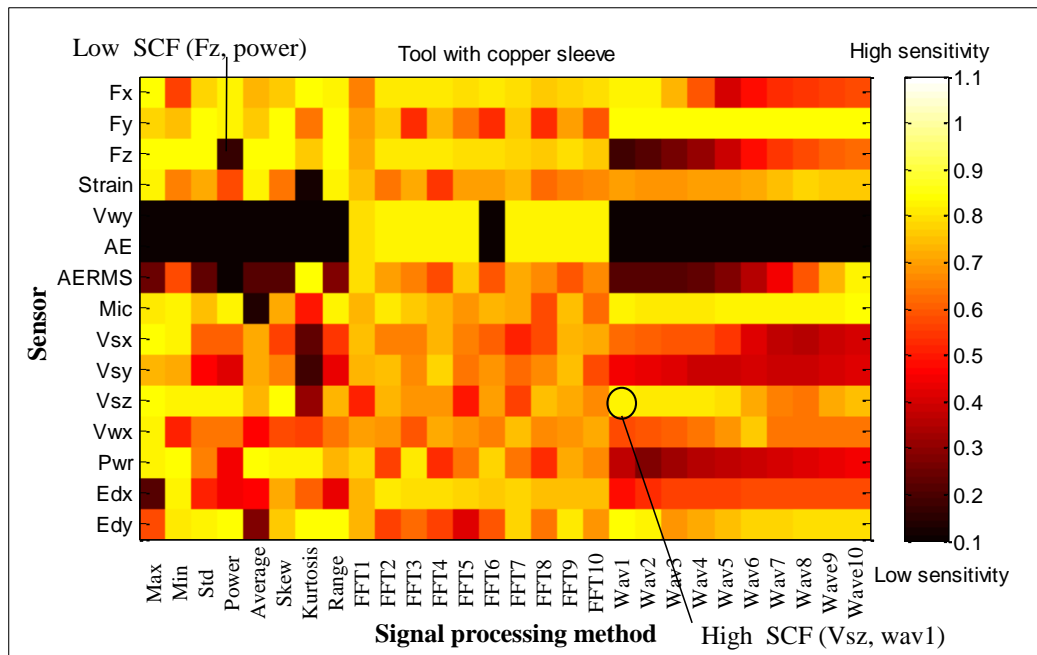


Figure L.5: A graphical presentation of the sensitivity for tool with broken one tooth, with copper sleeve using SCIV method.

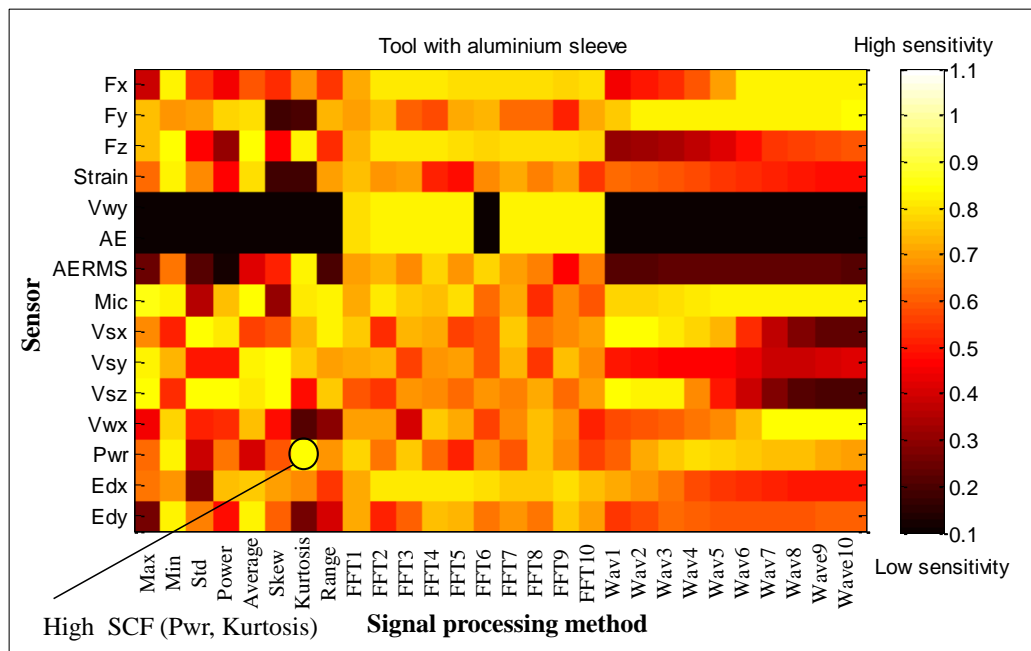


Figure L.6: A graphical presentation of the sensitivity for tool with broken one tooth, with aluminium sleeve using SCIV method.

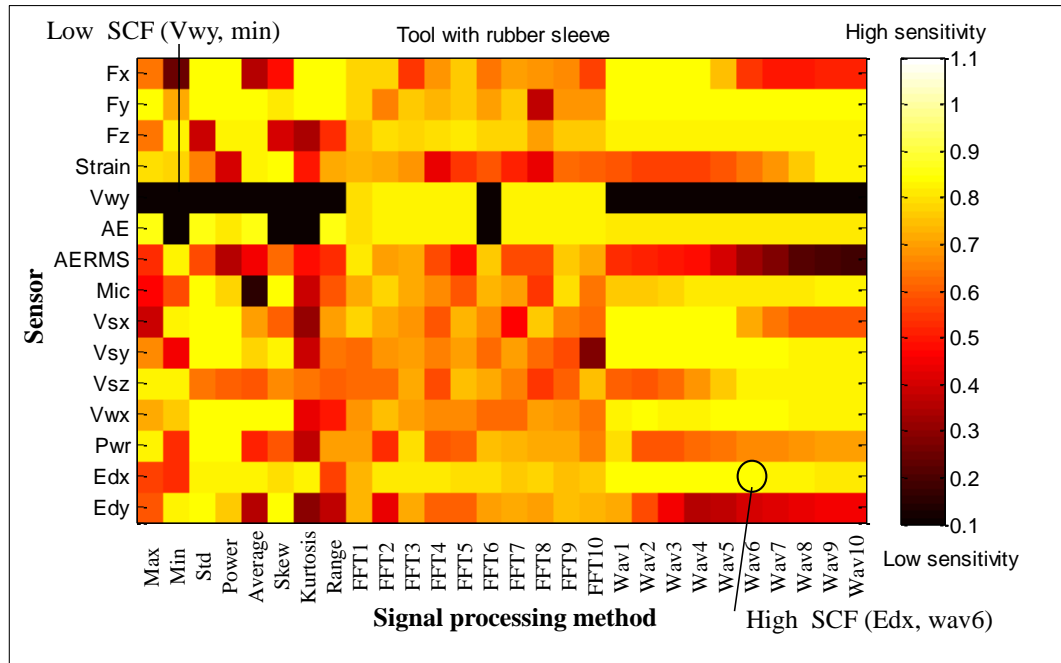


Figure L.7: A graphical presentation of the sensitivity for tool with broken two teeth, with rubber sleeve using SCIV method.

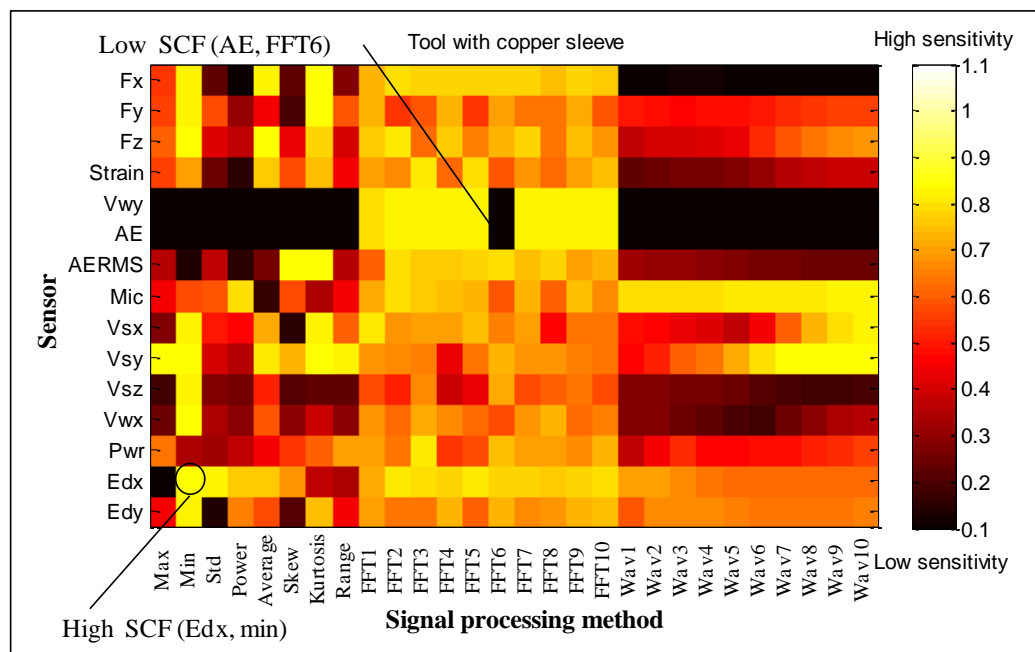


Figure L.8: A graphical presentation of the sensitivity for tool with broken two teeth, with copper sleeve using SCIV method.

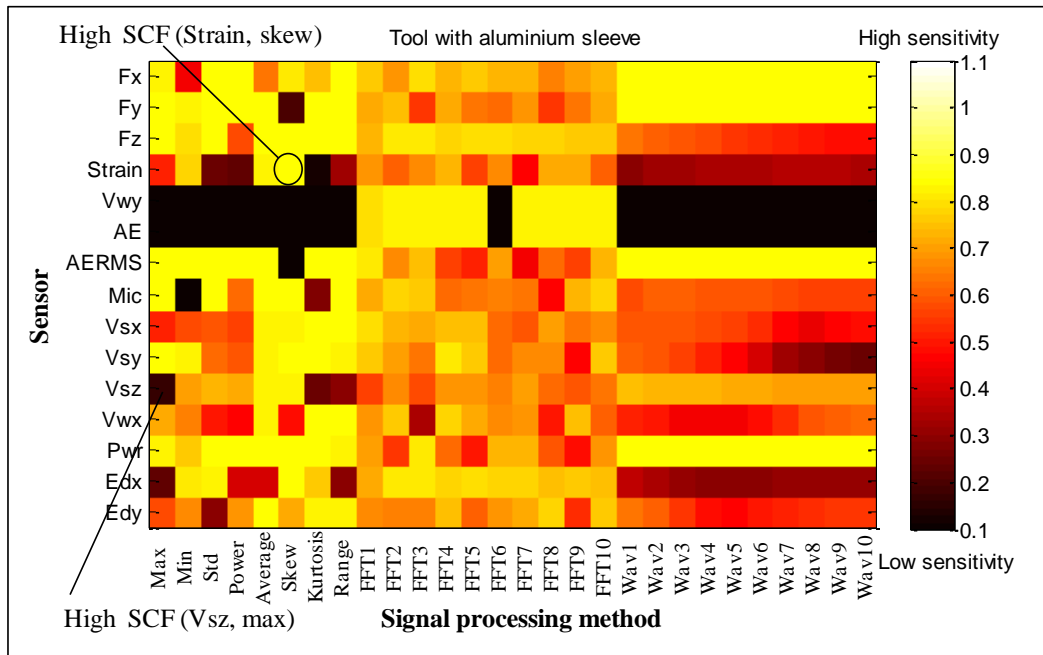


Figure L.9: A graphical presentation of the sensitivity for tool with broken two tooth, with aluminium sleeve using SCIV method.

Appendix M: Signal Simplification (For Chapter 10)

10.3.4 Correlation Coefficient (CCX3) method

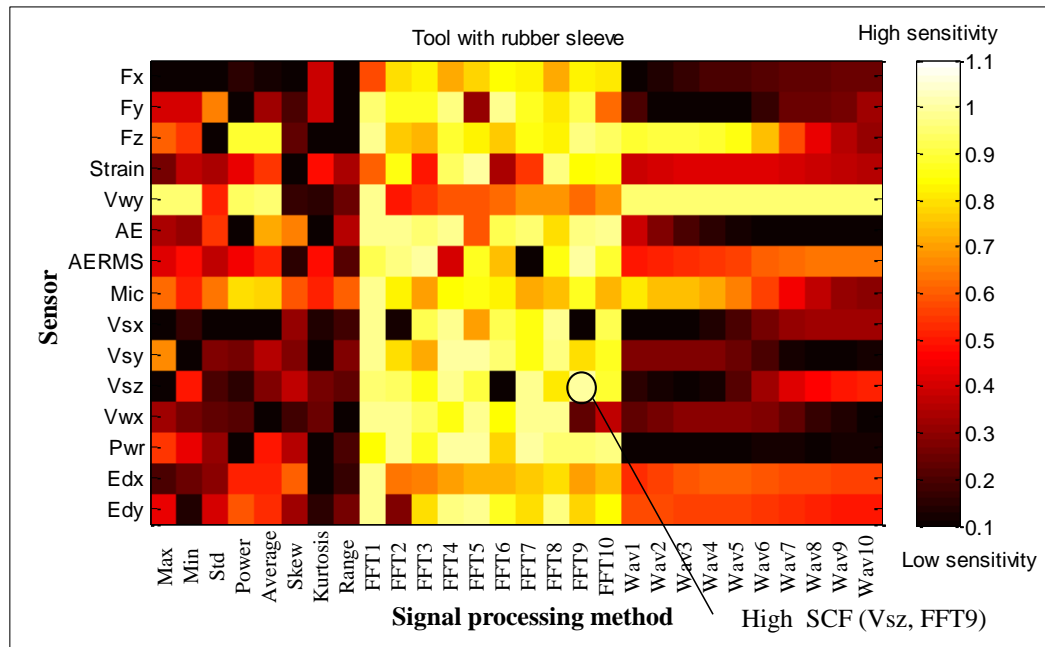


Figure M.1: A graphical presentation of the sensitivity for fresh tool with rubber sleeve using CCX3 method.

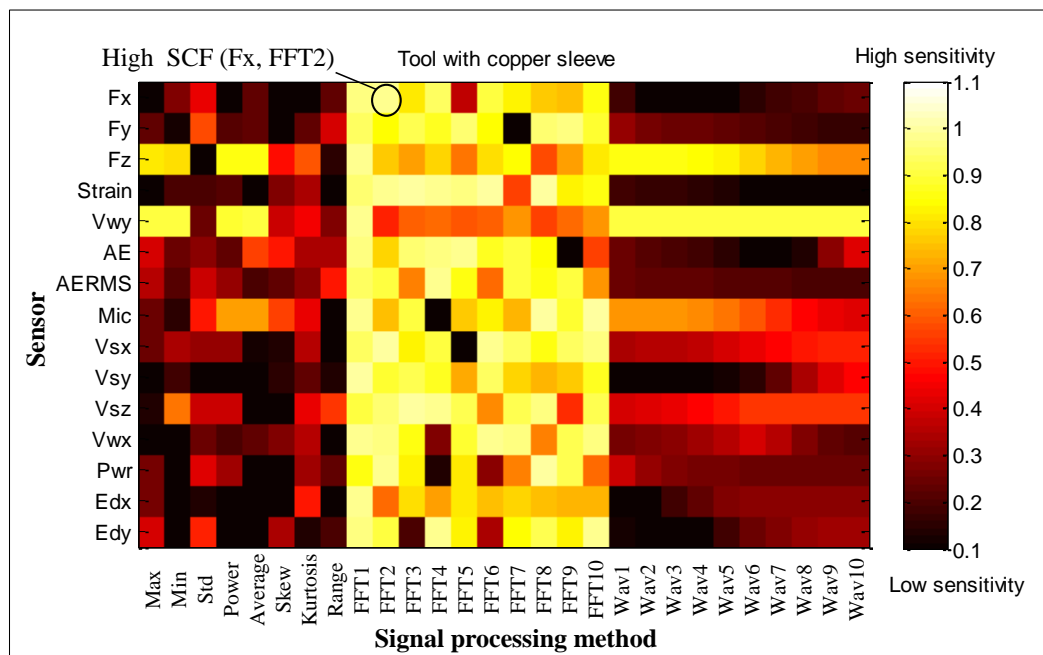


Figure M.2: A graphical presentation of the sensitivity for fresh tool with copper sleeve using CCX3 method.

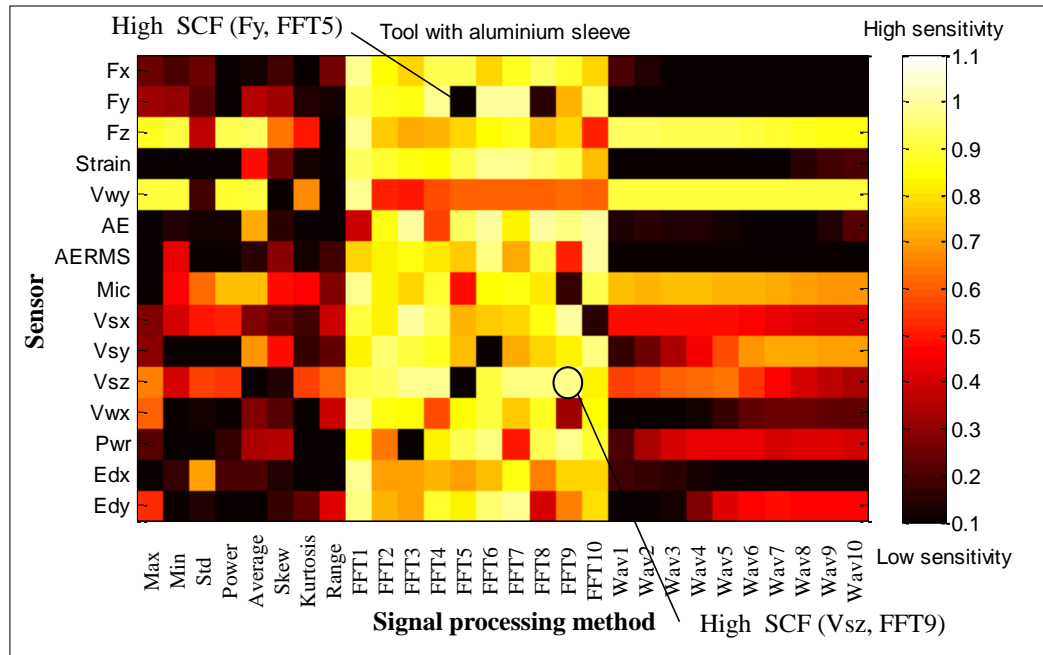


Figure M.3: A graphical presentation of the sensitivity for fresh tool with aluminium sleeve using CCX3 method.

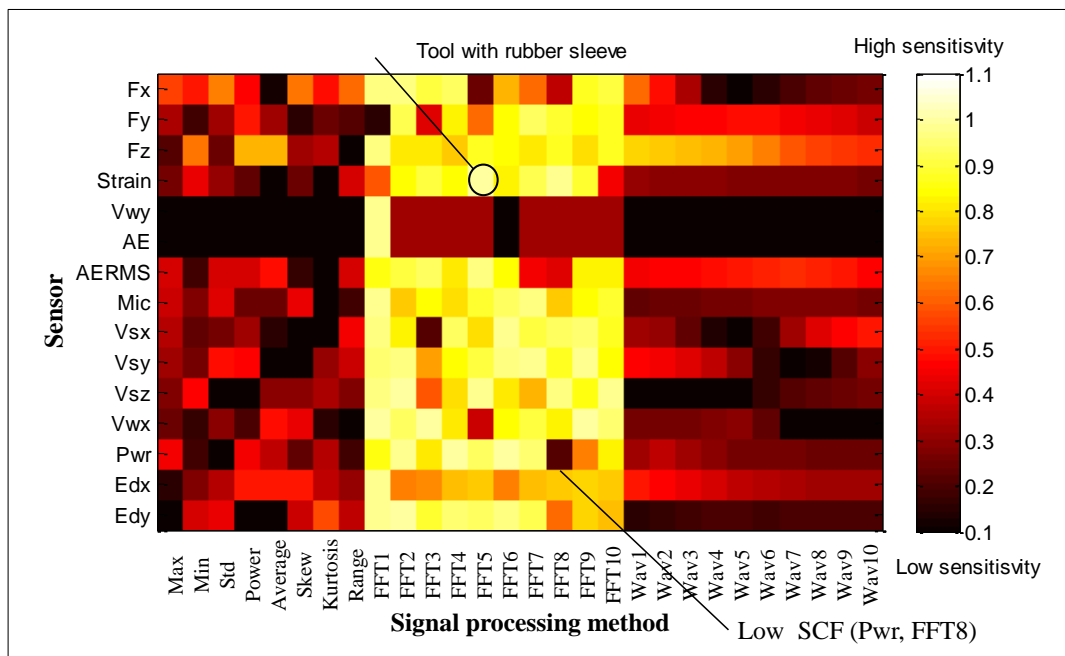


Figure M.4: A graphical presentation of the sensitivity for tool with one broken tooth, with rubber sleeve using CCX3 method.

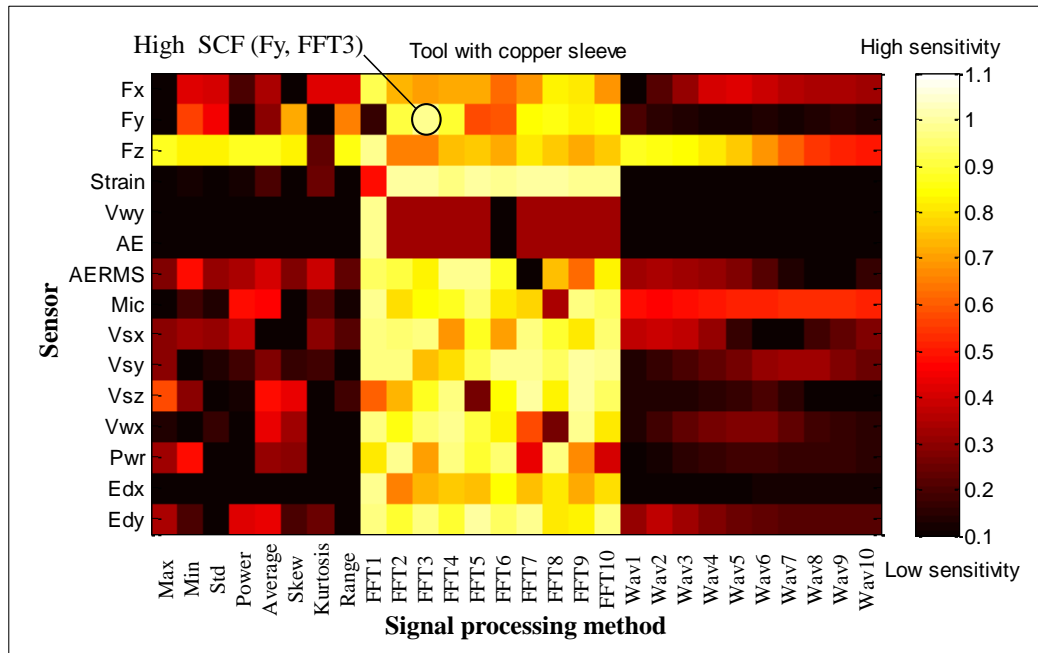


Figure M.5: A graphical presentation of the sensitivity for tool with one broken tooth, with copper sleeve using CCX3 method.

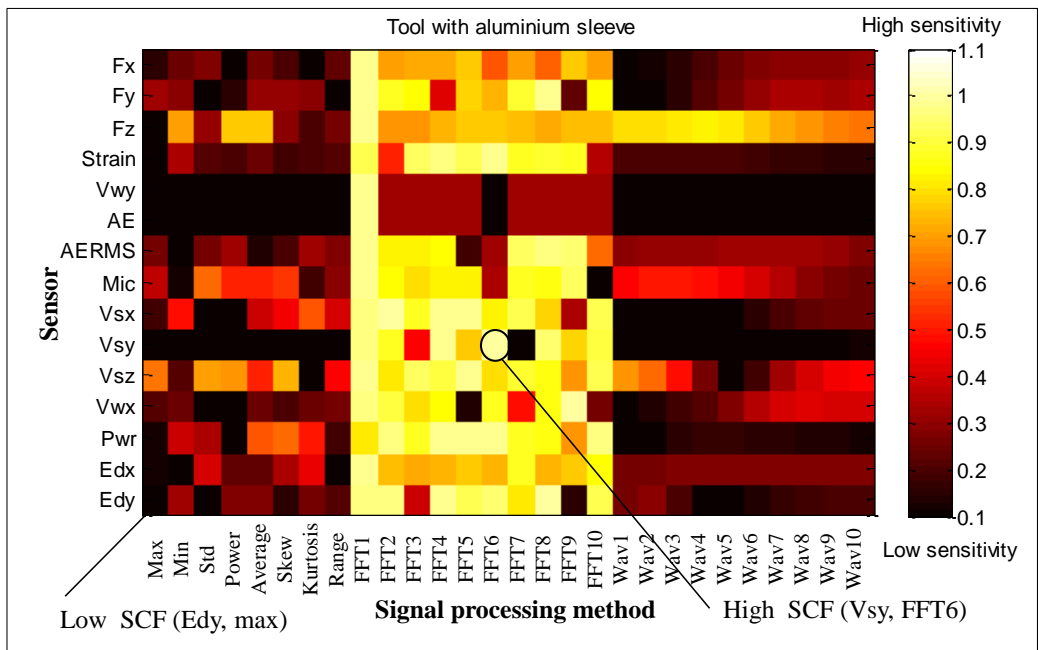


Figure M.6: A graphical presentation of the sensitivity for tool with one broken tooth, with aluminium sleeve using CCX3 method.

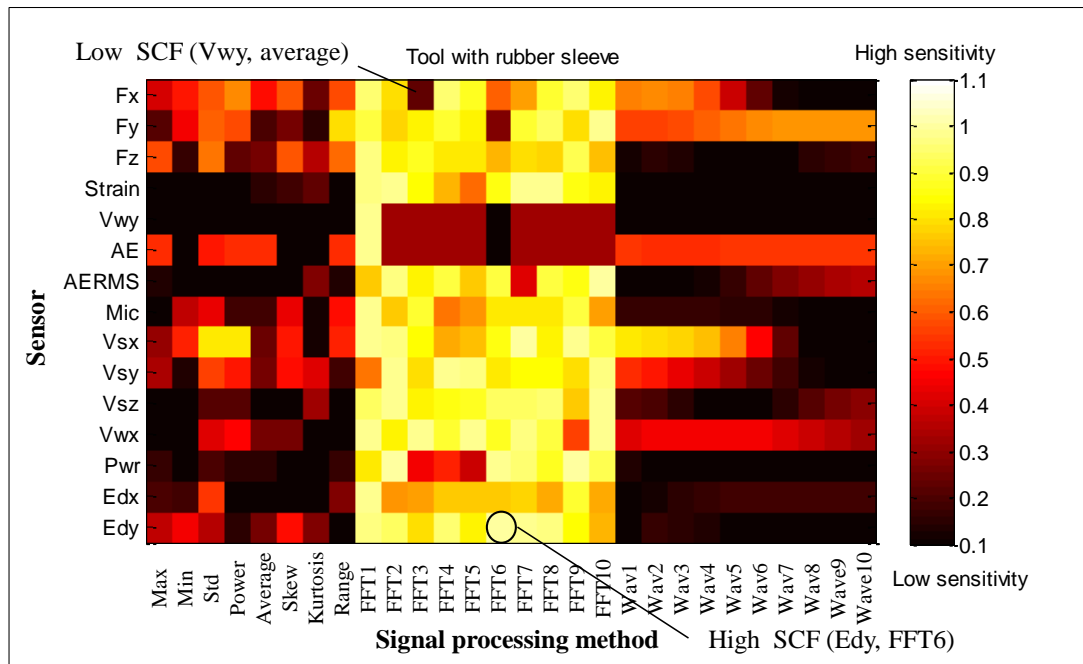


Figure M.7: A graphical presentation of the sensitivity for tool with two broken teeth, rubber sleeve using CCX3 method.

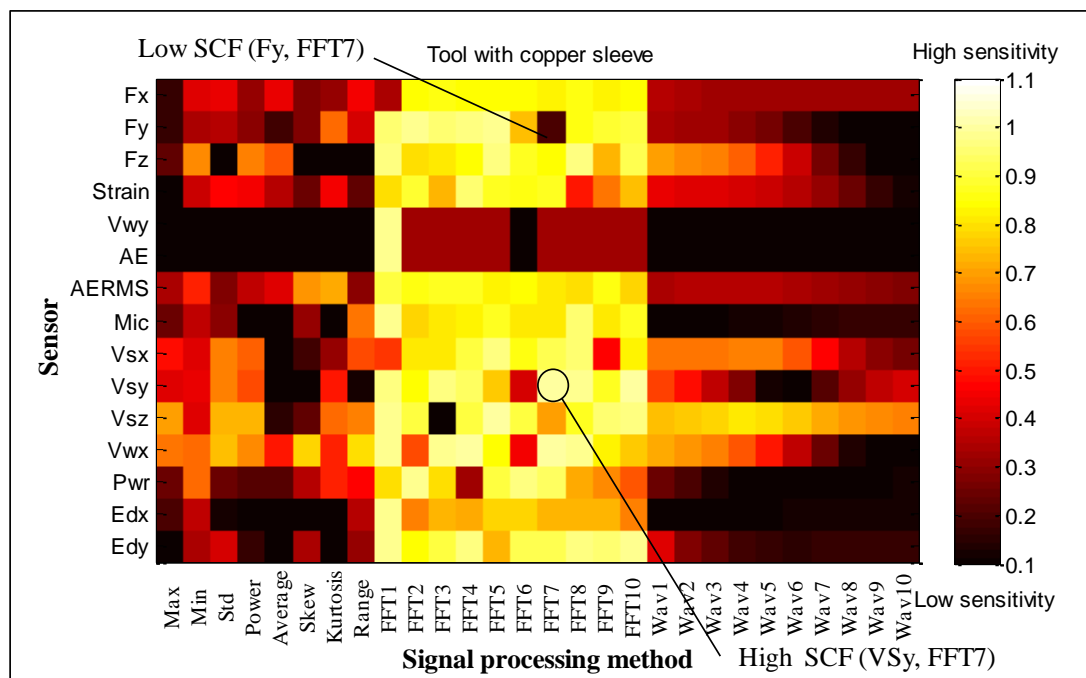


Figure M.8: A graphical presentation of the sensitivity for tool with two broken teeth, copper sleeve using CCX3 method.

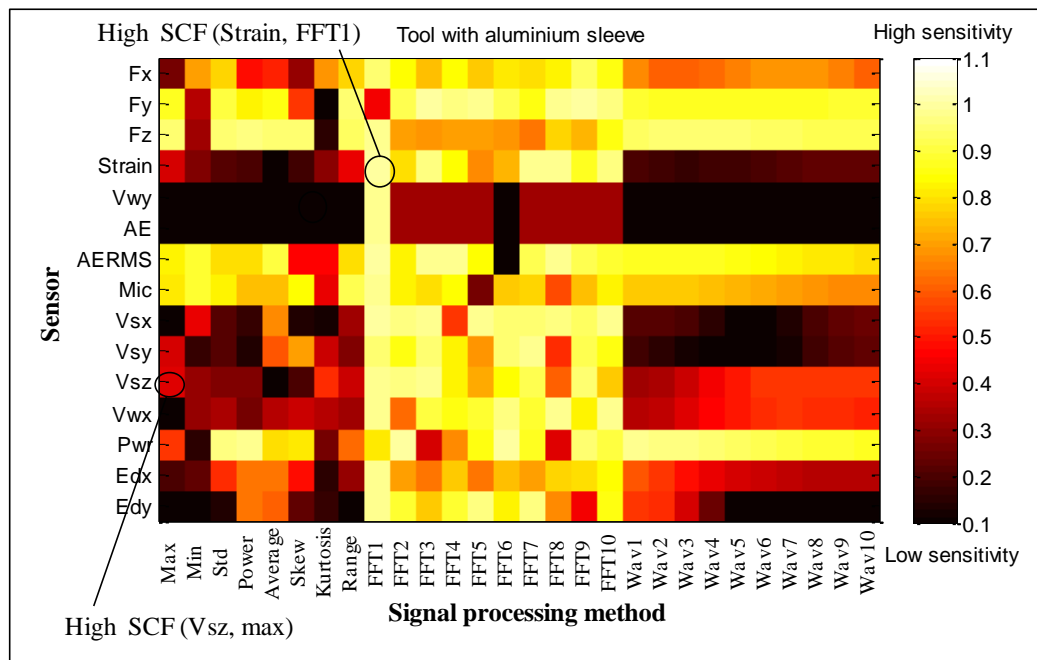


Figure M.9: A graphical presentation of the sensitivity for tool with two broken teeth, with aluminium sleeve using CCX3 method.

Appendix N: Signal Simplification (For Chapter 10)

10.3.4 Correlation Coefficient (CCX20) method

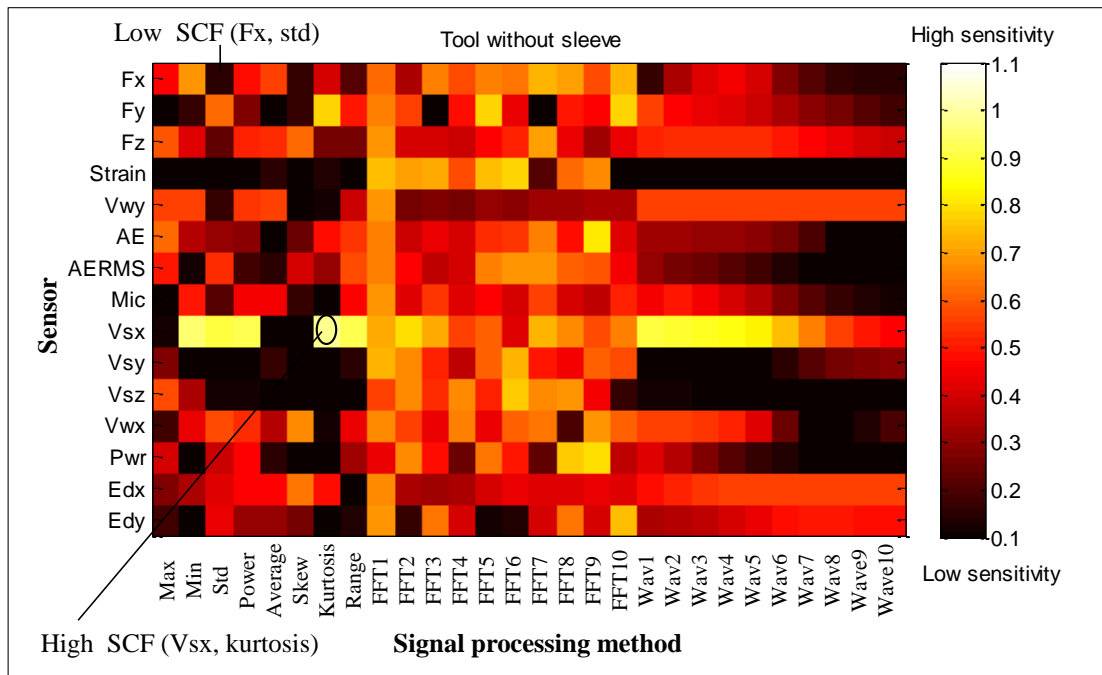


Figure N.1: A graphical presentation of the sensitivity for fresh tool without sleeve using CCX20 method.

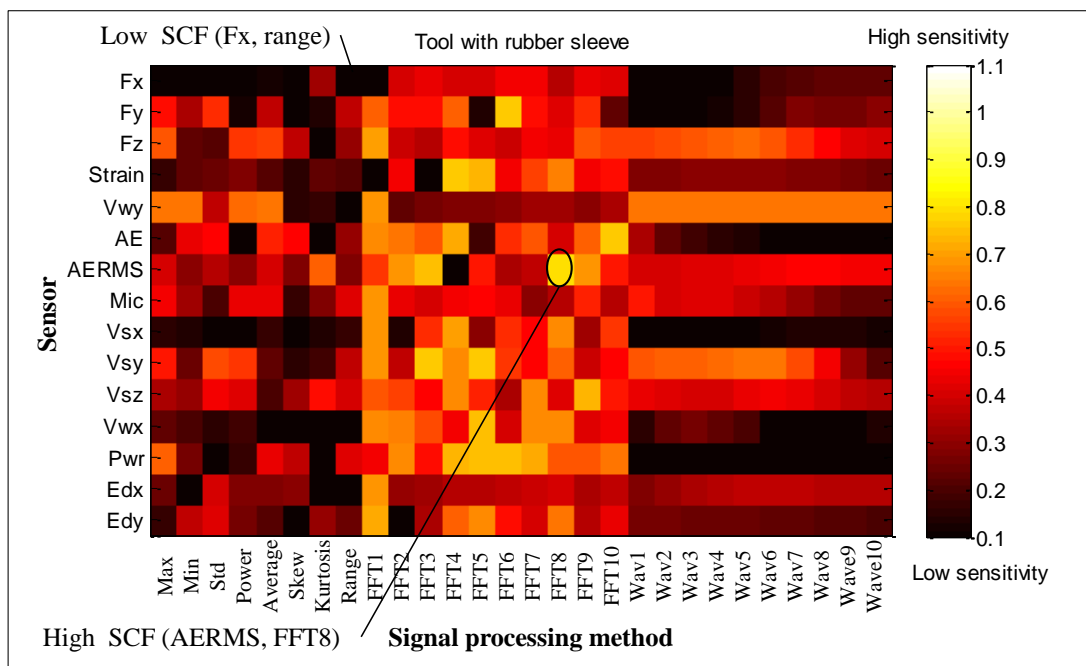


Figure N.2: A graphical presentation of the sensitivity for fresh tool with rubber sleeve using CCX20 method.

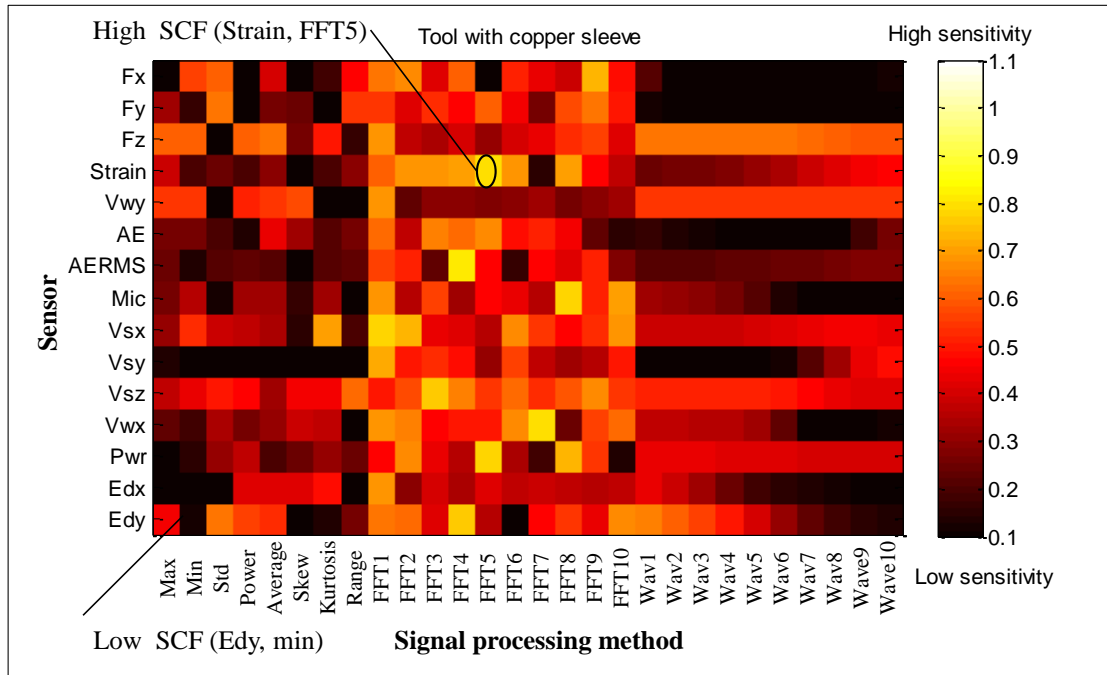


Figure N.4: A graphical presentation of the sensitivity for fresh tool with copper sleeve using CCX20 method.

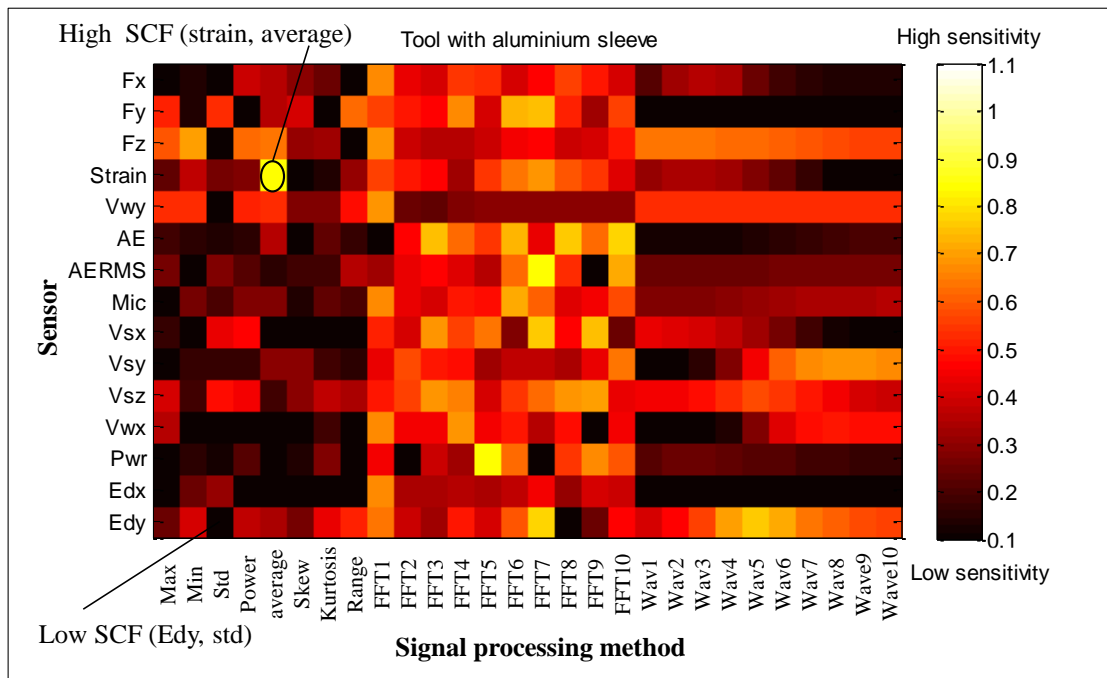


Figure N.5: A graphical presentation of the sensitivity for fresh tool with aluminium sleeve using CCX20 method.

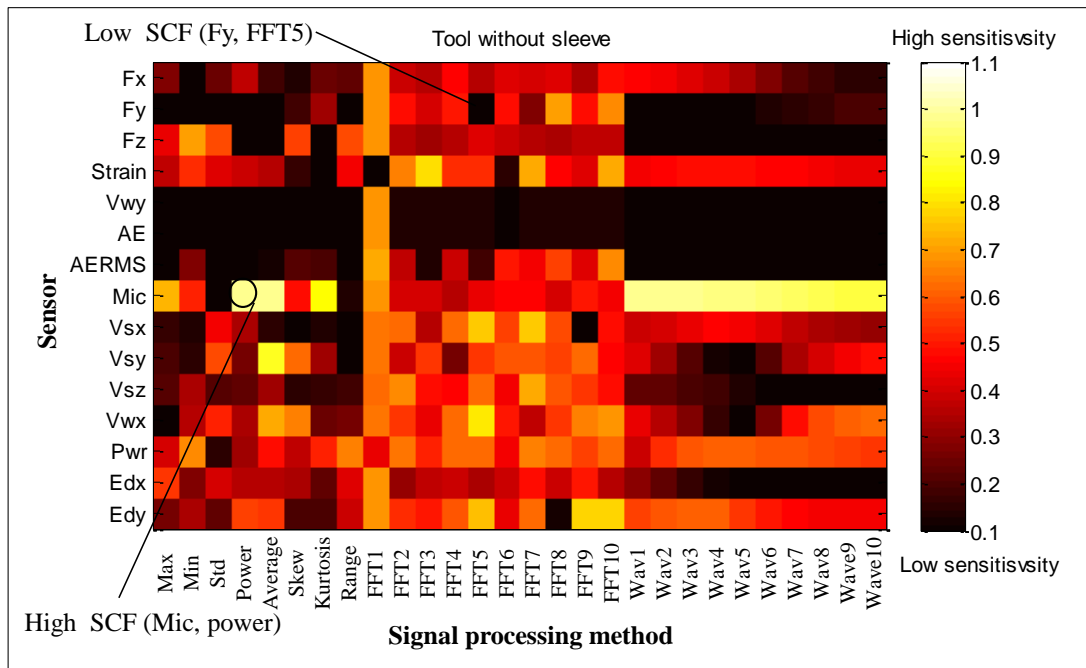


Figure N.6: A graphical presentation of the sensitivity for tool with one broken tooth, without sleeve using CCX20 method.

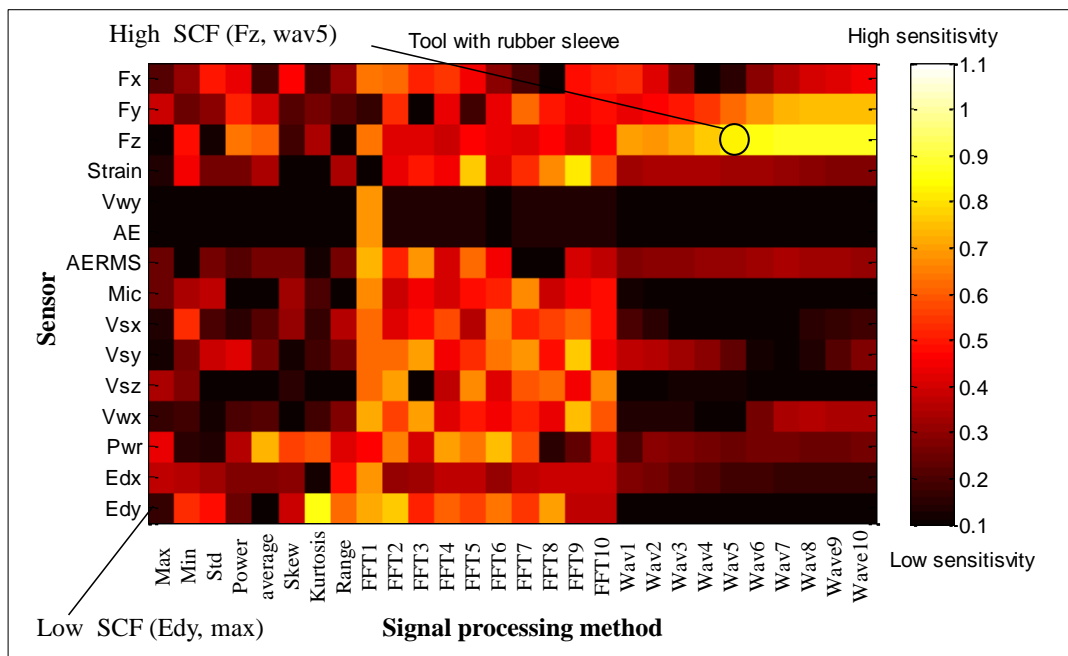


Figure N.7: A graphical presentation of the sensitivity for tool with one broken tooth, with rubber sleeve using CCX20 method.

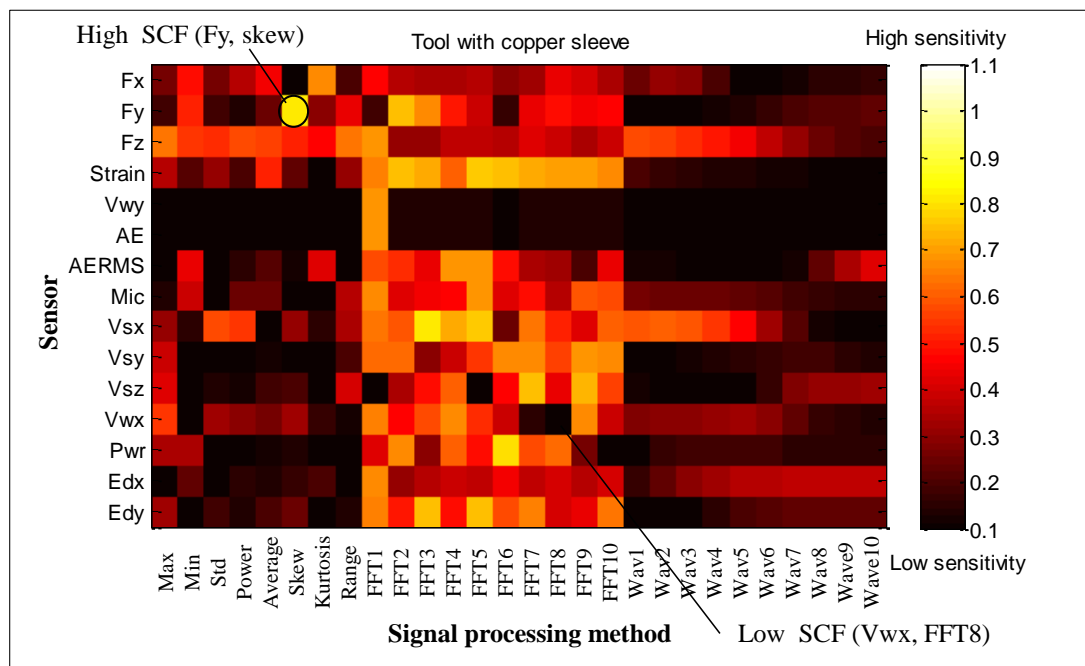


Figure N.8: A graphical presentation of the sensitivity for tool with one broken tooth, with copper sleeve using CCX20 method.

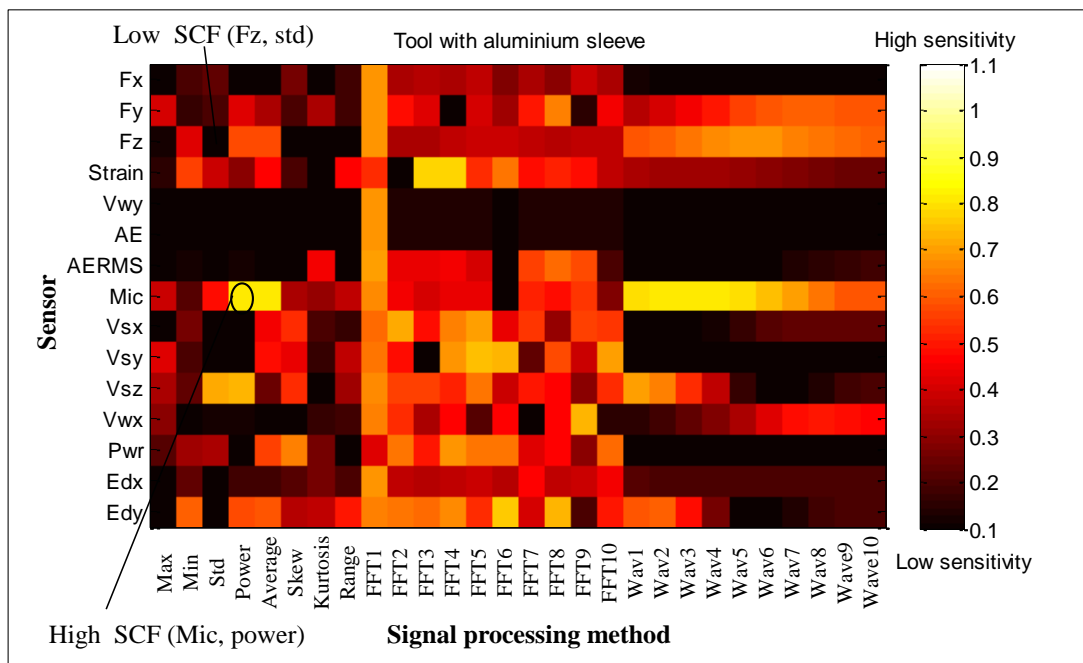


Figure N.9: A graphical presentation of the sensitivity for tool with one broken tooth, with aluminium sleeve using CCX20 method.

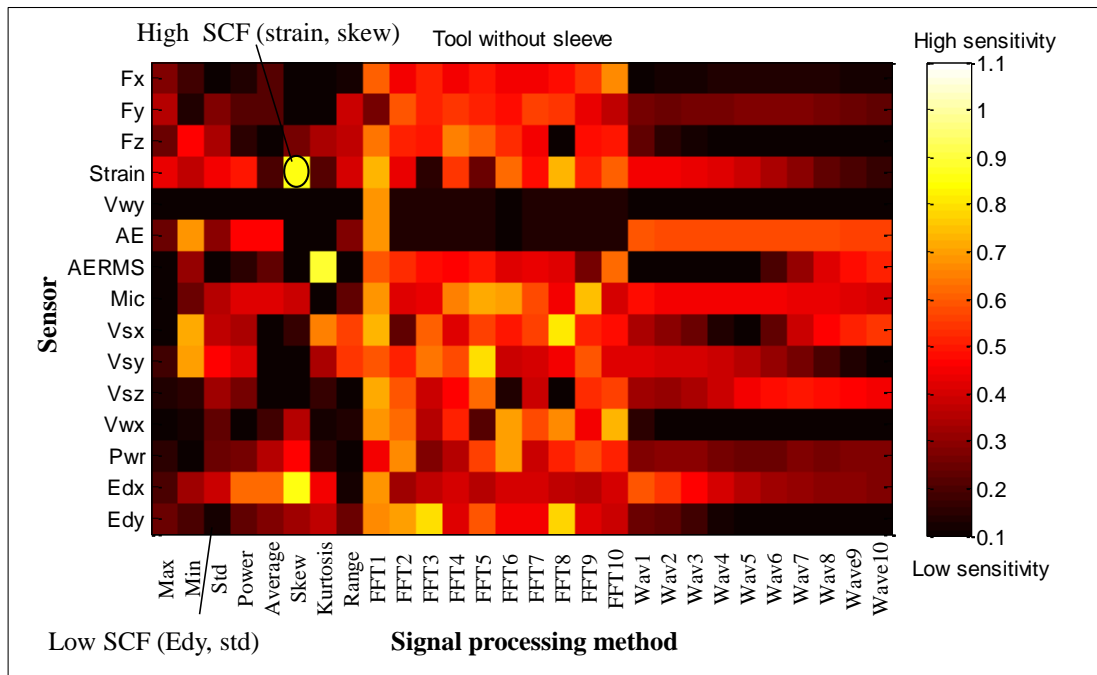


Figure N.10: A graphical presentation of the sensitivity for tool with two broken teeth, without sleeve using CCX20 method.

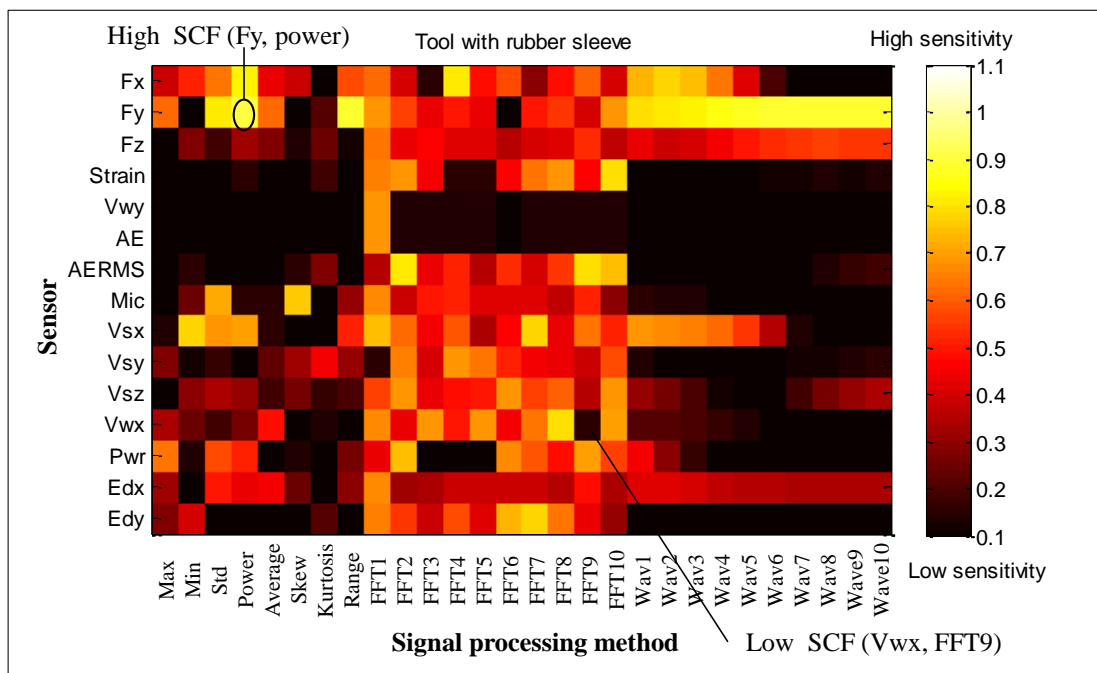


Figure N.11: A graphical presentation of the sensitivity for tool with two broken teeth, with rubber sleeve using CCX20 method.

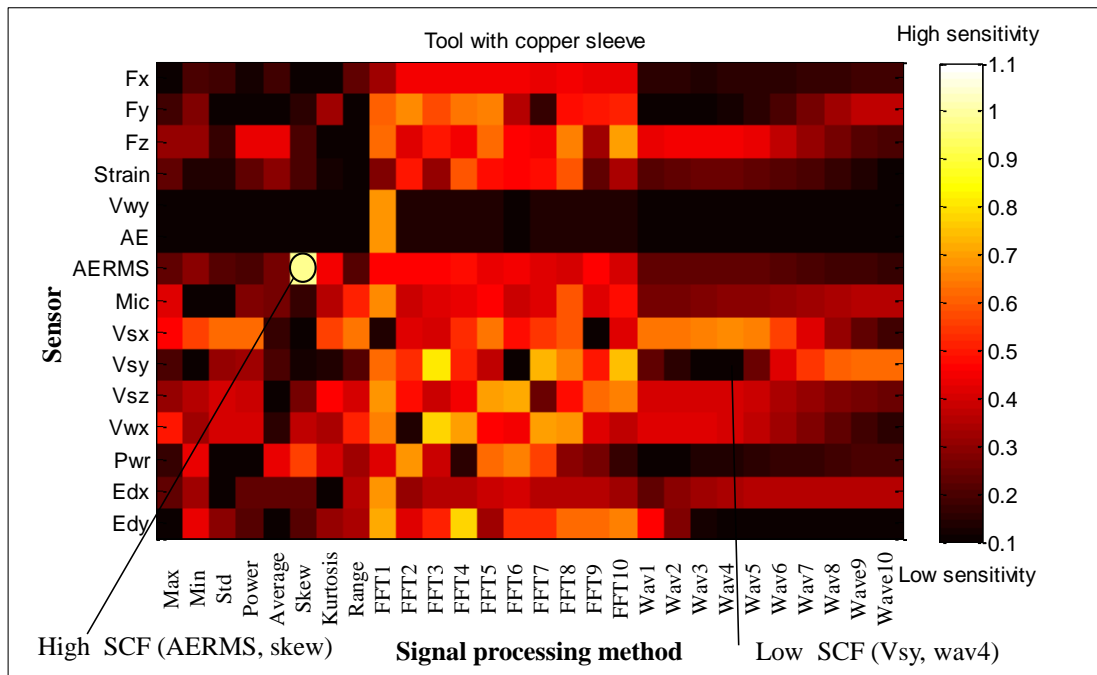


Figure N.12: A graphical presentation of the sensitivity for tool with two broken teeth, with copper sleeve using CCX20 method.

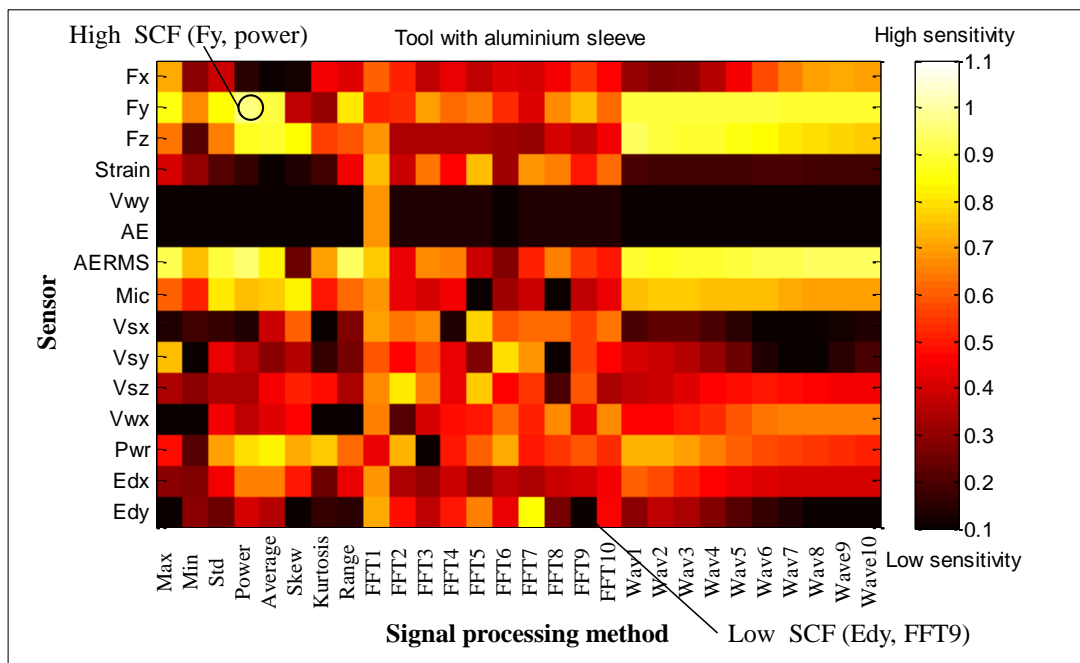


Figure N.13: A graphical presentation of the sensitivity for tool with two broken teeth, with aluminium sleeve using CCX20 method.

Appendix O: Signal Simplification (For Chapter 10)

10.3.6 Fuzzy Logic (FL) method

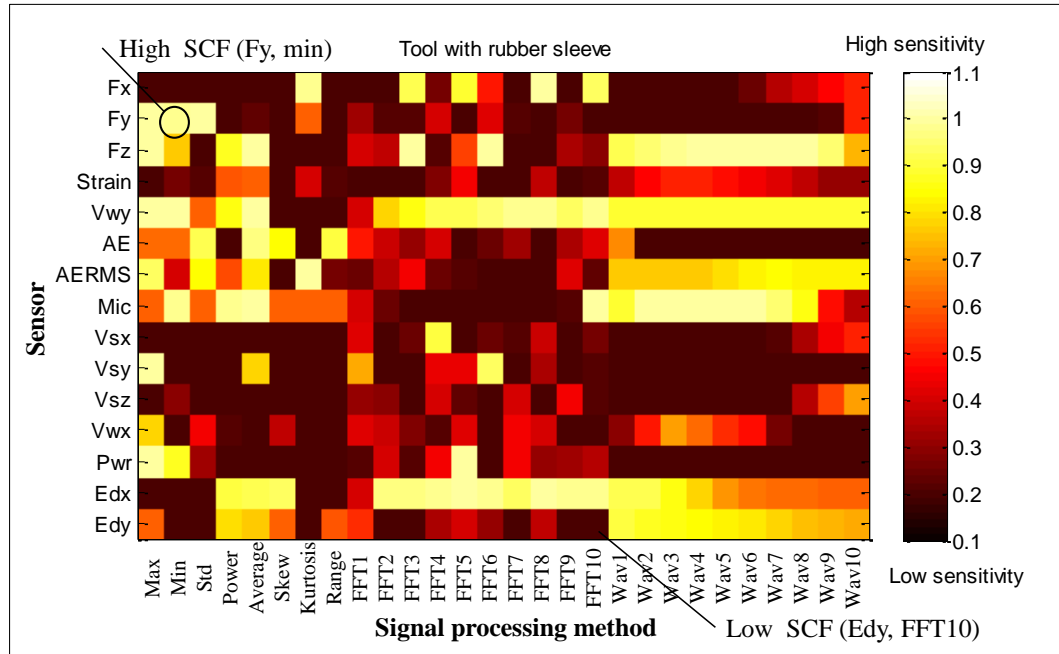


Figure O.1: A graphical presentation of the sensitivity for fresh tool with rubber sleeve using fuzzy logic method.

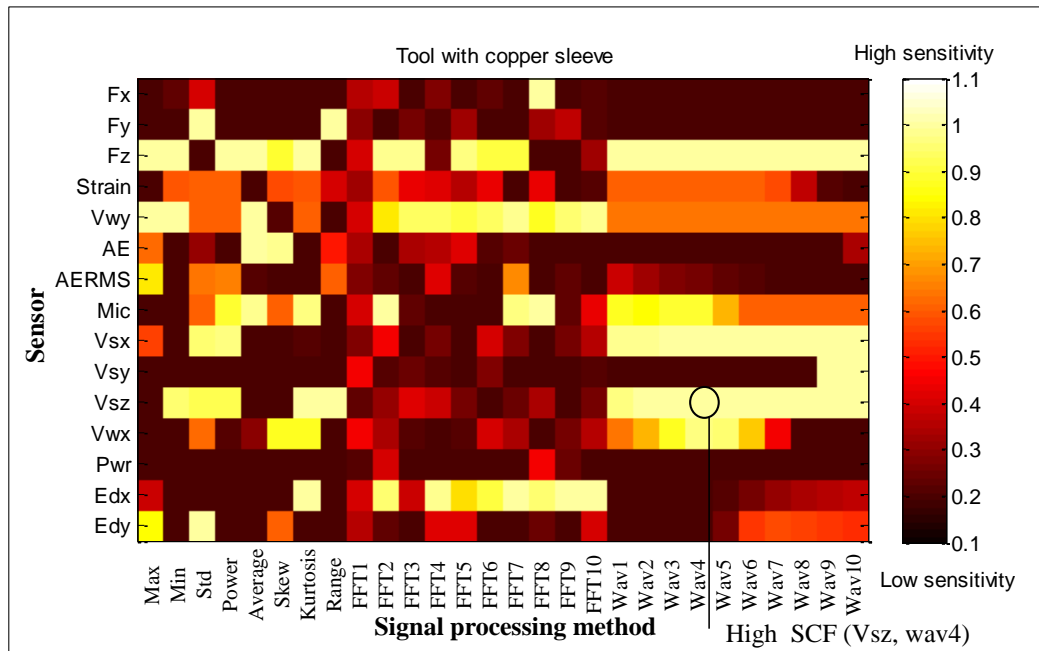


Figure O.2: A graphical presentation of the sensitivity for fresh tool with copper sleeve using fuzzy logic method.

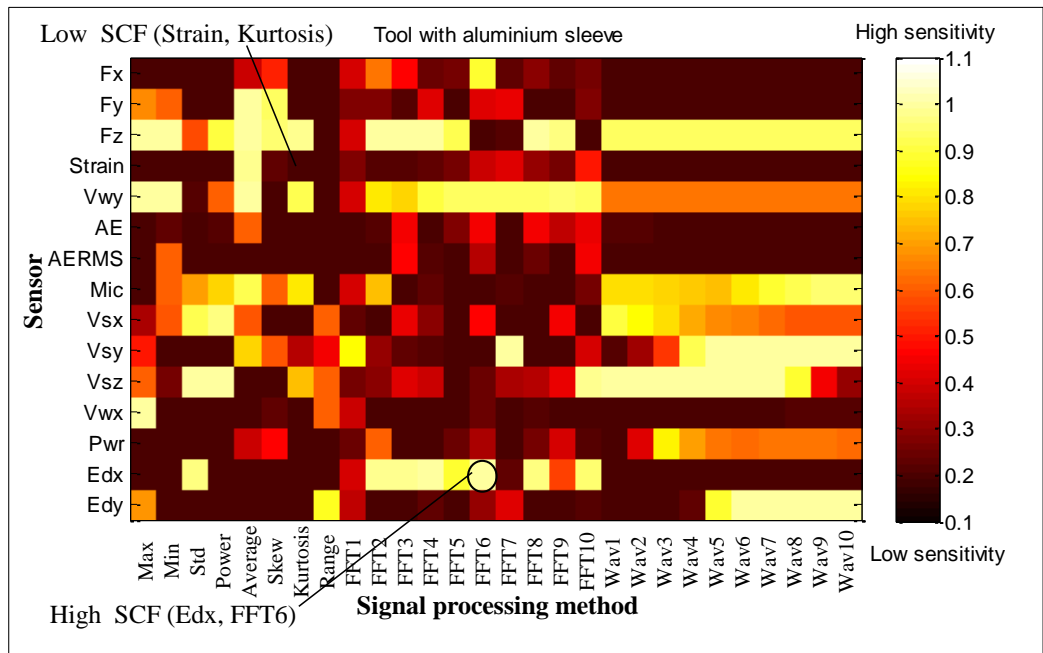


Figure O.3: A graphical presentation of the sensitivity for fresh tool with aluminium sleeve using fuzzy logic method.

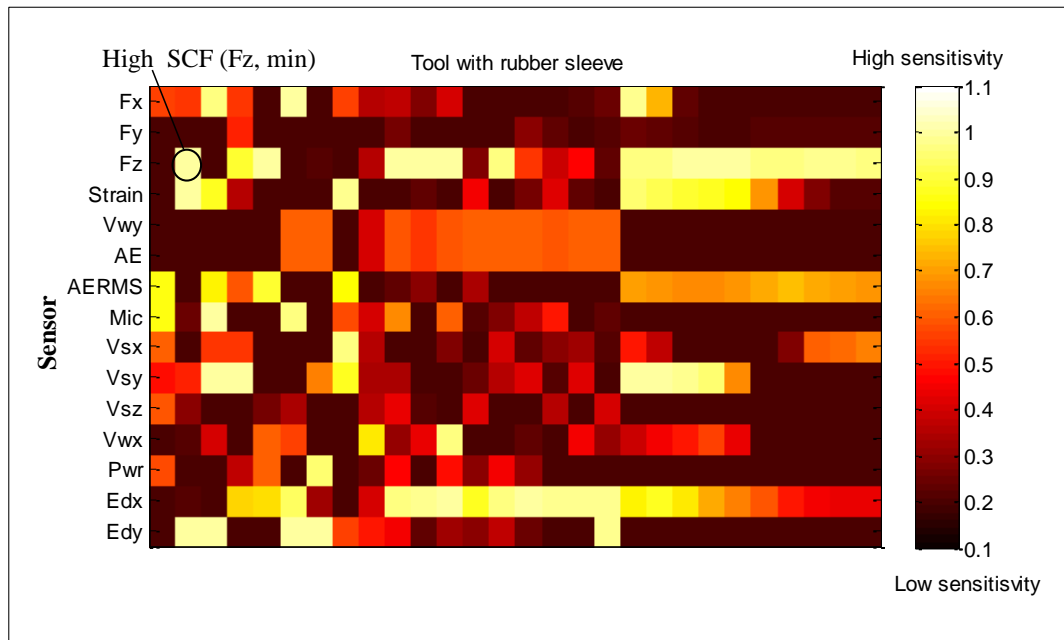


Figure O.4: A graphical presentation of the sensitivity for tool with broken one tooth, with rubber sleeve using fuzzy logic method.

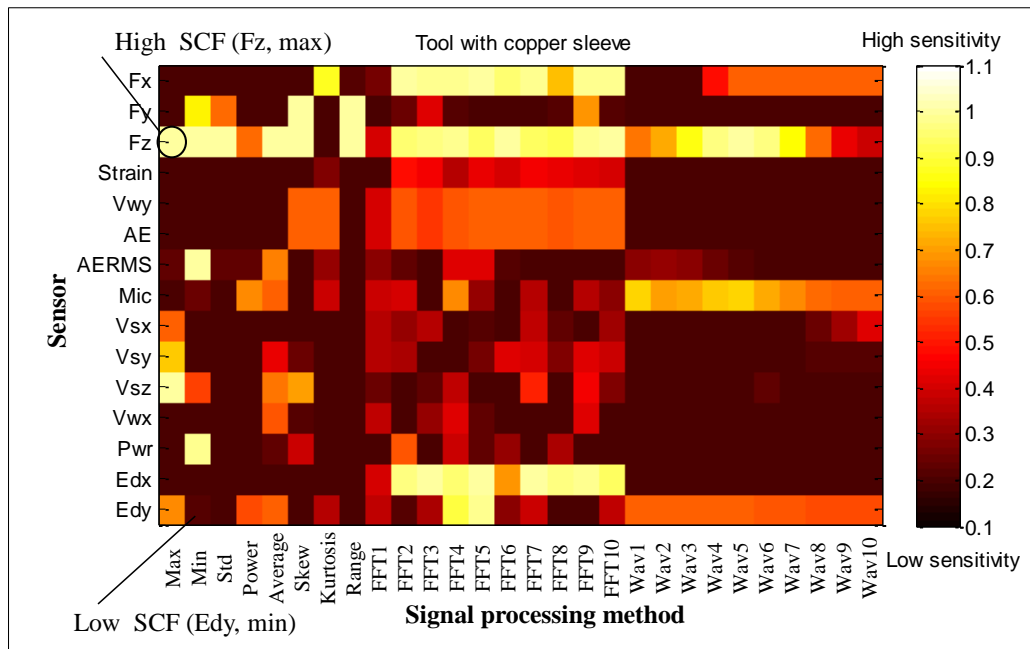


Figure O.5: A graphical presentation of the sensitivity for tool with one broken tooth, with copper sleeve using fuzzy logic method.

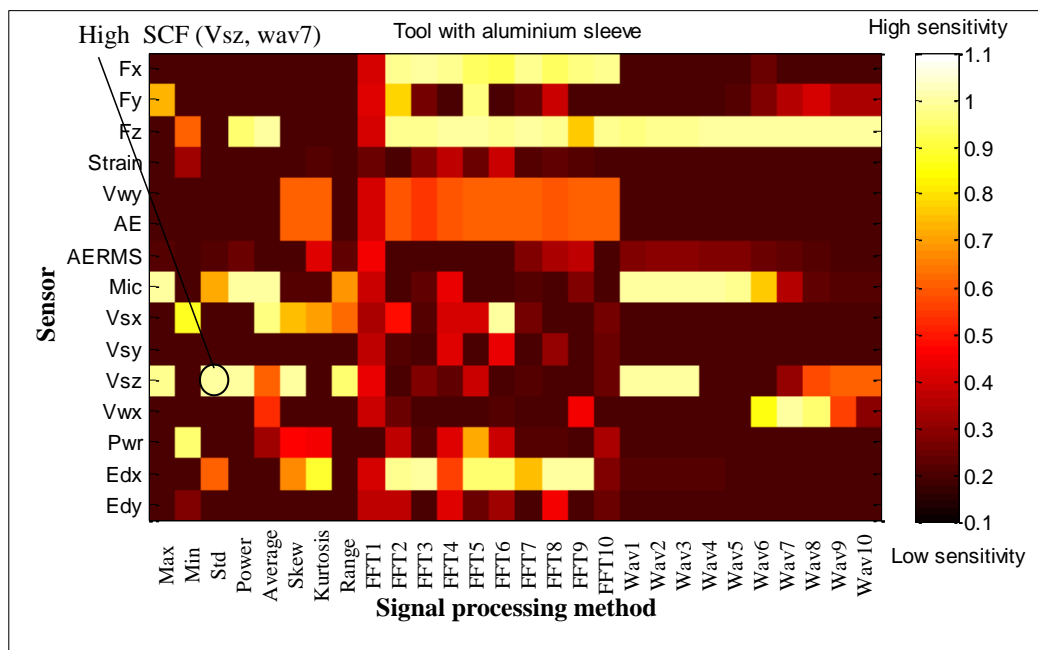


Figure O.6: A graphical presentation of the sensitivity for tool with one broken tooth, with aluminium sleeve using fuzzy logic method.

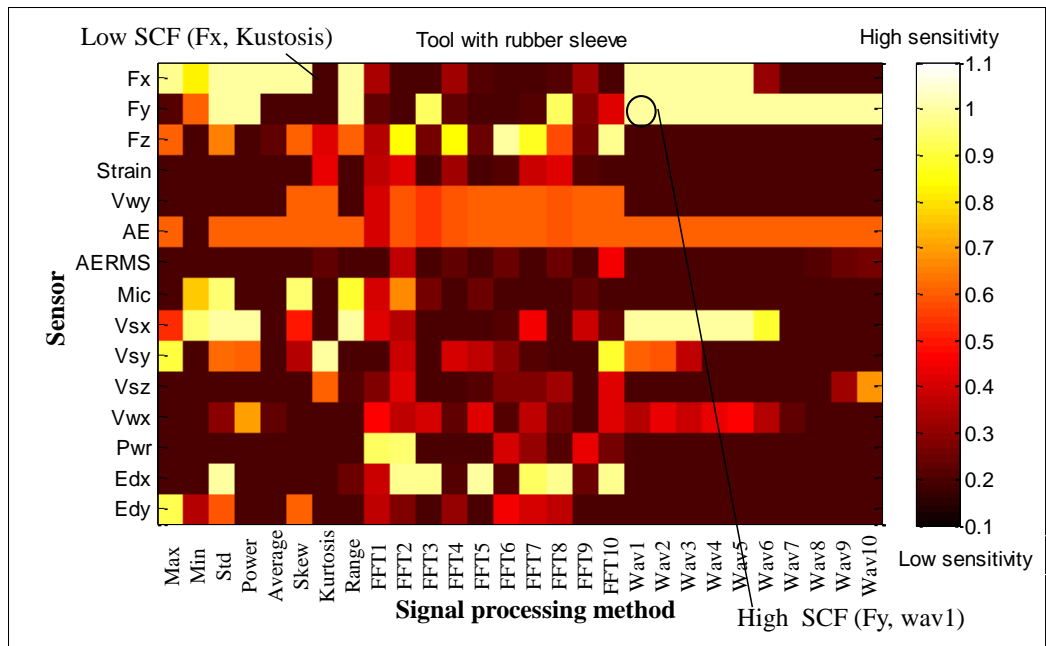


Figure O.7: A graphical presentation of the sensitivity for tool with two broken teeth, with rubber sleeve using fuzzy logic method.

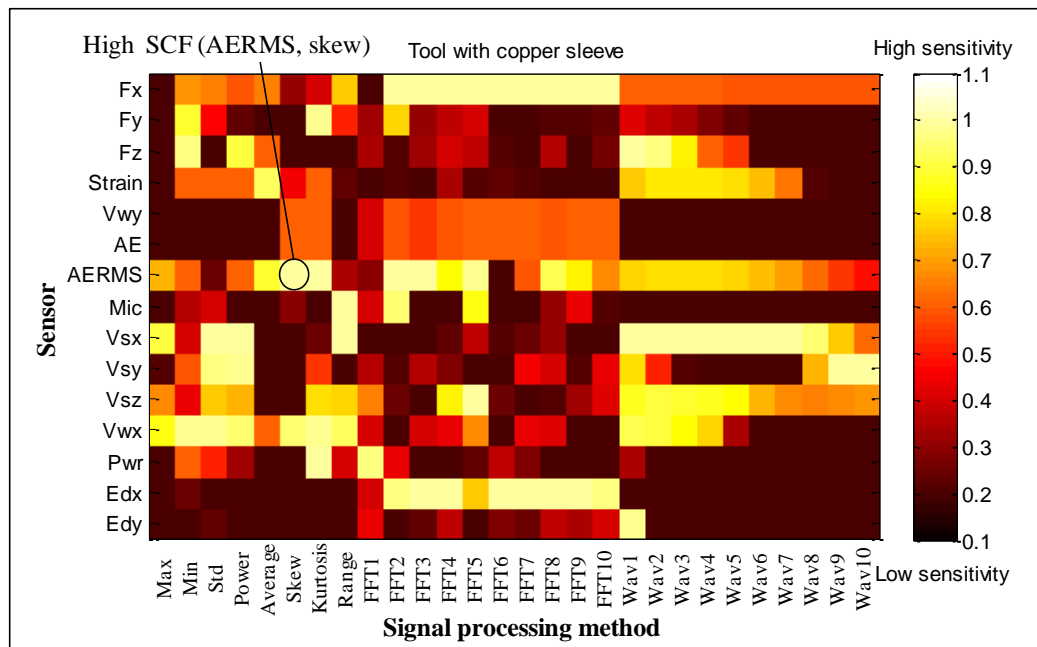


Figure O.8: A graphical presentation of the sensitivity for tool with two broken teeth, with copper sleeve using fuzzy logic method.

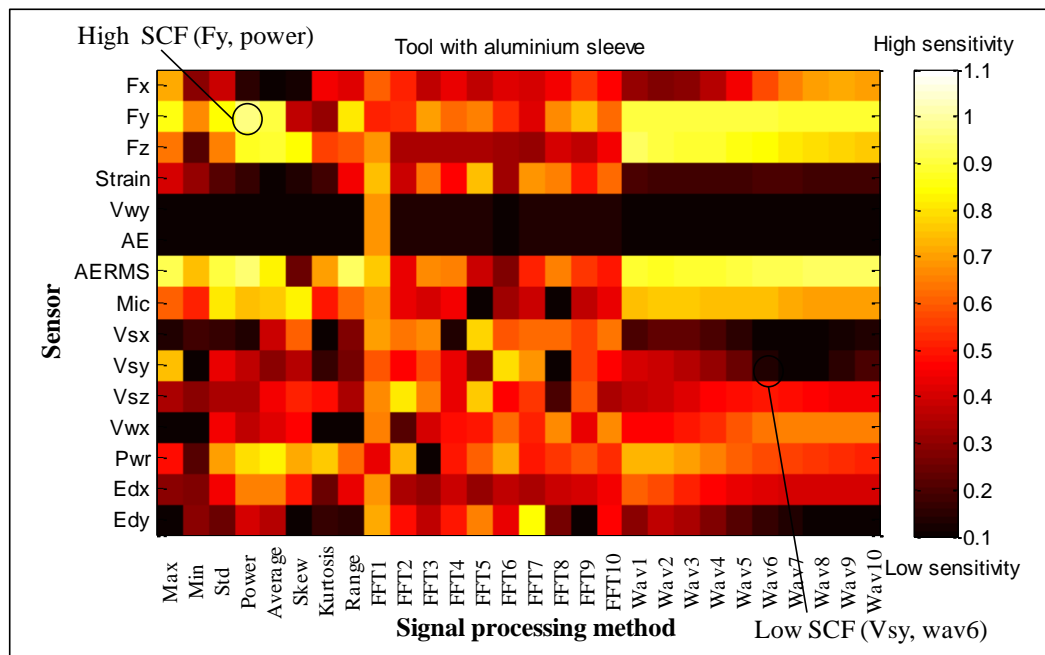


Figure O.9: A graphical presentation of the sensitivity for tool with two broken teeth, with aluminium sleeve using fuzzy logic method.